ACTA CHIMICA

ACADEMIAE SCIENTIARUM HUNGARICAE

ADIUVANTIBUS

M. BECK, R. BOGNÁR, V. BRUCKNER,
GY. HARDY, K. LEMPERT, F. MÁRTA,
K. POLINSZKY, E. PUNGOR,
G. SCHAY, Z. G. SZABÓ, P. TÉTÉNYI

REDIGUNT

B. LENGYEL et GY. DEÁK

TOMUS 92 FASCICULUS 1

AKADÉMIAI KIADÓ, BUDAPEST

1977

ACTA CHIM. (BUDAPEST) ACASA2 92 (1) 1–103 (1977)

ACTA CHIMICA

A MAGYAR TUDOMÁNYOS AKADÉMIA
KÉMIAI TUDOMÁNYOK OSZTÁLYÁNAK
IDEGEN NYELVŰ KÖZLEMÉNYEI

FŐSZERKESZTŐ
LENGYEL BÉLA

SZERKESZTŐ
DEÁK GYULA

TECHNIKAI SZERKESZTŐ
HARASZTHY-PAPP MELINDA

SZERKESZTŐ BIZOTTSÁG
BECK MIHÁLY, BOGNÁR REZSŐ, BRUCKNER GYŐZŐ,
HARDY GYULA, LEMPERT KÁROLY, MÁRTA FERENC,
POLINSZKY KÁROLY, PUNGOR ERNŐ, SCHAY GÉZA,
SZABÓ ZOLTÁN, TÉTÉNYI PÁL

Acta Chimica is a journal for the publication of papers on all aspects of chemistry, in the English, French, German and Russian languages.

Acta Chimica is published in 4 volumes per year. Each volume consists of 4 issues of varying size.

Manuscripts should be sent to

Acta Chimica
H-1521 Budapest, Hungary

Correspondence with the Editors should be sent to the same address. Manuscripts are not returned to the Authors.

Subscription rate $ 32.00 per volume.

Hungarian subscribers should order from Akadémiai Kiadó, 1363 Budapest, P.O. Box 24. Account No. 215 11488.

Orders from other countries are to be sent to "Kultúra" Foreign Trade Company for Books and Newspapers (H-1389 Budapest 62, P.O. Box 149. Account No. 218 10990) or to its representatives abroad.

ACTA CHIMICA

ACADEMIAE SCIENTIARUM HUNGARICAE

ADIUVANTIBUS

M. BECK, R. BOGNÁR, V. BRUCKNER,
GY. HARDY, K. LEMPERT, F. MÁRTA,
K. POLINSZKY, E. PUNGOR,
G. SCHAY, Z. G. SZABÓ, P. TÉTÉNYI

REDIGUNT

B. LENGYEL et GY. DEÁK

TOMUS 92

AKADÉMIAI KIADÓ, BUDAPEST

1977

ACTA CHIMICA

ТОМ 92 – ВЫП. 4

РЕЗЮМЕ

Механика радиолиза циклопентана

Ч. КЕСЕИ, Л. ВОЙНАРОВИЧ и Г. ФЁЛЬДИАК

Радиолиз циклопентана был исследован с помощью акцепторов, электроно- и положительных ионов. Были определены основные составляющие величины $G(H_2)$ (унимолекулярного выделения водорода: H_2: 1,5, а термических и горячих атомов водорода: 1,6 и 2,3, соответственно), выходы осколочных углеводородов и циклопентильных радикалов, образующихся за счет дегидрогенизации ~(5,2), а также отношения k_d/k_c последних радикалов (1,0). Суммарный выход ионов, образующихся под влиянием облучения, $G_{fi} = G_{fi} + G_{gi} = 4{,}4$, где выход свободных ионов равен всего G_{fi}-0,12, т. е. составляет всего ~3% от общего выхода. Значительные изменения в продуктах реакции акцепторов ионов, могут быть связаны с разными ионными процессами: унимолекулярное образование циклопентена на 60–80%-ов является такой реакцией. Было установлено, что около 90%-ов осколочных углеводород образуется в унимолекулярной реакции. Для расчета эффекта акцепторов было предложено уравописывающее явление и свободное от противоречий, с помощью которого и на основе результатов измерений была рассчитана величина α, характеризующая эффективность добавки, которая равна 3,9 для CCl_4 ловушки электронов и 0,086 M^{-1} для циклопропана ловушки положительных ионов.

Возможности соединения поляризационных измерений с адсорбционными измерениями радиоактивной техникой для исследований окислительных и восстановительных процессов, протекающих на платиновом электроде

ДЬ. ХОРАНИ

Рассматриваются теоретические вопросы, связанные с возможностями одновременного применения поляризационных измерений с адсорбционными измерениями радиоактивной техникой.

На нескольких примерах — электрогидрирование фенилуксусной кислоты, окисление щавелевой кислоты, восстановление и окисление п-нитрофенола, электрогидрирование ацетона — иллюстрировали использование теоретических соображений.

Итерационный расчет β-интегралов

Й. СЁКЕ и А. И. КИШ

С помощью ППП-алгоритмов из энергий синглетного возбуждения произвели обратный расчет точного значения β-интегралов моно- и гомодвузамещенных производных бензола. Отклонения энергии первого перехода, полученных для подобных типов связей как экспериментально, так и методом обратного счета средневзвешенных значений β-интегралов находятся в пределах 0,7–1,5%. Причины относительно большого разброса (примерно 10–15%) обратно вычисленных β-интегралов можно отчасти объя-

снить ненадежностью экспериментальных данных и фиксированных значений атомных параметров, а также аппроксимированным характером интегралов Кулона и ППП-алгоритмов.

Кинетика образования комплекса между железом (III) и α-окси-α--дибутилфосфиноксидопропионовой кислотой

А. Х. МИФТАХОВА, Л. ДОЖА и М. Т. БЭК

Кинетика реакции α-окси-α-дибутилфосфиноксидо пропионовой кислоты (ОДФП) с железом(III) была исследована спектрофотометрически с помощью метода «остановленной струи» в водных растворах с ионной силой 0,2 при pH-1,4—2,2 и температурах 20, 25 и 30°С. При постоянном pH скорость изменяется по следующему закону:

$$w = \kappa_H \, c_{Fe} \, c_{ОДФП}$$

С увеличением концентрации водородных ионов кажущаяся константа скорости (κ_H) уменьшается. При pH-2,00 и 25°С она равна 8,0 • 10^2 дм^{3}моль$^{-1}$сек$^{-1}$. Для кажущейся энергии активации, при этом pH, была получена величина 12,3 ккал • моль$^{-1}$ (51,5 кдж • F моль$^{-1}$). При обсуждении механизма реакции полагалось существование предварительных равновесий протонирования и депротонирования.

Идентификация донорных атомов в комплексах N,N'-дизамещенных тиомочевины с галоидами олова (IV)

С. А. А. ЗАИДИ, Т. А. ХАН и К. С. СИДДИКИ

Были описаны получение и характеристика комплексов типа $SnX_4 \cdot 2L$ (X-Cl, Br, I; L- N,N'-диаллилтиомочевина, N,N'-диэтилтиомочевина, N,N'-дибутилтиомочевина, N,N'-диизопропилтиомочевина и N,N'-дифенилтиомочевина). Их молярная проводимость в нитробензоле и нитрометане указывает на то, что они ковалентны по своей природе. ИК спектроскопические данные (4000—200 см$^{-1}$) указывают на координацию через азот иминогруппы.

Псевдосточный параметрический метод анализа внутримолекулярного силового поля: применение к вырожденным колебаниям некоторых молекул

Т. Р. АНАНТАКРИШНАН

Трансформационная матрица в нормальных координатах L, связанная с колебаеельной проблемой порядка n может быть выражена в параметрической форме так, что те элементы становятся функциями угловых параметров Φ_{ij}. Возможность набора принуждений к этим параметрам была проанализирована в свете спаривания. Они допускаются между различными координатами симметрии в нормальном состоянии с целью решения колебательных проблем более высокого порядка, обладающих ненадежными экспериментальными данными. Было показано, что допущения подобно Φ_{12}-Φ_1-0 наиболее справедливы в случае вырожденных колебаний молекул типа $XY_3Z(C_{3v})$ и $XY_5(D_{3v})$ с экспериментальными величинами кориолисовых постоянных спаривания ξ_{11}, приблизительно равными J_{11}, величина которого может быть рассчитана из молекулярной геометрии и атомных масс. Применимость принуждений проиллюстрирована на примере CH_3F, силовое поле которого хорошо определено, и распространяется для фиксирования силового поля E' молекулы AsF_5, силовое поле которого все еще не определено достаточно, вследствие ненадежных экспериментальных данных.

Химия хелатов лантанидов

М. МОХАН

Взаимодействие 2-п-толиламино-4-п-толилимино-2-пентена с нитратом лантанида(III) в безводном ацетонитриле приводит к твердым соединениям типа $Ln(L)_n(NO_3)_3$, где Ln^{+3}-La, Pr, Nd, Sm, Gd, Dy, Er и Yb, L-2-п-толиламино-4-п-толилимино-2-пентен и n-3 или 4. Эти соединения были охарактеризованы на основе данных элементарного анализа, магнитных и спектральных исследований. Величина магнитной восприимчивости новых комплексов, измеренной при комнатной температуре, лишь слегка отклоняется от величин Ван Влека. Электронные спектры, снятые при комнатной температуре и температуре жидкого азота, обладают небольшим, но явным различием в интенсивности полос. Координация нитратных ионов в некоторых комплексах определена на основе ИК спектров.

Избыточные термодинамические свойства смешения за счет диполярных взаимодействий

Я. ЛИСИ

Используя сумму состояний двойных жидких смесей, были выведены формулы расчета диполярных частей избытка свободной энергии, внутренней энергии и избытка энтропии смешения. Формулы распространялись и для случая многокомпонентных систем.

Оксазепины и тиазепины, III

А. ЛЕВАИ и Р. БОГНАР

Взаимодействие 2-аминотиофенола с двенадцатью халконами (I—XII), замещенными различным образом в кольце А, проводили в горячем безводном толуоле. Было найдено, что в зависимости от заместителей в кольце А образуются либо β-фенил-β-(2-аминофенилмеркапто)пропиофенионы (XIII—XVIII), либо 2,3-дигидро-2,4-дифенил-1,5-бензотиазепины (XXV—XXVIII). β-Фенил-β-(2-аминофенилмеркапто)пропиофеноны (XIII—XVIII) кипячением их в метанольном растворе и в присутствии уксусной кислоты, как катализатора, были превращены в 2,3-дигидро-2,4-дифенил-1,5-бензотиазепины (XIX—XXIV).

Исследование ацилирования 4,6-О-бензилиден-2-бензилоксикарбониламино--2-деокси-D-глюконовой кислоты

ДЬ. ДЕАК, К. ГАЛ-ИШТОК, Й. ХАШКО-БРОЙЕР и П. ШОХАР

При обычном ацилировании 4,6-О-бензилиден-2-бензилоксикарбонил-D-глюкозаминовой кислоты с хорошим выходом образуется 2-бензилоксикарбониламино-4,6-О-бензилиден-2,3-дидезокси-D-эритро-гек-2-ено-1,5-лактон (*б*).

Acta Chimica Academiae Scientiarum Hungaricae, Tomus 92 (1), pp. 1—8 (1977)

ION-EXCHANGE BEHAVIOUR OF STANNIC ANTIMONATE

SEPARATION OF SOME METAL IONS OF ANALYTICAL IMPORTANCE

J. MATHEW and S. N. TANDON

(Department of Chemistry, University of Roorkee, India)

Received March 1, 1976

In revised form June 20, 1976

Introduction

Samples of stannic antimonate have been prepared under varying conditions of precipitation; properties, composition, ion-exchange behaviour and surface functionality are reported. The plots between log K_d and pH have been drawn for Rb^+, Cs^+, Tl^+, Ca^{2+}, Zn^{2+} and Tl^{3+}. Distribution coefficients of 27 metal ions are determined and several separations of analytical and radiochemical importance achieved. The data obtained for stannic antimonate have been compared with other antimonates.

Inorganic ion exchangers are gaining popularity, specially in the field of radiochemical technology [1—3]. Their stability at high temperature and high levels of ionizing radiations makes them attractive alternatives to organic resins. Moreover, many of these exchangers show high selectivity to particular ions.

Amongst the acidic salts of multivalent elements the antimonates [4—10] of quadrivalent elements have shown useful ion exchange properties. Many of these exchangers have been prepared by precipitation with pyroantimonate. In our laboratory we observed that the antimonates prepared by the precipitation with antimonic acid have a higher exchange capacity and a better mechanical strength than those prepared by pyroantimonate [8—10]. This observation is supported by the stannic antimonate reported herein. By varying the metal to antimonate ratio in the reacting mixture and using antimonic acid as a precipitating reagent we have synthesized stannic antimonate with an exchange capacity about two times higher than that reported by earlier workers [6, 7]. The material has reproducible exchange properties and high mechanical, chemical and thermal stability.

The present paper reports our findings on the exchange behaviour of stannic antimonate and based on the sorption data some binary and ternary separations of analytical and radiochemical interest have been achieved. Besides this the data obtained for stannic antimonate have been compared with other antimonates.

Experimental

1. Stannic antimonate samples were synthesized by the metathesis of Sn^{4+} and $[Sb(OH)_6]^-$ at room temperature ($30 \pm 5°$ C). Antimonic acid was prepared by passing a potassium pyroantimonate solution through a bed of Dowex — 50×8 (H^+ form). Other details are given in Table I. The precipitate was filtered and washed several times with deionized water. The air-dried particles were then broken down to the required mesh size by grinding. Finally they were converted to the H^+ form by treatment with dilute mineral acid.

2. The composition of the samples was determined by dissolving known amounts of stannic antimonate in hot concentrated hydrochloric acid and determining tin and antimony spectrophotometrically [11] and titrimetrically [12], respectively.

3. The exchange capacity of all the different samples with respect to Na^+ ions was determined by batch method. The results are given in Table I. Since sample No. 4A has the highset exchange capacity all other studies were done on this sample only.

Table I

Method of preparation, composition and ion-exchange capacity

Sample, No.	Concentration of reagents in mixed solution		Volume of mixed solution, ml	Sb(V)/ Sn(IV)	Hydrogen liberation capacity, meq/g
	Sn^{4+}, M	$[Sb(OH)_6]^-$, M			
1A	0.01	0.01	400	1.41	0.70
1B	0.01	0.01	400	2.84	0.68
2A	0.01	0.02	200	1.98	1.03
2B	0.01	0.02	200	1.84	0.94
3A	0.01	0.03	400	4.02	1.33
3B	0.01	0.03	400	4.16	1.10
4A	0.008	0.032	400	5.10	1.60
4B	0.008	0.032	400	5.62	1.48
5A	0.007	0.035	400	4.49	1.60
5B	0.007	0.035	400	6.51	1.46

A — Samples with antimonic acid

B — Samples with pyroantimonate

Table II

Chemical stability of stannic antimonate in various solvents

B. S. S. mesh size of stannic antimonate	Reagent	Temperature	Time	Exchanger dissolved (g/l)	
				Sn	Sn
100—200	0.1 N HCl	ambient	7 days	0.001	0.012
100—200	0.1 N NaOH	ambient	7 days	0.004	0.034
100—200	4.0 N H_2SO_4	ambient	7 days	—	0.008
100—200	6.0 N HNO_3	ambient	7 days	0.001	0.022
50—100	H_2O	reflux	4 hr	0.006	0.016
50—100	6.0 N HNO_3	reflux	4 hr	0.001	0.085

The exchange capacity of sample No. 4A for Rb^+ and Cs^+ was also determined using a radioactive tracer technique [13]. The results are given in Table III.

4. The chemical stability of sample No. 4A was examined in various solvents by immersing ~ 0.2g of the exchanger in 50 ml of the solution. At higher temperatures, the solubility was investigated by refluxing the sample. Estimation of Sb(V) and Sn(IV) was carried out spectrophotometrically using Rhodamine B[14] and pyrocatechol violet [11], respectively.

Table III

Exchange capacity for various alkali and alkaline earth metal ions

Exchanging ion	Exchange capacity, meq/g
Li^+	0.88
Na^+	1.60
K^+	1.09
NH_4^+	1.94
Rb^+	0.72 (0.79)
Cs^+	0.56 (0.61)
Mg^{2+}	1.18
Ca^{2+}	1.55
Ba^{2+}	1.76

Values given in parentheses are obtained by radioactive tracer technique under the same experimental condition

5. The IR spectra of stannic antimonate in H^+ and alkali metal forms were recorded on a Beckman IR—20 infrared spectrophotometer in KBr.

6. Stoichiometric uptake of cations was checked by plotting log K_d *vs*, pH for Rb^+, Cs^+, Tl^+, Ca^{2+}, Zn^{2+} and Tl^{3+} using almost carrier-free radioisotopes.

7. Distribution coefficients of 27 metal ions were determined by batch operation. The exchanger (approximately 100 mg) was equilibrated with 20 ml of 0.005 *M* metal ion solution. The initial pH was adjusted between 2—3 with perchloric acid. Each solution was then analysed for metal ion by spectrophotometric method, complexometric titration or radiotracer techniques. ^{45}Ca, ^{54}Mn, ^{58}Co, ^{86}Zn, ^{86}Rb, ^{110m}Ag, ^{115}Cd, ^{134}Cs, ^{203}Hg and ^{204}Tl procured from BARC, Trombay were used as radiotracers. γ-counting of ^{54}Mn, ^{65}Zn, ^{86}Rb ^{110m}Ag, ^{134}Cs, ^{203}Hg was done with a scintillation counter and β-counting of ^{45}Ca, ^{115m}Cd and ^{204}Tl using a G. M. counter. The K_d values of the metal ions were calculated using the following expression:

$$K_d = \frac{\text{m-equiv. } M^+/\text{g of the exchanger}}{\text{m-equiv. } M^+/\text{ml solution}}$$

The results are tabulated in Table IV.

8. Separations of metal ions were carried out on stannic antimonate column (50—100 B. S. S. mesh size exchanger; i.d. 0.58 cm; column length 5—6 cm).

Table IV

Distribution coefficient of some cations on stannic antimonate (pH 2—3)

Cation	Taken as	K_d, ml/g
Rb(I)	Chloride	129
Cs(I)	Chloride	183
Tl(I)	Sulphate	1096
Ag(I)	Nitrate	1.5×10^4
Hg(II)	Nitrate	1.8×10^4
Zn(II)	Nitrate	43.4
Cd(II)	Sulphate	4764
Co(II)	Chloride	382
Ni(II)	Sulphate	228
Mn(II)	Chloride	199
Mg(II)	Nitrate	98
Cu(II)	Sulphate	447
Pb(II)	Nitrate	2273
Ca(II)	Nitrate	5000
Ba(II)	Nitrate	1424
Sr(II)	Nitrate	6300
Bi(III)	Nitrate	1810
Tl(III)	Nitrate	315
Al(III)	Sulphate	250
Fe(III)	Ammonium sulphate	565
La(III)	Nitrate	6558
Ga(III)	Sulphate	504
In(III)	Chloride	454
Th(IV)	Nitrate	711
Ce(IV)	Sulphate	3376
ZrO^{2+}	Chloride	4000
UO_2^{2+}	Acetate	1349

Results and discussion

As evident from Table I, the exchange capacity increases with the increasing Sb/Sn ratio in the reacting mixture reaching a maximum value at Sb/Sn ratio 4. This is true for the samples prepared from antimonic acid as well as pyroantimonate. A similar trend was also observed in the case of antimonates of Ti(IV) and Zr(IV) [9, 10] where a maximum exchange capacity was reached at an anion to metal ratio of 4. The exchange capacity of the samples

obtained with antimonic acid is systematically higher than those obtained with pyroantimonate. Even though this trend is not as marked as observed in the case of other antimonates but from the point of view of mechanical strength the samples prepared from antimonic acid are much better. The sample can be prepared with reproducible exchange properties and the exchange capacity for the sample 4A shows a standard deviation of $\pm$ 0.034 (based on 7 determinations). The exchange capacity of different antimonates of quadrivalent elements for Na^+ follows the order:

titanic antimonate $\approx$ stannic antimonate $>$ ceric antimonate $\approx$ zirconium antimonate $\gg$ thorium antimonate

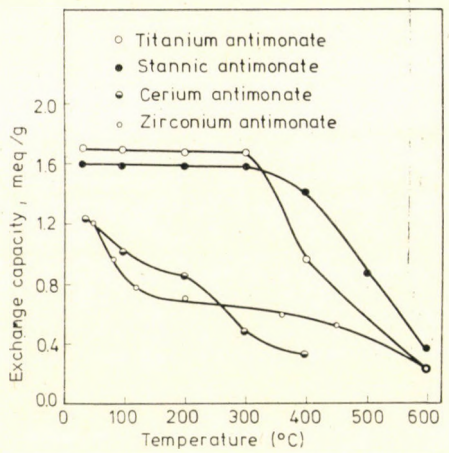

Fig. 1. Effect of drying temperature on the ion-exchange capacity of various antimonates

The effect of size and charge of the ingoing ion is shown in Table III. No regular trend is observed in the case of alkali metals; however in the case of alkaline earth metals the exchange capacity increases with increasing ionic radii. No systematic trends were observed in the case of other antimonates.

From the solubility data (Table II) it is clear that stannic antimonate is fairly stable to chemical attack. A comparison of solubility reveals that stannic antimonate is chemically the most stable of all the antimonates of quadrivalent elements.

Stannic antimonate is thermally very stable. It does not lose its exchange capacity even after drying at 300 °C. This behaviour parallels the behaviour of titanium antimonate. A comparison of the effect of drying temperature on the exchange capacity of various antimonates is given in Fig. 1.

Stannic antimonate can be regenerated up to three cycles without much loss in exchange capacity after which there is a substantial loss in the exchange capacity.

The character of the potentiometric titration curve and the approach of

the capacity value to the maximum reveals that the product is not purely a mixture of oxides but an ion exchanger containing incorporated Sb—OH groups capable of exchanging the H^+ ions. The fairly good agreement in the capacity data obtained titrimetrically and those measured by tracer technique support the mechanism of ion exchange.

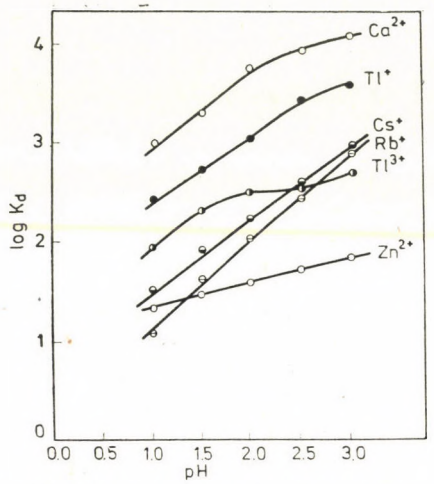

Fig. 2. K_d values on stannic antimonate as function of the pH of the solution

The infrared spectra of stannic antimonate in H^+, Na^+, K^+, NH_4^+, Rb^+ and Cs^+ forms are given in Fig. 2. A comparison of these spectra throws some light on the surface functionality [15] of stannic antimonate; this collectively refers to the functional groups on the bulk structure of the solid and their environment. The spectra of stannic antimonate in the sodium form was similar to that of the spectra in H^+ form except that the deformation band of Sb—OH between 1100 and 1350 cm^{-1} was shifted to a lower vibration frequency. This can be explained by assuming that an increase in the reduced mass occurs near the surface groups by conversion to sodium form. However, little change in the intensity was observed by conversion to sodium form. If the H^+ ions in Sb—OH exchange to alkali metal ions in the external solution, the absorption intensity of Sb—OH should decrease. In the case of other alkali metal forms the absorption intensity of Sb—OH decreases thereby suggesting an exchange of hydrogen of Sb—OH with the alkali metal ions. In these the shift to a lower vibration frequency cannot be discerned.

The dependence of cation exchange on pH studied for Rb^+, Cs^+, Tl^+, Ca^{2+}, Zn^{2+} and Tl^{3+} reveals that only for Rb^+ and Cs^+ ions ion-exchange mechanism is operative (Fig. 3). The prominence of some other mechanism [3] like surface adsorption, precipitation, simultaneous adsorption of anions might be expected for the remaining metal ions.

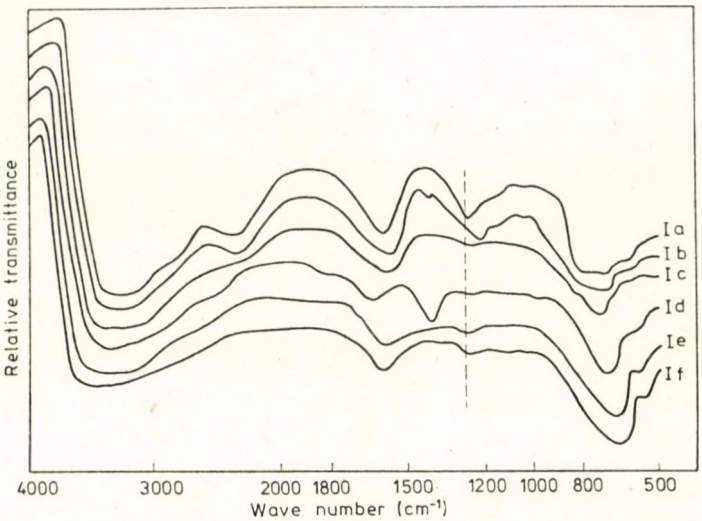

Fig. 3. **The infrared absorption patterns of stannic antimonate before and after exchange with alkali metals (KBr disk). Ia: H-form; Ib: Na-form; Ic: K-form; Id: NH_4-form; Ie: Rb-form; If: Cs-form**

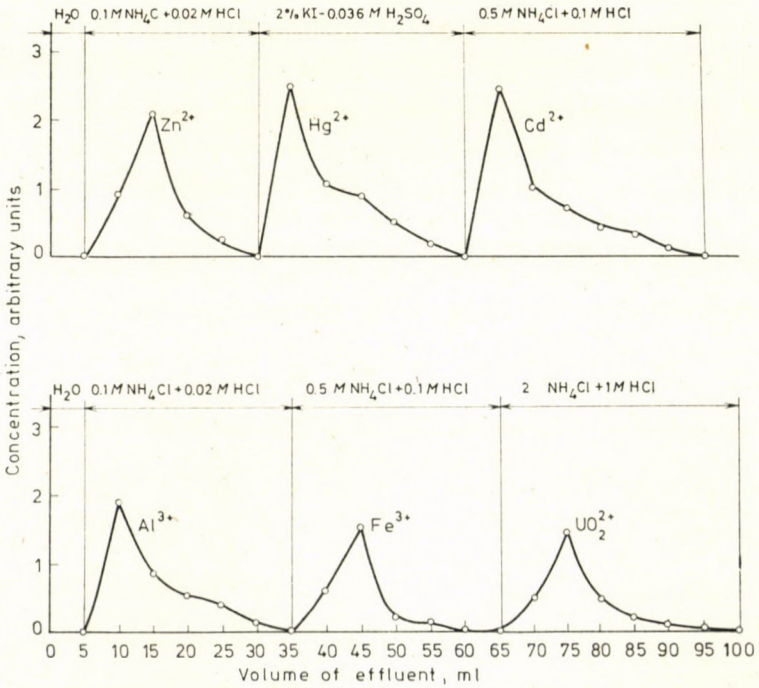

Fig. 4. **Separations on stannic antimonate column (i.d. 0.58 cm), flow rate 15 ml/hr**

The distribution studies of 27 metal ions have revealed that stannic antimonate shows high affinity for a number of metal ions of which Ag(I), Hg(II) and Pb(II) have high K_d values on other antimonates also [8—10]. The following binary and ternary separations of analytical and radiochemical importance have been achieved on stannic antimonate columns:

Zn^{2+}(0.1M NH_4Cl+0.02M HCl)—Cd^{2+}(0.5M NH_4Cl+0.1M HCl)
Hg^{2+}(0.5M NH_4Cl+0.1M HCl)—Bi^{3+}(1% KI+0.036 M H_2SO_4)
Cs^{+}(0.1M NH_4Cl+0.02M HCl)—UO_2^{2+}(2M NH_4Cl+1M HCl)
UO_2^{2+}(2M NH_4Cl+1M HCl)—ZrO^{2+}(0.1M citric acid)
Th^{4+}(2M NH_4Cl+1M HCl)—La^{3+}(4M NH_4NO_3+4M HNO_3)
Th^{4+}(2M NH_4Cl+1M HCl)—ZrO^{2+}(0.1M citric acid)
Mn^{2+}(0.1M NH_4Cl+0.01M HCl)—Fe^{3+}(0.5M NH_4Cl+0.1M HCl)
Mg^{2+}(0.5M NH_4Cl+0.1M HCl) —Ca^{2+}(4M NH_4Cl+4MHCl)
Zn^{2+}(0.1M NH_4Cl+0.02M HCl)—Hg^{2+}(2%KI+0.036M H_2SO_4)
—Cd^{2+}(0.5M NH_4Cl+0.1M HCl)
Al^{3+}(0.1M NH_4Cl+0.02 M HCl)—Fe^{3+}(0.5M NH_4Cl+0.1M HCl)
—UO_2^{2+}(2M NH_4Cl+1M HCl)

The metal ions were eluted in the indicated order using the eluents given in the parentheses against them. In all these cases the elution curves are fairly sharp. As a typical case, the elution curves of Zn^{2+}—Hg^{2}—$^{+}Cd^{2+}$ and Al^{3+}—Fe^{3+}— UO_2^{2+} separations are given in Fig. 4. Separations involving mercury are of particular interest to environmentalists.

*

The financial assistance of C. S. I. R. (India) is gratefully acknowledged.

REFERENCES

[1] Amphlett, C. B.: Inorganic Ion Exchangers, Elsevier, Amsterdam 1964
[2] Vesely, V., Pekarek, V.: Talanta **19,** 219 (1972)
[3] Pekarek, V., Vesely, V.: Talanta **19,** 1245 (1972)
[4] Phillips, H. O., Kraus, K. A.: J. Am. Chem. Soc. **84,** 2267 (1967)
[5] Abe, M., Kenjo, T., Ito, T.: Kogyo Kagaku Zasshi **70,** 291 (1967)
[6] Abe, M., Ito, T.: Kogyo Kagaku Zasshi **70,** 440 (1967)
[7] Qureshi, M., Kumar, V., Zehra, N.: J. Chromatog. **67,** 351 (1972)
[8] Gill, J. S., Tandon, S. N.: Tálanta **19,** 1355 (1972)
[9] Gill, J. S., Tandon, S. N.: J. Radioanal. Chem. **20,** 5 (1974)
[10] John Mathew, Tandon, S. N.: J. Radioanal. Chem. **27,** 315 (1975)
[11] Tanaka, K., Yamayoshi, K.: Japan Analyst **13,** 540 (1964)
[12] Furman, N. H.: Standard Methods of Chemical Analysis, Vol. 1, 5th ed., Van Nostrand, New York 1959
[13] Zsinka, L., Szirtes, L.: Acta Chim. (Budapest) **69,** 249 (1971)
[14] Sandell, E. B.: Calorimetric Determination of Traces of Metals, 3rd ed., Interscience, New York 1959
[15] McDonald, R. S.: J. Phys. Chem. **62,** 1168 (1958)

John Mathew, S. N. Tandon | Department of Chemistry, University of Roorkee, Roorkee — 247667, India.

Acta Chimica Academiae Scientiarum Hungaricae, Tomus 92 (1), pp. 9—16 (1977)

CRYSTAL AND MOLECULAR STRUCTURE OF DECAMETHYLBICYCLO-HEXASILOXANE, $Si_6O_7C_{10}H_{30}$

GY. MENCZEL

(Department of Solid State Physics, Eötvös L. University, Budapest)

Received January 15, 1976

The crystal and molecular structure of one isomer of the polycyclic methylsiloxane oligomers T_2D_4 ($Si_6O_7C_{10}H_{30}$) has been determined by X-ray diffraction. The crystal belongs to the monoclinic space group $P2_1/c$ with unit cell data a=8.32, b=12.72, c=23.24 Å, β=98.9°. The structure was solved by direct methods using the program LSAM [4]. A final residual of 0.10 has been attained for 817 photographically recorded reflexions with non-zero intensities. The low number of measured reflexions is due to the volatility of the substance. The molecule has a closed structure, being a combination of an eight-membered ring and a seven-membered half ring. It has a pseudo-symmetry near to mm2. The great value of one Si—O—Si angle (170°) is strikingly characteristic of the structure. The average of the remaining six Si—O—Si angles is 150°.

Several new polycyclic methylsiloxane oligomers have been prepared by GARZÓ *et al.* [1], by thermal decomposition of branched-chain polymers. The compounds were composed of $MeSiO_{3/2}$ (T) and Me_2SiO (D) units. The crystal and molecular structure of one of these substances with the composition T_2D_3 was determined by X-ray diffraction [2]. Three isomers with the composition T_2D_4 were isolated from the decomposition products; the X-ray structure determination of one of them is now reported.

Experimental

The crystals are extremely volatile and the samples — monoclinic prisms with lengths of about 0.3 mm in all directions — were sealed in thin-walled capillary tubes. Nevertheless, a decrease in the specimen size was observable after about a week. Two specimens were used for the 0kl → 3kl and the h0l → h2l layer Weissenberg photographs, respectively. The exposures were taken at 22—24°C; 1178 reflexions were measured visually, 817 of them had intensities higher than the background (classed as 'observed').

No absorption correction of the intensities was made.

Crystallographic data (with standard deviations in parentheses) ($Si_6O_7C_{10}H_{30}$), m.p. 54.5°C. The space group, given unambiguously by systematic absences, is $P2_1/c$ (monoclinic), a = 8.32(2), b = 12.72(2), c = 23.24(4) Å, β = 98.9(4)°. The density calculated with Z = 4 is 1.193, the density measured by flotation is 1.16(3) g cm^{-3}.

The structure was solved by direct methods. The symbolic addition procedure [3] making use of the program LSAM [4] provided four sets of signs for reflexions with $E \geq 1.35$. An E-map calculated with the best set of signs for 208 reflexions and two subsequent structure factor and Fourier calculations revealed the positions of the non-hydrogen atoms. The refinement started with a conventional R factor of 0.28, using the overall temperature factor B_T = = 2.8 Å^2 given by the Wilson plot. The structure was refined by two cycles of block-diagonal least squares calculations with isotropic and five cycles with anisotropic thermal parameters.

Table I

Final positional parameters ($\times 10^4$) and thermal parameters ($\times 10^4$) with estimated standard deviations in parentheses (a) Fractional co-ordinates

	x/a	y/b	z/c
Si(1)	5340 (9)	2316 (7)	2142 (3)
Si(2)	6120 (9)	4239 (6)	1395 (3)
Si(3)	2375 (9)	4378 (6)	1041 (3)
Si(4)	1809 (10)	3136 (7)	2149 (3)
Si(5)	2365 (10)	2396 (6)	227 (3)
Si(6)	4597 (11)	841 (6)	1075 (3)
O(7)	6196 (22)	3199 (14)	1782 (7)
O(8)	4308 (19)	4634 (13)	1197 (7)
O(9)	1702 (21)	3984 (14)	1622 (6)
O(10)	3700 (20)	2746 (14)	2320 (8)
O(11)	2064 (24)	3492 (15)	536 (8)
O(12)	3558 (24)	1700 (15)	687 (7)
O(13)	5077 (23)	1298 (15)	1741 (7)
C(14)	6756 (32)	1954 (23)	2830 (10)
C(15)	7188 (31)	3872 (23)	744 (11)
C(16)	7217 (28)	5278 (21)	1844 (8)
C(17)	1361 (30)	5609 (18)	756 (10)
C(18)	1186 (34)	3804 (26)	2800 (10)
C(19)	352 (32)	1984 (21)	1897 (13)
C(20)	350 (29)	1747 (21)	37 (12)
C(21)	3356 (37)	2676 (24)	—442 (11)
C(22)	6508 (29)	526 (24)	756 (11)
C(23)	3301 (41)	—392 (23)	1138 (12)

The great number of cycles was necessary because only the last cycle produced good shift/standard deviation ratios (all below 0.5 and, on the average, 0.2 for the positional parameters).

The final residual is 0.10 for the observed and 0.15 for all reflexions. Atomic scattering factors were taken from International Tables for X-ray Crystallography [5]; the scattering factor of carbon atom was replaced by that of N [6], as no hydrogen positions were determined. The final atomic parameters are listed in Table I. The schematic drawings of two parts of the molecule with bond distances and Si—O—Si angles are shown in Fig. 1 and Fig. 2. Other angles are listed in Table II. A list of structure factors is available from the author.

Table I (*contd.*)

b) Anisotropic thermal parameters in the form exp $[-(h^2b_{11}+hkb_{12}+hlb_{13}+k^2b_{22}+klb_{23}+l^2b_{33})]$

	b_{11}	b_{12}	b_{13}	b_{22}	b_{23}	b_{33}
Si(1)	139 (16)	23 (21)	5 (8)	86 (6)	8 (6)	13 (1)
Si(2)	54 (14)	0 (19)	3 (8)	61 (6)	15 (6)	19 (1)
Si(3)	107 (15)	32 (19)	—2 (8)	47 (5)	—2 (6)	16 (1)
Si(4)	94 (15)	41 (22)	7 (9)	88 (7)	30 (7)	22 (2)
Si(5)	200 (18)	34 (21)	—40 (9)	59 (6)	—19 (6)	20 (2)
Si(6)	257 (21)	41 (22)	—31 (10)	59 (6)	0 (7)	21 (2)
O(7)	124 (39)	—45 (51)	—7 (23)	124 (17)	46 (16)	33 (4)
O(8)	98 (31)	—2 (46)	32 (20)	72 (14)	29 (15)	35 (4)
O(9)	163 (37)	59 (50)	47 (22)	114 (16)	78 (15)	34 (4)
O(10)	185 (36)	—45 (47)	1 (20)	86 (15)	30 (14)	20 (4)
O(11)	328 (47)	47 (55)	—8 (25)	107 (18)	—16 (17)	29 (5)
O(12)	293 (46)	136 (53)	—102 (24)	110 (17)	—6 (16)	31 (4)
O(13)	395 (46)	120 (53)	—41 (23)	99 (17)	—32 (15)	17 (4)
C(14)	321 (63)	17 (81)	—41 (31)	185 (29)	44 (23)	26 (5)
C(15)	235 (61)	147 (80)	46 (37)	165 (27)	8 (27)	44 (7)
C(16)	235 (54)	63 (71)	—109 (37)	117 (24)	—10 (26)	59 (8)
C(17)	338 (57)	86 (62)	—42 (27)	98 (20)	14 (18)	18 (4)
C(18)	460 (74)	217 (99)	81 (37)	223 (36)	0 (29)	35 (7)
C(19)	282 (61)	—167 (70)	8 (41)	120 (23)	22 (28)	67 (10)
C(20)	195 (56)	—118 (56)	—159 (34)	145 (24)	—52 (26)	66 (8)
C(21)	422 (79)	30 (94)	48 (38)	184 (31)	31 (27)	30 (6)
C(22)	236 (51)	204 (80)	14 (33)	217 (33)	—39 (28)	48 (7)
C(23)	437 (82)	—257 (86)	—97 (44)	159 (29)	11 (29)	55 (8)

Discussion

Four kinds of connections are possible between T and D units in T_2D_4. The present work has shown that the actual structure corresponds to scheme No. IV in Ref. [1]. The siloxane skeleton of the molecule consists of an eight-membered ring of the atoms Si(1) → Si(4) and O(7) → O(10) coupled with a seven-membered half ring of Si(1), Si(3), Si(5), Si(6) and 0(11) → 0(13). The contour of Fig. 1 is the eight-membered ring, while the half ring is shown in Fig. 2. A distorted symmetry close to *mm2* is characteristic of the molecule. A mirror plane coincides with the half ring, the other is formed by the atoms Si(2), Si(4) and O(12). Figure 1 represents a projection of the eight-membered

Table II

Bond angles around the Si atoms (°). Estimated standard deviations range from 1.0 to 1.3°

O (7)-Si(1)-O(10)	111.0	O(9)-Si(4)-O(10)	108.3
O (7)-Si(1)-O(13)	106.9	O (9)-Si(4)-C(18)	108.5
O(10)-Si(1)-O(13)	112.8	O (9)-Si(4)-C(19)	108.4
O (7)-Si(1)-C(14)	109.7	O(10)-Si(4)-C(18)	108.3
O(10)-Si(1)-C(14)	108.2	O(10)-Si(4)-C(19)	112.1
O(13)-Si(1)-C(14)	107.9	C(18)-Si(4)-C(19)	110.4
O (7)-Si(2)-O (8)	112.2	O(11)-Si(5)-O(12)	107.6
O (7)-Si(2)-C(15)	104.9	O(11)-Si(5)-C(20)	107.1
O (7)-Si(2)-C(16)	107.8	O(12)-Si(5)-C(20)	110.7
O (8)-Si(2)-C(15)	112.4	O(11)-Si(5)-C(21)	108.7
O (8)-Si(2)-C(16)	107.6	O(12)-Si(5)-O(21)	110.1
C(15)-Si(2)-C(16)	111.8	C(20)-Si(5)-C(21)	112.1
O (8)-Si(3)-O (9)	109.4	O(12)-Si(6)-O(13)	108.9
O (8)-Si(3)-O(11)	110.0	O(12)-Si(6)-C(22)	109.7
O (9)-Si(3)-O(11)	110.5	O(12)-Si(6)-C(23)	110.0
O (8)-Si(3)-C(17)	106.9	O(13)-Si(6)-C(22)	110.2
O (9)-Si(3)-C(17)	111.3	O(13)-Si(6)-C(23)	105.9
O(11)-Si(3)-C(17)	108.4	C(22)-Si(6)-C(23)	111.7

Averages

O-Si-O 109.7

O-Si-C 108.8

C-Si-C 111.6

ring along the line of intersection of the pseudo-mirror planes. Striking deviation from this pseudo-symmetry is shown by the significant difference between the angles at O(11) and O(13).

The most interesting feature of the structure is the large value of the angle at O(12). Such large Si—O—Si angles, up to 180° were reported for open-chain siloxanes [7] and inorganic silicate compounds [8—10]. The average of the other Si—O—Si angles in T_2D_4 is 150° and agrees well with the value measured in α-crystoballite, but it is higher than the averages found in siloxanes with six-membered and eight-membered rings (130° and 145°, respectively) [7]. The non-bonded Si . . .Si distances and the angles formed by them represent important information about the structure of the molecule (Fig. 3). The asymmetry of the seven-membered half ring is shown by the difference between the Si (1) . . .Si(6) and Si(3) . . .Si(5) distances.

The averages of the Si—O and Si—C bond lengths (1.61 and 1.89 Å, respectively), as well as those of the angles around the Si atoms (see Table II)

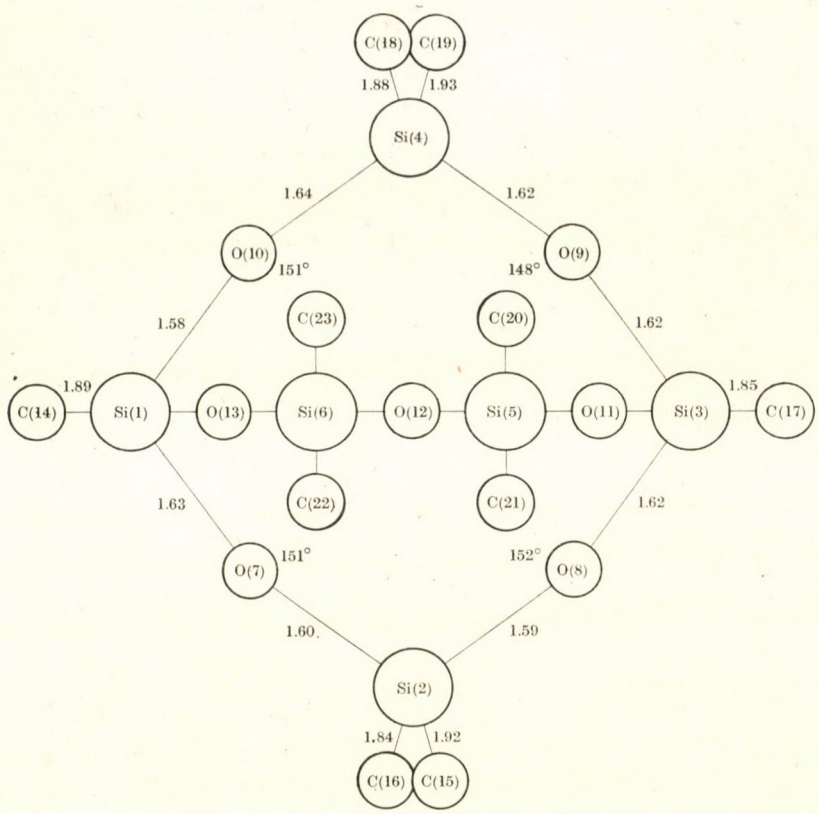

Fig. 1. Schematic drawing of the molecule with bond distances (Å) and Si—O—Si angles in the eight-membered ring. E.s.d.'s for Si—O 0.02, for Si—C 0.03 Å, for Si—O—Si 1.2°

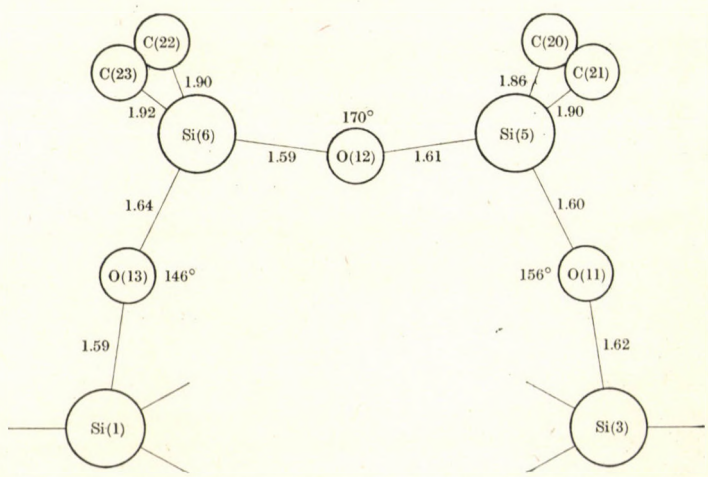

Fig. 2. Schematic drawing of the seven-membered half ring with bond distances (Å) and Si—O—Si angles. E.s.d. values are given at Fig. 1

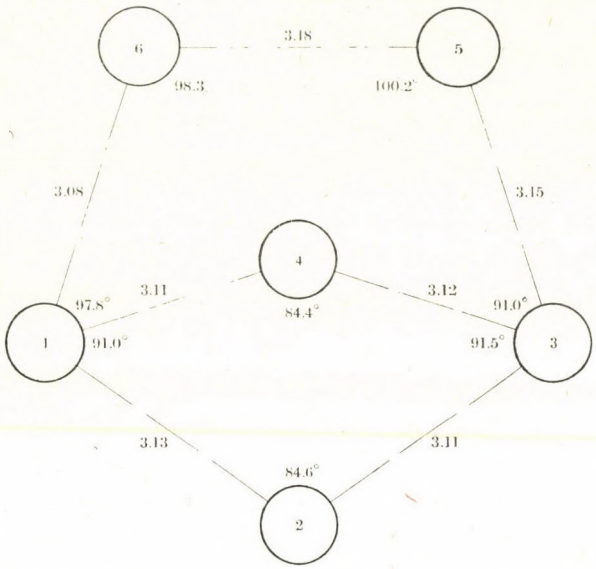

Fig. 3. Geometry of the Si atoms in the molecule (distances in Å). Angles not indicated in the figure: Si(2)..Si(1)..Si(6) 93.6°, Si(2)..Si(3)..Si(5) 91.4°. E.s.d for Si...Si 0.01 Å.

agree well with the values found in similar compounds. From the lengths of the *Si-tetrahedron edges* the O . . .C distances fall into the interval 2.77—2.97 Å, showing great deviations from the mean value of 2.89 Å. The C . . .C distance limits are 3.12—3.16 Å, while eight of the ten O . . .O edges range from 2.63—2.66 Å. The two others (0(7) . . .0(13) and 0(11) . . .0(12)) have a common value of 2.58 Å.

Table III

Least squares planes in the molecule. The plane constants ($Ax + By + Cz = D$) are multiplied by 10^4 and are referred to crystallographic axes

The co-ordinates are in Å

Plane	Atoms	A	B	C	D
P1	Si(1) → Si(4)	544	7132	6820	60,312
P2	O(7) → O(10)	1205	7063	6705	63,674
P3	Si(1) → Si(4), O(7) → O(10)	830	7092	6788	61,921
P4	Si(1), Si(3), Si(5), Si(6)	8700	3505	—4773	25,202
P5	Si(1), Si(3), Si(5), Si(6), O(11) → O(13)	8764	3500	—4625	25,461

Planes in the molecule. The equations of some least squares planes formed by the atoms of the molecule are listed in Table III. The Si atoms of the eight-membered ring do not form a plane, Si(1) and Si(3) are shifted "upward" (if the atoms Si(5), Si(6) and O(12) are regarded as the upper part of the molecule), while the atoms Si(2), Si(4) deviate in the opposite direction from their least squares plane (P1) by 0.30 Å. The distances of the O atoms from their least squares plane P2 are 0.09 Å. This plane almost coincides with the least squares plane of the Si atoms forming a dihedral angle of 3.8° with one another. So the symmetry of the eight-membered ring is approximately $\bar{4}2m$ (D_{2d}). In the half ring, the Si atoms lie in the same plane within 0.01 Å, while the O atoms deviate by 0.06 — 0.13 Å from this plane (P4). P3, the least squares plane of the eight-membered ring and that of the half ring P5 form nearly right angle (84.9°) with each other.

The shortest intermolecular distances were found between two Me groups, between a Me group and an O atom of adjacent molecules and are listed in Table IV.

Table IV

Intermolecular distances less than 4.0 Å

From atom at x, y, z	To atom	at position	Distance (Å)
O (7)	C(19)	1 + x, y, z	3.76
O (8)	C(14)	1—x, 1/2 + y, 1/2—z	3.90
O (9)	C(15)	—1 + x, y, z	3.99
O(10)	C(16)	1—x, 1/2 + y, 1/2—z	3.83
O(11)	C(17)	—x, 1—y, —z	3.97
C(14)	C(19)	1 + x, y, z	3.96
C(15)	C(17)	—1—x, 1—y, —z	3.92
C(16)	C(19)	—1—x, 1/2 + y, 1/2—z	3.94
C(17)	C(20)	—x, 1—y, —z	3.99

*

The calculations were performed on the ODRA—1304 computer at the Computer Center of the Faculty of Sciences, Eötvös L. University; the author thanks the staff of the Computer Center.

REFERENCES

[1] GARZÓ, G., TAMÁS, T., SZÉKELY, T., UJSZÁSZI, K.; Acta Chim. (Budapest) **69,** 273 (1971)
[2] MENCZEL, Gy., KISS, J.: Acta Cryst., **B31,** 1214 (1975)
[3] KARLE, I. L., KARLE, J.: Acta Cryst., **16,** 969 (1963)
[4] MAIN, P., WOOLFSON, M. M., GERMAIN, G.: LSAM, University of York and Louvain, 1968.
[5] International Tables for X-ray Crystallography Vol. III, Kynoch Press, Birmingham 1962.
[6] PEYRONEL, G.: Atti. Accad. Nazl. Lincei, **16,** 231 (1954)
[7] BOKII, N. G., STRUCHKOV, YU. T.: Zh. Str. Khim., **9,** 722 (1968)
[8] NÁRAY-SZABÓ, I., KÁLMÁN, A.: Silikattechnik, **12,** 316 (1961)
[9] CRUICKSHANK, D. W. J., LYNTON, H., BARCLAY, G. A.: Acta Cryst., **15,** 491 (1962)
[10] SMOLIN, YU. J., SHEPELEV, YU. F.: Acta Cryst., **B26,** 484 (1970)

György MENCZEL, H—1088 Budapest, Múzeum krt. 6—8.

Acta Chimica Academiae Scientiarum Hungaricae, Tomus 92 (1), pp. 17—25 (1977)

STRUCTURE OF VANADIUM–PHOSPHORUS OXIDE CATALYSTS

K. C. KHULBE and R. S. MANN

(Department of Chemical Engineering University of Ottawa, Ottawa, Canada)

Received March 1, 1976

X-ray, infra-red and electron spin resonance (ESR) studies were made on vanadium–phosphorus oxide catalysts. A new phase was observed for P/V ratios greater than 0.5. The IR study indicated the formation of a new compound of V—P—O, in which P—O stretching vibrations bands suggest the phosphoric ions to have a variety of degrees of condensation. It has been observed that though the V—O—V band (at 822 cm^{-1}) disappeared when the phosphate ion was added to V_2O_5, no appreciable effect was observed in the V = O band (at 1020 cm^{-1}) up to a P/V ratio of 0.5. The addition of phosphate as an impurity to V_2O_5, gave an ESR signal which is attributed to VO^{2+} ions. Its intensity and shape depended on the phosphate concentrations. For P/V ratios greater than 2, a hopping affect was observed on the ESR signal. It is concluded that the new compound is a vanadyl phosphate type.

Introduction

Catalysts based on vanadium pentoxide have found ever increasing use in the oxidation of hydrocarbons. Phosphate or phosphorus is mixed with vanadium pentoxide in order to either improve the selectivity and activity [1—4] or sometimes to increase the melting point of the catalyst so the yield of the product is increased. Despite the great amount of work done on the catalytic behaviour of vanadium–phosphorus catalysts, little work has been done on the structure of this catalyst.

The catalyst system vanadium–phosphorus oxide was studied using infra-red absorption, X-ray diffraction and ESR technique in order to obtain some information regarding the structure of the catalyst. By studying the ESR spectrum, when a small amount of phosphate dopant is used, we are able to show that the spectrum is due to VO^{2+} ion, enabling the determination of accurate values of the pertinent Spin Hamiltonian parameters.

Experimental

(a) Catalysts: The mixed oxide catalysts of vanadium and phosphorus were prepared by weighing purified ammonium metavanadate (Baker Analyzed) and ammonium dihydrogen phosphate in amounts to give the desired phosphorus vanadium ratios (atomic). Ammonium dihydrogenphosphate and ammonium metavanadate were dissolved in the minimum quantity

of warm water (50 °C) and the resulting mixture was evaporated over a hot plate at low heat with a magnetic stirrer. The residue was dried for 12 hours at 70 °C and for 4 hours at 150 °C and calcined at 500 °C. Pure vanadium pentoxide was obtained from ammonium meta vanadate by the same method as used for the mixed oxides. Samples of different phosphorus vanadium (P/V) ratios were prepared and studied (Table I).

The technique for X-ray diffraction studies, infrared absorption spectra and ESR measurements are described elsewhere[5].

Results

X-ray analysis: Samples B, C and D gave nearly the same pattern as that of pure vanadium pentoxide (Sample A). At higher ratios, *i.e.*, P/V > 0.75, other phase was present which could not be identified. Table I shows the results of the X-ray analysis of the samples. Table II indicates the intensities of different lines observed for sample I (P/V = 3).

Table I

Sample	P/V (Atomic ratio)	Detected phases
A	V=100%, P=0%	V_2O_5
B	0.1	V_2O_5
C	0.25	V_2O_5
D	0.5	V_2O_5
E	0.75	$V_2O_5 + VPO_5$
F	1.0	Unidentified + V_2O_5
G	1.5	Amorphous
H	2.0	Amorphous
I	3.0	Unidentified

Infra-red absorption: Figure 1 shows the infra-red absorption spectrum for all the samples. The infra-red spectrum of V_2O_5 (sample A) is characterized by a narrow but very intense band at 1020 cm^{-1} and a broad intense band at 822 cm^{-1}, and a region of continuous absorption in the range 640—400 cm^{-1} (Fig. 1). This spectrum was similar to those observed by TARAMA *et. al.* [6] and others [7]. The spectra of the vanadium—phosphorus oxide system, specially of samples B and C show few changes relative to the spectrum of the original V_2O_5 (Sample A), (Fig. 1). However, the 822 cm^{-1} band is displaced by 5—10 cm^{-1} towards higher frequency and its shape is slightly different. Further addition of phosphate yielded spectra that differed markedly from that of V_2O_5; the band at 822 cm^{-1} disappeared completely. The nature of the observed changes in the spectra suggests the formation of a chemical compound.

Table II

Powder diffraction data for $P/V = 3$

d	I	d	I
8.151	20	1.575	10
5.476	40	1.537	10
5.202	10	1.518	20
4.688	30	1.463	10
4.199	10	1.403	30
3.860	100	1.358	20
3.597	20		
3.411	70	Few other faint lines	
3.225	20		
3.077	30		
2.864	10		
2.761	10		
2.706	20		
2.578	10		
2.430	50		
2.347	20		
2.261	10		
2.012	30		
1.833	20		
1.773	20		
1.712	40		
1.683	30		

d = interplanar spacing
I = relative peak intensity

ESR measurement: Pure vanadium pentoxide (sample A), prepared by calcination at 500 °C, gave a paramagnetic resonance signal (Fig. 2) due to V^{4+} ions[3]. On the addition of a phosphate as an impurity in V_2O_5, an ESR signal was observed whose intensity and the shape depended on the phosphate content. When the phosphorus/vanadium ratio was 0.5 or less, the signal had a hyperfine structure (broadened) (HFS) consisting of two groups of lines with eight components in each group having different intensities. A similar spectrum was observed when MoO_3 was doped with V_2O_5[5]. The resolution of spectrum was best when P/V ratio was 0.25 (Fig. 3). The appearence of two groups of lines in the spectrum is due to the pronounced anisotropy of the hyperfine structure [5] and the anisotropy of the field (H)

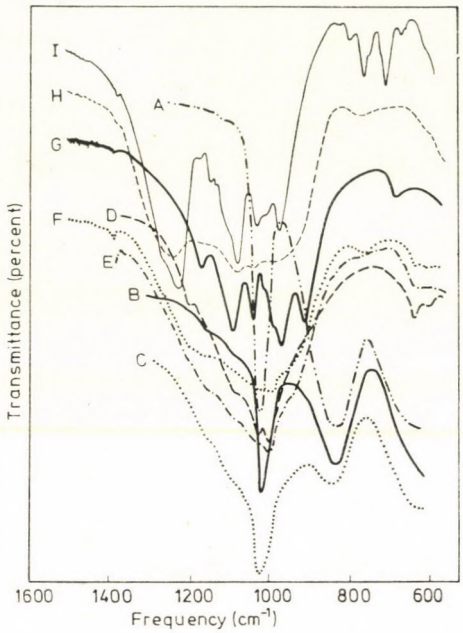

Fig. 1. IR spectrum of; A—V_2O_5, B-sample B (P/V = 0.1), C-sample C (P/V = 0.25), D-sample D (P/V = 0.5), E-sample E (P/V = 0.75), F-sample F (P/V = 1.0), G-sample G (P/V = = 1.5), sample H (P/V = 2), I-sample I (P/V = 3)

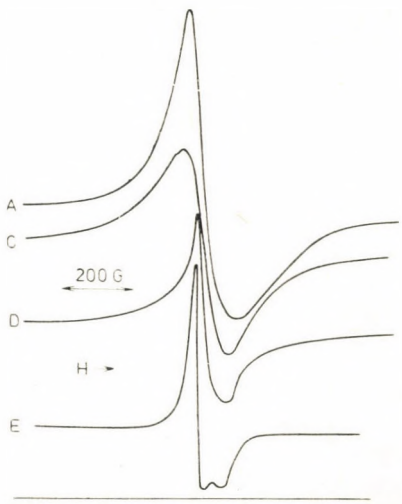

Fig. 2. ESR spectrum; A—V_2O_5, C-sample G (P/V = 1.5), D-sample H (P/V = 2), E-sample I (P/V = 3)

and the electrical field (E) of the catalyst microcrystals, whereas the weaker lines correspond to parallel orientation of (H) and (E).

The pattern of lines observed is a characteristic of the VO^{2+} vanadyl ion which originates in a V^{4+}. $6O^{2-}$ distorted octahedral complex [5]. The best one can say from the observed spectrum of the powder is that the site has an axial symmetry with the parallel direction (Z-axis) along the V = O direction of the VO^{2+}, vanadyl ion.

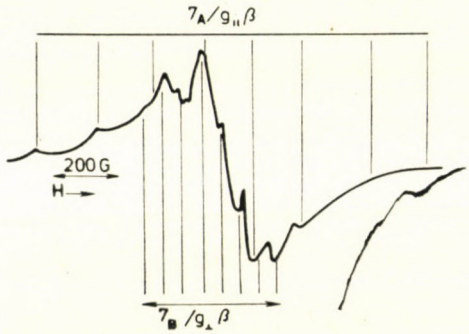

Fig. 3. ESR spectrum of sample C (P/V = 0.25)

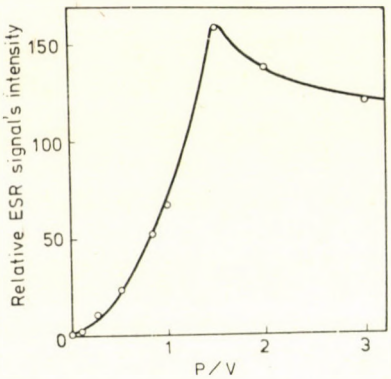

Fig. 4. Relative intensities of the ESR spectra *vs.* P/V ratios

The Spin Hamiltonian parameters were calculated [5] to be $g_{||} = 1.940 \pm 0.005$, $g_{\perp} = 1.990 \pm 0.005$, average $\langle g \rangle = 1/3\ (2g_{\perp} + g_{||}) = 1.973$, $|A| = 165.7 \times 10^{-4}$ cm^{-1} and $|B| = 56.6 \times 10^{-4}$ cm^{-1}.

In studying the sequence of spectra for samples A to G, it was observed that the individual hyperfine lines broadened to form a single large broad line near the centre of the spectral pattern (Fig. 2, Sample G). While the individual hyperfine lines broadened and gradually disappeared, their position did not appear to shift. Fig. 2 shows the ESR spectra of the samples H(P/V = 2), and I(P/V = 3). While the lines became narrow, the 'g' value for both lines

remained 1.965, which is a characteristic 'g' value for V^{4+} ions. The narrowing may not be due to a decrease in the number of V^{4+} ions, but might be attributed to hopping of electrons.

The integrated line intensities of the spectra increased with the increase in the P/V ratios between 0.1 and 1.5 and then decreased with further increase, up to P/V = 3.0 (Fig. 4).

Discussion

The X-ray analysis did not reveal any new phase in the V_2O_5–P_2O_5 system up to a ratio of V/P = 0.5. A new crystalline phase was observed at higher P/V ratios, *i.e.*, P/V = 3 (Table I.) However, this could not be identified conclusively. Though several compounds of vanadium phosphides are reported in the literature [8, 9, 10, 11] none could be identified in the present system. This does not preclude the presence of small amounts of the other known phases which might have been present below the X-ray detection limit. NÁDOR [8] studied the system vanadium pentoxide—phosphorus pentoxide prepared by melting various mixtures of vanadium pentoxide and phosphorus pentoxide and reported that the system consisted of two 3 phase and one 2 phase systems. No X-ray data were reported. EZHKOVA *et al.* [11] prepared mixed oxides of V_2O_5–P_2O_5 by mixing solutions of vanadyl oxalate with solutions of the salts of phosphorus and decomposing the dried residues at temperatures of 400—500° for 4 to 6 hours. They reported a chemical compound VPO_x was formed, but no X-ray data were given.

The composition of vanadium and phosphides in the vanadiumphosphate oxide mixtures studied in the present investigation represents a limit for phosphate concentration. On heating above 250 °C, the excess of P_2O_5, the final product obtained in the thermal decomposition of ammonium dihydrogenphosphate, sublimes. Consequently, no other stable oxides of phosphorus could exist at temperatures higher than 250 °C. In the vanadium—phosphorus oxide mixture, no other phases except V_2O_5 were detected up to a P/V ratio of 0.5.

In Figures 1 and 2, bands at 1020 cm^{-1} and 822 cm^{-1} are due to the stretching vibrations of the V = O and V–O–V respectively. The broad region of absorption between 640 and 400 cm^{-1} is usually assigned to the lattice vibration [12, 13]. Samples B and C do not show any new sharp bands; however the band at 822 cm^{-1} is displaced by 5—10 cm^{-1} towards higher frequency. A small shoulder appeared around 1200—1250 cm^{-1}. This became more pronounced in other samples as the phosphate concentration increased and was attributed to V–O–P bending. It appears that while P gradually replaces V in V–O–V, it does not affect the V = O group in samples B and C. With the increase in the phosphate concentration, the lattice vibrations also disappear.

Other samples D, E, F, G, H and I give broad and single bands in the 900—1300 cm^{-1} region. Samples G, H, and I also gave some small bands in the region 600—800. In each of these spectra, while an absorption band at about 1010 cm^{-1} is attributed to a V = O stretching vibration, a broad band in the region 1000—1300 cm^{-1} is ascribed to ortho, pyro, tri and higher linear metaphosphates [14, 15]. Pyrophosphates (OP—O—PO) give absorption bands in the region 870—930, and 670—710 cm^{-1} and the tetrahedral phosphate ion has four fundamental frequencies around 1082, 980, 515 and 363 cm^{-1} [17, 18]. Therefore, the broadness of the P–O stretching vibration bands suggests that the phosphide ions have a variety of degree of condensation. In each of the samples D to I, the band at 980—990 cm^{-1} is attributed to V^{2+} : O [19]. It can thus be concluded that the compound is a vanadyl-phosphate type.

The X-ray diffraction data showed that while only V_2O_5 is present in samples B, C and D, other phases besides V_2O_5 were present in samples E and F. The IR spectra on the other hand did not give all the frequencies of V_2O_5 due to some unknown reasons. It is possible that the samples B, C and D may be a homogeneous solid compound.

Ezhkova *et al.* [11] studied the V_2O_5–P_2O_5 system by ESR and observed that the catalyst containing more than 5 mole % P_2O_5 gave a single line with a width of approximately 200 G. Catalysts containing small quantities of P_2O_5 (less than 5 mole % P_2O_5) gave a spectrum with a hyperfine structure. No ESR spectrum was observed for pure V_2O_5. Also no Hamiltonian parameters of the spectrum were reported. In our present studies we obtained an ESR spectra for even pure V_2O_5 [5].

The paramagnetic impurity which produces the ESR signal in the system V_2O_5–P_2O_5 is the VO^{2+} ion. The anisotropy in the g values, $g_{||}$ and $g_{\perp}$ and the hyperfine parameters, A and B are indicative of a V^{4+} ion, surrounded by six oxygen ligands forming a distorted octahedron. The main part of the distortion is due to the V^{4+} ion being strongly bonded to one of the neighbouring oxygens with the Z axis of the distortion being along the V = O bond direction.

The V_2O_5 structure can be regarded as being built of distorted VO_6 octahedra [5, 20]. The ESR signal obtained from pure V_2O_5 shows that some of the vanadium ions are in the V^{4+} state. When V_2O_5 is doped by a phosphate, the P^{5+} ion enters the V_2O_5 structure. This is confirmed by the IR studies where —V—O—V band disappeared as the P concentration increased in samples B, C and D. The possible mechanism for the formation of P^{5+} and V^{4+} ions could be as follows:

$$P^{3+} + \text{heat} \rightarrow P^{5+} + 2e^-$$

and

$$2e^- + 2V^{5+} \rightarrow 2V^{4+}$$

The spectrum given by P/V = 0.25 is shown in Fig. 3. It contains HFS of

VO^{2+} ions ($V^{4+} + O^{2-} \rightarrow V : O^{2+}$). The hyperfine broadening can be due to either of the following reasons:

(i) Dipole — dipole interaction between V^{4+} ions (due to concentration of V^{4+});
(ii) strains or dislocations in the sample;
(iii) different sites of V^{4+} giving slightly different A and B values [5];
(iv) some hopping of electrons at V^{4+} ions site.

At higher ratios of P/V (2—3) a narrow line was observed, with a g value of 1.965, indicating that the line was due to vanadyl ions. The intensity of ESR signal is also decreased. This narrowing is not due to fewer V^{4+} ions, since in this case, one would expect to see the appearance of hyperfine structure, which does not occur. For high enough donor impurity concentrations, there is a probability of electrons hopping from one donor to another because of the overlap of the donor wave functions [21]. In such cases, the donor hyperfine interaction is averaged out and a single motionally narrowed line appears. This phenomenon is observed in the present investigation at higher ratios of P/V($2 \sim 3$). Isotropic spectra of amorphous samples are supposed to be due to unusual vanadyl complexes, vanadyl phosphate in this case.

It is possible that VO^{2+} ions in V_2O_5–P catalysts play an important role in improving the selectivity and the activity for the oxidation of hydrocarbons. It was observed that 20% V_2O_5 + 20% MoO_3 contained the maximum selectivity for the formation of formaldehyde in the oxidation of methanol [22].

*

The authors are grateful to Dr. A. MANOOGIAN, Physics Department, University of Ottawa for helpful discussions and are indebted to the National Research Council of Canada for providing funds through a research grant (A—1125).

REFERENCES

[1] MOLDAVASKII, B. L., KERNES, Yu-D., BELOSTOTSKAYA, I. L., KHABIBULINA, A. Sh.: Izobret. Prom. Obraztsy, Tovernye Znaki, **45** (14), 12, 1968 (C. A. 46 400 h, **69,** 1968)
[2] MAMORU, A.: Kogyo Kagaku Zasshi, **73** (5), 946, 1970
[3] MATSUURA, T., KAMIMURA, S., MIYAJIMA, S.: Jap. Pat. 7888, 1965
[4] MARSHALL, D.: Brit. Pat. 1, 070, 642, 1967
[5] KHULBE, K. C., MANN, R. S., MANOOGIAN, A.: J. Chem. Phys. 60 (12), 4810, 1974
[6] TARAMA, K., TERANISHI, S., YOSHIDA, S., TAMURA, N.: Proc. 3rd Int. Cong. Amsterdam, 1964, North-Holland, Publ., Amsterdam 1965, p. 202
[7] KHULBE, K. C., MANN, R. S.: Can. J. Chem. **53,** 2917, 1975
[8] NÁDOR, B.: Acta. Chim. Acad. Sci. Hung., **40** (1), 1, 1960
[9] NÁDOR, B.: Magyar Kém. Foly. **65,** 443, 1959
[10] ZAITSEV, B. E., EZHKOVA, Z. I., IOFFE. I. I.: Kinetika i Kataliz **5,** 861, 1964
[11] EZHKOVA, Z. I., IOFFE, I. I., KAZANSKII, V. B., KRYLOVA, A. V. LYUBARSKII, A. G., MARGOLIS, L-Ya.: Kinetika i Kataliz **5,** 861, 1964
[12] ZAITSEV, B. E., EZHKOVA Z. I., Ioffe, I. I.: Kinetika i Kataliz **7,** 755, 1966
[13] KERRA, Y., KERRA, S., TERATANI, S., KOZOHIROTO: Bull. Chem. Soc. Japan, **40,** 2458 1967

[14] CORBRIDGE, D. E. C., LOWER, E. J.: J. Chem. Soc. 493, 1954
[15] NAKAMURA, M., KAWAI, K., FUZIWARA, Y.: J. Cat. **34,** 1974
[16] CORBRIDGE, D. E. C.: J. Appl. Chem. **6,** 456, 1956
[17] HERZBERG, G.: "Infra-red and Raman Spectra of Polyatomic Molecules", Van Nostrand, Princeton, New Jersey, 1956
[18] HERZBERG, G.: "Spectra of Diatomic Molecules", Van Nostrand, Princeton, New Jersey 1950
[19] YOSHIDA, S.: Shokubai (Tokyo) **10,** 90, 1968
[20] BALLHAUSEN, G. J., GRAY, H. B.: Inorg. Chem. **1,** 111, 1962.
[21] ANDERSON, P. W., WEISS, P. R.: Rev. Mod. Phys. **25,** 269, 1953
[22] MANN, R. S., DOSI, M. K.: Cat. **28,** 282, 1973

K. C. KHULBE, R. S. MANN } Department of Chemical Engineering University of Ottawa, Ottawa, Canada K1N 6N5.

Acta Chimica Academiae Scientiarum Hungaricae, Tomus 92 (1), pp. 27—30 (1977)

BIS-VANILLIN *o*-PHENYLENE DIAMINE COMPLEXES OF RARE-EARTHS

M. SHAMEEM ANSARI and NASEER AHMAD

(Department of Chemistry, Aligarh Muslim University, Aligarh, U. P. India)

Received March 26, 1976

Bis-vanillin-*o*-phenylene diamine reacts with yttrium (III) and lanthanide (III) (except promethium and lutecium) ions to give 1:1 products having the composition $C_{22}H_{18}N_2O_4M\ Cl \cdot 3H_2O$. The molar conductance shows them to be 1:1 electrolytes and thermogravimetric analysis curves show that the three water molecules are co-ordinated. The infrared spectrum reveals the shifting of the C = N and C–O bands to higher frequencies on complexation. The co-ordination thus occurs through the two nitrogen atoms and both the oxygens of the phenolic OH groups making the rare earth ions heptaco-ordinate in these complexes.

A review of the present day chemical literature evinces the inadequacy of research on lanthanide (III) complexes of Schiff bases [1—2]. In previous papers [3—4] we have reported the lanthanide (III) and yttrium (III) complexes of tetradentate Schiff bases, bis vanillin-benzidine and bis salicylaldehyde-*o*-dianisidine.

The present communication deals with the synthesis of lanthanide (III) (except Pm and Lu) and yttrium (III) complexes of bis vanillin-*o*-phenylene diamine, which were characterized by their elemental and thermogravimetric analyses, melting points, molar conductances and infrared spectra.

Experimental

Rare-earth (III) chlorides (Leico Chemicals, U.S.A.) and yttrium (III) chloride (E. Merck, Germany) were used to prepare the complexes. The Schiff base bis-vanillin-*o*-phenylene diamine was prepared by the condensation of vanillin (Bush Boake Allen, London) and *o*-phenylene diamine in the molar ratio of 2:1 in ethanol, and purified by recrystallization from the same solvent.

The crystalline complexes were obtained by mixing the rare earth chlorides and the Schiff base in the stoichiometric ratio of 1:1 in ethanol and dried in vacuo.

The complexes were subjected to microanalysis for carbon, hydrogen and nitrogen, and chloride was estimated as silver chloride after fusing the complex with caustic soda in a platinum crucible.

The thermograms of six complexes (La, Pr, Sm, Tb, Ho and Yb) were taken at slow scan speed between ambient and 800 °C and the weight loss was plotted *versus* the temperature.

The molar conductances of $10^{-3}M$ solutions of these complexes in dimethyl sulphoxide were measured on a Philips PR 9500 conductivity bridge using a dip type cell.

The infrared spectra of the Schiff base and the complexes were recorded in the range of 4000—6000 cm^{-1} in KBr discs on a Perkin Elmer Infra Cord Model 137 B spectrophotometer.

Results and discussion

Bis-vanillin-*o*-phenylene diamine interacts with trivalent yttrium and lanthanide ions in the molar ratio of 1:1 giving products having the composition:

$$[C_{22}H_{18}N_2O_4M]\,Cl \cdot 3H_2O$$

Table I

Elemental analyses and some other data

Compounds	% C	% H	% N	% Cl	M. P. °C	Λ M ohm^{-1} cm^2 mole^{-1}
1. $LaLCl \cdot 3H_2O$	(43.85) 44.19	(3.983) 4.18	(4.647) 4.53	(5.883) 5.99	215—18°	69.1
2. $CeLCl \cdot 3H_2O$	(43.763) 45.21	(3.975) 4.03	(4.637) 4.72	(5.87) 5.76	218°	60.6
3. $PrLCl \cdot 3H_2O$	(43.70) 44.89	(3.975) 4.11	(4.631) 4.80	(5.864) 5.98	225—27°	49.8
4. $NdLCl \cdot 3H_2O$	(43.466) 44.0	(3.948) 4.13	(4.606) 4.80	(5.83) 5.90	225°	36.9
5. $SmLCl \cdot 3H_2O$	(43.034) 43.94	(3.908) 4.25	(4.560) 4.70	(5.773) 5.88	226.28°	40.5
6. $EuLCl \cdot 3H_2O$	(42.926) 44.11	(3.89) 4.13	(4.548) 4.66	(5.758) 5.90	178°	59.3
7. $GdLCl \cdot 3H_2O$	(42.555) 43.7	(3.883) 4.00	(4.509) 4.71	(5.709) 5.82	270°	65.4
8. $TbLCl \cdot 3H_2O$	(42.441) 43.92	(3.871) 4.09	(4.497) 4.50	(5.694)	168—70°	63.9
9. $DyLCl \cdot 3H_2O$	(42.198) 40.81	(3.833) 4.13	(4.471) 4.61	(5.66)	220—25°	46.3
10. $HoLCl \cdot 3H_2O$	(42.035) 41.95	(3.818) 4.11	(4.554) 4.38	(5.639) 5.80	215—20°	36.7
11. $ErLCl \cdot 3H_2O$	(41.878) 40.93	(3.804) 4.10	(4.438) 4.61	(5.619)	226—30°	27.5
12. $TmLCl \cdot 3H_2O$	(41.763) 43.25	(3.794) 4.02	(4.426) 4.33	(5.604)	230°	29.7
13. $YbLCl \cdot 3H_2O$	(40.557) 40.77	(3.769) 4.13	(4.303) 4.20	(5.568) 5.70	225—30°	29.6
14. $YLCl \cdot 3H_2O$	(47.639) 48.15	(4.325) 4.55	(5.067) 5.20	(6.414) 6.59	230—35°	40.1

L = Bis-vanillin benzidine calculated values are given in parentheses

Where M stands for lanthanide elements (except promethium and lutecium) and yttrium, according to elemental analyses for carbon, hydrogen, nitrogen and chlorine. The formation of these complexes involves the ionization of the two phenolic hydroxyl groups.

The molar conductances of these complexes at $10^{-3}M$ concentration in dimethyl sulphoxide are in the range of 27.5—69.1 ohm^{-1} cm^2 mole^{-1}. GREENWOOD [5] *et al.* reported 50—70 ohm^{-1} cm^2 mole^{-1} as the range for 1 : 1 electrolytes in this solvent and BROOMHEAD and KUNE-MAGUIRE [6] reported 24 and 27 ohm^{-1} cm^2 mole^{-1} molar conductances for ethylene diamine complexes of cobalt (III) and ruthenium (III) under the same conditions. It can be concluded that these complexes are 1 : 1 electrolytes and the chloride is in the outer co-ordination sphere.

Table II

Thermogravimetric analyses data

Compounds	Removal of one water molecule, % wt. loss			Removal of three water molecule, % wt. loss			Metal formation, % wt. loss		
	Theo.	Obs.	Temp. °C	Theo.	Obs.	Temp. °C	Theo.	Obs.	Temp. °C
1. $LaLCl \cdot 3H_2O$	2.987	3.0	100°	8.96	9.0	160°	76.95	80.0	550°
2. $PrLCl \cdot 3H_2O$	2.983	3.1	98°	8.949	9.0	168°	76.71	79.5	560°
3. $Sm \cdot Cl \cdot 3H_2O$	2.931	2.5	96°	8.793	8.5	150°	75.52	77.5	568°
4. $TbLCl \cdot 3H_2O$	2.892	2.5	110°	8.676	8.4	155°	74.48	78°	560°
5. $HoLCl \cdot 3H_2O$	2.86	3.0	108°	8.59	8.5	156°	73.77	79.5	566°
6. $YbLCl\ 3H_2O$	2.824	2.5	108°	8.472	8.4	150°	72.82	80.5	554°

The thermograms yield useful information. One water molecule is eliminated between 96° and 100 °C and all the three water molecules are lost up to 150—168 °C (Table II). The three water molecules seem to be co-ordinated to the lanthanide ions. The total weight loss observed is greater by 2.5—7% than the loss calculated for the removal of the ligand, water molecules and the chloride. Perhaps because the complex species volatilizes at various stages leaving less metal than required on the basis of stoichiometric considerations.

The infrared spectrum of bis-vanillin-*o*-phenylene diamine shows a medium intensity band at 3448 cm^{-1} which is also present in its complexes in the region of 3448—3534 cm^{-1} and is assigned to antisymmetric OH stretching mode. The IR spectra of complexes do not show any band near 1630 cm^{-1} which may be assigned to lattice water.

In bis-vanillin-*o*-phenylene diamine a medium intensity band appears at 1585 cm^{-1} which is the stretching frequency of the C = N bond. A strong band at 1428 cm^{-1} is the C–O stretching frequency of the phenolic part of vanillin. HENRY and DEHN [7] have reported the IR spectra of Schiff bases

and suggested that C = N absorption occurs at 1630 cm.$^{-1}$ GOLDBERG and NACE [8] have assigned very strong bands at 1630 and 1661 cm^{-1} for C = N stretching absorption. ROSE *et al.* [9] have reported C = N stretching frequencies at 1650(s) and 1660(s) cm.$^{-1}$ ROBSON *et al.* [10] assigned a broad band at 1610 cm^{-1} to imine C = N stretching frequency. BIRADAR and KULKARNI [11] have assigned the strong band at 1620—1610 to C = N stretching in Schiff base and found that this is shifted to higher frequency, 1650—1630 cm^{-1}, on complexation with titanium (IV). In our studies on lanthanide complexes of bis vanillin benzidine [12] it was observed that the two strong bands 1626 cm^{-1} (C = N stretching) and 1425 cm^{-1} (C — O stretching) shift to higher frequencies on complexation. In similar studies [4] on the complexes of bis-salicylaldehyde-*o*-dianisidine we observed that the 1613 cm^{-1} band shifted to higher frequency (1654—1629 cm^{-1}). The 1585 cm^{-1} and (CN stretching) and 1428 cm^{-1} band (C–O stretching) in bis-vanillin-*o*-phenylene diamine are shifted to higher frequency on complexation (1680—1613 and 1481—1494 cm^{-1} respectively).

The phenolic OH deformation occurring at 1389 cm^{-1} (medium) in the ligand disappears in the complexes.

A band appearing in the region of 865—873 cm^{-1} (strong) in the complexes is absent in the ligand and can be assigned to co-ordinated water.

On the basis of the shift of CN and C–O vibrations to higher frequencies, and the disappearance of the phenolic OH deformation, it is concluded that co-ordination occurs through both the phenolic oxygen atoms and the nitrogen atoms. The three water molecules are also co-ordinated making the rare-earth ions hepta-co-ordinate.

*

Authors express their gratitudes to Prof: W. RAHMAN, Head of the Department for providing necessary research facilities. One of the authors (M.S.A.) is thankful to C.S.I.R. New Delhi, for a senior fellowship.

REFERENCES

[1] YAMADA, S., YAMANOUCHI, J., KUMA, H.: Bull. Chem. Soc., Japan, **44,** (5) 1448 (1971)
[2] DATT, N. K., NAG, K.: J. Inorg. Nucl. Chem., **30,** 7—9, 2493—99 (1968)
[3] ANSARI, M. S., AHMAD, N.: J. Inorg. Nucl. Chem. accepted for publication,
[4] ANSARI, M. S., AHMAD, N.: Acta Chim. (Budapest), **86**(1), pp. 47—51 (1975)
[5] GREENWOOD, N. N., STRANGHAM, B. P., WILSON, A. E.: J. Chem. Soc., (A) **2209** (1968)
[6] BROOMHEAD, J. A., KANE-MAGUIRE, L. A.: J. Chem. Soc., (A), **548** (1967)
[7] HENRY, R. A., DEHN, W. M.: J. Chem. Soc., **71,** 2297 (1949)
[8] GOLDBERG, E. P., NACE, H. R.: J. Chem. Soc., **75,** 6260 (1953)
[9] ROSE, N. J., ELDER, M. S., BUSCH, O. H.: Inorg. Chem, **6,** 1964 (1967)
[10] MCFADYEN, W. D., ROBSON, R., SCHAAP, H.: Inorg. Chem, **11,** 1777, (1972)
[11] BIRADAR, N. S., KULKARNI, V. H.: J. Inorg. Nucl. Chem, **33,** 3847 (1971)
[12] ANSARI, M. S., AHMAD, N.: J. Inorg. Nucl. Chem, accepted for publication

N. SHAMEEM ANSARI
MASEER AHMAD
Department of Chemistry, Aligarh Muslim University
Aligarh, U.P. India.

Acta Chimica Academiae Scientiarum Hungaricae, Tomus 92 (1), pp. 31–47 (1977)

EMPIRICAL CORRELATION BETWEEN THE POTENTIAL ENERGY OF BOND DISSOCIATION AND BOND LENGTH

T. BÉRCES

(Reaction Kinetics Research Group of the Hungarian Academy of Sciences, Szeged)

Received April 22, 1976

The concept of potential energy of dissociation (V^0_{AB}) has been defined as the change in the potential energy during the increase of the length of an A–B bond of a polyatomic molecule to infinity. The existence of an unambiguous correlation between V^0_{AB} and the equilibrium bond length R^0_{AB} was verified:

$$I_1 V^0_{AB} + \ln V^0_{AB} = -I_2 R^0_{AB} + I_3$$

The values of the parameters I_1 and I_2 were expressed by means of the Morse constants for the investigated bond (β_{AB}) and for the appropriate Lennard-Jones molecule (β_X):

$$I_1 = C_1(\beta_X/\beta_{AB}) \text{ and } I_2 = C_2(\beta_X/\beta_{AB})^{1/2},$$

where C_1 and C_2 are constants with values depending on the position (on the row) occupied by the bonded atoms in the periodic table. The validity of the suggested correlation was tested for 13 types of chemical bonds, including C–C and C–H.

For the change of the potential energy of dissociation with bond length in case of a given bond, the relation

$$I_1(V_{AB} - V^0_{AB}) + \ln(V_{AB}/V^0_{AB}) = -I_2(R_{AB} - R^0_{AB})$$

was suggested. This relation, permitting the estimation of the energy or the length of an extended bond, may be used in semi-empirical and empirical treatments of reaction kinetic problems.

I. Introduction

Considerable progress has been made during the last one and a half century in the theoretical calculation of the energy of interaction between atoms. Potential energies calculated [1] for various states of H_2 are accurate enough for most physicochemical applications, and promising results were obtained also for other diatomic molecules. The situation is, however, not so favourable regarding calculation of interaction energies of polyatomic species. Adjustable parameters have to be introduced often in the quantum mechanical treatments, and the accuracy of the calculations is not satisfactory. Therefore, kinetic, and other physicochemical considerations, requiring the knowledge of the correlation between interaction energies and interatomic distances, generally have to rely on empirical relationships. In this paper we intend to

suggest a correlation which might be used in semi-empirical and empirical methods developed for the estimation of the potential energy of activation of atom-transfer reactions.

II. Formulation of the problem

The "*ab initio*" calculation of the potential energy surface for the simplest

$$A + B - C \rightarrow A - B + C \tag{1}$$

type atom-transfer process (for the $H + H_2 \rightarrow H_2 + H$ reaction) can be carried out with reasonable accuracy [2]. However, the theoretical treatments of metathetical reactions involving polyatomic groups or of reactions different from the type symbolized by Eq. (1), are not expected in the near future to supply results comparable in accuracy with that of the experimental activation energies. Therefore, semi-empirical calculations of potential energy surfaces and semi-empirical or empirical estimations of the activation energies will maintain their importance for a long time in predicting kinetic parameters or examining the reliability of experimental kinetic data.

A number of semi-empirical methods developed for the calculation of potential energy surfaces and for the estimation of activation energies use relationships between bond energy and bond length or between bond dissociation energy and bond length. Among the semi-empirical potential energy surface calculation methods based on the LONDON equation [3], the LONDON—EYRING—POLANYI (LEP) treatment [4] and the SATO (LEPS) procedure [5] express the relationship between bond energy and bond length by the MORSE function [6]:

$$^1E = V^0[\{1 - \exp(-\beta(R - R^0))\}^2 - 1] \tag{2}$$

where ^1E denotes the bond energy at an interatomic distance R, V^0 is the classical dissociation energy (the potential energy of dissociation) at the equilibrium interatomic distance R^0, and β stands for the Morse constant.

The Morse function is used also in the semi-empirical activation energy calculation method of ZAVITSAS [7]. However, the BEBO (bond energy — bond order) method developed by JOHNSTON and PARR [8, 9] — which has been widely used to estimate activation energies for atom-transfer reactions — is based on a relationship between the bond energy and bond order:

$$D = D_s n^p \tag{3}$$

where D_s designates the bond energy of the single bond, and p is a parameter characteristic for the given bond, obtainable from the energy and interatomic

distance of the appropriate Lennard-Jones "molecule" (see Eq. (15)). In Eq. (3), n denotes the "chemist's bond order", and D is the energy of a partial bond characterized by the bond order n. The bond order playing an important role in the BEBO theory, is an intuitive concept defined by PAULING's relation [10]

$$R = R_s - 0.26 \ln n \tag{4}$$

where R and R_s designate the bond lengths of the partial and the single bonds, respectively. Eliminating n from Eq. (3) by using PAULING's Eq. (4),

$$\ln (D/D_s) = -\frac{p}{0.26}(R - R_s), \tag{5}$$

it appears that the BEBO method too is based on a relationship of the bond energy and the bond length.

Both the Morse function and Eq. (5) are empirical correlations derived on the basis of known bond energy and bond length data. However, if activation energies of atom-transfer reactions involving polyatomic groups have to be estimated (*i.e.* if one deals with the reaction type (1) where A or C or both represent polyatomic groups), it is desirable to rely on relationships between bond-dissociation energies and bond lengths (instead of bond energy *vs.* bond length correlations). More precisely — since the semi-empirical methods referred to above calculate the potential energy of activation (*i.e.* the classical activation energy) — the correlation between the potential energy of dissociation and the interatomic distance is of major interest from kinetic point of view.

The concept of potential energy of dissociation will be defined in connection with the

$$AB \rightarrow A + B \tag{6}$$

dissociation of a polyatomic molecule, as the change in the potential energy during the increase of the length of the A–B bond from the original value to infinity. The potential energy of dissociation shall be denoted by V^0_{AB} if the length of the A–B bond in the considered molecule equals the equilibrium R^0_{AB} value. In order to be able to deal with partial bonds, the potential energy of dissociation for an AB molecule characterized by a partial A–B bond (where $R_{AB} \neq R^0_{AB}$) shall be denoted by V_{AB}.

The value of V^0_{AB} may be given by means of D^0_0 (A–B), the bond-dissociation energy at O K:

$$V^0_{AB} = D^0_0(A - B) + \frac{1}{2}\sum h\nu_{AB} - \frac{1}{2}\sum h\nu_A - \frac{1}{2}\sum h\nu_B . \tag{7}$$

The second, third and fourth terms on the right hand side of Eq. (7) represent the zero-point energies of species AB, A and B, respectively; summation is to

be extended to all v frequencies of the given species. The quantity D_0^0(A–B) is connected with the bond-dissociation energy at 298 K [11]:

$$D_0^0(A - B) = DH_{298}^0(A - B) - \frac{1}{2} RT(\Delta + 2), \tag{8}$$

where Δ denotes the change in the number of transitional and vibrational degrees of freedom in process (6). (The value of Δ is 1,3 and 6 if both A and B are atoms, if B is an atom and A a polyatomic group, and if both A and B are polyatomic groups, respectively.) Substituting $D^0(A - B)$ from Eq. (8) into Eq. (7), one obtains

$$V_{AB}^0 = DH_{298}^0(A - B) + \left\{ \frac{1}{2} \Sigma h \nu_{AB} - \frac{1}{2} \Sigma h \nu_A - \frac{1}{2} \Sigma h \nu_B \right\} - \frac{1}{2} RT(\Delta + 2) \tag{9}$$

According to Eq. (9), the potential energy of dissociation related to the A–B bond characterized by the equilibrium R_{AB}^0 interatomic distance can be given by means of DH_{298}^0 (A — B) and the zero-point energies of A, B and AB. However, the vibrational frequencies required to calculate the zero-point energies are available only for a few polyatomic molecules and for even fewer free radicals. The use of average frequencies may introduce, in most cases, considerable errors. Therefore, we replace arbitrarily on the right hand side of Eq. (9) all terms but the first by the bond zero-point energy, ZPE_{A-B}, calculated from the A–B stretching frequency. Thus,

$$V_{AB}^0 = DH_{298}^0(A - B) + ZPE_{A-B} \tag{10}$$

We retain the symbol V_{AB}^0 for the value calculated according to the approximate equation (10), but call this quantity as the potential energy of bond dissociation (in order to differentiate from the potential energy of dissociation obtained from the accurate equation (9)). In order to be able to extend the applicability of the correlation suggested in this work (see below) to a bond-length range as wide as possible, we have calculated arbitrarily bond dissociation energies for multiple bonds by means of the well-known equation

$$DH^0(A - B) = \Delta H_f^0(A) + \Delta H_f^0(B) - \Delta H_f^0(AB) \tag{11}$$

where the symbols ΔH_f^0 designate the heats of formation of the given species.

Approximations similar to that included in Eq. (10) were previously used in semi-empirical calculations of activation energies [7—9, 12, 13]. The error in this approximation is different if A and B are atoms or polyatomic groups as may be seen from Table I. The most important bonds, from our point of

Table I

Comparison of values of V^0_{AB} calculated from Eqs (9) and (10)

A—B	DH°_{298}(A—B) kcal/mol	V°_{AB}—DH°_{298}(A—B) kcal/mol	
		Eq. (9)	Eq. (10)
H—H	103.2	5.5	6.4
CH_3—H	104.0	7.2	4.2
CH_3—CH_3	88.2	6.2	1.4

view, are the bonds between polyatomic groups and atoms. For these, Eq. (10) is a reasonable approximation. Among the three vibrational degrees of freedom disappearing during the decomposition, only one is taken into account in Eq. (10) when correcting for the zero-point energies, however, the error is largely compensated by the neglection of the last term in Eq. (9). In case of bonds between two polyatomic groups, the neglection of five vibrational degrees of freedom and that of the term RT $(\Delta + 2)/2$ brings about only partial compensation of the errors. In spite of this, the use of equation (10) is expected to be acceptable in our work for all types of bonds, because in the correlation suggested below relative values of the potential energies of bond dissociation appear yielding a further compensation of the errors.

The lengths of certain bonds (or the interatomic distances) change considerably during the chemical reaction, therefore, the problem to be solved is to find a general correlation, of the form

$$V_{AB} = f(R_{AB}), \tag{12}$$

valid in a very wide range of bond lengths. Since experimental V_{AB} and R_{AB} values for partial bonds are not available, we first establish the correlation

$$V^0_{AB} = f(R^0_{AB}) \tag{13}$$

for each class of bonds (as for instance C–C, C–H, etc.), and then assume that correlation (12) has the same form.

III. The empirical correlation

In a recent paper [14] Szabó and Konkoly Thege showed that a linear correlation exists between the strengths and lengths of single C–C bonds:

$$DH^0_{298}(C—C) = 696 — 400\ R \tag{14}$$

For the 37 substituted ethanes with C–C bond lengths varying from 1.38 to 1.56 Å, the suggested equation was found to fit the experimental data very well.

Since experimental results or reliable theoretical data for the lengths and energies of partial bonds are not available, progress can be made only by introducing a suitable postulate. In order to be able to deal with partial bonds characterized by bond orders less than 1, JOHNSTON and PARR assumed [8, 9] that the applicability of a correlation valid for normal molecules may be extended to the appropriate LENNARD—JONES cluster, and in the BEBO procedure [8, 9] they calculated the energies of the extended (loose) bonds by the correlation of bond energy and bond length given by Eq. (5). The parameter p appearing in this equation may be obtained from

$$p = \frac{0.26 \ln (D_s/\varepsilon_x)}{R_x - R_s} \tag{15}$$

where R_x and ε_x is the bond length and the depth of the potential-energy well for the appropriate LENNARD—JONES noble-gas diatomic cluster. It was realized that deviations occur from the linearity predicted by Eq. (5); the deviations were found to be positive for certain classes of bonds and negative for others.

A preliminary examination of available experimental data led us to the conclussion that *an unequivocal correlation exists between* R^0_{AB} *and* V^0_{AB} *in a wide range of bond lengths*, extending from the lengths of multiple bonds to those of the LENNARD—JONES molecules, *and that the expression for the bond length contains both a logarithmic term and a first order term with respect to the potential energy of bond dissociation.* Thus, the correlation function for given types of bonds (*i.e.* C–C, C–H, *etc.* bonds) could be written as

$$I_1 V^0_{AB} + \ln V^0_{AB} = - I_2 R^0_{AB} + I_3 \tag{16}$$

where I_1, I_2 and I_3 are constants. If the validity of Eq. (16) can be extended to the LENNARD—JONES molecule corresponding to the position in the periodic table of the bonded atoms forming a given type of bond (*i.e.* to Ne–Ne in case of C–C bonds, to Ne–He in case of C–H bonds, etc.), then

$$I_1 V^0_x + \ln V^0_x = - I_2 R^0_x + I_3 \tag{17}$$

where R^0_x and V^0_x is the interatomic distance and the depth of the potential-energy well for the appropriate LENNARD—JONES noble-gas diatomic cluster. Equations (16) and (17) yield the two-parameter relationship

$$I_1(V^0_{AB} - V^0_x) + \ln(V^0_{AB}/V^0_x) = - I_2(R^0_{AB} - R^0_x) \tag{18}$$

which is more suitable for experimental test and for certain practical applications.

IV. Experimental verification of the empirical correlation

The linearized form of Eq. (18),

$$\frac{\ln (V^0_{AB}/V^0_x)}{R^0_x - R^0_{AB}} = I_2 - I_1 \frac{V^0_{AB} - V^0_x}{R^0_x - R^0_{AB}}, \tag{19}$$

is most suitable for the verification of the suggested empirical correlation and for the evaluation of the parameters I_1 and I_2. According to Eq. (19), a plot of $\ln(V^0_{AB}/V^0_x)/(R^0_x - R^0_{AB})$ against $(V^0_{AB} - V^0_x)/(R^0_x - R^0_{AB})$ for a given type of bonds should give a straight line; I_2 and $-I_1$ are obtained as the intercept and the slope of the line, respectively. However, if the correlation between V^0_{AB} and R^0_{AB} is similar to that suggested by JOHNSTON and PARR (see Eq. (5)), *i.e.* if the relationship may be formulated as

$$\ln V^0_{AB} = -J_2 R^0_{AB} + J_3 \tag{20}$$

and

$$\ln (V^0_{AB}/V^0_x) = -J_2(R^0_{AB} - R^0_x), \tag{21}$$

then the ratio on the left hand side of Eq. (19) should be constant for a given type of bonds.

The verification of Eq. (18) has been carried out for 13 different types of bonds given below: C–H, N–H, O–H, C–C, C–N, C–O, N–N, N–O, O–O, C–F, C–Cl, C–Br, C–I. Those organic (and a few inorganic) molecules and free radicals were examined for which the required bond lengths, bond-dissociation energies and vibrational frequencies were available in the literature. Regarding the 121 molecules and free radicals examined and the sources of the data used, see the Appendix.

Verification of the suggested empirical correlation for C–H and C–C bonds is shown in Fig. 1 and 2, respectively. In case of C–C bonds where bond lengths and bond dissociation energies vary in a wide range and experimental data are more reliable, it is evident that the linearity expected from Eq. (19)

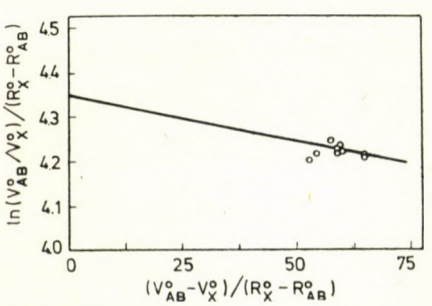

Fig. 1. Verification of the linearized form of Eq. (18) in case of C–H bonds. (Experimental points belong to C—H bonds given in the Appendix)

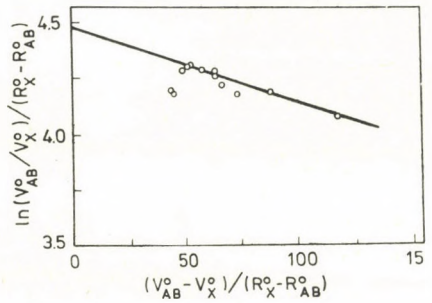

Fig. 2. Verification of the linearized form of Eq. (18) in case of C–C bonds. (Experimental points belong to C–C bonds given in the Appendix)

Table II

Experimental values for parameters of Eqs (16) and (18)

Type of bonds	$I_1 \times 10^3$ mol/kcal	I_2 Å^{-1}	I_3
C—H	1.5	3.98	9.21
N—H	1.2	3.78	8.57
O—H	0.8	3.73	8.41
C—C	3.6	4.62	11.85
C—N	3.2	4.36	11.04
C—O	2.8	4.35	11.01
C—F	4.9	4.47	11.38
N—N	4.2	4.18	10.48
N—O	7.2	4.15	10.39
O—O	4.4	4.13	10.33
C—Cl	9.6	4.30	12.81
C—Br	7.7	4.04	12.55
C—I	6.7	3.94	12.85

holds. In spite of the greater scatter of the experimental data and the limited range of available bond lengths, it may be seen that the ratio $\ln(V^0_{AB}/V^0_x)/(R^0_x - R^0_{AB})$ for C–H bonds in not constant and the change is in accordance with Eq. (19). Conclusions similar to those given above were obtained also for the rest of chemical bonds studied.

Plots of experimental data according to Eq. (19) allowed us to estimate I_1 and I_2 for various types of bonds. With these and with the R^0_x and V^0_x data

of the appropriate diatomic noble-gas molecules (see Table IV) we could calculate I_3 from Eq. (17). The values of the parameters I_1, I_2 and I_3 are summarized in Table II. The 13 types of bonds included in the table were divided in 6 groups in accordance with the position of the bonded atoms occupied in the MENDELEEV periodic table. The bonds of the second row elements with hydrogen are to be found in the first group. The bonds of the second row elements with each other were put in the second and third groups. (The reason for differentiating between these two groups will be given below.) Bonds of C-atoms with the 3rd, 4th and 5th row halogens are to be found in the 4th, 5th and 6th groups, respectively.

V. Consideration of the parameters of Eqs (16) and (18)

In each group of Table II, the bonds were given in order of increasing atomic number of the atoms forming the bond. In this succession, the values of the experimental parameters I_1, I_2 and I_3 show a definite decreasing tendency, which is opposite to that of the change of the Morse constants, as may be seen from the comparison with the β values given in Table III. In Table

Table III

Basic compounds, and the R^0_{AB}, V^0_{AB} and β_{AB} data for their given bonds

Type of bonds	Basic compound	R^0_{AB} Å	V^0_{AB} kcal/mol	β_{AB} Å^{-1}
C—H	CH_3—H	1.106	108.2	1.785
N—H	H_2N—H	1.012	114.9	2.000
O—H	HO—H	0.957	124.2	2.101
C—C	CH_3—CH_3	1.532	89.6	1.676
C—N	CH_3—NH_2	1.474	87.9	1.843
C—O	CH_3—OH	1.428	92.6	1.830
C—F	CH_3—F	1.385	107.9	1.771
N—N	H_2N—NH_2	1.449	72.5	2.023
N—O	H_2N—OH	1.46	77.3	2.024
O—O	HO—OH	1.49	51.9	2.242
C—Cl	CH_3—Cl	1.781	84.6	1.549
C—Br	CH_3—Br	1.939	70.7	1.528
C—I	CH_3—I	2.139	56.9	1.523

III given are characteristic representatives for the various bond types (the so-called basic compounds which are the simplest molecules containing the given bonds), R^0_{AB} and V^0_{AB} values for the studied bonds of the basic compounds, and their Morse constants. The latter can be estimated from

$$\beta_{AB} = 2^{1/2}\,\pi\,\nu_{AB}(\mu/V^0_{AB})^{1/2} \tag{22}$$

where ν_{AB} designates the stretching frequency of the A–B bond, and the reduced mass μ may be obtained from the masses of the end atoms of the bond.

Examining the relationship between the experimental values of I_1 and I_2 and the Morse constants given in Table III, we came to the conclusion that within each group of Table II *the values of I_1 and I_2 are inversely proportional to the Morse constants and to the square roots of the Morse constants, respectively*. Accordingly, we suggest the following expressions for the parameters I_1 and I_2:

$$I_1 = C_1(\beta_x/\beta_{AB}) \tag{23}$$

and

$$I_2 = C_2(\beta_x/\beta_{AB})^{1/2} \tag{24}$$

where β_x stands for the Morse constant of the noble-gas molecule appropriate to the position of the bonded atoms occupied in the MENDELEEV periodic table. The C_1 and C_2 are constants whose values depend — in the first approximation — only on the row of the periodic table where the two bonded atoms belong to; C_1 and C_2 are characteristic for the groups of Table II. Our suggested values are summarized in Table IV.

As more reliable data for bond lengths and bond dissociation energies become available, the values given for C_1 and C_2 in Table IV may require minor amendments. This might affect first of all C_1 which is less accurate than C_2

Table IV

Suggested values for the constants of Eqs (23) and (24), and data for the noble-gas molecules [35]

Type of bonds	$C_1\times10^3$ mol/kcal	C_2 Å^{-1}	Noble-gas analogue			
			Bonds	R^0_x Å	V^0_x kcal/mol	β_x Å^{-1}
C—H, N—H, O—H	1.7	4.4	Ne—He	3.21	0.0284	1.449
C—C, C—N, C—O	2.9	4.2	Ne—Ne	3.10	0.0835	2.034
C—F, N—N, N—O, O—O	4.3	4.2	Ne—Ne	3.10	0.0835	2.034
C—Cl	7.7	3.9	Ne—Ar	3.43	0.1430	1.924
C—Br	6.0	3.6	Ne—Kr	3.58	0.1480	1.955
C—I	4.8	3.3	Ne—Xe	3.75	0.1490	2.109

since in Eqs (16) and (18) the term containing the first power of V^0_{AB} is less important than the logarithmic term even at the shortest interatomic distances. On the basis of our results obtained for C_1 we found it necessary to divide the bonds of the second row elements into two groups, as it was done in Table IV and in the previous tables.

Table V

Calculated values for parameters of Eqs (16) and (18)

Type of bonds	$I_1 \times 10^3$ mol/kcal	I_2 Å^{-1}	I_3
C—H	1.4	3.96	9.15
N—H	1.2	3.75	8.48
O—H	1.2	3.65	8.16
C—C	3.5	4.63	11.88
C—N	3.2	4.41	11.20
C—O	3.2	4.43	11.26
C—F	4.9	4.50	11.48
N—N	4.3	4.21	10.58
N—O	4.3	4.21	10.58
O—O	3.9	4.00	9.93
C—Cl	9.6	4.35	12.98
C—Br	7.7	4.07	12.66
C—I	6.7	3.88	12.63

In table V are given the values of I_1 and I_2 calculated from Eqs (23) and (24), respectively, by means of C_1 and C_2 taken from Table IV. Table V also reports I_3 values calculated from Eq. (17). Comparison of the calculated parameters with the experimental ones (see Table II) shows that I_1 and I_2 can be estimated within the limits of experimental error from Eqs (23) and (24), respectively.

VI. Comparison of Eq. (16) with other empirical relationships

In this chapter we compare V^0_{AB} *vs.* R^0_{AB} plots obtained from Eq. (16) with experimental data, and discuss the relation of Eq. (16) to Eq. (20) based on the work of JOHNSTON and PARR, and to Eq. (14) suggested by SZABÓ and

KONKOLY THEGE. In calculating the curves shown below, the parameters I_1, I_2 and I_3 were taken from Table V, and the constants J_2 and J_3 of Eq. (20) were estimated from R^0_{AB} and V^0_{AB} data of the basic compounds and of the appropriate noble gas molecules (see Tables III and IV).

As examples from among the bonds of the second row elements, we present calculated V^0_{AB} *vs.* R^0_{AB} curves and experimental data for C–C, C–N and N–N types of bonds in Figs 3, 4 and 5, respectively. Curves calculated by Eq. (16) agree better with experiment than those obtained by Eq. (20). This can be seen specially well for the C–C bonds where the experimental data are more accurate.

For the limited bond length range where experimental data are available, the curve obtained with Eq. (16) is only mildly bent and may be approximated by a straight line in accordance with Eq. (14) suggested by SZABÓ and KONKOLY THEGE with the aim of establishing the relationship between bond strengths

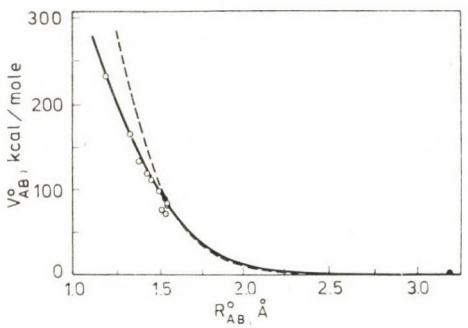

Fig. 3. Calculated V^0_{AB} *vs.* R^0_{AB} curves and experimental data for C–C bonds. ——, calculated from Eq. (16); – – –, calculated from Eq. (20); ○, experimental data; ●, data of the basic compound and of the appropriate noble-gas molecule

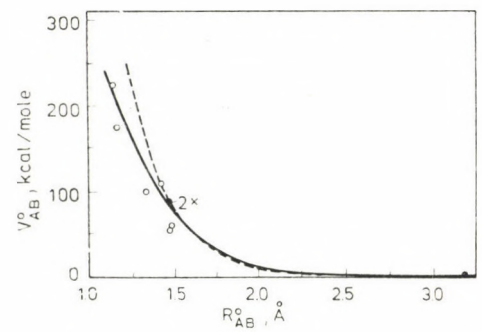

Fig. 4. Calculated V^0_{AB} *vs.* R^0_{AB} curved and experimental data for C–N bonds. ——, calculated from Eq. (16); – – –, calculated from Eq. (20); ○, experimental data; ●, data of the basic compound and of the appropriate noble-gas molecule

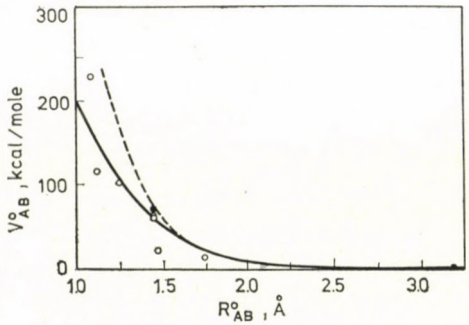

Fig. 5. Calculated V^0_{AB} *vs.* R^0_{AB} curves and experimental data for N–N bonds. ——, calculated from Eq. (16); – – –, calculated from Eq. (20); ○, experimental data; ●, data of the basic compound and of the appropriate noble-gas molecule

and bond lengths of C–C single bonds. Differentiating Eq. (16), one obtains

$$\frac{dV^0_{AB}}{dR^0_{AB}} = -\frac{I_2}{I_1 + 1/V^0_{AB}} \tag{25}$$

which may be used to show that in the experimental C–C bond length range of 1.20—1.54 Å the differential quotient dV/dR changes from — 580 to — 290 kcal/mol. Å. In the middle of the range (at $R^0_{AB} = 1.37$ Å) $dV^0_{AB}/dR^0_{AB} =$ — 430 kcal/mol. Å which agrees very well with the parameter — 400 appearing in Eq. (14).

From among the bonds of the second row elements with hydrogen we present the V^0_{AB} plots for C–H and N–H in Figs 6 and 7, respectively, while from the bonds of C with halogens the C–Cl bonds are shown in Fig. 8. The bond length range of bonds of polyatomic groups with atoms (especially with hydrogen atoms) is very narrow. In spite of this fact, the results presented in Figs 6, 7 and 8 show that the increase of V^0_{AB} with decreasing R^0_{AB} is not so

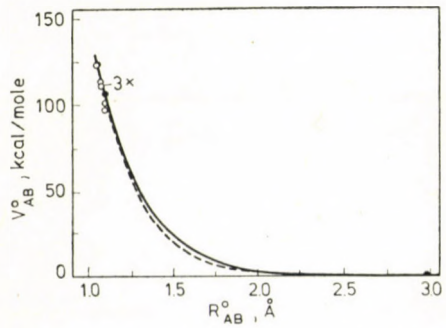

Fig. 6. Calculated V^0_{AB} *vs.* R^0_{AB} curves and experimental data for C–H bonds. ——, calculated from Eq. (16); – – –, calculated from Eq. (20); ○, experimental data; ●, data of the basic compound and of the appropriate noble-gas molecule

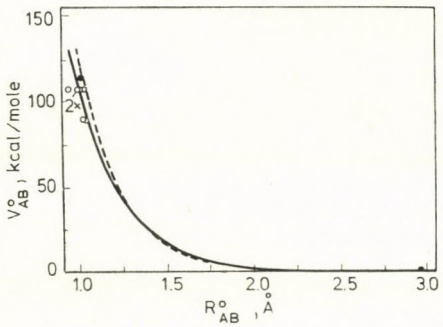

Fig. 7. Calculated V^0_{AB} *vs.* R^0_{AB} curves and experimental data for N–H bonds. ——, calculated from Eq. (16); – – – calculated from Eq. (20); ○, experimental data; ●, data of the basic compound and of the appropriate noble-gas molecule

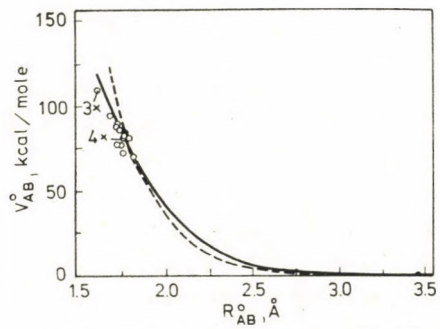

Fig. 8. Calculated V^0_{AB} *vs.* R^0_{AB} curves and experimental data for C–Cl bonds. ——, calculated from Eq. (16); – – –, calculated from Eq. (20); ○, experimental data; ●, data of the basic compound and of the appropriate noble-gas molecule

steep as expected from Eq. (20). Equation (16) is in accordance with the experimental data; the deviations being less than the estimated experimental errors.

In the narrow range of experimental bond lengths for bonds of polyatomic groups and atoms, the relationship between V^0_{AB} and R^0_{AB} may be described very well by a straight line. Thus, for the type of C–H bonds, the value of dV/dR changes only between — 440 and — 360 kcal/mol Å while the bond lengths increase from 1.06 to 1.11 Å. At the average bond length of 1.09 Å, $dV^0_{AB}/dR^0_{AB} = -400$ kcal/mol Å. The latter value is very close to that obtained for the C–C bonds indicating that the change in the potential energy of bond dissociation caused by a unit change of the bond length is very similar for the C–C and C–H types of bonds.

VII. Applications of Eq. (16)

Equation (16) establishes connection between equilibrium values of bond lengths and potential energies of bond dissociation. The correlation in its original form or even more so in a form similar to Eq. (18),

$$I_1(V^0_{AB} - V^0_{A'B}) + \ln (V^0_{AB}/V^0_{A'B'}) = - I_2(R^0_{AB} - R^0_{A'B'}) \qquad (26)$$

(where the relationship is concerned with the same type of bonds in molecules AB and A'B'), may be used either for the estimation of potential energies of bond dissociation from known bond lengths, or for obtaining R^0 data from V^0 values.

The main object of this work is, however, the formulation of a correlation describing for a given bond the change of V_{AB} with bond length. This problem can be solved by introducing a postulate stating that *the validity of the correlation obtained on the basis of equilibrium data may be extended to non-equilibrium bond lengths* (*i.e.* to partial bonds). The universal verification of this postulate would be possible only if reliable quantum mechanical calculations of the energies of interaction of polyatomic groups as a function of the interatomic distances could be carried out. Lacking such calculations, yet we feel plausible the assumption that the postulate is correct for small deviations from the equilibrium interatomic distances. One should point out that it is just the property of the slightly extended bond which is required in kinetic considerations of certain very important types of chemical reactions. Such reactions are, for instance, the atom-transfer reactions characterized by tight activated complexes.

On the basis of the postulate introduced, the change of the potential energy of dissociation with bond length can be given by

$$I_1(V_{AB} - V^0_{AB}) + \ln (V_{AB}/V^0_{AB}) = - I_2(R_{AB} - R^0_{AB}) \qquad (27)$$

where the parameters I_1 and I_2 may be obtained from Eqs (23) and (24), respectively, or may be taken from Table IV.

Appendix

Studied chemical bonds, and the sources of data

C—H bonds: CH_3—H, C_2H_5—H, $C_2H_5CH(CH_3)$—H, $CH_2 : CHCH_2$—H, $CH_2 : CH$—H, $CH_2 : C(CH_3)$—H, $CH_3CH : CH$—H, C_6H_5—H, $CH : C$—H, $CH_3C : C$—H;

N—H bonds: H_2N—H, HN—H, N—H, CH_3NH—H, H_2NNH—H, $O : CHNH$—H, $H_2NC(O)\,NH$—H, $N \vdots CNH$—H;

O—H bonds: O—H, HO—H, CH_3O—H, HCOO—H;

C—C bonds: CH_3—CH_3, $(CH_3)_2CH$—CH_3, $(CH_3)_3C$—CH_3, $CH_2 : CHCH_2$—CH_3, $CH_2 : C(CH_3)CH_2$—CH_3, $CH_2 : CH$—CH_3, $CH_2 : CH$—$CH : CH_2$, $CH : C$—CH_3, $CH : C$—$CH : CH_2$, $CH \vdots C$—$C \vdots CH$, $CH_2 = CH_2$, $CH \equiv CH$;

C—N bonds: $CH_3—NH_2$, CH_3NHCH_3, $CH_3—NO_2$, $CH_3—N:NCH_3$, $CH_3—N:C$, $O:CH—NH_2$, $CH{\equiv}N$, $\dot{C}H \equiv N(^2\Sigma^+)$;

C—O bonds: $CH_3—OH$, $CH_3—OCH_3$, $O:CH—OH$, $CH_2=O$, $CH_3CH=O$, $(CH_3)_2C=O$, $HOCH=O$, $CH_3C(OH)=O$, $C\equiv O$, $\dot{C}H=O$;

N—N bonds: $H_2N—NH_2$, $F_2N—NF_2$, $(CH_3)_2N—NH_2$, $CH_3NH—NHCH_3$, $O_2N—NO_2$, $FN=NF$, $N\equiv NO$, $N\equiv N$;

N—O bonds: $H_2N—OH$, $H_2N—OCH_3$, $ON—OH$, $ON—OCH_3$, $O_2N—OH$, $HN=O$, $FN=O$, $ON=O$, $N\equiv O$;

O—O bonds: $HO—OH$, $O=O$;

C—F bonds: $CH_3—F$, $CH_2F—F$, $CHF_2—F$, $CF_3—F$, $CCl_3—F$, $C_2H_5—F$, $(CH_3)_3C—F$, $CH_3C(O)—F$, $CH_2:CH—F$, $C_6H_5—F$;

C—Cl bonds: $CH_3—Cl$, $CH_2Cl—Cl$, $CHCl_2—Cl$, $CCl_3—Cl$, $CH_2F—Cl$, $CF_3—Cl$, $C_2H_5—Cl$, $CH_3CH_2CH_2—Cl$, $(CH_3)_2CH—Cl$, $(CH_3)_3C—Cl$, $CH_3C(O)—Cl$, $ClC(O)—Cl$, $CH_2:CH—Cl$, $CH_2:CHCH_2—Cl$, $C_6H_5—Cl$, $CH:C—Cl$, $CH_3C:C—Cl$, $N:C—Cl$;

C—Br bonds: $CH_3—Br$, $CH_2Br—Br$, $CF_3—Br$, $C_2H_5—Br$, $(CH_3)_2CH—Br$, $CH_2:CH—Br$, $CH_2:CHCH_2—Br$, $CH_3C(O)—Br$, $C_6H_5—Br$, $CH:C—Br$, $CH_3C:C—Br$, $N:C—Br$;

C—I bonds: $CH_3—I$, $CH_2I—I$, $CF_3—I$, $C_2H_5—I$, $CH_2:CHCH_2—I$, $CH_3C(O)—I$, $C_6H_5—I$, $CH_3C:C—I$, $N:C—I$.

Source of bond length data: Interatomic distances for noble-gas molecules were taken from scattering results [35]. Most bond lengths were taken from compilations [15, 16], and in a few cases other literature sources [17—26] were used.

Source of bond dissociation energies: The bond energies of the noble-gas molecules originate from scattering results [35]. Bond strengths were exceptionally estimated on the basis of known dissociation energies of analogous bonds, and were generally calculated by Eq. (11) from known heats of formation of radicals and molecules. The heats of formation of free radicals were taken from a table compiled by critical examination of data found in literature compilations [27—30] and recently published papers. The heats of formation of molecules were obtained from three sources [31—33].

Source of vibrational frequencies: In the calculation of the zero-point energy related to the bond considered (ZPE_{A-B}), the appropriate stretching frequency (or average of stretching frequencies) was used. Frequencies were taken from compilations [34, 17, 18], or in a few cases were estimated on the basis of known data of similar bonds.

REFERENCES

[1] Kolos, W., Wolniewicz, L.: J. Chem. Phys., **43,** 2429 (1965)
Kolos, W., Wolniewicz, L.: Chem. Phys. Let., **24,** 457 (1974)
Kolos, W., Roothaan, C. C. J.: Rev. Mod. Phys., **32,** 219 (1960)
[2] Liu, B.: J. Chem. Phys., **58,** 1925 (1973)
[3] London, F.: Z. Electrochem., **35,** 552 (1929)
[4] Eyring, H., Polanyi, M.: Z. physik. Chem. (Leipzig), **B12,** 279 (1931)
[5] Sato, S.: Bull. Chem. Japan **28,** 450 (1955)
Sato, S.: J. Chem. Phys., **23,** 592, 2465 (1955)
[6] Morse, R. M.: Phys. Rev., **34,** 57 (1929)
[7] Zavitsas, A. A.: J. Amer. Chem. Soc., **94,** 2779 (1972)
[8] Johnston, H. S., Parr, C.: J. Amer. Chem. Soc., **85,** 2544 (1963)
[9] Johnston, H. S.: Gas Phase Reaction Rate Theory. The Ronald Press Co., New York 1966.
[10] Pauling, L.: J. Amer. Chem. Soc., **69,** 542 (1947)
[11] Benson, S. W.: J. Chem. Educ., **42,** 502 (1965)
[12] Carmichael, H., Johnston, H. S.: J. Chem. Phys., **41,** 1975 (1964)
[13] Arthur, N. L., McDonell, J. A.: J. Chem. Phys., **56,** 3100 (1972)

[14] SZABÓ, Z., KONKOLY THEGE, I.: Magy. Kém. Folyóirat, **80,** 317 (1974)
SZABÓ, Z. G., KONKOLY THEGE, I.: Acta Chim., (Budapest) **86,** 127 (1975)
[15] SUTTON, L. E.: Tables of Interatomic Distances. Special Publ. No. 11, The Chemical Society, London 1958.
[16] SUTTON, L. E.: Tables of Interatomic Distances. Supplement 1956—1959. Special Publ. No. 18, The Chemical Society, London 1965.
[17] HERZBERG, G.: Spectra of Diatomic Molecules. Second Edition, Van Nostrand Co., New York 1950.
[18] HERZBERG, G.: Infrared and Raman Spectra of Polyatomic Molecules. Van Nostrand Co., New York 1949.
[19] BARTELL, L. S., KUTCHITSU, K., DE NENI, R. J.: J. Chem. Phys., **35,** 1211 (1961)
[20] BARTELL, L. S., HIGGINBOTHAM, H. K.: J. Chem. Phys., **42,** 851 (1965)
[21] LIDE, Jr. D. R., CHRISTENSEN, D.: J. Chem. Phys., **35,** 1374 (1961)
[22] FAST, H., WELSH, H. L.: J. Mol. Spectroscopy, **41,** 203 (1972)
[23] KUTCHITSU, K.: J. Chem. Phys., **49,** 4456 (1968)
[24] HAUGEN, W., TRAETTEBERG, M.: Acta Chem. Scand., **20,** 1726 (1966)
[25] BARTELL, L. S., ROTH, E. A., HOLLOWELL, C. D., KUTCHITSU, K., YOUNG, Jr. J. E.: J. Chem. Phys., **42,** 2683 (1965)
[26] GLOCKLER, G.: J. Chem. Phys., **19,** 124 (1951)
[27] EGGER, K. W., COCKS, A. T.: Helvetica Chim. Acta, **56,** 1516 (1973)
[28] BENSON, S. W., O'NEAL, H. E.: Kinetic Data on Gas Phase Unimolecular Reactions. NSRDS-NBS 21, 1970.
[29] BENSON, S. W.: Thermochemical Kinetics. John Wiley and Sons, New York 1968.
[30] KERR, J. A.: Chem. Revs., **66,** 465 (1966).
[31] COX, J. D., PILCHER, G.: Thermochemistry of Organic and Organometallic Compounds. Adademic Press, New York, 1970.
[32] STULL, D. R., WESTRUM, Jr. E. F., SINKE, G. C.: The Chemical Thermodynamics of Organic Compounds, John Wiley and Sons, New York 1969.
[33] LANDOLT-BÖRNSTEIN: Kalorische Zustandsgrössen, Springer-Verlag, Berlin 1961.
[34] SHIMANOUCHI, T.: Tables of Molecular Vibrational Frequencies. Consolidated Volume I. NSRDS-NBS 39, 1972.
[35] FARRAR, J. M., LEE, Y. T.: J. Chem. Phys., **56,** 5801 (1972)
CHEN, C. H., SISKA, P. E., LEE, Y. T.: J. Chem. Phys., **59,** 601 (1973)
FARRAR, J. M., LEE, Y. T., GOLDMAN, V. V., KLEIN, M. L.: Chem. Phys. Lett., **19,** 359 (1973)
NG, C. Y., LEE, Y. T., BARKER, J. A.: J. Chem. Phys., **61,** 1996 (1974)
PARSON, J. M., SISKA, P. E., LEE, Y. T.: J. Chem. Phys., **56,** 1511 (1972)
BARKER, J. A., WATTS, R. O., LEE, J. K., SCHAFER, T. P., LEE, Y. T.: J. Chem. Phys., **61,** 3081 (1974)

Tibor BÉRCES, H—6701 Szeged, Pf. 105.

Acta Chimica Academiae Scientiarum Hungaricae, Tomus 92 (1), pp. 49—55 (1977)

SPECTRAL AND MAGNETIC STUDIES ON COPPER (II) COMPLEXES OF INDAZOLES

S. A. A. ZAIDI, A. S. FAROOQI and NEELAM SINGHAL

(Department of Cemistry, Aligarh Muslim University, Aligarh 202001, INDIA)

Received April 29, 1976

A number of complexes of general formula Cu $L_m X_2$ have been prepared. In this formula L stands for indazole, 5-nitroindazole or 5-aminoindazole, and X for Cl^-, Br^-, NO_3^-, 1/2 SO_4^{2-} and CH_3COO^-. The value of *m* varies from 1—4. An inner indazolate complex of copper (II) has also been prepared. The complexes have been characterized by chemical analyses, infrared and electronic spectral studies and magnetic measurements. In most of the complexes the metal ion is in a tetragonally distorted octahedral environment.

Introduction

Indazole and its derivatives have long been known to be corrosion inhibitors for copper [1,2]. The chemistry of indazole which is an isomer of the biologically important molecule benzimidazole [3] could have a vast potential in the field of bioinorganics. The co-ordination chemistry of indazole, has virtually remained unexplored excepting for two sketchy reports of complex forming ability of indazole with Co(II) [4] and Cu(II) [1]. However, only one complex of indazole *viz.* bis (indazole) copper(II) chloride has been studied in some detail, but even in this work no infrared studies have been made [5]. Recently the results of studies on the complexes of 5-aminoindazole with a few transition metals have been reported from this laboratory [6, 7]. It was considered worth-while to undertake a systematic study of the co-ordination chemistry of indazole and its derivatives. As a part of this programme, the preparation and physicochemical studies of Cu(II) complexes of indazole, 5-nitroindazole and 5-aminoindazole (below) are being reported here.

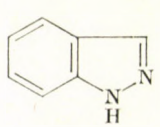

Indazole

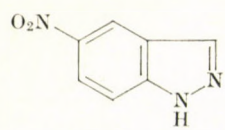

5-nitroindazole

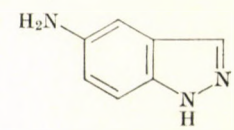

5-aminoindazole

Experimental

Starting materials: Indazole, 5-nitroindazole and 5-aminoindazole (Koch-Light) m.p. 146 °C, 205 °C and 175 °C, respectively were recrystallized from methanol. All the copper salts were B.D.H. (A.R. quality) reagents. Nitromethane (Eastman Kodak) and DMSO (Koch-Light) were used as such.

Physical measurements and analyses

Diffuse reflectance spectra were recorded on a Carl Zeiss VSU—2—P spectrophotometer. Elemental analyses were done by the microanalytical techniques. The estimation of halogen and sulphur were done gravimetrically and that of copper by complexometric titration [8]. Conductivity measurements were performed on a systronix 321 bridge at 30 °C. The IR spectra in KBr disks (4000—650 cm^{-1}) and far IR spectra in nujol mull (650—250 cm^{-1}) were recorded on a Perkin-Elmer 521 spectrophotometer. Magnetic measurements were done on a Gouy balance at 27 °C.

Preparation of complexes: ligands and copper salts were allowed to react in suitable ratios in either ethanol or water. The complexes formed were filtered off, washed with water, ethanol and ether and dried in vacuo. Most of the indazole complexes were recrystallized in organic solvents.

Results and discussion

The analytical results of all the complexes (Table I) are in good agreement with the expected values. Their apparent magnetic moments (Table II) are characteristic of one unpaired electron. The molar conductance values of the complexes indicate them to be non-electrolytes (Table II). In DMSO medium, however, a few complexes seem to be dissociated. This may be due to partial substitution of anions by the solvent molecules, as has been found in the case of l-benzyl-2-phenyl benzimidazole complexes [9].

Nature of bonding from IR data. While the nitrato bands in $Cu(Inz)_2(NO_3)_2$ and $Cu(5\text{-}NInz)_2(NO_3)_2$ occur at 1581 $cm^{-1}(\nu_1)$ and 1271 $cm^{-1}(\nu_1)$, and 1529 $cm^{-1}(\nu_4)$ and 1292 $cm^{-1}(\nu_1)$, respectively suggesting bidentate co-ordination [9, 10] the bands at 1511 $cm^{-1}(\nu_4)$ and 1315 $cm^{-1}(\nu_1)$ in Cu (5-AInz) $(NO_3)_2$ are attributed to a monodentate co-ordination of nitrato group [10].

Though it is difficult to distinguish a unidentate acetato group from an asymmetric bidentate one depending on their O — C — O frequencies, the bands in Cu(5-NInz) $(CH_3COO)_2$ observed at 1570 cm^{-1} (ν_{as}) and 1415 cm^{-1} (ν_s) and in Cu(5-AInz) $(CH_3COO)_2$ at 1568 $cm^{-1}(\nu_{as})$ and 1413 cm^{-1} (ν_s) have been assigned to a unidentate acetate group [9, 11].

The sulphato bands are observed at 1244, 1100 and 1000 cm^{-1} (ν_3) and 950 cm^{-1} (ν_1) for indazole complex, at 1244, 1080 and 980 cm^{-1} (ν_3) and 940 cm^{-1} (ν_1) for 5-nitroindazole complex and at 1164, 1102 and 1056 cm^{-1} (ν_3) and 998 cm^{-1} (ν_1) for 5-aminoindazole complex [9, 12]. Though the sulphato bands have been assigned and suggested to be bidentate bridging, this assignment is only tentative due to the fact that the ligand bands also overlap with some of these bands.

A strong band at 1507 cm^{-1} in Inz, at 1499 cm^{-1} in 5-NInz and at 1516 cm^{-1} in 5—AInz has been assigned to C = N stretching frequency. This assignment seems to be reasonable as the C = N band in the closely related benzimidazoles also has been reported in this region [13, 14]. Even

Table I

Analytical data and other physical properties of copper(II) indazole complexes

Complex	Colour	M. P. (°C)	% Cu Calc. (obs.)	% N Calc. (obs.)	% C Calc. (obs.)	% H Calc. (obs.)	% Anion Calc. (obs.)
$Cu(Inz)_2Cl_2$	Light green	230	17.14 (17.21)	15.10 (15.11)	45.31 (45.40)	3.24 (3.27)	19.15 (19.10)
$Cu(Inz)_2Br_2$	Yellowish brown	292	13.81 (13.82)	11.90 (11.93)	36.52 (36.51)	2.55 (2.58)	34.77 (34.73)
$Cu(Inz)_4Br_2$	Bright green	195	9.13 (9.08)	16.10 (16.10)	48.28 (48.20)	3.45 (3.45)	22.99 (22.97)
$Cu(Inz)_2(NO_3)_2$	Deep green	196	15.01 (15.00)	19.86* (19.89)	39.66 (39.67)	2.83 (2.82)	— —
$Cu(Inz)_2SO_4$	Blue	276	16.06 (16.08)	14.16 (14.20)	42.45 (42.47)	3.03 (3.04)	8.09 (8.11)
$Cu(Inz)_2$	Deep green	216	21.32 (21.60)	18.79 (18.72)	56.37 (56.41)	3.36 (3.39)	— —
$Cu(5\text{-}NInz)_2Cl_2$	Yellow	272	13.78 (13.79)	18.23 (18.30)	36.44 (36.42)	2.17 (2.25)	15.40 (15.35)
$Cu(5\text{-}NInz)_2Br_2$	Yellowish brown	276	11.55 (11.61)	15.27 (15.28)	30.54 (30.60)	1.82 (1.89)	29.09 (29.10)
$Cu(5\text{-}NInz)_2(NO_3)_2$	Bright green	200[d]	12.37 (12.40)	21.80* (21.78)	32.76 (32.72)	1.95 (1.88)	— —
$Cu(5\text{-}NInz)_2SO_4$	Bright green	294	13.08 (13.12)	17.29 (17.19)	34.57 (34.28)	2.06 (2.12)	6.44** (6.43)
$Cu(5\text{-}Ninz)\ (CH_3COO)_2$	Deep green	265[d]	18.44 (18.48)	12.18 (12.21)	38.29 (38.30)	3.19 (3.21)	— —
$Cu(5\text{-}AInz)_2Br_2$	Deep brown	208	12.97 (12.99)	17.14 (17.23)	34.29 (34.18)	2.89 (2.98)	32.65 (32.63)
$Cu(5\text{-}AInz)\ (NO_3)_2$	Blackish brown	300	19.80 (19.83)	21.81* (21.82)	26.17 (26.21)	2.18 (2.31)	— —
$Cu(5\text{-}AInz)\ SO_4$	Deep brown	300	21.70 (21.65)	14.35 (14.41)	28.70 (28.61)	2.39 (2.50)	10.93** (10.86)
$Cu(5\text{-}AInz(\ (CH_3COO)_2$	Brownish black	300	20.13 (20.30)	13.33 (13 28)	41.91 (42.00)	4.13 (4.13)	— —

* Total nitrogen including that of NO_3^- groups; d = decomposition
** Refers to % sulphur

Table II

Molar conductance, magnetic moment and electronic spectra (cm^{-1}) of the copper(II) complexes of indazoles

Complex	Molar conductance of 0.001 M solution, (ohm^{-1} cm^2 $mole^{-1}$		Magnetic moment (μ_{eff})	Electronic spectra cm^{-1}
	Nitromethane	DMSO	B. M.	
Inz				23,810 : 29,000
$Cu(Inz)_2Cl_2$	27.4	28.5	2.02	13,510
$Cu(Inz)_2Br_2$	21.2	60.4	1.94	13,860
$Cu(Inz)_4Br_2$	25.7	44.6	1.97	14,930
$Cu(Inz)_2(NO_3)_2$	30.8	63.0	1.88	14,800
$Cu(Inz)_2SO_4$	—	8.1	1.88	14,925
$Cu(Inz)_2$	—	2.0	1.98	16,950
5-NInz				29,000
$Cu(5\text{-}NInz)_2Cl_2$	—	54.2	1.84	13,330
$Cu(5\text{-}NInz)_2Br_2$	—	47.3	1.73	14,000
$Cu(5\text{-}NInz)_2(NO_3)_2$	—	65.6	1.82	14,100
$Cu(5\text{-}NInz)_2SO_4$	—	7.8	1.60	12,500
$Cu(5\text{-}NInz)\ (CH_3COO)_2$	—	0.9	1.83	16,670
5-A-Inz				29,850
$Cu(5\text{-}AInz)_2Br_2$	—	—	1.79	21,000
$Cu(5\text{-}AInz)\ (NO_3)_2$	—	62.7	1.73	22,000
$Cu(5\text{-}AInz)SO_4$	—	17.0	1.76	21,000
$Cu(5\text{-}AInz)\ (CH_3COO)_2$	—	—	1.67	20,000

— = Insoluble

though after complexation there is a very small decrease in this freqeuency (Table III), co-ordination is suggested through the pyridyl nitrogen. In pyrazole complexes also co-ordination through the pyridyl nitrogen has been suggested even though C = N bands have not been assigned [15, 16].

A comparison of the N—H stretching frequency of the ligands indazole, 5-aminoindazole and 5-nitroindazole with that of their complexes shows a decrease in this frequency (Table III). This has been attributed to the involvement of the pyrrole nitrogen in hydrogen bonding with the anions. The N—H stretching frequency increase with decreasing possibility of hydrogen bonding upon proceeding from the more electronegative anion to the less electronegative anions.

$$Cl^- < Br^- < NO_3^-$$

A similar pattern of hydrogen bonding has also been found in the complexes of pyrazoles [17]. However, in the case of sulphato and acetato complexes and all 5-AInz complexes the position of N–H stretching frequency cannot be unambiguously related to the anion effect as in some of these cases either the pyrrole or more likely the amino nitrogen is also involved in co-ordination. The nitro bands appearing at 1535 cm^{-1} and 1341 cn^{-1} in 5-NInz do not show any notable shift in the complexes suggesting their non-involvement in the co-ordination as has been noted in Cu(II) complexes of nitropyrazole [16].

The reaction of an aqueous solution of copper acetate (pH = 4) with indazole solution at room temperature, yielded an inner complex having anionic ligand. The IR spectrum of the complex did not show any N—H or acetato bands.

The far IR spectra of all the complexes compared with that of the free ligand (Table III) reveal only one strong band in the 570—482 cm^{-1} range which is tentatively assigned to Cu—N absorptions.

Table III

N—H, C=N and Cu—N stretching frequencies in indazoles and their complexes

Compound	N—H	C=N	Cu—N
Inz	3450^{*}_{s}	1507_{s}	—
$Cu(Inz)_2Cl_2$	3305_{s}	1497_{s}	530_{m}
$Cu(Int)_2Br_2$	3340_{s}	1498_{s}	535_{m}
$Cu(Inz)_4Br_2$	3205_{s}	1499_{s}	532_{m}
$Cu(Inz)_2(NO_3)_2$	$3220_{s,b}$	1505_{s}	539_{m}
$Cu(Inz)_2SO_4$	$3210_{s,b}$	1500_{s}	531_{m}
$Cu(Inz)_2$	—	1493_{m}	548_{sh}
5-NInz	3450^{*}_{m}	1499_{s}	—
$Cu(5\text{-}NInz)_2Cl_2$	3367_{s}	1496_{sh}	482_{s}
$Cu(5\text{-}NInz)_2Br_2$	3401_{s}	1498_{sh}	453_{s}
$Cu(5\text{-}NInz)_2(NO_3)_2$	$3328_{s,b}$	1498_{s}	454_{s}
$Cu(5\text{-}NInz)_2SO_4$	$3334_{s,b}$	1500_{s}	$490_{s,b}$
$Cu(5\text{-}NInz)(CH_3COO)_2$	3340_{s}	1506_{s}	$492_{s,b}$
5-AInz	3350_{m}	1516_{s}	—
	$3200_{s,b}$		
$Cu(5\text{-}AInz)_2Br_2$	3289_{s}	1515_{m}	520_{m}
$Cu(5\text{-}AInz)(NO_3)_2$	3300_{s}	1515_{m}	$570_{m,b}$
$Cu(5\text{-}AInz)SO_4$	$3320_{s,b}$	1514_{m}	560_{m}
$Cu(5\text{-}AInz)(CH_3COO)_2$	$3328_{s,b}$	1512_{m}	$562_{s,b}$

* in $CHCl_3$ s = strong, m = medium, w = weak, b = broad, sh = shoulder.

Electronic spectra and the structure: — To obtain further information regarding the geometry of the complexes ligand-field spectra were recorded. Most of the complexes show a strong band attributable to $^2E_g \leftarrow {}^2T_{2g}$ transition (Table III) indicating an octahedral environment for the Cu(II) ion. This octahedron must be distorted. It is proposed that four of the co-ordination sites required for an octahedral geometry of copper are provided by the two bridging anions and the remaining two by the indazoles presumably in transposition to each other. LAWSON [5] has proposed such a polymeric structure for $Cu(Inz)_2Cl_2$.

All of the complexes excepting the $Cu(Inz)_4Br_2$ and $Cu(5\text{-}AInz)_2Br$ appear to be polymeric. In general the polymerization is presumably through anion bridges but in a few cases where the indazoles behave as bidentate ligands the ligand bridging seems to be more likely. In the case of dibromotetrakis(indazole)copper(II) the four indazole molecules should be in the xy plane and the bromides on the z axis. A similar structure for dibromotetrakis-(benzimidazole)copper(II) has also been reported [18].

The octahedral geometry of the sulphato complexes of Inz and 5-NInz requires bidentate ligand co-ordination and a dimeric complex having anion bridges.

All the 5-AInz complexes are four co-ordinated but it is difficult to assign a geometry to these complexes. Its bromo-complexes appear to be monomeric while the nitrato-, sulphato- and the acetato-complexes are dimeric having ligand bridges. The corresponding acetato complex of benzimidazole [18] has also been shown to be dimeric in nature.

The polymeric 'inner complex' bis(indazolato) copper(II) is suggested to have an octahedral geometry with considerable distortion. The lower μ_{eff} values indicate some antiferromagnetic interaction.

*

Professor W. RAHMÅN is thanked for providing facilities. A.S.F. and N.S. thank the C.S.I.R. (New Delhi) for a senior and junior fellowship, respectively.

REFERENCES

[1] COTTON, J. B.: Int. Congr. Metal Corrosion, 2nd Ed. 590 New York (1966) p.
[2] COTTON, J. B., SHOOLS, I. R.: Br. Corros. Ji., **2,** 1 (1967)
[3] ROBINSON, F. A.: The Vitamin B Complex, Chapman and Hall Ltd. London p. 533 (1951)
[4] CAMBI, L., CANONICA, L.: At. Accad. naz. Lincei Re. **20,** 17 (1956)
[5] LAWSON, M. B.: Diss. Abst. Int. B., **32,** 143 (1971)
[6] ZAIDI, S. A. A., FAROOQI, A. S.: J. Inorg. Nucl. Chem., **35,** 4320 (1973)
[7] ZAIDI, S. A. A., FAROOQI, A. S., VARSHNEY, D. K.: J. Inorg. Nucl. Chem., (in press).
[8] REILLEY, C. N., SCHMID, R. W., SADAK, F. A.: Chem. Edn., **36,** 555 (1959)
[9] BOSE, K. S., PATEL, C. C.: J. Inorg. Nucl. Chem., **32,** 1141 (1970)
[10] FIELD, B. O., HARDY, C. J.: Quart. Rev. (London), **18,** 361 (1964)
[11] CURTIS, N. F.: J. Chem. Soc., A, 1579 (1968)

[12] NAKAMOTO, K.: Infrared Spectra of Inorganic Coordination Compounds, London p. 161 (1963)
[13] GHOSH, S. P., MISRA, L. K.: J. Indian Chem. Soc., **47**, 1154 (1970)
[14] ELDER, M. S., NELSON, G. A., BUSCH, D. H.: Inorg. Chem., **5**, 74 (1966)
[15] REEDIJK, J.: Rec. Trav. Chim., **88.** 1451 (1969)
[16] REEDIJK, J., WINDHORST, J. C. A., VAN HAM, N. H. M., GROENEVELD, W. A.: Rec. Trav. Chim., **111**, 234 (1971)
[17] REEDIJK, J.: Rec. Trav. Chim., **90**, 117 (1971)
[18] GOODGAME, M., HAINES, L. I. B.: J. Chem. Soc., A, **174** (1966)

S. A. A. ZAIDI
A. S. FAROOQI
NEELAM SINGHAL
Aligarh Muslim University, Aligarh—202001, India.

Acta Chimica Academiae Scientiarum Hungaricae, Tomus 92 (1), pp. 57–64 (1977)

IONIZATION OF INORGANIC ACID ANHYDRIDES AND ACID HALIDES IN CHLOROSULPHURIC ACID

FORMATION OF OXYCATIONS

S. A. A. ZAIDI and Z. A. SIDDIQI

(Department of Cchemistry, Aligarh Muslim University, Aligarh)

Received, August 23, 1975

In revised form May 12, 1976

Electrical conductivities of solutions of the oxides of As, Sb, Bi, P, V, Se and Te and of the oxyhalides of Sb, Bi, P and V in chlorosulphuric acid have been measured with a view, investigating their modes of ionization involving possible formation of oxycations. The trioxides of arsenic, antimony and bismuth, the oxychloride of antimony and the oxyhalides of bismuth form the oxychlorosulphates. It appears that at low concentrations antimony and bismuth oxychlorosulphates partly ionize yielding respectively the hithertofore elusive cations SbO^+ and BiO^+. The dissociation constant of these oxychlorosulphates has been calculated.

Phosphorous pentoxide forms protonated phosphoric acid whereas phosphoryl chloride is incompletely protonated.

Vanadium pentoxide and vanadyl chloride behave as weak electrolytes and presumably form $H[VO(SO_3Cl)_4]$. The dioxide of Se and Te are simply protonated, the latter being more basic.

Introduction

The formation of the oxycations of nitrogen *viz;* NO^+ and NO_2^+ in sulphuric, fluorosulphuric and disulphuric acids by the ionization of the anhydrides of the respective oxyacids of nitrogen, N_2O_3 and N_2O_5 is well known [1—3]. Similar attempts to prepare in strong acidic media, the oxycations of other elements of groups V and VI have been successful only in the case of As_2O_3 in H_2SO_4 [4]. Although chlorosulphuric acid is a stronger acid than sulphuric acid no such study has so far been reported in this solvent. It was therefore considered worth-while to study the behaviour of the oxides of As, Sb, Bi, P, V, Se, and Te in chlorosulphuric acid with a view to exploring the possibility of the formation and stabilization of the oxycation of these elements. As another possible new route to the formation of such oxycations appeared to be the direct ionization of the oxyhalides, the behaviour of the oxyhalides of Sb, Bi, P and V in HSO_3Cl has also been examined.

Experimental

Reagent grade chlorosulphuric acid (B.D.H.England) was used. Arsenic trioxide, bismuth trioxide, antimony trioxide, vanadium pentoxide, phsophorus pentoxide and niobium pentoxide were commercially pure samples and were used after drying in an oven at 100 °C. Phosphoryl chloride was redistilled and the fraction distilling at 108 °C was used. Bismuth oxychloride, bismuth oxybromide, bismuth oxyiodide, antimony pentoxide, tellurium dioxide and vanadyl chloride were prepared and purified by standard methods [5]. The design of the conductivity cell used has been described elsewhere [6]. The infrared spectra of solutions in HSO_3Cl were recorded at room temperature on a Perkin Elmer 337 spectrophotometer by using envelope cell made of thin polyethylene sheets.

Meaning and significance of the symbols γ and ω

Chlorosulphuric acid undergoes self-ionization by the formation of chlorosulphuric acidium ($H_2SO_3Cl^+$) and the chlorosulphate (SO_3Cl^-) ions;

$$2HSO_3Cl \rightleftharpoons H_2SO_3Cl^+ + SO_3Cl^-$$

According to solvosystem definition of acids and bases all the substances that either generate or increase the concentration of $H_2SO_3Cl^+$ ion are acids and those that generate or increase the concentration of SO_3Cl^- ion are bases in chlorosulphuric acid solvent system. It has been established [7] that in HSO_3Cl solutions all other ions which conduct by diffusion mechanism are unable to compete with ions of solvent self-dissociation and almost all the current is carried by SO_3Cl^-, or $H_2SO_3Cl^+$ ions which conduct by a Grothus type proton-jump mechanism.

The symbol γ is defined as the number of moles of SO_3Cl^-, (or $H_2SO_3Cl^+$) produced by each mole of solute in HSO_3Cl. Its value can be readily determined from conductometric measurements. Since it is known that KCl being a strong electrolyte is fully ionized in HSO_3Cl [7] producing one mole of SO_3Cl^- per mole of the solute *i.e.* having $\gamma = 1$ according to the reaction given below,

$$KCl + HSO_3Cl \rightarrow K^+ + SO_3Cl^- + HCl \uparrow$$

the γ value of a base is determined from the specific conductance concentration curves by comparing the concentration of the base with the concentration of KCl giving the same specific conductance.

For the usual molal and molar concentration units it is assumed that the solutes do not undergo any chemical change in the solvent. In strong acidic solvents when a solute is dissolved it undergoes some chemical reaction with the solvent hence these two units can not be adopted for precise studies. Furthermore, because of the reaction of the solvent with solutes, some fraction of the solvent is consumed and hence true weight or volume of the solvent can

not be estimated after each addition of the solute. The most convenient unit therefore is the molon (ω) first introduced by GILLESPIE [8, 9] and defined as moles of the solute per kg of the solution. It can be seen that the molon unit is approximately the same but a refinement over the molal unit and hence is widely used in dealing with equilibria in strong acid solvent systems.

Discussion

Arsenic trioxide was extensively soluble in HSO_3Cl yielding a very low conducting solution (Fig. 1) having a γ value of 0.05. Its mode of ionization could be represented by either Eq. (1) or (2) given below:

$$As_2O_3 + 9HSO_3Cl = 2As(SO_3Cl)_3 + 3H_2SO_4 + 3HCl \uparrow \quad (1)$$

$$As_2O_3 + 3HSO_3Cl = 2AsO \cdot SO_3Cl + H_2SO_4 + HCl \uparrow \quad (2)$$

The species $As(SO_3Cl)_3$ if formed should behave as a weak acid of chlorosulphuric acid solvent system by consuming a chlorosulphate ion according to Eq. (3)

$$As(SO_3Cl)_3 + SO_3Cl^- = As(SO_3Cl)_4^- \quad (3)$$

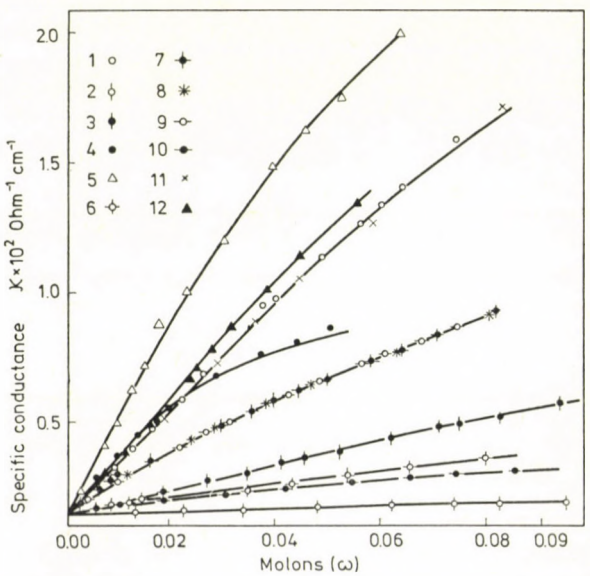

Fig. 1. Specific conductance concentration curve of the compounds in chlorosulphuric acid at 35 °C. 1. Potassium chloride; 2. arsenic trioxide; 3. antimony trioxide; 4. bismuth trioxide; 5. phosphorus pentoxide; 6. antimony oxychloride; 7. bismuth oxychloride; 8. bismuth oxybromide; 9. bismuth oxyiodide; 10. phosphoryl chloride; 11. selenium dioxide; 12. tellurium dioxide.

causing a decrease in the conductance of the solution with the passage of time. As there is no such decrease in conductance, ionization of As_2O_3 according to Eq. (1) must be ruled out. The low conductance of the solution should be only due to the formation of the very weak bases H_2SO_4 and HCl [7] of chlorosulphuric acid solvent system. The low conductance further suggests that $AsO \cdot SO_3Cl$ formed does not ionize appreciably to produce the cation AsO^+.

There is some evidence for the formation of the hithertofore elusive oxycations SbO^+ and BiO^+ on dissolving Sb_2O_3 and Bi_2O_3, respectively, in HSO_3Cl. Antimony trioxide was fairly soluble in HSO_3Cl and gave solutions having stable conductivities for about 24 hours. The following mode of ionization is suggested for its reaction:

$$Sb_2O_3 + 3HSO_3Cl \rightleftharpoons 2SbO \cdot SO_3Cl + H_2SO_4 + HCl \uparrow$$
$$2SbO \cdot SO_3Cl \rightleftharpoons 2SbO^+ + 2SO_3Cl^- \qquad (4)$$

Table I

The average value of γ and K_b for the compounds in HSO_3Cl at 35°C

Compound	γ	$K_b \times 10^3$ mole kg^{-1}
Arsenic trioxide	0.05	—
Antimony trioxide	0.25	1.56
Antimony oxychloride	0.18	1.40
Bismuth trioxide	0.90	19.43
Bismuth oxychloride	0.61	22.84
Bismuth oxybromide	0.57	22.82
Bismuth oxyiodide	0.58	22.77
Phosphorus pentoxide	2.00	—
Selenium dioxide	1.00	—
Tellurium dioxide	1.10	—
Phosphoryl chloride	0.15	0.81

The observed lower value of γ (Table I) from that expected by ionization according to Eq. (4) *i. e.* $\gamma = 2.00$, suggests that $SbO \cdot SO_3Cl$, formed in the first step of the reaction, is only partly ionized to produce the SbO^+ cation. A decrease in the γ value from 0.26 to 0.22 with the increasing concentrations of Sb_2O_3 was observed which may presumably be due to the polymerization of the unionized oxychlorosulphates. The dissociation constant (K_b) of $SbO \cdot SO_3Cl$ could be evaluated from the observed γ value by the use of the relationship given below:

$$K_b = \frac{[SbO^+]\,[SO_3Cl^-]}{[SbO \cdot SO_3Cl]} \text{ or } \frac{[SO_3Cl^-]\,\gamma}{(2-\gamma)} \qquad (5)$$

the average value of K_b obtained within the concentration range studied has been shown in Table I.

Bismuth trioxide also gave stable and highly conducting solution ($\gamma = 0.90$) in HSO_3Cl. Its ionization may also be represented according to Eq. (4):

$$Bi_2O_3 + 3HSO_3Cl = 2BiO \cdot SO_3Cl + H_2SO_4 + HCl \uparrow$$
$$2BiO \cdot SO_3Cl = 2BiO^+ + 2SO_3Cl^- \quad (6)$$

A decrease in the γ value from 1.30 to 0.70 with increasing concentration of the solute has been observed. At concentrations above 0.02 molons the appearance of a solid was also observed which was separated but could not be characterized as it could not be isolated free from the acid. These observations suggest that at low concentrations (below 0.02 molons) there is apparently the ionization of $BiO \cdot SO_3Cl$ to give the cationic species BiO^+. The average value of the dissociation constant of $BiO \cdot SO_3Cl$ (Table) has been evaluated using Eq. (5). However, at concentrations above 0.02 molons, this species polymerizes to give probably a long chain polymer $(BiO \cdot SO_3Cl)_n$ which is insoluble in HSO_3Cl and separates out of the solution.

Antimony oxychloride and bismuth oxyhalides were soluble and gave solutions having stable conductances. The mode of ionization of these compounds in HSO_3Cl may be given in the following:

$$SbOCl + HSO_3Cl = SbO \cdot SO_3Cl + HCl \uparrow$$
$$SbO \cdot SO_3Cl = SbO^+ + SO_3Cl^- \quad (7$$

$$BiOX + HSO_3Cl = BiO \cdot SO_3Cl + HX \uparrow$$
$$BiO \cdot SO_3Cl = BiO^+ + SO_3Cl^-$$
$$X = Cl, Br, I \quad (8)$$

where the oxychlorosulphates formed in the first step of the reaction undergo incomplete ionization ($\gamma < 1.00$) to produce the oxycations similar to those observed for their trioxides. The decrease in the γ value with the increasing concentrations of the solutes in these cases also is attributed to the polymerization of the unionized oxychlorosulphates. At higher concentrations solids were separated out of the solutions but could not be characterized. The dissociation constant (K_b) of the oxychlorosulphates of Sb and Bi produced according to Eqs (7) and (8) have been evaluated from the relation.

$$K_b = \frac{[SO_3Cl^-]\gamma}{(1-\gamma)} \quad (9)$$

The magnitude of the K_b values obtained from both, the ionization of oxyhalides and the corresponding trioxides are quite comparable (Table I), and support their suggested mode of ionization.

Due to strong background absorption of the acid and polyethylene in the 1500—1000 cm^{-1} region where BiO^+ and SbO^+ cations are also expected to absorb, it was not possible to obtain IR evidence of the existence of these ions in solutions of Sb_2O_3, Bi_2O_3 SbOCl and BiOX in HSO_3Cl. The IR spectra of such solutions recorded in the region 3000—1000 cm^{-1} did not show any other band.

Arsenic pentoxide and antimony pentoxide which were also considered to produce AsO_2^+ and SbO_2^+ ions in HSO_3Cl, however, remained insoluble indicating no interaction with the acid.

Phosphorus pentoxide gave highly conducting solutions (Figure 1) in chlorosulphuric acid with the evolution of hydrogen chloride gas. The ionization of phosphorus pentoxide is represented by Eq. (10) as given below:

$$P_2O_5 + 11HSO_3Cl = 2H_4PO_4^+ + 4S_2O_5Cl_2 + H_2SO_4 + 2SO_3Cl^- + HCl \uparrow \quad (10)$$

Recently ^{31}P n.m.r. studies[10] on concentrated solution of P_2O_5 in HSO_3Cl have revealed that the solution contains protonated phosphoric and trimetaphosphoric acids. At higher concentrations presumably the protonated phosphoric acid formed in Eq. (10) is condensed to give higher acids.

Phosphoryl chloride which is a non-electrolyte in H_2SO_4[4] gave conducting solutions in HSO_3Cl. It is reasonable to suggest that there is simple partial protonation at oxygen atom to give the conjugate acid HO^+PCl_3 according to the following reaction:

$$O = PCl_3 + HSO_3Cl \rightleftharpoons HO^+ = PCl_3 + SO_3Cl^- \quad (11)$$

The dissociation constant (K_b) of the conjugate acid was obtained by using the expression,

$$K_b = \frac{[HO^+PCl_3]\,[SO_3Cl^-]}{[POCl_3]} = \frac{\alpha^2 \cdot \omega}{(1-\alpha)} \quad (12)$$

where ω and α are the concentration and the degree of ionization of the base, respectively. The latter can be found by comparing the concentrations of the base with that of KCl (reference electrolyte) that give the same specific conductivity. The average value of K_b obtained within the concentration range is shown in Table I.

Vanadium pentoxide was found to have a limited solubility in HSO_3Cl and a solution of up to 0.03 molon concentration only could be obtained. It gave a brown-red coloured solution with evolution of hydrogen chloride

gas and produced a very small change in the conductance of the solvent unlike its behaviour in sulphuric acid where it gave highly conducting solutions [11, 12]. Vanadyl chloride also gave brown-red coloured solutions with no appreciable change in the conductance of solvent. The following solvolytic reactions are suggested:

$$V_2O_5 + 11\ HSO_3Cl = 2\ H\ [VO\ (SO_3Cl)_4] + 3\ H_2SO_4 + 3\ HCl\ \uparrow \qquad (13)$$

$$VOCl_3 + 4\ HSO_3Cl = H\ [VO\ (SO_3Cl)_4] + 3\ HCl\ \uparrow \qquad (14)$$

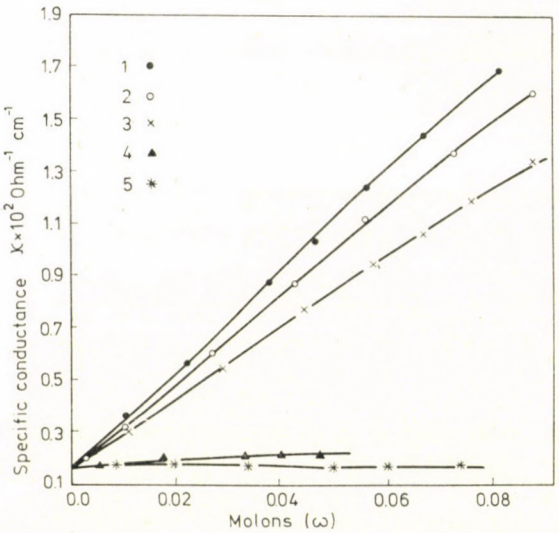

Fig. 2. Specific conductance concentration curve of the compounds in chlorosulphuric acid at 35 °C. 1. Potassium chloride; 2. potassium chloride in 0.01 ω vanadium pentoxide; 3. potassium chloride in 0.17 ω vanadyl chloride; 4. vanadium pentoxide; 5. vanadyl chloride.

The solvolysed species H $[VO\ (SO_3Cl)_4]$ was found to behave as a weak acid of the chlorosulphuric acid solvent system. This has been shown by the specific conductance concentration curves (Fig. 2) of a known base KCl in (a) neat HSO_3Cl and (b) in a solution of V_2O_5 and in $VOCl_3$ in HSO_3Cl containing the species H $[VO\ (SO_3Cl)_4]$. The curve obtained from the solution (b) was found to be point by point lowered from that of (a). To check whether this behaviour is due the non-electrolytic nature of the solute or is it really due to its acidic nature, in another experiment KCl was added to the solution of a non-electrolyte *viz.* $SOCl_2$ in HSO_3Cl. In this case no change in the slope of the curve was observed supporting the above proposed behaviour of the solvolysed species H $[VO\ (SO_3Cl)_4]$.

Niobium pentoxide remained insoluble in HSO_3Cl without producing any change in the conductance of the solvent suggesting no interaction whatsoever.

Both selenium dioxide and tellurium dioxide are extensively soluble in HSO_3Cl yielding highly conducting solutions. The average values of γ are 1.00 and 1.10, respectively, which suggest a complete monoprotonation of SeO_2 and a partial diprotonation of TeO_2 according to the following equations:

$$SeO_2 + HSO_3Cl \rightleftharpoons HO^+ = Se = O + SO_3Cl^- \quad (15)$$

$$TeO_2 + 2HSO_3Cl \rightleftharpoons HO^+ = Te = OH^+ + 2SO_3Cl^- \quad (16)$$

*

Professor W. RAHMAN is thanked for providing all the facilities for this work. One of us (Z.A.S) is grateful to C.S.I.R. New Delhi for financial assistance.

REFERENCES

[1] GILLESPIE, R. J., HUGHES, E. D., INGOLD, C. K.: J. Chem. Soc., **2473,** (1950)
[2] PAUL, R. C., SHARMA, S. K., SHARMA, R. D., PAUL, K. K., MALHOTRA, K. C.: J. Inorg. Nucl. Chem., **33,** 2905 (1971)
[3] PAUL, R. C., KAPILA, V. P., PURI, J. K., MALHOTRA, K. C.: J. Chem. Soc. (A), **2127,** (1971)
[4] GILLESPIE, R. J., ROBINSON, E. A.: Can. J. Chem., **41,** 450 (1963)
[5] GEORGE BRAUER, Handbook of Preparative Inorganic Chemistry V. I. Academic press New York 1963
[6] ZAIDI, S. A. A., SIDDIQI, Z. A.: J. Inorg. Nucl. Chem., **37,** 1806 (1975)
[7] ROBINSON, E. A., CIRUNA, J. A.: Can. J. Chem., **46,** 1719, (1968)
[8] GILLESPIE, R. J., SOLOMONS, C.: J. Chem., Soc., **1796,** (1957)
[9] FLOWERS, R. H., GILLESPIE, R. J., OUBRIDGE, J. V., SOLOMONS, C.: J. Chem., Soc. **667,** (1958)
[10] DILLION, K. B., WADDINGTON, T. C.; J. Chem. Soc. (A), **1146,** (1970)
[11] GILLESPIE, R. J., KAPOOR, R., ROBINSON, E. A.,; Can. J. Chem. **44,** 1203 (1966)
[12] MISHRA, H. C., SYMONS, M. C. R.: J. Chem. Soc., **4411,** (1962)

S. A. A. ZAIDI, Z. A. SIDDIQI } Department of Chemistry Aligarh Muslim University, Aligarh, 202001 India.

Acta Chimica Academiae Scientiarum Hungaricae, Tomus 92 (1), pp. 65–72 (1977)

THE RELATION BETWEEN RESONANCE ENERGY AND MOLECULAR STRUCTURE

I. GUTMAN

(Institute "Rudjer Bošković", Zagreb, Croatia, Yugoslavia)

Received May 31, 1976

The dependence of resonance energy *RE* on the molecular structure is discussed on the basis of the Coulson integral representation of total pi-electron energy (Eq. (7)) and *RE* (Eq. (12)). The integral (12) is solved approximately and a simple topological formula (16) for *RE* is obtained.

Analysis of this formula leads to several general rules relating *RE* to certain structural and combinatorial properties of the molecule.

Resonance energy (*RE*) is one of the central concepts in the theory of conjugated compounds, closely related to the 'evergreen' problem of aromaticity. Although nowadays *RE* is a commonly accepted notion which is treated in any textbook of theoretical organic chemistry, numerous recent investigations [1—4] show that not all aspects of it are completely elucidated. In the present paper the 'classical' resonance energy

$$RE = E - n_{=} E_{=} \tag{1}$$

will be analysed, where E is the total pi-electron energy of the molecule, $E_{=}$ is the pi-electron energy of an isolated ('ethylene-like') double bond and $n_{=}$ is the number of double bonds contained in a KEKULÉ structure of the considered molecule. This definition of resonance energy applies only to conjugated molecules, all pi-electrons of which can be formally considered as belonging to double bonds. Therefore, conjugated radicals, polyradicals and ions are not tractable by this formula, as well as systems with pi-electrons belonging to localized lone pairs. Nevertheless, Eq. (1) is important because it reflects the actual content of *RE*, namely that it measures the energy gain of the delocalization of pi-electrons over the whole conjugated network. (Note that *RE* is often named "delocalization energy".)

In the present paper we shall consider conjugated hydrocarbons only. This is justified because we are mainly interested in the dependence between *RE* and molecular structure, which can be most clearly seen when other disturbing effects (the presence of heteroatoms, substituents etc.) are avoided. However, extension to heteroconjugated systems should be straightforward.

Now, if RE is calculated within the Hückel molecular orbital (HMO) approximation and is expressed in β units, $E_{=} = 2$ and $RE = E - 2n_{=} = E - N = E - N_e$, where N and N_e are the number of carbon atoms and pi-electrons in the conjugated hydrocarbon. Note that $\beta < 0$. Then the relation

$$RE = E - N_e \tag{2}$$

can be used for the calculation of RE's of arbitrary conjugated hydrocarbons.

The concept of RE has been subjected to serious criticism from various viewpoints [5,6]. In particular, there exist numerous examples of molecules having large RE values but being rather unstable (antiaromatic). If RE is understood as a measure of aromaticity of a molecule, almost all conjugated systems are predicted to be of a much higher stability than it is actually the case. The opinion [5] that these violations have their origin in the crudeness of the HMO model, was recently shown [7] to be unjustified. Namely, several quantities [7—9] which can be calculated from HMO total pi-electron energy are demonstrated to be rather good measures for aromaticity (and antiaromaticity). These are also named as different variants of resonance energy, but have nothing common with its classical definition (Eqs (1) and (2)). The discussion about these various resonance energies goes, however, beyond the scope of the present work.

In fact, if RE is defined as in Eqs (1) and (2), it necessarily depends on the structure (topology) of the molecule in a way which cannot be straightforwardly connected with aromaticity. Therefore, it seems to be interesting to investigate the details of this dependence.

The first important contribution along these lines was given by McClelland [2], who has shown that

(a) the RE of a conjugated hydrocarbon is grossly determined by only two topological parameters — the number of carbon atoms N and the number of carbon–carbon bonds M.

However, two-parametric topological expressions for RE are chemically insufficient, since they predict equal RE's for isomers [10]. Independently of McClelland's work, England and Ruedenberg [3] posed the questions

(b) why is RE almost always positive (when expressed in β units), and

(c) why is RE proportional to the size of the molecule (that is to N).

They rationalized (b) and (c) by means of an intuitive, but physically profound argument based on localizability of MO's. Finally, Hall [4] demonstrated that

(d) there exists a simple (linear) correlation between the number of Kekulé structures, K, and RE in benzenoid systems.

In the present work we offer a result which generalizes (*a*)-(*d*). A number of further properties of RE will be also deduced.

Before starting with our analysis, we would like to draw the reader's attention that in spite of the seemingly complicated mathematical formalism which shall be used in the subsequent sections, our final conclusions (*a*)—(*h*) are quite simple and can be straightforwardly "translated" into the common terminology of organic chemistry. In order to avoid any ambiguity, we remember that N_e = number of pi-electrons, N = number of (conjugated) carbon atoms, M = number of carbon–carbon bonds, N_0 = number of non-bonding molecular orbitall and $\tilde{N} = N - N_0$. Practically all conjugates substanced, which are stable in a classical chemical sense, have $N_0 = 0$. Accordingly, systems with $N_0 > 0$ are, in the large majority of cases, very reactive, short living and thermodynamically unstable species, which can be synthetized only under severe conditons. Therefore we suggest the reader, not familiar with details of HMO theory, to assume $N_0 = 0$ an $\tilde{N} = N$ for molecules usually occurring in the chemistry of conjugated compounds and $N_0 = 1$ and $\tilde{N} = N - 1$ for free radicals. Similarly, these readers can identify $|a_{\tilde{N}}|$ with the square of the number of KEKULÉ structures, except in the case of non-benzenoid systems (see (*e*)).

Notations and definitions

The investigation of the dependence of chemical and physical properties of a compound on molecular structure is a fundamental problem in all chemical theories. When this problem is treated within the framework of the HMO model, graph theory [9, 11, 12] proved to be an especially convenient mathematical formalism. Thus, a conjugated molecule is presented [11, 12] by a graph G with N vertices and M edges, the adjacency matrix of which is $\mathbf{A}$. The characteristic polynomial of G is

$$P(G, x) = \det(x\,\mathbf{I} - \mathbf{A}) = \sum_{j=0}^{N} a_j\, x^{N-j}\,. \tag{3}$$

The roots $x_1 \geq x_2 \geq \ldots \geq x_N$ of this polynomial form the spectrum of the graph G. The relation between this spectrum and the HMO energy levels is well known [11—13]. Thus, the total pi-electron energy E (in β units) is given by

$$E = \begin{cases} 2 \sum_{j=1}^{N_e/2} x_j & \text{if } N_e \text{ is even} \\ x_{(N_e+1)/2} + 2 \sum_{j=1}^{(N_e-1)/2} x_j & \text{if } N_e \text{ is odd} \end{cases} . \tag{4}$$

If all bonding levels ($x_j > 0$) are doubly occupied and all antibonding levels ($x_j < 0$) are unoccupied,

$$E = \sum_{j=1}^{N} |\, x_j \,| \quad . \tag{5}$$

Throughout this paper Eq. (5) will be assumed to hold, at least as a good approximation.

Let in the spectrum of G there be N_0 zeros. Then the characteristic polynomial can be written as

$$P(G, x) = x^{N_0} \tilde{P}(G, x) = x^{N_0} \sum_{j=0}^{\tilde{N}} a_j\, x^{\tilde{N}-j} \tag{6}$$

where $\tilde{N} = N - N_0$. Since the quantities N_0 and $\tilde{N}$ will play a considerable role in the following considerations, it is to be noted that relatively simple graph-theoretical algorithms are known for their determination [14].

Eq. (6) implies $a_{\tilde{N}} \neq O$. If $N_0 = O$, $a_{\tilde{N}} = (-1)^N \det \mathbf{A}$. Simple procedures are known for evaluation of $\det \mathbf{A}$ [15]. If $N_0 \neq O$, $a_{\tilde{N}}$ can be calculated by a method developed in [16].

Coulson-type integral formula for RE and its approximation

COULSON [17] has obtained the following expression which relates the characteristic polynomial with total pi-electron energy

$$N = (1/\pi) \int_{-\infty}^{+\infty} [N - ix\, P'(G, ix)/P(G, ix)]\, dx \tag{7'}$$

where $i = \sqrt{-1}$ and $P'(G, x)$ is the first derivative of $P(G, x)$. It is convenient to write Eq. (7') in an abbreviate form [18]

$$E = \langle N - ix\, P'(G, ix)/P(G, ix) \rangle_i^{\infty}. \tag{7''}$$

After suitable transformations, Eq. (7) becomes

$$E = \left\langle \tilde{N} - x \frac{d}{dx} \log | \tilde{P}(G, ix) | \right\rangle. \tag{8}$$

The characteristic polynomial of the reference structure (RS) containing $N/2$ isolated double bonds is $P(RS, x) = (x^2-1)^{N/2}$, which gives $|P(RS, ix)| = (x^2 + 1)^{N/2}$. Therefore, from Eq. (8),

$$N = \left\langle N - x \frac{d}{dx} \log (x^2 + 1)^{N/2} \right\rangle \tag{9'}$$

since, evidently, $E(RS) = N$. Substituting in the formula (9') $\tilde{N}$ instead of N, we obtain

$$\tilde{N} = \left\langle \tilde{N} - x \frac{d}{dx} (x^2 + 1)^{\tilde{N}/2} \right\rangle \tag{9''}$$

which combined with Eqs (2) and (8) gives

$$RE = E - \tilde{N} - (N_e - \tilde{N}) = -\left\langle x \frac{d}{dx} W(x) \right\rangle - (N_e - \tilde{N}) \tag{10}$$

where

$$W(x) = \log | \tilde{P}(G, ix) | (x^2 + 1)^{-\tilde{N}/2} \tag{11}$$

Note that for non-charged species, $N_e - \widetilde{N} = N_0$. Partial integration of Eq. (10) gives

$$\mathrm{RE} = \langle W(x) \rangle - (N_e - \widetilde{N}). \tag{12}$$

Essentially the same result has been derived by COULSON many years ago [19].

Taking into account that for all molecular graphs $a_0 = 1$, $a_1 = 0$ and $a_2 = -M$, it can be proved that for large values of $|x|$,

$$W(x) \sim (M - \widetilde{N}/2)\, x^{-2} \tag{13'}$$

while for small values of $|x|$,

$$W(x) \sim \log |a_{\widetilde{N}}| \,. \tag{13''}$$

Of course, $M - \widetilde{N}/2 > 0$ is in all cases of interest in chemistry.

Table I

Resonance energies (in β units) of selected conjugated hydrocarbons; (a) exact HMO values [20]; (b) RE's from eq. (16)

No.	Molecule	(a)	(b)	Error (%)
1	benzene	2.00	2.04	+2.0
2	naphthalene	3.68	3.63	—1.4
3	anthracene	5.31	5.00	—6.0
4	phenanthrene	5.45	5.38	—1.2
5	chrysene	7.19	7.06	—1.8
6	triphenylene	7.27	7.26	—0.2
7	pentacene	8.54	7.33	—14.2
8	picene	8.94	8.77	—1.9
9	coronene	10.57	10.95	+3.5
10	ovalene	14.50	14.00	—3.5
11	cyclobutadiene	0.00	0.04	—
12	biphenylene	4.51	4.19	—6.9
13	biphenyl	4.38	4.41	+0.5
14	tetraphenylethylene	9.72	9.42	—3.1
15	1,2 benz-fulvene	3.33	2.88	—13.5
16	dibenz-fulvene	5.22	5.00	—4.4
17	azulene	3.36	2.88	—14.3
18	acenaphthylene	4.62	4.19	—9.2
19	pentalene	2.46	2.38	—3.0
20	allyl	—0.172	—0.167	—2.4
21	pentadienyl	0.46	0.48	+3.9
22	benzyl	1.72	1.79	+4.0
23	triphenyl-methyl	6.80	7.00	+3.0
24	acenaphthenyl	4.83	4.99	+3.4

It is easily seen that W is an even function. Hence, $W(0)$ is an extreme of W. In the subsequent section it will be shown that if $|a_{\tilde{N}}|$ is large enough, $W(0)$ is a maximum. Then $W(x)$ monotonously decreases in the interval $(0, +\infty)$. A simple algebraic function $V(x)$, like

$$V(x) = (M - \tilde{N}/2) \log |a_{\tilde{N}}| (M - \tilde{N}/2 + x^2 \log |a_{\tilde{N}}|)^{-1} \qquad (14)$$

has identical asymptotic behaviour as $W(x)$ for both small and large values of $|x|$, and its only extreme is a maximum for $x = 0$. Therefore, it is to be expected that $\langle V(x) \rangle$ will present a fair approximation of $\langle W(x) \rangle$. Elementary integration gives

$$\langle V(x) \rangle = \left[(M - \tilde{N}/2) \log |a_{\tilde{N}}| \right]^{1/2} \qquad (15)$$

since $\langle (1 + x^2)^{-1} \rangle = 1$. Finally, we obtain a simple approximate topological formula for resonance energy

$$RE \doteq \left[(M - \tilde{N}/2) \log |a_{\tilde{N}}| \right]^{1/2} - (N_e - \tilde{N}). \qquad (16)$$

The validity of this approximation is illustrated in Table 1. Of course, only structures having $|a_{\tilde{N}}| > 1$ are included in Table. The HMO total pi-electron energy data are taken from [20].

Discussion

An inspection of Table I shows that formula (16), although extremely simple, reproduces RE with an error of only few per cents. The calculated RE's seem to be of equal accuracy for both benzenoids (Nos 1—10), cyclobutadiene containing systems (Nos 11, 12), polyphenyls (Nos 13, 14), nonalternants (Nos 15—19) and free radicals (Nos 20—24). In the great majority of the cases the exact RE's are underestimated. Hence, the introduction of a (least squares) fitting parameter could substantially increase the accuracy of formula (16). However, the present form of our topological relation has the great advantage of being independent of any fitting parameter.

The examples of coronene ($N = 24$), tetraphenylethylene ($N = 26$) and ovalene ($N = 32$) show that Eq. (16) gives fair results for large conjugated systems as well.

The calculated RE values for the isomeric pairs anthracene–phenanthrene, chrysene–triphenylene and especially pentacene–picene indicate that the larger is $|a_{\tilde{N}}|$, the smaller is the error in Eq. (16). Similarly, errors are considerably large in molecules which have relatively small $|a_{\tilde{N}}|$ in comparison with $\tilde{N}$ (Nos 7,15 and 17). This occurs because in the derivation of (16) it has been assumed that $W(x)$ is maximal for $x = 0$.

A detailed analysis shows that $W(x)$ has the following asymptotic behaviour for small values of $|x|$:

$$W(x) \sim \log |a_{\tilde{N}}| + Q\, x^2 \tag{17}$$

with

$$Q = 2 \mid a_{\tilde{N}-2}/a_{\tilde{N}}| + (a_{\tilde{N}-1}/a_{\tilde{N}})^2 - \tilde{N}. \tag{18}$$

The coefficients $a_{\tilde{N}-1}$ and $a_{\tilde{N}-2}$, necessary for the evaluation of Q, can be determined using a general graph-theoretical procedure of sachs [12]. However, this is by no means simple in all cases.

Hence, $Q < 0$ is a necessary condition for the validity of the approximation (14). If $|a_{\tilde{N}}| > 1$, $\tilde{N}$ is usually large enough to provide the above inequality. However, if $|a_{\tilde{N}}| = 1$ or if $\tilde{N}$ is small, $Q > 0$ and the function $W(x)$ has a minimum for $x = 0$ and another maximum in the interval $(0, +\infty)$. Then instead of $V(x)$ another model function

$$V_1(x) = (M - \tilde{N}/2)\,(Qx^2 + \log |a_{\tilde{N}}|)\,(M - \tilde{N}/2 + Qx^4 + x^2 \log |a_{\tilde{N}}|)^{-1} \tag{19}$$

is to be used. Although the integral $\langle V_1(x) \rangle$ can be calculated, it results in a rather complicated expression. This expression leads, moreover, to the same general consequences as Eq. (16).

Concluding our discussion, we would like to emphasize the following general properties of RE which can be deduced from Eqs (12) and (16).

(a) The most important topological factors which determine RE are M, N, N_0 and $|a_{\tilde{N}}|$.

(b) If $N_e - \tilde{N} = N_0 = 0$, RE is necessarily positive (except in the trivial case of ethylene, for which $RE = 0$). RE can be negative only if $N_0 > 0$ and besides if $\tilde{N}$ is small enough. But only two chemically relevant graphs have such properties — the allyl- and the cyclobutadiene-graph. (Of course, there exist further anionic species which have negative RE.)

(c) If there are R rings contained in the molecule, $M = N + R - 1$. Therefore, in the case of $N_0 = 0$, $M - \tilde{N}/2 = N/2 + R - 1$. Since $N/2 \gg R - 1$, RE should be grossly proportional to $\sqrt{N}$. Similarly, the mere presence of rings will increase RE.

(d) In benzenoid systems $|a_N| = K^2$. Hence, the proportionality between RE and K [4] is well reproduced by Eq. (16).

(e) This regularity is no more valid for nonbenzenoid molecules. For alternant nonbenzenoids, $|a_N| = (ASC)^2$, where $ASC = K^+ - K^-$ is the algebraic structure count [15]. K^+ and K^- are the number of KEKULÉ structures of even and odd parity, respectively. Since $K^+ + K^- = K$, $ASC \leq K$ and a nonbenzenoid conjugated system should always have smaller RE than its benzenoid isomer.

(f) Among isomeric benzenoid systems, the one with maximal (minimal) *RE* is that with maximal (minimal) K. In the general case, within a set of isomeric conjugated molecules, the larger are the $|a_{\widetilde{N}}|$'s, the larger are their *RE* values.

(g) If there exist non-bonding *MO*'s, *RE* is no more a function of N, but of a fictive "reduced" number of vertices, $\widetilde{N}$. The fact that the presence of non-bonding *MO*'s ($N_0 > 0$) decrease *RE* is evident from both Eqs (12) and (16).

(h) It follows from (*b*) and (*c*) that *RE* cannot be utilized as a measure of aromaticity. Namely, a satisfactory topological index of aromaticity should be independent of (or at least not much dependent on) the molecular size. Such an index (the "topological resonance energy") has been proposed in [9].

*

The author thanks Dr. GÁBOR NÁRAY-SZABÓ (Budapest) for useful comments and suggestions.

REFERENCES

[1] For some recent work in this field see: GEORGE, P., TRACHTMAN, M., BOCK, C. W., BRETT, A. M.: Theoret. Chim. Acta, **38,** 121 (1975); HERNDON, W. C.: J. Org. Chem., **40,** 3583 (1975); RANDIĆ, M.: Chem. Phys. Letters, **38,** 68 (1976); EPIOTIS, N. D., YATES, R. L.: J. Amer. Chem. Soc., **98,** 461 (1976)
[2] MCCLELLAND, B. J.: J. Chem. Phys., **54,** 640 (1971)
[3] ENGLAND, W., RUEDENBERG, K.: Amer. Chem. Soc., **95,** 8769 (1973)
[4] HALL, G. G.: Internat. J. Math. Educ. Sci. Technol., **4,** 233 (1973)
[5] DEWAR, M. J. S.: The Molecular Orbital Theory of Organic Chemistry, & McGraw-Hill, New York 1969
[6] BINSCH, G.: Naturwissenschaften, **60,** 369 (1973)
[7] HESS, B. A., SCHAAD, L. J.: J. Amer. Chem. Soc., **93,** 305 (1971) and numerous later publications; MILUN, M., SOBOTKA, Ž., TRINAJSTIĆ, N.: J. Org. Chem., **37,** 139 (1972)
[8] AIHARA, J.-I.: Bull. Chem. Soc. Japan, **47,** 3169 (1974); *ibid.*, **48,** 517, 3637 (1975); WILCOX, C. F.: Croat. Chem. Acta, **47,** 79 (1975)
[9] GUTMAN, I., TRINAJSTIĆ, N.: Acta Chim. (Budapest), **91,** 203 (1976)
[10] GUTMAN, I., MILUN, M., TRINAJSTIĆ, N.: J. Chem. Phys., **59,** 2772 (1973)
[11] For review on application of graph theory in the theoretical chemistry of conjugated compounds see: GUTMAN, I., TRINAJSTIĆ, N.: Topics Curr. Chem., **42,** 49 (1973); Croat. Chem. Acta, **47,** 507 (1975)
[12] GRAOVAC, A., GUTMAN, I., TRINAJSTIĆ, N., ŽIVKOVIĆ, T.: Theoret. Chim. Acta, **26,** 67 (1972)
[13] GÜNTHARD, H. H., PRIMAS, H.: Helv. Chim. Acta, **39,** 1645 (1956)
[14] CVETKOVIĆ, D., GUTMAN, I.: Matematicki vesnik (Beograd), **9,** 141 (1972); ŽIVKOVIĆ, T.: Croat. Chem. Acta, **44,** 351 (1972); CVETKOVIĆ, D., GUTMAN, I., TRINAJSTIĆ, N.: Croat. Chem. Acta, **44,** 365 (1972); Theoret. Chim. Acta, **34,** 129 (1974); J. Mol. Struct., **28,** 289 (1975)
[15] WILCOX, C. F.: J. Amer. Chem. Soc., **91,** 2732 (1969) and references therein
[16] GUTMAN, I., TRINAJSTIĆ, N., WILCOX, C. F.: Tetrahedron, **31,** 143 (1975)
[17] COULSON, C. A.: Proc. Cambridge Phil. Soc., **36,** 201 (1940)
[18] GRAOVAC, A., GUTMAN, I., TRINAJSTIĆ, N.: Chem. Phys. Lett., **35,** 555 (1975); *ibid.*, 37, 471 (1976)
[19] COULSON, C. A.: J. Chem. Soc., **3111** (1954); see also: MARCUS, R. A.: J. Chem. Phys., **43,** 2643 (1965)
[20] COULSON, C. A., STREITWIESER, A.: Dictionary of Pi-Electron Calculations, Pergamon Press, Oxford 1965

Ivan GUTMAN 4100 Zagreb. P. O. Box 1016 Croatia, Yugoslavia.

Acta Chimica Academiae Scientiarum Hungaricae, Tomus 92 (1), pp. 73—83 (1977)

ON THE MECHANISM OF THE HYDROGENATION AND ISOTOPIC EXCHANGE IN THE ALKYLAROMATIC HYDROCARBONS–SUBSTITUTED CYCLOALKANES SYSTEM ON NICKEL

L. M. MAMALADZE, N. V. NEKRASOV, B. S. GUDKOV, and S. L. KIPERMAN

(Zelinskii Institute of Organic Chemistry, Academy of Sciences of the U.S.S.R.)

Received November 3, 1975

The regularities of hydrogenation and isotope exchange with deuterium on nickel catalysts have been studied in the series benzene, toluene, ethylbenzene, *meta*-, *para*- and *ortho*-xylene and mesitylene and the characteristics of isotopic exchange in the series cyclohexane, methylcyclohexane, 1,1- and 1,2-dimethylcyclohexane. The hydrogenation characteristics of benzene and toluene were found to be closely similar, demonstrating the identical mechanism of these processes. Within the series of alkylaromatic compounds, the rate of hydrogenation decreases regularly, while the rate of isotopic exchange remains approximately constant in both the aromatic ring and the alkyl substituents. This finding indicates that different surface forms must be responsible for hydrogenation and isotopic exchange. In contrast to alkylbenzenes, no significant difference was detected between exchange rates in the ring and in the alkyl groups in the case of substituted cyclohexanes.

Earlier studies on the kinetics and mechanism of benzene hydrogenation in the range of reversibility of the process [1] demonstrated the utility of a complex approach, making use of kinetic, isotopic exchange and other methods, for determining the characteristics of catalytic reactions. It therefore appeared expedient to study in a similar manner the hydrogenation of toluene to methylcyclohexane

$$C_7H_8 + 3H_2 = C_7H_{14} \qquad (1)$$

Further useful information regarding the mechanism of the process might be expected from a comparison of the hydrogenation rates of a series of alkylbenzenes as well as their isotopic exchange rates with deuterium. A study of these problems was the object of the present work.

Experimental

The hydrogenation of toluene and its isotopic exchange with deuterium under the conditions of reaction (1) were investigated in a flow-circulation system in the temperature range of 43—270 °C at an overall pressure of 1 atm. The partial pressures of toluene, hydrogen and added methylcyclohexane were varied within the ranges of 36—139, 373—720 and 0—126 Torr, respectively. The same apparatus was used for determining the rates of hydrogenation of a

series of alkylbenzenes at 225 °C. Under the given experimental conditions side reactions (*e. g.* hydrodemethylation) were practically absent. In rate calculations we introduced correction factors accounting for the reverse reaction [2].

Isotopic exchange reactions of alkylbenzenes and substituted cycloalkanes were studied in a quasi-static circulation system [3] connected with a type MI—1305 mass spectrometer. Measurements were carried out at 30 °C. Under the given experimental conditions practically no hydrogenation of the alkylbenzenes on the catalyst (nickel on zinc oxide support) occurred. The partial pressure of the hydrocarbons was 1—2 Torr, that of deuterium 24—48 Torr.

In the hydrogenation experiments with toluene and in the hydrogenation and isotopic exchange experiments with a series of alkylbenzenes we used a nickel catalyst on zinc oxide support (66.8% Ni) prepared by the method described in Ref. [4]. Its specific surface area was 11 m^2/g. In the isotopic exchange experiments with cycloalkanes a nickel catalyst on silica gel support (11.9% Ni, specific surface area 18 m^2/g) was used [5].

An ionization voltage of 13—22 V was used for establishing the isotope composition of the different hydrocarbons. Calculations were performed for the molecular ions, introducing the usual correction for the natural isotope content.

For details of the experimental technique, *cf.* [6, 7].

Results

Kinetics of toluene hydrogenation

The temperature dependence of the rate of reaction (1) is represented by curve I in Fig. 1, showing that the rate passes through a temperature-dependent maximum. The reversibility range of the reaction is located on the descending part of the curve, *i. e.* it formally corresponds to a negative apparent activation energy E. It is essential that the decrease in the rate of reaction is not related to the approach towards equilibrium, but follows from the particular mechanism, and is due to the decreasing surface coverage by toluene with increasing temperatures, after having passed the maximum rate at 180 °C [6].

We studied the kinetics of the reaction in detail in the reversibility range. The rate was found to depend solely on the concentrations of the starting materials, while the concentration of the product methylcyclohexane had no effect on the rate. We investigated the agreement between experimental data and various kinetic equations of the general form

$$W = \frac{k P_{C_7H_8}^m P_{H_2}^n}{(1 + k_1 P_{C_7H_8} + k_2 P_{H_2})^l} \,. \tag{2}$$

A preliminary graphical analysis and subsequent computations performed on a Minsk-22 computer, using non-linear programming, demonstrated that the set of data obtained in the temperature range of 200—270 °C agreed best with the equation

$$W = k P_{C_7H_8}^{0,5} P_{H_2}^3 \tag{3}$$

where $k = 1.15 \times 10^{-10}$ exp (18 500/RT) mol/h $atm^{2.5}$ cm^3. The mean deviation of the computed and experimental values was 9.3%.

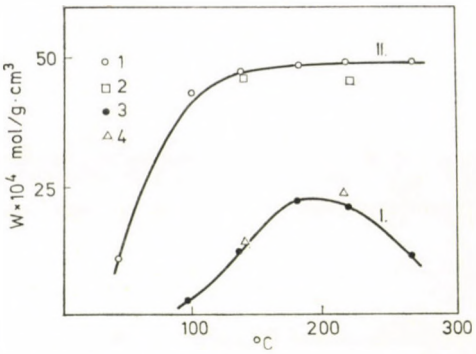

Fig. 1. Hydrogenation rate (I) and isotopic exchange rate (II) of toluene *vs.* temperature. ○–Isotopic exchange rate; □ — isotopic exchange rate in the presence of 68% methylcyclohexane added; ● — hydrogenation rate; △ — hydrogenation rate in the presence of 68% methylcyclohexane added

Isotopic exchange in toluene

Curve II in Fig. 1 represents the termperature dependence of the rate of hydrogen–deuterium exchange in toluene, demonstrating that this rate is higher than the rate of hydrogenation within the whole investigated temperature range. The nature of temperature dependence is different for hydrogenation and the isotopic exchange. IR spectroscopy of the products at various temperatures demonstrated that — in agreement with literature data [8] — the easiest to exchange are the hydrogen atoms of the methyl group, followed by those in the *meta-* and *para-* positions of the aromatic ring, while the hydrogen atoms in the *ortho*-position are the most difficult to exchange. The ease of exchange in the methyl group explains the finding that already at relatively low temperatures practically no toluene molecules are left that do not contain at least one deuterium atom, that is, the extent of isotope exchange under these conditions is close to 1.

Earlier, a similar comparison of istopic exchange and hydrogenation rates had been made with benzene [20]. The analogous nature of the results obtained allows to extend the conclusions made in the earlier paper to the present case, *i. e.* to assume that isotope exchange and hydrogenation of toluene take place through different intermediates possibly *via* the initial formation of some common intermediate.

Kinetic isotope effects

Kinetic isotope effects were measured for the protium-to-deuterium substitution in different positions of the toluene molecule, and also in hydrogen. The results are listed in Table I. The value of β was calculated as the ratio of

Table I

Kinetic isotope effects, β, in the hydrogenation of toluene at 240 °C

Reactants	β	Reactants	β
$C_6H_5CH_3 + 3H_2$ $C_6D_5CH_3 + 3H_2$	0.9	$C_6H_5CH_3 + 3H_2$ $C_6D_5CD_3 + 3D_2$	0.4
$C_6H_5CH_3 + 3H_2$ $C_6D_5CD_3 + 3H_2$	0.7	$C_6H_5CH_3 + 3H_2$ $C_6H_5CH_3 + 3D_2$	0.4

the rate constants obtained by means of Eq. (3). The β values obtained with deuterotoluenes may be distorted by the superposition of isotope exchange with excess H_2. When the reaction was carried out in deuterium excess, *i. e.* when substituted by exchanged for deuterium, the rate increased rather significantly. Similar reverse isotope effects, that is, an increase instead of a decrease of the rate of reaction after the substitution of the light isotope by the heavy isotope have been observed earlier in the hydrogenation of benzene [1], ethylene [9] and acetone [10]. The phenomenon is apparently caused by different changes in the rates of the slow stages and in the equilibrium constants of the fast stages, as well as by different changes in the zero-point energies of the starting materials and activated complexes when protium is substituted by deuterium [1, 21]. Here we only wish to emphasize that the existence of an isotope effect in itself indicates the participation of hydrogen in the slow step of toluene hydrogenation.

Mechanism of toluene hydrogenation

The experimental data indicate the similarity of the hydrogenation regularities of toluene and benzene. On this basis it appears permissible to extend the concept of the mechanism of benzene hydrogenation to the hydrogenation of toluene. This mechanism consists of the following steps:

$$\text{(i)}\quad H_2 = (H_2)$$

$$\text{(ii)}\quad C_7H_8 + (Ni) = C_7H_8\,(Ni)$$

$$\text{(iii)}\quad C_7H_8\,(Ni) + 3\,(H_2) = [C_7H_8\,(Ni)] \cdot 3\,H_2 \qquad (4)$$

$$\text{(iv)}\quad [C_7H_8\,(Ni)] \cdot 3\,H_2 = [C_7H_{10}\,(Ni)] \cdot 2\,H_2$$

$$\text{(v)}\quad [C_7H_{10}\,(Ni)] \cdot 2\,H_2 = [C_7H_{12}\,(Ni)] \cdot H_2$$

$$\text{(vi)}\quad [C_7H_{12}\,(Ni)] \cdot H_2 = C_7H_{14} + (Ni)$$

According to this mechanism, toluene forms a strong surface complex with nickel in fast step (ii). Its formation is not hindered by hydrogen weakly bounded to the surface (formed in equilibrium reaction (i)). In the subsequent slow step (iii) toluene reacts with this hydrogen and forms a molecular co-ordinated compound, in which then fast rearrangements take place, leading finally to the appearance of methylcyclohexane. It should be noted that among all examined models, only the above mechanism appeared to be free of contradictions. Other variants did not agree neither with isotopic exchange data nor with kinetic data [1]. The formation of a reactive complex with six hydrogen atoms also appears improbable. Kinetic analysis shows that Eq. (3) follows from mechanism (4). Experimentally found kinetic isotope effects are also in agreement with mechanism (4).

Isotopic exchange, however, occurs by a different mechanism, which the dissociative adsorption of toluene must be included (*e. g.* according to the dissociative mechanism of π-complex substitution, like that in benzene [1]) after the formation of the intermediate compound C_7H_8 (Ni) in step (ii).

Comparison of hydrogenation and isotopic exchange rates in a series of alkylbenzenes

The similarity in the hydrogenation characteristics of toluene and benzene allows to expect an analogous behaviour in the hydrogenation of other representatives of alkylaromatic compounds. The results presented in Table II demonstrate that the rate of hydrogenation decreases with increasing number of substituents.

As to isotopic exchange, the characteristic feature of the alkylbenzenes studied is that the exchange rate is approximately the same in all compounds, in both the aromatic ring and the methyl groups (Table II). The composition of the groups in which the hydrogen atoms are susceptible to isotope exchange was established by determining the isotope distribution of the products in successive moments of time [7, 8]. In addition, as mentioned earlier, IR spectroscopic data confirm the distribution of hydrogen atoms in toluene regarding their readiness to isotopic exchange.

Isotopic exchange in the listed alkylbenzenes was measured at 30 °C only. However, apparently, the succession of the different hydrogen atoms regarding their readiness to exchange remains unchanged at higher temperatures too. This is confirmed by the similarity of isotopic distribution in the exchange products of toluene in the static system at 30 °C and in the flow-circulation system at 96 °C where hydrogenation proceeds up to 5%. On the other hand, the order of hydrogenation rates obtained in the present work for the compounds studied is qualitatively the same as that observed by

Table II

Relative hydrogenation and isotopic exchange rates in alkylaromatic compounds

Compound	Relative hydrogenation rate		Relative isotopic exchange rate		
	Results obtained in this work 225 °C	Literature results [11] 143.5 °C	Overall	In the aromatic ring*	In the side chain
Benzene	1.0	1.0	1.0	1.0	—
Ethylbenzene	0.6	0.5	1.9	1.3**	0.6***
Toluene	0.3	0.9	4.0	1.0	3.0
m-Xylene	0.2	—	4.2	0.9	3.3
p-Xylene	0.2	0.5	4.2	0.7	3.4
o-Xylene	0.2	—	4.3	1.1	3.1
Mesitylene	0.1	0.3	3.6	—	3.6

* This includes only those hydrogen atoms in the aromatic ring that are capable of appreciable isotopic exchange. Hence, two H atoms in *ortho*-positions in toluene and *o*-xylene, and one H atom in *ortho*-position in *m*-xylene are left out of consideration

** In this value, the two H atoms in the CH_2 group and the three H atoms in the *meta*- and *para*-positions of the ring are included

*** This value refers to the three H atoms in the CH_3 group

VÖLTER *et al.* [11, 12] at a lower temperature (*cf.* Table II). This fact also justifies the comparison of the charateristics of hydrogenation and isotope exchange.

As shown, the alkylbenzenes studied do not assume any regular succession either with respect to overall rate of exchange or with respect to rate of exchange for definite groups of hydrogen atoms, whereas a regular succession concerning the rate of hydrogenation is observed. This serves as confirmation for the difference in the nature and properties of the intermediates responsible for isotopic exchange and hydrogenation of alkylbenzenes, and for the different mechanisms of these processes.

Comparison of isotopic exchange rates in a series of alkyl-substituted cycloalkanes

The diagrams representing the isotopic distributions of the exchange products of cycloalkanes (Fig. 2) demonstrate that in this case, in contrast to alkylbenzenes, the hydrogen atoms in the methyl groups do not significantly differ, regarding the easiness of exchange, from the hydrogen atoms in the ring. The primary factor determining the ease of isotopic exchange is not the position of the hydrogen atom in the ring or in the substituent, but the stereochemistry of the hydrocarbon molecule. Isotopic distribution in methyl-

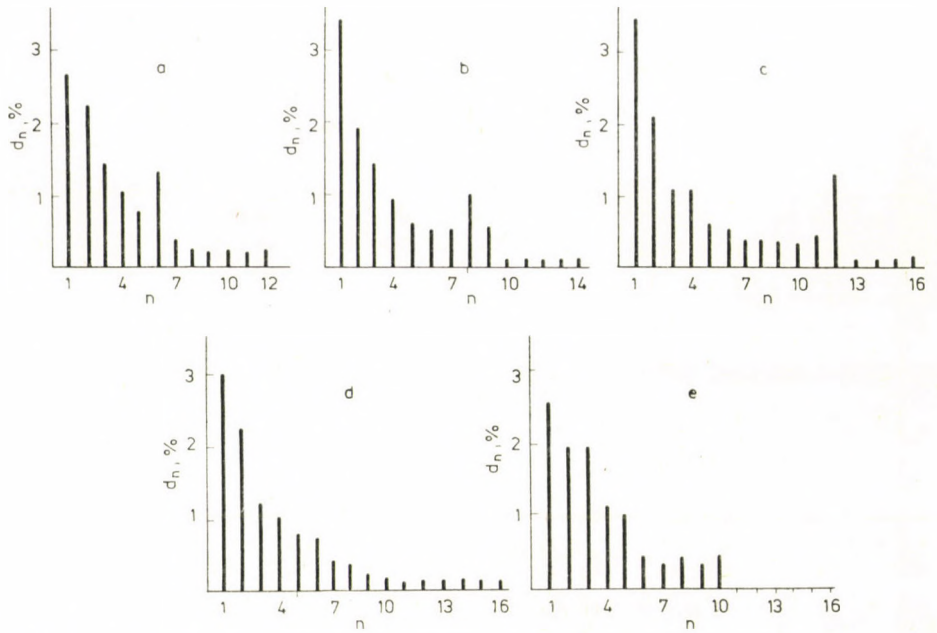

Fig. 2. Isotopic distribution in the exchange products of cyclohexane and its derivatives. Ni/SiO_2 catalyst, 30 °C: a — cyclohexane; b — methylcyclohexane; c — *cis*-1,2-dimethylcyclohexane; d — *trans*-1,2-dimethylcyclohexane; e — 1,1-dimethylcyclohexane. Extent of exchange: 11% for all compounds

cyclohexane (Fig. 2b) is very similar to that in cyclohexane (Fig. 2a), differing only insofar as the intermediate maximum is shifted by 2 or 3 units. In cyclohexane, as established earlier [13, 14], 6 H-atoms located on one side of the assumed ring plane and belonging to the surface will exchange rather rapidly, while the exchange of further H-atoms requires additional energy. This explains the appearance of an intermediate maximum d_6. In the case of methylcyclohexane, the first group of exchanging atoms includes, 3 H-atoms of the methyl group, and 5 or 6 H-atoms of the ring, depending on the initial orientation of the molecule on the surface. *Cis*-1,2-dimethylcyclohexane (*cis*-1,2-C_8H_{16}) behaves analogously, but the maximum in this case is further shifted to d_{12} (Fig. 2c), because the hydrogen atoms of both methyl groups are involved, in addition to those of the ring, in the exchange. In contrast, only one methyl group of *trans*-1,2-C_8H_{12} (Fig. 2d) is capable of participating in each single exchange act, so that not more than 8 H-atoms (3 from the methyl group and 5 from the ring) exchange simultaneously. The maximum at d_6 is possibly connected with some other process in which either both CH_3 groups participate, or 6 H-atoms from one side of the ring after isomerization of the *trans* compound into the *cis* compound. This latter assumption appears more probable. An analogous process in the case of *cis*-1,2-C_8H_{16}

could be covered up by the rapid exchange reaction in which 12 H-atoms participate, that is, owing to the absence of an energy barrier when passing from exchange in the ring to exchange in both substituents. In 1,1-C_8H_{16} (Fig. 2e) the maximum number of atoms participating in the exchange does not exceed 10. A comparison of molecular and fragment ion distributions [15] has shown that in the given case, no deuterium is found in the methyl groups, *i. e.* the hydrogen atoms of the latter do not participate in the exchange. In contrast, the methyl groups in *cis-* and *trans*-1,2-C_8H_{16} do contain deuterium, and the close similarity between the distributions in molecular ions and ions having lost one methyl group allows to assume that the exchange rate of the H-atoms in the ring and in the methyl groups must be nearly identical. Thus, as noted earlier [15], *trans*-1,2-C_8H_{16} appears to occupy an intermediate position, with respect to the character of exchange, between *cis*-1,2-C_8H_{16} and 1,1-C_8H_{16}. In the latter compound, the methyl groups, separated from the hydrogen atoms in the ring by a quaternary carbon atom, form a separately exchanging group, whereas in *cis*-1,2-C_8H_{16} the extension of exchange from the ring to the methyl groups (or inversely) does not run into any obstacles.

Table III

Rate of isotopic exchange in substituted cyclohexanes at 30 °C

Compound	Rate of exchange (Torr/min)	
	$P^0_{C_nH_{2n}} = 1$ Torr, $P^0_{D_2} =$ $= 48$ Torr	$P^0_{C_nH_{2n}} = 2$ Torr, $P^0_{D_2} =$ $= 48$ Torr
C_6H_{12}	14.2	18.6
C_7H_{14}	21.2	28.4
cis-1,2-C_8H_{16}	37.7	56.6
trans-1,2-C_8H_{16}	16.9	23.1
1,1-C_8H_{16}	10.8	16.2

This is also reflected in the exchange rates of the corresponding compound (the rate of disappearance of the 'light' molecules, *cf.* Table III). The presence of one methyl group (C_7H_{14}) and even more so, that of two methyl groups (*cis*-1,2-C_8H_{16}) readily participating in exchange leads to a substantial increase in the rate of isotopic exchange. On the other hand, the obstacle in extending exchange to methyl groups in *trans*-1,2-C_8H_{16} and, all the more so, in 1,1-C_8H_{16}, results in the decrease of the rate of isotopic exchange.

Discussion

The comparison of the hydrogenation and isotopic exchange characteristics of benzene and of the dehydrogenation and isotopic exchange characteristics of cyclohexane, on the one hand, with the hydrogenation and isotopic exchange characteristics of toluene and other alkylaromatic compounds and the isotopic exchange characteristics of methyl-substituted cycloalkanes, on the other hand, allows to point out that the mechanisms of the reversible hydrogenation–dehydrogenation processes are closely similar in all cases. To explain the mechanism of the reversible hydrogenation of benzene and of the isotopic exchange in benzene and cyclohexane, we proposed, in our earlier work [1], the following scheme:

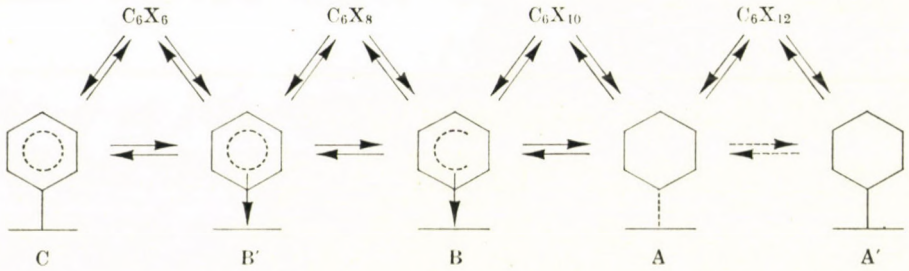

(5)

where symbol X stands for hydrogen or deuterium (the form in which it participates in the reaction will not be considered). The results obtained in the present work justify the extension of this scheme to the systems studied.

According to scheme (5), benzene (and analogously, alkyl-substituted aromatic compounds) forms, with nickel, a strongly bound compound (B') of the π-complex type. Hydrogenation takes place through this compound. It can either, in the course of hydrogenation, be transformed successively into other π-complexes (marked in the scheme by symbol B), in agreement with the scheme proposed by ROONEY and WEBB [16, 17], or, according to the dissociative mechanism of π-complex substitution [18], be converted into compound C, held by a σ-bond, simultaneously splitting off hydrogen. The latter reaction is responsible for isotopic exchange in the aromatic compound. Cyclohexane (and substituted cyclohexane), as a result dissociative adsorption, will form the surface compound A held by σ bonds, this process being responsible for isotopic exchange. The formation of another surface compound A', responsible only for isotopic exchange, is also possible, especially at low temperatures. The different character of isotopic exchange in the case of 1,1-C_8H_{16} and other dimethylcyclohexanes may be explained by the π-allyl nature of the intermediate, allowing participation in the reaction only of those methyl groups which are not separated by quaternary carbon atoms from the hydrogen atoms in the ring [19].

Hence, it is assumed in scheme (5) that isotopic exchange in benzene and its analogues, on the one hand, and their hydrogenation, on the other hand, proceed through different surface compounds. An equilibrium can be established between these compounds, which will be shifted towards one or the other side depending on the temperature. An analogous assumption can be made relating to isotopic exchange and dehydrogenation of cyclohexane and its analogues. These assumptions are in agreement with the experimentally found independence of the characteristics of the different processes taking place in the systems studied.

The observed qualitative analogy of the character of each process in the series of benzene and its homologues, as well as in the series of cyclohexane and its substituted derivatives allows to draw some general conclusions, namely that the nature of the aromatic or polymethylene ring has a decisive effect on the characteristics of the process when the alkyl substituents do not have a significant part in it (hydrogenation and dehydrogenation). In this case, similar kinetics and mechanisms may be expected, in the series considered, as was actually found in the hydrogenation of benzene and toluene, where the differences found were merely quantitative. When, however, substituents of the same type participate directly in the process, their effect on the characteristics of the process may be decisive (isotopic exchange). However, the effects caused by the substituents may either be small (benzene derivatives), or, in other cases, they may not lead to monotonous changes. It should be noted that the qualitative differences observed in the kinetics of isotopic exchange in cycloalkanes are related to this latter case and require further investigations.

REFERENCES

[1] KIPERMAN, S. L., SHOPOV, D., ANDREEV, A., ZLOTINA, N., GUDKOV, B.: Izv. Otd. Khim. Nauk Bolg. Akad. Nauk, **4**, 237 (1971)
[2] KIPERMAN, S. L., GADZHI-KASUMOV, V. S.: Izv. Akad. Nauk. SSSR, Ser. Khim., 1110 (1965)
[3] NEKRASOV, N. V., GUDKOV, B. S.: Izv. Akad. Nauk. SSSR, Ser. Khim., 25 (1973)
[4] RUBINSHTEIN, A. M., SLINKIN, A. A., FEDOROVSKAYA, E. A., KLYACHKO-GURVICH, A. L., SAGALOVICH, A. V., SHASHKIN, D. P., ASHAVSKAYA, G. A., MELNIKOVA, I. V.: Sbornik "Metody issledovaniya katalizatorov i kataliticheskikh reaktsii", Vol. 2, p. 39. Izd. Sib. Otd. Akad. Nauk SSSR, Novosibirsk 1965.
[5] SLINKIN, A. A. LOKTEV, M. I., RUBINSHTEIN, A. M.: Kinet. Katal., **13**, 464 (1972)
[6] MAMALADZE, L. M., KIPERMAN, S. L.: Kinet. Katal., **16**, 1601 (1975)
[7] GUDKOV, B. S., MAMALADZE, L. M., KIPERMAN, S. L.: Izv. Akad Nauk SSSR, Ser. Khim., 757 (1975); Sbornik "Kinetika-2" Vol. 2, p. 112. Novosibirsk 1975
[8] CRAWFOWD, E., KEMBALL, C.: Trans. Faraday Soc., **58**, 2452 (1962)
[9] HORIUTI, J., MIYAHARA, K.: Hydrogenation of Ethylene on Metallic Catalysts. Ed. NSR DS-NBS 13, Washington 1971
[10] GEGENAVA, T. P., KIPERMAN, S. L.: Vses. konferentsiya po mekhanizmu get.-kat. reaktsii, Moscow 1974, Preprint 55
[11] VÖLTER, J., LANG, B., KUHN, W.: Z. anorg. allg. Chem., **340**, 253 (1965)
[12] VÖLTER, J., HERMANN, M., HEISE, K.: J. Catal., **12**, 307 (1968)

[13] ANDERSON, J. R., KEMBALL, C.: Proc. Roy. Soc., A **226,** 472 (1954)
[14] NEKRASOV, N. V.: Dissertation, Moscow, 1974
[15] GUDKOV, B. S., SAVIN, E. P.: Izv. Akad. Nauk. SSSR, Ser. Khim., 585 (1969)
[16] ROONEY, J. J.: J. Catal., **2,** 53 1163
[17] ROONEY, J. J., WEBB, G.: J. Catal., **3,** 488 (1964)
[18] GARNETT, J. L., SOLLICH-BAUMGARTNER, W. A.: Adv. in Catalysis V. 16, p. 95 (1966)
[19] GAULT, F. G., ROONEY, J. J., KEMBALL, C.: J. Catal. **1,** 255 (1962)
[20] ZLOTINA, N. E., GUDKOV, B. S.: Izv. Akad. Nauk. SSSR, Ser. Khim., 1940 (1967)
[21] KIPERMAN, S. L.: Teor. Eksp. Khim., **12,** 16 (1976)

L. M. MAMALADZE
N. V. NEKRASOV
B. S. GUDKOV
S. L. KIPERMAN

Zelinskii Institute of Organic Chemistry, Academy of Sciences of the U. S. S. R.

Acta Chimica Academiae Scientiarum Hungaricae, Tomus 92 (1), pp. 85—87 (1977)

NITROXIDES, I

SULFONIC ESTERS OF 4-HYDROXY-2,2,6,6-TETRAMETHYL-PIPERIDINE 1-OXYL AND THEIR REACTION WITH NUCLEOPHILIC REACTANTS

K. HIDEG, O. H. HANKOVSZKY and J. TIGYI

(Central Laboratory of Chemistry and Biophysical Department, University of Pécs)

Received March 1, 1976

2,2,6,6-Tetramethylpiperidine-1-oxyl-4-sulfonates react with nucleophiles (sodium azide, sodium thiocyanate and potassium cyanide) in dimethylformamide to give the corresponding 4-substituted-2,2,6,6-tetramethylpiperidine-1-oxyl.

Researches into free radical compounds of the stable nitroxide type [1—3] and their application in biological studies [4—8] have become increasingly frequent in recent years. For these investigations, the preparation of new derivatives are desirable. We aimed at developing a synthesis by which substituents coupled directly to the hetero ring can be introduced.

4-Hydroxy-2,2,6,6-tetramethylpiperidine-1-oxyl (**1**) [3] in pyridine can readily be converted with sulfonic chlorides (**2**) into sulfonic esters(**3**). These products, when allowed to react with nucleophilic reagents in dimethylformamide, give 4-substituted derivatives (**4**). Besides the substitution reaction an elimination reaction takes place and a tetrahydropyridine derivative (**5**) is also formed.

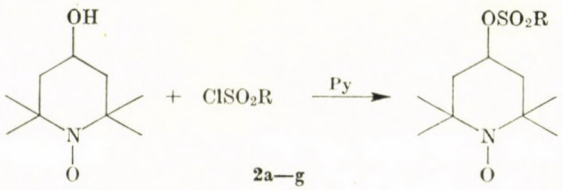

R	
a	CH_3
b	CF_3
c	CH_2CF_3
d	Ph
e	p-ClC_6H_4
f	p-BrC_6H_4
g	p-$CH_3C_6H_4$

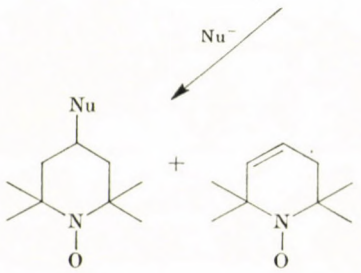

Nu	
4a	N_3
b	SCN
c	CN

Table I

Compd.	Formula (Mol. Wt.)	M. p., °C or b. p. °C/mm	Method	Yield, %	Analyses % Calcd./Found				IR[e] [cm^{-1}]
					C	H	N	S	
3a	$C_{10}H_{20}NO_4S$ (250.34)	89—90	A	85	47.98 48.10	8.05 8.02	5.60 5.49	12.81 12.76	1350, 1165—1190, (ν OSO_2—)
3b	$C_{10}H_{17}F_3NO_4S$ (304.31)	71—72	A	35	39.47 39.35	5.63 5.76	4.60 4.54	10.54 10.10	1245, 1170—1125, (ν OSO_2—)
3c	$C_{11}H_{19}F_3NO_4S$ (318.32)	98—99	A	62	41.53 41.44	6.02 6.09	4.40 4.31	10.07 10.30	1330, 1170—1135, (ν OSO_2—)
3d	$C_{15}H_{22}NO_4S$ (312.41)	121—122	A	90	57.67 57.72	7.10 7.18	4.48 4.39	10.27 10.32	1360, 1190—1170 (ν OSO_2—)
3e	$C_{15}H_{21}ClNO_4S$ (346.86)	108—110	A	92	51.94 51.98	6.10 6.45	4.04 4.13	9.25 9.45	1350, 1180—1120, (ν OSO_2—)
3f	$C_{15}H_{21}BrNO_4S$ (391.32)	122—123	A	75	46.04 46.19	5.41 5.39	3.59 3.22	8.19 8.58	1350, 1175—1119, (ν OSO_2—)
3g	$C_{16}H_{24}NO_4S$ (326.44)	114—115[a]	A	86	58.87 58.76	7.41 7.46	4.29 4.32	9.82 9.78	1350, 1180—1170, (ν OSO_2—)
4a	$C_9H_{17}N_4O$ (197.26)	70—71	B	50—70[b]	54.81 54.99	8.68 8.77	28.40 28.32	—	2110 (ν N_3)
4b	$C_{10}H_{17}N_2OS$ (213.27)	146—147	B	40—60[c]	56.32 56.65	8.04 8.06	13.13 13.04	15.01 14.89	2030 (ν SCN)
4c	$C_{10}H_{17}N_2O$ (181.26)	68—70/1 mm	B	37[d]	66.26 66.24	9.45 9.37	15.46 15.12	—	2180 (ν CN)

[a] in Ref. [1]: m. p. 115°C; [b] starting compd. (yields): **3a** (54), **3b** (60), **3c** (56), **3d** (68), **3f** (70)
[c] starting compd. (yields): **3a** (50), **3c** (40), **3f** (60). [d] from **3a**. [e] N—O appear at 1335—1370 cm^{-1}

Experimental

M.p.'s were determined with a Büchi apparatus Type SMP—20 and were uncorrected. IR spectra were recorded in Nujol mulls using a Zeiss Specord 71 spectrometer.

Method A

4-Hydroxy-2,2,6,6-tetramethylpiperidine-1-oxyl (**1**) (1.72 g; 0.01 mole) was allowed to react in dry pyridine (10 ml) with the appropriate sulfonic acid derivative (**2a-g**) (0.01 mole) at 0—10 °C, under stirring. After allowing the reaction mixture to stand for 24 hr, it was poured onto ice (300 g), stirred, and the precipitated orange solid was filtered off, washed with water and petroleum ether, and dried. The crude products can be used in the subsequent reaction without any purification. For analytical purposes the compounds were recrystallized from a mixture of chloroform and hexane. The constants of the obtained products (**3a-g**) are listed in Table I.

Method B

The appropriate sulfonic ester derivative (**3a-g**) was heated in a mixture of dimethyl formamide and water (20 ml, 1:1) with the nucleophilic reactant (NaN_3, NaSCN, or KCN) at 80 °C for 3 hr. in a flask equipped with a reflux condenser and gas outlet tube. The reaction mixture was then evaporated in vacuum. In all the three substitution reactions also a reddish oil distilled over with the solvent. This oil, which floated on the surface of the distillate in the receiver, was subjected to fractional crystallization (from hexane and petroleum ether). The resulting substance, 2,2,6,6-tetramethyl-1,2,5,6-tetrahydropyridine-1-loxyl (**5**), proved to be identical with an authentic sample synthesized in another way; m.p. 31—33 °C (lit. [9] m.p. 33 °C). The residual red oil obtained from the evaporation was diluted with water (15 ml), and extracted several times with chloroform and shaken with water (3×5 ml). The combined chloroform extracts were dried over sodium sulfate and filtered. Removal of the solvent in vacuum left an orange-red crystalline solid. The crude products (**4a-b**) were recrystallized from ether-hexane; product (**4c**) was distilled as a red oil.

The constants of the obtained products are listed in Table I.

*

Thanks are expressed to the Reanal Factory of Laboratory Chemicals, Budapest, for the support of this research and for supplying the intermediates.

REFERENCES

[1] Rozantsev, E. G.: Free Nitroxyl Radicals, Plenum Press, New York 1970
[2] Rozantsev, E. G., Sholle, V. D.: Synthesis **1971,** 190
[3] Rozantsev, E. G., Sholle, V. D.: Synthesis **1971,** 401
[4] Hamilton, C. L., McConnell, H. M.: In: Structural Chemistry and Molecular Biology (Ed. A. Rich. N. Davison), W. H. Freeman and Co., San Francisco 1968.
[5] Griffith, H. O., Waggoner, A. S.: Accounts Chem. Res., **2,** 17 (1969)
[6] McConnell, H. M., McFarland, B. G.: Quart. Rev. Biophys., **3,** 91 (1970)
[7] Chignell, C. F.: Life Sci., **13,** 1299 (1973)
[8] Likhtenshtein, G. I.: Method spinovükh metok v molekularnoj biologii. (Publisher: Izdatelstvo Nauka) Moskva, 1974
[9] Rozantsev, E. G., Goluber, V. A., Neiman, M. B.: Izv. Akad. Nauk. SSSR, Ser. Khim., **1965,** 391

Kálmán Hideg
Olga H. Hankovszky
Joseph Tigyi

H-7643 Pécs, Szigeti út 12.

Acta Chimica Academiae Scientiarum Hungaricae, Tomus 92 (1), pp. 89–97 (1977)

A NOVEL SYNTHESIS OF 12H-BENZO[A] PHENOTHIAZIN-5-OLS AND THEIR ESTERS

N. L. AGARWAL and R. L. MITAL

(Chemical Laboratories, University of Rajasthan, Jaipur-302004, India)

Received July 8, 1975;

in revised form March 21, 1976

A number of substituted 5H-benzo[a]phenothiazin-5-ones have been synthesized by the condensation reaction of 2,3-dichloro-1,4-napthoquinone with zinc mercaptides of substituted 2-aminobenzenethiols in alcohol. The substituted 12H-benzo[a]phenothiazin-5-ols were obtained in almost quantitative yields by reduction of 5H-benzo[a]-phenothiazin-5-ones. The esters of 12H-benzo[a]phenothiazin-5-ols have been synthesized by two different routes. IR and TLC data are also presented.

Though benzophenothiazine derivatives are of interest as potential carcinostatic agents [1, 2], little attention has been directed to benzophenothiazines. In the present paper we report a novel route for the synthesis of substituted hydroxybenzo[a]phenothiazines and their N-acyl and O,N-diacyl derivatives. Thin-layer chromatographic and infrared data are also presented.

It has been found that 2,3-dichloro-1,4-naphthoquinone (**I**) reacts with zinc mercaptides of substituted 2-amino benzenethiols in alcohol to give the substituted 5H-benzo[a]phenothiazin-5-ones(II) (Scheme I). These 5H-benzo [a]phenothiazin-5-ones were further reduced to the corresponding substituted

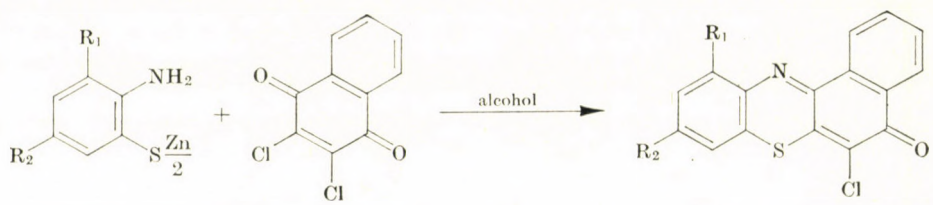

I **II**

Scheme I

12H-benzo[a]phenothiazin-5-ols (III) in very good yields with sodium hydrosultite in acetone (Scheme II).

The synthesis of esters of hydroxybenzo[a]phenothiazines have been carried out in very good yields by following two methods: (A) acetylating hydroxybenzo[a]phenothiazines with acetic anhydride and pyridine (Scheme II), (B) by the reductive acetylation of substituted 5H-benzo[a]-phenothiazin-5-ones (Scheme II).

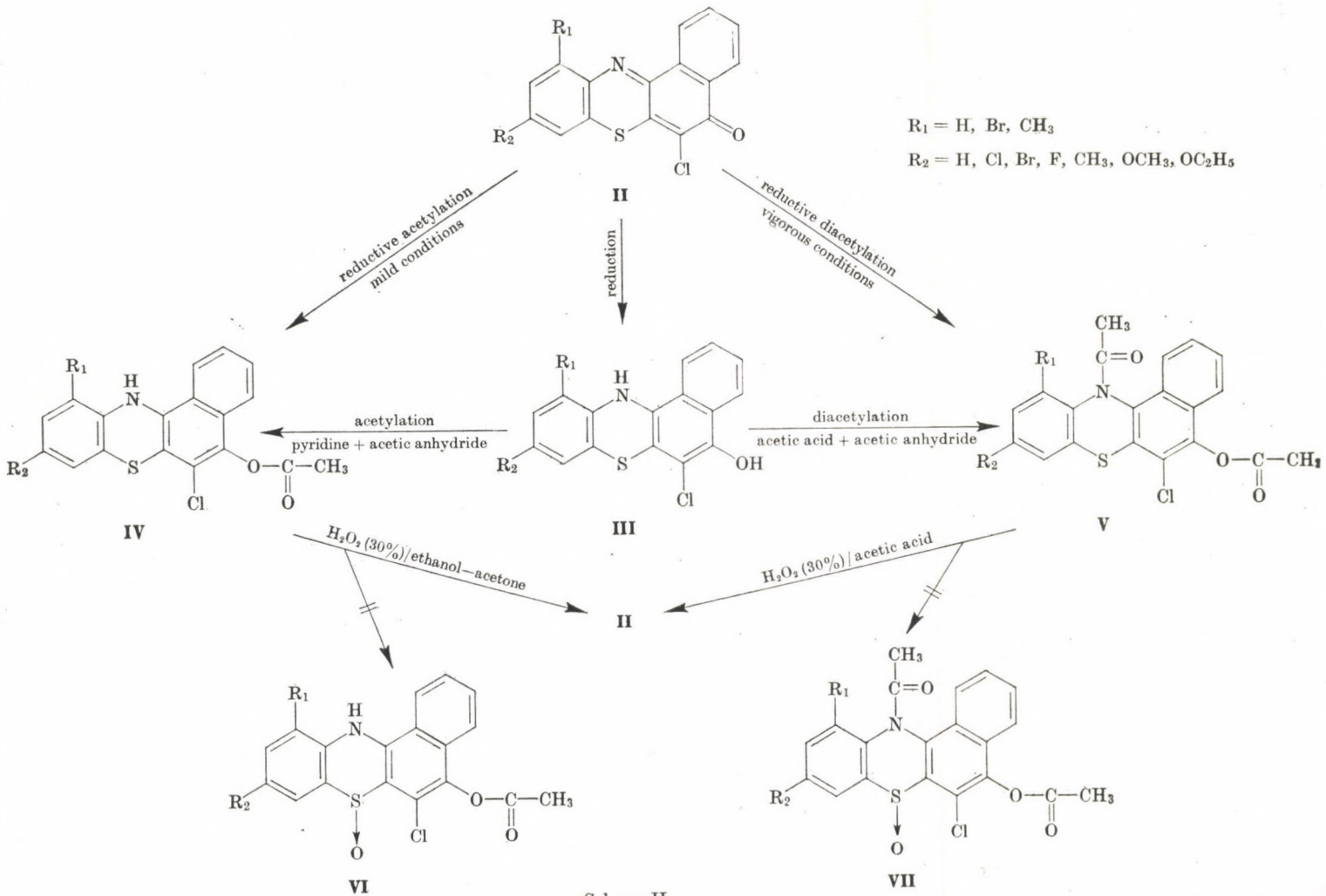
R1 = H, Br, CH3
R2 = H, Cl, Br, F, CH3, OCH3, OC2H5
reductive acetylation
mild conditions
reduction
reductive diacetylation
vigorous conditions
acetylation
pyridine + acetic anhydride
diacetylation
acetic acid + acetic anhydride
H2O2 (30%)/ethanol–acetone
H2O2 (30%)/acetic acid
II
III
IV
V
VI
VII

Scheme II

The reductive acetylation of the substituted 5 H-benzo[a]phenothiazin-5-ones (**II**) gives two series of benzo[a]phenothiazine derivatives, in which the degree of acetylation depends upon the reaction conditions. Under mild conditions, (second method A) substituted 5-acetoxy-12H-benzo[a]phenothiazines (**IV**) are obtained. However, under relatively less mild conditions (second method B) the reaction gives 5-acetoxy-6-chloro-9-methoxy-12H-benzo[a]-phenothiazine (**IVf**) and 5-acetoxy-6-chloro-9-ethoxy-12H-benzo[a]phenotiazine (**IVg**) from **IIf** and **IIg**, respectively.

The structures were established on the basis of the IR absorptions at 1742;1779 cm^{-1} (aromatic acetate) and at 3398—3470 cm^{-1} (NH, *cf.* phenothiazine 3340 cm^{-1}). More vigorous conditions (method B, yielding 5-acetoxy-12-acetyl-12H-benzo[a]phenothiazines, **V**), are required to achieve acetylation of the ring nitrogen atom (transparent in the 3μ region). The substituted 5-acetoxy-12-acetyl-12H-benzo[a]phenothiazines (**V**) have been also synthesized by the diacetylation of **III** (Scheme II, Method A). The identity of these compounds made by two different routes was substantiated by comparison of the infrared spectra, mixed melting points, and R_f values.

O,N-Acylation of **IIIh** and **IIIi** is, of course, rendered more difficult by the presence of a substituent in position 11. The loss of the N-acyl group occurs even on pouring the reaction mixture into water. This is probably owing to steric effects.

Attempts were made to convert **IV** into the corresponding substituted 5-acetoxy-12H-benzo [a] phenothiazin-7-oxides (**VI**) with H_2O_2 (30%) in ethanol–acetone under varied reaction conditions [3]. Instead of obtaining the desired product (**VI**), oxidative deacetylation occurred in each case, with the formation of **II**. When oxidation of **V** with H_2O_2 (30%) in acetic acid was tried, again oxidative deacetylation occurred, with the formation of the corresponding 5 H-benzo[a]phenothiazin-5-one (**II**) in almost quantitative yields (Scheme II). A similar conversion of 3-methoxyphenothiazine was encountered previously [4].

Experimental

The IR spectra were determined with a Beckman IR—4 and a Perkin-Elmer 337 grating infrared spectrophotometer in KBr discs and nujol mulls, respectively. All m.p.'s are uncorrected. The purity of compounds was the checked by TLC on Silica Gel G (Merck) in various non- aqueous solvent systems. Acetone, 1,4-dioxane, tetrahydrofuran, *n*-butanol, carbon tetrachloride, isopropyl alcohol, *o*-dichlorobenzene, toluene, benzene, hexane and cyclohexane were carefully dried and purified. TLC was done by the standard method. [5].

Substituted 5H-benzo [a] phenothiazin-5-ones (II)

A mixture of 2,3-dichloro-1,4-naphthoquinone (0.01 mole) and the zinc thiolate of the appropriate substituted 2-aminobenzenethiol (0.005 mole) in dry ethanol (100 ml) was stirred for 1 hr at room temperature. In most cases the colour of the solution changed to orange-red; it was then refluxed for 2 hrs. The solid which deposited on cooling was filtered off, washed with 5% hydrochloric acid (ca. 500 ml) and water. Analytical samples were obtained by recrystallization from a suitable solvent (Table I.)

Table I

Substituted 5H-benzo[a]phenothiazin-5-ones (II)

No.	R_1	R_2	M. p. °C	Solvent of recrystn.	Yield, %	Formula***
IIa	H	H	232	benzene	84	$C_{16}H_8ClNOS$
IIb	H	Cl	282	benzene	82	$C_{16}H_7Cl_2NOS$
IIc	H	Br	274	benzene	80	$C_{16}H_7BrClNOS$
IId	H	F	277	toluene	81	$C_{16}H_7ClFNOS$
IIe	H	CH_3	242	toluene	87	$C_{17}H_{10}ClNOS$
IIf	H	OCH_3	298	acetone	75	$C_{17}H_{10}ClNO_2S$
IIg	H	OC_2H_5	292	chloroform	77	$C_{18}H_{12}ClNO_2S$
IIh	Br	CH_3	dec. 262—265	benzene	70	$C_{17}H_9BrClNOS$
IIi	CH_3	CH_3	254	toluene	83	$C_{18}H_{12}ClNOS$

νmax., cm^{-1}*						R_f value			Spot colour in sunlight
A	B	C	D	E	F	X**	Y	Z	
3040	1645	1520	1289	—	760	0.58	0.70	0.69	orange-red
3050	1645	1520	1304	815	770	0.60	0.74	0.62	orangre-red
3050	1645	1520	1305	825	775	0.57	0.72	0.64	orange-red
3050	1645	1529	1300	822	774	0.58	0.71	0.63	orange-red
3100	1645	1520	1300	820	745	0.59	0.73	0.64	bronze
3050	1645	1520	1295	820	775	0.55	0.69	0.62	bronze
3100	1645	1520	1300	825	775	0.57	0.70	0.63	orange-red
3050	1645	1520	1300	—	775	0.53	0.61	0.58	bronze-red
3050	1645	1520	1305	—	770	0.54	0.68	0.59	bronze-red

* A: aromatic C—H stretching; B: C = O stretching; C: C = N stretching; D: Ph—N stretching in tertiary amines; E: 1, 2, 4-trisubstitution; F: 1, 2-disubstitution

** Solvent systems X: chlorobenzene–1,4-dioxane (90 : 10); Y: chlorobenzene–*n*-butanol (50 : 50); Z: chlorobenzene–*n*-butanol (80 : 20)

*** Satisfactory C, H, N and S analyses have been obtained in all cases

Table II

Substituted 12H-benzo[a]phenothiazin-5-ols (III)

No.	R_1	R_2	M. p., °C	Yield, %	Formula***	A	B
IIIa	H	H	165	90.5	$C_{16}H_{10}ClNOS$	3425	3040
IIIb	H	Cl	167	90.6	$C_{16}H_9Cl_2NOS$	3448	3058
IIIc	H	Br	152	92.8	$C_{16}H_9BrClNOS$	3425	2040
IIId	H	F	157	95.5	$C_{16}H_9ClFNOS$	3413	3049
IIIe	H	CH_3	166	84.6	$C_{17}H_{12}ClNOS$	3360	3049
IIIf	H	OCH_3	168	85.4	$C_{17}H_{12}ClNO_2S$	3448	3040
IIIg	H	OC_2H_5	155	79.1	$C_{18}H_{14}ClNO_2S$	3410	3030
IIIh	Br	CH_3	180	80.4	$C_{17}H_{11}BrClNOS$	3413	3040
IIIi	CH_3	CH_3	144	81.6	$C_{18}H_{14}ClNOS$	3435	3049

νmax. (cm^{-1})*					R_f value			Spot colour in sunlight
C	D	E	F	G	X**	Y	Z	
1302	1030			751	0.73	0.64	0.57	light yellow
1292	1031	882	882	752	0.78	0.67	0.59	light yellow
		868		731				
1299	1031	883	820	755	0.83	0.66	0.56	yellow
		860		725				
1292	1030	883	828	775	0.84	0.69	0.61	yellow
			813	752				
1290	1029	880	840	772	0.82	0.65	0.57	light pink
			820	754				
1299	1066	880	846	772	0.72	0.55	0.56	pink
			820	753				
1299	1042	885	847	773	0.76	0.63	0.58	light yellow
		866	828	730				
1289	1075	883		752	0.74	0.60	0.60	yellow
1305	1006	892		776	0.75	0.61	0.59	pink
				753				
				725				

* A: N—H and O—H stretching; B: aromatic C—H stretching; C: C—N stretching; D: C—O linkage; E: an isolated ring hydrogen atom; F: vicinal pair of hydrogen atom; G: 1,2-disubstitution

** Solvent systems X: acetone–cyclohexane (50 : 50) Y: tetrahydrofuran–benzene (30 : 70) Z: 1,4-dioxane–toluene (30 : 70)

*** Satisfactory C, H and N analyses have been obtained in all cases

Substituted 12H-benzo[a]phenothiazin-5-ols (III)

A mixture of the substituted 5H-benzo[a]phenothiazin-5-one (0.005 mole), sodium hydrosulfite (2 g) water (5 ml) and acetone (50 ml) was refluxed for 80 min. The mixture, which had turned from orange-red to colourless, was allowed to cool and poured into a solution of sodium dithionite (5 g) in cold water (1 litre). The resulting yellow-white solid was washed with water, dried in vacuum and crystallized from toluene to give the corresponding substituted 12H-benzo[a]phenothiazin-5-ol.

Recrystallization from benzene-ligroin gave samples of analytical purity as white or yellow needles (Table II). The above experiments were carried out under dry nitrogen and in the absence of strong, direct light. The compounds were stored in specially designed coloured tubes to avoid contact with air and light.

Substituted 5-acetoxy-12H-benzo[a]phenothiazines (IV) First method: acetylation of the substituted 12H-benzo[a]phenothiazin-5-ols (III)

A mixture of the substituted 12H-benzo[a]phenothiazin-5-ol (0.005 mole), pyridine (40 ml), sodium dithionite (3g) and acetic anhydride (1.58 ml) was stirred for 2.5 hr at room temperature, concentrated to 30 ml and poured into 500 ml of cold water. The resulting solid was collected, washed with water, dried and recrystallized from benzene–petroleum ether (b.p. 60—80 °C) to obtain **IV**.

Second method (A): reductive acetylation of the substituted 5H-benzo[a]phenothiazin-5-ones (II)

A mixture of **II** (0.005 mole), acetic anhydride (35 ml) and pyridine (2 ml) was shaken with zinc dust (2 g), stirred at room temperature for 15 min and then warmed on a water bath at 100 °C for 3 min. The pale yellow solution was separated from the excess of zinc dust by filtration and poured on ice to obtain a light yellow precipitate.

The solid was extracted in chloroform and the solution washed with saturated aqueous sodium hydrogen carbonate and water, and then dried (Na_2SO_4). Evaporation of the solvent gave a crystalline residue, which after recrystallization from benzene–petroleum ether (b.p. 60—80 °C) provided an analytical sample of the substituted 5-acetoxy-12H-benzo[a]phenothiazine (Table III).

Second method (B): 5-Acetoxy-6-chloro-9-methoxy- and 5-acetoxy-6-chloro-9-ethoxy-12H-benzo[a]phenothiazines

The appropriately substituted 5H-benzo[a]phenothiazin-5-one (0.005 mole) in acetic anhydride (30 ml) and pyridine (2 drops) was shaken with zinc dust (500 mg) at room temperature for 30 min. The colourless solution was separated from the excess zinc dust by decantation and poured on ice; the resulting solid was purified in the usual way (Table III).

5-Acetoxy-12-acetyl-12H-benzo[a]phenothiazines (V) method A: O,N-Diacetylation of substituted 12H-benzo[a]phenothiazin-5-ols (III)

A mixture of the substituted 12H-benzo[a]phenothiazin-5-ol (0.01 mole), acetic anhydride (25 ml), glacial acetic acid (25 ml) and sodium dithionite (3 g) was refluxed for 3 to 5 hr; it was then poured on crushed ice and allowed to stand for 12 hr at 5 °C. The solid was collected by filtration and washed with sodium carbonate solution. Analytical samples were obtained by recrystallization from benzene–petroleum ether (b.p. 60—80 °C).

Method B: Reductive diacetylation of the substituted 5H-benzo[a]phenothiazin-5-ones (II)

A mixture of the 5H-benzo[a]phenothiazin-5-one (0.01 mole), acetic anhydride (50 ml) and pyridine (5 ml) was stirred with an excess of zinc dust at room temperature for 10 min. The pale yellow liquid was then refluxed for 45 min. The hot solution was filtered into crushed ice, where upon a solid precipitated. This was extracted with chloroform and the solution washed

Table III

Substituted 5-acetoxy-12H-benzo[a]phenothiazines (IV)

No.	R_1	R_2	M. p., °C	Yield, %	Formula***	νmax. (cm⁻¹)*	
						A	B
IVa	H	H	211	75.6[a]	$C_{18}H_{12}ClNO_2S$	3400	1762
IVb	H	Cl	220	80.4[a]	$C_{18}H_{11}Cl_2NO_2S$	3470	1779
IVc	H	Br	222	73.5[a]	$C_{18}H_{11}BrClNO_2S$	3410	1748
IVd	H	F	215	82.4[a]	$C_{18}H_{11}ClFNO_2S$	3450	1742
IVe	H	CH_3	212	82.6[a]	$C_{19}H_{14}ClNO_2S$	3415	1750
IVf	H	OCH_3	186	79.6[b]	$C_{19}H_{14}ClNO_3S$	3428	1764
IVg	H	OC_2H_5	185	78.6[b]	$C_{20}H_{16}ClNO_3S$	3450	1745
IVh	Br	CH_3	187	71.5[a]	$C_{19}H_{13}BrClNO_3S$	3398	1762
IVi	CH_3	CH_3	174	69.4[a]	$C_{20}H_{16}ClNO_2S$	3448	1767

νmax. (cm⁻¹)*				R_f value			Spot colour in sunlight
C	D	E	F	X**	Y	Z	
1210			757	0.47	0.80	0.63	yellow
			750				
			721				
1205	907	855	743	0.45	0.84	0.64	light yellow
		810	710				
1200	906	855	746	0.50	0.87	0.65	light yellow
		806	710				
1209	893	833	760	0.47	0.86	0.64	light yellow
	877	825	745				
1200	885	845	750	0.48	0.83	0.67	yellow
		825	720				
			700				
1206	909	830	741	0.38	0.82	0.64	yellow
	873	792	724				
1217	910	791	741	0.44	0.84	0.66	yellow
	866		719				
1200	910		770	0.62	0.84	0.80	yellow
			750				
1196	909		746	0.58	0.79	0.77	pink
	878		719				

* A: N—H stretching; B: C = O stretching; C: C—O linkage; D: an isolated ring hydrogen atom; E: 1,2,4-trisubstitution; F: 1,2-disubstitution

** Solvent systems; X: tetrahydrofuran–hexane (40 : 60); Y: isopropyl alcohol–benzene–carbon tetrachloride (40 : 40 : 20); Z: *n*-butanol–*o*-dichlorobenzene–hexane (10 : 20 : 70)

*** Satisfactory C, H analyses have been obtained in all cases

[a] yields by second method A; [b] yields by second method B

Table IV

5-Acetoxy-12-acetyl-12H-benzo[a]phenothiazines (V)

No.	R^1	R^2	M. p., °C	Yield, %	Formula****	A	B
Va	H	H	137—139*	89.4[a]	$C_{20}H_{14}ClNO_3S$	1778	1682
Vb	H	Cl	158	69.9[a]	$C_{20}H_{13}Cl_2NO_3S$	1779	1689
Vc	H	Br	125—127*	85.4[a]	$C_{20}H_{13}BrClNO_3S$	1783	1695
Vd	H	F	205	87.5[a]	$C_{20}H_{13}ClFNO_3S$	1757	1667
Ve	C	CH_3	172	85.3[a]	$C_{21}H_{16}ClNO_3S$	1742	1669
Vf	H	OCH_3	182	80.4[a]	$C_{21}H_{16}ClNO_4S$	1773	1684
Vg	H	OC_2H_5	126—28*	78.8[a]	$C_{22}H_{18}ClNO_4S$	1786	1681

νmax. (cm^{-1})**				R_f value			Spot colour in sunlight
C	D	E	F	X***	Y	Z	
1180			749	0.70	0.86	0.87	pink
			690				
1190	891	835	768	0.74	0.87	0.88	light pink
	870	820	762				
		794	735				
1190	890	820	762	0.72	0.85	0.84	light pink
	867		735				
1206	908	859	755	0.71	0.84	0.70	light pink
	871		746				
			717				
1196	905	833	758	0.65	0.87	0.65	pink
	886	806	741				
			719				
1190	892	838	761	0.55	0.82	0.52	pink
	867	827	742				
1189	866	826	758	0.57	0.85	0.55	yellow
		793	741				
			722				

* Foaming

** A: C = O (aromatic acetate); B: C = O (N-acetyl); C: C—O linkage; D: an isolated ng hydrogen atom; E: 1, 2, 4-trisubstitution; F: 1, 2-disubstitution

*** Solvent systems; X: tetrahydrofuran–hexane (40 : 60); Y: isopropyl alcohol–benzene -carbon tetrachloride (40 : 40 : 20); Z: *n*-butanol–*o*-dichlorobenzene–hexane (10 : 20 : 70)

**** Satisfactory C, H and N analyses have been obtained in all cases

[a] Yields by method B

with saturated aqueous sodium hydrogen carbonate and water, and then dried (Na_2SO_4). Evaporation of the solvent left a crystalline residue, which after repeated recrystallization from petroleum ether (b.p. 80 —100 °C) provided a sample of analytical purity of the substituted 5-acetoxy-12-acetyl-12H-benzo[a]phenothiazine (Table IV).

Oxidative deacetylation of substituted 5-acetoxy-12H-benzo[a]phenothiazines (IV)

A solution, of the substituted 5-acetoxy-12H-benzo[a]phenothiazine (0.016 mole) 30% H_2O_2 (11.6 ml), ethanol (50 ml) and acetone (100 ml) was refluxed for 3 hr, concentrated and poured into water. The precipitate was filtered off and washed with hot water to give, in each instance, an almost quantitative yield of the corresponding 5H-benzo[a]phenothiazin-5-one. These phenothiazones were identical in every respect with the authentic samples.

Oxidative deacetylation of substituted 5-acetoxy-12-acetyl-12H-benzo[a]phenothiazines (V)

A cooled solution of **V** (0.01 mole) in glacial acetic acid (50 ml) was mixed with 30% H_2O_2 (11.6 ml). The mixture was then refluxed for 4 hr and the resulting solution was poured in water to give, in each case, an almost quantitative yield of the corresponding 5H-benzo[a] phenothiazin-5-one.

REFERENCES

[1] SHIRLEY, D. A., GILMER, J. C., WATERS, W. D.: J. Chem. Soc., **1964,** 5260
[2] SHIRLEY, D. A., SEN, K., GILMER, J. C.: J. Org. Chem., **26,** 3587 (1961)
[3] NODIFF, E. A., HAYAZAKI, T., ITO, T., SHARMA, H. L., KOHNO, T., UEDA, T., MOROSAWA, S., MANIAN, A. A.; Unpublished work
[4] BODEA, C., RAILEANU, M.: Acad. Rep. Populare, Romîne, Filiali Cluji, Studii cercetari chim., **11,** 325 (1960)
[5] AGARWAL, N. L., MITAL, R. L.: J. Chromatogr., **115,** 264 (1975)

NAND LAL AGARWAL
R. L. MITAL
B-30, Prabhu Marg, Tilak Nagar Jaipur
302004, India.

RECENSIONES

An Introduction to Spectrometric Methods for the Identification of Organic Compounds

Vols 1 and 2. Edited by F. SCHEINMANN, Pergamon Press, London 1970 and 1974, pp. 201+345. US $ 8.50+12.00 (hard cover); 5.00+7.00 (flexi).

This compilation written by a team of specialists is meant for post-graduate students and interested non-specialists. It covers the most important spectroscopic techniques generally accessible in a well-equipped department: NMR, ESR, IR, UV and MS. The presentation is very practical: for each technique there is a short introduction to the pertinent theory, then applications, worked examples, seminar problems with amply commented answers and finally correlation tables and data collections follow. This latter is a very useful feature which keeps the book on the shelf even after the text has been read and the problems solved. The theoratical introductions, though short are free of oversimplifications and there are several useful comments on how misinterpretations and unjustified conclusions can be avoided.

In the Referee's opinion the chapters on NMR, IR and MS are the best. That on UV is marred by several small errors and sections on ESR go beyond the general scope of the book.

In summary the volumes can be recommended not only to those who wish to get an introduction to spectroscopic methods in organic chemistry but also to those who would like to obtain a reference book on this subject at a very reasonable price.

M. NÓGRÁDI

Topics in Flavonoid Chemistry and Biochemistry

Proceedings of the Fourth Hungarian Bioflavonoid Symposium, Keszthely 1973

Edited by L. FARKAS, M. GÁBOR and F. KÁLLAY

Akadémiai Kiadó, Budapest and Elsevier Publ. Co., Amsterdam 1975, 286 pages.

Hungarian chemists have traditionally played a prominent part in flavonoid chemistry. Recognition of this work is reflected by the international attendance at the Bioflavonoid Symposia held periodically in Hungary.

The collection of papers presented at the Fourth Symposium covered many topics of current interest. MARINI-BETTÓLO reported the isolation of novel compounds in the recently discovered group of natural prenylated flavonoids. Hungarian chemists made important contributions to flavonoid synthesis, such as the development of a new isoflavone synthesis (FARKAS *et al.*) and a comprehensive study of the oxidation of flavonoids (BOGNÁR *et al.*). Some novel reactions on the flavonoid C-4 atom (KÁLLAY) and on the isoflavonoid C-4 atom (SZABÓ *et al.*), as well as in the field of N-containing rings (JANZSÓ, BOGNÁR *et al.*) should to be mentioned. DONELLY's review gives a complete and up-to-date picture of the interconversion of the neoflavonoids and of the isoflavonoids.

Papers on ^{13}C—NMR (WEINGES) and mass spectroscopy (WAGNER *et al.*) illustrate the modern techniques applied to flavonoid research.

Up-to-date accounts are given on the biochemistry of plant proanthocyanidins (HASLAM), on the metabolism (GRIFFITHS, GÁBOR, FÖRSTER), the biological behaviour (SCHULTZ *et al.*, BÉLÁDI *et al.*) and on the antioxidant effects (SZ. GÁBOR) of flavonoids.

The many facets of flavonoid chemistry presented at the symposium well illustrates the growing interest of chemists for this field, first of all for the biological aspects.

Á. GOTTSEGEN

M. G. HALPERN: *Synthetic Paper from Fibers and Films*

Noyes Data Corp. New Jersey—London 1975. (Chemical Technology Review No. 52) 265 pages

Synthetic papers still represent at present an insignificant part in paper manufacture. However, since artificial and synthetic fibers are also used in addition to wood pulp and cotton for their manufacture, the end-product can be provided with special properties. This explains why, in spite of the small amount manufactured, synthetic papers are already today of great importance for certain purposes. Such advantageous properties are the high wet strength, toughness, chemical resistance, resistance to weather, stability of colour and excellent dimensional stability. The most important fields of application are map paper, industrial filter paper, etc.

In recent years, many publications appeared in the literature on the manufacture of synthetic papers. However, the present book has the great merit of covering 122 patents relevant to the manufacture of synthetic paper. Owing to its quick publication, it includes up to the end of 1974 practically all of the recent patents. Similarly to other publications of the Noyes Data Corporation, the single patents are described in detail. Patents are discussed in a grouping, so as to give an overall picture on the various raw materials and technologies used.

The book covers the following subjects:
Cellulose derivatives;
Synthetic papers manufactured from polyacrylnitril fibers;
Paper manufactured from polyamide fibres;
The use of other synthetic fibers;
The paper manufacturing technology of various synthetic fibers;
Synthetic paper made of films containing olefinic resins;
Synthetic paper made of films containing other resins.

The manufacturing technologies and part of the additives of synthetic paper production can be used also in classical paper manufacture, so that the book will be of interest to a broad field of readers.

The handling of the book is facilitated by the fact that the patents are listed according to the manufacturing firm, the inventor and the number.

P. LENGYEL

C. L. KHETRAPAL, A. C. KUNWAR, A. S. TRACEY: *Lyotropic Liquid Crystals*

Basic Principles and Progress, Vol. 9.

Editors: P. DIEHL, E., FLUCK, R. KOSFELD. Springer-Verlag, Berlin 1975.

Lyotropic liquid crystals have been poorly understood. This review summarizes the results obtained recently by NMR studies of such systems.

The first part (16 pages) of the book is an introduction dealing with the characteristics of lyotropic liquid crystals and with the basic principles of NMR spectroscopy applied to this field.

Part I acquaints the reader with the spectra and spectral parameters of lyotropic phases and of molecules dissolved in nematic lyotropic phases. The problems of the Hamiltonian,

of direct and dipolar couplings, the structural informations obtained from the chemical shift anisotropy, anisotropic contribution, indirect spin–spin couplings and the quadrupole interactions are discussed.

The experimental part of this chapter reviews the preparation of samples for NMR measurements. (Commonly available high-resolution, wide-line, pulsed and Fourier transform spectrometry is used.)

In Part II (27 pages) studies of lyotropic liquid crystals are described in detail.

The investigation of lyotropics is particularly important since these systems have fairly well-defined physical and chemical properties, and can serve as models for the more complicated biological systems. Studies of the state of water molecules, their motion and diffusion, the mobility of the alkyl chains and binding of small ions in the various phases have been made.

Line shape and line width, chemical shift and dipole coupling, relaxation time and quadrupolar interaction data have been used in the structure elucidation and in attempts to understand these systems. PMR and DMR spectra provide informations on the state of water adsorbed on fibrous materials. This part also includes chapters devoted to self-diffusion in lyotropic liquid crystals (soaps, synthetic polypeptides and lecithin systems), interactions of ions in anisotropic media (ion bonding, ion competition, halide ions, alkali ions, proton, deuterium and anisotropic phases).

The last chapter of part II is a brief introduction to sonicated lamellar systems. An appendix to this part gives a very well arranged table of the reported systems.

Part III (27 pages) contains NMR studies of molecular and ionic species dissolved in the nematic mesophase of lyotropic liquid crystals. Order in nematic lyotropic phases as well as some general comments concerning the order parameter can be found here as well. A chapter of molecular and ionic species in aqueous phases provide some interesting data concerning the preferred orientations of benzenes and related compounds. An appendix belonging to this part lists the compounds studied.

At the end of the book 461 references are given.

Though this book deals with a special application of NMR spectroscopy, the biological importance of lyotropic liquid crystals, occurring abundantly in all living systems, predicts an accelarating development and increasing interest for this topic. The first review of this field will be useful for all scientists, who wish to expand their knowledge in this direction.

P. SOHÁR

Topics in Current Chemistry, Vol. 59

Springer-Verlag, Berlin, Heidelberg, New York 1975. 136 pages

Volume 59 of the series deals with four subjects. Although the subject-matter of the book is not homogeneous, the distribution is very proportional: two chapters are characterized by rather practical importance and the two others are of more theoretical character.

The first review ("Use of Activated Metals in Organic and Organometallic Synthesis") is devoted to a topic of organic chamistry that is always actual, also at the level of the synthetic laboratory. Of the most frequently used activated metals (Mg, Zn) the reader obtains an abundant list of references and a good review of their reactions. The more rarely used metals (Cd, Tl) are also discussed; *e.g.*, the direct preparation of organocadmium reagents that previously have been made in general, by means of an intermediate Grignard reaction, is particularly interesting.

The second chapter of the book ("New Directions in Aromatic Nucleophilic Substitution") reflects two principal trends. One of them is the use of such substances that ensure relatively very mild circumstances for reactions requiring forced conditions when carried out in the classical way (use of crown ethers; aprotic polar solvents). The other dominant topic of the chapter is the transfer to heterocycles of particular reactions known firstly in benzene chemistry; an example is the excellent review on hetarynes.

The third chapter ("Formation and Reactions of Aminyloxides") is a section of organic chemistry that can owe its development first of all to ESR spectroscopy. An interesting feature of this group of compounds is that the energy content of the aminyloxides is very low, thus they are readily formed and retain their free radical character in the course of reactions.

The last chapter of the book ("Cyclobutadienoids") deals also with a relatively new field of organic chemistry. The reader obtains a review about the most recent developments of the "cyclobutadiene problem" and, in addition, about all the possibilities of structural stabilization (substitutions, benzo- and heterocyclobutadienes). Another detailed section is devoted to the biphelylenes. However, the number of examples illustrating the reactions of cyclobutadienoid compounds is relatively low.

In conclusion it can be stated that this book, like the previous volumes of the series, presents several topics of actual interest for both the theoretical and the practical organic chemist. The chapters are generally lucid and easy to survey; it appears, however, that the review on aminyloxides may contain a redundant number of examples that make the review a little complex, particularly as far as conciseness is concerned.

E. KASZTREINER

Analytical Aspects of Mercury an Other Heavy Metals in the Environment

Editors Roland W. FREI and O. HUTZINGER, Gordon and Breach Sci. Publ. 1975, pp. 196

The book belongs to the series Current Topics in Environmental and Toxicological Chemistry, a collection of papers published in Int. J. Environmental Chemistry Vol. 1, and in Toxicological and Environmental Chemistry Reviews Vol. 1.

Compounds of mercury and other heavy metals like lead, cadmium, antimony, etc., give rise to pollution of the environment in increasing amounts owing to their industrial application and the enormous progress in the chemistry of agricultural production. This process may lead to unpredictable consequences, owing to their action on human organism, and the same holds for the balance in the whole living system on the earth, since most of these metals are seriously toxic. The book consists of twelve chapters, each being an indepedent article in itself. Five of them deal with the utilization and application of organic and inorganic mercury compounds, their detection in air, waste water and the environment (J. G. SAHA). The application of mercury in both industry and agriculture is discussed in detail, and the degree of pollution in the environment and in food products today in the economically developed countries all over the world is estimated. Literature data are used to illustrate the individual analytical methods and these are compared and their applicability evaluated.

A separate chapter is devoted to the mass spectrometric detection of organic mercury compounds (mainly methylmercury dicyandiamide) used as fungidices in corn, since direct utilization of treated corn for consumption has led to large-scale poisoning several times, therefore, special attention must be paid to the determination of the "no-effect level". Other chapters deal with the detection of mercury in air, water and waste water. The paper written by A. ZDROJEWSKI reviews new methods of the determination of lead, that is, the new radiochemical selective method developed in order to substitute for the neutron activation method. The new procedure is suitable for the detection of 0.01 μg of lead in air. The other new technique described is the ASP method (anodic stripping polarography) suitable for the determination of lead, cadmium, copper and zinc in biological materials, too. B. E. SCHREIBER described the atomic absorption spectroscopic technique elaborated for the determination of trace amounts of antimony. Two other papers deal with the determination of transition metals by the atomic absorption technique and the detectability of trace elements in biological materials. The most comprehensive article in the book describes activation analysis and the application of this technique in research on the contamination of the environment with metals.

The book is a valuable help for all researchers engaged in determination and detection of heavy metals in the field of biology, geology, toxicology or pharmacology.

K. LEHOTZKY

Quantitative Structure–Activity Relationships.

Proceedings of the Conference on Chemical Structure–Biological Activity Relationships: Quantitative Approaches
Edited by M. TICHY, Akadémiai Kiadó, Budapest 1976. pp. 265.

Biology is becoming more and more quantitative. This book provides a proof through more than 30 original contributions on methods and models of quantitative structure–activity relationships. Five plenary lectures, followed by special reports, treat the various aspects of the field.

Mathematical empirical models (Free–Wilson, four-parameter equation, Hansch approach) are introduced by W.P. PURCELL. Protein binding, the role of dissolution rate, substructural analysis, toxicity, and the activity of several types of compounds are discussed in the subsequent papers.

Statistical approaches in fitting models are dealt with by S. WOLD.

In the third chapter correlations between various physicochemical properties and biological activities are treated. An introductory talk is given by V. A. FILOV.

The fourth chapter deals with correlations between electronic indices and biological activity. L. B. KIER gives here a survey on his conformational studies using the extended Hückel method. MO-methods, like the simple Hückel, EHT, CNDO/2 and the precise but elaborate *ab initio* one, are applied to a lot of problems.

The last section (introductory talk by R. ZAHRADNIK on calculations of Henry constants and partition coefficients) discusses some characteristics used in the correlations, from the quantum chemical point of view.

Nobody, working on any field of molecular biology or pharmacology, will find this work uninteresting. The reliability of the biological models given here, may need, in general, further confirmation. However, it is proved that statistics and quantum chemistry can be applied with success in biology.

G. NÁRAY-SZABÓ

INDEX

ANALYTICAL CHEMISTRY

Ion-Exchange Behaviour of Stannic Antimonate, Separation of Some Metal Ions of Analytical Importance, J. MATHEW, S. N. TANDON 1

PHYSICAL AND INORGANIC CHEMISTRY

Crystal and Molecular Structure of Decamethylbicyclo-Hexasiloxane, $Si_6O_7C_{10}H_{30}$, GY. MENCZEL 9

Structure of Vanadium–Phosphorus Oxide Catalysts, K. C. KHULBE, R. S. MANN 17

Bis-vanillin-*o*-phenylene Diamine Complexes of Rare-Earths, M. SHAMEEM ANSARI, NASEER AHMAD 27

Empirical Correlation Between the Potential Energy of Bond Dissociation and Bond Length, T. BÉRCES 31

[illegible] and Magnetic Studies on Copper (II) Complexes of Indazoles, S. A. A. ZAIDI, A. S. FAROOQI, NEELAM SINGHAL 49

Ionization of Inorganic Acid Anhydrides and Acid Halides in Chlorosulphuric Acid. Formation of Oxycations, S. A. A. ZAIDI, Z. A. SIDDIQI 57

The Relation Between Resonance Energy and Molecular Structure, I. GUTMAN 65

ORGANIC CHEMISTRY

On the Mechanism of the Hydrogenation and Isotopic Exchange in the Alkylaromatic Hydrocarbons–Substituted Cycloalkanes System on Nickel, L. M. MAMALADZE, N. V. NEKRASOV, B. S. GUDKOV, S. L. KIPERMAN 73

Nitroxides, I. Sulfonic Esters of 4-Hydroxy-2,2,6,6-tetramethyl-piperidine 1-oxyl and Their Reaction with Nucleophilic Reactants, K. HIDEG, O. H. HANKOVSZKY, J. TIGYI 85

A Novel Synthesis of 12H-Benzo[a]Phenothiazin-5-ols and Their Esters, N. L. AGARWAL, R. L. MITAL 89

Recensiones 99

Printed in Hungary

A kiadásért felel az Akadémiai Kiadó igazgatója. Műszaki szerkesztő: Zacsik Annamária

A kézirat nyomdába érkezett: 1976. IX. 28. — Terjedelem: 9,45 (A/5) ív, 28 ábra

77.3654 Akadémiai Nyomda, Budapest — Felelős vezető: Bernát György

ACTA CHIMICA

ТОМ 92 — ВЫП. 1.

РЕЗЮМЕ

Ионнообменное поведение антимоната олова(IV)

ДЖ. МАТЬЮ и С. Н. ТАНДОН

Образцы антимоната олова(IV) были приготовлены в различных условиях высаждения. Приводятся их свойства, состав, ионнообменное поведение и функциональность поверхности. Были построены графики зависимости log K_d от pH в случае ионов Rb^+, CS^+, Tl^+, Ca^{+2}, Zn^{+2} и Tl^{+3}. Были определены коэффициенты распределения для 27 ионов металлов и достигнуты некоторые разделения, важные как с аналитической, так и с радиохимической точек зрения. Данные, полученные для антимоната олова(IV), сравнивались с данными для других антимонатов.

Кристаллическое и молекулярное строение декаметилбициклогексасилоксана

ДЬ. МЕНЦЕЛ

Кристаллическое и молекулярное строение одного изомера полициклических метилсилоксановых олигомеров T_2D_4 ($Si_6O_7C_{10}H_{30}$) было определено с помощью рентгенодифракционного анализа. Кристалл относится к моноклинической группе типа $P2_1/c$ со следующими данными ячейки: a = 8,32, в = 12,72, c = 23,24Å, β = 98,9°. Строение было определено прямым методом, используя программу LSAM [4]. Конечный остаток 0,1 был достигнут для 817 фотографически зарегистрированных рефлексий с ненулевой интенсивностью. Малое число измеренных рефлексий вызвано летучестью вещества. Молекула имеет закрытую структуру. Это комбинация восьмичленных колец с семичленными полукольцами. Молекула обладает псевдосимметрией около мм2. Большая величина угла Si—O—Si (170°) является особенно характерной для данной структуры. Средняя величина остальных углов шести Si—O—Si равна 150°.

Структура катализаторов ванадий — окись фосфора

К. С. ХУЛЬБЕ и Р. С. МАНН

Были произведены рентгенографические, ИК и ЭПР исследования с катализаторами ванадий — окись фосфора. Наблюдалось образование новой фазы при отношении P/V, превышающем 0,5. ИК исследования указывают на образование нового соединения V—P—O. Исходя из наблюдаемых растягивающих колебаний P—O, фосфорные ионы имеют различные степени конденсации. Было найдено, что при добавлении фосфатного иона к V_2O_5 полоса V—O—V (при 822 $см^{-1}$) исчезает, однако, никакого заметного эффекта не наблюдалось в полосе V = O (при 1020 $см^{-1}$) вплоть до отношений P/V, равным 0,5. Добавление фосфата как примеси к V_2O_5 дает сигнал ЭПР, приписываемый ионам VO^{+2}. Его интенсивность и форма зависят от концентрации фосфата. Для отношений P/V, бóльших 2, наблюдалось суживание сигнала ЭПР. Было заключено, что новое соединение представляет собой фосфат ванадия.

Комплексы бис-ванилин-о-фенилендиамина с редкоземельными металлами

М. Ш. АНСАРИ и Н. МАХАД

Бис-ванилин-о-фенилендиамин реагирует с ионами иттрия(III) и лантанидов(III) (за исключением прометия и лютеция), давая продукты с составом 1 : 1 и с общей формулой $C_{22}H_{18}N_2O_4MCl \cdot 3H_2O$. Молярная проводимость указывает на то, что это электролиты 1 : 1 и кривые термогравиметрического анализа свидетельствуют о трех координированных молекулах воды. На ИК спектрах обнаружен сдвиг полос C=N и C—O к более высоким частотам при комплексообразовании. Координирование происходит таким образом через два атома азота и оба кислорода фенольных (OH) групп, делая ионы редкоземельных металлов гептакоординированными.

Эмпирическая зависимость между потенциальной энергией диссоциации связи и длиной связи

Т. БЕРЦЕШ

Понятие потенциальной энергии диссоциацяи (V°_{AB}) определяется как изменение потенциальной энергии при увеличении длины связи A—B многоатомной молекулы до бесконечности. Существование однозначной корреляции между V°_{AB} и равновесной длиной связи R°_{AB} было проведено в широком интервале, включая как длины многократных связей, так и длины связей в соответствующих диатомных кластерах благородных металлов:

$$I_1 V_{AB} + \ln V^0_{AB} = - I_2 R^0_{AB} + I_3$$

Величина параметров I_1 и I_2 может быть выражена с помощью констант Морзе рассматриваемой связи (β_{AB}) и соответствующей молекулы Леннард—Джонса (β_X):

$$I_1 = C_1(\beta_X/\beta_{AB}); \quad I_2 = C_2(\beta_X/\beta_{AB})^{1/2},$$

где C_1 и C_2 — постоянные, величины которых зависят от места связанных атомов (ряда) в периодической системе. Величина I_3 была рассчитана из энергии и межатомного расстояния молекулы Леннард—Джонса. Справедливость этих зависимостей проверялась на 13 типах химических связей, включая связи C—C и C—H.

Для изменения потенциальной энергии диссоциации с длиной связи в случае заданной связи предлагается следующая зависимость:

$$I_1 (V_{AB} - V^\circ_{AB}) + \ln (V_{AB}/V^\circ_{AB}) = - I_2 (R_{AB} - R^\circ_{AB})$$

С помощью этого соотношения можно определить энергию или длину растянутой связи. Оно может быть также использовано в полуэмпирической и эмпирической обработке проблем реакционной способности.

Ионизация ангидридов неорганических кислот и галидов кислот в хлористом сульфуриле

Образование оксикатионов

С. А. А. ЗАИДИ и З. А. СИДДИКИ

Электропроводность растворов окислов AS, SB, Bi, P, V, Se и Te и оксигалидов Sb, Bi, P и V в хлористом сульфуриле была измерена с целью выяснения путей их ионизации и возможного получения оксикатионов. Трехокиси мышьяка, сурьмы, висмута, оксихлорид сурьмы и оксигалиды висмута образуют оксихлорсульфаты. Оказалось, что при низких концентрациях оксихлоросульфаты сурьмы и висмута частично ионизируются, давая со-

ответственно гипотетические катионы SbO^+ и BiO^+. Были рассчитаны константы диссоциации этих оксихлоросульфатов.

Пятиокись фосфора образует протонированную фосфорную кислоту, в то время как хлористый фосфорил протонируется неполностью.

Пятиокись ванадия и хлористый ванадий ведут себя как слабые электролиты и образуют, вероятно, соединение с формулой $H[VO(SO_3Cl)_4]$. Двуокись Se и Te просто протонируются, причем последняя является более основной.

Спектральные и магнитные исследования комплексов меди(II) с индазолами

С. А. А. ЗАИДИ, А. С. ФАРУКИ и Н. СИНГАЛ

Было приготовлено несколько комплексов с общей формулой CuL_mX_2, где L означает индазол, 5-нитроиндазол или 5-аминоиндазол, а X — Cl^-, Br^-, NO_3^-, 1/2 SO^{-2} и CH_3COO^-. Величина m изменяется от 1 до 4. Был приготовлен также внутренний комплекс индазолята с медью(II). Комплексы были охарактеризованы данными химического анализа, ИК и электронной спектроскопии, а также магнитными измерениями. Было обнаружено, что в большинстве комплексов ион металла находится в октаэдрическом окружении, деформированном тетрагонально.

Связь между энергией резонанса и молекулярной структурой

И. ГУТМАН

Зависимость резонансной энергии (РЭ) от молекулярной структуры обсуждается на основе представления общей π-электронной энергии (уравнение (7)) и РЭ (уравнение (12)) с помощью интеграла Кулсона. Интеграл (12) был решен приближенно и простая топологическая формула (16) была получена для РЭ.

Анализ этой формулы приводит к некоторым основным правилам, связывающим РЭ с некоторыми структурными и комбинаториальными свойствами молекулы.

О механизме гидрирования алкилароматических углеводородов, дегидрирования образующихся циклоалканов и изотопного обмена их с дейтерием на никеле

Л. М. МАМАЛАДЗЕ, Н. В. НЕКРАСОВ, Б. С. ГУДКОВ и С. Л. КИПЕРМАН

Проведено комплексное исследование закономерностей гидрирования и изотопного обмена с дейтерием на никелевых катализаторах в ряду бензол — толуол-этилбензол — м-, п- и о-ксилолы — мезитилен, а также изотопного обмена в ряду циклогексан — метилциклогексан — 1,1- и 1,2-диметилциклогексаны в области температур 30—270°С. Закономерности гидрирования бензола и толуола весьма близки, что свидетельствует о совпадении механизмов процессов. Скорости гидрирования в ряду алкилароматических углеводородов закономерно снижаются, а скорость изотопного обмена в ароматическом кольце и в алкильных заместителях сохраняется приблизительно постоянной, что свидетельствует о различии поверхностных форм, ответственных за оба процесса. В отличие от алкилбензолов, у замещенных циклогексанов не обнаружено значительного расхождения в скоростях обмена кольцевых и алкильных атомов водорода.

Нитроксиды, I

Сульфоновые эфиры 4-гидрокси-2,2,6,6-тетраметилпиперидин-1-оксила и их реакции с нуклеофильными реагентами

К. ХИДЕГ, Х. ХАНКОВСКИ и Й. ТИДИ

2,2,6,6-Тетраметилпиперидин-1-оксил-4-сульфонаты реагируют с нуклеофильными реагентами (азидом натрия, тиоцианатом натрия и цианидом калия) в диметилформамиде, давая соответствующие 4-замещенные 2,2,6,6-тетраметилпиперидин-1-оксила.

Новые синтезы 12H-бензо[a]фенотиазин-5-олов и их эфиров

Н. Л. АГАРВАЛ и Р. Л. МИТАЛ

Ряд замещенных 5H-бензо[2]фенотиазин-5-онов был синтезирован реакцией конденсации 2,3-дихлор-1,4-нафтохинона с цинковыми меркаптидами замещенных 2-аминобензотиолов в спирте. Замещенные 12H-бензо[a]фенотиазин-5-олы были получены в почти количественных выходах восстановлением 5H-бензо[a]фенотиазин-5-онов. Сложные эфиры 12H-бензо[a]фенотиазин-5-олов были синтезированы двумя различными путями. Приводятся ИК спектроскопические и ТСХ данные этих соединений.

Les Acta Chimica paraissent en français, allemand, anglais et russe et publient des mémoires du domaine des sciences chimiques.

Les Acta Chimica sont publiés sous forme de fascicules. Quatre fascicules seront réunis en un volume (4 volumes par an).

On est prié d'envoyer les manuscrits destinés à la rédaction à l'adresse suivante:

Acta Chimica
H-1521 Budapest, Hongrie

Toute correspondance doit être envoyée à cette même adresse.

La rédaction ne rend pas de manuscript.

Le prix de l'abonnement est de $ 32,00 par volume.

Abonnement — en Hongrie à l'Akadémiai Kiadó (1363 Budapest, P.O.B.24. C.C.B. (Bankszámla) 215 11488, à l'étranger à l'Entreprise pour le Commerce Extérieur de Livres et Journaux «Kultúra» (1389 H-Budapest 62, P.O.B. 149 Compte-courant No. 218 10990) ou à l'étranger chez tous les représentants ou dépositaires.

Die Acta Chimica veröffentlichen Abhandlungen aus dem Bereich der chemischen Wissenschaften in deutscher, englischer, französischer und russischer Sprache.

Die Acta Chimica erscheinen in Heften wechselnden Umfanges. Vier Hefte bilden einen Band. Jährlich erscheinen 4 Bände.

Die zur Veröffentlichung bestimmten Manuskripte sind an folgende Adresse zu senden:

Acta Chimica
H-1521 Budapest, Ungarn

An die gleiche Anschrift ist auch jede für die Redaktion bestimmte Korrespondenz zu richten.

Manuskripte werden nicht zurückerstattet. Abonnementpreis pro Band: $ 32,00.

Bestellbar für das Inland bei Akadémiai Kiadó (1363 Budapest, Postfach 24, Bankkonto Nr. 215 11488), für das Ausland bei dem Buch- und Zeitungs-Außenhandels-Unternehmen »Kultúra« (1389 Budapest 62, P.O.B. 149. Bankkonto Nr. 218 10990) oder bei seinen Auslandsvertretungen und Kommissionären.

«Acta Chimica» издают статьи по химии на русском, английском, французском и немецком языках.

«Acta Chimica» выходят отдельными выпусками разного объема, 4 выпуска составляют один том и за год выходят 4 тома.

Предназначенные для публикации рукописи следует направлять по адресу:

Acta Chimica
H-1521 Budapest, ВНР

Всякую корреспонденцию в редакцию направляйте по этому же адресу.

Редакция рукописей не возвращает.

Подписная цена — $ 32,00 за том.

Отечественные подписчики направляйте свои заявки по адресу Издательства Академии Наук (1363 Budapest, P.O.B. 24, Текущий счет 215 11488), а иностранные подписчики через организацию по внешней торговле книг и газет «Kultúra» (1389 H-Budapest 62, P.O.B. 149. Текущий счет 218 10990) или через ее заграничные представительства и уполномоченных.

Reviews of the Hungarian Academy of Sciences are obtainable at the following addresses:

AUSTRALIA
C.B.D. LIBRARY AND SUBSCRIPTION SERVICE, Box 4886, G.P.O., *Sydney N.S.W.2001*
COSMOS BOOKSHOP, 145 Ackland Street, *St. Kilda (Melbourne), Victoria 3182*

AUSTRIA
GLOBUS, Höchstädtplatz 3, *1200 Wien XX*

BELGIUM
OFFICE INTERNATIONAL DE LIBRAIRIE, 30 Avenue Marnix, *1050 Bruxelles*
LIBRAIRIE DU MONDE ENTIER, 162 Rue du Midi, *1000 Bruxelles*

BULGARIA
HEMUS, Bulvar Ruszki 6, *Sofia*

CANADA
PANNONIA BOOKS, P.O.Box 1017, Postal Station "B", *Toronto, Ontario M5T 2T8*

CHINA
CNPICOR, Periodical Department, P.O.Box 50, *Peking*

CZECHOSLOVAKIA
MAD'ARSKÁ KULTURA, Národní třida 22, *115 66 Praha*
PNS DOVOZ TISKU, Vinohradská 46, *Praha 2*
PNS DOVOZ TLAČE, *Bratislava 2*

DENMARK
EJNAR MUNKSGAARD, Norregade 6, *1165 Copenhagen*

FINLAND
AKATEEMINEN KIRJAKAUPPA, P.O.Box 128, *SF-00101 Helsinki 10*

FRANCE
EUROPÉRIODIQUES S. A., 31 Avenue de Versailles, *78170 La Celle St.-Cloud*
LIBRAIRIE LAVOISIER, 11 rue Lavoisier, *75008 Paris*
OFFICE INTERNATIONAL DE DOCUMENTATION ET LIBRAIRIE, 48 rue Gay Lussac, *75240 Paris Cedex 05*

GERMAN DEMOCRATIC REPUBLIC
HAUS DER UNGARISCHEN KULTUR, Karl-Liebknecht-Strasse 9, *DDR-102 Berlin*
DEUTSCHE POST, ZEITUNGSVERTRIEBSAMT, Strasse der Pariser Kommüne 3—4, *DDR-104 Berlin*

GERMAN FEDERAL REPUBLIC
KUNST UND WISSEN, ERICH BIEBER, Postfach 46, *7000 Stuttgart 1*

GREAT BRITAIN
BLACKWELL'S PERIODICALS DIVISION, Hythe Bridge Street, *Oxford OX1 2ET*
BUMPUS, HALDANE AND MAXWELL LTD., Cowper Works, *Olney, Bucks MK46 4BN*
COLLET'S HOLDINGS LTD., Denington Estate, *Wellingborough, Northants NN8 2QT*
WM. DAWSON AND SONS LTD., Cannon House, *Folkestone, Kent CT19 5EE*
H. K. LEWIS AND CO., 136 Gower Street, *London WC1E 6BS*

GREECE
KOSTARAKIS BROTHERS, International Booksellers, 2 Hippokratous Street, *Athens-143*

HOLLAND
MEULENHOFF-BRUNA B.V., Beulingstraat 2, *Amsterdam*
MARTINUS NIJHOFF B.V., Lange Voorhout 9—11, *Den Haag*
SWETS SUBSCRIPTION SERVICE, 347b Heereweg, *Lisse*

INDIA
ALLIED PUBLISHING PRIVATE LTD., 13/14 Asaf Ali Road, *New Delhi 110001*
150 B-6 Mount Road, *Madras 600002*
INTERNATIONAL BOOK HOUSE PVT. LTD., Madame Cama Road, *Bombay 400039*
THE STATE TRADING CORPORATION OF INDIA LTS., Books Import Division, Chandralok, 36 Janpath, *New Delhi 110001*

ITALY
EUGENIO CARLUCCI. P.O.Box 262, *70100 Bari*
INTERSCIENTIA, Via Mazzé 28, *10149 Torino*
LIBRERIA COMMISSIONARIA SANSONI, Via Lamarmora 45, *50121 Firenze*
SANTO VANASIA, Via M. Macchi 58, *20124 Milano*
D. E. A., Via Lima 28, *00198 Roma*

JAPAN
KINOKUNIYA BOOK-STORE CO. LTD., 17-7 Shinjuku 3 chome, Shinjuku-ku, *Tokyo 160-91*
MARUZEN COMPANY LTD., Book Department, P.O.Box 5050 Tokyo International, *Tokyo 100-31*
NAUKA LTD. IMPORT DEPARTMENT, 2-30-19 Minami Ikebukuro, Toshima-ku, *Tokyo 171*

KOREA
CHULPANMUL, *Phenjan*

NORWAY
TANUM-CAMMERMEYER, Karl Johansgatan 41—43, *1000 Oslo*

POLAND
WĘGIERSKI INSTYTUT KULTURY, Marszałkowska 80, *Warszawa*
CKP I W ul. Towarowa 28 *00-958 Warsaw*

ROUMANIA
D. E. P., *Bucureşti*
ROMLIBRI, Str. Biserica Amzei 7, *Bucureşti*

SOVIET UNION
SOJUZPETCHATJ — IMPORT, *Moscow*
and the post offices in each town
MEZHDUNARODNAYA KNIGA, *Moscow G-200*

SPAIN
DIAZ DE SANTOS, Lagasca 95, *Madrid 6*

SWEDEN
ALMQVIST AND WIKSELL, Gamla Brogatan 26, *101 20 Stockholm*
GUMPERTS UNIVERSITETSBOKHANDEL AB, Box 346, *401 25 Göteborg 1*

SWITZERLAND
KARGER LIBRI AG, Petersgraben 31, *4011 Base*

USA
EBSCO SUBSCRIPTION SERVICES, P.O.Box 1943, *Birmingham, Alabama 35201*
F. W. FAXON COMPANY, INC., 15 Southwest Park, *Westwood, Mass, 02090*
THE MOORE-COTTRELL SUBSCRIPTION AGENCIES, *North Cohocton, N. Y. 14868*
READ-MORE PUBLICATIONS, INC., 140 Cedar Street, *New York, N. Y. 10006*
STECHERT-MACMILLAN, INC., 7250 Westfield Avenue, *Pennsauken N. J. 08110*

VIETNAM
XUNHASABA, 32, Hai Ba Trung, *Hanoi*

YUGOSLAVIA
JUGOSLAVENSKA KNJIGA, Terazije 27, *Beograd*
FORUM, Vojvode Mišiča 1, *21000 Novi Sad*

ACTA CHIMICA

ACADEMIAE SCIENTIARUM HUNGARICAE

ADIUVANTIBUS

M. BECK, R. BOGNÁR, V. BRUCKNER,
GY. HARDY, K. LEMPERT, F. MÁRTA,
K. POLINSZKY, E. PUNGOR,
G. SCHAY, Z. G. SZABÓ, P. TÉTÉNYI

REDIGUNT

B. LENGYEL et GY. DEÁK

TOMUS 92 FASCICULUS 2

AKADÉMIAI KIADÓ, BUDAPEST

1977

ACTA CHIM. (BUDAPEST) ACASA2 92 (2) 105–209 (1977)

ACTA CHIMICA

A MAGYAR TUDOMÁNYOS AKADÉMIA KÉMIAI TUDOMÁNYOK OSZTÁLYÁNAK IDEGEN NYELVŰ KÖZLEMÉNYEI

FŐSZERKESZTŐ

LENGYEL BÉLA

SZERKESZTŐ

DEÁK GYULA

TECHNIKAI SZERKESZTŐ

HARASZTHY-PAPP MELINDA

SZERKESZTŐ BIZOTTSÁG

BECK MIHÁLY, BOGNÁR REZSŐ, BRUCKNER GYŐZŐ, HARDY GYULA, LEMPERT KÁROLY, MÁRTA FERENC, POLINSZKY KÁROLY, PUNGOR ERNŐ, SCHAY GÉZA, SZABÓ ZOLTÁN, TÉTÉNYI PÁL

Acta Chimica is a journal for the publication of papers on all aspects of chemistry, in English, German, French and Russian languages.

Acta Chimica is published in 4 volumes per year. Each volume consists of 4 issues of varying size.

Manuscripts should be sent to

Acta Chimica
H-1521 Budapest, Hungary

Correspondence with the Editors should be sent to the same address. Manuscripts are not returned to the Authors.

Subscription rate $ 32.00 per volume.

Hungarian subscribers should order from Akadémiai Kiadó, 1363 Budapest, P.O. Box 24. Account No. 215 11488.

Orders from other countries are to be sent to „Kultúra" Foreign Trade Company for Books and Newspapers (H-1389 Budapest 62, P.O. Box 149. Account No. 218 10990) or to its representatives abroad.

Acta Chimica Academiae Scientiarum Hungaricae, Tomus 92 (2), pp. 105–112 (1977)

DETERMINATION OF SULFUR IN ORGANIC COMPOUNDS BY THE HYDROPYROLYSIS METHOD

L. MÁZOR

(Department of General and Analytical Chemistry, Technical University, Budapest)

Received September 1, 1975

The 'hydropyrolysis' method, described in an earlier communication for the micro-determination of halogens in organic compounds, has now been found suitable for the determination of the sulfur content.

The vapours or pyrolysis products of the organic sulfur compounds are passed with nitrogen carrier gas saturated with water vapour through a platinum catalyst bed at 800—1000 °C, where they are completely decomposed under the formation of hydrogen sulfide and/or sulfur dioxide. The gas stream is introduced into 0.02 *N* iodine standard solution, which oxidizes hydrogen sulfide to elementary sulfur, and sulfur dioxide to sulfate. Since, referred to sulfur, the stoichiometry of the two oxidation reactions is identical, titration of the excess of the iodine standard solution allows the calculation of the sulfur content, independently of the ratio of the two sulfur compounds formed.

Introduction

In our previous paper [1] a method has been described for the determination of the fluorine, chlorine, bromine and iodine content of organic halogen compounds. According to this method, the pyrolysis products or vapours of the compounds are passed with a nitrogen gas stream saturated with water vapour through a platinum catalyst bed at 800—1100 °C, where they are completely converted into halogen hydrogen acids and carbon oxides. After the condensation of water vapour, the acids or the halide ions are determined by a suitable analytical method in the condensate of relatively small volume and high concentration.

It has been found that organic sulfur compounds can be similarly completely decomposed by hydropyrolysis.

However, while organic halogen compounds gave in the case of each halogen element and each halogen compound a uniform hydropyrolysis product, the corresponding halogen hydrogen acid, organic sulfur compounds are converted to different simple, inorganic sulfur compounds, depending on the oxidation number of their sulfur atom, the mode of bonding and on the structure of the compound. From certain compounds hydrogen sulfide, whereas from others sulfur dioxide, or both hydrogen sulfide and sulfur dioxide are formed.

Discussion

The thermal decomposition of organic sulfur compounds starts, in general, at lower temperatures than that of fluorine and chlorine compounds. The energy of the carbon–sulfur bond is nearly equal to that of the carbon–bromine bond (67 kcal/mole). The energy of the C=S double bond is higher (117 kcal/mole), and experience also shows that the thermostability of sulfides is higher than that of, *e.g.*, mercaptans.

Reviews in the literature [2, 3] describe the thermal decomposition of some inorganic and simple organic sulfur compounds and their reactions with water vapour.

Elementary sulfur reacts with water vapour at temperatures between 200 and 600 °C to give hydrogen sulfide and sulfur dioxide:

$$3\,S + 2\,H_2O = 2\,H_2S + SO_2.$$

Thiosulfuric acid, pentathionic acid, etc. may also be formed in secondary reactions.

Carbon disulfide decomposes into its elements at a temperature of about 800 °C; at 400 to 450 °C it reacts with steam:

$$CS_2 + 2\,H_2O = CO_2 + 2\,H_2S.$$

Thiophosgene and isothiocyanates are decomposed at higher temperatures by steam, to yield hydrogen sulfide.

However, unlike the case of halogen compounds, no reaction of general validity is known, in the course of which the carbon–sulfur bond would break to be replaced by another group, as in the rather frequent nucleophilic substitution reactions of halogen compounds. There are only a few compounds which react similarly, *e.g.* tertiary mercaptans decompose on heating to give hydrogen sulfide and the corresponding olefin. Primary and secondary straight-chain alkylmercaptans are decomposed at 260 °C by alkali (possibly also by water vapour). It was found that three reactions may proceed simultaneously: substitution of the mercapto group by hydroxyl group:

$$CH_3CH_2CH_2SH + HOH \rightarrow CH_3CH_2CH_2OH + H_2S,$$

the formation of a thioether:

$$CH_3CH_2CH_2SH \rightarrow CH_3SCH_2CH_3,$$

and the formation of unsaturated hydrocarbon:

$$CH_3CH_2CH_2SH \rightarrow CH_2{=}CHCH_3 + H_2S.$$

Several disulfides are liable to hydrolytic decomposition, the first step being disproportionation:

$$R—S—S—R \rightarrow RS^{\ominus} + {}^{\oplus}SR$$

From the group with negative charge, a thiol is formed:

$$RS^{\ominus} + H^{+} \rightarrow R—SH,$$

while the group with positive charge gives elementary sulfur:

$${}^{\oplus}SR + H^{+} \rightarrow R—H + S^{0};$$

yet, mercaptide can also be formed from the group with negative charge. Thiols are unstable, they decompose with the formation of hydrogen sulfide.

In sulfides (thioethers) the C–S bond is more resistant, *e.g.* to acid hydrolysis, than the C–O bond of ethers. Thioacids are decomposed by steam to give hydrogen sulfide. Thiocarboxylic acid esters undergo hydrolysis:

$$\begin{matrix} R—CS—R \\ \quad\| \\ \quad O \end{matrix} + HOH = R—COOH + R—SH\,.$$

It can be seen from the examples given that the predominant part of organic sulfur compounds (the exceptions being sulfonic acids and sulfones, which suffer decomposition with the formation of sulfur trioxide) are decomposed by water vapour mostly at temperatures as low as 500—600 °C, and in the course of this process the sulfur content is converted to hydrogen sulfide or sulfur dioxide. When sulfur trioxide is formed from the compounds, this is also decomposed at temperatures higher than 700 °C:

$$2\ SO_3 = 2\ SO_2 + O_2.$$

Thus, the thermal decomposition even of organic sulfates gives eventually sulfur dioxide as the end-product, if the pyrolysis products are passed through a platinum catalyst bed at a temperature higher than 700 °C. If the catalyst bed is heated to about 1000 °C, the other decomposition products of the compound will also burn giving the oxides of carbon, by reaction with the oxygen of water vapour. If the carrier gas contains also water vapour, hydrogen sulfide can pass the high temperature catalyst bed without decomposition.

Without the addition of reducing agents, conditions under which sulfur dioxide is also reduced to hydrogen sulfide could not be ensured.

Our experiments have shown that hydrogen sulfide is the sole product from low molecular weight aliphatic and aromatic mercaptans. The reaction is probably nucleophilic substitution, similar to their decomposition on the action of alkali [4]:

$$R—SH + HOH = R—OH + H_2S.$$

The alcohol formed is further decomposed at higher temperatures, but hydrogen sulfide passes through the catalyst bed. Hydrogen sulfide was the only product in the decomposition of, *e.g.*, benzyl mercaptan if the temperature did not exceed 500 °C:

$$C_6H_5CH_2SH + HOH = C_6H_5CH_2OH + H_2S;$$

however, at higher temperatures, sulfur dioxide was also present among the decomposition products of the hydropyrolysis reaction:

$$3\ C_6H_5CH_2SH + 4\ HOH = 3\ C_6H_6 + 3\ CH_4 + H_2S + SO_2.$$

Similarly, hydrogen sulfide was formed in the decomposition of methionine:

$$CH_3\,SCH_2\,CH_2\,\underset{\displaystyle NH_2}{\underset{|}{C}}HCOOH \rightarrow CH_3\,.\,CH_3 + H_2S + NH_3 + CO_2 + 2\,C\,.$$

As can be seen, this reaction is only a thermal decomposition; according to our experiments, the same decomposition products are obtained in the absence of water vapour. The reaction scheme also fulfills the condition that the decomposition products are low molecular weight compounds, and thus thermally stable.

In the thermal decomposition of dithizone (diphenylthiocarbazone) with water vapour, in addition to the preponderant formation of hydrogen sulfide, a small quantity of sulfur dioxide was also obtained. The sulfide form of this compound is:

$$S{:}C{:}(N{:}N.C_6H_5).(NHNHC_6H_5),$$

and this decomposes presumably to hydrogen sulfide and diphenylcarbazone. The mercaptide form,

$$HSCN{:}NC_6H_5{:}N{:}NHC_6H_5,$$

similarly gives diphenylcarbazone in the course of thermal decomposition, the other decomposition product being elementary sulfur; the latter reacts with water vapour to yield hydrogen sulfide and sulfur dioxide in a secondary reaction.

The decomposition of disulfides starts probably with the rupture of the sulfur–sulfur bond. The sulfur atom carrying a positive excess charge in one half of the molecule is stabilized by the formation of sulfur dioxide, and the sulfur atom with negative excess charge gives rise to hydrogen sulfide. For cystine, the following decomposition scheme can be written:

$$\begin{matrix} HOOCH_2\,NHCH_2\,CS^{\ominus} \\ \vdots \\ HOOCH_2\,NHCH_2\,CS^{\oplus} \end{matrix} + 2\,HOH \rightarrow 2\,CH_3\,CHNH_2\,COOH + H_2S + SO_2\,,$$

Sulfinic acids gave only sulfur dioxide on thermal decomposition; the first step may be disproportionation or simple decomposition:

$$C_6H_5SO_2H \rightarrow C_6H_6 + SO_2.$$

Sulfur trioxide was the product from sulfonic acids if the temperature of the platinum catalyst was less than 700 °C. For example, the decomposition of benzenesulfonic acid can be written as follows:

$$C_6H_5SO_3H \rightarrow C_6H_6 + SO_3,$$

or that of sulfanilic acid:

$$NH_2C_6H_4SO_3H\,.\,H_2O \rightarrow NH_2C_6H_5 + H_2SO_4.$$

When the temperature of the platinum catalyst is about 800 °C, only sulfur dioxide is formed, because, as it has been mentioned, sulfur trioxide is decomposed to sulfur dioxide and oxygen. In this way, the sulfur content of organic sulfates, *e.g.* that of benzidine sulfate, was converted into sulfur dioxide. Evidently, sulfonic acid salts did not decompose.

Procedure

The hydropyrolytic decomposition of organic sulfur compounds was carried out in the apparatus described in detail and illustrated in our preceding paper [1]. However, instead of the Liebig condenser, a more efficient cooling coil shown in Fig. 1 was connected to the end of the reaction tube. The gas mixture leaving the hot reaction tube is cooled immediately in this condenser preventing *e.g.*, the interaction of hydrogen sulfide with sulfur dioxide giving elementary sulfur, which can only at elevated temperatures. The gases were absorbed without loss in the flask attached to the outlet tube of the condenser.

The selective determination of hydrogen sulfide was also possible in the absorbing solution. For this purpose, the gases were absorbed in a known volume of 0.01 *M* zinc acetate solution of pH 10. Zinc sulfide precipitated by the hydrogen sulfide was compacted by heating, filtered off, washed, and the zinc ion content in the filtrate was determined by titration, in the presence of Eriochrom Black T indicator, with 0.01 *M* EDTA standard solution. The sulfur content was calculated from the difference in the volumes of the standard solution consumed. The zinc ion content of the isolated zinc sulfide precipitate could also be titrated after dissolution. No reliable results were obtained for the sulfite ion content in the filtrate, because a substantial part of the sulfite ions suffered oxidation during the heating and filtration.

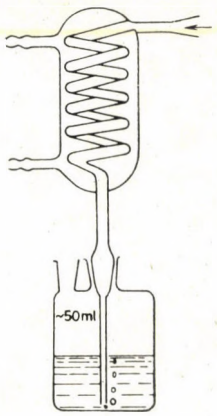

Fig. 1. Coil condenser, receiver and titration flask

Iodometry offered the possibility of a procedure allowing the determination of the sulfur content of organic compounds independently of the fact, whether hydrogen sulfide, sulfur dioxide or both were formed from the organic sulfur during the pyrolytic decomposition.

Hydrogen sulfide is oxidized in acid solution by iodine, giving rise to iodide ions:

$$H_2S + I_2 = 2\,I^- + 2\,H^+ + S^0. \qquad (1)$$

Elementary sulfur, even in the colloidal state, is resistant to the oxidative action of iodine.

Sulfur dioxide, or in aqueous solution sulfurous acid, react with iodine similarly, also producing iodide ions:

$$SO_2 + I_2 + H_2O = SO_4^{2-} + 4\,H^+ + 2\,I^-. \qquad (2)$$

As can be seen from Equations (1) and (2), the equivalent weight of sulfur, referred to iodide, is in both cases identical and equal to half the atomic weight of sulfur.

In carrying out the determination, a known volume of 0.01 or 0.02 *N* iodine standard solution is introduced into the absorber vessel with a pipette and 0.5—1.0 g of potassium iodide is dissolved in the solution in order to decrease further the tension of iodine. Depending on the sulfur content, 5—15 mg of the substance to be analyzed is weighed into a micro combustion boat; liquids are sucked up in a glass capillary, weighed, and placed into the reaction tube of the apparatus. The combustion furnace heating the catalyst bed is then heated up to 900 °C, and the moving mantle is kept at 400—600 °C. Carrier gas saturated with water vapour is passed at a rate of 5—8 ml/min through the reaction tube, and the pyrolysis of the sample to be analyzed is begun. After 20—30 min, when the pyrolysis products have been completely absorbed by the iodine solution using a total of about 150 ml of carrier gas, the excess of iodine in the vessel is titrated with 0.01—0.02 *N* sodium thiosulfate standard solution. Starch solution is used to indicate the end-point of the titration.

The sulfur content of the sample analyzed is calculated from the difference of the titrations. One ml of 0.01 *N* iodine solution is equivalent to 0.16 mg of sulfur.

Elementary sulfur and a few organic sulfur-containing substances have been investigated. The results are listed in Table I.

Table I

Compound	Theoretical sulfur content, %	Mean value of the results of 10 determinations, %	Standard deviation, %
Elementary sulfur	100.0	100.98	3.41 (0.034)
Thioacetamide, CH_3CSNH_2	42.60	42.09	1.41 (0.033)
D-Cystine $(SCH_2CHNH_2COOH)_2$	26.69	26.31	0.90 (0.034)
Benzyl mercaptan, $C_6H_5CH_2SH$	25.81	25.81*	0.86 (0.033)
L-Methionine, $CH_3SCH_2CH_2CHNH_2COOH$	21.49	21.49	1.12 (0.052)
DL-Cystine hydrochloride, $(SCH_2CHNH_2COOH)_2.2\ HCl$	20.54	20.31	0.63 (0.031)
Sulfanilic acid, $NH_2C_6H_4SO_3H.H_2O$	16.77	16.16	0.20 (0.012)
5-Sulfosalicylic acid, $C_6H_3OHCOOHSO_3H$	14.67	14.05	1.48 (0.10)
Diphenylthiocarbazone (Dithizone) $C_{13}H_{12}N_4S$	12.51	12.44	0.42 (0.034)
Benzidine sulfate, $NH_2C_6H_4C_6H_4NH_2.H_2SO_4$	11.31	11.17	0.83 (0.075)

* Mean value of 5 determinations

The values of the standard deviation given in parenthes were calculated by dividing the preceding value by the percentage sulfur content of the compound. This 'relative standard deviation' is a better measure of the scattering of the results.

The maximum deviation of the single results from the mean value was —10 to +6%.

REFERENCES

[1] MÁZOR, L.: Acta Chim. (Budapest) **89,** 289 (1976)
[2] HOUBEN—WEYL: Methoden der Organischen Chemie, Vol. IX. Schwefel-, Selen-, Tellurverbindungen. Eugen Müller, Tübingen, 1955
[3] GMELINS Handbuch der Anorganischen Chemie. Syst. No. 9, Schwefel, Part A, p. 692. Verlag-Chemie, Braunschweig, 1953
[4] BILLHEIMER, E. C., REED, E. E.: J. Am. Chem. Soc. **52,** 4338 (1930)

László MÁZOR H-1111 Budapest, Gellért tér 4.

Acta Chimica Academiae Scientiarum Hungaricae, Tomus 92 (2), pp. 113—116 (1977)

KINETIC EQUATIONS OF MULTISTEP ELECTRODE PROCESSES, III

L. Kiss

(Department of Physical Chemistry and Radiology, Eötvös Loránd University, Budapest)

Received July 11, 1975

A correlation is given which describes the polarization curve of a multistep electrode process controlled purely by diffusion.

In former communications [1, 2] we have described a method for calculating the polarization curves of metal ionization and metal ion neutralization proceeding by charge transfer in several successive steps (multistep process). We have discussed cases in which the kinetics of the reactions are affected by charge transfer only [1] or by charge transfer and diffusion [2]. The correlation deduced permits also to discuss electrode processes that proceed as consecutive first order reactions, in which the first step is the diffusion of the initial component and the last step the diffusion of the final product, and both chemical and electrochemical (charge transfer) reactions [3] are involved.

In this paper a relationship between the current density and the other parameters of the process will be given for pure diffusion polarization, assuming that the ionization of the metal and the neutralization of the metal ions proceed according to the stepwise mechanism described previously [1].

The following reaction scheme shows the essence of the process studied.

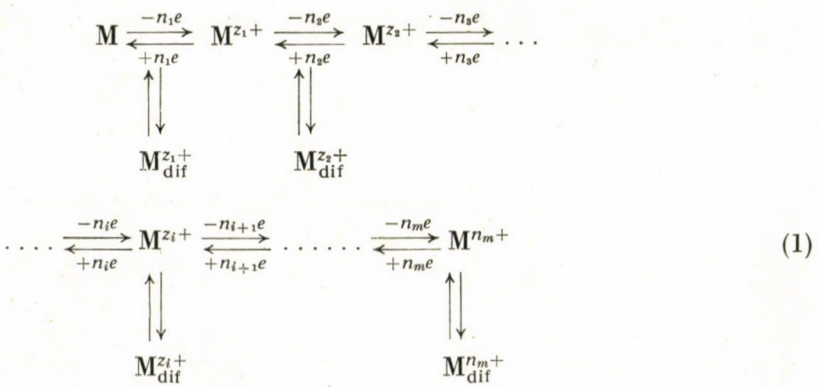

(1)

According to this scheme the intermediate ion M^{z_i+} $(i = 1, 2, \ldots (m—1))$ is removed from the electrode surface in two ways, *viz.* either it is transformed

into ion $M^{z(i+1)+}$ or into ion $M^{z(i-1)+}$ by an electrochemical reaction involving the loss of n_{i+1} electrons, or the gain of n_i electrons, respectively, or it diffuses into the bulk of the solution ($M^{z_i+}_{\text{diff}}$). In this scheme thus no account is taken of the possibility that the ion M^{z_i+} may react with a component of the solution. The multistep process is governed by diffusion kinetics if the diffusion of the product formed in an electrochemical reaction is much slower than the electrochemical step (charge transfer) in which it is formed. In this case — supposing that the product due to the electrochemical process is transported into the solution and that the ions which will undergo reaction at the electrode surface are transported to the electrode by stationary diffusion — for current density j, after a stationary state is attained, the following correlation can be written,

$$j = j_1' + j_2' + \ldots + j_i' + \ldots + j_m' \tag{1}$$

The partial current densities j_1' due to the diffusion of ions M^{z_1+}, M^{z_2+} ... ... M^{z_i+} in Eq. (1) can be defined as

$$\begin{aligned} j_1' &= z_1 X_1 (c_{1,0} - c_{1,\infty}) \\ j_2' &= z_2 X_2 (c_{2,0} - c_{2,\infty}) \\ &\vdots \\ j_i' &= z_i X_i (c_{i,0} - c_{i,\infty}) \\ &\vdots \\ j_m' &= z_m X_m (c_{m,0} - c_{m,\infty}) \end{aligned} \tag{2}$$

where $z_i = \sum_{i=1}^{i} n_i$ and, for a rotating disc electrode $X_i = 0.62\, F D_i^{2/3} \nu^{-1/6} \omega^{1/2}$; F is Faraday's constant, D_i is the diffusion coefficient of the i-th ion, ν is the kinematic viscosity of the solution, and ω the angular velocity of the electrode ($\omega = 2\pi f/60$, f = r.p.m. of the electrode), $c_{i,0}$ and $c_{i,\infty}$ are the concentrations of the i-th ion at the electrode surface and in the bulk of the solution, respectively.

On the basis of Eqs (1) and (2), the following correlation can be deduced for the current density

$$j = \sum_{i=1}^{m} z_i X_i (c_{i,0} - c_{i,\infty}) \tag{3}$$

Since, as comparison with the corresponding electrode reactions, the diffusion of the ions is a much slower process, concerning ion concentration at its surface, the electrode can be regarded as being in equilibrium. At equilibrium the following correlation is valid

$$k_{a_i} \cdot c_{(i-1),0} = k_{k_i} \cdot c_{i,0} \tag{4}$$

where k_{a_i} and k_{k_i} are rate constants of the corresponding electrode processes, depending on the electrode potential φ; $i = 1, 2 \ldots i \ldots m$, and $c_{0,0} = 1$.

$$k_{a_i} = k'_{a_i} \exp\left(\frac{\alpha_i n_i F\varphi}{RT}\right)$$

$$k_{k_i} = k'_{k_i} \exp\left[-\frac{(1-\alpha_i) n_i F\varphi}{RT}\right] \tag{5}$$

The value of the rate constants k'_{a_i} and k'_{k_i} depends also on the potential of the reference electrode chosen; α_i is the transfer coefficient of the i-th step, φ is the electrode potential against the given reference electrode. It must be noted that Eq. (4) is valid to a good approximation only if

$$k_{k_{(i-1)}} \gg k_{a_i} . \tag{6}$$

If Eq. (4) holds true then for the concentration of the i-th intermediate at the electrode, the following can be written

$$c_{i,0} = \prod_{p=1}^{i} \frac{k_{a_p}}{k_{k_p}} . \tag{7}$$

When this term is substituted into Eq. (3), we get

$$j = \sum_{i=1}^{m} \left\{ z_i X_i \left[\left(\prod_{p=1}^{i} \frac{k_{a_p}}{k_{k_p}} \right) - c_{i,\infty} \right] \right\}_i . \tag{8}$$

If we assume that

$$\prod_{p=1}^{l-1} \frac{k_{a_i}}{k_{k_i}} \ll \frac{k_{a_l}}{k_{k_l}} \gg \frac{k_{a_{(l+1)}}}{k_{k_{(l+1)}}} \tag{9}$$

then Eq. (8) becomes simpler, and in the case of anodic dissolution, the rate of the process is determined only by the diffusion of the l-the component from the electrode surface into the bulk of the solution. Then, in the steady state, the polarization curve is described by

$$j = z_l X_l \left(\prod_{i=1}^{l} \frac{k_{a_i}}{k_{k_i}} - c_{l,\infty} \right) . \tag{10}$$

Taking Eq. (5) into account, from Eq. (10) the correlation of electrode potential and current density can be deduced as follows,

$$\varphi = \frac{RT}{z_l F} \ln \prod_{i=1}^{l} \frac{k'_{k_i}}{k'_{a_i}} - \frac{RT}{z_l F} \ln z_l X_l + \frac{RT}{z_l F} \ln (j - j_{hl}) \tag{11}$$

where j_{hl} is cathodic limiting current of the l-th ion.

If $c_{l,\infty} = 0$, there is a linear correlation between the logarithm of electrode potential φ and the logarithm of current density.

Thus in the case discussed the ionization of the metal at the electrode surface proceeds up to charge number z_l only. If $l = m$, *i.e.* ionization produces the ion with the maximum possible charge, then the polarization curve does not give any indication of a stepwise mechanism.

If $l < m$, or it is not the ion with the maximum possible charge number that goes into solution, further oxidation by an oxidizing agent, *e.g.* oxygen, in the solution may occur as a homogeneous reaction [4]. This happens for instance with a copper electrode in an aqueous solution in the presence of ammonia, in acid solutions containing chloride, or in anhydrous acetic acid solutions containing chloride or perchlorate [5, 6]. If the reduction of the ions of higher charge formed in the bulk of the solution *via* a homogeneous reaction is on the surface of metal sufficiently rapid, then this phenomenon, in the case of spontaneous dissolution due to an oxidizing agent (oxygen), may lead to an autocatalytic acceleration of spontaneous dissolution [5, 7]. This can be observed when copper is spontaneously dissolved in an aqueous medium containing ammonia or in an acid solution containing chloride [5]. However, no autocatalytic effect is apparent in acetic acid solutions.

REFERENCES

[1] Kiss, L., Farkas, J.: Magy. Kém. Foly. **80,** 542 (1974); Acta Chim. (Budapest) **84,** 161 (1975)
[2] Kiss, L., Farkas, J.: Electrokhim. **7,** 1744 (1971)
[3] Kiss, L., Varsányi, L. M.: Magy. Kém. Foly. **81,** 446 (1975); Acta Chim. (Budapest) **88,** 259 (1976)
[4] Pchelnikov, A. P., Losev, V. V.: Zasch. Metal., **8,** 673 (1972)
[5] Kiss, L.: 74th Manif. of the Eur. Feder. of Corrosion, II., p. 49. Budapest 1974
[6] Kiss, L., Varsányi, L. M.: Magy. Kém. Foly. **80,** 29 (1974); **80,** 225 (1974); Acta Chim. (Budapest) **81,** 61 (1974); **83,** 165 (1974)
[7] Molodov, A., Markosyan, G., Yanov, P.: Pjataja Mezhdunarodnaya Konf. po probleme CEB, Praha, 21—26. Apr. 1975, Sbornik dokl. sekc. I, p. 293.

László Kiss H-1088 Budapest, Puskin u. 11—13.

Acta Chimica Academiae Scientiarum Hungaricae, Tomus 92 (2), pp. 117–128 (1977)

STUDY OF THE MECHANISM OF HEXENE RADIOLYSIS, I

INVESTIGATION OF CYCLOHEXENE IN THE PRESENCE OF ADDITIVES

A. KOVÁCS, GY. CSERÉP and G. FÖLDIÁK

(Institute of Isotopes of the Hungarian Academy of Sciences, Budapest)

Received October 11, 1975

The γ-radiolysis of cyclohexene has been studied in the presence of electron, positive ion and radical scavengers. In contrast to earlier suggestions [14], it has been shown that the role of electron–ion recombination processes cannot be neglected in hydrogen formation; at the same time, the importance of such processes in cyclohexane production has been confirmed.

Whereas the role of radical processes in hydrogen formation is insignificant, cyclohexyl radicals are of paramount importance in cyclohexane and dimer formation. The effect of conjugated dienes on monoalkene radiolysis is similar to that of the latter compounds on the radiolysis of alkanes.

Not only are various products of cyclohexene radiolysis produced according to different pathways but also more than one reaction path may exist to form the same product; in addition, both products and intermediates can compete with each other.

Introduction

The study of low molecular weight products formed in the radiolysis of unsaturated hydrocarbons has received relatively little attention as compared with the investigation of polymerization. Fewer studies have dealt with the formation of such products from alkenes in the presence of additives, as compared with similar studies on alkanes. This is attributed mainly to the very low yields, implying that the determination of changes would require exceptionally accurate and sensitive analysis.

Since this problem has not been studied so far with the application of scavengers, this approach was aimed at both supporting earlier views and establishing new reaction mechanisms.

Literature survey

Radiolysis of cyclohexene has been studied both with and without scavengers by a number of authors. FREEMAN *et al.* [1] have determined the yields of methane, ethylene, acetylene and total C_4 hydrocarbons in addition to C_6 and C_{12} yields (Table I) and suggested the decomposition of the ring into two or three unsaturated hydrocarbons, giving one ethylene and one butadiene molecules, or two ethylene and one acetylene molecules.

This hypothesis has been verified and extended by CSERÉP and FÖLDIÁK [2] who have found ethylene and 1,3-butadiene as fragments with the highest yields; this effect has been attributed to the directing effect of the π-bond.

SATO *et al.* [3] have found that the $G(H_2)$ value of cyclohexene does not change considerably in the presence of N_2O as electron scavenger. WAKEFORD and FREEMAN [4] have studied cyclohexene radiolysis in the presence of cyclic dienes (1,3-cyclohexadiene, 1,4-cyclohexadiene) and benzene. They assumed that only about 1/3 of the product cyclohexane has been formed in disproportionation reactions of cyclohexyl radicals, the further 2/3 being produced presumably in ion–molecule reactions. Dimer formation has been interpreted in terms of radical combination processes. This is supported by the results of HOLROYD and SEVILLA [5], reporting the existence of methyl, allyl, cyclohexyl and cyclohexenyl radicals in photochemical processes. BURNS, HOLROYD and KLEIN [6] have studied the radiolysis of cyclohexene in the presence of $^{14}CH_3I$ and have found 3-cyclohexenyl, 1-cyclohexenyl and cyclohexyl radicals.

Experimental

The radiolysis of cyclohexene has been studied in the presence of additives with electron scavenging (CCl_4, SF_6) positive ion scavenging (C_2H_5OH, NH_3) or radical scavenging (*p*-benzoquinone, O_2) properties. In some experiments two different additives have been applied simultaneously (*p*-benzoquinone + CCl_4; *p*-benzoquinone + C_2H_5OH; CCl_4 + C_2H_5OH). In these last three cases the concentration of scavengers was 0.05 mol l^{-1} for each additive. In systems containing one scavenger, its concentration varied as follows: for CCl_4 and C_2H_5OH: 0.005, 0.05, 0.1 and 0.2; for SF_6, O_2 and *p*-benzoquinone: 0.005, 0.01 and 0.05; for NH_3: 0.005, 0.01, 0.05 and 0.2 mol l^{-1}, respectively.

Cyclohexene was a FLUKA product ('purum' grade, of 99% purity). SF_6 and NH_3 were FLUKA 'purum' and 'purissimum' grade, respectively, CCl_4 manufactured by BIOGAL (Hungary) was of 99% purity, O_2 was a commercial grade cylinder gas purified, *p*-benzoquinone and C_2H_5OH have been supplied by REANAL (Hungary).

Gaseous additives were dosed volumetrically on the basis of OSTWALD's solubility coefficients [7] so that the gas volume in the ampoules over the liquid be negligibly small.

Sample preparation was performed as described earlier [2].

Irradiations took place in the ^{60}Co γ-irradiation facility of the Institute with a nominal activity of 80 kCi, ($3 \cdot 10^{15}$ Bq) at a temperature of 30—35 °C. Dose rate was 1.44 Mrd h^{-1} (8.98×10^{19} eV g^{-1} h^{-1}) integrated dose was 8 ± 0.5 Mrd ($5 \cdot 10^{20}$ eV g^{-1}). Doses were determined using alcoholic chlorobenzene dosimetry [8].

Hydrogen formed during irradiation was measured volumetrically by an automatic Toepler pump. Hydrocarbon fragments were determined qualitatively and quantitatively by a Perkin—Elmer F-7 gas chromatograph using a dimethylsulfolane column at 20 °C. C_6 and C_{12} products were determined on the same gas chromatograph, at 67 and 120 °C, respectively, using a 100 m capillary column coated with squalane.

Results

It has been found that the yields of fragments of irradiated pure cyclohexene are nearly the same as the data given by FREEMAN [1] or CSERÉP and FÖLDIÁK [2]. At the same time, however, additional products have been identified and determined. Due to analytical difficulties, it was not possible

Table I

Products of radiolysis of cyclohexene

Product	G (molecule/100 eV)		
	Literature data		Present study
	[1]	[2]	
Hydrogen	1.28	1.190	1.200
Methane	0.001	0.005	0.004
Ethane	—	0.001	0.001
Ethylene	0.160	0.140	0.170
Acetylene	0.022	0.017	0.022
Propane	—	0.001	0.001
Propene	—	0.005	0.004
Butane	—	0.001	0.001
1-Butene	—	0.005	0.004
2-Butene	—	0.001	0.001
1,3-Butadiene	0.1	0.060	0.055
trans-2-Hexene	—	—	tr.
cis-2-Hexene	—	—	tr.
1,5-Hexadiene	0.02	—	0.026
trans-1,4-Hexadiene	—	—	tr.
cis-1,4-Hexadiene	—	—	tr.
trans-1,3-Hexadiene	—	—	0.040
Cyclohexane	0.95	—	0.962
1,3-Cyclohexadiene	0.10	—	0.141
1,4-Cyclohexadiene	0.05	—	tr.
Methylcyclopentane	—	—	0.040
Benzene	0.05	—	0.022
Dicyclohexyl	0.21	—	0.051
Dimer (retention index 1308.7)	—	—	0.564
Dimer (retention index 1310.3)	—	—	0.426
2,2′-Dicyclohexenyl	1.90	—	—
3-Cyclohexylcyclohexene	0.58	—	—

* tr.: $G < 0.001$

to identify all C_{12} products formed in the radiolysis; thus, some of them were distinguished only on the basis of retention indices taken from the literature.

Yields obtained have been summarized in Table I.

The effect of additives is illustrated by plotting G-values as a function of scavenger concentration.

Hydrogen formation

The mechanism of hydrogen formation from irradiated cyclohexene was studied in the presence of electron scavengers. It has been found that an appreciable decrease of the yield can only be observed at higher scavenger concentrations (Fig. 1). Positive ion scavengers brought about a yield increase the extent of which was within the limits of experimental errors but showed a definite tendency; with radical scavengers a slight decrease of $G(H_2)$ was observed.

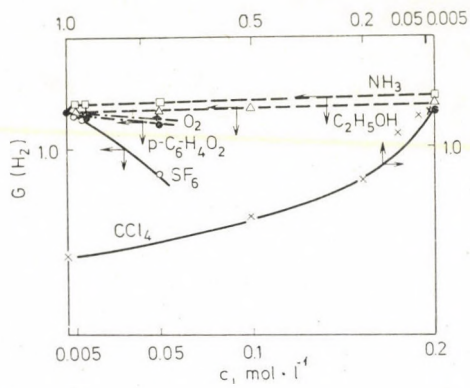

Fig. 1. $G(H_2)$ values as a function of the concentration of various scavengers

With binary scavenger systems, the combination of electron and radical scavengers as well as of electron and positive ion scavengers caused only a slight decrease in $G(H_2)$ values: 0.13 and 0.10, respectively. At the same time, the simultaneous application of positive ion and radical scavengers did not alter the yield of hydrogen as compared with that of pure cyclohexene, presumably due to a compensation of the effects.

Formation of fragments

Of fragments, ethylene and 1,3-butadiene have been found in the highest amounts, due to the directing effect of the π-bond, *i.e.* to the differences in bond energies. Electron and positive ion scavengers cause the yield of 1,3-butadiene (and to a lesser extent, that of ethylene) to decrease; with *p*-benzoquinone, the *G*-values of ethylene and acetylene somewhat increased.

The most marked feature was the increase of 1,3-butadiene yield in the presence of a radical scavenger (Fig. 2). At the same time, however, the yields of saturated hydrocarbons (ethane, propane and butane) decreased in the presence of radical scavengers, although to different extents.

The yields of methane, 1-butene, *trans*- and *cis*-2-butenes were not affected by any of the additives used.

With the simultaneous application of two scavengers the only change to be observed was the increase of the yield of 1,3-butadiene in such cases when the system contained a radical scavenger.

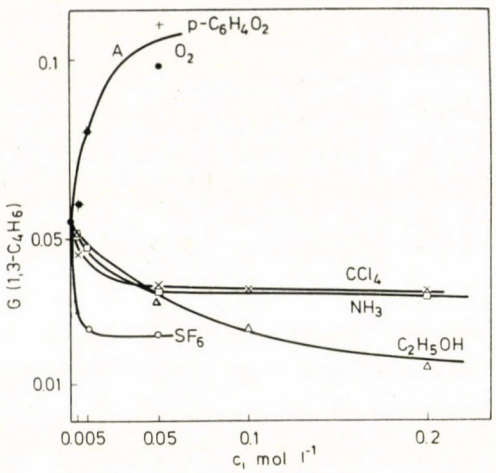

Fig. 2. G(1,3-butadiene) as a function of the concentration of various scavengers (Measured values: + *p*-benzoquinone, ● O_2; calculated values: curve A)

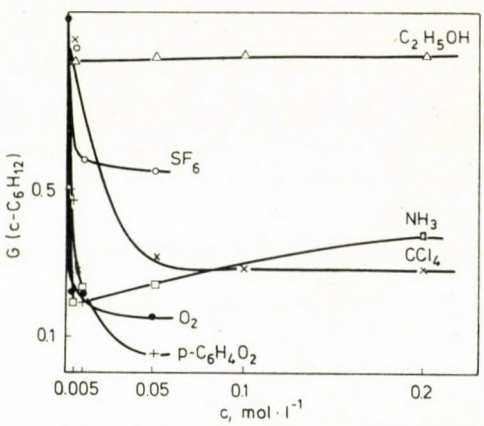

Fig. 3. G-values of cyclohexane as a function of the scavenger concentration

Formation of C_6-products

Of these, the yield of cyclohexane was the highest and also the amount of this product was influenced most markedly by various scavengers. Every scavenger type decreased the yield of cyclohexane: in addition to this, also the character of the concentration dependence of G-values varied with individual additives, even with those belonging to the same group (Fig. 3).

Of positive ion scavengers, ethanol brought about a decrease not more than 10%, at the same time, NH_3 80%. Both curves have a minimum, after which the yield decrease has a limiting value equal to about 8% for ethanol and 60% for ammonia. The decrease of the cyclohexane yield was about 90% with radical scavengers and 60% with electron scavengers.

The application of two different type scavengers simultaneously caused a similar effect. With mixtures containing *p*-benzoquinone, the decrease of the *G*-value was $\Delta G = 0.72$, whereas with ($CCl_4 + C_2H_5OH$) $\Delta G = 0.30$.

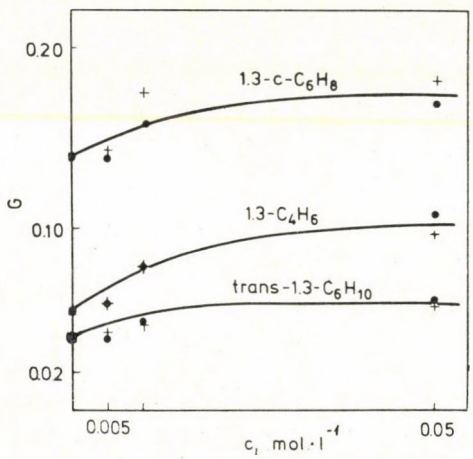

Fig. 4. G-values of conjugated dienes as a function of the scavenger concentration (Measured values: + *p*-benzoquinone, ● O_2; calculated values: continuous lines)

The *G*-value of 1,3-cyclohexadiene is suppressed by CCl_4 and — in high concentrations — by NH_3. In systems containing radical scavengers, the *G*-values of 1,3-cyclohexadiene and *trans*-1,3-hexadiene as well as that of 1,3-butadiene are higher (Fig. 4).

The yield of methylcyclopentane decreases in the presence of radical scavengers, that of benzene decreases with CCl_4 addition.

Formation of C_{12} products

The yield of dicyclohexyl decreased gradually in the presence of increasing amounts of electron scavengers and increased with positive ion scavengers. The addition of radical scavengers eliminated this dimeric product almost entirely.

Unfortunately, we did not succeed in identifying two other dimeric products with retention indices of 1308.7 and 1310.3, respectively. It is probable that these are 3-cyclohexylcyclohexene and 2,2′-dicyclohexenyl.Their behaviour

under the effect of scavengers was the same as observed for dicyclohexyl: *p*-benzoquinone decreased, whereas O_2, positive ion and electron scavengers increased their yields (Fig. 5).

The *G*-value of these dimers decreased in binary scavenger systems with *p*-benzoquinone as one of the additives. The simultaneous application of CCl_4 and C_2H_5OH caused a yield increase.

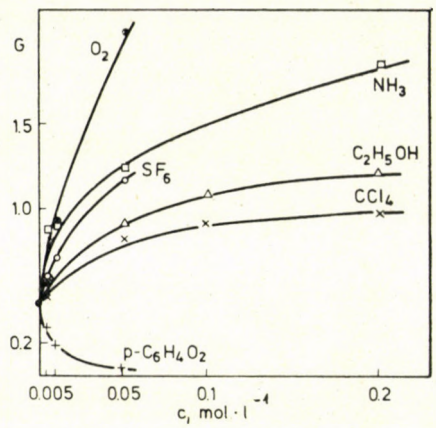

Fig. 5. Yield of the dimeric product with a retention index of 1308.7 as a function of scavenger concentration

Discussion

Processes involving C–H bond rupture

The decrease of $G(H_2)$ under the effect of CCl_4 is due presumably to the hindrance of electron–ion neutralization processes leading to excited molecules, by partial electron capture:

$$e^- \begin{cases} \xrightarrow{c-C_6H_{10}^+} c-C_6H_{10}^* & (1a) \\ \xrightarrow[CCl_4]{} CCl_4^- & (1b) \end{cases}$$

A fraction of both directly excited cyclohexene molecules and those excited in process (1a) can transfer their energy to CCl_4, resulting also in decreasing $G(H_2)$ values:

$$c-C_6H_{10}^* \begin{cases} \rightarrow H_2 + C_6H_8 & (2a) \\ \rightarrow H + c-C_6H_9^\cdot & (2b) \\ \rightarrow CCl_4 & \\ \rightarrow c-C_6H_{10} + CCl_4^* & (2c) \end{cases}$$

FREEMAN and SINGH [9] have already suggested processes of this kind.

The increase of hydrogen yield observed in the presence of positive ion scavengers may also be due to more than one elementary process. On the one

hand, the $G(H_2)$-value of ethanol (4.85) receiving the transferred charge, is higher than that of cyclohexene; on the other hand, H-atoms formed in reactions (3) and (4) can interact with cyclohexene in abstraction reaction (5a) thus increasing further the value of $G(H_2)$ [10]:

$$c\text{—}C_6H_{10}^+ + C_2H_5OH \rightarrow c\text{—}C_6H_9^{\bullet} + C_2H_5OH_2^+ \quad (3)$$

$$C_2H_5OH_2^+ + e^- \rightarrow C_2H_5OH_2^* \rightarrow C_2H_5OH + H \quad (4)$$

$$c\text{—}C_6H_{10} + H\text{—} \begin{cases} \rightarrow c\text{—}C_6H_9^{\bullet} + H_2 & (5a) \\ \rightarrow c\text{—}C_6H_{11}^{\bullet} & (5b) \end{cases}$$

Since these reactions compete with (1a), the resulting yield increase allows us to conclude that the rate of process (1a) is lower than those of (3)—(5).

The decrease of $G(H_2)$ under the effect of radical scavengers is not large and it may be due to the capture of thermal H-atoms. This is in agreement with the previous suggestion [11] that the yield determined with irradiated pure alkenes is the so-called 'molecular' yield corresponding to the limiting concentration of the radical scavenger since π-bonds present in high concentration capture the majority of thermal H-atoms. On the other hand, this also indicates that added O_2 or p-$C_6H_4O_2$ are more efficient scavengers than the cycloalkene itself, thus, in spite of their low concentration, they are able to capture further thermal H-atoms.

The relatively high decrease of yield caused by electron plus radical scavengers is presumably due to the superposition of the above processes. The simultaneous application of electron and positive ion scavengers brings about a $G(H_2)$ decrease as low as $\Delta G = 0.1$, indicating the relative unimportance of recombination processes as well as the fact that the effects of various additives may compensate each other.

The most probable further reactions of the $c\text{—}C_6H_{11}^{\bullet}$ radical formed as a result of addition of a H-atom (produced in C–H bond rupture reactions) to the double bond of cyclohexene are abstraction, disproportionation and combination [12]:

$$c\text{—}C_6H_{11}^{\bullet} + c\text{—}C_6H_{10} \rightarrow c\text{—}C_6H_{12} + c\text{—}C_6H_9^{\bullet} \quad (6)$$

$$2\ c\text{—}C_6H_{11}^{\bullet} \longrightarrow c\text{—}C_6H_{12} + c\text{—}C_6H_{10} \quad (7)$$

$$c\text{—}C_6H_{11}^{\bullet} + c\text{—}C_6H_9^{\bullet} \rightarrow c\text{—}C_6H_{12} + c\text{—}C_6H_8 \quad (8)$$

The decrease of $G(C_6)$ observed with electron scavengers can be interpreted in terms of competition of reactions (1a) and (1b) and, consequently, of the decrease in the rate of reaction (2b).

The plot of G(cyclohexane) against the concentration of positive ion scavengers exhibiting a minimum must be due to not less than two simultaneous effects: the hindrance of recombination processes (1a) decreases the amount of cyclohexyl radicals [reaction (2b)] but, with increasing amount of NH_3 and C_2H_5OH the number of H-atoms produced in the system according to (3) and (4) increases; this, in turn, results in an increase of the amounts of $c-C_6H_{11}^{\cdot}$ and $c\text{-}C_6H_9^{\cdot}$ radicals according to (5).

The decrease of the G-value of 1,3-cyclohexadiene in the presence of CCl_4 may, presumably, be due to the competition between (1a) and (1b), whereas that caused by NH_3 in high concentrations can be attributed to the capture by 1,3-cyclohexadiene of thermalized H-atoms formed originally from NH_3.

The increase of yields of 1,3-cyclohexadiene and *trans*-1,3-hexadiene in the presence of *p*-benzoquinone may be attributed to the fact that additives react more rapidly with various radicals than do conjugated dienes, thus the latter decompose to a lesser extent or not at all in secondary reactions.

The effect of dose on the radiolysis of cyclohexene has been reported earlier [13]; the decrease of the yields of conjugated dienes with increasing dose has been explained in terms of competing reactions. It has been suggested that various conjugated dienes react more rapidly with radicals present in the system as compared with the starting alkene.

The phenomena observed in the presence of radical scavengers have been explained by the following reactions:

$$E^* \xrightarrow{k_c} R^{\cdot} + H \tag{9}$$

$$E^* \xrightarrow{k_a} CDE + H_2 \tag{10}$$

$$E + R^{\cdot} \xrightarrow{k_e} ER^{\cdot} \tag{11}$$

$$S + R^{\cdot} \xrightarrow{k_d} SR^{\cdot} \tag{12}$$

$$CDE + R^{\cdot} \xrightarrow{k_b} CDE - R^{\cdot} \tag{13}$$

where E denotes the alkene molecules to be studied, S the radical scavengers added, R·, H and CDE radicals, hydrogen atoms and conjugated diene molecules, respectively, produced during radiolysis.

The rate of formation of various radicals (R·) can be characterized by Eq. (14):

$$\frac{d[R^{\cdot}]}{dt} = k_c[E^*] - k_e[E]\,[R^{\cdot}] - k_d[S]\,[R^{\cdot}] - k_b[CDE]\,[R^{\cdot}] \cong 0 \tag{14}$$

In the steady state, $d[R^{\cdot}]/dt$ should be zero, therefore, the steady state concentration of the radicals is as follows [Eq. (15)]:

$$[R\cdot]_s = \frac{k_c[E^*]}{k_e[E] + k_d[S] + k_b[CDE]} \tag{15}$$

The actual concentration of conjugated dienes is determined by the rates of their formation in monomolecular reactions as well as of their further reactions in bimolecular processes with the radicals present

$$\frac{d[CDE]}{dt} = k_a[E^*] - k_b[CDE]\,[R\cdot] \tag{16}$$

From Eqs (15) and (16):

$$\frac{d[CDE]}{dt} = k_a[E^*] - k_b[CDE]\,\frac{k_c[E^*]}{k_e[E] + k_d[S] + k_b[CDE]} \tag{17}$$

and, since $k_b[CDE] \ll k_e[E] + k_d[S]$ in the denominator, we can write

$$\frac{d[CDE]}{dt} = k_a[E^*] - \frac{\frac{k_b k_c}{k_d}[E^*]}{\frac{k_e}{k_d}[E] + [S]}[CDE] \tag{18}$$

Equation (18) can be written in a simpler form:

$$\frac{d[CDE]}{dt} = k_a[E^*] - \frac{A}{B + [S]}[CDE] \tag{19}$$

where

$$A = \frac{k_b k_c}{k_d}[E^*]\,; \quad B = \frac{k_e}{k_d}[E]\,;$$

Finally, after substituting G-values and integrating, we obtain

$$G = G_0\,\frac{1 - \exp\left(-\frac{A}{B + [S]}t\right)}{\frac{A}{B + [S]}t} = G_0\,\frac{1 - \exp\left(-\frac{A'}{B + [S]}\right)}{\frac{A'}{B + [S]}}, \tag{20}$$

where G denotes the CDE yield determined in the presence of a scavenger of given concentration, G_0 a G-value extrapolated to zero irradiation dose, [S] is the concentration of the scavenger, $A' = At$ since t (the duration of irradiation) is constant in our case.

Since the experimental data and the calculated function agree sufficiently well (see Figs 2 and 4 where the lines correspond to the calculated functions and points denoted by + and • to experimental data measured in the presence of *p*-benzoquinone and oxygen, respectively) it can be regarded as verified that the competition between the alkene studied and the radical scavenger during radiolysis can be described by a mathemathical model (Table II) and the equations derived by us are suitable for characterizing radical scavenging processes.

Table II

Conjugated diene formation from cyclohexene

Product	A (mol h^{-1})	B (mol)	G_0
trans-1,3-C_6H_{10}	1.75×10^{-3}	10^{-2}	0.065
1,3-c-C_6H_8	9.8×10^{-4}	10^{-2}	0.185
1,3-C_4H_6	3×10^{-3}	10^{-2}	0.120

The decrease of methylcyclopentane yield under the effect of radical scavengers indicates the role of cyclohexyl radicals in its formation.

The decreased yield of benzene in the presence of CCl_4 is presumably due to an excitation transfer process but there are no exact data available to characterize the reaction mechanism in a more detailed manner.

The decrease of the yields of dicyclohexyl and the unidentified dimers in the presence of radical scavengers supports the earlier suggestions [12] about the importance of radical combination processes in radiation chemical dimerization of cyclohexene. The increase of yields in the presence of positive ion scavengers is also in favour of radical type dicyclohexyl formation, see *e.g.* reactions (21)—(24):

$$c-C_6H_{10}^+ + NH_3 \rightarrow c-C_6H_9^{\cdot} + NH_4^+ \quad (21)$$

$$NH_4^+ + e^- \rightarrow NH_3 + H \quad (22)$$

$$c-C_6H_{10} + H \rightarrow c-C_6H_{11}^{\cdot} \quad (23)$$

$$2\ c-C_6H_{11}^{\cdot} \rightarrow c-C_{12}H_{22} \quad (24)$$

The decrease of the yield with electron scavengers can be explained by hindrance of process (25) following recombination (1a):

$$c-C_6H_{10}^* \rightarrow c-C_6H_9^{\cdot} + H \quad (25)$$

The yields of two other dimers (R.I. = 1308.7 and 1310.3) with fairly high *G*-values increase in the presence of electron scavengers; this may be due to ionic processes.

Processes involving C–C bond rupture

The decrease of the yields of alkanes (ethane, propane, butane) caused by radical scavengers indicates the role of C_1–C_4 monoradicals.

The decrease of the yields of 1,3-butadiene (and partly also ethylene) under the effect of electron and positive ion scavengers can be attributed to the importance of electron–ion neutralization processes in the formation of these products. This observation supports the earlier suggestion [1, 2] on the formation of these two products *via* direct decomposition of excited cyclohexene:

$$c\text{—}C_6H_{10}^* \rightarrow C_2H_4 + 1,3\text{-}C_4H_6 \qquad (26)$$

The slight increase of ethylene and acetylene yields in the presence of *p*-benzoquinone can be interpreted in terms of competing reactions: the radical scavenger reacts more rapidly with radicals,thus 'protects' unsaturated products by preventing them from reacting with these radicals.

The yield of 1,3-butadiene shows a similar behaviour in the presence of radical scavengers as do the conjugated hexadienes mentioned above. In this case, too, a competition should be supposed between the conjugated diene produced in radiolysis and the radical scavenger added to the system.

By comparing Tables I and II it can be established that the G_0 values of conjugated dienes extrapolated to zero dose are higher than the *G*-values determined without additive, applying a dose of about 8 Mrd. This increase can be attributed to a supposed competition between radical scavengers and conjugated dienes. The application of radical scavengers with appropriate structure and inappropriate concentrations may lead to the fixation of a considerable (or predominant) part of intermediates which would act without radical scavengers as agents decreasing the yields of conjugated dienes.

REFERENCES

[1] FREEMAN, G. R.: Rad. Res. Rev., **1,** 1 (1968)
[2] CSERÉP, GY., FÖLDIÁK, G.: Proc. 3rd Tihany Symposium on Radiation Chemistry, (Eds.) DOBÓ J. and HEDVIG P., Vol. 1. p. 287 Akadémiai Kiadó, Budapest 1972
[3] SATO, S., YUGETA, R., SHINSAKA, K., TERAO, T.: Bull. Chem. Soc. Japan, **39,** 150 (1966)
[4] WAKEFORD, B. R., FREEMAN, G. R.: J. Phys. Chem., **68,** 2992 (1964)
[5] SEVILLA, N. D., HOLROYD, R. A.: J. Phys. Chem., **74,** 2459 (1970)
[6] BURNS, W. G., HOLROYD, R. A., KLEIN, G. W.: J. Phys. Chem., **70,** 910 (1966)
[7] KOURIM, P.: Int. J. Rad. Phys. Chem., **1,** 345 (1969)
[8] HORVÁTH, ZS., BÁNYAI, É., FÖLDIÁK, G.: Radiochim. Acta, **13,** 150 (1970)
[9] SINGH, A., FREEMAN, G. R.: J. Phys. Chem., **69,** 666 (1965)
[10] ADAMS, G. E., SEDGWICK, R. D.: 2nd Intern. Congr. Rad. Research, Abstracts of Papers, p. 80, Harrogate 1962
[11] FÖLDIÁK, G. *et al.:* A kémia újabb eredményei, Vol. 20, Akadémiai Kiadó, Budapest 1974
[12] FREEMAN, G. R.: Can. J. Chem., **38,** 1043 (1960)
[13] KOVÁCS, A., CSERÉP, GY., FÖLDIÁK, G.: Radiochem. Radioanal. Lett., **22** (3), 221 (1975)
[14] HATANO, Y., SHIDA, S., SATO, S.: Bull. Chem. Soc. Japan, **41,** 1120 (1968)

András KOVÁCS
György CSERÉP
Gábor FÖLDIÁK
H-1525 Budapest 114, POB 77.

Acta Chimica Academiae Scientiarum Hungaricae, Tomus 92 (2), pp. 129–142 (1977)

INFRARED SPECTROPHOTOMETRIC STUDIES ON ALUMINIUM OXIDE LAYERS PREPARED BY ANODIC OXIDATION

A. B. KISS* and E. SZONTÁGH

*(*Research Institute of Tungsram Ltd., Budapest, Research Institute for the Metal Industry, Budapest)*

Received November 5, 1975

The possibilities were established for the studies on amorphous oxide layers produced by anodic oxidation on aluminium surfaces by applying the infrared spectrophotometric technique. ATR and regular reflection techniques were employed, furthermore, spectra of separated oxide films were also recorded in KBr pellets.

The vibration frequencies of chemical bonds and other characteristics of the spectra were studied and on this basis the structure and composition of amorphous aluminium oxide layers formed in inorganic and organic electrolytes, as well as the size of co-ordination units, the degree of "polymerization" of the crosslinked structure can be estimated.

It was stated that the Al^{3+} ions formed temporarily during the anodic oxidation and not taking part in oxide formation will react with sulfosalicylic acid having the greatest complexing power of all the components of the bath, and some of the complex will be retained in the pores or bound at the surface.

The characteristics of the interference spectra produced by reflection of light on thin layers indicate the porosity of amorphous layers, their morphological properties, as well as the structure of the interface layers between the metallic substrate and the oxide layer. In the knowledge of the layer thickness the refractivities of the oxide layers produced by a. c. and d. c. oxidation were calculated from the interference waves.

Introduction

Within the technique of anodic oxidation, the various processes can yield oxide layers of widely different properties on aluminium surfaces. The great practical importance of these oxide layers, the uncertainties in respect of their formation and properties justify the interest taken by experts in this field employing various techniques of structure elucidation.

In the studies on the structure of different aluminium oxide layers the amorphous composition of these layers is of decisive importance. In connection with this problem we refer to the difficulties arising in X-ray diffraction studies and to the fact that the amorphous character, the complex composition of the layers and the various chemical bonds present render more difficult the thorough recognition of these oxide systems and exact elucidation of the formation processes.

Since in the investigation of amorphous materials the infrared spectrophotometric technique may be a powerful tool, first the main possibilities of the application of this method in the case of aluminium oxide layers developed by anodic oxidation will be surveyed.

I. *The structure of amorphous oxide layers* produced by different methods can be studied on the basis of characteristic chemical bonds (Al—O, Al—O—Al, Al—OH, Al—O . . ., HOH, etc., producing characteristic vibrational frequencies, bond interactions, etc.). In this field, the two most important techniques are:

a) direct investigation of the layer by the regular and ATR reflection techniques, and

b) recording transmission spectra after separation, grinding and pressing of oxide layers.

II. Detection of components from the electrolyte bath retained within the layer or on the substrate in unchanged, reduced, oxidized or occasionally in reacted state.

Such studies can be carried out in three ways:

a) direct recording of the reflection spectrum of the oxide layer and its evaluation,

b) recording the spectrum of the oxide layer in KBr pellets after separation, and

c) recording the spectrum of substances obtained from the layer by extraction and concentration, employing the KBr pellet technique.

III. Physical characteristics of light reflection on thin layers provide information on the porosity of the oxide, the dimensions of the particles and crystal cells, the diffraction properties, as well as on the morphological structure of the interface layer between the substrate and the oxide film. The interference waves appearing in the reflection spectra can be used *e.g.*, for calculating the refractive index of the sample when the layer thickness is known.

Experimental

In the present work three kinds of oxide layers were studied. These were prepared by the following procedures.

Sample A: Gold-coloured layer prepared by the direct colouring procedure AUTOKOLOR-HSH anodic processes in organic acid electrolyte using alternating current.

Sample B: Red-coloured layer; the basic layer was prepared with direct current sulfuric acid procedure, coloured in copper-containing electrolyte by the ELEKTROKOLOR-KRB process.

Sample C: Brown-coloured layer prepared according to the AUTOKOLOR-HSH direct colouring anodic procedure in organic acid electrolyte (the same as that applied to Sample A) using direct current.

The infrared spectra were recorded with a Zeiss UR 10 spectrophotometer. The reflection spectra were recorded by employing the Zeiss regular and multiple ATR reflection equipment. In the former case, the angle of incident light was 20° and 55°. In the measurements with 20° angle of incidence the area of the layer examined was usually 26×16 mm; in the studies on interference waves the area was 20×10 mm. The ATR spectra were recorded with a 45° KRS 5 prism of 3.5 mm thickness, the area of sample surface was 49×20 mm. Number of reflections was 14. Satisfactory transmission spectra of the oxide separated from the aluminium surfaces could be obtained in pellets with 8 mg sample/1 g KBr concentration.

Results and discussion of IR spectra

I. Composition of the amorphous layer, characteristics of the chemical bonds

Regular reflection spectra of samples A and B recorded at two different angles of incidence are shown in Figs 1 and 2. Here, as usual in studies on thin layers, the separation of spectral characteristics produced by chemical bonds and by reflection phenomena presents difficulties. Since the interference waves are superimposed on the absorption bands due to the vibrations of che mica

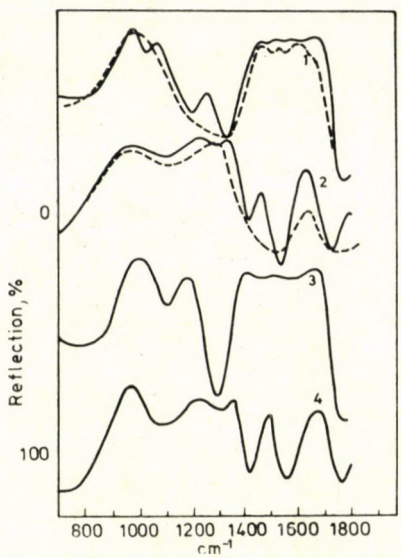

Fig. 1. Regular reflection spectra of aluminium oxide layers. 1. Sample A, angle of incidence 20°; 2. sample B, angle of incidence 20°; 3. sample A, angle of incidence 55°; 4. sample B, angle of incidence 55°

bonds rendering the interpretation of the bands more difficult. In the spectra recorded at 55° angle of incidence the bands in the region of OH vibrations (Fig. 2) are significantly less intense, thus the spectra recorded at 20° angle of incidence were found to be more useful in the evaluation work.

Interpretation of regular reflection spectra from chemical points of view can be attempted in two ways. On one hand, the ATR spectra of the samples may be recorded yielding the pure absorption spectra of the oxide layers free from interference waves, on the other hand, removing the oxide layer from the aluminium substrate by an appropriate method and suitable pieces of the layer are used either directly or mixed with KBr for recording the transmission spectrum (Fig. 3).

With respect to the amorphous nature of the oxide layers, exact analysis of the bands obtained according to crystal classes cannot be carried out.

Spectra of crystalline systems show characteristic sharp, distinct bands and band systems, however, amorphous systems yield spectra comprising mainly only broad and flat bands owing to the presence of various bond energies and

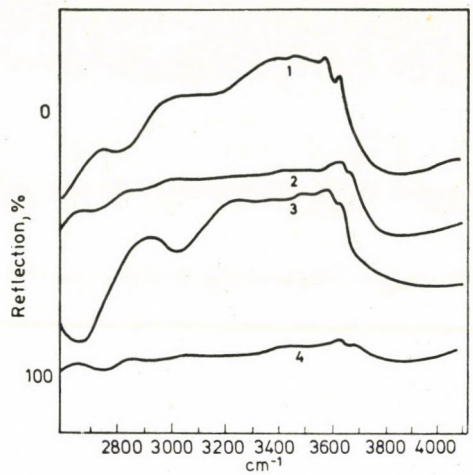

Fig. 2. Regular reflection spectra of aluminium oxide layers. Notations 1, 2, 3 and 4 are the same as in Fig. 1

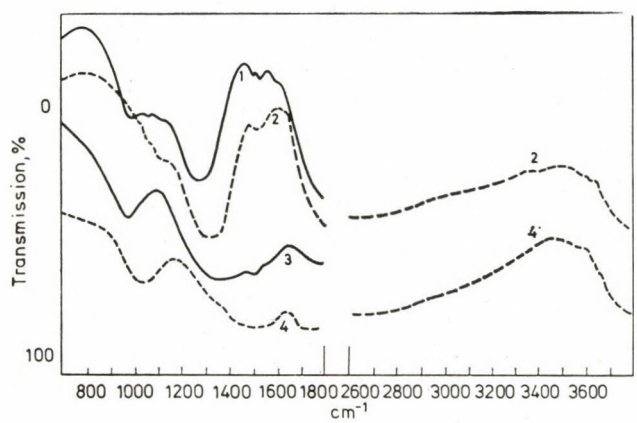

Fig. 3. ATR reflection and transmission spectra of amorphous aluminium oxide layers 1. Layer A, ATR reflection; 2. layer A, separated and recorded in KBr pellet; 3. layer B, ATR reflection; 4. layer B, separated and recorded in KBr pellet

bond distances. These broad and flat bands represent ultimately the statistic averages of vibrational states strongly scattered around a mean value.

The amplitudes of interference waves caused by reflection of light decrease with increasing frequency, thus at wavenumbers above 3000 cm^{-1} the conditions are favourable for undisturbed appearance of the OH bands. Consequently, the regular reflection spectra show OH bands similar to those

in the absorption spectra in this range. In practice, the advantage provided by this phenomenon is that bond relations and other characteristics of structural OH groups in anodic oxide layers, and of HOH groups bound by chemical or physical forces can be studied very simply without the degradation of the layers by the regular reflection technique.

The ATR reflection spectra and the transmission spectra recorded in KBr pellets (Fig. 3) are very similar, in accordance with the statement made by HARRICK [1] that the ATR reflection and the transmission spectra are the same in character. The slight displacement of the bands in the transmission spectrum of Sample A towards higher frequencies is a usual phenomenon in the case of layers much thicker (10—12 μm) than the depth of penetration of the light beam (1—2 μm) and in our case, too [1]. However, the frequency shifts in the spectrum of Sample B as compared to the bands in the ATR spectrum are greater than expected. Thus, for example, the maximum found at 1090 cm^{-1} in the ATR spectrum appears at 1160 cm^{-1} in the transmission spectrum which indicates differences of rather chemical in nature. It must therefore be assumed that during the separation of the layer from the carrier aluminium substrate, its grinding and pressing, changes can occur in the oxide yielding the above-mentioned frequency shift. Since separation of the oxide layer requires the production of a layer with considerably larger thickness than the usual, it cannot be excluded either that the structure of the layer prepared by the same technology but having an increased thickness will be different and this is reflected in the changes in the spectrum shown in Fig. 3 (Spectra 3 and 4).

On the basis of the above facts, the reflections due to chemical and physical reasons can easily be distinguished in the reflection spectrum shown in Fig. 1. The dotted line in Fig. 1 obtained by taking into account the ATR spectrum thus represents the spectrum of the amorphous layer free from interference waves.

The interpretation of the bands was based on the fundamental work of FICHTER [2] and DORSEY [3]. In connection with Table I it must be noted that the assignation of νOH bands has been supported by IR spectroscopic studies not only on aluminium oxides formed by anodic oxidation but by the results obtained in connection with several other inorganic compounds, too [4—9].

The most striking differences in the spectra of samples obtained in organic and inorganic electrolytes appear in the 1400—1700 cm^{-1} region.

In the spectra of oxide layers obtained in organic electrolytes the bands appearing at 1465, 1520 and 1560 cm^{-1} can be attributed to the valence vibrations of Al=O bonds, since their frequency range is between 1345 and 1696 cm^{-1} as demonstrated by DORSEY [3]. The δOH vibration superimposed on these vibrations appears only as a shoulder.

Table I

Layer A, cm^{-1}			Layer B, cm^{-1}			Assignation	
Reflection Abs.			Reflection Abs.			Vibration character	Bond type
Regular	ATR	in KBr	Regular	ATR	in KBr		
	800	820		700	700	νAlO	Al ↔ O–Al
	1050	1100		1090	1160	δAlOH	Al ↔ OH
					1350	νAlO	
	1465	1500		(1480)		νAlO	
	1520			(1520)		νAlO	Al ⇔ O
	1520	1600				νAlO	
	1610	1625		1650	1645	δOH	AlO . . . H_2O
3300		3320				νOH	Al–OH . . . OH_2
3440		3450	3420		3425	νOH	AlO . . . H_2O
3580		3580	3590		3590	νOH	AlO ↔ H
3650		3630	3640		3640	νOH	AlO ↔ H

In the spectrum of the oxide of type B, a slight absorption appears at 1350 cm^{-1} being the frequency indicated by DORSEY [3] for layers obtained in sulfuric acid medium only in the transmission spectrum, and this can be assigned to the νAlO(Al=O) vibration. It is striking that in the 1500—1600 cm^{-1} range, where the νAl–O vibration bands would appear, only a very weak absorption is observed. The band at 1640 cm^{-1} is due to the δOH vibration of water molecules.

In the other characteristic range, between 1050 and 1150 cm^{-1}, the band produced by the oxide of type A is complex. According to DORSEY [3], this range can be assigned to the frequency of the δAl ↔ OH vibration, and the smaller partial maxima are due to the presence of the organic electrolyte as it will be demonstrated later. In the spectrum of the oxide produced in sulfuric acid medium no partial maxima appear at this band.

Of course, exact structural conclusions cannot be drawn on the basis of the IR spectra alone, since the relationship between the band systems in the spectra and the construction of the amorphous layers has not been established unambiguously yet. Combined application of fundamental molecular spectroscopic correlations and experimental observations, however, allow some realistic deductions. Thus, for example, the higher frequency of the valence vibration of the Al–O–Al chain indicates the stronger interaction of Al–O bonds in the network of chains which may accompany a more frequent break in the cross-linked structure, its higher compactness [3]. In the case of Sample A thus the higher frequency of the band mentioned above and the simultaneous appearance of the bands due to Al=O double bonds indicates a more compact

structure of the 'polymeric' oxide layer formed in the organic electrolyte, being formed from smaller co-ordination units as compared with the layer obtained in sulfuric acid medium, which represents a more loose system with a higher 'degree of polymerization'. The presence of the Al=O bonds (Sample A) in itself proves that in the crosslinked structure chain terminals with double bonds frequently develop. At the same time, their absence and the lower frequency of the Al–O–Al chain vibrations can be regarded as definite indication of more extensive crosslinking.

The spectrum of the oxide layer formed in sulfuric acid-containing electrolyte comprises only two broad and flat vibration bands — disregarding the νOH and δOH bands — while the oxide layer produced in organic medium shows several well-defined intense maxima.

In the spectrum of the latter, a definite and characteristic system of Al–O vibration bands appear, consequently the atomic distances and bond relations are more defined within the aluminium–oxygen co-ordination units in the layer formed in organic media, although X-ray studies show the same amorphous structure for both systems [10].

The evaluation of the OH bands is rendered somewhat difficult by the fact that in the spectrum of Sample A the OH deformation band overlaps the band of Al–O bonds (Fig. 3, 1 and 2), and makes the determination of the shape and exact frequency of the δOH band questionable. The small maxima appearing between 3580 and 3640 cm^{-1} show that in both kinds of oxide layer OH groups with approximately free hydroxyl nature are strongly bound to the central aluminium atoms of the co-ordination units. In the crosslinked layer structure of oxide B the H_2O molecules present participate in a somewhat stronger hydrogen bond as compared to Oxide A, since in the former the frequency of the respective νOH band is lower, while that of the δOH band is higher. Here the δOH band is rather broad and flat (Fig. 3, 3) which can be explained by a stronger distortion of the asymmetry of the H_2O molecule due to the hydrogen bond [4]. It is noteworthy that in layer A another band appears at an even lower frequency and, on the analogy of other metal–OH bonds [8], it is probably due to the absorption of H_2O molecules attached to Al–OH bonds by hydrogen bonds.

In the case of layer B, where the second step in the preparation is the deposition of copper with alternating current, the formation of copper oxide beside metallic copper could also be supposed. The spectra shown in Fig. 4 do not confirm this assumption, since they do not indicate the presence of Cu(II)O which could be detected by IR spectrophotometry. This statement is in agreement with the results of X-ray diffraction examinations on these layers, too [11].

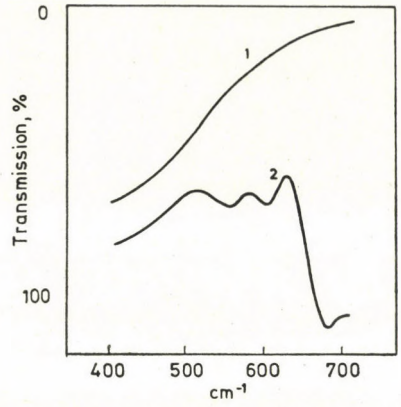

Fig. 4. 1. Regular reflection spectrum of sample B; 2. Transmission spectrum of Cu(II) oxide in KBr pellet

II. Studies on residual organic electrolytes

Direct detection of the organic electrolyte bound in the oxide layer by adsorption, capillary or chemical forces was carried out in the layer separated from Sample A in KBr pellets. The spectra of samples rinsed with cold water after the preparation then washed thoroughly with cold water or treated in hot water for 10 minutes are shown in Fig. 5. On the effect of these operations, the disappearance of smaller peaks and inflection points could be observed in the spectra. When comparing these frequencies with the well-known spectra of sulfosalicylic acid and formic acid used as organic electrolytes, none of the bands disappeared could be statisfactorily identified. The suggestion of TAJIMA *et al.* [12, 13] also seems doubtful, according to them, compounds of

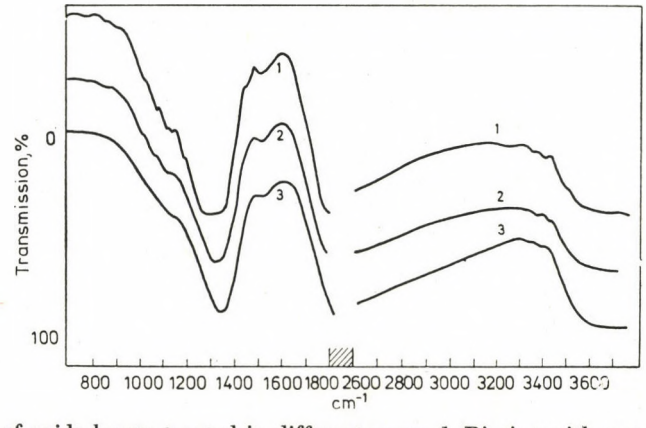

Fig. 5. Spectra of oxide layers treated in different ways. 1. Rinsing with water; 2. prolonged washing in cold water; 3. boiling in hot water

phenolic and quinoidal type are retained in the layer produced in sulfosalicylic acid baths, since identification on the basis of one single weak band may lead to unreliable conclusions.

The spectra of the aluminium complexes prepared by us, as well as the evaporation residue of the hot water extraction fraction (Fig. 6) provide a firm evidence that the majority of the compound searched for is aluminium sulfosalicylate and that formation of aluminium formate should not be expected. In Table II the wavenumbers of the spectra shown in Figs 5 and 6 are listed which strongly support the above conclusions.

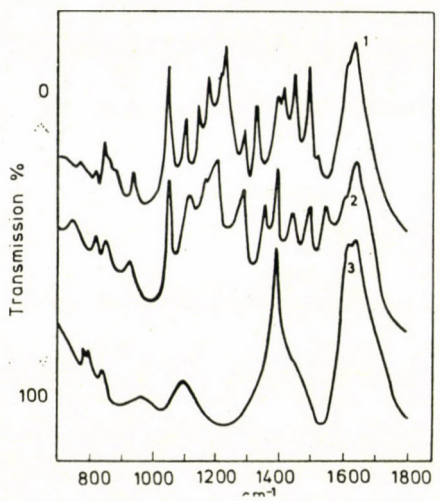

Fig. 6. Spectra of aluminium complexes. 1. The evaporation residue of the hot water fraction; 2. aluminium sulfosalicylate (1 : 2); 3. aluminium formate (1 : 3)

The difference appearing in columns 1 and 3 in Table II yields information on the frequencies attributable to organic material bound at the surface. These frequencies can be compared with the respective frequencies of aluminium sulfosalicylate, thus the agreement between the most intense bands definitely proves the correctness of identification of the unknown substances as discussed above.

On the basis of experimental data, it can be assumed that in the course of anodic oxidation the Al^{3+} ions formed temporarily and excluded from the oxide formation reaction react with sulfosalicylic acid having the strongest complexing power of the components of the electrolytic bath, and some of the complex is retained in the pores or bound at the surface.

This phenomenon is in agreement with the high stability constant of aluminium sulfosalicylate ($\log k_1 = 13.2$) [14]. The slight deviation in the frequencies underlined in Table II is probably caused by the difference in the states of free and at the surface chemically bound aluminium complex.

Table II

Aluminium oxide layer (cm^{-1})				Complexes (cm^{-1})	
Untreated	Washed in cold water	Washed in hot water	Residue of hot water phase	Al-sulfo-salicylate	Al-formate
820	800	800	767	740	780
880			816	817	797
			840	845	835
950			936	927	950
1040	1040		1048	1048	
1096	1090		1100	1103	1100
1140	1140		1142	1140	
1175	1175	1175	1170	—	
1210			1208	1204	
			1221	1240	
			1285	1280	
			1326	1330	
			1393	1390	
			1410	—	
1455			1445	1447	
1500	1500	1500	1492	1490	1492
			1520	1525	
			1608	1590	
1625	1625	1625	1630	1630	1625
			3200	3200	3160
3300	3300		3430	3430	3440
3480	3450				
		3500			
3585	3580	3580			
3630	3630	3630			

III. Interference waves

The complex nature of reflection spectra of oxide layers formed on aluminium is due to the fact that the light absorption caused by the vibration of chemical bonds, the light scattering phenomena caused by morphological properties and the interference waves related to the layer thickness together result in the shape of the spectrum. Interference waves appear when the wave-number range examined is transparent for the layer and the carrier of the layer has dielectric constant and optical characteristics different from those of the layer. These criteria are usually fulfilled for aluminium oxide layers produced by anodic oxidation on aluminium surfaces. The optical path occurring

in the system examined is shown in Fig. 7. When following the paths of the incident light (1), the partly reflected light (2) and the departing light (3), the phenomenon of interference is observed. Interference waves are obtained at wave lengths where the difference in path length, $L = C - D$, is an integer multiple of the half-wave length, that is,

$$L = \left(m + \frac{1}{2}\right) \lambda_m$$

where $m = 0, 1, 2 \ldots$ and λ_m is the wave length belonging to the maximum of the mth order (μm). The interference method has been employed by several

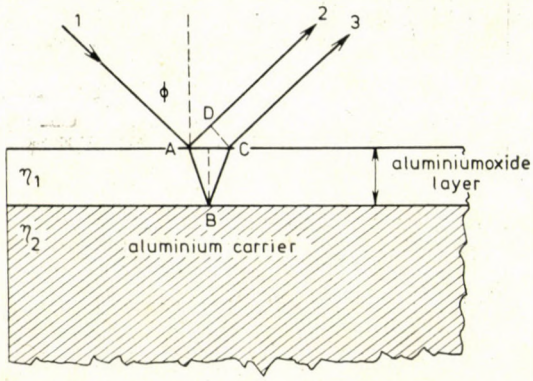

Fig. 7. Optical path in the oxide layer

authors [15—17] for measuring the thickness of epitaxial layers of semiconductors. On the basis of these works, in our system the number of interference maxima (n) between wave lengths λ_m and λ_{m+x} is:

$$n = 2T \frac{\lambda_m - \lambda_{m+x}}{\lambda_m \cdot \lambda_{m+x}} \cdot \frac{1}{(\eta^2 - \sin^2 \Phi)^{-1/2}}$$

where T is the thickness of the oxide layer (μm), η is its refractive index and Φ is the angle of incidence. Thus, when the thickness of the layer is known, its refractive index is determined by the following correlation:

$$\eta = \sqrt{\sin^2 \Phi + \left(\frac{n}{2T} \cdot \frac{\lambda_m \cdot \lambda_{m+x}}{\lambda_m - \lambda_{m+x}}\right)^2} .$$

The interference method was used to determine the refractive indices of the two kinds of layers produced in electrolytes of identical composition with a.c. and d.c. technique (Samples A and C). For this purpose the layer thickness

of the oxide samples was determined on a 2 cm^2 area at 40 different sites with an instrument operated on the basis of the eddy current principle in a non-destructive way, and the results were averaged. The same area was used for recording the infrared spectra (Fig. 8). The frequency values of maxima of the mth order and the refractive indices calculated in the knowledge of thickness are shown in Table III.

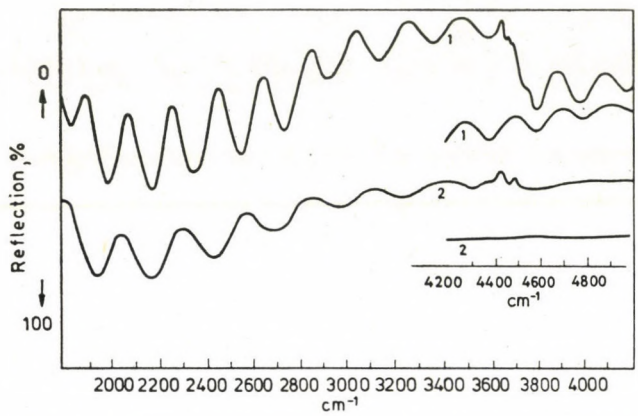

Fig. 8. Infrared interference waves. 1. sample A; 2. sample C

Table III

	Sample A, T = 17.20 μm, Ø = 20°					Sample C, T = 13.10 μm, Ø = 20°			
m + x	m	m + 1	m + 2	m + 3	m + 4	m	m + 1	m + 2	m + 3
Wave length μ	4.618	4.251	3.933	3.633	3.407	4.629	4.132	3.731	3.389
Wavenumber cm^{-1}	2165	2352	2542	2730	2935	2160	2420	2680	2950
Refractive index η	1.608	1.583	1.560	1.583		1.507	1.507	1.454	
$\bar{\eta}$ (2000—3000 cm^{-1})	1.583					1.490			

In the calculations the 2000—3000 cm^{-1} range was considered, since, strictly speaking, the conditions of the applicability of the above correlation are ensured in this region only. The correlation cannot be applied between 3000 and 3800 cm^{-1}, since partly the development of interference waves is disturbed by the appearance of OH bands, partly the refractivity value changes abruptly in the vicinity of absorption maxima and this would lead to false results. The

range of higher frequency was neglected, since sample C does not show any interference phenomenon there, thus comparison cannot be made. The results clearly reveal that the refractive index of the sample prepared by d.c. anodic oxidation (Sample C) is lower than that of the a.c. sample (Sample A). The refractive indices calculated by the interference method are in good agreement with the series of values measured for similar systems with other methods [18] and this confirms the reality of the data obtained by us.

On the basis of Fig. 8, conclusions can be drawn regarding other properties of the layers, too. The sharper appearance of interference waves and the higher intensity of the maxima indicate that in the sample produced by a.c. technique the transition between the aluminium substrate and the oxide layer is rather sharp. On the other hand, a less sharp and less distinct interference picture is obtained in the oxide layer prepared with the d.c. method, shows the presence of a more broad interface layer between the two materials of different refractivities. The higher refractivity of the a.c. sample refers to the higher density (compactness) of the layer, since the refraction

$$\frac{\eta^2 - 1}{\eta^2 + 2} = \frac{4\pi}{3} \cdot N\alpha$$

— which also increases with the refractivity — is proportional to the number of oscillators in unit volume, assuming that the polarizability of molecules (α) in the two kinds of layers does not differ. This conclusion is in accordance with the statements made in Chapter I. There is also an important morphological difference between the two systems. In Fig. 8 in the high-frequency range the transmission of the d.c. sample is very low caused by the strong light scattering in the layer. Consequently, the d.c. layer shows a morphologically more uniform structure [19]. The porosity of the a.c. sample is considerably lower and the layer produces sharp interference waves up to 5000 cm^{-1}.

Finally, it is to be noted that examination of several samples made by the same methods (A, B, C) yielded identical, reproducible results.

REFERENCES

[1] HARRICK, N. J.: Internal Reflection Spectroscopy, John Wiley, New York 1967. pp. 60—65
[2] FICHTER, R. F.: Helv. Phys. Acta **19,** 21 (1946)
[3] DORSEY, G. A.: J. Electrochem. Soc. **113,** 169 (1966)
[4] GLEMSER, O.: Angew. Chem. **73,** 785 (1961)
[5] SCHWARZMANN, E., MARSMANN, H.: Naturwiss. **53,** 349 (1966)
[6] HENNING, O.: Wissenschaftliche Zeit. der Hochschule für Architektur und Bauwesen Weimar, **15,** 53 (1968)
[7] SATO, T.: J. Appl. Chem. **11,** 207 (1961); *ibid.* **12,** 553 (1962); *ibid* **14,** 303 (1964)
[8] KISS, B. A.: Acta Chim. (Budapest) **75,** 351 (1973)

[9] NAKAMOTO, K.: Infrared Spectra of Inorganic and Coordination Compounds, John Wiley, New York 1963. pp. 157—159.
[10] GADÓ, P.: Unpublished results
[11] GADÓ, P., LICHTENBERGER-BAJZA, E., DÖMÖLKI, F., IMRE-BAÁL, I.: Acta Techn. **80,** 303 (1975)
[12] TAJIMA, S., BABA, N., MORI, T., SHIMURA, M.: Proc. Int. Symp. on Anodising (Birmingham, 1967), Aluminium Federation London (1967), pp. 37—42.
[13] TAJIMA, S., BABA, N., SHIMURA, M.: Electrochim. Acta **12,** 955 (1967)
[14] BANKS, C. V., SINGH, R. S.: J. Am. Chem. Soc. **81,** 6159 (1960)
[15] SPITZER, W. G., TANNENBAUM, M.: J. Appl. Phys. **32,** 744 (1961)
[16] ALBERT, M. P., COMBS, J. F.: J. Electrochem. Soc. **109,** 709 (1962)
[17] FEJES, L., KISS, A., KOMLÓS, J.: Híradástechnikai Ipari Kutató Intézet Közl. **6,** 15 (1966)
[18] TAJIMA, S.: Anodic Oxidation of Aluminium, Advances in Corrosion Sciences and Technology, Plenum Press. Vol. 1, p. 288 (1970)
[19] SZONTÁGH, E.: Aluminium (Düsseldorf) **49,** 807 (1973)

András B. KISS H-1044 Budapest, Váci út 77.
E. SZONTÁGH H-1116 Budapest, Fehérvári út 144.

Acta Chimica Academiae Scientiarum Hungaricae, Tomus 92 (2), pp. 143—146 (1977)

STUDIES ON SOME SQUARE PLANAR COMPLEXES OF N-5-ACETOACENAPHTHYLIDENE-O-AMINO-PHENOL WITH Cu(II) Pt(II) AND Pd(II)

P. SINGH, B. P. SINGH, V. SINGH and R. L. GOEL

(Chemical Laboratories, S. S. V. College, Hapur, Meerut, India)

Received January 13, 1976

Complexes of composition $[M(C_{20}H_{16}N\,O)_2]$ [M = Cu(II), Pt(II) or Pd(II)] with N-5-acetoacenaphthylidene-O-aminophenol (HAAAP) have been studied. Analytical, magnetic, IR and electronic spectral data show that all these complexes possess square planar configurations. On the basis of electronic spectral studies it has been shown that bonding increases in the order $3d_\sigma < 4d_\sigma < 5d_\sigma$.

Introduction

Square planar complexes of C_{4v} symmetry have been discussed in recent years [1—6]. The five degenerate *d*-orbitals of the uncomplexed metal ion split into four different levels of symmetries [5] $d_{x^2-y^2}$ (b_{1g}), $d_{xy}(b_{2g})$, $d_{z^2}(a_{1g})$ and $d_{xz,\,yz}(e_g)$ as shown in Fig. 1.

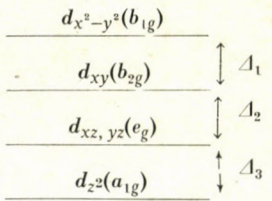

Fig. 1. Metal *d*-orbital energies for typical square planar complexes

The three orbital parameters Δ_1, Δ_2 and Δ_3 describe the ligand field splitting in such complexes. In this paper the magnetic and spectral properties of typical square planar complexes of N-5-acetoacenaphthylidene-O-aminophenol with Cu(II), Pd(II) and Pt(II) will be described.

Experimental

N-5-acetoacenaphthylidene-O-aminophenol (HAAAP), a bidentate ligand, was prepared by refluxing a mixture of 5-acetylacenaphthene and O-aminophenol in ethanol in the presence of a few drops of glacial acetic acid on the water bath for 5.5 hrs. The contents after cooling were poured into water, the gummy mass separating out was dried and crystallized from ethanol (yield 70%, m. p. 71 °C). Anal. $[C_{20}H_{17}N\,O]$. Calcd. C 83.62; H 5.92; N 4.87. Found C 83.30; H 5.75; N 4.68%. 75% ethanolic solutions of the ligand were used throughout. Metal chlorides of A. R. quality were used.

Table I

Electronic spectral data (nujol mull, cm^{-1})

Complex compound	Observed bands and their assignments	Δ_1	Δ_2	Δ_3
[Cu $(C_{20}H_{16}N\,O)_2$]	16,000 $^2B_{1g} \rightarrow {}^2A_{1g}$			
	19,000 $^2B_{1g} \rightarrow {}^2E_g$			
	21,500 Charge-transfer			
[Pd $(C_{20}H_{16}N\,O)_2$]	30,000 $^1A_{1g} \rightarrow {}^1A_{2g}$, ^1E_g, $^1B_{1g}$	33 500	1500	500
	48,000 $\rightarrow C^1E_u$			
[Pt $(C_{20}H_{16}N\,O)_2$]	32,150 $^1A_{1g} \rightarrow {}^3E_g$, $^3A_{2g}$	44 500	1500	3000
	41,000 $\rightarrow {}^1A_{2g}$, ^1E_g			
	43,500 $\rightarrow {}^1B_{1g}$			
	47,000 $\rightarrow C^1E_u$			

Orbital parameters were calculated taking $B = 500\ cm^{-1}$ and $C = 3500\ cm^{-1}$

Magnetic studies of the complexes were made on a Guoy balance using mercury(II) tetrathiocyanatocobaltate(II) as a standard. The electronic spectra of the complexes were recorded in nujol mull on a Cary-14 recording spectrophotometer. The bands and relevant ligand field parameters are listed in Table I. The IR spectra of the complexes were recorded on a Model 521 Perkin—Elmer Infracord Spectrophotometer in KBr pellets.

The complexes of Cu(II), Pd(II) and Pt(II) were isolated by refluxing a stoichiometric mixture of the metal chloride and the ligand in ethanol solution on the water bath for 2.0—4.5 hrs. On refrigeration for a few days the reaction mixture yielded brown, grey and yellow crystals of complexes which were washed with water, ethanol and ether and dried in vacuum (yield 60—70%, decomposition points 200—250 °C).

(a) [Cu$(C_{20}H_{16}N\,O)_2$], brown compound. Calcd. C 75.53; H 5.03; N 4.40; Cu 9.99. Found C 75.33; H 4.88; N 4.29; Cu 9.79%.

(b) [Pd$(C_{20}H_{16}N\,O)_2$], grey compound. Calcd. C 70.80; H 4.72; N 4.13; Pd 15.61. Found C 70.56; H 4.58; N 4.00; Pd 15.36%.

(c) [Pt$(C_{20}H_{16}N\,O)_2$], yellow compound. Calcd. C 62.57; H 4.17; N 3.65; Pt 25.42. Found C 62.37; H 4.08; N 3.50; Pt 25.20%.

Results and discussion

Analytical data show a 1:2 (metal : ligand) stoichiometry in all cases, Copper(II) complexes are considered to exhibit magnetic moments close to the spin-only value (1.73 B.M.), irrespective of the stereochemistry [7]. The observed magnetic moment (1.76 B.M.) is very close to the predicted spin-only value; it shows that orbital contribution is almost quenched by the ligand fields. Magnetic data on copper(II) complexes are therefore not helpful in deciding the stereochemistry.

In the electronic spectrum of the Cu(II) complex three bands are observed at 16,000, 19,000 and 21,500 cm^{-1} which correspond to square planar stereochemistry [8]. The first two bands are assigned to the transitions $^2B_{1g} \rightarrow {}^2A_{1g}$ (16,000 cm^{-1}) and $^2B_{1g} \rightarrow {}^2E_{1g}$ (19,000 cm^{-1}), whereas the third band is assigned to a charge-transfer transition. One of the interesting features of

electronic spectra studies is that the ratio $^{o}Cu/^{o}Ni$ between the wavenumber (^{o}Cu) of the principal band of the Cu(II) complex and ^{o}Ni, the wavenumber of the first spin-allowed band of the high-spin octahedral Ni(II) complex $[Ni(C_{20}H_{16}NO)_2(H_2O)_2]$, (9540 cm^{-1}, 14,030 cm^{-1}, 24,560 cm^{-1}) with the same ligand would be 1.6—1.8 for a highly tetragonal distortion of Cu(II) [9]. This ratio is in conformity with the present Cu(II) complex ($^{o}Cu/^{o}Ni \sim 1.67$) having a square planar stereochemistry, the extreme case of tetragonal distortion.

The complexes of Pd(II) and Pt(II) are diamagnetic. Three spin-allowed *d–d* transitions are anticipated corresponding to transitions from the three lower lying *d*-levels to the empty $d_{x^2-y^2}$ orbital; two-electron transitions would be very weak and are neglected. Energies corresponding to these transitions are determined as described by MARTELL [10].

In the electronic spectrum of $[Pt(C_{20}H_{16}NO)_2]$, four bands are observed at 32,150 cm^{-1}, 41,000 cm^{-1}, 43,500 cm^{-1} and 47,000 cm^{-1}. The first spin-allowed transition $^1A_{1g} \rightarrow {}^1A_{2g}$ in azomethine $CH_3—C=N$-complexes has been reported to be about 18,500 cm^{-1} higher in energy than in halide complexes, owing to the spectrochemical differences of azomethine and halide ligands in several octahedral complexes of third row transition series [11]. GRAY and MASON [5] have reported the transition $^1A_{1g} \rightarrow {}^1A_{2g}$ at about 25,500 cm^{-1} in $[PtCl_4]^{-2}$. The corresponding transition in the present Pt(II) complex of HAAAP has been observed at 41,000 cm^{-1}, lying 15,500 cm^{-1} higher in energy than the corresponding transition of $[PtCl_4]^{-2}$. Since the difference between the energies of $d_{xy}(b_{2g})$ and $d_{xz,yz}(e_g)$ levels should be very small for simple σ donor azomethine ligands, the above bands may also be assigned as a combination of both $^1A_{1g} \rightarrow {}^1A_{2g}$ and $^1A_{1g} \rightarrow {}^1E_g$ transitions, whereas the maxima at 43,500 cm^{-1} may be spin-allowed $^1A_1g \rightarrow {}^1B_{1g}$ transition. Consequently, the first band appearing at 32,150 cm^{-1} is a spin-forbidden $^1A_{1g} \rightarrow {}^3E_g$, $^3A_{2g}$ transition. Due to the large ligand field splitting and relative stability of the σ donor level of the azomethine group, charge transfer transitions of the type $L\sigma_u \rightarrow d\sigma_g$ are not expected to fall below 55,000 cm^{-1}. The lowest predicted allowed transition is in fact a $d \rightarrow p$ type $e_g \rightarrow a_{2u}\pi$ transition as the $a_{2u}\pi$ orbital is nonbonding and should be relatively stable. Therefore the band observed at 47,000 cm^{-1} may be considered to have arisen due to the $^1A_{1g} \rightarrow C^1E_u$ transition [4].

In contrast to the spectra of the Pt(II)—HAAAP complex, only two bands are observed for the Pd(II) complex. In the electronic spectrum of $[Pd(C_{20}H_{16}NO)_2]$ the bands appear at 30,000 cm^{-1} and 48,000 cm^{-1}. Following the assignment of GRAY and MASON [5] for the electronic spectrum of the square planar $[Pd(NH_3)_4]^{+2}$, we may presume that the former is a combination of all three spin-allowed transitions. This means that in the case of Pd(II) complex, the $a_{1g}(z^2)$ level has moved to higher energy relative to the corre-

sponding Pt(II) complex. The other band at 48,000 cm^{-1} has also shifted to the red with respect to the Pt(II) complex and has been assigned to the transition $^1A_{1g} \rightarrow C^1E_u$.

Table I summarizes the values of the ligand field parameters Δ_1, Δ_2 and Δ_3 derived from the *d–d* spectra of Pt(II) and Pd(II) complexes under investigation. The values of Δ_1 are found to be larger than the combined values of Δ_2 and Δ_3. Further, since Δ_1[Pt(II) complex] $>$ Δ_1[Pd(II) complex], it is interesting to note that this increase is similar to that observed for the corresponding octahedral complexes [12] [Co(III); Δ (21,000 cm^{-1})] $<$ [Rh(III); Δ (21,400 cm^{-1})] $<$ [(Ir(III); Δ (25,000 cm^{-1})] $<$ [Pt(IV); Δ (31,000 cm^{-1})] with HAAAP and may therefore be interpreted to indicate increasing σ bonding in the order $3d\sigma < 4d\sigma < 5d\sigma$.

IR spectral studies

In the IR spectrum of the ligand two significant peaks due to azomethine ($CH_3C=N-$, 1650 cm^{-1}) and hydroxyl (—OH, 3480 cm^{-1}) groups are observed. In the spectra of the chelates the stretching frequencies of the above groups are lowered to the range 1500—1560 cm^{-1} and 3300—3400 cm^{-1} respectively. Further, the appearance of bands around 400—470 cm^{-1} and 475—525 cm^{-1} in the IR spectra of the chelates due to the formation of M–N and M–O bonds indicates complex formation through nitrogen and oxygen donors of subsequent groups.

*

The authors are thankful to Dr. G. L. MAHESHWARI, Dr. R. P. MAHESH and Dr. R. S. KAPIL (C. D. R. I. Lucknow) for their co-operation in this work.

REFERENCES

[1] GRAY, H. E., BALLHAUSEN, C. J.: J. Amer. Chem. Soc. **85,** 260 (1963)
[2] BALLHAUSEN, C. J., BJERRUM, N., DINGLE, R., ERIKS, K., HARE, C. R.: Inorg. Chem., **4,** 514 (1965)
[3] COTTON, F. A., HARRIS, C. B.: Inorg. Chem., **6,** 369 (1967)
[4] MASON, W. R., GRAY, H. B.: Inorg. Chem., **7,** 55 (1968)
[5] MASON, W. R., GRAY, H. B.: J. Amer. Chem. Soc., **90,** 5721 (1968)
[6] CHATT, J., GAMLEM, G. A., ORGEL, L. E.: J. Chem. Soc., **1958,** 486
[7] KEETON, M., LEVER, A. B. P., RAMASWAMY, B. S.: Can. J. Chem., **48,** 3185 (1970)
[8] FIGGIS, B. N.: Introduction to Ligand Fields p. 316, Interscience, New York 1967
[9] JØRGENSEN, C. K.: Absorption Spectra and Chemical Bonding. In: Complexes, p. 123, Pergamon Press, New York 1962
[10] MARTELL, A. E.: Co-ordination Chemistry, ACS Monograph, Vol. 1, p. 67. Van Nostrand-Reinhold, New York 1971
[11] JØRGENSEN, C. K.: Absorption Spectra and Chemical Bonding, Chapter 13. Addison—Wesley, Reading, Mass. 1962
]12] SINGH, P., SINGH, V., SINGH, B. P., GOEL, R. L.: J. Inorg. Nucl. Chem. (In press)

P. SINGH
B. P. SINGH
V. SINGH
R. L. GOEL
Mohalla Ram Nagar Gulaothi (Bulandshahr) U. P. India.

Acta Chimica Academiae Scientiarum Hungaricae, Tomus 92 (2), pp. 147—156 (1977)

ELECTROCHEMICAL INVESTIGATIONS ON SUPPORTED PALLADIUM CATALYSTS

É. POLYÁNSZKY, T. MALLÁT and J. PETRÓ

(Department of Organic Chemical Technology, Technical University of Budapest)

Received January 25, 1976

Potentiodynamic polarization studies already applied to non-supported noble metal powder catalysts have been extended to supported palladium catalysts.

After determining the optimum conditions of measurement, a series of active carbon-supported catalysts containing 0, 1, 5, 10, 20 and 100% by weight of palladium was prepared in a similar way, and the changes in the sorption and catalytic properties with the metal content were studied.

According to the potentiodynamic investigations, at low metal content the character of hydrogen sorption resembles that of pure carbon, and at higher metal content that of pure palladium black. The amount of sorbed hydrogen increases with increasing metal content, as well as the ratio of weakly and strongly bonded hydrogen and the apparent activities measured in hydrogenation reactions (reduction of acetophenone and cyclohexene).

The potentiodynamic measurements have also indicated that the preparation method of the catalyst substantially influences the average bonding energy of strongly bonded hydrogen.

Introduction

Potentiodynamic polarization methods can be applied to advantage for the investigation of the metal—hydrogen systems of noble metals. Experiments were recently reported on the extension of measurements from compact electrodes (smooth and blackened metal) to powder catalysts [1—3]. In the potentiodynamic investigations of supported noble metal catalysts of industrial importance the design of the measuring electrode is problematic for technical reasons, since it is difficult to ensure the contact already between non-supported powder catalysts and the measuring electrode, and these difficulties become even more serious in the presence of supports. The problem was solved by KINOSHITA *et al.* [4, 5] by embedding the graphite-supported platinum catalyst into teflon, and immersing the leading-out electrode into this system. In order to improve reproducibility, anodic—cathodic pre-polarization was applied before the measurements.

By an appropriate choice of experimental conditions we endeavoured to make the results pertain to the active ('live') powder catalyst. Therefore, stabilization was avoided, and the catalyst was not embedded into electrical conductor medium.

When choosing the support three criteria were taken into account: it had to be a good electrical conductor, indifferent towards the electrolyte, and, finally, available in industrial quantities.

Some data can be found on the investigation of carbon-supported and inorganic salt-supported noble metal systems worth considering in view of the conductivities (Pt/C [4, 5] and $Pd/CaCO_3$ [6]). Of these systems only active carbon has industrial importance, and thus, after determining the optimum conditions of measurements, active carbon-supported noble metals, primarily palladium were studied in detail.

Experimental

Preparation of catalysts

The catalysts were prepared from chemicals of analytical purity using distilled water. The metal contaminations of commercial palladium were removed by twofold precipitation with dimethylglyoxime and subsequent digestion.

$Pd/BaSO_4$ with 5% Pd content:

The catalyst was prepared by co-precipitation, by adding 200 ml solution of 0.062 g $PdCl_2$ and 0.65 g Na_2SO_4, of pH = 5 dropwise to 200 ml aqueous solution of 0.845 g of $BaCl_2$ of pH = 5. The pH of the solution was maintained between 7 and 8 by the simultaneous addition of 1% by weight NaOH solution. (At the end of the precipitation the solution contains an excess of sulfate ions.)

The resulting palladium oxide–barium sulfate precipitate mixture was reacted with 100 ml of 1% by weight $NaBH_4$ solution at room temperature. The obtained $Pd/BaSO_4$ precipitate was filtered off, washed and dried at 60 °C.

Active carbon-supported Pd catalysts

To prepare catalysts containing 1, 5, 10 and 20% by weight of metal, 2 g of carbon (Carbo C-extra) were impregnated with an appropriate amount of 4% by weight $PdCl_2$ solution at 60 °C in vacuo, under shaking. The dry, impregnated support was fed into 300 ml 3% by weight solution of $NaHCO_3$ at 60 °C, and after half an hour of stirring, it was reduced with atmospheric hydrogen under shaking. The filtered and washed catalyst was dried in vacuo at room temperature.

To prepare non-supported (100% by weight) palladium catalyst, the same procedure was applied except that 20 ml 10% by weight solution of $PdCl_2$, rather than the impregnated support, was fed into the alkali.

Pd/C catalysts of 5% metal content were prepared both by $NaBH_4$ reduction (a) and by formaldehyde reduction (b).

(a) The support impregnated as above and 100 ml of 0.5% by weight solution of $NaBH_4$ were added at room temperature, under stirring, to 10 ml of a 0.5% by weight solution of $NaBH_4$.

(b) 4 g of NaOH was dissolved in 100 g of water, 5 ml of 40% formaldehyde was added, and the impregnated support was fed portionwise, at 25 °C, into this solution.

After reductions (a) and (b) the suspension was stirred for half an hour. The catalysts were filtered off, washed with distilled water, and dried in vacuo at room temperature.

Measurement of activity

The apparent activities of catalysts were measured in liquid-phase by hydrogenation (and expressed in millilitres of hydrogen consumed under 1 min pro 1 g of catalyst). The measurements were carried out with 100 mg of catalyst in 9 ml of 90% ethanol, using acetophenone and cyclohexene as reactants. The temperature was 25 °C, and the rate of shaking was 330 r. p. m.

By plotting hydrogen consumption against time, the apparent activity was determined from the differential hydrogen consumption (ml/min) extrapolated to time = 0.

Electrochemical measurements

These measurements were performed initially in a three-electrode cell described in one of our previous publications [7]. Since this cell could be applied for only very well sedimenting supported catalysts, it was modified in a manner that the three electrode spaces communicated only via ground joints (Fig. 1).

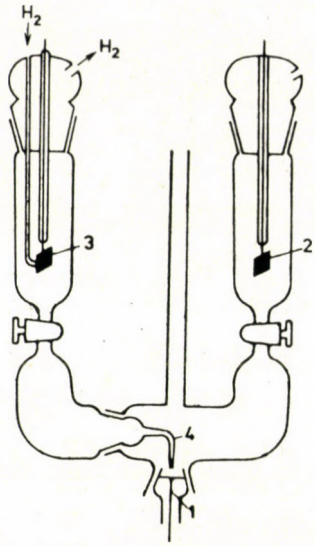

Fig. 1. Electrochemical measuring cell 1 — smooth Pt measuring electrode, 2 — smooth Pt polarizing electrode, 3 — platinized Pt-hydrogen reference electrode, 4 — Luggin capillary

The catalyst powder was placed on the measuring electrode of smooth platinum sheet (1), and the apparatus was filled with 1 *N* sulfuric acid. From the space of the reference electrode, platinized platinum/hydrogen (3), a Luggin capillary (4) leads down to the surface of the measuring electrode. The polarizing electrode (2) is a smooth platinum sheet.

Since the samples stored in air contain oxygen on their surfaces, they were saturated with hydrogen by cathodic polarization before recording the anodic glavanostatic and potentiodynamic curves in the range of 50—60 mV to 800—1000 mV. Polarization was performed with an AMEL 551/SU potentiostat.

In the galvanostatic measurements 5—10 mg samples of catalyst were used. Current densities of 20 to 250 μA were applied, depending on the weight and hydrogen content of the catalyst. Under these conditions the plots can be regarded as equilibrium curves to good approximation.

Potentiodynamic curves were taken at a potential rate of 20—50 mV/min, generally using 1—5 mg of catalyst. To discuss the hydrogen sorption of *non-supported* Pd *catalysts*, the following approximation can be used in interpreting the curves: hydrogen adsorption can be neglected below 100 mV in comparison with the large amount of dissolved hydrogen, whereas between 100 and 300 mV the amount of dissolved hydrogen can be neglected in comparison with that of adsorbed hydrogen (particularly for catalysts with large surface areas).

In the case of *supported catalysts* superstoichiometric adsorption [8] must also be taken into account. Since the potential dependence of the latter is not exactly known, in the case of supported Pd catalysts it is more appropriate to refer to hydrogen with small or great bond energy rather than dissolved and adsorbed hydrogen.

On the basis of the well separated two sections of the hydrogen domain of the potentiodynamic curves, the first maximum below 100 mV will be regarded as belonging to loosely bonded hydrogen, and the 1 to 3 maxima between 100 and 300 mV as corresponding to strongly bonded hydrogen.

By integrating the difference between the potentiodynamic curves of supported palladium and pure carbon, taken under the same conditions, we determined the ratio of loosely

and strongly bonded hydrogen and the total amount of hydrogen. The latter result is less accurate, due to uncertainties in sample weight (a little, non-moistening portion of the sample fails to sediment on the surface of the measuring electrode) than the ratio of loosely and strongly bonded hydrogen.

It also decreases the accuracy of the measured total amount of hydrogen that at low metal content a relatively large proportion of the integrated area (*e.g.* about 80% at 1% Pd/C ratio) arises from pure carbon, which is taken into correction.

Results and discussion

We have been concerned with extending the potentiodynamic technique already applied on non-supported noble metal powder catalysts (Pt, Pd) to supported Pd catalysts.

Of the conventional supports only carbon and inorganic supports could be taken into consideration.

The optimum conditions of electrochemical measurements were determined with 5% by weight Pd/C and Pd/$BaSO_4$ catalysts. The aim was to develop an appropriate cell, and to determine the optimum amount of catalyst and rate of potential change.

The potentiodynamic curve of 5% by weight Pd/$BaSO_4$ catalyst taken at a rate of 50 mV/min is shown in Fig. 2. The curve has only one maximum below 100 mV, corresponding to hydrogen with low binding energy, and hydrogen sorption is negligible between 100 and 300 mV.

The activity of the catalyst in the reduction of acetophenone and cyclohexene is not significantly different from that of active carbon-supported catalysts with 5% by weight of Pd content (Table I), the activities being 24 and 83 ml H_2/min × g of catalyst.

Carbon-supported catalysts containing 5% by weight of Pd were prepared by three different methods: reduction with (a) hydrogen, (b) $NaBH_4$

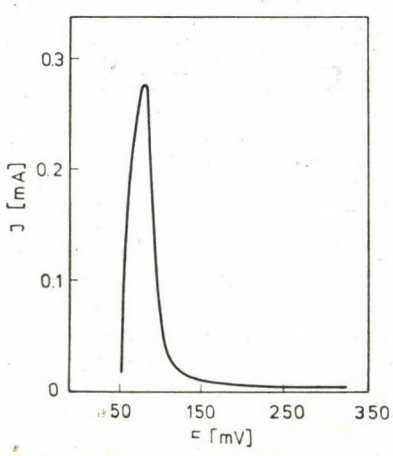

Fig. 2. The potentiodynamic curve of 5 w/w % Pd/$BaSO_4$ catalyst; $m \sim 19$ mg, $v = 50$ mV/min

Table I

The activities, measured at 25 °C, *of* 5 w/w % Pd/C *catalysts prepared by various methods*

Reductant	Activity $\frac{\text{ml of hydrogen}}{\text{min.} \times \text{g of catalyst}}$	
	on acetophenone	on cyclohexene
H_2	34	126
$NaBH_4$	8	120
HCHO	8	92

and (c) formaldehyde. The potentiodynamic curves of these catalysts are shown in Fig. 3. It can be seen that the maxima of loosely bonded hydrogen are between 70 and 80 mV in all the three cases, but the curves are remarkably different in the region above 100 mV. The maxima of hydrogen desorption appear at 200 mV, ca. 230 mV and 240 mV for the catalysts reduced with formaldehyde, hydrogen and sodium borohydride, respectively, indicating that the bonding energy of hydrogen sorbed on the metal increases in this order.

The activities of these catalysts were measured in the liquid-phase reduction of acetophenone and cyclohexene (Table I), but no correlations were found to exist between the bonding energy of sorbed hydrogen and the apparent catalytic activity.

After these experiments, the sorption and catalytic properties of carbon-supported catalysts reduced with hydrogen were investigated as a function of their metal content. The measurements were extended to catalysts containing 0, 1, 5, 10, 20 and 100% by weight of Pd.

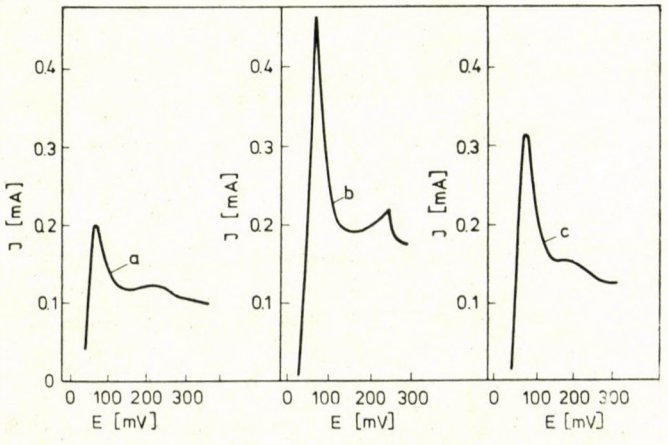

Fig. 3. The potentiodynamic curves of 5 w/w % Pd/C catalysts prepared by various methods; $v = 20$ mV/min; (a) $m \sim 3$ mg; reductant: hydrogen; (b) $m = 5$ mg; reductant: $NaBH_4$; (c) $m \sim 3$ mg; reductant: HCHO

According to the *potentiodynamic investigations*, hydrogen sorption at low metal content is similar in character to that of the pure support, whereas at higher metal content to that of pure Pd black. The potentiodynamic curve of carbon (Fig. 4) exhibits a blurred peak corresponding to hydrogen sorption at about 100—150 mV (Table II), which is marked with an arrow in the figure. At a metal content of 1% by weight (Fig. 5) a maximum appears already at ca. 70 mV, and the amount of sorbed hydrogen increases. The polarization

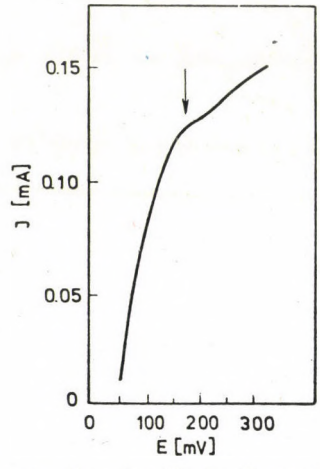

Fig. 4. The potentiodynamic curve of carbon (Carbo C extra) in 1 *N* H_2SO_4; $m \sim 5$ mg, $v = 20$ mV/min

curve of the catalyst containing 10% by weight of Pd (Fig. 6) is already very similar to that of pure palladium: the maximum of strongly bonded hydrogen (260 mV) coincides with the most characteristic maximum of Pd found in a

Table II

Hydrogen sorption on C, Pd/C *and* Pd *catalysts on the basis of the potentiodynamic curves in* 1 *N sulfuric acid*

Pd content (w/w %)	Location of maxima in the hydrogen region (mV)	Ratio of weakly and strongly bonded hydrogen	Total amount sorbed hydrogen (ml/g of catalyst)
0 (pure C)	100—150	—	—
1	70, about 150	30 : 70	0.6
5	70, about 230	55 : 45	1.3
10	70, 260	50 : 50	6.4
20	70, 180, 260	45 : 55	10
100	90, 170, 255, 265*	87 : 13	100

* Shoulder rather than maximum

similar region. At 20% a further weak adsorption maximum appears at ca. 180 mV.

The peak corresponding to loosely bonded hydrogen can be found at ca. 20 mV higher potential for pure palladium than for supported catalysts (Fig. 7)

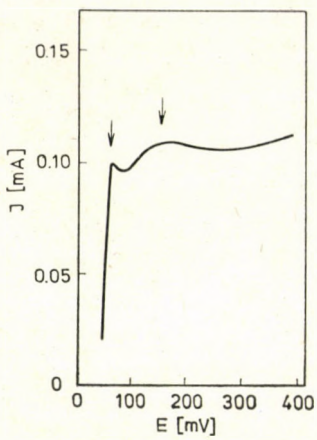

Fig. 5. The potentiodynamic curve of 1 w/w % Pd/C catalyst in 1 *N* H_2SO_4; $m \sim 3$ mg, $v =$ = 20 mV/min

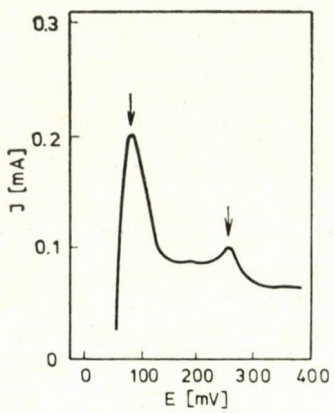

Fig. 6. The potentiodynamic curve of 10 w/w % Pd/C catalyst in 1 *N* H_2SO_4; $m \sim 1$ mg, $v =$ = 20 mV/min

since the former measurement was performed at a higher rate of potential change. (By decreasing the scan speed appropriately, the maximum of hydrogen with low bonding energy can be shifted to about 60—65 mV [2]).

The calculations have shown that the ratio of weakly and strongly bonded hydrogen increases in tendency with increasing metal content (Table II), and the total amount of sorbed hydrogen increases simultaneously.

Galvanostatic measurements on hydrogen sorption were also performed in all cases. Fig. 8 shows the charging curves of catalysts containing 1, 5, 10, 20 and 100% by weight of Pd. In the curve of the sample with 20% of Pd, the two distinct regions of hydrogen sorption are still clearly visible. The curve of the catalyst with 5% Pd already shows only one step, whereas the curves of the catalysts with lower Pd content are practically useless, since the charge required to remove sorbed hydrogen is too small relatively to that necessary to re-charge the double layer.

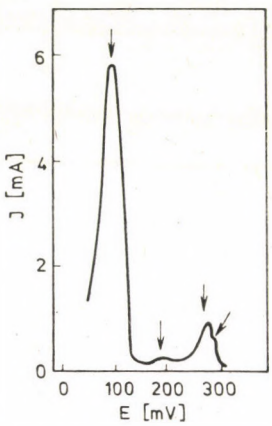

Fig. 7. The potentiodynamic curve of Pd catalyst in 1 N H_2SO_4; $m \sim 2$ mg, $v = 100$ mV/min

The *apparent activities* of carbon-supported catalysts containing 0—100% by weight of Pd and reduced with hydrogen, measured in the hydrogenation of acetophenone and cyclohexene are given in Table III. The specific activities increase in tendency with the metal content between 0 and 20% by weight for both reactants, and reach their maxima at 20% by weight. In the reduction

Table III

The apparent activities at 25 °C *of* Pd/C *catalysts reduced by hydrogenation*

Pd-content (w/w %)	Activity $\frac{\text{ml of hydrogen}}{\text{min.} \times \text{g of catalyst}}$		Activity $\frac{\text{ml of hydrogen}}{\text{min.} \times \text{g of Pd}}$	
	on acetophenone	on cyclohexene	on acetophenone	on cyclohexene
0	0	0	0	0
1	11	67	1100	6700
5	34	126	680	2520
10	16	114	160	1140
20	78	167	390	835
100	11	—	11	—

of acetophenone the maximum activity is greater than the activity of pure palladium. The total amount of hydrogen sorbed by supported catalysts changes in a similar manner between 0 and 20% by weight. This agrees with the widespread opinion that there is a positive correlation between the hydrogenation activity and the hydrogen content of the catalyst. It can also be seen that the amount of loosely bonded hydrogen and the average bonding

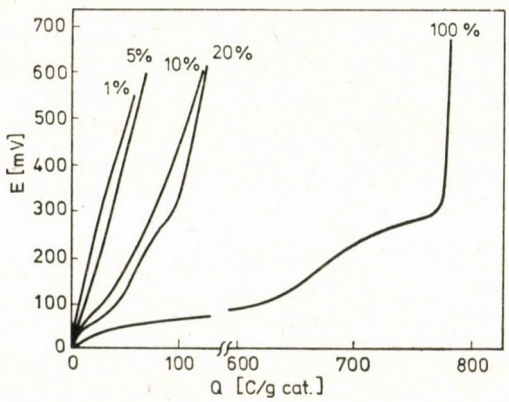

Fig. 8. The charging curves of Pd/C catalysts of various metal content (1, 5, 10 and 20 w/w %) and of non-supported (100 w/w %) Pd catalyst in 1 N H_2SO_4

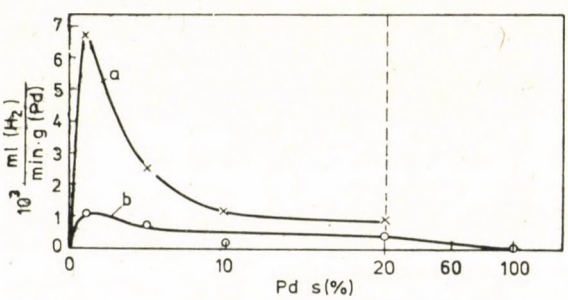

Fig. 9. The apparent activities of Pd/C catalysts related to the metal content as a function of Pd content; a — cyclohexene; b — acetophenone

energy of strongly bonded hydrogen increase with the metal content (*cf.* Figs 5—7). This might also influence the variation of activity. If the results measured on supported catalysts are compared to the activity and hydrogen content of pure palladium, it can be seen that the activity of the catalyst containing 1% of metal is the same as that of pure palladium which contains two orders greater amount of hydrogen. No doubt, the reason is the effect of the support.

Plotting the apparent activities related to the metal content of the catalysts against the composition, a maximum can be obtained at 1% of Pd.

Summary

The potentiodynamic method applied successfully for the investigation of the metal–hydrogen system with powder catalysts has been extended to supported noble metal catalysts of industrial importance (Pd). Of the usual supports only the relatively good electrical conductors could be investigated and the ones indifferent with respect to the electrolyte.

Taking these aspects into account, the parameters of the potentiodynamic measurements were determined on 5% by weight Pd/C and $Pd/BaSO_4$ catalysts prepared under various conditions.

It has been found that $BaSO_4$ supported catalysts contain only weakly bonded hydrogen, whereas with carbon-supported catalysts both weakly and strongly bonded hydrogen occur, and the bonding energy of the latter depends considerably on the conditions of preparation.

According to the investigation of carbon-supported palladium catalysts with metal contents of 0, 1, 5, 10, 20 and 100% by weight prepared by the same method, the potentiodynamic curves of catalysts with low metal content resemble, in the hydrogen region, that of the support, and the curves of catalysts with higher metal content are similar to that of palladium black. Whereas in the case of pure Pd catalyst the amount of sorbed hydrogen is simple to calculate from the galvanostatic curve, the galvanostatic curves of supported catalysts are useless owing to the great capacity of the double layer, confining these calculations to the potentiodynamic curves. It has been found that between 0 and 20% by weight the ratio of weakly and strongly bonded hydrogen, the total amount of sorbed hydrogen as well as the apparent activity in the liquid-phase hydrogenation of acetophenone and cyclohexene increase in tendency.

The apparent activity related to the metal content of the catalyst reaches its maximum at 1% of Pd for both reactants.

REFERENCES

[1] PETRÓ, J., POLYÁNSZKY, É.: Acta Chim. (Budapest) **87,** 385 (1975)
[2] MALLÁT, T., POLYÁNSZKY, É., PETRÓ, J.: J. Catalysis **44,** 345 (1976)
[3] ENTINA, V. S., PETRIJ, O. A.: Elektrokhimiya **3,** 1237 (1967); **4,** 111 (1968)
[4] KINOSHITA, K., LUNDQUIST, J., STONEHART, P.: J. Catalysis **31,** 325 (1973)
[5] KINOSHITA, K., LUNDQUIST, J., STONEHART, P.: J. Electroanal. Chem. Interf. Electrochem., **48,** 157 (1973)
[6] BELOSYUDOVA, T. M.: Elektrokhimiya **10,** 1558 (1974)
[7] PETRÓ, J., POLYÁNSZKY, É., CSŰRÖS, Z.: J. Catalysis **35,** 289 (1974)
[8] BAGOTZKII, V. S., KANEVSKII, L. S., PALANKER, V. SH.: Electrochim. Acta **18,** 473 (1973)

Éva POLYÁNSZKY
Tamás MALLÁT
József PETRÓ
H-1111 Budapest, Műegyetem rkp. 3.

Acta Chimica Academiae Scientiarum Hungaricae, Tomus 92 (2), pp. 157—167 (1977)

СМАЧИВАЕМОСТЬ ГЕЛЕЙ ЖЕЛАТИНЫ

Э. ВОЛЬФРАМ и Х. СТЕРГИОПУЛОС

(Кафедра Коллоидной Химии Университета им. Л. Ётвёша, Будапешт)

(1. III. 1976)

В случае гелей, образующихся при застывании водных желатиновых растворов, на основе измерений краевых углов их поверхности, соприкасающейся с воздухом, можно сделать заключение, что последняя ведет себя как гидрофобная низкоэнергетическая поверхность. Свежий внутренний слой, полученный сколом, как и ожидалось, обладает гидрофильным характером. Додецилсульфат натрия, растворенный в геле, уменьшает, в зависимости от его концентрации, гидрофобность внешней поверхности.

Концентрационные изотермы краевых углов на внешней поверхности для смесей этилового или пропилового спиртов с водой имеют нормальный — монотонно понижающийся — ход. В случае же водных растворов додецилсульфата натрия или бромистого додецилтриметиламмония, однако, имеем — до сих пор еще не наблюдавшуюся — кривую с явно выраженным минимумом. Этот минимум находится практически при концентрации, соответствующей c_M поверхностно-активного вещества.

Результаты интерпретируются, с одной стороны, на основе конформационных изменений поверхности желатины и взаимодействиями с поверхностно-активными веществами, а с другой стороны, адсорбцией дифильных молекул спиртов и ПАВ на различных поверхностях раздела системы.

Введение

Многие гидрофильные полимеры и природные макромолекулярные вещества образуют такие гели, поверхность которых гидрофобна, т. е. низкоэнергетична. Так например, в случае студня желатины, получаемого застыванием из водного раствора, краевой угол воды на поверхности, соприкасающейся с воздухом, приближается по своему значению к измеренному на парафине. Эту кажущуюся аномалию качественно можно объяснить тем, что желатин и другие гелеобразующие вещества, ведущие себя подобным образом, в водных растворах являются поверхностно-активными (это подтверждается и данными поверхностного натяжения) и т. о., поверхность обогащается молекулами, взаимодействующими с водой, в результате чего их конформации отличаются от конформаций внутри раствора. В качестве рабочей гипотезы, во всяком случае, можно полагать, что разматывание, обычно сопровождающее адсорбцию, приводит к тому, что на поверхности образуются структуры с неполярными группами, ориентированными в сторону неполярной окружающей фазы, что и сохраняется в студне.

Интересно отметить, что с такого рода исследованиями редко встречаемся в литературе [1, 2], хотя биологическая важность поверхностных свойств студней широко известна [3]. Эти исследования принципиально важны и потому, что влияние геометрических неравномерностей в этих случаях на смачиваемость либо совсем отсутствует, либо им можно пренебречь, в противоположность компактным низкоэнергетическим поверхностям.

Поэтому в данной работе смачиваемость студней желатины исследовалась, применяя чистые жидкости и водные растворы, с целью получения количественной характеристики структуры поверхностей студней. Эти студни приготовлялись либо из чистых водных растворов, либо из водных растворов, содержащих поверхностно-активные вещества. Были исследованы смачиваемости помимо действительных внешних — продолжительно соприкосающихся с воздухом — поверхностей, также и внутренних „nascens" — полученных свежим сколом — поверхностей.

Теоретическая часть

Характеристика полярности поверхности с помощью данных краевых углов

Для правильного описания контактой конфигурации, формирующейся на студнях, строго подходя к вопросу, необходимо использовать термодинамическую трактовку, относящуюся к деформируемым твердым телам [4, 5]. Для случая высококонцентрированных студней, использованных в наших исследованиях, в первом приближении, однако, можно не считаться с незначительными искажениями поверхности студня за счет помещения на нее капли жидкости. Т. о., могут быть использованы методы расчета энергии жестких твердых поверхностей с помощью различных приближений, исходным началом которых является уравнение Юнга [6]:

$$\gamma_{SV} - \gamma_{SL} = \gamma_{LV} \cos \Theta \tag{1a}$$

и

$$\gamma_{SO} - \gamma_{SL} = \gamma_{LV} \cos \Theta + \pi_{SV}\,, \tag{1b}$$

где γ — поверхностное натяжение на границе раздела соотвествующих фаз, Θ — равновесный макроскопический краевой угол [6], π — поверхностное давление, а индексы S, L, V относятся к твердой, жидкой и газовой фазам, индекс же 0 означает вакуум.

Основой вышеупомянутых способов служит то, что *межфазное натяжение* на поверхности раздела любых двух фаз или свободная энергия, принимая в расчет подходящим образом межмолекулярные взаимодействия, могут быть выражены через *свободные поверхностные натяжения* соприкасающихся фаз или через их свободные энергии. Таким образом, в случае по-

верхности раздела твердое вещество/жидкость, принимая во внимание уравнение Юнга, для γ_{SO} (в дальнейшем сокращенно γ_S) получаем выражение в явной и неявной форме. На основе расчета π_{SV} или приблизительной оценки, может быть получено выражение для γ_{SV} — реальной величины, характеризующей контактную конфигурацию.

Можно исходить из соображений Гуда [7], которые, используя параметр взаимодействия Φ, определяемый уравнением (2)

$$\Phi = \frac{\gamma_{ij} - (\gamma_i + \gamma_j)}{2(\gamma_i\gamma_j)^{1/2}} \tag{2}$$

приводят к уравнению (3):

$$\gamma_S = \frac{[\gamma_{LV}(1 + \cos\Theta) + \pi_{SV}]^2}{4\Phi^2\gamma_{LV}}. \tag{3}$$

С другой стороны, можно использовать соображения Фаукеса [8], согласно которым свободное поверхностное натяжение любой фазы может быть представлено в виде суммы компонента, обязанного дисперсионным силам (с верхним индексом d), и компонента, происходящего за счет взаимодействий, обобщенных под названием полярных (с верхним индексом p):

$$\gamma_i = \gamma_i^d + \gamma_i^p \tag{4}$$

Такое разложение — как это делали Ву [9] и Келбл [10] — можно применять и для обратимой адгезионной энергии типа Дюпре:

$$W_a = W_a^d + W_a^p \tag{5}$$

откуда, исходя из формулы, выведенной первоначально Фаукесом, имеем:

$$\gamma_{LV}(1 + \cos\Theta) + \pi_{SV} = 2(\gamma_L\gamma_S)^{1/2}\,[d_L d_S^{1/2} + p_L p_S]^{1/2}, \tag{6}$$

здесь $\mathrm{d}_i = \gamma_i^d/\gamma_i$ и $p_i = \gamma_i^p/\gamma_i$ ($i = L$ или S), т. е. $d_i + p_i = 1$. Величина p т. наз. *поверхностная полярность*, приближенно может быть представлена как степень относительной гидрофильности рассматриваемой фазы.

С другой стороны, значения γ_S и γ_S^d могут быть рассчитаны из величины критического поверхностного натяжения типа Зисмана (γ_c), определяемого непосредственно, экспериментальным путем:

$$\gamma_S = \gamma_c/\Phi^2 \tag{7}$$

и

$$\gamma_S^d \approx \gamma_c \quad (\gamma_S^d = \gamma_c^d). \tag{8}$$

Условием выполнимости уравнений (7) и (8) является пренебрежение двухмерным давлением пленки поверхности раздела твердое вещество/пар,

т. е. адсорбция насыщенного пара на низкоэнергетической поверхности должна быть достаточно малой. Уже ранее было указано, что это допущение является справедливым [11]; на основе новейших расчетов [12], величина π_{SV} в случае компактных полимеров имеет величину порядка лишь нескольких mNm^{-1}. Т. к. с полной уверенностью можно утверждать, что адсорбцией водяного пара на гидрофобной поверхности студней с высоким содержанием воды можно пренебречь, то вышеупомянутые приближения могут быть использованы и для сравнений, т. е. для относительной оценки.

Роль адсорбции

На основе более ранних исследований [13] и новейших результатов [14] известно, что для одинаковых низкоэнергетических поверхностей величина γ_c принимает различные значения в зависимости от того, что при экстраполяции функции $\cos\Theta = f(\gamma_L)$ ($\gamma_L \to \gamma_c$, если $\cos\Theta \to 1$) графики строятся на основе данных, полученных в чистых жидкостях или в растворах. Несомненно, что причиной отклонения является адсорбция растворенных компонентов на различных поверхностях раздела системы, включая и поверхность раздела фаз S/V, на что уже ранее было указано, опираясь на факт кажущегося аномального растекания [15]. В случае гелей, строго судя, в круг адсорбции следует включать и адсорбцию гелеобразующих макромолекул, однако при качественной оценке явления последней сейчас не занимаемся.

Адсорбция гелеобразующего компонента на поверхности раздела гель/воздух является первостепенным фактором при установлении данной структуры поверхности, поэтому последнюю для данной системы считаем уже готовой. Возможную диффузию гелеобразующих макромолекул в смачивающую жидкость и их адсорбцию на поверхности раздела L/V строго следует рассматривать как смачиваемость твердых поверхностей химически неинертными жидкостями. Сравнивая с инертными жидкостями, в предыдущем случае имеем гораздо более значительное изменение краевого угла во времени, нежели это можно ожидать на основе отклонения динамического поверхностного натяжения от равновесного при размазывании растворов. Следует однако отметить, что сама польза принятия в учет адсорбции гелеобразующих макромолекул при рассмотрении явления весьма сомнительна т. к. применение равновесной термодинамики к поверхности, изменяющейся по своим химическим свойствам, является простым формализмом.

Если, таким образом, ограничимся рассмотрением влияния адсорбции веществ, растворенных в смачивающей жидкости, то уравнение Юнга в форме, дифференцированной по логарифму концентрации, при сравнении с уравнением Гиббса (8), приводит к следующей зависимости:

$$\gamma_{LV} \sin\Theta(\mathrm{d}\Theta/\mathrm{dln}\, c) = \mathrm{RT}(\Gamma_{SV} - \Gamma_{SL} - \Gamma_{LV}\cos\Theta)\,, \qquad (8)$$

где Γ — поверхностный избыток, относящийся к соответствующим поверхностям раздела. Т. к. $\sin \Theta$ в действительном интервале углов смачивания является положительным, то выражение в скобках в правой и левой части уравнения имеет один и тот же знак. Это означает, что зависимость краевого угла от концентрации, т. е. полная качественная картина смачивания определяется относительными величинами отдельных избытков поверхностей раздела. Исходя из этого, можно сделать следующее приближение. Если концентрация растворенного в смачивающей жидкости вещества (в нашем случае капиллярно-активного) мала, то обе величины Γ_{SV} и Γ_{SL} пренебрежимо малы (однако, Γ_{LV} естественно нет); т. о., направление хода изменения краевого угла с концентрацией однозначно определяется тем, что краевой угол растворителя (воды) больше или меньше 90°. При повышенных концентрациях первостепенную роль играет разница ($\Gamma_{SV}-\Gamma_{SL}$), а если величина Γ_{SV} во всей области концентраций пренебрежимо мала, то решающим является отношение величин Γ_{SL} и Γ_{LV}. Как ранее было указано [16], эти две величины могут в некоторых случаях практически совпадать, и тогда несмотря на наличие зависимости краевого угла от концентрации, энергия адгезии является неизменной во всем интервале концентраций. В этом случае натяжение смачивания $\gamma_{LV} \cos \Theta$ линейно изменяется с изменением поверхностного натяжения раствора, что можно рассматривать как специальный случай уравнения (6), выведенного из теории Фаукеса.

Экспериментальная часть

Вещества

Средний молекулярный вес фотожелатины, измеренный на основе светорассеяния в растворе с KSCN (конц. 1 мольдм$^{-3}$) равен 6 . 10^5; pH, соответствующая ИЭТ, на основе измерений вязкости равна 4,78, а на основе потенциометрического титрования 5,0.

Измеряемыми жидкостями были: дистиллированная вода, формамид, метиленйодид, этанол, н-пропанол и изопропанол. Поверхностное натяжение измерялось методом веса капли при 20,0 $\pm$ 0,1°C.

Были использованы два типа поверхностно-активных веществ: анионактивным веществом служил додецилсульфат натрия (NaDS, Merck), а катионактивным — бромистый додецилтриметиламмоний (DTAB, Ferak). Их очистка производилась уже ранее описанным методом [17]. Критические концентрации мицеллообразования (c_M) определялись из данных электропроводности при 25,0 $\pm$ 0,1°C и имели очень хорошее совпадение с литературными данными [18]: для NaDS c_M=8,1 ммольдм$^{-3}$, а для DTAB c_M=15,0 ммольдм$^{-3}$.

Приготовление студней

Воздушно-сухую желатину растворяли в дистиллированной воде, а также в водных растворах ПАВ с различной концентрацией (2,0 и 20,0 ммольдм$^{-3}$). Согласно полученной практике, хотя концентрация гелеобразователя невелика, однако его влиянием на поверхностную структуру нельзя пренебрегать. Поэтому это влияние было предварительно исследовано на

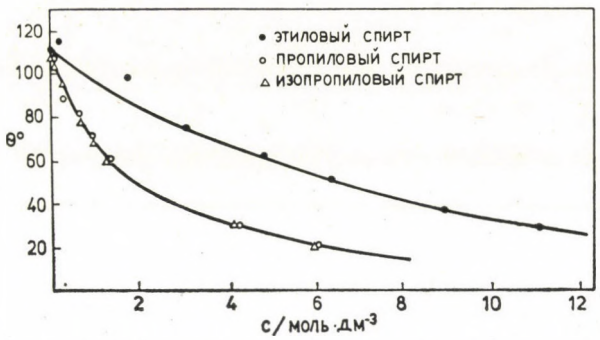

Рис. 1. Изменение краевого угла натекения водно-спиртных смесей на поверхности геля желатины в зависимости от концентрации спирта

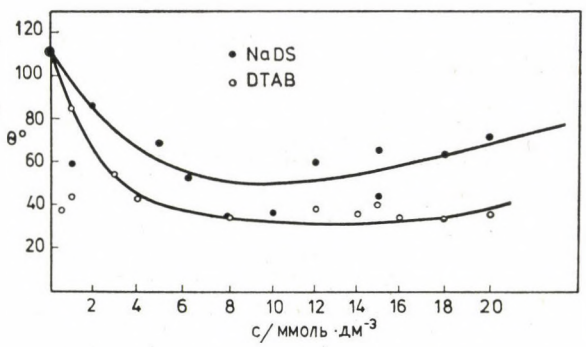

Рис. 2. Изменение краевого угла натекания ПАВ в водных растворах на поверхности геля желатины в зависимости от концентрации поверхностно-активного вещества

основе измерений краевых углов чистой воды. Оказалось, что студни с концентрацией, превыщающей 25%, не пригодны вследствие синерезиса, а более разбавленные, чем 12%, не пригодны потому, что вследствие относительно быстрого всасывания воды ими, измерение краевых углов было ненадежным. Поэтому во всех случаях приготовляли 20%-ые растворы (200 гдм$^{-3}$), которые выливались в плексиглазные посуды с размерами $5 \times 10 \times 0{,}3$ см; при застывании на воздухе образуются листообразные блочные образцы. Помимо измерений краевых углов на внешней поверхности студня, соприкасающейся с воздухом, были произведены измерения и на внутренних поверхностях, приготовленных сколом.

Определение краевого угла

Величины краевых углов на поверхности студней, вследствие диффузии, а в случае растворов и вследствие адсорбции, сильно изменяются во времени (обычно уменьшаются). Поэтому в каждом случае казалось необходимым снять кривые $\Theta = \Theta(t)$. Естественно, что экспериментальные значения Θ т. о. представляют собой краевые углы натекания. Вследствие этой временной зависимости, конкретные значения Θ, характерные для отдельных систем и используемые в дальнейших расчетах, были получены двумя путями: либо экстраполированием, либо представлением данных, относящихся к определенному моменту времени. Как известно, экстраполирование к $t \to 0$ в случае растворов в принципе — из-за динамического характера величины — не справедливо, а экстраполирование к $t \to \infty$ не может быть произведено в нашем случае вследствие значительного набухания. Так, исходя из опытных наблюдений, согласно которым после нанесения капли смачивающей жидкости на пятой минуте все еще не наблюдается набухания, принимали значения краевых углов, относящихся к моменту времени, равному 1 минуте.

Измерения проводились гониометрическим методом, комбинированным с фотографированием, описанным подробно нами уже ранее [19]. В определенные моменты времени на поверхность студней наносили по 3—5 капель с объемом каждой 0,002 см³. Для каждой капли определяли изменяющийся краевой угол на протяжении 120 минут так, что на первом часу измерения проводились через каждые 3—5 минут, а на втором часу — через 10—15 минут, в зависимости от наблюдаемых изменений. Погрешность измерения угла составляла $\pm 0{,}5°$, а воспроизводимость $\pm 2°$. Для расчетов использовались средние величины краевых углов при $t = 1$ минуте, измеренные вышеописанным методом на поверхности, по крайней мере, двух образцов. В таблице приводятся эти значения. Здесь следует отметить, что в случае смесей спирт-вода, при концентрации спирта, превыщающей 50 об.%, надежных данных краевых углов получить не удалось.

Экспериментальные данные и их оценка

Экспериментальные и расчетные данные, относящиеся к студням в чистых водных средах (не содержащих поверхностно-активных веществ) собраны в таблице 1.

Под внешней поверхностью подразумевается свободная поверхность, соприкасающаяся с воздухом, а под внутренней поверхностью — поверхность, образующаяся за счет свежего скола. Значения $d_L (= \gamma_L^d)$, фигурирующие в таблице, являются литературными данными [4]; для расчета d_S и p_S ($d_S + p_S = \gamma_{SO}$) было использовано уравнение (6) при условии $\pi_{SV} = 0$. Для

подтверждения соблюдения этого условия, обычно, как в случае низкоэнергетических поверхностей, так, в особенности и для гелей с высоким содержанием жидкости, получение надежных экспериментальных данных особенно затруднено, даже едва ли осуществимо. Для оценки порядка допускаемой таким образом ошибки исходным началом может служить величина γ_{SO}, определенная каким-либо независимым методом [20], напр., экстраполированием поверхностного натяжения жидкой системы, измеряемого непосредственно на основе температурной зависимости. Так на основе данных такого рода измерений для γ_{SO} желатиновых растворов в интервале температур 50—40°C нами была получена величина 30 mNm^{-1}, что находится в очень хорошем согласии с расчетной величиной, полученной, естественно, для внешней поверхности (29,8 mNm^{-1}). Подобным образом хорошее согласие наблюдалось между величинами критического поверхностного натяжения Зисмана, (γ_c) и расчетной величиной γ_{SO} для внешней поверхности студня. Итак, для жидкостей, перечисленных в таблице 1 имеем величину 31 mNm^{-1}, а для смесей трех спиртов с водой, на основе их концентрационного ряда величина $\gamma_c = 28—30$ mNm^{-1}, используя при этом экстраполяцию зависимости $\cos \Theta = f(\gamma_{LV})$ к $\Theta \to 0$. Следует отметить, что — как на это уже было нами неоднократно указано [13, 16], — вышеупомянутые зависимости не линейны, в противоположность распространенным в литературе представлениям.

Наиболее важным заключением из данных таблицы 1 является то, что две разные поверхности студня проявляют весьма различающееся поведение: внешняя поверхность несомненно гидрофобна, полярные взаимодействия можно почти полностью исключить; внутренняя поверхность гидрофильна по сравнению с внешней, полярные взаимодействия приобретают явное значение, хотя ролью лондоновских сил также нельзя пренебрегать.

Причина этого расхождения заключается в том, что конформация молекул белков на поверхности отличается от конформации внутри студня, причем гидрофобная основная цепь, содержащая белковые цепочки, ориентируется, естественно в направлении воздуха. В результате этого изменяется и энер-

Таблица 1

Краевой угол чистых жидкостей на поверхности студней желатины

Жидкость	γ_{LV}	d_L	Внешняя поверхность			Внутренняя поверхность		
			θ	d_S	p_S	θ	d_S	p_S
	mNm^{-1}		град.	mNm^{-1}		град.	mNm^{-1}	
Вода	72,8	21,8	111			36		
Формамид	58,2	39,5	74	29,2	0,6	31,5	14,5	43,3
Метилениодид	50,8	48,5	59			64		

гетическое состояние молекул воды в поверхностном слое. Согласно представлениям Слонимского [2], структура воды в поверхностном слое студней с высоким содержанием воды подобна структуре в чистой воде, а это также играет роль в гидрофобности поверхностей студней.

Интересный результат был получен относительно смачиваемости внешних поверхностей студней, приготовленных застыванием растворов, содержащих NaDS. Как видно из данных таблицы 2, поверхность студней, образующихся из растворов с концентрацией как меньшей, так и большей c_M более гидрофильна по сравнению со студнями из чистой воды. В случае $c > c_M$ поверхностная энергия меньше, а ее дисперсионный компонент больше, чем в случае $c > c_M$. Этот эффект обусловлен конформационными изменениями на поверхности, происходящими за счет гидрофобных взаимодействий белков с цепями ионов DS^-, подробности молекулярной природы которых следует выяснить более подробными исследованиями.

Смачиваемость внешних поверхностей чистых водных студней смесями вода-спирт и водными растворами двух ионных ПАВ отражает сложное сочетание условий, как это видно из концентрационных изотерм, представленных на рисунках 1 и 2. Степень смещения двух кривых, представленных на рис. 1, с хорошим приближением соответствует требуемой, согласно правилу Траубе. Это однозначно указывает на то, что уменьшение краевого угла обусловлено, в первую очередь, уменьшением поверхностного натяжения смеси, хотя и нельзя полностью пренебрегать собцией спирта, происходящей за счет взаимодействий гидрофобных групп белков и молекул спиртов на границе раздела студень/раствор, а даже на границе раздела студень/пар. В результате посленего величина γ_c в случае растворов может оказаться меньшей, чем в случае чистых жидкостей [21]. Качественно явление подобно смачиваемости компактных низкоэнергетических поверхностей водно-спиртовыми смесями. Так Фаукес и Харкинс [22] изменение краевого угла с концентрацией для смесей метанол-вода на парафине объясняли тем, что ориентация спиртовых молекул на поверхности раздела парафин/раствор

Таблица 2

Влияние растворенного додецилсульфата натрия на гидрофобность внешней поверхности студня желатины (c — концентрация поверхностно-активного вещества)

Жидкость	$c=0$			$c=2$ ммоль. дм$^{-3}$			$c=20$ ммоль дм$^{-3}$		
	θ	d_S	p_S	θ	d_S	p_S	θ	d_S	p_S
	град.	mNm^{-1}		град.	mNm^{-1}		град.	mNm^{-1}	
Вода	111			56			54,5		
Формамид	74	29,2	0,6	59	14,1	27,0	60	17,2	20,4
Метиленйодид	59			66			64		

одинакова с ориентацией на поверхности раздела раствор/воздух. В более ранних работах для систем парафин-вода-спирты нами было установлено, что площадь, приходящаяся на молекулу спирта, одинакова на двух вышеупомянутых поверхностях раздела [23].

Картина изменяется в случае поверхностно-активных веществ, где концентрационная изотерма — как это видно из рис. 2 — уже не монотонна, а обладает явным минимумом. В случае обоих изученных веществ этот минимум наблюдается при концентрациях, близких к их собственному значению c_M. Для объяснения этого хода (до сих пор неизвестного) изотермы смачивания следует исходить из того, что вследствие взаимодействия ПАВ с белком, экспериментально обнаруженного [24], первый преимущественно адсорбируется на поверхности раздела студень/ раствор. Полярность поверхности студня благодаря этому возрастает до тех пор (на что указывают студни из растворов с поверхностно-активными веществами), пока гидрофобное взаимодействие доминирует среди прочих взаимодействий макромолекулы с амфипатическими молекулами. Однако, при таких концентрациях, для которых электростатическая часть становится доминирующей, поверхность снова гидрофобизуется. Последнее, в принципе, протекает до тех пор, пока не образуется второй адсорбционный слой за счет взаимодействий амфипатических молекул. Этого же, в свою очередь, нельзя достигнуть в пределах осуществимых концентраций. Во всяком случае, из обеих кривых рис. 2 ясно видно, что за сильной гидрофилизацией, протекающей вплоть до достижения значения c_M, следует сильно различающаяся для двух поверхностно-активных веществ гидрофобизация: в обоих случаях минимум краевого угла находится вблизи 30°, а с дальнейшим увеличением концентрации Θ для NaDS достигает величины 70°, а для DTAB повышается лишь до значения 35—40°. Для интерпретации этих различий требуются дополнительные исследования.

Авторы признательны М. Ковач, дипл. химику, за проведение измерений.

Summary

According to contact angle measurements, the surface of hydrogels formed upon solidification of aqueous gelatine solutions, if contacted with air, behaves as a strongly hydrophobic, low-energy surface. Fresh internal surfaces created by breaking the gel mechanically show the expected hydrophilic character. Sodium dodecyl sulfate dissolved in the gel decreases the hydrophobicity of the external surface to an extent depending on its concentration.

The concentration isotherms of the contact angle at the external surface with aqueous ethanol and propanol show the normal behaviour (monotonous decrease). However, in the case of aqueous sodium dodecyl sulfate and dodecyltrimethylammonium bromide the curves show a distinct minimum not observed thus far. The minimum appears in the vicinity of the concentration corresponding to the c_M value of the surfactant.

The results are interpreted in terms of changes in the surface conformation of gelatine aod its interaction with the surfactant, as well as by the adsorption of amphipathic alcohol and molecules on various boundary surfaces of the system.

ЛИТЕРАТУРА

[1] Е. Е. БРАУДО, В. Б. ТОЛСТОГУЗОВ, Е. А. НИКИТИНА: Коллоидн. ж., *36*, 208 (1974)
[2] Е. Е. БРАУДО, В. Б. ТОЛСТОГУЗОВ, В. А. ЕРШОВА, Г. Л. СЛОНИМСКИЙ: Коллоидн. ж., *33*, 653 (1971)
Е. Е. БРАУДО, В. Б. ТОЛСТОГУЗОВ, Г. Л. СЛОНИМСКИЙ: Высокомолек. соед. *Б9*, 796 (1967)
[3] F. J. Holly, M. F. Refojo: J. Biomed. Mater. Res., **9**, 315 (1975)
[4] G. L. Lester: J. Colloid Sci., **16**, 315 (1961); Nature, **209**, 1126 (1966); SCI Monograph No. **25**,„Wetting". London, p. 57, 1967
[5] A. I. Rusanov: Proc. IUPAC Intern. Conf. Colloid Surface Sci., Vol. **1**, Budapest, p. 125, 1975
[6] J. D. Eick, R. J. Good, A. W. Neumann: J. Colloid Interface Sci., **53**, 235 (1975)
[7] L. A. Girifalco, R. J. Good: J. Phys. Chem., **61**, 904 (1957)
[8] F. M. Fowkes: J. Phys. Chem., **59**, 2538 (1963); Advan. Chem. Ser., **43**, 99 (1964); Soc. Chem. Ind. Monograph **25**, 3 (1967); J. Colloid Interface Sci., **28**, 439 (1968); Chemistry and Physics of Interfaces II. Washington, p. 154, 1971
[9] S. Wu: J. Phys. Chem., **72**, 3332 (1968)
[10] D. H. Kaelble: Physical Chemistry of Adhesion. Wiley-Interscience, New York, 1971
[11] E. Wolfram: Kontakt nedvesedés. Akad. Kiadó, Budapest 1971
[12] J. Klobek: J. Adhesion, **6**, 293 (1974)
[13] E. Wolfram: Kémiai Közlemények, **27**, 383 (1967)
[14] W. J. Murphy, M. W. Roberts, J. R. H. Ross: J. Chem. Soc. Faraday Transactions I., No. 7, 1190 (1972)
[15] E. Wolfram: Kolloid-Z. Z. Polymere, **211**, 89 (1966); Abh. Deut. Akad. Wiss. Berlin, **66**, 82 (1967)
[16] E. Wolfram: Proc. 3rd Intern. Congr. Surf. Activity, **2**, 435 (1960)
[17] E. Wolfram: Proc. 4th Intern. Congr. Surf. Activity, **2**, 351 (1964)
[18] P. Mukerjee, K. J. Mysels: Critical Micelle Concentrations of Aqueous Surfactant Systems. NSRDS—NBS 36, Washington 1971
[19] E. Wolfram: Kolloid-Z., **182**, 75 (1962)
[20] L. H. Lee: J. Polymer Science, Ä **2**, 1103 (1967); Advan. Chem. Ser., **87**, 85 (1968); J. Colloid Interface Sci., **27**, 751 (1968)
[21] J. R. Dann: J. Colloid Interface Sci., **32**, 302, 321 (1970); W. J. Murphy, M. W. Roberts, J. R. H. Ross: J. Chem. Soc. Faraday Transactions I. No. 7, 1190 (1972)
[22] F. M. Fowkes, W. D. Harkins: Am. Chem. Soc., **62**, 3377 (1940)
[23[E. Wolfram: Akad. doktori értekezés. Budapest, 1966
[24] H. Moravetz: Macromolecules in Solution, Wiley 1965. A. Veis: The Macromolecular Chemistry of Gelatin, AP 1964

Ervin Wolfram
Ch. Stergiopoulos
H-1088 Budapest, Puskin u. 11—13.

Acta Chimica Academiae Scientiarum Hungaricae, Tomus 92 (2), pp. 169–173 (1977)

THE REACTION OF CARBON DIOXIDE AND DIOXYGEN WITH DINITROGENTRIS (TRIPHENYLPHOSPHINE) COBALT(O)

G. SPEIER, Á. SIMON and L. MARKÓ

(Department of Organic Chemistry, Veszprém University of Chemical Engineering and Research Group for Petrochemistry of the Hungarian Academy of Sciences, 8201 Veszprém)

Received May 11, 1976

The reactions of $[Co(N_2)(PPh_3)_3]$ with CO_2 and O_2 have been investigated. Solid complexes were isolated; the CO_2 complex is very air sensitive and the O_2 complex is thermally stable only up to 0°. Assignments of structures are based on elemental analyses, IR spectra, analogies with established reactions and chemical degradation. Evidence is presented for the formulas $[Co(CO_2)(PPh_3)_2]_n$ and $[(PPh_3)_3Co(O_2)Co(PPh_3)_3]$.

Introduction

It has been reported by MISONO *et al.* [1] that the cobalt complex $[CoH(N_2)(PPh_3)_3]$ reacts with CO_2 to give the cobalt formate complex $[CoOOCH(PPh_3)_3]$. The same compound was found by YAMAMOTO *et al.* [2, 3] in the reaction products of $[CoH_3(PPh_3)_3]$ and $[CoH(N_2)(PPh_3)_3]$ with CO_2.

The very air sensitive complexes $[CoH_3(PPh_3)_3]$ and $[CoH(N_2)(PPh_3)_3]$ are active catalysts for the oxygenation of triphenylphosphine to triphenyl phosphine oxide [3]. A cobalt dioxygen complex was assumed as intermediate but could not be isolated.

We report now on the reaction of $[Co(N_2)(PPh_3)_3]$ with CO_2 and O_2, where no insertion of the substrate molecules into the Co—H bond is possible.

Results and discussion

Gaseous carbon dioxide reacts with $[Co(N_2)(PPh_3)_3]$ in ether or toluene at 0° according to the equation shown in Fig. 1. During the reaction the orange colour of the suspended starting complex turns to brownish yellow. Using one mole of the dinitrogen cobalt complex nearly one mole CO_2 is taken up and one mole N_2 set free. The carbon dioxide cobalt complex is very air sensitive and has to be handled carefully under dry argon or dinitrogen. In the IR spectrum a sharp absorption band at 1890 cm^{-1} and weaker bands at 1980; 1715; 1835 and 1775 cm^{-1} could be found. No correct assignments of these bands were possible. Since the compound is only poorly soluble in ether and hydrocarbon solvents, a polymeric structure is suggested.

Thermal degradation of the carbon dioxide complex liberated ~0.66 mole CO_2, decomposition with sulfuric acid 0.8 mole CO_2 per mole of $[Co(CO_2)(PPh_3)_2]$. No carbon monoxide could be found in the gaseous products evolved. Treatment of the benzene solution with an excess of methyl iodide afforded a considerable quantity of methyl acetate. Since in the case of the cobalt formate complex only methyl formate was formed [4] this supports a structure containing a metal–carbon bond. Treating $[Co(CO_2)(PPh_3)_2]_n$ in toluene with dioxygen at 20° $CoCO_3$ was deposited and the triphenylphosphine was oxidized to phosphine oxide. No phosphine cobalt carbonate complexes could be obtained as found in similar reactions of platinum [5, 6].

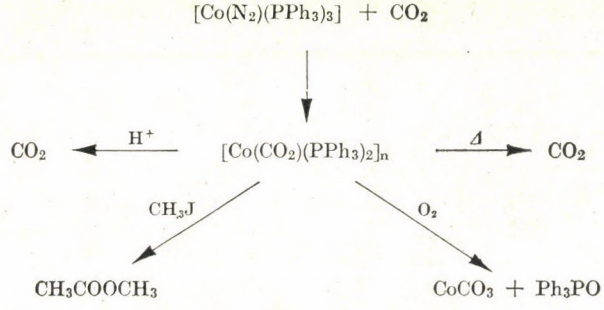

Fig. 1. The preparation and reactions of the carbon dioxide cobalt complex

As already described earlier $[Co(N_2)(PPh_3)_3]$ and $[CoH_2(PPh_3)_3]$ are not so air sensitive as the corresponding $[CoH(N_2)(PPh_3)_3]$ and $[CoH_3(PPh_3)_3]$ [7]. We have now observed, that the oxygenation of triphenylphosphine to phosphine oxide is catalyzed by the $[Co(N_2)(PPh_3)_3]$ and $[CoH_2(PPh_3)_3]$ complexes at room temperature. A typical experiment is shown in Fig. 2. Kinetic measurements suggest a complicated mechanism for this reaction.

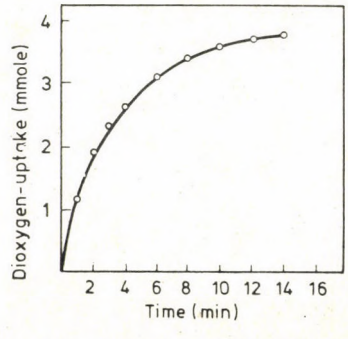

Fig. 2. Oxygenation of triphenylphosphine by $[Co(N_2)(PPh_3)_3]$; catalyst: 0.59 mmole; triphenylphosphine: 11.4 mmole; benzene: 10 ml; temperature: 20°; dioxygen pressure: 1 atm

$[Co(N_2)(PPh_3)_3]$ suspended in ether reacted with dioxygen already at —50°; in 8 hs the orange colour of the starting cobalt complex turned to yellow and μ-peroxo-hexakis (triphenylphosphine)dicobalt(I) was formed (see Fig. 3) which is stable up to 0°. Above this temperature it decomposes to phosphine oxide and probably a Co(II) species. For this reason the elemental analyses could not be carried out. The structure proposed for the dioxygen cobalt complex in Fig. 3 is therefore based on the determination of dioxygen uptake and hydrogen peroxide formation following acidic hydrolysis. No triphenylphosphine dissociation could be established by filtrating off the oxygenated product at —10° and determining the amount of triphenylphosphine in the filtrate by evaporating the ether.

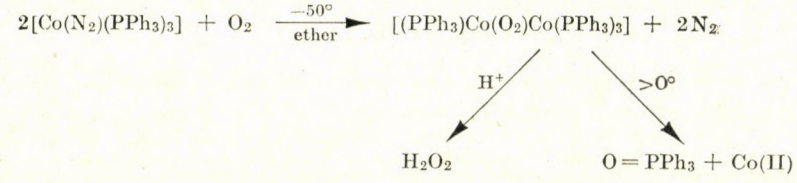

Fig. 3. The preparation and degradation of $[(PPh_3)_3Co(O_2)Co(PPh_3)_3]$

The reaction of dioxygen with the hydrido cobalt complexes $[CoH(N_2)(PPh_3)_3]$, $[CoH_3(PPh_3)_3]$ and $[CoH_2(PPh_3)_3]$ at low temperature resulted in brown products, the structures of which were not further investigated.

Experimental

General procedures

All reactions were carried out in an atmosphere of dry dinitrogen. Hydrocarbon and ether solvents were freshly distilled before use from sodium–potassium alloy. IR spectra were recorded on a UR-20 (Carl Zeiss, Jena) spectrometer.

The compounds $[Co(N_2)(PPh_3)_3]$ [7], $[CoH_2(PPh_3)_3]$ [7], $[CoH(N_2)(PPh_3)]$ [8, 9], $[CoH_3(PPh_3)_3]$ [8, 9] were obtained by standard methods.

Reaction of $[Co(N_2)(PPh_3)_3]$ with dioxygen at —50°

A suspension of dinitrogentris (triphenylphosphine)cobalt(O) (0.3—0.5 mmol) in *ca.* 5 ml ether was cooled to —50° and reacted with dioxygen. The reaction was carried out in a thermostated vessel connected to a gas buret. The amount of dioxygen absorbed in three separate experiments was found to be 0.21 mmole O_2/0.37 mmole Co; 0.19 mmole O_2/0.42 mmole Co and 0.27 mmole O_2/0.24 mmole Co. After 8 hs the orange colour of the suspension changed to lemon yellow. On warming up the yellow product decomposed at 0° and turned brown.

Determination of the P : Co ratio of the dioxygen cobalt complex

Dinitrogentris(triphenylphosphine)cobalt(O) (0.76 g, 0.87 mmole) were suspended in 15 ml ether and reacted with dioxygen at −50° for 8 hs. The yellow dioxygen complex was filtered at −10° and washed with 5 ml precooled ether. Evaporating the solvent from the joint filtrate 0.057 g of a residue was obtained, which was identified by mixed melting point as triphenylphosphine (0.22 mmole).

The acidic hydrolysis of $[(PPh_3)_3Co(O_2)Co(PPh_3)]$ to hydrogen peroxide

Dinitrogentris(triphenylphosphine)cobalt(O) (0.56 g 0.64 mmole) in 10 ml ether was reacted with dioxygen for 8 hs. The dioxygen was pumped off and acetyl acetone (2 ml), ether saturated with water (25 ml) and $HgCl_2$ (0.53 g, 1.96 mmole) dissolved in ether were added to the suspension. The mixture was allowed to warm up to room temperature. A white precipitate was formed, which was filtered off and the H_2O_2 content of the filtrate was determined iodometrically. H_2O_2 formed 0.25 mmole (yield 78%).

Reaction of $[Co(N_2)(PPh_3)_3]$ with dioxygen at 25°

Dinitrogentris(triphenylphosphine)cobalt(O) (0.87 g 1 mmole) was sealed in a small bulb and placed in a thermostated Schlenk-tube containing 10 ml ether and connected to a thermostated gas buret. After reaching vapour–liquid equilibrium the bulb was broken by a magnetic stirring bar and the amount of dioxygen absorbed measured (the amount of dinitrogen evolved was taken into correction). The dioxygen uptake was found in two parallel experiments to be 2.15 mole O_2 *per* 1.02 mole Co and 2.17 mole O_2 *per* 1.01 mole Co.

Catalytic oxidation of PPh_3 by dioxygen in the presence of $[Co(N_2)(PPh_3)_3]$

Triphenylphosphine (3.0 g 11.4 mmole) and benzene (10 ml) were placed into a thermostated Schlenk-tube which was connected to a thermostated gas buret filled with dioxygen and was equipped with a magnetic stirring bar and a bulb containing dinitrogentris(triphenylphosphine)cobalt(O) (0.51 g 5.8 mmole). After the bulb was broken with the magnetic stirrer the consumption of dioxygen was measured as shown on Fig. 2.

Reaction of $[Co(N_2)(PPh_3)_3]$ with carbon dioxide

Dinitrogentris(triphenylphosphine)cobalt(O) (4.37 g 5.0 mmole) was suspended in ether (30 ml), cooled to 0° and stirred under carbon dioxide for 2 hs and then at 25° for 10 hs. The orange colour of the starting material changed to yellow-brown. The product obtained was filtered off, washed with a small amount of ether and dried in vacuo. Yield (2.43 g, 77.5%); m. p. 80—100° (not sharp) (Found: Co 9.65%. $C_{37}H_{30}CoP_2O_2$; calcd. Co 9.38%). The compound is very air sensitive and only slightly soluble in ether and hydrocarbon solvents.

The determination of CO_2-uptake and N_2-loss in the reaction of $[Co(N_2)(PPh_3)_3]$ with carbon dioxide

In a closed system dinitrogentris(triphenylphosphine)cobalt(O) (0.6279 g, 0.72 mmole) dissolved in toluene (10 ml) was reacted with carbon dioxide at 0° and 1 atm pressure. The red solution turned to brown-yellow during 3 hs. The total amount of gas above the reaction mixture was pumped off and the CO_2- and N_2-contents were determined by GLC (3 m molecular sieve A-5, 25°). In two parallel experiments the CO_2-uptake was found to be 1.14 and 1.58 mole CO_2/mole Co. Simultaneously 0.677 respectively, 0.94 mole N_2/mole Co was given off.

Thermal decomposition of $[Co(CO_2)(PPh_3)_2]_n$

Small amounts of carbon dioxidebis(triphenylphosphine)cobalt(O) were in a Schlenksube connected to a gas buret slowly warmed up to 140° using a metal bath. The volume of the gas evolved was measured and the composition determined by GLC (2 m Porapak N)

Complex weighed in (mmole Co)	Carbon dioxide evolved (mmole)	CO_2/Co
0.18	0.097	0.54
0.25	0.19	0.76
0.16	0.11	0.69

Decomposition of $[Co(CO_2)(PPh_3)_2]_n$ with sulfuric acid

Carbon dioxidebis(triphenylphosphine)cobalt(O) (0.75 g, 1.2 mmole Co) in a Schlenk-tube was reacted with 1.0 ml cc. sulfuric acid and the gas evolved was found to be 0.95 mmole consisting of carbon dioxide (97% by GLC). No carbon monoxide could be detected in the mixture.

Reaction of $[Co(CO_2)(PPh_3)_2]_n$ with dioxygen

Dinitrogentris(triphenylphosphine)cobalt(O) (0.534 g, 0.61 mmol) in toluene (8 ml) was transformed to carbondioxidebis(triphenylphosphine)cobalt(O) as described previously and then reacted with dioxygen at 20°. A purple precipitate deposited from the brown solution. This was filtered off, washed with toluene and dried in vacuo to give $CoCO_3$ (0.060 g, 82%) (Found: Co 49.1; $CoCO_3$ calcd.: Co 49.55; authentic IR spectrum).

Reaction of $[Co(CO_2)(PPh_3)_2]_n$ with methyl iodide

Carbon dioxidebis(triphenylphosphine)cobalt(O) (0.76 g, 1.21 mmole Co) was suspended in toluene (5 ml) and cooled to −78°. Methyl iodide (0.45 ml, 7.22 mmole) was added and the mixture stirred for 3 hs during which it warmed up to room temperature. Analysing the reaction mixture by GLC (2 m polyethylene glycol, 100°) methyl acetate could be identified.

REFERENCES

[1] Misono, A., Ushida, G., Hidai, M., Kuse, T.: Chem. Commun., **1968,** 981
[2] Pu, L. S., Yamamoto, A., Ikeda, S.: J. Amer. Chem. Soc., **90,** 3896 (1968)
[3] Yamamoto, A., Kitazume, S., Pu, L. S., Ikeda, S.: J. Amer. Chem. Soc., **93,** 371 (1971)
[4] Kolomnikov, I. S., Stepovska, H., Tyrlik, S., Vol'pin, M. E.: Zh. Obshch. Khim., **42,** 1952 (1972)
[5] Nyman, C. J., Wymore, C. E., Wilkinson, G.: Chem. Commun., **1967,** 407
[6] Nyman, C. J., Wymore, C. E., Wilkinson, G.: J. Chem. Soc. A, (London) **1968,** 561
[7] Speier, G., Markó, L.: Inorg. Chim. Acta **3,** 127 (1969)
[8] Yamamoto, A., Pu, L. S., Kitazume, S., Ikeda, S.: J. Amer. Chem. Soc., **89,** 3071 (1967)
[9] Pu, L. S., Yamamoto, A., Ikeda, S.: Chem. Commun., **1969,** 189

Gábor Speier
Ákos Simon
László Markó
H-8201 Veszprém, Schönherz Z. u. 8.

Acta Chimica Academiae Scientiarum Hungaricae, Tomus 92 (2), pp. 175—186 (1977)

STEREOCHEMICAL STUDIES, XXVII* STUDIES ON CYCLIC 2-HYDROXYCARBOXYLIC ACIDS, VI**

NEIGHBOURING HYDROXYL GROUP CATALYSIS IN THE ALKALINE HYDROLYSIS OF ETHYL *CIS*- AND *TRANS*-2-HYDROXYCYCLOPENTANE-, CYCLOHEXANE-, CYCLOHEPTANE- AND CYCLOOCTANECARBOXYLATES***

G. BERNÁTH, P. SOHÁR+, K. L. LÁNG, GY. GÖNDÖS, L. GERA and A. PÁL

(Institute of Organic Chemistry, Attila József University, Szeged and +Pharmaceutical Research Institute, Budapest)

Received November 26, 1975

The kinetics of the alkaline hydrolysis of ethyl *cis*- and *trans*-2-hydroxycyclopentanecarboxylates (**1**, **2**), as well as of their cyclohexane (**4**, **5**), cycloheptane (**7**, **8**) and cyclooctane (**10**, **11**) homologues was investigated in 70% aqueous dioxane. The hydrolysis is accelerated by the neighbouring hydroxyl group by a factor of 10 to 21 compared with the corresponding ethyl cycloalkane carboxylates (**3**, **6**, **9**, **12**). The rate of hydrolysis is about the same in the case of cyclopentane and cycloheptane isomers, while in cyclohexane derivatives the *trans*, in cyclooctane derivatives the *cis* compound reacts about twice as fast as the other isomer. The $\Delta E^{\ddagger}$, $\Delta H^{\ddagger}$, $\Delta S^{\ddagger}$ and $\Delta G^{\ddagger}$ values of the reactions were determined. The isokinetic temperature of the hydrolysis of the *cis*- and *trans*-2-carbethoxycyclanols was computed and found to be $\beta = 251 \pm 12$ *K* with a correlation coefficient $r = 0.99$. For the ethyl cycloalkanecarboxylates the slope of the plot is steeper, showing that the two reactions occur by different mechanism. The IR and NMR spectra of methyl and ethyl *cis*- and *trans*-2-hydroxycycloalkanecarboxylates are discussed. It can be concluded that in the rate enhancing effect of the neighbouring hydroxyl group in alkaline ester hydrolysis the solvent sorting due to the neighbouring hydroxyl group is the deciding factor, though the different hydrogen bonding in the *cis* and *trans* isomers must also be taken into consideration.

Introduction

Following the observation of the anchimeric assistance of the hydroxyl group in ester hydrolysis[1], numerous papers have dealt with the participation of the neighbouring hydroxyl group in the alkaline hydrolysis of esters (*e.g.* [2—9]). The reaction was reviewed [10, 11].

More recent investigations were promted by the fact that related anchimeric assistance has a decisive role also in biological processes [12, 13]. Very thorough studies of enzyme-catalyzed ester hydrolysis led to the expla-

* Part XXVI: BERNÁTH, G., GERA, L., GÖNDÖS, GY., PÁNOVICS, I. and ECSERY, Z.: Acta Chim. (Budapest) **89**, 61 (1976)

** Part V: JANCKE, H., ENGELHARDT, G., BERNÁTH, G., GÖNDÖS, GY. and TICHÝ, M.: J. prakt. Chem. **317**, 1005 (1975).

*** A preliminary announcement of this work was made in the lecture of BERNÁTH, G., LÁNG, K. L., GÖNDÖS, GY. and KOVÁCS, K. presented at the Meeting of the Hungarian Chemical Society in Debrecen, 1 September, 1971 (See: Proceedings, p. 136). Part of this work is described in the Diploma Thesis submitted by A. PÁL to the József Attila University, Szeged in 1972. See also Ref. [31].

nation that the proximity of appropriate groups, *e.g.* a hydroxyl group of a seryl residue and an imidazol group of a hystidyl residue, is involved in the rate enhancement.

Earlier investigations on the neighbouring hydroxyl group participation in the alkaline hydrolysis of esters chiefly dealt with diol monoesters; esters of β-hydroxycarboxylic acids were treated only in some cases (*e.g.*, the saponification of alkaloids containing methyl 2-hydroxycyclohexanecarboxylate moiety [3, 4]), and the results obtained were only qualitative owing to the complexity of the compounds (yohimbine, corynanthine, etc.).

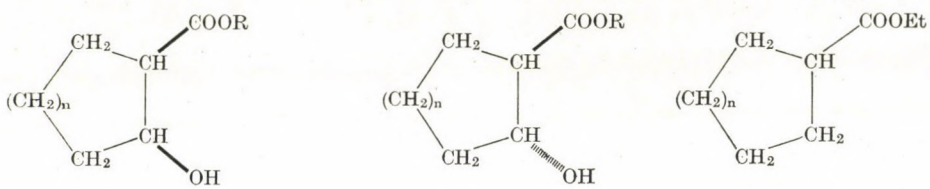

n = 1: **1** (R = Et) and **17** (R = Me)	n = 1: **2** (R = Et) and **18** (R = Me)	n = 1: **3**
n = 2: **4** (R = Et) and **19** (R = Me)	n = 2: **5** (R = Et) and **20** (R = Me)	n = 2: **6**
n = 3: **7** (R = Et) and **21** (R = Me)	n = 3: **8** (R = Et) and **22** (R = Me)	n = 3: **9**
n = 4: **10** (R = Et) and **23** (R = Me)	n = 4: **11** (R = Et) and **24** (R = Me)	n = 4: **12**

Fig. 1

Recently CAPON *et al.* have shown [7] that lactonizations in 2-hydroxyphenylacetic acid, 3-(2-hydroxyphenyl)propionic acid, 4-hydroxybutyric acid and 5-hydroxyvaleric acid occur with substantial anchimeric assistance. CAPON and PAGE also published a comprehensive study [8] on the kinetics and mechanism of hydrolysis of *cis*- and *trans*-2-hydroxycyclopentanecarboxylates.

Hydrolysis experiments on homologous cyclic β-hydroxycarboxylates affording the possibility to study conformational effects seem very promising. Therefore, as a continuation of our work on the reaction mechanism of alicyclic 1,3-bifunctional compounds [15—17], the present series of compounds (Fig. 1) was studied to obtain data concerning the accelerating influence on the reaction rate of a neighbouring hydroxyl group, and the effects of ring size, configuration and conformation.

Materials and kinetic method

Ethyl *cis*- and *trans*-2-hydroxycyclopentanecarboxylate (**1**, **2**) [18] and their cyclohexane (**4**, **5**) [19] and cycloheptane (**7**, **8**) [20] homologues were synthesized by PASCUAL *et al.* On elaborating methods for the preparation of larger quantities, we found [21, 22] the vacuum fractionation on a column of 30 theoretical plates suitable for separating the isomers, including the cyclooctane derivatives (**10**, **11**) [22]. This method is more convenient than fractional crystallization of the dinitrobenzoates applied earlier [18] for the separation of **1** and **2**, or the more recently used continuous countercurrent distribution [23], or preparative gas chromatog-

raphy [8]. As the efficiency of the fractionation depends on the isomer ratio, we studied [22] the catalytic (Raney Ni/H_2) and $NaBH_4$ reduction of homologous alicyclic ethyl β-ketocarboxylates, too.

Kinetic measurements were made with gas chromatographically stereohomogeneous ethyl β-hydroxycarboxylates (stationary phase: polyethylene glycol adipate 20%; column height 2 m; diameter 0.4 cm; temp.: 160 °C).

The ethyl cycloalkanecarboxylates (**3**, **6**, **9**, **12**) were prepared by standard methods. The IR, NMR data and microanalysis of the compounds were consistent with the structures.

The rates of the hydrolysis were measured in 70% dioxane–water mixture, the concentration of the compounds being about 0.02 mole/l; the system contained NaOH in 50% excess (approx. 0.03 *M*), prepared in the following way. A 0.06 *M* NaOH solution and 0.04 *M* ester solution, kept in ultrathermostate, were mixed in equal quantity after having reached the temperature required. 5 ml aliquots were withdrawn from time to time and put immediately into 10 ml ice-cool 0.02 *M* HCl solution. After warming the samples to room temperature, the excess of HCl was titrated with 0.02 *M* NaOH in water in the presence of phenolphthalein indicator. Blanks were prepared for each series of measurements.

The second order rate constants were calculated from the following equation:

$$k_2 = \frac{2.303}{(a-b)\,t} \cdot \log \frac{(a-x)\,b}{(b-a)\,a}$$

where: a = conc. of NaOH (mole/l); b = conc. of the compound (mole/l); x = conc. of the hydrolysed ester (mole/l); t = time (in seconds).

The activation energies were obtained from the Arrhenius equation and the activation entropies calculated from the following expression:

$$\Delta S^{\ddagger} = 4.576 \log k + \frac{\Delta H^{\ddagger}}{4.576\,T} - (10.31886 - \log T)$$

Results and discussion

The second order rate constants of the hydrolysis of 2-hydroxycycloalkanecarboxylates (**1**, **2**, **4**, **5**, **7**, **8**, **10**, **11**) and of cyclic ethyl carboxylates (**3**, **6**, **9**, **12**), together with the $\Delta E^{\ddagger}$, $\Delta H^{\ddagger}$, $\Delta S^{\ddagger}$ and $\Delta G^{\ddagger}$ values of the reactions, are listed in Table I. Some rate constants determined at different temperatures are collected in Table II. The rates of hydrolysis of **1** and **2** — in accordance with recent data [8] — are nearly the same and about 10 times as high as that of **3**, containing no neighbouring hydroxyl group. In the case of cyclohexane derivatives, the rate of hydrolysis of the *trans* isomer **5** is about twofold compared with the *cis* isomer **4**. The reaction rate of **4** is about 10 times, that of **5** about 19 times as high as the rate of hydrolysis of **6**. Interestingly, the reaction rates of *cis*- and *trans*-2-carbethoxycycloheptanol (**7**, **8**) are also nearly equal, while the accelerating effect of the hydroxyl group is about 11-fold as compared with **9**. In cyclooctane derivatives, the rate of hydrolysis of the *cis* isomer **10** is twice as high as that of the *trans* isomer; contrary to the relation for cyclohexane isomers, the accelerating effect of the hydroxyl group is 21-fold for **10** and 11-fold for **11**.

Though several earlier investigations attempted to determine the nature of the neighbouring aliphatic and aromatic hydroxyl group facilitation in the

Table I

Second order rate constants ($k_2 \cdot 10^{-2} \cdot \mathrm{sec}^{-1}$, $t = 25$ °C) *and activation parameters of the alkaline hydrolysis of ethyl cis- and trans-2-hydroxycyclopentane-, cyclohexane-, cycloheptane- and cyclooctanecarboxylates* (**1, 2, 4, 5, 7, 8, 10, 11**) *and of ethyl cyclopentane-, cyclohexane-, cycloheptane- and cyclooctanecarboxylates* (**3, 6, 9, 12**)

Compound	k_2	$\frac{k_{OH}}{k_H}$	$\Delta E^{\ddagger}$, kcal/mole	$\Delta H^{\ddagger}$, kcal/mole	$\Delta S^{\ddagger}$, e.u.	$\Delta G^{\ddagger}$, kcal/mole
1	4.11	8.38	11.4	10.9	−26.2	19.1
2	3.56	7.26	12.6	12.0	−22.3	19.1
3	0.49		10.9	10.3	−32.5	20.6
4	2.89	12.4	12.3	10.7	−27.8	19.3
5	4.72	19.67	11.5	10.9	−25.9	19.2
6	0.24		12.4	11.8	−28.9	21.0
7	1.57	11.20	9.66	9.10	−34.4	19.6
8	1.52	10.86	12.6	12.0	−24.0	19.6
9	0.14		12.9	12.4	−28.2	21.4
10	1.58		11.4	10.9	−27.7	19.6
11	0.82		7.7	7.2	−42.2	20.1
12	0.17*		12.48	11.9	−30.6	21.4

* $t = 35$ °C

Table II

Second order rate constants ($k_2 \cdot 10^2 \cdot \mathrm{sec}^{-1}$) *of the alkaline hydrolysis of ethyl cis- and trans-2-hydroxycyclopentane-, cyclohexane-, cycloheptane- and cyclooctanecarboxylates* (**1, 2, 4, 5, 7, 8, 10, 11**) *and of ethyl cyclopentane-, cyclohexane-, cycloheptane- and cyclooctanecarboxylates* (**3, 6, 9, 12**)

Compound	Temperature, °C					
	10	15	20	25	30	35
1	1.60	1.80	3.34	4.11		
2	1.65	2.28	3.34	3.46		
3				0.49	0.66	0.90
4	1.16	1.39	2.30	2.89		
5	2.10	2.67	4.24	4.72		
6			0.25	0.24	0.31	0.48
7	0.67	0.93	1.15	1.57		
8	0.61	0.96	1.34	1.51		
9			0.09	0.14		0.26
10	0.75	1.07	1.52	1.58		
11		0.52	0.62	0.82		
12		0.06	0.07			0.17

alkali-catalyzed ester hydrolysis [10—12], the problem still awaits an unambiguous interpretation.

The results of HANSEN [24] on the kinetics of the alkaline hydrolysis of catechol monoacetate and some related esters suggested that the rate increase is due to intramolecular hydrogen bonding. A series of further investigations (*e.g.* [25—27]) supported these conclusions. The reaction rates of the different monoesters of cathecol are 200 to 800 times higher than those of corresponding phenyl or *o*-methoxyphenyl esters. The most probable mechanism for the reaction is intramolecular general base catalysis.

The acceleration of the reaction rate by the alcoholic hydroxyl group in the ester hydrolysis is less distinct; the rate enchancement is about 10 to 20-fold, and is probably due to internal solvation of the transition state, facilitating the attack of the hydroxide ion on the carbonyl group [10, 11].

On the basis of qualitative IR analysis, a hydrogen-bonded structure (**13**) involving the ether oxygen was supposed [1] to explain assistance by the hydroxyl group, known as the Henbest—Kupchan effect [5, 28]. WEST, KORST and JOHNSON studied thoroughly [28] the IR spectra of several polycyclic 1,3-diol monoacetates in the νOH region under high resolution, and found that intramolecular hydrogen bond exists between the hydroxyl hydrogen and the ether oxygen of the acetate group (**13**). Explanation for hydrogen bonding to the more weakly basic ether oxygen atom might be in this case the large entropy effect favouring the six-membered ring hydrogen bonded system (**13**) over the eight-membered ring (**14**) (Fig. 2).

The differentiation between those two possibilities in the case of monoacetates of 1,2-diols is not so obvious, because the energetic differences between the five- and seven-membered structures are not so pronounced. In fact, the explanation proposed for the hydrolysis of monoacetates of 1,2-diols was that the acceleration should be due to hydrogen bonding to the ester carbonyl oxygen [2]. In the ethyl β-hydroxycarboxylates studied by us, both types of the intramolecular hydrogen bond structures are of the same ring size (**15**, **16**).

It was suggested [5, 28] that though the hydrogen bond to the ether oxygen may be dominant in the ground state, the kinetically important species should be that with hydrogen bonding to the carbonyl oxygen. According to BRUICE and FIFE [5], the most reasonable explanation for the hydroxyl assistance is the influence of the neighbouring hydroxyl group in the solvatation of the transition state, facilitating the nucleophilic attack of the hydroxide ion on the ester carbonyl.

It has been established [29] that the transition state in the basic hydrolysis of esters has a negative charge localized on the carbonyl oxygen, which becomes thereby a good acceptor for hydrogen bonding. Recent results [9] obtained in the saponification of glycol monobenzoates demostrated a remarkable solvent dependency in the ester hydrolysis occurring with anchimeric

assistance, and the relative reactivity was interpreted in terms of the different solvation of the transition state.

This seems to be in accordance with the results of CAPON and PAGE [8]. The IR spectra of ethyl and 2-naphthyl *cis*- and *trans*-2-hydroxycyclopentanecarboxylates showed that the only species present in solutions of *cis* esters are those in which the intramolecular hydrogen bond involves the carbonyl

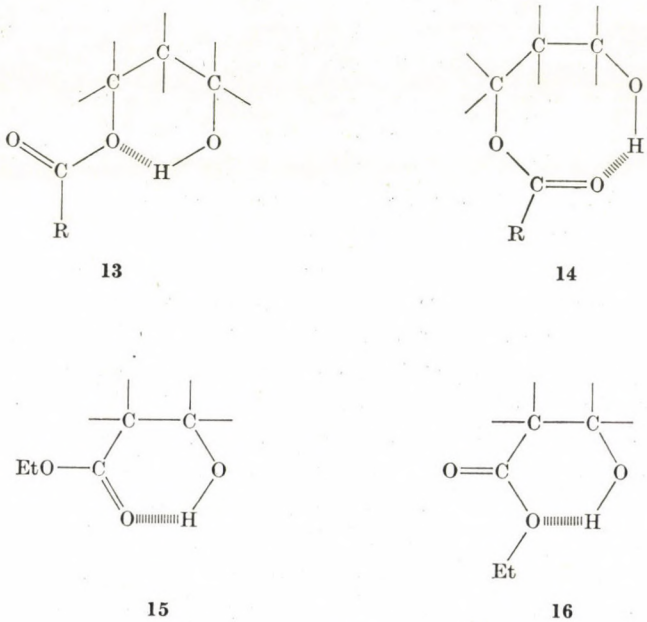

Fig. 2

oxygen. The shortest distance between the hydroxyl and ester carbonyl oxygens in the *trans* isomers is 3 Å, whereas hydrogen bonds hardly exist in the case of distances greater than 2.8 Å [30]. Since the reaction rate of the *trans* ester is as high as, or higher than, that of the *cis* isomer, the accelerating effect of the intramolecular hydrogen bond does not seem probable in the case of the *cis* ester either. Therefore, CAPON and PAGE attributed the accelerating effect to the solvent sorting [8] in the cybotactic region of the hydroxy-esters, though mentioning that "in view of the complexity of the physical chemistry of water–dioxane mixtures, it is difficult to be certain that it is the correct explanation". They consider it rather as a reasonable working hypothesis.

Though the above interpretation of the hydrolysis of ethyl cis- and *trans*-2-hydroxycyclopentanecarboxylates seems to be quite reasonable, our studies on a more complete series, of model compounds, performed simultaneously with the work of CAPON and PAGE (see footnote on page 175 and [31]), appeared interesting.

Table III

IR and NMR data of ethyl cis- and trans-2-hydroxycyclopentane-, cyclohexane-, cycloheptane- and cyclooctanecarboxylates (**1, 2, 4, 5, 7, 8, 10, 11**) *and of the corresponding methylates* (**17—24**)

Compound	IR*, cm^{-1}		NMR**	
	νOH KBr (CCl_4)	νC=O KBr (CCl_4)	δ(H-1), ppm	line width, Hz
1	3460 (~3510)	~1720 (1710 s, 1735 sh)	~4.33	20
2	~3400 (3600 s, 3600—3200)	~1725 (1730)	~4.33	20
4	~3490 (~3515)	~1720 (1710 s, 1730 sh)	~4.1	15
5	~3420 (3580 s)	~1725 (1720 s)	~3.65	30
7	~3470 (~3540)	1720 (1710 s, 1735 sh)	4.2	20
8	~3440 (3580 s)	~1720 (1720)	3.90	30
10	~3470 (~3530)	~1720 (1710 s, 1730)	~4.1	20
11	~3460 (3580 s)	1720 (1720)	~3.95	20
17	3510 s (3420 s, ~3520)	~1730 (1725)	4.40	10
18	~3400 (3600—3200)	~1730 ~1715 sh, (1740)	4.35	16
19	3500 s 3420 s (~3540)	~1730 (1730)	4.10	10
20	~3410 (3600—3200)	~1735 1720 sh (1735)	~3.7	***
21	3500 s 3420 (~3550)	~1730 (1730)	4.20	13
22	~3420 (3600—3200)	~1735 1720 sh (1740)+	3.90	25
23	3500 s, ~3420 (~3550)	~1725 (1730)	4.10	17
24	~3420 (—)	~1730, ~1720 (—)	4.00	22

* In brackets: data in CCl_4. s = sharp; sh = shoulder; ~ = broad
** In CCl_4 solution
*** Not measured because of overlap of the CH(OH) and OCH_3 signals
\+ Decomposed in CCl_4 solution (1790 cm^{-1})

The IR and NMR data of the model compounds are given in Table III. Though the IR spectra obtained in CCl_4 solution or in KBr pellets cannot be transferred without reserve to the transition states existing in water–dioxane

mixture, they afford information about the ground states. It follows from the IR spectra that in the case of the esters investigated, besides intramolecular hydrogen bonds, intermolecular association must also be taken into account. Intermolecular association is also in accordance with the relative reaction rates of the hydrolysis at different ester concentrations. In the ethylates, the evaluation of the signal CH—OH (H—1) is impeded by the methylene quartet of the ethoxy group, therefore, the NMR spectra of the corresponding methylates (**17**—**24**) were also measured.

There is no difference in the values of δ(H—1) in the case of **1** and **2**. This is in accordance with the conformational equilibrium of the parent compounds discussed by BAUMANN, FRANKLIN and MÖHRLE [32], as well as by us [33]. IR data, too, point to intra- and intermolecular hydrogen bonding.

In **4**, in the preferred conformation the hydroxyl group is *axial* and the COOEt *equatorial* [$(\delta H—1)_{trans} < (\delta H—1)_{cis}$]. In the *cis* isomer (**4**) there is an intramolecular hydrogen bond, while in the *trans* isomer (**5**) the hydrogen bonding is intermolecular.

The difference in association diminishes with increasing ring size, *i.e.* the proportion of the intramolecular association of the *cis* isomers decreases. Accordingly, the splitting of the νOH and νC=O bands gradually decreases and the νOH band broadens. Sharper νOH lines and higher νOH frequencies are characteristic of the intramolecular hydrogen bond. In accordance with earlier data [23], the intermolecular hydrogen bond is probably of the type $CH_3O \cdots HO$ ($C_2H_5O \cdots HO$), while the intramolecular bridge contains $C=O \cdots HO$ bonds. (The νC=O frequencies of the *cis* isomers are lower, as compared with the νC=O frequencies of the *trans* isomers.)

The chemical shift difference of the H—1 signals in the *cis* and *trans* isomer pairs, *i.e.* the value of $\Delta\delta$(H—1) gradually decreases in the case of the isomer pairs **4**—**5**, **7**—**8** and **10**—**11** (0.45, 0.3 and 0.15 ppm), in accordance with the pseudorotation of the corresponding ring systems and with the decreasing difference in the dihedral angles of the most preferred conformations of the 1,2-disubstituted *cis* and *trans* cycloheptane and cyclooctane derivatives [26—28]. On this basis, the existence of the intramolecular hydrogen bonding would be possible also in the *trans* cycloheptane and cyclooctane isomers; this, however, does not follow from the IR data.

In this respect some earlier studies on 1,2-disubstituted alicyclic systems are also to be mentioned. KUHN studied the intramolecular hydrogen bonding of alicyclic *cis*- and *trans*-1,2-diols of different ring size [37] and found that the torsional angles between the C—O bonds of the *cis*- and *trans*-cycloheptane-1,2-diols are 42° and 51°, respectively, *i.e.* the difference in the dihedral angles of the *cis* and *trans* isomers is negligible. SICHER *et al.* studied [38] the strength of the intramolecular hydrogen bonds of alicyclic 1,2-aminoalcohols as a function of the ring size. By considering the difference between the frequencies

νOH_{free} and νOH_{bonded}, *i.e.* the $\Delta\nu OH$ values of the cyclic 1,2-aminoalcohols, they demonstrated that the 'cross-over' of the *cis* and *trans* curves is located between the seven- and eight-membered rings. The $\Delta\nu OH$ value of cyclic 1,2-aminoalcohols is about 140 cm^{-1}. In the case of cyclic 1,2-diols the "cross-over" of the $\Delta\nu OH$ curves appears between the nine- and ten-membered rings. This was rationalized by the much smaller energy of the O—H · · · O bond as compared with the O—H · · · N bond; namely the $\Delta\nu OH$ values of diols are only about 40 cm^{-1}. Thus the functional groups in *trans*-1,2-aminoalcohols might more easily reach coplanarity by hydrogen bonding than in diols. Hydrogen bonding to the carbonyl oxygen, playing a part in the acceleration of the ester hydrolysis, is also stronger than the bonding to the ether oxygen of the carboxyl group.

By comparing the calculated and measured dipole moments of alicyclic ethyl 2-hydroxy-1-cycloalkanecarboxylates, we deduced [33] that an intermolecular hydrogen bond exists in the *cis* isomers **1** and **4**. In the *trans* isomer **5**, PASCUAL *et al.* supposed intermolecular hydrogen bonding on the basis of viscosity measurements [18].

In order to clarify the importance of intermolecular hydrogen bondings, it seemed reasonable to perform experiments at different ester concentrations. The hydrolysis of **1** and **2**, **4** and **5**, as well as of the compounds **3** and **6** used for comparison, was studied in 70% dioxane containing 50% excess of KOH at 4 °C and 0.12, 0.02 and 0.002 *M* ester concentration.

Sixfold increase in the concentration of **1** reduced the reaction rate to 0.93-fold of its original value, while the reaction rate of the *trans* isomer **2** showed an 1.35-fold increase. In the cyclohexane homologues, the decrease of the reaction rate for the *cis* isomer **4**, and the increase for the *trans* isomer **5** are somewhat more distinct. Tenfold decrease in the concentration (0.002 *M* ester) resulted in a less pronounced rate increase for the *trans* isomer in the case of cyclopentane and cyclohexane derivatives, supposedly owing to a decrease in intermolecular association compared with the *cis* derivatives in which the intramolecular association remained unchanged.

It follows that intramolecular hydrogen bonding cannot be the decisive factor in the rate accelerating effect of the neighbouring hydroxyl group. If the hydrogen bonding, present in *cis* and absent in *trans* isomers, were the only, or at least the determining, factor influencing the reaction rate, then, similarly to other 1,3-difunctional cyclopentane derivatives, the reactivities of the *cis* and *trans* isomers should differ by orders of magnitude, like in the N → O acyl migration reaction of *cis*- and *trans*-1,3-aminoalcohols [16], where the hetero ring in the transition state of the reaction is also six-membered, like the structure of the intramolecular hydrogen bonding in ethyl 2-hydroxycarboxylates.

It is worth mentioning that in the N → O acyl migration reaction of N-benzoyl-2-aminomethylcyclanols and N-benzoyl-2-hydroxymethyl cyclic

amines such a definite difference is found only in the reactivity of the *cis* and *trans* cyclopentane derivatives. In the case of cyclohexane, cycloheptane and cyclooctane derivatives it is always the reactivity of the *trans* isomers which is higher; however, the difference in the reactivity of *cis* and *trans* isomers is much less than in cyclopentane derivatives, k_{trans}/k_{cis} being only about 4—5.

Only very few 1,3-difunctional homologous compounds with ring size higher than six, in which the transitorily formed hetero ring is six-membered, have been investigated kinetically; therefore, it is hardly possible to draw further analogies.

In the ester hydrolysis discussed, the k_{cis}/k_{trans} ratio for cyclopentane and cycloheptane derivatives is nearly 1, while in cyclohexanes it is the *trans*, in cyclooctanes the *cis*-isomer which undergoes faster hydrolysis.

It is striking that the $\Delta S^{\ddagger}$ values of **7—8** and **10—11** *cis* and *trans* isomers differ by 10.4 and 14.5 e.u., respectively (Table I), furthermore, that in the case of cycloheptane derivatives the activation entropy of the *cis* isomer, for cyclooctane derivatives the activation entropy of the *trans* isomer is the more negative. The activation entropies of the hydrolysis of the ethyl 2-hydroxycarboxylates investigated are in the range -23.2 — -42.2 e.u., while the activation entropies of the four cyclic ethyl carboxylates are close to each other, varying between -28.2 and -32.5 e.u.

Such differences in the activation entropies of the *cis* and *trans* isomer pairs are hardly to be interpreted merely by the effect of intramolecular association, if in both the *cis* and *trans* isomers *equatorial* carbethoxy groups in rotamers *syn*-planar with the ring [34, 35] are assumed to be preferred.

The highly negative activation entropy values found are not surprising, considering the findings in related reactions, *e.g.*, in the cyclization of 3-amino-2-hydroxymethylbenzamide [36] a transition state with one or more water molecules was brought into connection with the highly negative entropy value determined. In the course of the hydrolysis of ethyl 2-hydroxyphenylcarbonate $\Delta S^{\ddagger} = -41.0$ e.u. was calculated, which may be attributed to the necessity of a proper orientation of the solvent molecules in the transition state [39].

Consequently, the transition state of the alkaline hydrolysis of the ethyl 2-hydroxycycloalkanecarboxylates discussed must be very complex. It seems noteworthy that in our model compounds, in which both substituents are connected to the same alicyclic ring, the accelerating effect on ester hydrolysis exerted by the β-hydroxyl group is 10 to 21-fold. This value is closely similar to that found for the enhancing effect of the alcoholic hydroxyl group in other, different reactions. CUNNINGHAM and SMIR found that introduction of a hydroxyl group in γ-position of the butyramide increases the reaction rate of the alkaline hydrolysis of the anilide function by a factor of 11 [40]. 4-Hydroxybutyramide was found to be 22 times as reactive as butyramide in alkaline hydrolysis [41].

Taking into account what has been said above it seemed desirable to check the validity of the isokinetic correlation. For the homologous ethyl *cis*- and *trans*-2-hydroxycycloalkanecarboxylates the $\Delta H^{\ddagger}$ and $\Delta S^{\ddagger}$ values gave a very good linear plot (Fig. 3). For the ethylates, not containing hydroxyl group in β-position, the slope of the plot is higher, showing that the two reactions occur by different mechanism.

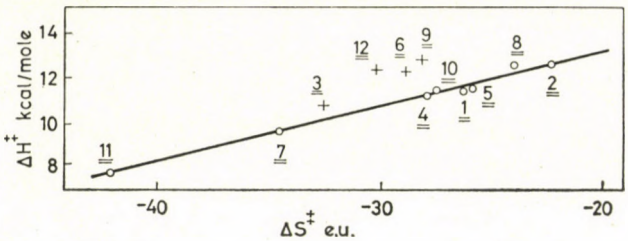

Fig. 3

Using the $\Delta H^{\ddagger}$ and $\Delta S^{\ddagger}$ values for the alkaline hydrolysis of ethyl 2-hydroxycycloalkanecarboxylates, the isokinetic temperature of the reaction was computed. We obtained $\beta = 251 \pm 12$ K with a correlation coefficient $r = 0.99$, showing that the experiments were performed above the isokinetic temperature (*i.e.* $T > \beta$). $\Delta G^{\ddagger}$ was found to be 19,513 $\pm$ 369 cal/mole. In the temperature range higher than β, the reactivity of the compounds is controlled by the activation entropy. This may be interpreted by the solvent effect [42].

Summing up, it can be stated that under the experimental conditions applied, the hydroxyl group in β-position accelerates the alkaline hydrolysis of ethyl 2-hydroxycycloalkanecarboxylates 10—21 times. This enhancing factor is closely similar to the value found for the alcoholic hydroxyl group in other processes. Activation entropies of homologous and isomeric ethyl 2-hydroxycycloalkanecarboxylates vary over a broad range, while those of the hydrolysis of homologous ethyl cycloalkanecarboxylates lie very near to each other. The isokinetic relation is valid for the ethyl 2-hydroxycycloalkanecarboxylates. Solvent sorting due to the neighbouring hydroxyl group plays an important role in the accelerating effect. However, intramolecular hydrogen bonding in the *cis* isomers and intermolecular association of the *trans* isomers must also be taken into consideration. The ratio of the rates of the reaction occurring with and without participation of the hydroxyl group depends on the ester concentration.

*

The authors wish to express their thanks to Mrs. É. Tomori (Pharmaceutical Research Institute, Budapest) for gas chromatographic analyses, to Pharmaceutical Works CHINOIN, Budapest, and to REANAL Factory of Laboratory Chemicals, Budapest, for supplying chemicals and starting materials.

REFERENCES

[1] HENBEST, H. B., LOVELL, B. J.: J. Chem. Soc. **1957,** 1965
[2] ZACHAU, H. G., KARAU, V.: Chem. Ber. **93,** 1830 (1960)
[3] ALLEN, M. J.: J. Chem. Soc. **1960,** 4904
[4] ALLEN, M. J.: J. Chem. Soc. **1961,** 4252
[5] BRUICE, T. C., FIFE, T. H.: J. Am. Chem. Soc. **84,** 1973 (1962)
[6] YAMANAKA, T., ICHIHARA, A., TANABE, K., MATSUMOTO, T.: Tetrahedron **21,** 1031 (1965)
[7] CAPON, B., MCDOWELL, S. T., RAFTERY, W. V.: Chem. Commun. **1971,** 389
[8] CAPON, B., PAGE, M. I.: J. Chem. Soc. (B) **1971,** 741
[9] BALAKRISHNAN, M., VENKOBA RAO, G., VENKATASUBRAMANIAN, N.: Tetrahedron Letters **1972,** 4617
[10] CAPON, B.: Quart. Rev. **18,** 45 (1964)
[11] EURANTO, E. K.: Esterification and ester hydrolysis. In: The Chemistry of Carboxylic Acids and Esters (Ed.: S. PATAI) p. 505. Interscience Publ., London—New York—Sydney—Toronto 1969
[12] BRUICE, T. C., BENKOVIC, S. J.: Bioorganic Mechanism, Vol. 1, p. 146. Benjamin, New York, N. Y. 1966
[13] JENCKS, W. P.: Catalysis in Chemistry and Enzymology, MacGraw-Hill Co., New York, N. Y. 1969
[14] GRIFFITS, D. W., BENDER, M. L.: Bioorganic Chemistry **4,** 84 (1975)
[15] BERNÁTH, G., GÖNDÖS, GY., LÁNG, K. L.: Acta Chim. (Budapest) **81,** 187 (1975)
[16] BERNÁTH, G., KOVÁCS, K., LÁNG, K. L.: Acta Chim. Acad. Sci. Hung. **65,** 347 (1970)
[17] BERNÁTH, G., LÁNG, K. L., GÖNDÖS, GY., MÁRAI, P., KOVÁCS, K.: Acta Chim. (Budapest) **74,** 479 (1972)
[18] PASCUAL, J., SISTARÉ, J., REGÁS, A.: J. Chem. Soc. **1949** (1952)
[19] PASCUAL, J., CASTELLS, J.: J. Am. Chem. Soc. **74,** 2899 (1952)
[20] PALAU, J., PASCUAL, J., RÁFOLS, J. M.: Bull. soc. chim. France **1964,** 269
[21] BERNÁTH, G., GÖNDÖS, GY., MÁRAI, P., GERA, L.: Acta Chim. (Budapest) **74,** 471 (1972)
[22] BERNÁTH, G., GÖNDÖS, GY., GERA, L.: Acta Phys. et Chem. Szeged **20,** 139 (1974)
[23] MÖHRLE, H., BAUMANN, H.: Annalen **716,** 61 (1968)
[24] HANSEN, B.: Acta Chem. Scand. **17,** 1375 (1963)
[25] FULLER, E. J.: J. Am. Chem. Soc. **85,** 177 (1963)
[26] SHALTIN, Y., BERNHARD, S. A.: J. Am. Chem. Soc. **86,** 2291 (1964)
[27] CAPON, B., GOSH, B. C.: J. Chem. Soc. (B) **1966,** 472
[28] WEST, R., KORST, J. J., JOHNSON, W. S.: J. Org. Chem. **25,** 1976 (1960)
[29] HABERFIELD, P., FRIEDMAN, J., PINKSTON, M. F.: J. Am. Chem. Soc. **94,** 71 (1972)
[30] PIMENTAL, G. L., MCCLELLAN, A. L.: The Hydrogen Bond, p. 260. W. H. Freeman and Co., San Francisco 1960
[31] BERNÁTH, G., GÖNDÖS, GY., LÁNG, K. L., GERA, L., KOVÁCS, K.: Lecture presented at the Meeting of the Hungarian Chemical Society at Pécs, 22 August, 1973. See: Proceedings, p. 136
[32] BAUMANN, H., FRANKLIN, N. C., MÖHRLE, H.: Tetrahedron **23,** 4331 (1967)
[33] BERNÁTH, G., SOHÁR, P., LÁNG, K. L., TORNYAI, L., KOVÁCS, Ö. K. J.: Acta Chim. Acad. Sci. Hung. **64,** 81 (1970)
[34] DUNITZ, J., STRICKLER, P.: Tetrahedron Letters **1966,** 3933
[35] ABRAMOVITCH, R. A., SINGER, S. S., ROGIC, M. M., STRUBLE, D. L.: J. Org. Chem. **40,** 34 (1975)
[36] FIFE, T. H., BENJAMIN, B. M.: J. C. S. Chem. Commun. **1974,** 525
[37] KUHN, L. P.: J. Am. Chem. Soc. **76,** 4323 (1954)
[38] SICHER, J., HORÁK, M., SVOBODA, M.: Coll. Czechoslov. Chem. Commun. **24,** 950 (1959)
[39] TILLETT, J. G., WIGGINS, D. E.: Tetrahedron Letters **1971,** 911
[40] CUNNINGHAM, B. A., SMIR, G. L.: J. Am. Chem. Soc. **89,** 917 (1967)
[41] BRUICE, T. C., MARQUARDT, F. H.: J. Am. Chem. Soc. **84,** 365 (1962)
[42] LEFFLER, J. E.: J. Org. Chem. **20,** 1202 (1955)

Gábor BERNÁTH
Kornélia L. LÁNG
György GÖNDÖS
Lajos GERA
Anikó PÁL
} H-6720 Szeged, Dóm tér 8.

Pál SOHÁR H-1045 Budapest, Szabadságharcosok útja 47—49.

Acta Chimica Academiae Scientiarum Hungaricae, Tomus 92 (2), pp. 187—199 (1977)

OPTIMIERUNG FERMENTATIONSPROZESSE MIT HILFE DER VERMEHRUNGSKURVEN VON MIKROORGANISMEN-KULTUREN

K. Polinszky, T. Blickle, J. Fülöp, R. Tőrös und T. Vajda

(Forschungsinstitut für Technische Chemie der Ungarischen Akademie der Wissenschaften)

Eingegangen am 5. Mai 1975

In unserer Arbeit interprätieren wir vorerst die Vermehrungskurve von Mikroorganismen-Kulturen auf Grund elementarer Überlegungen, wobei der Begriff der Teilungswahrscheinlichkeit eingeführt wird. Im Nachfolgenden wird gezeigt, auf welche Weise halbkontinuierliche Fermentationsprozesse auf Grund einer empirisch erhaltenen Vermehrungskurve der Mikroorganismen-Kultur optimiert werden kann, mit dem Ziel, eine maximale Ausbeute an Mikroorganismen zu gewinnen.

I. Einleitung

Es ist allgemein bekannt, daß die Fermentationsprozesse in den modernen intensiven chemischen Verfahren — vor allem in der pharmazeutischen und Lebensmittelindustrie — eine immer grössere Rolle spielen. Die Nachteile dieser Methode sind die relativ schmale Skala der Verwendbarkeit, eine große Empfindlichkeit Umwelteinflüssen gegenüber, sowie die Tatsache, daß die für die Prozeß-Steuerung wichtigen Parameter nur annähernd angegeben werden können. Dies alles ist eine logische Folge der Tatsache, daß bei den von uns untersuchten Prozessen das die Änderung verursachende Medium, die Mikroorganismen sich vom gewohnten ganz abweichend, viel komplizierter verhalten, und einem Modell schwerer anzupassen sind. Es gibt jedoch zahlreiche Verfahren, die ausschließlich mit Hilfe von Fermentationsprozessen durchführbar sind. Aus diesem Grunde ist jeder Versuch, dieses spezielle Verfahren einer mathematischen Behandlung näherzubringen und dessen Prozesse zu optimieren, von größter Bedeutung. In diesem Bestreben liegt — unserer Meinung nach — der Sinn vorliegender Arbeit.

Die Erfahrung hat gezeit, daß die Vermehrungskurve als das wichtigste quantitative Merkmal einer Zellkultur zu betrachten ist. Aus diesem Grunde haben wir die Untersuchung dieser Kurve in den Mittelpunkt unserer Studien gestellt. In dem uns bekannten, repräsentativen Schrifttum (z. B. [1—6]) ist die naheliegendste, die statistische Theorie der Vermehungskurve und ihre Anwendung in der Optimierung von Fermentationsprozessen nicht anzutreffen. Die Vermehrungskurve $c(t)$ gibt die im Einheitsvolumen eines vollständig durchmischten Fermentors vorhandene Zellmasse ($\equiv$ Biomasse) als

Funktion der Zeit an. Ihren typischen Verlauf sehen wir in Abb. 1. Da es sich hier bloß um eine Angabe von empirischem Wert handelt, verfolgen wir das Ziel, diese auch auf theoretischem Wege aus einer solchen elementaren Theorie abzuleiten, die wenige einfache Hypothesen enthält und deren Ableitung keinen komplizierten mathematischen Apparat erfordert. Das wichtigste Moment der Ableitung ist die Einführung des Begriffes der Teilungswahrscheinlichkeit. Diese gibt jene Wahrscheinlichkeit an, gemäß welcher die Teilung der im entsprechenden Alter befindlichen Mikroorganismen tatsächlich verläuft.

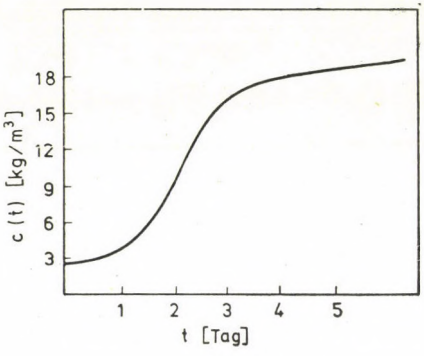

Abb. 1

Ein sehr häufiger Typ der Fermentationsprozesse ist das von uns als halbkontinuierlich bezeichnete Verfahren, bei welchem ein gewisser Teil des Volumens des Fermentors in bestimmten Perioden abgezapft, sodann eine Nährstofflösung desselben Volumens versetzt wird. Falls man die Hypothese akzeptiert, daß die Möglichkeit besteht, eine solche Nährungstofflösung-Mischung zu versetzen, bei welcher sich die Zellkonzentration (≡ Biomassen-Konzentration) in der Fermentationsflüssigkeit (Nährstofflösung + suspendierte Zellen) zwar vermindert, die Mikroorganismenpopulation sich aber — von der aktuellen Konzentration ausgehend — auf analoge Weise vermehren kann wie in der vorhergehenden Periode, so besteht auch die Möglichkeit, den Prozeß zu optimieren. Unsere Hypothese ist also die, daß es möglich ist, solche Verhältnisse zu schaffen, unter welchen die Vermehrungsgeschwindigkeit der Population bloß von der aktuellen Konzentration der Biomasse abhängt. Diese Abhängigkeit wird auf Grund der Vermehrungskurve als empirisch gegeben betrachtet.

Im ersten Teil der Arbeit wird gezeigt, daß die Vermehrungskurve die quantitativen Informationen über die Biomasse tatsächlich treu verfolgt, da sie ja in Kenntnis der bekannten vermehrungskinetischen Gesetzmässigkeiten der Mikroorganismen mathematisch abgeleitet werden kann. Die Verwendung der Kurve für die Optimierung von Fermentationsprozessen, bei welchen das Ziel eine maximale Ausbeute an Biomasse ist, erscheint daher als begründet.

II. Elementare Theorie der Vermehrungskurve

Wir betrachten die Vermehrungskurve als die bezeichnendsten quantitativen Kennzeichen von Mikroorganismen-Kulturen. Die Vermehrungskurve ist eine Größe vom Typ eines Integrals, daher definieren wir für unsere Untersuchungen erst einmal folgendes Altersspektrum.

Es sei $\nu(\tau, t)\mathrm{d}\tau$ die Zahl jener Mikroorganismen im Einheitsvolumen der Fermentationsflüssigkeit, deren Alter im Zeitpunkt t zwischen τ und $\tau + \mathrm{d}\tau$ fällt. Weiters sei $\nu_0(\tau)\mathrm{d}\tau$ die Zahl jener Mikroorganismen im Einheitsvolumen der Fermentationsflüssigkeit, deren Alter im Zeitpunkt $t = 0$ zwischen τ und $\tau + \mathrm{d}\tau$ fällt. Dann gilt

$$\nu(\tau, 0) = \nu_0(\tau)\,. \tag{1}$$

Aus dem Spektrum $\nu(\tau, t)$ können vielerlei die Kultur betreffenden Daten abgeleitet werden.

Bei der Bestimmung des Altersspektrums — was im Falle der von uns gewählten Methode ausschließlich im Wege der Logik möglich ist — werden folgende Voraussetzungen angenommen:

a) Keine der Altersklassen wird von irgendeinem der Faktoren zerstört;

b) die Mikroorganismen vom Alter $\tau = T$ (T ist die Generationszeit) teilen sich mit der Wahrscheinlichkeit p in zwei Mikroorganismen des Alters $\tau = 0$, sie bleiben mit der Wahrscheinlichkeit $1 - p$ weiter am Leben, teilen sich jedoch nicht mehr.

Faktor p wird als Teilungswahrscheinlichkeit bezeichnet, letztere ist natürlich eine Funktion der Zeit, also ist $p = p(t)$. Das Alter der teilungsfähigen Mikroorganismen liegt jederzeit zwischen $0 \leq \tau \leq T$, das Alter der nicht teilungsfähigen Mikroorganismen zwischen $T < \tau < +\infty$.

Unsere Aufgabe besteht nun darin, in Kenntnis obiger Gesetzmäßigkeiten ein Altersspektrum zu bestimmen, das der Voraussetzung (1) genüge leistet. Dies geschieht auf Grund wahrscheinlichkeits-theoretischer Überlegungen, sowie auf Grund der Transformation des Arguments der Funktionen abschnittsweise. Im Intervall $0 < t \leq T$ gilt:

$$\nu_1(\tau, t) = \begin{cases} 2p(t-\tau)\nu_0(T+\tau-t) & \text{wenn } 0 \leq \tau < t \\ \nu_0(\tau - t) & \text{wenn } t \leq \tau \leq T \\ \left[1 - p(T+t-\tau)\right]\nu_0(\tau - t) & \text{wenn } T < \tau < t + T \\ \nu_0(\tau - t) & \text{wenn } t + T \leq \tau < +\infty. \end{cases} \tag{2}$$

Obige Struktur (2) des Altersspektrums ist derart gewählt, daß die teilungsfähige Altersklasse von einem geschlossenen Intervall vertreten wird.

Im folgenden Intervall $T < t \leq 2T$ ist:

$$v_2(\tau, t) = \begin{cases} 2^2 p(t-\tau)\, p(-T+t-\tau)\, v_0(2T+\tau-t) & \text{wenn } 0 \leq \tau < t-T \\ 2p(t-\tau)\, v_0(T+\tau-t) & \text{wenn } t-T \leq \tau \leq T \\ 2\left[1-p(T+t-\tau)\right] p(t-\tau)\, v_0(T+\tau-t) & \text{wenn } T < \tau < t \\ \left[1-p(T+t-\tau)\right] v_0(\tau-t) & \text{wenn } t \leq \tau < t+\tau \\ v_0(\tau-t) & \text{wenn } t+T \leq \tau < +\infty. \end{cases} \tag{3}$$

Unter Zugrundelegung der Strukturen von (2) und (3) schreiben wir nun auf induktive Weise das im allgemeinen Intervall $(k-1)T < t \leq kT$ gültige Altersspektrum auf; ohne dessen Struktur ausführlich zu erklären, seine Richtigkeit ist nämlich ähnlich wie oben beschrieben einzusehen. Der folgende Ausdruck entspricht also der gesuchten allgemeinen Form:

$$v_k(\tau, t) =$$

$$= \begin{cases} 2^k \prod_{i=1}^{k} p\big((1-i)\,T + t - \tau\big) v_0(kT+\tau-t) \\ \qquad\qquad \text{wenn } 0 \leq \tau < t-(k-1)\,T \\ 2^{k-1} \prod_{i=1}^{k-1} p\big((1-i)\,T + t - \tau\big)\, v_0\big((k-1)\,T + \tau - t\big) \\ \qquad\qquad \text{wenn } t-(k-1)\,T \leq \tau \leq T \\ 2^{k-1}\left[1-p(T+t-\tau)\right] \prod_{i=1}^{k-1} p\big((1-i)T + t - \tau\big) v_0\big((k-1)\,T + \\ \qquad + \tau - t\big) \text{ wenn } T < \tau < t-(k-2)T \\ 2^{k-2}\left[1-p(T+t-\tau)\right] \prod_{i=1}^{k-2} p\big((1-i)\,T + t - \tau\big)\, v_0\big((k-2)\,T + \tau - t\big) \\ \qquad\qquad \text{wenn } t-(k-2)\,T \leq \tau < t-(k-3)\,T \\ \qquad\qquad \vdots \qquad\qquad \vdots \\ 2^{k-j}\left[1-p(T+t-\tau)\right] \prod_{i=1}^{k-j} p\big((1-i)\,T + t - \tau\big)\, v_0\big((k-j)\,T + \tau - t\big) \\ \qquad\qquad \text{wenn } t-(k-j)\,T \leq \tau < t-(k-(j+1))\,T \\ \qquad\qquad \vdots \qquad\qquad \vdots \\ 2\left[1-p(T+t-\tau)\right] p(t-\tau)\, v_0(T+\tau-t) \\ \qquad\qquad \text{wenn } t-T \leq \tau < t \\ \left[1-p(T+t-\tau)\right] v_0(\tau-t) \quad \text{wenn } t \leq \tau < t+T \\ v_0(\tau-t) \qquad\qquad \text{wenn } t+T \leq \tau < +\infty, \\ \qquad\qquad k = 1, 2, \ldots \end{cases} \tag{4}$$

Aus dem Altersspektrum (4) soll vorerst die Anzahl $n_k(t)$ der Mikroorganismen im Einheitsvolumen der Fermentationsflüssigkeit als Funktion der Zeit bestimmt werden. Hierzu ist folgendes Integral zu bilden:

$$n_k(t) = \int_0^\infty \nu_k(\tau, t)\, d\tau . \tag{5}$$

Es sollen daher folgende Bezeichnungen eingeführt werden:

$$\left.\begin{aligned} n_{0a} &= \int_0^T \nu_0(\tau)\, d\tau , \\ n_{0p} &= \int_T^\infty \nu_0(\tau)\, d\tau , \end{aligned}\right\} \tag{6}$$

mit deren Hilfe die Anzahl n_0 der im Augenblick $t = 0$ im Einheitsvolumen der Fermentationsflüssigkeit bereits vorhandenen Mikroorganismen in die teilungsfähige und in die nicht teilungsfähige Altersklasse geteilt aufgeschrieben werden kann: $n_0 = n_{0a} + n_{0p}$. Wir setzen nun (4) in (5) ein und betrachten die Teilungswahrscheinlichkeit p vorläufig als eine Konstante. Mit einer Funktion p von unbestimmter Form könnte man nämlich das Integral (5) nicht auswerten. Wir erhalten folgende Form:

$$\begin{aligned} n_k(t) = (2p)^k \int_0^{t-(k-1)T} \nu_0(kT + \tau - t)\, d\tau + (2p)^{k-1} \int_{t-(k-1)T}^{T} \nu_0\big((k-1)T + \tau - t\big)\, d\tau + \\ + (2p)^{k-1}(1-p) \int_T^{t-(k-2)T} \nu_0\big((k-1)T + \tau - t\big)\, d\tau + (1-p) \sum_{j=2}^{k} (2p)^{k-j} \int_{t-(k-j)T}^{t-(k-j-1)T} \\ \nu_0\big((k-j)T + \tau - t\big)\, d\tau + \int_{t+T}^{\infty} \nu_0(\tau - t)\, d\tau . \end{aligned} \tag{7}$$

Durch die Einführung neuer Integrationsvariablen, sowie unter Berücksichtigung von (6), wird (7) wie folgt umgestaltet:

$$n_k(t) = (2p)^{k-1}\Big(n_{0a} + p \int_{kT-t}^{T} \nu_0(\tau)\, d\tau\Big) + n_{0a}(1-p) \sum_{j=2}^{k} (2p)^{k-j} + n_{0p} . \tag{8}$$

Schließlich kann man — angenommen dass $p \neq 0{,}5$ ist — in (8) die Summierung vornehmen, dann wird (8) umgeformt und wir erhalten:

$$n_k(t) = (2p)^{k-1} \cdot p \left(\frac{n_{0a}}{2p-1} + \int_{kT-t}^{T} \nu_0(\tau) d\tau \right) - n_{0a} \frac{1-p}{2p-1} + n_{0p} . \tag{9}$$

(9) gibt die Formel für die Anzahl der Mikroorganismen im Zeitintervall $(k-1)\,T < t \leq kT$ an, die wir unter Annahme der konstanten Teilungswahrscheinlichkeit erhalten haben. Ist $p = 0{,}5$, so nimmt (8) einfach folgende Form an:

$$n_k(t) = \frac{1}{2}\left((k+1)\,n_{0a} + \int_{kT-t}^{T} v_0(\tau)\,\mathrm{d}\tau\right) + n_{0p}\,. \tag{10}$$

Es ist leicht einzusehen, daß wir auf folgende Weise die geglättete Näherungsvariante von Funktion (9) erhalten. Es wird die kontinuierliche

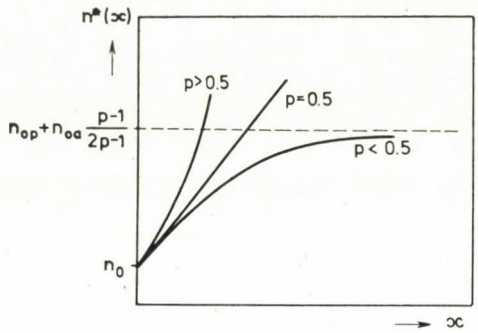

Abb. 2

Variable $\varkappa = \dfrac{t}{T}$ eingeführt, und wir erhalten Funktion

$$n^*(\varkappa) = (2p)^{\varkappa}\frac{pn_{0a}}{2p-1} - n_{0a}\frac{1-p}{2p-1} + n_{0p}\,, \tag{11}$$

welche in den Zeitpunkten $t = (k-1)T$ dieselben Werte hat wie (9), sonst aber nahezu parallel wie (9) verläuft. Eine ähnlich gebildete, geglättete Variante von (10) ist folgende Funktion:

$$n^*(\varkappa) = \frac{n_{0a}}{2}(\varkappa + 2) + n_{0p}. \tag{12}$$

Abbildung 2. zeigt die Veränderung der mit Hilfe von (11) und (12) hergestellten Mikroorganismen-Anzahl in den Fällen $p > 0{,}5$, $p = 0{,}5$ und $p < 0{,}5$. Man sieht, daß die Anzahl der Mikroorganismen in den ersten zwei Fällen eine sich exponentiell, bzw. linear erhöhende Menge ist, während sie sich im dritten Fall der Sättigung nähert.

Wenden wir nun der Ableitung der Vermehrungskurve zu, die wir aus folgendem Integral erhalten:

$$c(t) = \int_0^{\infty} \gamma(\tau)\,\nu(\tau, t)\,\mathrm{d}\tau\,. \tag{13}$$

Hier ist $\gamma(\tau)$ die Masse des Mikroorganismus des Alters τ, und diese Menge enthält gleichzeitig sämtliche, die Wachstumprozesse der einzelnen Mikro-

organismen betreffenden Informationen, welche — wie gleich zu sehen sein wird — in dem gegenwärtigen Modell der Vermehrungskurve nicht figurieren. Aus unserem Modell für die Vermehrung — aus der Erhaltung der gebildeten Mikroorganismenmasse — folgt jedoch, dass $\gamma(\tau)$ wie aus Abbildung 3. ersichtlich, im Intervall $T < \tau < +\infty$ konstant ist (γ_0), im Intervall $0 \leq \tau \leq T$

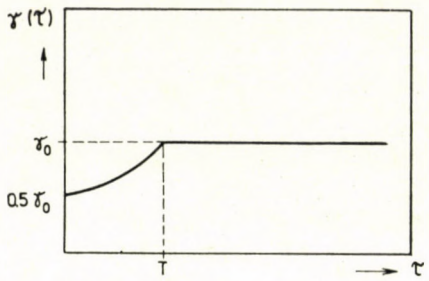

Abb. 3

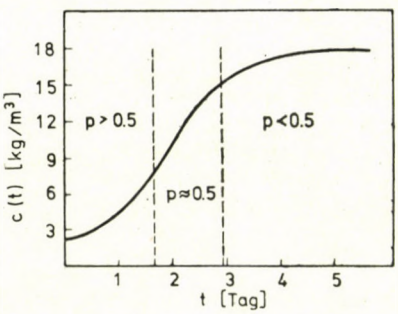

Abb. 4

jedoch mit dem Faktor 2 zunimmt (die zwei Teile bilden natürlich eine kontinuierliche Kurve). Es ist also mit der Genauigkeit des Modells vereinbar, wenn man auch als Resultate der Integration (13) die mit einer geeigneten Konstante multiplizierten Funktionen (11) und (12) wählt. Wesentlich ist aber die Feststellung, daß bei konstanter Teilungswahrscheinklichkeit die vom Modell gelieferten Vermehrungskurven ähnlich wie auf Abb. 2. verlaufen, also je nach dem Wert von p konvex, linear oder konkav sind, jedenfalls aber eine monoton wachsende Tendenz zeigen.

Wir versuchen nun, die auf Abb. 1. dargestellte empirische Kurve auf Grund unserer erhaltenen Resultate zu interprätieren. Es ist klar, daß die Voraussetzung eines konstanten p nicht der Wirklichkeit entspricht. Die konvexen, linearen und konkaven Abschnitte der empirischen Kurve können jedoch — im Vergleich mit den Typen der Vermehrungskurven, die aus unseren Modellen ableitbar sind — offensichtlich als den Fällen $p > 0{,}5$, $p = 0{,}5$ und $p < 0{,}5$ entsprechend betrachtet werden (Abb. 4). Auf Grund obiger

Überlegungen kann die Zeitfunktion der Teilungswahrscheinlichkeit aufgestellt werden, mit deren Verwendung das Modell eine solche Vermehrungskurve liefert, die der Praxis vollkommen entsprechend ist. Abb. 5. zeigt die annähernde Form derselben.

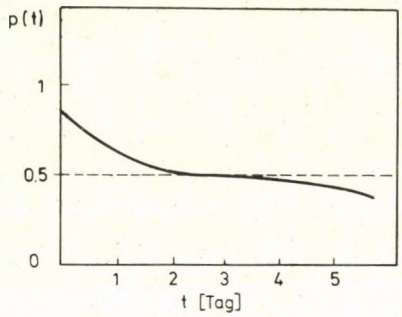

Abb. 5

Aus den empirischen Resultaten folgt also, daß die Teilungswahrscheinlichkeit während des Fermentationsprozesses mit der Zeit monoton abnimmt. Nachdem diese in unserem Modell der alleinige Träger der Information über die Art der Vermehrung ist, muß sie wahrscheinlich als eine Funktion zahlreicher Faktoren (Nährstoffkonzentration, Biomassen-Konzentration, Temperatur, Druck, usw.) betrachtet werden und so werden die im Laufe des Fermentationsprozesses sich verändernden Verhältnisse, so z. B. die Begrenztheit der Nährstoffe, von dieser repräsentiert. Die Bestimmung dieser Funktionsbeziehungen überschreitet aber den Rahmen unserer Untersuchungen. Zusammenfassend kann festgestellt werden, daß unser Modell für die Vermehrung bei der Wahl einer geeigneten, gut interprätierbaren Teilungswahrscheinlichkeit ein — unter (4) angegebenes — solches Altersspektrum liefert, aus welchem die Vermehrungskurve der Mikroorganismen-Kulturen in der Erfahrung entsprechender Form abgeleitet werden kann.

III. Optimierung halbkontinuierlicher Fermentationsprozesse

Im zweiten Teil unserer Arbeit wird eine Methode vorgeführt, auf welche Weise im Falle eines halbkontinuierlichen Fermentationsprozesses eine optimale Abzapfungszeit und ein optimales Volumen bezüglich der in der Zeiteinheit gewinnbaren Zellmasse, allein in Kenntnis der Vermehrungskurve, bestimmt werden kann.

Wir wollen folgende Annahme gelten lassen: die Mikroorganismen-Kultur kann — wie schon erwähnt — ihre Vermehrungskurve »reproduzieren«. Wenn man also aus dem Fermentor des Volumens V eine gewisse Menge Fermentationsflüssigkeit V_i abzapft, sodann der Fermentor mit Nährstofflösung

auf sein ursprünglisches Volumen wieder aufgefüllt wird, so kann sich die verdünnte Kultur — ausgehend von dem entsprechenden Punkt der Vermehrungskurve und dem Kurvenverlauf entsprechend — also nur auf eine Art vermehren. Da die Vermehrungskurve eine monoton wachsende Funktion ist, wird der Ausgangspunkt c_i' aus folgender Gleichung eindeutig angegeben:

$$c_i' = \frac{V - V_i}{V} c_i \,, \tag{14}$$

wobei c_i die Biomassen-Konzentration der Fermentationsflüssigkeit während des Abzapfens ist, i die Ordnungszahl der Abzapfung.

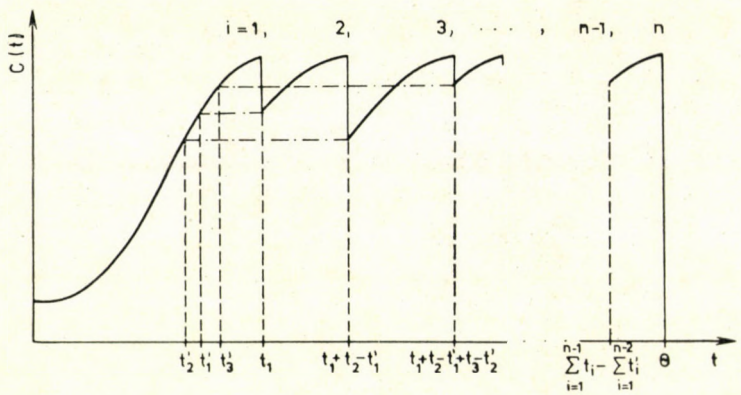

Abb. 6

Unsere Berechnung verfolgt jenen üblichen Gang des halbkontinuierlichen Betriebes, als zum Zeitpunkt $t = 0$ die Nährstofflösung im Fermentor mit einer entsprechenden Menge von Biomasse eingeimpft, dann ein Volumen V_i zu bestimmten Zeitpunkten t_i (insgesamt n-mal) abgezapft, sodann dieselbe Menge von Nährstofflösung nachgefüllt wird. Bei der n-ten Abzapfung wird die gesamte Fermentationsflüssigkeit abgelassen. Im Hinblick auf folgende Ausführungen wird (14) in folgender Weise ausgedrückt (dies bedeutet gleichzeitig eine Umskalierung der Zeitmessung):

$$c(t_i') = \frac{V - V_i}{V} c(t_i) \,. \tag{15}$$

Demnach sind die Abzapfzeitpunkte der Reihe nach t_1, $t_1 + t_2 - t_1'$, $t_1 + t_2 - t_1' + t_3 - t_2'$, usw., und die Länge des gesamten untersuchten Zeitintervalls beträgt:

$$\Theta = \sum_{i=1}^{n} t_i - \sum_{i=1}^{n-1} t_i' \,. \tag{16}$$

Abbildung 6. zeigt die oben beschriebene Berechnungs- und Skalierungsmethode. C bedeutet die im Fermentor bestehende Biomassen-Konzentration.

Es ist offensichtlich, daß im Falle einer entsprechend angegebenen Vermehrungskurve $c(t)$ bei beliebigem i die Angabe von t_i und t'_i mit dem Zeitpunkt und dem Volumen des i-sten Abzapfens identisch ist. Die in der Praxis vorkommenden Vermehrungskurven sind immer dieser Art. Unsere Aufgabe besteht nun in der Bestimmung der optimalen Abzapf-Parameter, d. h. in der Optimierung der Zellmassenerzeugung in der Zeiteinheit nach den Variablen t_i und t'_i. Wir definieren die Produktion P wie folgt:

$$P = \frac{\sum_{i=1}^{n} V_i c(t_i)}{\Theta} . \tag{17}$$

Es soll vorerst (17) unter Verwendung von (15) und (16) umgebildet werden. Auf diese Weise wird es klar, daß P tatsächlich nur von den Variablen t_i und t'_i abhängt:

$$P = V \frac{\sum_{i=1}^{n} \left(c(t_i) - c(t'_i)\right)}{\sum_{i=1}^{n} t_i - \sum_{i=1}^{n-1} t'_i} . \tag{18}$$

Die Optimierung der Produktion ist mit der Suche nach dem bedingten Extremum von P nach den Variablen t_i und t'_i identisch. Bedingt in dem Sinne, als uns bekannt ist, daß die letzte, n-te Abzapfung das Ablassen des gesamten Volumens des Fermentors bedeutet, also $V_n = V$. Auf Grund von (15) ist es leicht einzusehen, daß dies mit der bereits nach der Lagrange-Methode in (18) einfügbaren Bedingung $c(t'_n) = 0$ gleichbedeutend ist. Es soll nun aus (18) in diesem Sinne folgende Funktion aufgeschrieben werden:

$$\pi = P + \lambda c(t'_n) = V \frac{\sum_{i=1}^{n} \left(c(t_i) - c(t'_i)\right)}{\sum_{i=1}^{n} t_i - \sum_{i=1}^{n-1} t'_i} + \lambda c(t'_n) , \tag{19}$$

wobei λ eine neue Variable ist. Wir schreiben nun die partiellen Differentialquotienten von (19) nach den Variablen t_i, t'_i und λ (unter Berücksichtigung von (16)) auf:

$$\frac{\partial \pi}{\partial t_j} = V \frac{\Theta \left(\frac{\mathrm{d}c}{\mathrm{d}t}\right)_{t=t_j} - \sum_{i=1}^{n} \left(c(t_i) - c(t'_i)\right)}{\Theta^2} , \quad j = 1, 2, \ldots, n ; \tag{20a}$$

$$\frac{\partial \pi}{\partial t'_j} = V \frac{-\Theta \left(\frac{\mathrm{d}c}{\mathrm{d}t}\right)_{t=t'_j} + \sum_{i=1}^{n} \left(c(t_i) - c(t'_i)\right)}{\Theta^2} , \quad j = 1, 2, \ldots, n-1 ; \tag{20b}$$

$$\frac{\partial \pi}{\partial t'_n} = \left(\lambda - \frac{V}{\Theta}\right)\left(\frac{\mathrm{d}c}{\mathrm{d}t}\right)_{t=t'_n}; \tag{20c}$$

$$\frac{\partial \pi}{\partial \lambda} = c(t'_n). \tag{20d}$$

Den Regeln der Extremumberechnung gemäss sind die Werte der Differentialquotienten (20a) . . . (20d) im Maximum π gleich Null (bei den in der Praxis vorkommenden Vermehrungskurven $c(t)$ gibt es kein lokales Minimum). So erhalten wir aus (20a)—(20b) für die Differentialquotienten der Vermehrungskurve $c(t)$ zu den Zeitpunkten t_i und t'_i folgende Funktionen:

$$\left(\frac{\mathrm{d}c}{\mathrm{d}t}\right)_{t=t_j} = \frac{1}{\Theta}\sum_{i=1}^{n}\left(c(t_i) - c(t'_i)\right), \quad j = 1, 2, \ldots, n; \tag{21a}$$

$$\left(\frac{\mathrm{d}c}{\mathrm{d}t}\right)_{t=t'_j} = \frac{1}{\Theta}\sum_{i=1}^{n}\left(c(t_i) - c(t'_i)\right), \quad j = 1, 2, \ldots, n-1. \tag{21b}$$

Der Nullwert von (20d) bedeutet das Bestehen der Bedingungsgleichung, und aus (20c) kann — angenommen, daß der Differentialquotient von $c(t)$ an der Stelle $t = t'_n$ nicht gleich Null ist (was keine Limitation bedeutet) — der zum Maximum gehörende Wert der Variablen λ bestimmt werden; dieser Wert ist in den für uns wichtigen Gleichungen (21a)—(21b) von keiner Bedeutung. Dies bedeutet gleichzeitig, daß das letzte Ablassen der gesamten Fermentationsflüssigkeit die Werte der intermediären Abzapfzeiten und -volumen überhaupt nicht beeinflußt.

(21a) und (21b) können unter Berücksichtigung von (15) und (17) noch umgeformt werden:

$$\left(\frac{\mathrm{d}c}{\mathrm{d}t}\right)_{t=t_i} = \frac{P}{V}, \quad i = 1, 2, \ldots, n; \tag{22a}$$

$$\left(\frac{\mathrm{d}c}{\mathrm{d}t}\right)_{t=t'_i} = \frac{P}{V}, \quad i = 1, 2, \ldots, n-1. \tag{22b}$$

Wir wollen nun untersuchen, auf welche Weise das Ergebnis unter (22a)—(22b) interprätiert werden kann. Vor allem ist festzustellen, daß zur Gewinnung einer maximalen Biomassenmenge in der Zeiteinheit zweckmäßigerweise gleiche t_i und t'_i Werte gewählt werden müssen. Da notwendigerweise $t_i \geq t'_i$, müssen die auf der Zeitskala der Vermehrungskurve gemessenen t_i Abzapfzeiten, bzw. die das Abzapfvolumen bezeichnenden Parameter t'_i so gewählt werden, daß dort die Differentialquotienten der Vermehrungskurve identisch seien.

Außerdem ist es wegen der Proportionalität der Biomassenerzeugung in der Zeiteinheit mit den Differentialquotienten laut (22a)—(22b) erwünscht, daß der Wert des Differentialquotienten möglichst hoch sei.

Es sollen nun (22a)—(22b) mit Hilfe von (18) weiter umgebildet werden: Da die Zeitparameter t_i und t_i' vom Index i unabhängig sind, können die Summierungen von (18) vereinfacht und wie folgt geschrieben werden:

$$\left(\frac{dc}{dt}\right)_{t=t_i} = \left(\frac{dc}{dt}\right)_{t=t_i'} = \frac{c(t_i) - c(t_i')}{t_i - \frac{n-1}{n} t_i'} . \tag{23}$$

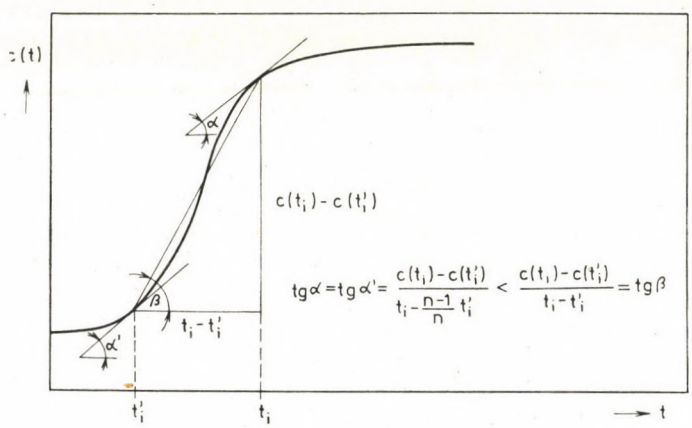

Abb. 7

Aus (23) geht bereits klar folgendes hervor: Falls die Vermehrungskurve $c(t)$ analytisch oder tabellarisch angegeben ist, so liefert (23) ein Gleichungssystem zur Bestimmung der Parameter t_i und t_i', welches mit Hilfe algebraischer bzw. numerischer Methoden gelöst werden kann. Aus der geometrischen Interprätation von (23) — daß nämlich in den Punkten t_i und t_i' die Differentialquotienten von $c(t)$ um einen festgesetzten, aber nicht bedeutenden Wert geringer sind als der zu obigen Punkten gehörende Differenzquotient — geht ebenfalls hervor, daß im Falle einer gegebenen Vermehrungskurve die beschriebenen Verhältnisse nur im Falle spezieller t_i und t_i' Werte erfüllt werden können. Die geometrischen Verhältnisse zeigt Abbildung 7.

Schließlich muß es — unter Hinweis auf vorhergehende Ausführungen — bemerkt werden, daß bei dem in der Praxis vorkommenden Typ der Vermehrungskurven (eine monoton wächsende, sich Asymptoten nähernde, einen Inflexsionspunkt enthaltende Kurve) das in der Zeiteinheit die maximale Biomassenproduktion sichernde Parameterpaar jederzeit gefunden werden kann. Verfolgen wir jedoch — auf Grund verschiedener wirtschaftlicher Über-

legungen — das Ziel, Parameter für sonstige optimale Produktionsverhältnisse zu bestimmen, so kann nach Aufschreiben einer entsprechenden Kostenfunktion mit obiger Methode die Optimierung des halbkontinuierlichen Fermentationsprozesses auf dieselbe Weise durchgeführt werden, falls unsere die Vermehrungsverhältnisse von Mikroorganismen betreffenden, bisherigen, grundlegenden Annahmen auch weiterhin akzeptiert werden. Die optimalen Verhältnisse werden wir aber in diesem Fall offensichtlich bei anderen t_i und t_i' Werten finden.

LITERATUR

[1] RÉNYI, A.: Valószínűségszámítás, Tankönyvkiadó, Budapest (1954)
[2] BARTLETT, M. S.: An Introduction to Stochastic Processes, Cambridge Univ. Press (1966)
[3] Proceedings of the Vth Berkeley Symposium on Mathematical Statistics and Probability IV. (1967)
[4] GOEL, N. S. *et al.:* Nonlinear Models of Interacting Populations, Academic Press, New York/London (1971)
[5] Mathematical Models in Biology and Medicine, edited by Bailey, N. T. J. et al., North-Holland/American Elsevier (1974)
[6] Foundations of Mathematical Biology, edited by Rosen, R., Academic Press, New York/London (1973)

Zeichenerklärung

c	Konzentration der Zellmasse (Vermehrungskurve) Kg/m^3
C	Biomassen-Konzentration im Fermentor während der halbkontinuierlichen Fermentation Kg/m^3
c_i	Abzapfskonzentration Kg/m^3
c_i'	Verdünnungskonzentration Kg/m^3
k, j	Summierungsindizes
n	Zahl der Abzapfen
n_k	Anzahl der Mikroorganismen
n_0	Anzahl der Mikroorganismen im Moment $t = 0$
n_{0a}	Anzahl der teilungsfähigen Mikroorganismen im Moment $t = 0$
n_{0p}	Anzahl der nicht teilungsfähigen Mikroorganismen im Moment $t = 0$
n^*	Geglättete Anzahl der Mikroorganismen
p	Teilungswahrscheinlichkeit
P	Mikroorganismen Produktion im Fermentor Kg/m^3 sec
t	Zeitkoordinate sec
t_i	Abzapfszeit sec
t_i'	"Verdünnungszeit" sec
T	Generationszeit sec
V	Volumen des Fermentors m^3
V_i	Abzapfvolumen m^3
γ	Masse des Mikroorganismus Kg
Θ	Gesamtlänge der Fermentationszeit sec
$\varkappa$	dimensionlose Zeit
ν	Altersspektrum $m^{-3} \cdot sec^{-1}$
ν_0	Altersspektrum im Moment $t = 0$ $m^{-3} \cdot sec^{-1}$
π	Lagrange-Funktion
τ	Alter des Mikroorganismus sec

Károly POLINSZKY
Tibor BLICKLE
János FÜLÖP
Róbert TŐRÖS
Tádé VAJDA

H-1056 Budapest, Szerb u. 23.

RECENSIONES

Topics in Current Chemistry / Fortschritte der chemischen Forschung, Volume 54

Triplet States I

Springer, Berlin, 1975, p. 163.

This volume comprises three reviews.

1. Quantum-Mechanical Calculations of the Potential Energy Surfaces of Triplet States
A. DEVAQUET

This theoretical review (comprising 71 pages) consists of two parts. Part I deals with the calculation of the potential energy surfaces of triplet states. In this section a brief account of the most important ab initio HF methods is given. It is a good idea that the same example, the formaldehyde molecule, is used to illustrate the results of the different methods thereby making possible a better comparison.

Part II shows some applications of the *ab inito* calculations in the study of photochemical processes. It is dealing with two types of problems: the use of potential energy surfaces of low-lying excited states in the study 1. of a single molecule and 2. of a reacting system. Concerning the first subject, the geometry of the lowest $\pi\pi^*$ triplet state of ethylene and the $\pi\pi^*$ and $n\pi^*$ triplet states of acrolein are discussed in detail. It should be emphasized that at present good numerical accordance cannot be expected in conformational calculations. Regarding the second topic some investigations of the photochemical dissociation processes of simple carbonyl compounds are presented as well as some photochemical reactions are considered. At the end, SALEM's classification of photochemical processes is given.

The subjects are clearly treated and the review is worth to read for all those who are interested in the current theoretical aspects of photochemistry.

2. Photochemistry of β,γ-Unsaturated Ketones
W. G. DAUBEN, G. LODDER and J. IPAKTSCHI

The central problem treated in this review (42 pages) is the photoisomerization of β,γ-unsaturated ketones via 1,3- or 1,2-acyl shifts. It is demonstrated on numerous examples that the former reaction occurs primarily via the singlet, the latter via the triplet state. A critical evaluation of the mechanism for both types of reactions is presented. In the subsequent sections short accounts are given for nine further types of reactions of the β,γ-unsaturated ketones. The main parameter considered is the $n - \pi^*$ absorption coefficient.

This review presents a general survey of the results obtained up to 1974.

3. Protein Triplet States
A. H. MAKI and J. A. ZUCLICH

This review (49 pages) is dealing with informations obtained by experimental methods on the triplet states of proteins and their precursors.

The longest section is devoted to the aromatic amino acids. First the phosphorescence spectra are discussed and compared with the fluorescence and absorption spectra. Further, the substituent and solvent effects as well as temperature dependence are briefly considered. The investigation of triplet states by electron paramagnetic resonance (EPR) and a recent technique optically detected magnetic resonance (ODMR) are reviewed. Regarding the latter technique, first the principles are summarized which seems to be useful.

Two shorter sections are devoted to the polypeptides and proteins, especially to the energy transfer between the aromatic residues of proteins. Finally, the experimental data obtained by phosphorescence, EPR and ODMR are given.

This is an up-to-date account on the title subject, giving good information for research in this field.

The presentation of the volume is of high quality, only a few misleading printing errors exist.

Á. KISS

Structure and Bonding vol. **22**. *Rare Earths*

Eds. J. D. DUNITZ, P. HEMMERICH, R. H. HOLM, J. A. IBERS, C. K. JØRGENSEN, J. B. NEILANDS, D. REINEN, R. J. P. WILLIAMS

Springer Verlag, Berlin, Heidelberg, New York 1975

The 22nd volume of the series "Structure and Bonding" consists of four articles which deal with the chemistry of rare earths.

In the first article entitled "The Lanthanide Ions as Structural Probes in Biological and Model Systems" a relatively new field of the application of lanthanides is reviewed by E. NIEBOER (47 pages with 235 references). In the study of the structure of macromolecules of biological interest the substitution of metal ions *(e.g.* Ca^{2+}) with lanthanides (which are easily detectable as a result of their optical and magnetic properties) has become a fruitful research tool. The article gives a good summary on the chemical and physical basis of the application of lanthanide(III) ions as structural probes discussing their electronic, magnetic properties and their effect on the resonance absorption of protons (dipolar and contact shift as well as relaxation enhancement properties). The experimental methods used to detect the lanthanide ions (fluorescence, difference absorption, chemical shift and relaxation studies) are also presented. The basic principles of the coordination chemistry of the lanthanides — coordination numbers, equilibrium properties and kinetic behaviour — are also reviewed. In this part there is an inaccurate generalization when it takes the rate of dissociation of complexes as a property independent of the atomic number of lanthanides. It is known that the rate of dissociation of complexes with multidentate ligands decreases with increasing atomic number.

In the article entitled "Partly Filled Shells Constituting Anti-bonding Orbitals with Higher Ionization Energy than their Bonding Counterparts" a review is given by C. K. JØRGENSEN on the results of the photo-electron spectra of metallic lanthanides and lanthanide compounds. The nephelauxetic parameters obtained from the photo-electron spectra are compared with those calculated from the visible and ultraviolet spectra. The results and difficulties of the theoretical treatment of the weak covalent interactions in the lanthanide compounds are also discussed (39 pages with 130 references).

"The Intensities of Lanthanide f ↔ f Transitions" is the following article in which R. D. PEACOCK discusses the Judd-Ofelt theory and its success in the interpretation of the spectra of lanthanides as well as the difficulties of the theory in the explanation of the spectra of praseodymium and europium. The attempts to elucidate the hypersensitive transitions on the basis of the Judd-Ofelt, the inhomogeneous dielectric and the dynamic coupling theories are also discussed (39 pages with 113 references).

R. REISFELD's review "Radiative and Non-Radiative Transitions of Rare-Earth Ions in Glasses" deals with a rapidly growing field of research. The studies in this field are very important in the development and application of rare-earth activated materials (phosphors, lasers, quantum counters, etc.). The experimental data have been correlated with the Judd-Ofelt model. This theory proved to be suitable to predict the electric dipole absorption intensities (to within 5—10%) and the radiative transition probabilities in a number of cases. The nonradiative transitions have been explained by a multiphonon process relaxation theory (55 pages with 56 references).

The first article of this volume of "Structure and Bonding" can be recomended to biochemists and chemists interested in the study of the structure of biological macromolecules, while the others to those dealing with the spectroscopy and application of lanthanides.

E. BRÜCHER

H. ENGELHARDT: *Hochdruck-Flüssigkeits-Chromatographie*

Springer-Verlag, Berlin—Heidelberg—New York 1975. 213 Seiten, 52 Abbildungen und 17 Tabellen

Die Hochdruck-Flüssigkeits-Chromatographie ist der jüngste Zweig der chromatographischen Methoden, ihre Entwicklung begann Ende der sechziger Jahre. Ihre gegenwärtige Lage ist mit der raschen Entwicklung der Gaschromatographie Ende der fünfziger Jahre vergleichbar. Die Bedeutung der Methode wird durch die Schätzung unterstrichen, daß etwa 20% der Stoffsysteme gaschromatographisch, dagegen bis zu 80% flüssigkeitschromatographisch getrennt werden kann.

Der Verfasser ist ein leitender Mitarbeiter eines der in der Entwicklung der Hochdruck-Flüssigkeits-Chromatographie eine wichtige Rolle spielenden Institute (Institut für Angewandte Physikalische Chemie, Universität des Saarlandes, Saarbrücken) und aktiver Teilnehmer an ihrer Entwicklung seit Ende der sechziger Jahre.

Grundlegendes Ziel des Buches ist es einen Überblick und eine praktische Anleitung zu den Apparaten, Trennungsmethoden und Anwendungsmöglichkeiten der Hochdruck-Flüssigkeits-Chromatographie zu geben. Das Buch besteht aus 12 Abschnitten.

Abschnitt I gibt einen kurzen Überblick über die verschiedenen chromatographischen Methoden und Techniken im allgemeinen.

In Abschnitt II sind die Grundlagen der chromatographischen Trennung zusammengefaßt, mit besonderer Rücksicht auf die praktische Anwendung. Es werden die Faktoren behandelt, die einen Einfluß auf die Trennung ausüben und es werden praktische Hinweise zur Wahl der optimalen Arbeitsbedingungen und der geeignetsten Trennsäulen gegeben.

Im Abschnitt III behandelt der Verfasser die Arbeitsweise der Hauptteile der Apparaturen für Hochdruck-Flüssigkeits-Chromatographie sowie die wichtigsten konstruktionsmäßigen Lösungen.

Abschnitt IV beschreibt die in der Hochdruck-Flüssigkeits-Chromatographie gebräuchlichen Detektoren und gibt einen Vergleich der wichtigsten Detektortypen.

Abschnitt V behandelt die Trägermaterialien und stationären Phasen verschiedener Typen. Die wichtigsten Handelstypen für die verschiedenen chromatographischen Methoden sowie ihre Eigenschaften sind in ausführlichen Tabellen zusammengestellt.

Abschnitt VI befaßt sich mit der Adsorptions-Chromatographie. Die Eigenschaften der verschiedenen Adsorbensfüllungen, die Wirkung des Feuchtigkeitsgehalts des Adsorbenten und der Natur der strömenden Phase auf die Trennung sowie die verschiedenen Techniken zum Verbessern der Trennung und die wichtigeren Anwendungsgebiete werden behandelt. Da der Verfasser hauptsächlich auf diesem Gebiet tätig ist, enthält dieser Abschnitt besonders reiche praktische Erfahrungen und nützliche Hinweise zur Lösung von praktischen Aufgaben.

Abschnitt VII behandelt die Verteilungschromatographie. Er faßt die in der Flüssigkeit-Flüssigkeit-Chromatographie verwendeten Füllungen und Flüssigkeitsphasen sowie die bei der Trennung verwendeten Arbeitsbedingungen zusammen und illustriert das Gesagte mit einigen Beispielen.

Im Abschnitt VIII erörtert der Verfasser die Grundlagen des Ionenaustausches, die verschiedenen Ionenaustauscher-Füllungen und die Wirkung bestimmter Faktoren auf die Trennung. Die Anwendungsmöglichkeiten werden anhand einiger Beispiele gezeigt.

Abschnitt IX gibt ein sehr kurzgefaßtes Bild über die Anwendungsmöglichkeit der Gelpermeations-Chromatographie mit Hochdruck-Flüssigkeits-Chromatographie. Mit Rücksicht auf die stets zunehmende Wichtigkeit dieses Gebiets hätte es eine umfangreichere Behandlung verdient (der Abschnitt enthält nur 9 Seiten was sich sowohl auf die Methoden als auch auf die Anwendungsmöglichkeiten bezieht).

Im Abschnitt X erläutert der Verfasser die wichtigsten Aspekte der Wahl des für die gegebene Trennungsaufgabe optimalen Trennsystems.

Abschnitt XI behandelt Spezialmethoden wie die Möglichkeiten der präparativen Trennung, der quantitative Analyse und der Spurenanalyse.

Im Abschnitt XII gibt der Verfasser nützliche praktische Hinweise für die Reinigung der bei der Trennung verwendeten Lösungsmittel.

Der Anhang enthält eine Liste der wichtigsten Firmen, die Apparate und Detektoren für die Hochdruck-Flüssigkeits-Chromatographie bauen und auf den Markt bringen.

Die Abbildungen und Tabellen des Buches sind klar und gut übersichtlich. Die Handhabung des Buches wird durch das gut zusammengestellte Sachregister wesentlich erleichtert.

Der Verfasser erörtert die Hochdruck-Flüssigkeits-Chromatographie als Trennungsmethode. Es wäre jedoch sehr nützlich gewesen, wenn er die Probleme der qualitativen und quantitativen Analyse ebenfalls ausführlich erläutert hätte. Auch eine tiefergehende Dar-

stellung der präparativen Anwendungsmöglichkeiten und Arbeitsverfahren wäre zweckmäßig gewesen, um die Leistungsfähigkeit der Methode voll vorzuführen.

Im Vorwort schreibt der Verfasser, daß er sein Buch für Anfänger, als Einleitung in die Technik der Hochdruck-Flüssigkeits-Chromatographie geschrieben hat. Die einheitliche und allgemeinverständliche Behandlungsart des Stoffes macht das Buch in der Tat höchst anziehend für solche, die die Methode erst jetzt kennen lernen. Darüber hinaus jedoch ist es ein nützliches Handbuch für Forscher auf anderen Gebieten der Chemie, weil es einen guten Überblick über die Möglichkeiten und wichtigsten Anwendungsgebiete der neuen Methode vermittelt. Selbst für die auf dem Gebiet der Hochdruck-Flüssigkeits-Chromatographie tätigen enthält das Buch viele nützliche Kenntnisse und praktische Hinweise.

L. SZEPESY

B. A. NÉMETH: *Chemical Tables* (in Hungarian)

Akadémiai Kiadó. Budapest 1975. 477 p.

The book of Béla A. NÉMETH consists of 256 tables. Of these, the most extensive is the table summarizing the properties of the elements and their compounds, which comprises in addition to the data of the elements also those of almost 1400 inorganic and a few organic compounds (in general, salts), in the alphabetic order of their formulas. These data are besides the formula (water of crystallization also indicated) and the name: atomic and molecular weight (calculated with the atomic weights of 1969), melting and boiling points, solubility in cold and hot water and in other solvents, and the appearance of the compound (element). The absence of serial numbers is unusual in the twin-page table, but this is compensated by the excellent typography, which helps to find data belonging together.

The tabular summarization of the atomic and molecular weights of elements, inorganic compounds and organic radicals often used, and of the multiples of these values is very useful. The analytical data listed include analytical factors over more than 30 pages and equivalent weights of volumetric analysis. More than 120 pages are occupied by the tables containing the densities of the aqueous solutions of acids, bases and alcohols, of which the data of the more important acids are listed both according to increasing density and whole number percent composition.

All the tables cannot be listed within this review, it will suffice to mention the tables summarizing the buffers, the solubility of inorganic compounds in water at different temperatures, analytical indicators, and various physico-chemical properties. Finally, the book discusses over 18 pages the toxic properties of organic and inorganic chemicals, the symptoms of poisoning, and the necessary first-aid.

It can be established in summary that the book of Béla A. NÉMETH is useful to chemists or technicians working in educational, research and plant laboratories, because it is of a size still easy to handle, but nevertheless it contains the most important data, with the exception of the properties of organic compounds.

L. FENICHEL

K. KOVÁCS and M. HALMOS: *Recent results in the chemistry of steroids* (in Hungarian)

Recent results in chemistry, Vol. 27

Editor: B. CSÁKVÁRI

Akadémiai Kiadó, Budapest, 1975. 197 pages

The publishing of the book fills a gap, because in spite of the fact that the various aspects of this branch of chemistry are studied by numerous research groups in Hungary, so far no survey on problems in steroid chemistry has appeared in Hungarian. Bells were tolled several times on steroid research, regarding steroid chemistry as an exploited and closed field. However, the manysided practical applicabilities continuously raise new problems, so that important new results are born, which invariably ensure a distinguished place for steroid chemistry in organic chemical research.

The book, arranged in 5 chapters, clearly summarizes the trends characteristic today of steroid research, so that attention is directed also to those fields, which are scarcely studied in Hungary (Chapters 4 and 5).

The first chapter very briefly surveys semi-synthetic processes. This briefness is justified by the fact that these industrial processes, developed earlier, have been modified only slightly in recent years. The larger part of the chapter deals with total syntheses, presenting the historical development of this research from its initial aim of structure proof, till the present requirement of possible industrial realization. The chapter gives fundamental stereochemical concepts, without which no stereoselective synthesis of steroids can be designed.

In the second chapter, the authors attempt to set things right in the baffling jungle of steroids with modified structure. The summary is concerned with steroids modified in the skeleton, sometimes also indicating the biological action. Owing to the limited compass of the book, non-natural steroids used in medicine have been omitted, or are partly discussed in the following chapter.

In this third chapter, grouped on the basis of biological actions, substances with anabolic, gestagenic and antihormonal action, attaining importance in the recent decades, are covered in addition to the conventional steroid drugs. The chapter also includes definitions of biological actions, and describes even one of the biosynthetic routes leading to corticosteroids. This chapter comprises mainly research results of the period from 1945 to 1965, yet it cannot be regarded as out-of-date, because it turns the attention on those works, which made the present therapeutic applications possible, or fall within the province of today's pharmaceutical industry.

The fourth chapter, dealing with the hormones of insect metamorphosis, highlights the potentialities of the most novel branch of steroid chemistry. The structure proof and the synthesis of the two first insect moulting hormones, α-ecdysone and crustecdysone, are the most striking results of steroid chemistry achieved in the sixties. The closing section of the chapter also indicates practical utilization, *i.e.* ecdysone antagonists. Research in this field has progressed so far that these hormones hold out promise for the control of insect pests.

The last chapter groups very briefly steroid liquid crystals, which have been known for a long time, but their practical utilization ensued mainly in the last twenty years. Information is given on the conditions of orientation in the liquid crystal state, on thermotropic substances, lyotropic systems, and on mixtures exhibiting hysteresis lag. The chapter does not aim at completeness, nevertheless it would have been great pity to leave it out, because at least it directs the attention to this interesting field of research.

By writing this book, Kálmán Kovács and the late Miklós Halmos, regrettably deceased early, contributed to the Hungarian chemical literature providing a greatly needed book. It is an almost impossible task to discuss each branch of steroid chemistry, in the detail it would merit, within the framework of a single monograph. Therefore, the aim of the authors to outline the main research objects in the fields discussed and to indicate practical utilizations, can only be approved by the recensor. Parts in conjunction with drug manufacture are treated in relatively greater detail, reflecting thus the drug-centered trends of steroid research in Hungary. This succinctly presented work, aided by many formulas, can be recommended to all readers interested in organic chemistry. Specialist in this field may obtain more detailed information from a total of 258 references listed at the end of each chapter.

I. Weisz-Vincze

F. H. A. Rummens: *Van der Waals Forces and Schielding Effects*

Springer Verlag, Berlin 1976

This book has been published in the series "Basic Principles and Progress" (Ed. P. Diehl, E. Fluck and R. Kosfeld) as the 10th Volume. The series provide excellent reviews about special fields of theoretical and practical n. m. r.-spectroscopy.

Origins and applications of solvent effects on n. m. r. chemical shifts have been published in great profusion. In contrast to other effects contributing to the solvent shifts (neighbour anisotropy, reaction field or complexation effect), no major direct use has yet been found for the Van der Waals effect. This effect is namely very complex and many parameters must be considered before a quantitative understanding may be expected. Van der Waals shielding effects are site-specific sensors of intermolecular forces and should therefore be useful as a

direct tool in structural or dynamic studies. Furthermore, it offers unique possibilites to study the intermolecular potentials and structures of liquids and gases in comparison to other physical techniques.

The review contains 16 Chapters, dealing with the following subjects.

The intermolecular shielding is measured by that "excess shift" which contributes to the gas-phase–liquid-phase (or infinitely diluted solution) shift-difference besides the "bulk susceptibility" shift due to the medium (solvent). This effect can be assigned to Van der Waals forces (σ_W). Its nature is dependent upon both the solute and the solvent properties. The growing empirical evidence and the first attempts for a theoretical explanation is treated in Ch. 1 (Historical Development, up to 1961) on 8 pages.

Two Chapters are devoted to the theoretical models which aim at calculating *(i.e.* predicting) the measurable σ_W values. In Ch. 2 (9 pages) on Continuum Models the shortcoming of any such model is clearly demonstrated by the contradiction of the continuous medium conception to the r^{-6} dependence of the Van der Waals forces restricting the interaction to the firs 'shell' of solvent molecules around the solute. Two particular continuum models (of LINDER and DE MONTGOLFIER) are discussed.

Three different Pair Interaction Models are put forward for calculating of σ_W in Ch. 3 (9 pages). The statistical mechanical binary collision gas model is an approach to find an appropriate pair interaction term which is than integrated over a Boltzmann distribution in the coordination space. The cage model forms the product of a pair-interaction term with an effective coordination number to find the average of the σ_W value. More sophisticated is the quantum mechanical theory of σ_W. Because of major simplifications in the assumptions and in the calculations the quantum mechanical model can be applied successfully only for atomic liquids. A comparison of the models discussed is included in this chapter too.

In Ch. 4 (7 pages) those experimental proton-σ_W data are collected which were not presented previously, to serve as an experimental basis for further discussion.

Relevant models put forward to explain the intermolecular shielding effects have different implications as to the physical nature of the averaged square of the electric field, and the associated excitation energy entering the expressions. This point makes the subject of Ch. 5 (6 pages).

Chapter 6 (7 pages) deals with different attempts to incorporate the site factor — which takes into consideration the fact that a measured nucleus lies generally out of the centre of mass of the molecule — into σ_W-calculations.

On theoretical grounds a shielding effect may be predicted due to repulsion of molecules being very close to each other. Ch. 7 (6 pages) concerns with the possibility of calculating and/or experimentally demonstrating such an effect.

In Ch. 8 the mostly ignorable effects of higher order dispersion terms are discussed briefly (2 pages).

The calculation or experimental determination of the pure solute bond, the so-called B parameter is essential in the quantum mechanical model (*c.f.* Ch. 3.) in calculating σ_W directly. The results of this field are detailed in Ch. 9 (10 pages).

Intermolecular shielding effects are arising not only in solute–solvent interactions but amongst molecules of the same substance as well. This can be observed by the density dependence of σ_W, and this point is discussed in Ch. 10 (3 pages).

In establishing the rather complex temperature dependence of σ_W — the subject of Ch. 11 (7 pages) — the experimenter has to devise sophisticated techniques in order to separate intramolecular temperature effects largely due to rotational excitation and centrifugal distortion, and intermolecular effects which arise from the temperature dependence of both the bulk properties and the dispersive terms.

The relatively large Ch. 12 is devoted to Factor Analysis (10 pages), a mathematical method for separating different shielding terms due to medium effects on the basis of the observation that intermolecular effects in many cases may be described by a product function of solute and solvent factors. As the Author demonstrates, however, the method fails to have an universal applicability to n. m. r. solvent effects.

The remaining 4 Ch.'s are related with various experimental and computational aspects of the determination of σ_W,. Ch. 13 and 14 (5 and 4 pages, resp.) collects all available experimental σ_W data for nuclei other than ^1H (^{19}F, ^{13}C, ^{29}Si, ^{31}P and ^{129}Xe, resp.). These nuclei generally have a larger solvent effect than that observed in ^1H-n.m.r. Details of obtaining reliable σ_W data through adequate referencing systems and appropriate corrections are presented in Ch. 15 (7 pages), which demonstrates the numerous sources of error the experimenter must cope with from his measurements up to presentation of acceptable data. The final Ch. 16 (9 pages) concerns with molecular parameters and physical constants required for σ_W calculations. It provides some useful functions in tabulated or graphical representation.

The review covers 143 references.

The critical and comprehensive review on such a complex field requires from its author a creative competence. This type of critical attitude may best be illustrated by the author's readiness to correct any errors to be found incidentally in literature calculations, or by the manner he recalculates all σ_W data using the most up-to-date bulk susceptibility data.

For spectroscopists with a special interest in the field reviewed, this book will be an useful source.

P. SOHÁR

International Review of Science. Organic Chemistry Series Two

Volume 5. Alicyclic Compounds

Edited by D. GINSBURG (Technion-Israel Institute of Technology, Haifa)

Butterworth & Co. (Publishers) Ltd., London, 1976. 431 pages. Price £ 13.45

The series of organic chemistry and the two companion series for physical and inorganic chemistry aim to provide periodic authoritative reviews of the entire discipline of chemistry.

The publication of Organic Chemistry Series One was completed in 1973 with ten volumes and one index volume. The present book, the 5th of the Series Two of the biennal reviews in the International Review of Science, mainly intends to cover work in the chemistry of alicyclic compounds published in the years 1972 and 1973.

The chapters, written by different authors, show well the trends in different fields of alicyclic chemistry during this period. Some special groups of alicyclic compounds, such as annulenes, fulvenes, terpenoids and steroids are excluded. (Steroids will be discussed separately in the 9th volume of this series.) Eac hchapter is preceded by an outline of contents and followed by extensive bibliography. An index is incorporated in the volume.

The first chapter by N. M. D. BROWN and D. J. COWLEY (New University of Ulster, Coleraine) deals with the geometric and electronic structure of alicyclic compounds. Priority has been given to those methods of structure elucidation which are unambiguous and relatively direct, *i.e.* X-ray, neutron and electron diffraction, and significant spectroscopical studies. Nearly fifty pages cover more than 500 references.

The second chapter of the volume, dealing with the synthesis of alicyclic compounds, contains 110 pages, and was written by J. MARTIN (Dow Chemical, Massachusetts). An emphasis is placed on new synthetic methods of resonable efficiency and general applicability. In the reviewer's oppinion, the subject is well-proportioned and clearly arranged: *i.e.* the bicyclo compounds are divided into bicyclo [n. m. 0], and the bridged, bicyclo [n. m. o] compounds, "since synthetic strategies for each type are usually different". Subdivisions are devoted to the very important prostaglandines and the interesting "alicycles with characteristic morphology" (adamantanes, cage compounds, propellanes, asteranes, rotanes). The great amount of work behind this chapter is shown by the successful selection of the 582 references.

The next chapter by B. FUTHS (Tel-Aviv University) deals with the conformational analysis of alicyclic compounds. Both static and dinamic conformational analysis are treated following a classification criterion by ring size. Subdivisions are devoted to the conformational analytical techniques and to the conformation-reactivity correlations. The chapter contains numerous spectroscopic and structural data.

Publications which appeared in the period 1972—1973 and deal with the pyrolysis of alicyclic systems are reviewed in the 4th chapter, written by D. BECKER and N. C. BRODSKY (Technion-Israel Institute of Technology, Haifa). The pyrolytic reaction of alicyclic compounds are interesting theoretically, and some of them may be used for preparative purposes too. The review is organized according to the structure of compounds undergoing thermolysis.

Chapter 5, on the photochemistry of alicyclic compounds, was compiled by M. B. RUBIN (Technion-Israel Institute of Technology, Haifa) in 43 pages, with 315 references. The author tries to give an as far as possible brief but manysided survey on recent results, published in 1972—1973.

Quantitative structure-reactivity correlations of alicyclic compounds is discussed in chapter 6, written by T. W. BENTLEY (University College of Swansea). The main part of review deals with the development and applications of MINDO (*M*odification of the *I*ntermediate *N*eglect of *D*ifferential *O*verlap) and related calculations. It is followed by survey of

molecular mechanics (empirical force field calculations) and by linear free energy relationships between two sets of kinetic data or between kinetic data and equilibrium constants. It is a concise summary of the recent results.

The last chapter, written by D. GINSBURG (Technion-Israel Institute of Technology, Haifa), dealing with propellanes, is a more special subject, as compared with the others. Propellanes are tricyclic systems conjoined in a single carbon–carbon bond, and seem to find increasing use as model substrates in conformational analysis. The synthesis, thermal and photochemical reactions, structure and stereochemistry of propellanes are discussed in 44 pages on the basis of 92 references published in 1971—1973.

In summary, the 5th Volume of Organic Chemistry Series Two (431 pp. 2204 references!) facilitates the work of the organic chemist interested in the development of the chemistry of alicyclic compounds.

Á. KUCSMAN

L. MÁZOR: *Analytical Chemistry of Organic Halogen Compounds* (in Hungarian)

Akadémiai Kiadó, Budapest, 1976. 291 pages

The new book by Dr. MÁZOR, entitled "Analytical Chemistry of Organic Halogen Compounds" has been published as a joint edition of Akadémiai Kiadó (The Publishing House of the Hungarian Academy of Sciences). Budapest, and Pergamon Press Ltd., England. The attractive small handbook comprises eight chapters presented on 291 pages.

Halogen-containing organic compounds are of great importance and significance from the aspect of both the analyst and the organic preparative chemist. Their identification and analysis require a thorough grounding and training on the part of the microanalyst. The book by Dr. MÁZOR represents a significant progress, and at the same time it affords great practical help to the reader in this respect. The moderate volume and the way of editing of the manual also serve well this practical object.

Chapter 1 describes the properties, the ways of preparation and the reactions of halogens and of organic halogen compounds. The detection of halogens in organic compounds is discussed in Chapter 2, whereas Chapter 3 is devoted to the determination of chlorine, bromine and iodine. Determinations of fluorine, meeting also special requirements, are described in Chapter 4. Ultramicro methods gaining increasing importance in up-to-date analysis, are summarized in Chapter 5. Chapter 6, in turn, deals with investigations based on differences in the reactivity of halogen-containing organic compounds. Chapter 7 is concerned with the ways of eliminating the interfering effect of halogens in the micro determination of C, H, N, O, S and other elements. In Chapter 8 the physical constants of 1317 halogen-containing organic compounds of importance from the aspect of the organicc hemical and drug industry are summarized in tabulated form. This is followed by a formula index.

References to the literature are given at the and of each Chapter. Though this is of great advantage when reading the text, it does not meet the requirements of retrieval (namely, the book has no author index).

This small handbook is recommended mainly for practical analysts and microanalysts, because the theoretical part and the practically useful information are balanced to form a well organized concord. Understanding of the text is facilitated by 38 figures. The editing, printing and presentation of the book are exemplary.

I. GYENES

Gy. HONTI: *The Nitrogen Industry* (in Hungarian)

Akadémiai Kiadó. Budapest 1976

The book "The Nitrogen Industry", consisting of monographs and written by György HONTI an coworkers, appeared in the care of Akadémiai Kiadó. The work of more than 1400 pages, published in two volumes in English, fills a gap. Though several monographs have appeared earlier which deal with nitrogen industry, ammonia synthesis, nitric acid manufacture, preparation of urea etc., the book edited by György HONTI is superior to these, not only on account of its up-to-dateness, presenting the development achieved by this industry until the

early 70s, but also because all chemical, mechanical, electric or building engineers, active in the field of nitrogen industry, can acquire knowledge from the book needed in their everyday work. Turning the pages of the same book, chemical engineers can get at the same time information on the solution of problems, forming the task of those working in other fields of engineering sciences.

The introductory chapter of the first volume of 876 pages of the book deals with the various methods of the binding of nitrogen gas and its conversion to compounds, and with the history of processes used earlier. The subjects of the following chapters are ammonia, nitric acid, ammonium nitrate, urea, ammonium sulfate, multi-nutrient fertilizers, and the handling and formulation of fertilizers. The single monographs comprise in addition to a listing of the chemical and physical properties of the above compounds also thermodynamical and reaction kinetic informations needed for their manufacture, further the fundamental principles of mass and heat transfer, and chemical unit operations, as well as their most important theorems needed for the solving of manufacturing problems. In these parts, an important place was reserved also for experiences gained in realized manufacturing technologies and in the operation of the single apparatuses. The numerous figures, tables and nomograms contained in the chapters mentioned can be utilized to good advantage in their work by both planning and process engineers. Ample bibliography at the end of each chapter is intended to facilitate the activity of those, who need for the solving of their task more detailed information than given in the book.

Materials of construction used in the nitrogen industry are also discussed in the first volume. The chapter summarizing the structural properties of various kinds of steels, knowledge needed for their working and the fields of application of various steels is followed by a chapter discussing non-ferrous metals and the properties of metal coatings. The book treats separately and in detail inorganic, non-metal materials of construction, plastics and other products serving as binding- and sealing-materials, and finally, linings and coatings to be prepared from non-metal substances.

The chapter on compressors and pumps is organized in the second volume of 587 pages of the book. The subject discussed is illustrated by numerous carefully prepared drawings, diagrams and photos. A separate chapter deals with refrigeration techniques, and within this, with the fundamentals of air liquefaction and industrial oxygen manufacture. The subject of this chapter is complemented by important knowledge relative to medium and high pressure apparatus and conduits and fittings.

A separate chapter deals with electric equipment, motors, their suitable selection and with the problems of power stations and nets.

The chapter discussing instrumentation, measuring and control equipment, and the optimation of processes is a valuable help to both planning and process engineers.

A relatively brief but very interesting chapter of only 11 pages discusses the siting, the lay-out concept of nitrogen works, of the factory, and presents the principles followed earlier and today.

The last chapter closing the volume, and at the same time the book, deals with the expected role of nuclear energy in the nitrogen industry.

Most certainly, "The Nitrogen Industry" will be a useful aid for engineers active in the nitrogen industry and will commend great interest. It is my opinion that the book is addressed not only to those actually working in the nitrogen industry, but can be used to good advantage also for the teaching of future engineers, who wish to work in this field, so that this book of two volumes can be recommended as a handbook of the libraries of experts of the nitrogen industry, of ammonia plants, research institutes and technical universities.

P. KÁLDI

INDEX

ANALYTICAL CHEMISTRY

Determination of Sulfur in Organic Compounds by the Hydropyrolysis Method, L. MÁZOR 105

PHYSICAL AND INORGANIC CHEMISTRY

Kinetic equations of Multistep Electrode Processes, III, L. KISS 113
Study of the Mechanism of Hexene Radiolysis, I. Investigation of cyclohexene in the presence of additives, A. KOVÁCS, GY. CSERÉP, G. FÖLDIÁK 117
Infrared Spectrophotometric Studies on Aluminium Oxide Layers Prepared by Anodic Oxidation, A. B. KISS, E. SZONTAGH 129
Studies on Some Square Planar Complexes of N-5-Acetoacenaphthylidene-O-aminophenol with Cu(II), Pt(II) and Pd(II), P. SINGH, B. P. SINGH, V. SINGH, R. L. GOEL 143
Electrochemical Investigations on Supported Palladium Catalysts, É. POLYÁNSZKY, T. MALLÁT, J. PETRÓ 147
Wettability of Gelatine Gels, (in Russian) W. WOLFRAM, CH. STERGIOPOULOS 157
The Reaction of Carbon Dioxide and Dioxygen with Dinitrogentris (Triphenylphosphine) Cobalt (O), G. SPEIER, Á. SIMON, L. MARKÓ 169

ORGANIC CHEMISTRY

Stereochemical Studies, XXVII. Studies on Cyclic 2-Hydroxycarboxylic Acids, VI. Neighbouring Hydroxyl Group Catalysis in the Alkaline Hydrolysis of Ethyl *Cis*- and *Trans*-2-hydroxycyclopentane-, cyclohexane-, cycloheptane- and cyclooctanecarboxylates, G. BERNÁTH, P. SOHÁR. K. L. LÁNG, GY. GÖNDÖS, L. GERA, A. PÁL 178

TECHNOLOGICAL CHEMISTRY

The Optimation of Fermentation Processes by Means of the Propagation Curves of Microorganism Cultures, K. POLINSZKY, T. BLICKLE, J. FÜLÖP, R. TŐRÖS, T. VAJDA (in German) 187

RECENSIONES 201

Printed in Hungary

A kiadásért felel az Akadémiai Kiadó igazgatója — Műszaki szerkesztő: Zacsik Annamária

A kézirat nyomdába érkezett: 1976. XI. 11. — Terjedelem: 9,45 (A/5) ív, 38 ábra

77.3817 Akadémiai Nyomda, Budapest — Felelős vezető: Bernát György

ACTA CHIMICA

Том 92 – вып. 2

РЕЗЮМЕ

Применение метода гидропиролиза для определения содержания серы в органических соединениях

Л. МАЗОР

Метод гидропиролиза, использованный для микроколичественного анализа органических соединений на галоген и описанный в предыдущем сообщении, оказался пригодным и для определения содержания серы.

Пары органических серных соединений или продукты их пиролиза пропускались в токе азота, насыщенного водяным паром, над платиновым катализатором при температуре 800—1000°C, разлагаясь при этом полностью либо до сероводорода, либо до двуокиси серы. Газовый поток пропускался через 0,01—0,02N йодный раствор, известной концентрации и объема, в котором сероводород окислялся до элементарной серы, а двуокись серы до сульфата. Т. к. стехиометрия этих двух окислительных реакций одинакова, то после обратного титрования избытка йода, содержание серы может быть рассчитано независимо от того, в каком отношении образуются эти два серных соединения.

О кинетических уравнениях многостадийных электродных процессов

Ш. Л. КИШ

Было выведено и рассмотрено уравнение поляризационной кривой для многостадийного электродного процесса, для случая чистого диффузионного перенапряжения.

Исследование механизма реакции радиолиза гексена, I

Исследование циклогексена с добавками

А. КОВАЧ, ДЬ. ЧЕРЕП и Г. ФЁЛЬДИАК

Был исследован γ-радиолиз циклогексена, применяя ловушки электронов, положительных ионов и радикалов.

В противоположность ранним представлениям, было доказано, что при образовании водорода нельзя пренебрегать процессами электронно-ионной рекомбинации, а также была подтверждена роль этих процессов в образовании циклогексана.

Если в образовании водорода важность радикальных процессов невелика, то при образовании димеров роль циклогексильных радикалов становится решающей. Сопряженные диены оказывают на радиолиз моноалкенов влияние, подобное влиянию моноалкенов на алканы.

При радиолизе циклогексена различные продукты образуются согласно различным механизмам, но отдельные продукты могут образовываться различными путями. Помимо этого, необходимо считаться также с конкурирующими реакциями, как конечных, так и промежуточных продуктов.

ИК спектрофотометрические исследования на слоях окиси алюминия приготовленных анодным окислением

Б. А. КИШ и Е. СОНТАГ

Были рассмотрены возможности исследования с помощью ИК спектрофотометрии аморфных слоев окиси, образующихся на поверхности алюминия при ее анодном окислении. После отделения окисной пленки, для последней в таблетках KBr снимались спектри регулярного и зеркального отражения.

На основе колебательных частот химических связей и других характеристик спектров были сделаны заключения относительно структуры аморфных алюмоокисных слоев, образующихся в органических и неорганических электролитах, размеров координированных звеньев, степени «полимеризации» сетчатой структуры и т. д.

Было установлено, что ионы Al^{+3}, образующиеся временно в процессе анодного окисления и незатронутые при образовании окиси, вступают во взаимодействие с сульфосалициловой кислотой, обладающей наиболее сильными комплексообразовательными свойствами по сравнению со всеми остальными компонентами ванны. Некоторая доля комплекса остается в связанном состоянии в порах или на поверхности.

Исходя из особенностей диффракционного спектра, полученного за счет отражения света с тонких слоев, были сделаны заключения относительно пористости аморфных слоев, морфологических свойств, а также относительно структуры поверхности раздела между основным металлом и окисной пленкой. Зная толщину слоя, из интерференционных полос были рассчитаны коэффициенты преломления окисных слоев, образующихся при окислении прямым и переменным током.

Исследование некоторых плоско квадратных комплексов N-5-ацетоаценафтилиден-о-аминофенола с Cu(II), Pt(II) и Pd(II)

П. СИНГ, Б. П. СИНГ, В. СИНГ и Р. Л. ГОЭЛ

Были исследованы комплексы состава $[M(C_{20}H_{16}NO)_2]$ (M *III* Cu(II), Pt(II) или Pd(II) и $C_{20}H_{16}NO$ = N-5-ацетоаценафтилиден-о-аминофенол). Данные аналитических, магнитных, ИК и электронно-спектроскопических исследований указывают на то, что все эти комплексы находятся в плоско квадратной конфигурации. На основе данных электронной спектроскопии было найдено, что сила связи увеличивается в порядке $3d_{\sigma} < 4d_{\sigma} < 5d_{\sigma}$.

Электрохимические исследования палладиевых катализаторов на носителях

Е. ПОЛЯНСКИ, Т. МАЛЛАТ и Й. ПЕТРО

Потенциодинамический поляризационный метод, использованный для порошковых катализаторов благородных металлов без носителей, был распространен для исследований палладиевых катализаторов на носителях.

После выяснения условий измерений, одинаковым образом была приготовлена серия катализаторов на активированном углероде, как носителе, с содержанием палладия 0, 1, 5, 10, 20 и 100%. Были исследованы их сорбционные и каталитические свойства в зависимости от содержания металла.

На основе потенциодинамических исследований было установлено, что характер сорбции водорода при небольших содержаниях металла подобен наблюдаемой на чистом углероде, а при повышенных содержаниях металла подобен наблюдаемой на чистой палладиевой черни. С увеличением содержания металла увеличивается количество сорбированного водорода, доля слабо и сильно связанного водорода и кажущаяся активность в реакциях гидрирования (восстановление ацетофенона и циклогексена).

На основе потенциодинамических исследований было также установлено, что изменение способа приготовления катализатора оказывает значительное влияние на среднюю энергию связи сильно связанного водорода.

Взаимодействие двуокиси углерода и молекулярного кислорода с динитрогентрис (трифенилфосфин) кобальт(о)

Г. ШПЕЙЕР, А. ШИМОН и Л. МАРКО

Было исследовано взаимодействие $[Co(N_2)(PPh_3)_3]$ с CO_2 и O_2. Были изолированы твердые комплексы. Комплекс с CO_2 очень чувствителен к воздуху, а комплекс с O_2 термически стабилен лишь до 0°. Заключения о структуре основаны на данных элементарного анализа, ИК спектров, аналогиях с уже установленными реакциями и химической деградацией. Приводятся доказательства в пользу формул $[Co(CO_2)(PPh_3)_2]_n$ и $[(PPh_3)_3Co(O_2)Co(PPh_3)_3]$.

Стереохимические исследования, XXVII

Исследование циклических 2-гидроксикарбоксильных кислот, VI. Катализ соседней гидроксильной группой щелочного гидролиза этил цис- и транс-2-гидроксициклопентанкарбоксилатов и их циклогексановых, циклогептановых и циклооктановых гомологов

Г. БЕРНАТ, П. ШОХАР, К. Л. ЛАНГ, ДЬ. ГЁНДЁШ, Л. ГЕРА и Л. ПАЛ

Кинетика щелочного гидролиза этил *цис-* и *транс*-2-гидроксициклопентанкарбоксилатов (*1, 2*), а также их циклогексановых (*4, 5*), циклогептановых (*7, 8*) и циклооктановых (*10, 11*) гомологов была исследована в 70% водном диоксане. Скорость гидролиза увеличивается под влиянием соседней гидроксильной группы в 10—21 раз, по сравнению с соответствующими этил циклоалканкарбоксилатами (*3, 6, 9, 12*). Скорость гидролиза почти одинакова для циклопентановых и циклогептановых изомеров, а в случае циклогексана *транс*-производное и циклооктана *цис*-производное реагируют почти в два раза быстрее, чем их стереоизомеры. Были определены значения $\Delta E^{\ddagger}$, $\Delta H^{\ddagger}$, $\Delta S^{\ddagger}$ и $\Delta G^{\ddagger}$ реакции. Изокинетическая температура гидролиза *цис-* и *транс*-2-карбетксициклоалканов была рассчитана с помощью ЭВМ и равна $\beta = 251 \pm 12$°К с коэффициентом корреляции $\gamma = 0{,}99$. Для этил циклоалканкарбоксилатов кривая имеет более крутой неклон, указывая тем самым на то, что механизм двух реакции различается. Обсуждаются ИК и ЯМР спектры метил и этил *цис-* и *транс*-2-гидроксициклоалканкарбоксилатов. Можно заключить, что определяющим фактором ускоряющего эффекта соседней гидроксильной группы в щелочно*3* гидролизе эфиров является сортировка растворителя за счет соседней гидроксильной группы, хотя следует принимать во внимание также и различные водородные связи *цис-* и *транс*-изомеров.

Использование кривых размножения культур ми кроорганизмов для оптималиэации ферментационных процессов

К. ПОЛИНСКИ, Т. БЛИКЛЕ, Й. ФЮЛЕП, Р. ТЁРЁШ и Т. ВАЙДА

Впервые обсуждается кривая размножения культур микроорганизмов на теоретической основе, т. е. с введением понятия вероятности размножения.

Далее показано, каким образом на основе взятой эмпирически кривой размножения выращиваемой культуры можно оптимализировать полунепрерывное ферментационное производство, если целью является выигрыш максимальной массы микроорганизмов.

Les Acta Chimica paraissent en français, allemand, anglais et russe et publient des mémoires du domaine des sciences chimiques.

Les Acta Chimica sont publiés sous forme de fascicules. Quatre fascicules seront réunis en un volume (4 volumes par an).

On est prié d'envoyer les manuscrits destinés à la rédaction à l'adresse suivante:

Acta Chimica
H-1521 Budapest, Hongrie

Toute correspondance doit être envoyée à cette même adresse.

La rédaction ne rend pas de manuscript.

Le prix de l'abonnement est de $ 32,00 par volume.

Abonnement — en Hongrie à l'Akadémiai Kiadó (1363 Budapest, P.O.B. 24. C.C.B. Bankszámla) 215 11488, à l'étranger à l'Entreprise pour le Commerce Extérieur de Livres et Journaux «Kultúra» (H-1389 Budapest 62, P.O.B. 149 Compte-courant No. 218 10990) ou l'étranger chez tous les représentants ou dépositaires.

Die Acta Chimica veröffentlichen Abhandlungen aus dem Bereich der chemischen Wissenschaften in deutscher, englischer, französischer und russischer Sprache.

Die Acta Chimica erscheinen in Heften wechselnden Umfanges. Vier Hefte bilden einen Band. Jährlich erscheinen 4 Bände.

Die zur Veröffentlichung bestimmten Manuskripte sind an folgende Adresse zu senden:

Acta Chimica
H-1521 Budapest, Ungarn

An die gleiche Anschrift ist auch jede für die Redaktion bestimmte Korrespondenz zu richten.

Manuskripte werden nicht zurückerstattet.

Abonnementpreis pro Band: $ 32,00.

Bestellbar für das Inland bei Akadémiai Kiadó (1363 Budapest, Postfach 24, Bankkonto Nr. 215 11488), für das Ausland bei dem Buch- und Zeitungs Außenhandels-Unternehmen „Kultúra" (H-1389 Budapest 62, P.O.B. 149. Bankkonto Nr. 218 10990) oder bei seinen Auslandsvertretungen und Kommissionären.

«Acta Chimica» издают статьи по химии на русском, французском, английском и немецком языках.

«Acta Chimica» выходит отдельными выпусками разного объема, 4 выпуска составляют один том и за год выходит 4 тома.

Предназначенные для публикации рукописи следует направлять по адресу:

Acta Chimica
H-1521 Budapest, ВНР

Всякую корреспонденцию в редакцию направляйте по этому же адресу.

Редакция рукописей не возвращает.

Подписная цена — $ 32,00 за том.

Отечественные подписчики направляйте свои заявки по адресу Издательства Академии Наук (1363 Budapest, P.O.B. 24, Текущий счет 215 11488), а иностранные подписчики через организацию по внешней торговле книг и газет «Kultúra» H-1389 Budapest 62, P.O.B. 149. Текущий счет 218 10990) или через ее заграничные представительства и уполномоченных.

Reviews of the Hungarian Academy of Sciences are obtainable at the following addresses:

AUSTRALIA
C.B.D. LIBRARY AND SUBSCRIPTION SERVICE, Box 4886, G.P.O., *Sydney N.S.W.2001*
COSMOS BOOKSHOP, 145 Ackland Street, *St. Kilda (Melbourne), Victoria 3182*

AUSTRIA
GLOBUS, Höchstädtplatz 3, *1200 Wien XX*

BELGIUM
OFFICE INTERNATIONAL DE LIBRAIRIE, 30 Avenue Marnix, *1050 Bruxelles*
LIBRAIRIE DU MONDE ENTIER, 162 Rue du Midi, *1000 Bruxelles*

BULGARIA
HEMUS, Bulvar Ruszki 6, *Sofia*

CANADA
PANNONIA BOOKS, P.O. Box 1017, Postal Station "B", *Toronto, Ontario M5T 2T8*

CHINA
CNPICOR, Periodical Department, P.O. Box 50, *Peking*

CZECHOSLOVAKIA
MAD'ARSKÁ KULTURA, Národní třida 22, *115 66 Praha*
PNS DOVOZ TISKU, Vinohradská 46, *Praha 2*
PNS DOVOZ TLAČE, *Bratislava 2*

DENMARK
EJNAR MUNKSGAARD, Norregade 6, *1165 Copenhagen*

FINLAND
AKATEEMINEN KIRJAKAUPPA, P.O. Box 128, *SF-00101 Helsinki 10*

FRANCE
EUROPÉRIODIQUES S. A., 31 Avenue de Versailles, *78170 La Celle St. Cloud*
LIBRAIRIE LAVOISIER, 11 rue Lavoisier, *75008 Paris*
OFFICE INTERNATIONAL DE DOCUMENTATION ET LIBRAIRIE, 48 rue Gay Lussac, *75240 Paris Cedex 05*

GERMAN DEMOCRATIC REPUBLIC
HAUS DER UNGARISCHEN KULTUR, Karl-Liebknecht-Strasse 9, *DDR-102 Berlin*
DEUTSCHE POST ZEITUNGSVERTRIEBSAMT, Strasse der Pariser Kommüne 3—4, *DDR-104 Berlin*

GERMAN FEDERAL REPUBLIC
KUNST UND WISSEN ERICH BIEBER, Postfach 46, *7000 Stuttgart 1*

GREAT BRITAIN
BLACKWELL'S PERIODICALS DIVISION, Hythe Bridge Street, *Oxford OX1 2ET*
BUMPUS, HALDANE AND MAXWELL LTD., Cowper Works, *Olney, Bucks MK46 4BN*
COLLET'S HOLDINGS LTD., Denington Estate, *Wellingborough, Northants NN8 2QT*
WM. DAWSON AND SONS LTD., Cannon House, *Folkestone, Kent CT19 5EE*
H. K. LEWIS AND CO., 136 Gower Street, *London WC1E 6BS*

GREECE
KOSTARAKIS BROTHERS, International Booksellers, 2 Hippokratous Street, *Athens-143*

HOLLAND
MEULENHOFF-BRUNA B.V., Beulingstraat 2, *Amsterdam*
MARTINUS NIJHOFF B.V., Lange Voorhout 9—11, *Den Haag*
SWETS SUBSCRIPTION SERVICE, 347b Heereweg, *Lisse*

INDIA
ALLIED PUBLISHING PRIVATE LTD, 13/14. Asaf Ali Road, *New Delhi 110001*
150 B-6 Mount Road, *Madras 600002*
INTERNATIONAL BOOK HOUSE PVT. LTD,. Madame Cama Road, *Bombay 400039*
THE STATE TRADING CORPORATION OF INDIA LTD., Books Import Division, Chandralok 36 Janpath, *New Delhi 110001*

ITALY
EUGENIO CARLUCCI, P.O. Box 252, *70100 Bari*
INTERSCIENTIA, Via Mazzé 28, *10149 Torino*
LIBRERIA COMMISSIONARIA SANSONI, Via Lamarmora 45, *50121 Firenze*
SANTO VANASIA, Via M. Macchi 58, *20124 Milano*
D. E. A., Via Lima 28, *00198 Roma*

JAPAN
KINOKUNIYA BOOK-STORE CO. LTD., 17-7 Shinjuku-ku 3 chome, Shinjuku-ku, *Tokyo 160-91*
MARUZEN COMPANY LTD., Book Department, P.O. Box 5050 Tokyo International, *Tokyo 100-31*
NAUKA LTD. IMPORT DEPARTMENT, 2-30-19 Minami Ikebukuro, Toshima-ku, *Tokyo 171*

KOREA
CHULPANMUL, *Phenjan*

NORWAY
TANUM-CAMMERMEYER, Karl Johansgatan 41—43, *1000 Oslo*

POLAND
WĘGIERSKI INSTYTUT KULTURY, Marszałkowska 80, *Warszawa*
CKP I W ul. Towarowa 28 *00-958 Warszawa*

ROUMANIA
D. E. P., *Bucureşti*
ROMLIBRI, Str. Biserica Amzei 7, *Bucureşti*

SOVIET UNION
SOJUZPETCHATJ — IMPORT, *Moscow*
and the post offices in each town
MEZHDUNARODNAYA KNIGA, *Moscow G-200*

SPAIN
DIAZ DE SANTOS, Lagasca 95, *Madrid 6*

SWEDEN
ALMQVIST AND WIKSELL, Gamla Brogatan 26 *101 20 Stockholm*
GUMPERTS UNIVERSITETSBOKHANDEL AB, Box 346, *401 25 Göteborg 1*

SWITZERLAND
KARGER LIBRI AG, Petersgraben 31, *4011 Basel*

USA
EBSCO SUBSCRIPTION SERVICES, P.O. Box 1943, *Birmingham, Alabama 35201*
F. W. FAXON COMPANY, INC., 15 Southwest Park, *Westwood, Mass. 02090*
THE MOORE-COTTRELL SUBSCRIPTION AGENCIES, *North Cohocton, N. Y. 14868*
READ-MORE PUBLICATIONS, INC., 140 Cedar Street, *New York, N. Y. 10006*
STECHERT-MACMILLAN, INC., 7250 Westfield Avenue, *Pennsauken, N. J. 080110*

VIETNAM
XUNHASABA, 32, Hai Ba Trung, *Hanoi*

YUGOSLAVIA
JUGOSLAVENSKA KNJIGA, Terazije 27, *Beograd*
FORUM, Vojvode Mišiča 1, *21000 Novi Sad*

ACTA CHIMICA

ACADEMIAE SCIENTIARUM HUNGARICAE

ADIUVANTIBUS

M. BECK, R. BOGNÁR, V. BRUCKNER,
GY. HARDY, K. LEMPERT, F. MÁRTA,
K. POLINSZKY, E. PUNGOR,
G. SCHAY, Z. G. SZABÓ, P. TÉTÉNYI

REDIGUNT

B. LENGYEL et GY. DEÁK

TOMUS 92 FASCICULUS 3

AKADÉMIAI KIADÓ, BUDAPEST

1977

ACTA CHIM. (BUDAPEST) ACASA2 92 (3) 211—328 (1977)

ACTA CHIMICA

A MAGYAR TUDOMÁNYOS AKADÉMIA KÉMIAI TUDOMÁNYOK OSZTÁLYÁNAK IDEGEN NYELVŰ KÖZLEMÉNYEI

FŐSZERKESZTŐ

LENGYEL BÉLA

SZERKESZTŐ

DEÁK GYULA

TECHNIKAI SZERKESZTŐ

HARASZTHY-PAPP MELINDA

SZERKESZTŐ BIZOTTSÁG

BECK MIHÁLY, BOGNÁR REZSŐ, BRUCKNER GYŐZŐ, HARDY GYULA, LEMPERT KÁROLY, MÁRTA FERENC, POLINSZKY KÁROLY, PUNGOR ERNŐ, SCHAY GÉZA, SZABÓ ZOLTÁN, TÉTÉNYI PÁL

Acta Chimica is a journal for the publication of papers on all aspects of chemistry, in English, German, French and Russian languages.

Acta Chimica is published in 4 volumes per year. Each volume consists of 4 issues of varying size.

Manuscripts should be sent to

Acta Chimica
H-1521 Budapest, Hungary

Correspondence with the Editors should be sent to the same address. Manuscripts are not returned to the Authors.

Subscription rate $ 32.00 per volume.

Hungarian subscribers should order from Akadémiai Kiadó, 1363 Budapest, P.O. Box 24. Account No. 215 11488.

Orders from other countries are to be sent to „Kultúra" Foreign Trade Company (H-1389 Budapest 62, P.O. Box 149. Account No. 218 10990) or to its representatives abroad.

Acta Chimica Academiae Scientiarum Hungaricae, Tomus 92 (3), pp. 211—221 (1977)

ELECTRONIC ABSORPTION SPECTRA OF SUBSTITUTED CARBAZOLOQUINONES

R. M. Issa, A. A. El-Samahy, I. M. Issa and S. H. Etaiw*

(Chemistry Department, Faculty of Science, Assiut University, A. R. Egypt.)

Received May 5, 1975
In revised form January 20, 1976

The U.V. and visible spectra of some carbazoloquinones are investigated in organic solvents and aqueous buffer solutions. Electronic transitions have been identified as either locally excited or predominatly charge transfer states. The spectral shifts are discussed in terms of medium effects and in relation to molecular structure. The variation of absorbance with pH is utilized for the determination of pK_a. The important bands in the IR spectra are assigned and discussed in relation to molecular structure.

Introduction

The absorption spectra of quinones were the subject of many investigations, however, few studies included heterocyclic quinones. In an investigation on substituted anthraquinone, Yoshida and Takabayaski [1] assigned all absorption bands to π–π^* transitions within the phenyl rings and the quinone nucleus. Similar assignments were given in studies of some hydroxy anthraquinones [2].

In previous studies [3—5] the absorption spectra of some carbazolo, 2,3-benzcarbazolo, and dibenzfuranoquinones were discussed. In such studies, it was found that substituents on the quinone ring influence considerably the quinone bands. Similarly some changes in the visible region were observed on changing the substituents and type of heterocyclic moieties. In the present investigation, the electronic absorption spectra of some substituted carbazoloquinones are studied in organic solvents and buffer solutions aiming to gain more knowledge concerning the spectral behaviour of these compounds. As the important bands in the IR spectra are discussed in relation to molecular structure.

Experimental

Carbazoloquinones of the type **I** and **II** were prepared by a method similar to that described by Inove *et al.* [6] and modified by Osman nad Hammam [7]. The products were crystallized several times from the appropriate solvent.

* Extracted from the Ph. D. thesis of Safaa El-Din Hassan Etaiw, March 1973

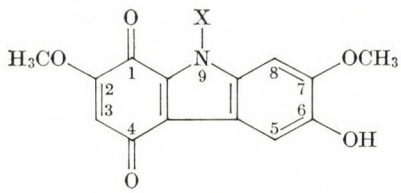

I

	X
a	H
b	CH_3
c	C_2H_5
d	C_4H_9

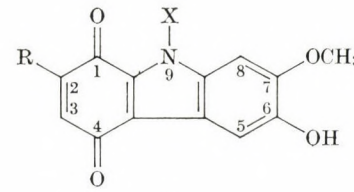

II

	X	R
a	CH_3	$NHCH_3$
b	C_4H_9	NHC_4H_9
c	phenyl	NHC_2H_5
d	anisyl	NHC_2H_5

The solvents used for spectral measurements were purified by recommended procedures [8]. The buffer solutions were prepared as given by BRITTON [9]. The absorption spectra were recorded on a UNICAM S.P. 8000 recording spectrophotometer using 1 cm matched quartz cells. The pH measurements were carried out by the aid of a RADIOMETER pH-meter model 28. The IR spectra were taken on a UNICAM S.P. 200 infrared spectrophotometer in KBr discs.

Results and discussion

I — *Spectra in organic solvents*

(A) *Band assignment:*

The spectra of **I** in ethanol can be considered as comprising five absorption bands. The spectra of **II**, on the other hand, Fig. 1, comprise six absorption bands (Table I). The three bands in the 230—241 nm, 239—259 nm and 263—

Table I

Spectra of $\mathbf{I}_b$ *and* $\mathbf{II}_a$ *in ethanol*

Ib		**IIa**		Band assignment
λ_{max}	$\varepsilon_{max} \cdot 10^{-4}$	λ_{max}	$\varepsilon_{max} \cdot 10^{-4}$	
232	2.63	236	2.30	$\pi-\pi^*$
258	1.79	258	1.60	transition of the indole
264	1.87	265	1.78	system
292	1.18	289	0.80	$\pi-\pi^*$
—	—	324	0.159+	transition of the qui-
321	0.87	374	0.69	nonoid system
486	0.65	482	0.53	CT

+: after making background correction

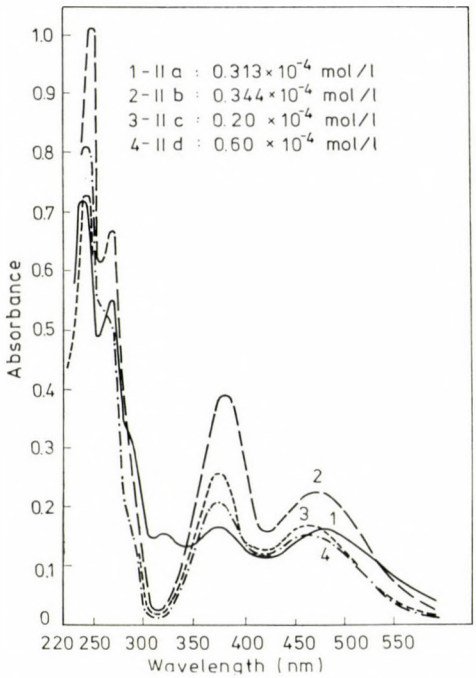

Fig. 1. Electronic absorption spectra of series **II** in ethanol

265 nm region can be assigned to π–π^* transitions in the indazole system. Comparable bands are observed in the spectrum of carbazoles however, exhibiting some shifts probably due to the influence of the substituents on the electronic transitions of the aromatic system.

The two bands appearing near 290 and 322 nm in the spectra of series **I** correspond to π–π^* transition in the quinone nucleus. Carbazole, phenol and anisole exhibit an absorption band within this spectral region and a band near 280 nm was ascribed by SPRUIT [10] and others to a π–π^* transition in quinones with three condensed rings which may be the case for carbazoloquinones.

The band near 290 nm is not affected by the nature of the substituent at position two while the second band in this region shifts to longer wave length (375 nm) on replacement the methoxy by an alkylamino group. This causes a higher delocalization of the π-electron clouds. Hence, an easier transition which is reflected in the red shift of the band.

In the spectra of substituted quinones, the band in the visible region is usually assigned to an intramolecular charge transfer (CT) from the substituent to the quinone nucleus [1—5]. In the compounds under investigation, the charge transfer seems to originate essentially from the indole part of the molecule to the quinone nucleus.

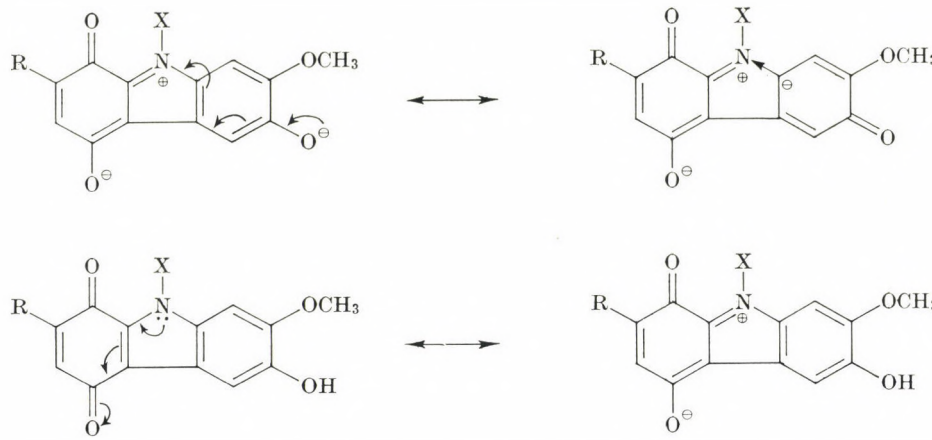

A change of the substituent directly bonded to the quinone ring does not significantly affect the band position.

The CT nature of the band located near 480 nm can be supported by considering the spectral behaviour in alkaline media. The solution in alkaline media acquires a bluish to bluish-green colour and the maximum absorption shifts to a longer wave length (*cf.* Fig. 2). The large red shift is mainly due to the increased electron density on the donor center resulting from a mesomeric interaction with the negative charge left on the phenolate ion.

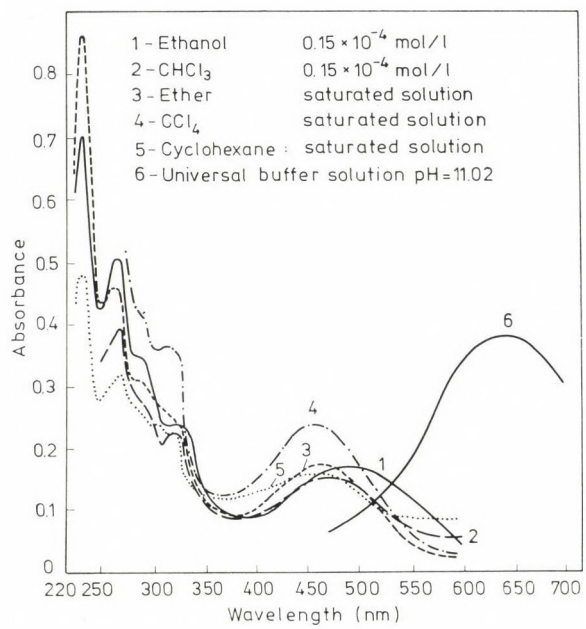

Fig. 2. Electronic absorption spectra of **Ic** in organic solvents

It is worthy to mention that the CT band shifts to shorter wave length on going from the first series to the second one. This may be ascribed to the easier migration of the *n*-electrons of the alkylamino group towards the quinone ring which antagonizes the CT from the heterocyclic ring.

(B) *Solvent effect:*

The bands display some changes in their position and extinction depending on the molecular structure and the polarity of the medium (*cf.* Table II and Fig. 2). The bands corresponding to π–π^* transitions in the aromatic system show no pronounced solvent shifts. The band due to π–π^* transition of the C = O group shows slight solvent effects on changing the solvent from a polar to a non-polar one. On the other hand, the band corresponding to the transition in the ethylenic system is red shifted on going from non-polar to polar solvents. The CT band is blue shifted on going from ethanol as a polar solvent to cyclohexane as non-polar one. The observed red shifts in case of ethanol, chloroform and ether are the resultant of the superposition of dipole–dipole forces as well as hydrogen bonding effects.

(C) *Effect of substitution:*

The electronic absorption spectra of carbazoloquinones in ethanol can be regarded as comprising two regions. The first one lying below 300 nm is more or less identical for the two series and being not very sensitive to substituent effect. The second region, above 300 nm is readily influenced by the nature of the substituent, especially on going from series **I** to series **II**. The band corresponding to the π–π^* transition in the ethylenic system of the quinone nucleus is highly affected by changing the substituent at position two.

In one and the same series, the CT band shifts to longer wavelength as the electron donor character of the substituent attached to the N-atom of the pyrrole ring increases. The increased donor character of the substituent increases the charge density on the nitrogen atom which favours the CT to the quinone nucleus. On the contrary, the increased charge density on the substituent group directly linked to the quinone ring hinders the CT and hence, causes a blue shift in the the band position.

(D) *The spectra in mixed organic solvents:*

The shift of the CT band to red in ethanol is much higher than corresponding to change of solvent polarity. The application of the equation given by GÁTI and SZALAY [11]

$$\Delta\nu = \left[\left(\frac{n^2-1}{2n^2+1}\right)(a-b)\right] + b\left(\frac{\varepsilon-1}{\varepsilon+1}\right)$$

Table II

Cumulative data obtained for series **I** *and* **II** *in different organic solvents*

λ_{max} = nm ε_{max} = $cm^2\ mole^{-1}$

Solvent	I_a		I_b		I_c		I_d		II_a		II_b		II_c			II_d
	λ_{max}	$\varepsilon_{max}\cdot10^{-4}$	λ_{max}	$\varepsilon_{max}\cdot10^{-4}$	λ_{max}	$\varepsilon_{max}\cdot10^{-4}$	λ_{max}	$\varepsilon_{max}\cdot10^{-4}$	λ_{max}	$\varepsilon_{max}\cdot10^{-4}$	λ_{max}	$\varepsilon_{max}\cdot10^{-4}$	λ_{max}	$\varepsilon_{max}\cdot10^{-4}$	λ_{max}	$\varepsilon_{max}\cdot10^{-4}$
Ethanol	232	3.32	232	2.63	232	4.669	233	3.65	236	2.30	—	—	—	—	—	—
	257	2.36	258	1.79	257	3.20	257	2.30	258	1.60	241	3.34	239	1.33	239	3.60
	264	2.48	264	1.87	265	3.40	265	1.45	265	1.78	264	1.92	265	0.85	265	2.55
	281	2.04	284	1.18	284	2.30	286	1.45	284	0.80	291	0.63	285	0.25	291	0.60
	—	—	—	—	—	—	—	—	324	0.159	—	—	—	—	—	—
	321	1.16	321	0.87	323	1.63	324	0.95	374	0.69	378	1.13	376	0.36	375	1.30
	490	1.12	486	0.65	491	1.16	492	0.90	482	0.535	476	0.65	472	0.25	467	0.83
$CHCl_3$	—	—	258	1.22	257	2.50	257	2.20	258	—	—	—	—	—	—	—
	—	—	266	1.26	266	2.66	266	2.35	266	—	266	1.45	—	—	266	2.50
	—	—	287	0.85	288	1.78	288	1.45	291	—	292	0.57	286	—	292	0.54
	—	—	—	—	—	—	—	—	321	—	—	—	—	—	—	—
	320	—	318	0.69	321	1.53	321	1.20	376	—	378	1.07	374	—	374	1.54
	474	—	474	0.46	475	1.10	473	1.50	468	—	465	0.55	460	—	457	0.83
Ether			—		233		—		—		—		—		—	
			258		257		257		—		—		—		—	
			264		265		264		265		263		266		265	
			288		291		289		293		292		290		292	
			—		—		—		320		—		—		—	
			315		318		317		370		372		388		368	
			466		465		464		463		459		445		444	
CCl_4			287		288		288		288		292		291		293	
			—		—		—		318		—		—		—	
			317		318		317		369		372		368		368	
			460		457		462		458		458		455		449	
Cyclohexane			—		232		232				239				—	
			258		256		256				—				—	
			263		265		263				262				263	
			287		286		288				290				291	
			315		315		315				367				364	
			454		458		459				455				450	

did not yield a linear relation between $\Delta\nu$ and $\varepsilon - 1/\varepsilon + 1$. The shift is thus not only due to changes in dielectric constant of the medium or altered solvation energy, but also accounts for the possible hydrogen bond formation between solute and solvent molecules.

The spectra of $\mathbf{I}_d$ in ethanol–CCl_4 mixture exhibit one absorption band in the 400—600 nm region (Fig. 3). The band is red shifted on increasing the

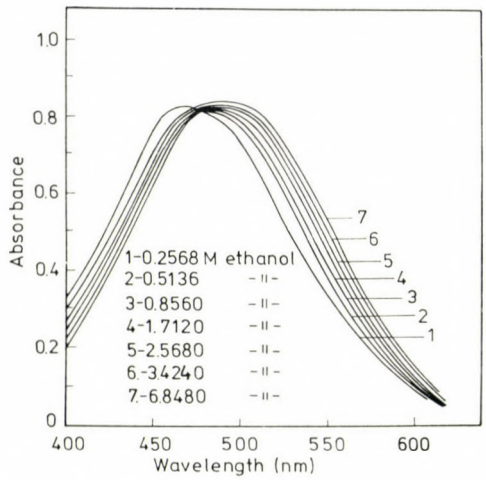

Fig. 3. Spectra of **Id** in CCl_4–Ethanol mixtures

proportion of polar solvent in solution. Above 0.65 *M* ethanol the red shift observed is small where the ethanol molecules are at least partly oriented around solute molecule causing a decrease in orientation strain found in solutions containing large proportions of CCl_4. The small red shift observed may be due to the tendency of ethanol molecules to orient themselves around the solute molecules causing a rapid reconstruction of the solvent cage. Above 2.0 *M* ethanol the frequency shift on increasing dielectric constant of the solution is no more apparent, indicating that the orientation strain attains a minimum value. Also, the solvent cage reaches its equilibrium state and the dipole–dipole interaction between solute and ethanol molecules assumes its maximum value.

A clear isobestic point is observed indicating that an equilibrium is set in solution between molecules solvated by the low polarity solvents and those bonded to ethanol through the intermolecular hydrogen bond forming a sort of molecular complex.

$$S + n\mathrm{ROH} \rightleftharpoons (\mathrm{ROH})_n \ldots\ldots S$$

For this equilibrium reaction

$$K_f = \frac{[(\mathrm{ROH})_n \ldots\ldots \mathrm{S}]}{(\mathrm{S})\,(\mathrm{ROH})^n}$$

The value of K_f can be determined from the variation of absorbance with ethanol concentration at a given wave length. The equation used is that given before [4, 5] namely.

$$\log \mathrm{C_{ROH}} = \frac{1}{n} \log K_f + \log \frac{A - A_0}{A_l - A}$$

in which A_0 = absorbance in low polarity solvent,
A = absorbance in CCl_4–ethanol mixture,
A_l = limiting absorbance in pure ethanol.

The values of n, pK and ΔG^* obtained for $\mathbf{I_b}$, $\mathbf{I_c}$, $\mathbf{I_d}$ and $\mathbf{II_b}$ are depicted in Table III. The strength of the hydrogen bond formed between solute and solvent molecules depends on molecular structure mainly the acidic character of the molecule.

Table III

Results obtained in mixed organic solvents

Compound	n	pK	ΔG^* Kcal/mole
I*b*	0.71	0.10	0.128
I*c*	0.60	0.37	0.498
I*d*	1.00	0.70	0.944
II*b*	0.65	0.19	0.256

II. *Spectra in buffer solutions*

The visible spectra in buffer solutions, represented in Fig. 4, show the normal behaviour, *i.e.* mainly two bands. The first band appearing at the lower wave length side is mainly due to the absorption of the neutral species of the dye. By gradually increasing the pH of the solution the ionization of the proton takes place and a new band appears at longer wave length. A clear isobestic point is observed indicating the existence of an equilibrium between the two species. The equilibrium present is accordingly of an acid–base type between the non-ionized and ionized forms. The absorbance-pH curves are typical dissociation and association curves. The dissociation constant of the acid–base equilibria was determined applying the methods considered previously [12, 14] namely:

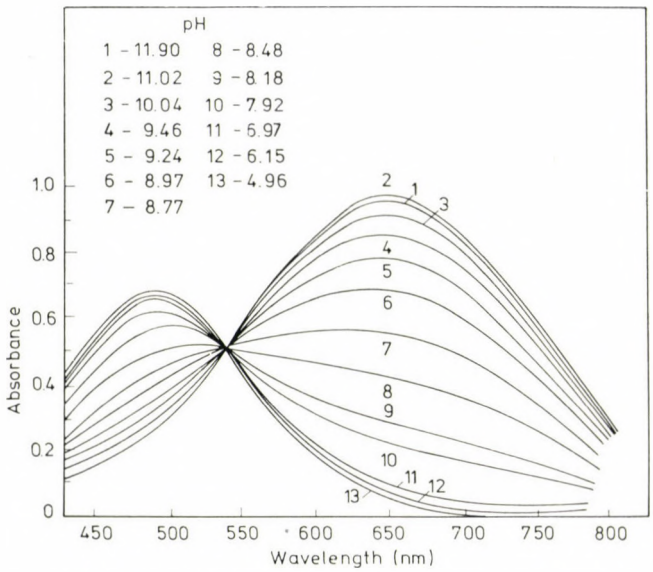

Fig. 4. Spectra of **Id** in universal buffer solutions

1. Half height method [12].
2. The limiting absorbance method as modified for stepwise equilibria.
3. The isobestic point method.
4. The COLLETER [13] method modified for acid–base equilibria [14].

The results obtained are given in Table IV. These results indicate that the pK value is dependent on the nature of the substituent at position 2 and

Table IV

Cumulative data obtained for series **I** *and* **II** *in universal buffer solutions*

λ_{max} = mm ε_{max} = cm^2 mole^{-1}

Compound	Nonionic form		Ionic form		Methods for calculation pK					ΔG^* Kcal/mole
	λ_{max}	$\varepsilon_{max} \cdot 10^{-4}$	λ_{max}	$\varepsilon_{max} \cdot 10^{-4}$	1	2	3	4	Average	
I*b*	485	0.457	642	0.602	8.80	8.78	8.34	7.72	8.66	11.67
I*c*	485	1.290	640	0.888	8.63	8.70	8.45	8.94	8.68	11.70
I*d*	492	0.670	650	0.960	8.66	8.66	9.40	8.81	8.63	11.63
II*a*	395	0.600	630	0.955	11.17	11.12	—	11.14	11.17	15.06
II*b*	505	0.770	650	0.950	9.30	9.25	—	9.26	9.27	12.49
II*c*	480	0.690	620	0.810	9.26	9.27	—	9.38	9.30	12.54
II*d*	479	0.530	615	0.880	9.29	9.30	9.24	9.30	9.28	12.51

1. Half height method
2. Modified limiting absorbance method
3. Isobestic point method
4. COLLETER method

at the nitrogen atom. Compounds of series **II** have pK values higher than that of series **I.** The alkylamino group antagonizes CT from the heteroatom to the quinone system through its high mesomeric effect. The basicity of the nitrogen atom increases and is reflected in a decreased charge transfer from the OH-group hence the acidity of the compound.

Generally, the pK increases as the donor character of the substituent increases. This can be ascribed to the increased charge transfer from both substituents to the hetero atom.

III. *IR-Spectra*

The band assignment is achieved using a method similar to that described by LOOKER [15]. The ν_{OH} band appears through the wide range 3200—3550 cm^{-1} while the broad ν_{NH} band locates near 3370 cm^{-1}. The spectra of all compounds exhibit three bands in the 1600—1680 cm^{-1} region which are characteristic of the quinone system (*cf.* Table V). The first two bands appearing near 1670 cm^{-1} and 1650 cm^{-1} correspond to the stretching vibrations of the non-polarized and polarized carbonyl groups, respectively.

The carbonyl group in position 4 is polarized under the influence of charge transfer from the hetero-atom and as well the substituent at position 2,

Table V

[*Solid state*[a] *infrared spectral data for series* **I** *and* **II**

$I_{a,b,c}$	I_b	I_c	I_d	II_a	II_b	II_c	II_d	Vibrational assignment
3540^m	3400^b	3360^b	3200^s	3530^b	3520^b	3550^s	3520^b	ν_{OH}
3120^b	—	—	—	3380^b	3380^s	3370^s	3370^s	ν_{NH}
1670^m	1670^{sh}	1655^{sh}	1665^m	1680^{sh}	1660^{sh}	—	1680^{sh}	$\nu_{C=O}$
1660^{sh}	1650^{sh}	1645^{sh}	1650^{sh}	1660^s	1650^w	1665^s	1668^s	$\nu_{polarized}$ C=O
—	—	—	—	1630^{sh}	1628^{sh}	1635^{sh}	1630^{sh}	δ_{NH}
1630^s	1622^s	1625^s	1620^s	1610^{sh}	—	1610^{sh}	1620^{sh}	$\nu_{C=C}$ conjugated with C=O
1250^s	1245^m	1240^m	1250^w	1210^b	1235^s	1245^s	1250^w	ν_{asy} = C—O—C
1110^s	1095^w	1112^m	1115^s	1085	1075^w	1085^w	1085^{sh}	$\nu_{C=OH}$
1020^w	1020^{sh}	1020^s	1030^s	1025^s	1015^w	1030^s	1030^s	ν_{sy} = C—O—C
858^s	860^w	865^s	880^s	880^s	867^s	875^s	878^s	γ isolated H-ring atom

a As KBr disc,

b Intensity of bands is given in s = strong, b = broad, m = medium, w = weak, sh = shoulder

c Absorption band frequencies are expressed in cm^{-1}

hence this group displays the lower frequency. The position of this band depends to an apparent extent on the substituents present while the band corresponding to the C=O group at position is slightly affected.

The nature of the substituents at position 2 and at the hetero atom thus affects the difference between the frequency of the two carbonyl groups. In case of the methoxy group at position 2 the difference is larger than if the substituent is an alkylamino group. This is due to higher antagonizing character of the alkylamino groups on the charge migration from the hetero atom leading to a decreased polarization of the carbonyl group in position 4. Also, on increasing the electron donating character of the substituents at the nitrogen atom, the polarization of the 4-carbonyl group increases leading to a shift of the band to lower frequency.

The carbonyl group at position 1 can form an intramolecular hydrogen bond with the hydrogen atom of the alkylamino group; a case which leads to decreased frequency of the band corresponding to this group.

The third band appearing near 1620 cm^{-1} — corresponds to stretching vibrations of the ethylenic bond in the quinone ring. The asymmetric and symmetric stretching bands of =C–O–C system appear near 1245 and 1020 cm^{-1}. Also, the ν_{C-OH} band can be observed in the range 1085—1115 cm^{-1}, while δ_{NH} band locates near 1630 cm^{-1}. On the other hand, the out-of-plane deformation bands of the aromatic ring hydrogen atoms are expected to appear below 1000 cm^{-1}.

REFERENCES

[1] Yoshida, Z., F. Takabayaski: Tetrahedron **24,** 933 (1968)
[2] Issa, R. M. and others: J. Chem. Soc. (1970) 1293, Egypt. J. Chem. (Special issue) **59** (1973)
[3] Hammam, A. S., Issa, R. M., Osman, A. M.: J. Chem. U.A.R. **15** (4), 391 (1970)
[4] Issa, R. M., Hammam, A. S., Ezzat, Inas I., Abd-el-Hamid, R.: J. Chem. U.A.R. **14** (5) 425 (1971)
[5] Issa, R. M., Hammam, A. S., Etaiw, S. H.: Z. Physik. Chem. **251,** 177 (1972)
[6] Inove, A., Nomira, Y., Kuraki, N., Koniski, K.: Yuksi Gasei-Kagakishi **16,** 536 (1958)
[7] Osman, A. M., Hammam, A. S.: Egypt J. Chem. **18,** 391 (1970)
[8] Vogel, A. I.: Practical Organic Chemistry, Longmans, London, 1956
[9] Britton, H. T. S.: Hydrogen Ions, Vol. I, 2nd Edit., Chapman and Hall, London, P. 365 (1952)
[10] Spruit, G. J. P.: Rec. Trav. Chim., **68,** 325 (1949)
[11] Gáti, L., Szalay L.: Acta Phys. Chem. **5,** 87 (1959)
[12] Issa, R. M. and others: Egypt. J. Chem. **14,** 113 (1971); Z. physik. Chem. N. F. **74,** 17 (1971)
[13] Colleter, J. C.: Ann. Chim. **5,** 415 (1960)
[14] Issa, R. M., El-Ezaby, M. S., Zewail, A. H.: Z. Physik. Chem. **244,** 155 (1970)
[15] Looker, J. H., Hanneman, Walter W.: J. Org. Chem. **27,** 381 (1962)

R. M. Issa
A. A. El-Samahy
I. M. Issa
S. H. Etaiw

Chem. Dep. Fac. of Science, Assiut University, Assiut A. R. Egypt.

Acta Chimica Academiae Scientiarum Hungaricae, Tomus 92 (3), pp. 223–236 (1977)

STUDY OF THE MECHANISM OF HEXENE RADIOLYSIS, II

INVESTIGATION OF *n*-HEXENE ISOMERS WITH ADDITIVES

A. KOVÁCS, GY. CSERÉP and G. FÖLDIÁK

(Institute of Isotopes of the Hungarian Academy of Sciences, Budapest)

Received October 11, 1975

The conclusions about the mechanism of formation of hydrogen and conjugated dienes and about the complex character of the process drawn from a study of cyclohexene radiolysis in the presence of scavengers [5] can be extended to *n*-hexene isomers, too. By investigations with radical and electron scavengers, the decomposition of 1-hexene involving a radical–ion intermediate and the internal rearrangement of the latter assumed earlier have been verified. These processes result in the formation of ethene and propene. Both radical and ionic reactions play a role in dimer formation but the importance of radical processes is greater in the radiolysis of hexenes with an internal double bond than assumed earlier [2]. It has been shown that isomerization also takes place during radiolysis of *n*-hexenes.

Introduction

The formation of both hydrogen and fragments from irradiated *n*-hexenes have already been studied in this laboratory: various mechanisms have been suggested for the formation of different products [1]. Our scavenger studies are aimed at verifying these hypotheses as well as at proving new mechanistic suggestions.

Literature survey

BRASH and GOLUB have determined the *G*-values of hydrogen, methane and dimers formed from *n*-hexene isomers [2]. They have found that in the dose range between 0 and $1.9 \cdot 10^{22}$ eV $\cdot$ g^{-1} the yields of these products are proportional to the dose, that is the *G*-values are dose independent. The dissolution of 2% iodine in 2-hexene resulted in the drop of $G(H_2 + CH_4)$ from 1.25 to 1.07. It has been assumed, therefore, that a considerable fraction of the gas (about 80%) is formed as a result of nonradical processes. CHANG *et al.* [3] studied the radiolysis of 1-hexene. The *G*-value of hydrogen plus methane was found to be 0.8—0.9, in a rather good agreement with the results mentioned above. At the same time, their $G(\text{dimer}) = 1.9$ value was different from that of BRASH and GOLUB, being $G(\text{dimer}) = 4.6$.

The radiolysis of *n*-hexene isomers has also been studied by CSERÉP and FÖLDIÁK [1]. Their data for hydrogen and methane yields are in a fairly

Table I

G-values of hydrogen and hydrocarbon fragments produced from n-hexene isomers

	1-hexene		2-hexene		3-hexene	
	Ref. [1]	This work	Ref. [1]	This work	Ref. [1]	This work
Hydrogen	0.900	0.956	1.370	1.357	1.640	1.610
	0.90*		1.17*		1.61*	
Methane	0.030	0.034	0.132	0.099	0.233	0.202
Ethane	0.028	0.030	0.107	0.092	0.160	0.120
Ethene	0.133	0.131	0.122	0.113	0.073	0.055
Acetylene	0.091	0.100	0.049	0.038	0.045	0.031
Propane	0.043	0.044	0.003	0.054	0.008	0.007
Propene	0.113	0.111	0.063	0.072	0.035	0.031
Cyclopropane	0.015	0.017	—	—	—	—
Propadiene	0.031	0.010	0.003	tr.	0.004	0.001
Butane	0.035	0.033	0.008	0.006	0.002	0.002
1-Butene	0.044	0.042	0.022	0.021	0.074	0.060
2-Butene	0.005	tr.	0.006	0.008	0.002	0.001
1,2-Butadiene	—	tr.	tr.	tr.	0.002	0.001
1,3-Butadiene	0.003	0.006	0.003	0.005	0.004	0.002
Pentane	0.001	tr.	0.001	0.008	0.002	0.008
1-Pentene	0.003	0.020	0.003	0.078	0.040	0.007
2-Pentene	0.004	0.001	0.001	0.050	—	0.007
1,3-Pentadiene	—	—	—	tr.	—	tr.
1,4-Pentadiene	—	—	—	tr.	—	—
2-Methyl-1-butene	—	—	—	tr.	—	—
3-Methyl-1-butene	—	—	—	tr.	—	—
2-Methyl-pentene	—	tr.	—	—	—	—
3-Methyl-1-pentene	—	0.020	—	—	—	—
4-Methyl-2-pentene	—	—	—	tr.	—	tr.
1-Hexene	—	—	—	0.190	—	—
trans-2-Hexene	—	tr.	—	—	—	—
cis-2-Hexene	—	tr.	—	—	—	—
trans-1,3-Hexadiene	—	—	—	—	—	0.053
1,5-Hexadiene	—	0.054	—	0.049	—	0.141
cis-1,3-Hexadiene	—	tr.	—	—	—	0.041

* Ref. [2]
tr.: $< 0.001\ G$

good agreement with those of BRASH and GOLUB, in addition, yields for several fragments have been reported. The influence of the position of the π-bond on the product yields has been demonstrated, together with the effects of the

terminal carbon atom and unpaired electrons of radicals produced during radiolysis. As a result, it has been verified that the relative bond energies have a decisive importance in determining the product composition.

Experimental

The present work involved the study of radiolysis of 1-hexene, *trans*-2-hexene and *trans*-3-hexene in the presence of electron (CCl_4), positive ion (C_2H_5OH) and radical (*p*-benzoquinone) scavengers. The concentrations of additives were 0.005, 0.05 and 0.2 mol l^{-1} for carbon tetrachloride and ethanol, whereas for *p*-benzoquinone, the corresponding values were 0.005, 0.01 and 0.05 mol l^{-1}.

Alkenes have been supplied by FLUKA; they were of "purum" grade, with a purity of 99%. Carbon tetrachloride (of 99% purity) was purchased from "Biogal" (Hungary), ethanol and *p*-benzoquinone from "Reanal" (Hungary).

Sample preparation, irradiation and analysis have been described earlier [4, 5].

Irradiations have been carried out in the ^{60}Co γ-facility of the Institute, with a nominal radioactivity of 3.10^{11}Bq (80.000 Ci). The dose rate was 2.5×10^{11} $eVg^{-1}s^{-1}$ the integral dose $(5 \pm 0.3) \times 10^{22}$ eVg^{-1}. Alcoholic chlorobenzene dosimetry was used for dose determinations [6].

Results

Table II

G-values of dimeric products of radiolysis of n-hexene isomers

Retention index of dimer	1-hexene	2-hexene	3-hexene	Retention index of dimer	1-hexene	2-hexene	3-hexene
1008.7	—	—	tr.	1093.6	—	0.028	0.071
1040.2	—	0.038	—	1098.3	0.090	—	—
1041.2	—	0.069	0.273	1099.1	—	0.070	—
1044.5	—	0.044	—	1101.1	—	0.070	—
1048.6	—	0.087	0.489	1103.8	0.050	—	—
1050.0	—	0.136	0.534	1104.4	—	0.180	—
1051.9	—	—	0.353	1109.2	—	0.026	0.035
1052.5	—	0.044	—	1111.0	—	0.036	—
1054.1	—	—	0.092	1112.8	—	0.088	0.038
1056.8	—	tr.	0.189	1117.6	—	tr.	—
1059.9	—	0.044	0.453	1122.7	—	—	0.165
1062.0	—	0.057	0.546	1127.3	—	0.084	—
1066.1	—	0.058	0.617	1133.0	0.054	—	—
1068.6	—	0.029	0.368	1137.7	0.022	—	—
1072.7	—	tr.	tr.	1148.3	0.035	—	—
1075.7	—	—	0.021	1152.2	0.118	—	—
1081.5	—	0.045	0.360	1160.7	0.054	—	—
1084.9	—	—	0.038	1163.6	0.087	—	—
1092.1	—	—	0.058	1179.6	0.390	—	—

Conditions of analysis: 100 m capillary column coated with squalane at 120 °C
tr.: < 0.001 *G*

The product yields obtained in the present work — together with literature data [1] — are listed in Tables I and II. The product spectrum contains several compounds not reported in the literature so far (*e.g.* 1,5-hexadiene, 1,3-hexadiene). Owing to analytical difficulties, not every dimeric product could be identified in all cases.

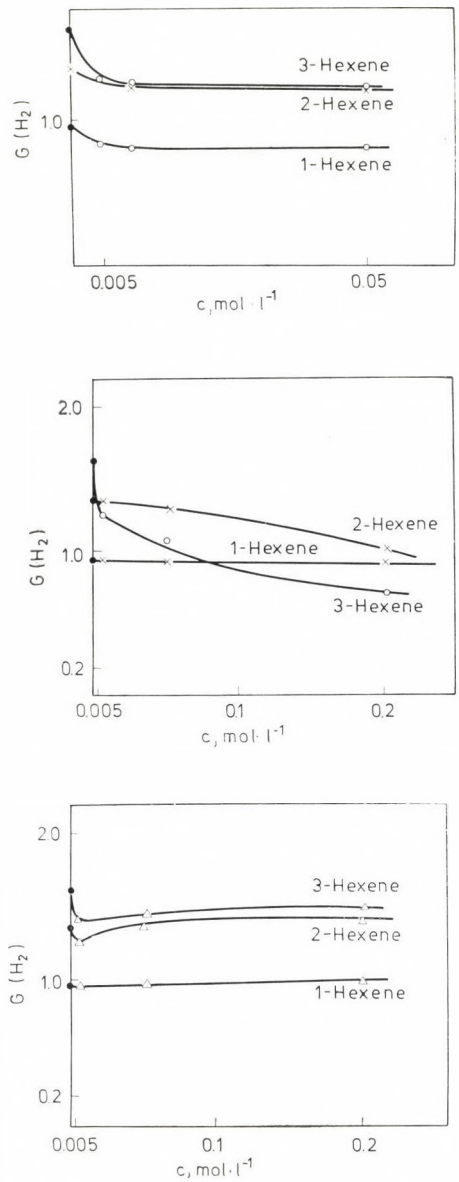

Fig. 1. The yield of hydrogen produced from irradiated *n*-hexene isomers as a function of the concentration of *a*) *p*-benzoquinone; b) carbon tetrachloride; c) ethanol

Hydrogen formation

As can be seen from the results reported (Fig. 1), the $G(H_2)$ value of hexene isomers increases with the shift of double bond towards the center of the molecule. CSERÉP and FÖLDIÁK have attributed this phenomenon to the different number of allylic hydrogen atoms in various hexene isomers [4].

The electron scavenger (CCl_4) decreased the hydrogen yield from all hexene isomers. At the same time, the addition of a positive ion scavenger causes a minimum in the $G(H_2)$ value as a function of ethanol concentration in 2- and 3-hexene; the minimum is close to 0.005 mol l^{-1} ethanol. Hardly any change is observed in 1-hexene under the effect of ethanol.

The radical scavenger (*p*-benzoquinone) decreases the $G(H_2)$ values of all hexene isomers: by about 10% for 1- and 2-hexene and by about 25% for 3-hexene.

Fragmentation

The yield of hydrocarbon fragments from *n*-hexenes is about three times higher than from cyclohexene [5]. The methane yield increases in the following order: 1-, 2-, 3-hexene. Earlier work [1] attributes this effect to the increase of the number of terminal methyl groups as well as to the directing effect of the π-bond.

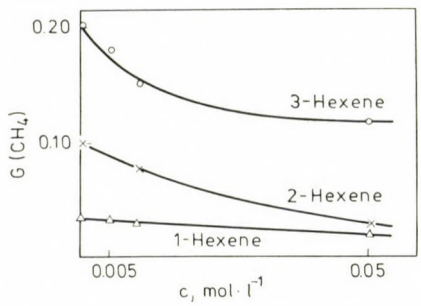

Fig. 2. The yield of methane from hexenes as a function of *p*-benzoquinone concentration

With increasing concentration of radical scavenger, the methane yield from all hexene isomers gradually decreases (Fig. 2). Both the electron and positive ion scavengers decrease the yield of methane from 1- and 3-hexene, while in the case of 2-hexene, only CCl_4 in high concentration causes a considerable drop of the yield (Fig. 3).

While the ethane yield from 3-hexene decreases under the effect of the electron and positive ion scavengers, $G(C_2H_6)$ from each isomer decreases considerably in systems containing *p*-benzoquinone (Fig. 4).

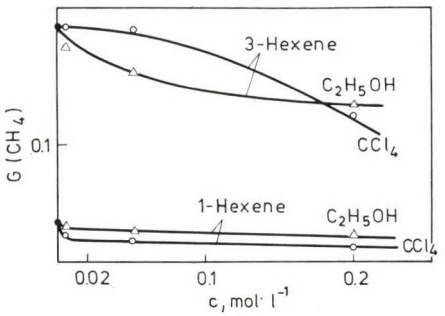

Fig. 3. The yield of methane from 1- and 3-hexene as a function of carbon tetrachloride and ethanol concentration

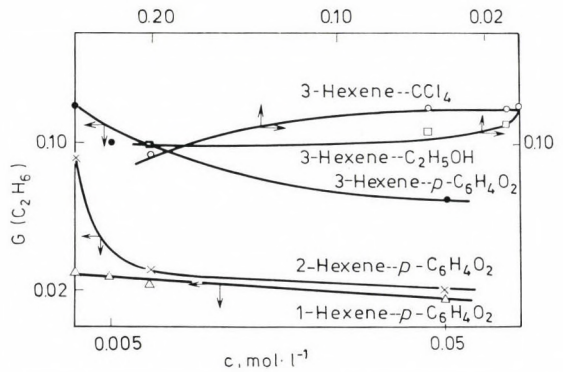

Fig. 4. The effect of scavengers on the yield of ethane from *n*-hexene isomers

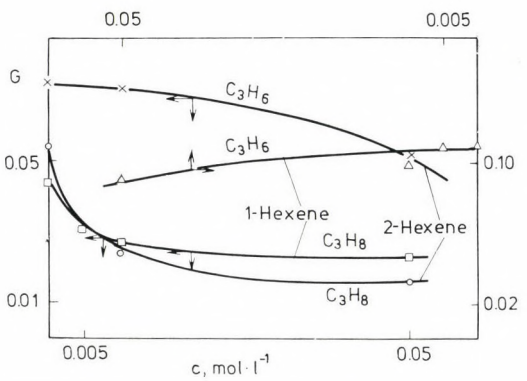

Fig. 5. The yield of propane and propene from 1- and 2-hexene in the presence of the radical scavenger

Electron and positive ion scavengers decrease the ethene yield from 1-hexene; *p*-benzoquinone exerts and analogous effect on 2-hexene radiolysis.

Of C_3 products, the yield of propene from 1- and 2-hexene decreases in the presence of CCl_4, and so do the yields of propane and propene from 1- and 2-hexene in the presence of *p*-benzoquinone (Fig. 5); no change has been observed with 3-hexene.

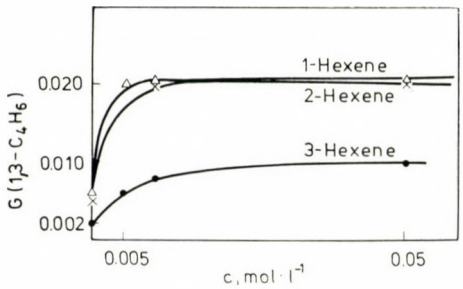

Fig. 6. The yield of 1,3-butadiene from irradiated hexene isomers as a function of *p*-benzoquinone concentration. (Points represent experimental data, curves were fitted by calculation)

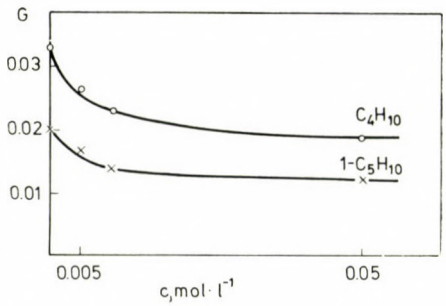

Fig. 7. The yields of butane and 1-pentene from 1-hexene in the presence of *p*-benzoquinone

Whereas the electron and positive ion scavengers have no effect on the yield of 1,3-butadiene, its yield increases considerably from each hexene in the presence of *p*-benzoquinone (Fig. 6).

The electron and positive ion scavengers have practically no effect on the yields of other C_4 and all C_5 products. With the radical scavenger, however, the yields of butane, 1-butene and 1-pentene from 1-hexene (Fig. 7), butane, 1-butene and 1-pentene from 2-hexene and 1- and 2-pentene from 3-hexene decrease.

The yields of other products included into Table 1 but not mentioned above were hardly or not at all influenced by the scavengers applied.

Formation of C_6 products

The yield of 3-methyl-1-pentene formed from 1-hexene decreases in the presence of the radical scavenger.

Both electron and radical scavengers decrease considerably the yield of 1,5-hexadiene in the case of all hexene isomers (Fig. 8). C_2H_5OH causes a similar effect in the radiolysis of 1-hexene.

The *G*-values of two conjugated dienes formed from 3-hexene (*trans*- and *cis*-1,3-hexadiene) increase in the presence of *p*-benzoquinone (Fig. 9).

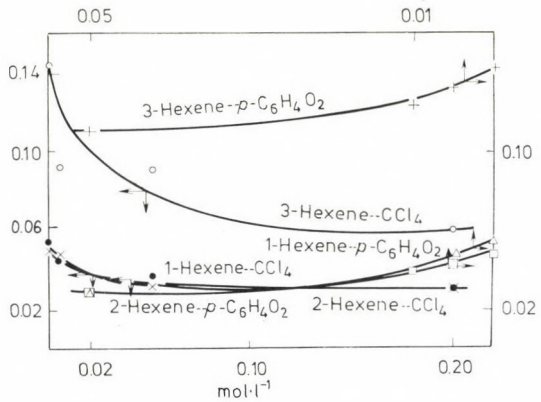

Fig. 8. The yields of 1,5-hexadiene as a function of the concentration of various additives

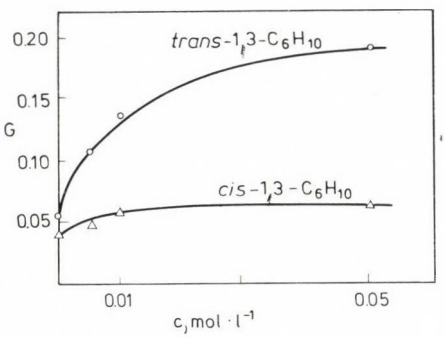

Fig. 9. The yields of *trans*- and *cis*-1,3-hexadiene from 3-hexene as a function of *p*-benzoquinone concentration, (Points represent experimental values, continuous line: calculated curve)

Formation of dimers

The yield of dimers from 1- and 2-hexene is about twice lower, from 3-hexene, about twice higher than that from cyclohexene [5].

The study of the mechanism of formation of dimers in hexene radiolysis has been rendered more difficult by the lack of reliable reference substances;

thus various dimers have been characterized by their retention indices only. The dimers will be discussed as a group, rather than as individual compounds.

Much less dimer have been formed from 1-hexene than from the other two isomers. The total G-value of dimers ($G = 0.9$) is closer to CHANG's value of $G = 1.9$ [3] than to the $G = 4.6$ reported by BRASH and GOLUB [2] although the agreement cannot be regarded as good in the former case, either.

Four compounds were found among the products whose yields increase in the presence of CCl_4 and p-benzoquinone and decrease in the presence of

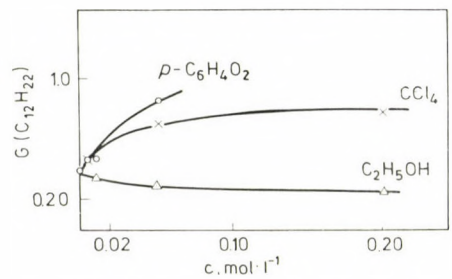

Fig. 10. The yield of ($C_{12}H_{22}$) dimer with R.I. = 1179.6 as a function of the additive concentration

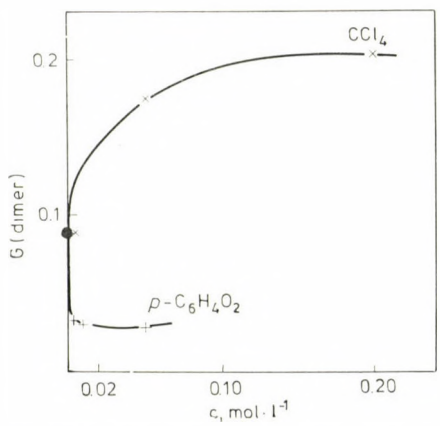

Fig. 11. The yield of dimer with R.I. = 1098.3 ($C_{12}H_{24}$), as a function of carbon tetrachloride and p-benzoquinone concentration

C_2H_5OH. Our assumption that these compounds contain two double bonds could be verified by mass spectrometry for one of them having a retention index (R. I.) of 1179.6, the formula found for this product being $C_{12}H_{22}$. The yields observed in the presence of various scavengers are shown in Fig. 10.

The formula of two other dimers could also be determined. The dimer with R.I. = 1152.2 is $C_{12}H_{22}$; its yield decreases under the effect of radical

scavenger. At the same time, the dimer with R.I. = 1098.3 has a composition of $C_{12}H_{24}$; its yield is increased by CCl_4 and decreased by p-$C_6H_4O_2$ (Fig. 11).

The behaviour of dimers from 2- and 3-hexene in the presence of various scavengers is more or less analogous.

22 components could be separated in the dimer range from irradiated 2-hexene; their total G-value was 1.23. BRASH and GOLUB, on the other hand, reported as few as 7 dimers but with a total G-value of 4.6 [2]. The yield of dimers from 3-hexene was $G = 4.7$, being only little higher than the value reported in Ref. [2]: $G = 4.1$.

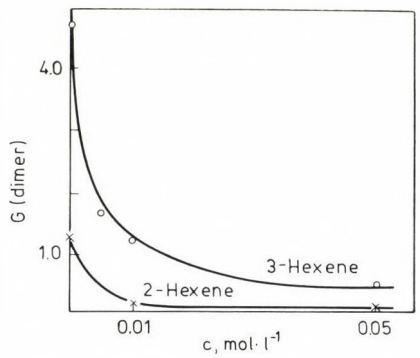

Fig. 12. The total dimer yield from 2- and 3-hexene as a function of p-benzoquinone concentration

The yield of some dimers increases in the presence of CCl_4 and decreases in the presence of ethanol; other dimers show a reverse behaviour. The admixture of the radical scavenger causes a considerable decrease in the yields of several dimeric products from both 2-hexene and 3-hexene radiolysis (Fig. 12).

Discussion

Isomerization processes

Of the products identified, *cis*-2-hexene and *cis*-3-hexene from *trans*-2-hexene, and *cis*- and *trans*-2-hexene from 1-hexene are due to isomerization processes.

The formation of 1-hexene from 2-hexene may be attributed partly to isomerization; in addition, disproportionation of hexenyl and hexyl radicals formed *via* dehydrogenation and addition, respectively, produces also 1-hexene.

The formation of 3-methyl-1-pentene involves a radical skeletal isomerization of 1-hexene, as shown by the decrease of its yield in the presence of p-benzoquinone.

Processes involving C–H bond rupture

As judged from the effect of various additives, similar reaction mechanisms of hydrogen formation from *n*-hexenes can be proposed as has been done for cyclohexene [5].

The character of the dependence of $G(H_2)$ on the concentration of the positive ion scavenger for 2- and 3-hexene (*cf.* Fig. 1/c) lends direct support to the assumption put forward for cyclohexene earlier [5], *viz.* that the overall process observed is the result of various competitive processes:

— the decrease of $G(H_2)$ in the presence of C_2H_5OH in low concentration may be attributed to the inhibition of electron–ion recombination by ethanol, decreasing thus the number of excited alkene molecules which are precursors of hydrogen;

— the increase of the yield at higher concentrations is due partly to H_2 originating from abstraction reactions between H-atoms, formed in the positive ion scavenging reaction and hexene molecules.

It can be concluded that hydrogen formation from *n*-hexenes involves two important reactions: electron–ion neutralization and — as assumed on the basis of data obtained in the presence of *p*-benzoquinone — radical processes.

1,5-Hexadiene is formed from all three hexene isomers: for 1-hexene it can be assumed that carbon tetrachloride and ethanol inhibit excitation, the radical scavenger, in turn, captures monoradicals formed *via* dehydrogenation; all these processes lead to the inhibition of combination reactions of C_3H_5 radicals formed as a result of the directing effect of the π-bond. Thus, the role of both ion recombination and radical processes can be regarded as verified in the formation of the compound in question.

On the basis of molecular structure and the scavenger studies, it is probable that the disproportionation of hexenyl radicals, formed in dehydrogenation steps, gives 1,5-hexadiene from 2- and 3-hexene since *p*-benzoquinone captures hexenyl radicals and carbon tetrachloride inhibits its precursor excited state; both processes decrease the hexadiene yield.

The yields of conjugated dienes: *trans*- and *cis*-1,3-hexadiene from 3-hexene increase upon admixture of *p*-benzoquinone. This can be explained by competitive reactions with various radicals in the system, analogously to cyclohexene [5] (*cf.* Fig. 9).

The data obtained by fitting a curve to the experimental points according to Eqs (19) and (20) in our previous paper [5] have been compiled in Table III.

The scavenger study of dimeric products obtained from hexene isomers allows to state, that 1-hexene with a terminal π-bond and 2- and 3-hexene with internal double bonds behave differently [2].

With 1-hexene, the addition of the radical scavenger leads to the decrease

Table III

Characteristics of conjugated diene formation from n-hexene isomers

Hexene isomer	Product	A(mol h^{-1})	B(mol)	G_0
1-Hexene	1,3-C_4H_6	3.4×10^{-4}	5×10^{-4}	0.025
2-Hexene	1,3-C_4H_6	3.24×10^{-4}	4.5×10^{-4}	0.022
	1,3-C_4H_6	1.51×10^{-3}	1.66×10^{-3}	0.011
3-Hexene	*trans*-1,3-C_6H_{10}	1.96×10^{-3}	3.2×10^{-3}	0.200
	cis-1,3-C_6H_{10}	1.7×10^{-4}	$5 \times 10^{-}$	0.061

of the yield of some dimers; thus they have been attributed to reactions of various radicals, first of all, hexyl and hexenyl radicals. The yields of dimers with R.I. = 1098.3, 1103.8 and 1163.6 increase upon CCl_4 and decrease upon *p*-$C_6H_4O_2$ addition: thus, it can be assumed that radical–ion intermediates also have an important role in their formation. The increase of the yields of dimers with R.I. = 1133.0, 1152.2, etc., under the effect of ethanol suggests that they involve radical type intermediates since, according to Eqs (3) and (4) in Ref. [5], a positive ion scavenger exchanges ion pairs into radicals; this is also supported by the decrease of their yields in the presence of the radical scavenger.

Supplementary studies have shown that the composition of products with R.I. = 1152.2 and 1179.6 is the same: $C_{12}H_{22}$; nevertheless, scavenger studies indicate different mechanisms of formation for them. Whereas a radical mechanism of formation is probable for the former, the role of ion–molecule reactions in the production of the latter is supported by the increase of the *G*-value upon CCl_4, and the decrease of the yield upon ethanol addition; the increase of its yield in the presence of the radical scavenger can be attributed to competing reactions.

The decrease of the *G*-value by ethanol and its increase under the effect of carbon tetrachloride in the case of some of the dimers of 2- and 3-hexene indicate ion–molecule condensation.

At the same time, several other dimers are formed *via* radical mechanisms, as supported by the decrease of their yields in the presence of the radical scavenger and carbon tetrachloride and the respective increase in the presence of the positive ion scavenger; this is analogous to the phenomena discussed in connection with cyclohexene dimerization [5].

On this basis it can be concluded that the importance of radical processes is greater, and that of ionic processes is less in the dimerization of 2- and 3-hexene than assumed previously [2].

Processes involving C–C bond rupture

The decrease of $G(CH_4)$ values in the presence of radical scavengers suggested a radical pathway for methane formation, involving mainly methyl radicals [4]. Thus, for 1-hexene processes (1a) and (2), for 2-hexene (1a), and for 3-hexene reactions (1a) and (1b) are probable:

$$C_6H_{12}^{*} \longrightarrow \begin{cases} CH_3 + C_5H_9 & (1a) \\ 2CH_3 + C_4H_6 & (1b) \\ C_2H_5 + C_4H_7 & (1c) \\ C_3H_7 + C_3H_5 & (1d) \end{cases}$$

$$C_3H_7 \longrightarrow CH_3 + C_2H_4 \qquad (2)$$

The importance of methyl radicals is supported also by the decrease of methane yield from 1- and 3-hexene under the effect of CCl_4 and C_2H_5OH and the same for 2-hexene in the presence of CCl_4, because these two scavengers decrease the number of excited hexene molecules by inhibiting electron–ion neutralization, thus decreasing the amount of methane produced.

The radical scavenger decreases the yield of ethane from 1- and 3-hexene by about 50%, and from 2-hexene by about 80%. This can be interpreted in terms of inhibition of methyl radicals produced in processes (1a) and (2) as well as of disproportionation and abstraction reactions with the participation of ethyl radicals formed in reaction (1c).

The decrease of $G(C_2H_6)$ in the radiolysis of 3-hexene indicates partly excitation transfer processes, partly neutralization reactions, supported also by the decrease of the yield in the presence of ethanol (Fig. 4).

The yield of ethylene from 1-hexene decreases in the presence of both CCl_4 and p-$C_6H_4O_2$, presumably owing to reactions (2)—(4) as well as radical–ion processes:

$$2C_2H_5 \longrightarrow C_2H_6 + C_2H_4 \qquad (3)$$

$$C_4H_7 \longrightarrow C_2H_4 + C_2H_3 \qquad (4)$$

Since none of the additives influences the yield of acetylene from any of the hexene isomers, it is presumably produced from directly excited alkene molecules in very rapid processes.

The yields of propane and propene from 1- and 2-hexene decrease in the presence of the radical scavenger; this phenomenon verifies the role of mono-radicals produced in process (1d) and their disproportionation.

At the same time, the decrease of propane yield from 1-hexene in the presence of CCl_4 points to a pathway involving an internal rearrangement of the transition state as suggested Ref. [1].

The presence of the radical scavenger resulted in a considerable increase of the yield of 1,3-butadiene from all three hexene isomers. This is analogous to diene formation from cyclohexene and hexadiene formation from *n*-alkenes and can be explained by competition between the conjugated dienes formed and the radical scavenger admixed. The characteristic values calculated on the basis of Eqs (19)—(20) of Ref. [5] are shown in Table III. On this basis it can be stated that the initial butadiene yield (G_4) is higher than that determined from the final product spectrum, owing to the further reactions of these rather reactive compounds.

The radical way of formation of C_4-C_5 products has been verified by the yield drops of butane, 1-butene and 1-pentene from 1-hexene, of butane and 2-butene from 2-hexene and of 2-pentene from 3-hexene in the presence of *p*-benzoquinone.

REFERENCES

[1] Cserép, Gy., Földiák, G.: Acta Chim. (Budapest) **83** 171 (1974)
[2] Brash, J. L., Golub, M. A.: Can. J. Chem., **46,** 594 (1968)
[3] Chang, P. C., Yang, N. C., Wagner, C. D.: J. Amer Chem. Soc., **81,** 2060 (1959)
[4] Földiák, G. et al.: „A kémia újabb eredményei". Vol. 20, Akadémiai Kiadó, Budapest, 1974
[5] Kovács, A., Cserép, Gy., Földiák, G.: Acta Chim. (Budapest) Inpress
[6] Horváth, Zs., Bányai, É., Földiák, G.: Radiochim. Acta, **13,** 150 (1970)
[7] Sato, G., Yugeta, R., Shinsaka, K., Terao, T.: Bull. Chem. Soc. Japan, **39,** 150 (1966)
[8] Nakagawa, T., Takamuku, S., Sakurai, H.: Bull. Chem. Soc. Japan, **40,** 2773 (1967)
[9] Hatano, Y., Shida, S., Sato, S.: Bull. Chem. Soc. Japan, **41,** 1120 (1968)

András Kovács
György Cserép
Gábor Földiák

H-1525 Budapest, Pf. 77.

Acta Chimica Academiae Scientiarum Hungaricae, Tomus 92 (3), pp. 237—247 (1977)

TPD STUDY OF THE "STABILITY" OF H_2 CHEMISORBED ON Al_2O_3 AND PT

D. MÓGER, G. BESENYEI, G. KOVÁCS and F. NAGY

(Central Research Institute for Chemistry, Hungarian Academy of Sciences)

Received November 1, 1975

In a TPD study of hydrogen chemisorption on Al_2O_3 and Pt catalysts above room temperature the following has been established.
(1) If the adsorption is carried out according to an adequate program, then, in the case of a Pt catalyst, in contrast to the literature, not two but three peaks are found in the thermodesorptogram. The new peak appears between those of hydrogen types γ and δ described in the literature.
(2) In the case of both Al_2O_3 and Pt we have worked out adsorption programs which ensure the appearance of only a single peak at a time, *i.e.* the catalyst contains only one type of adsorbed hydrogen.
(3) The stability of catalysts and adsorption states with respect to time, described in the previous paragraph permits to examine the role of adsorbed hydrogen assigned to the various desorption peak maxima in catalytic reactions.

Introduction

Since the advent of the temperature programmed desorption (TPD) technique [1], the chemisorption of hydrogen on various adsorbents and catalysts has been studied extensively. Attempts have been made to find a relationship between TPD characteristics (*viz.* the temperature at which a desorption peak appears, the peak area, etc.) and the catalytic activity [2]. Al_2O_3 and Pt, as well as platinum supported on Al_2O_3 catalyze several reactions in which hydrogen is involved as a reactant. This is the reason why numerous papers deal with the TPD study of hydrogen chemisorption on both Al_2O_3 and Pt [3, 4, 5]. Relatively few communications report on the role of adsorbed hydrogen corresponding to the different peak maxima in certain catalytic reactions. Examinations of this kind should provide information on whether a catalyst containing hydrogen attributed to a single peak maximum can be obtained, and whether this chemisorption state may be considered as "stable" compared with the time required by usual laboratory kinetic measurement. In the present paper we report on the results of our experiments in this field.

Experimental

The instrument was designed according to general principles applied in the construction of TPD apparatus. A thermal conductivity cell was used as detector. Al_2O_3 was used in the form of extrusions (CK-300 KETJEN, specific surface area 180 m^2/g). The Pt catalyst was prepared by reduction of a 0.16 *M* aqueous solution of H_2PtCl_6 with hydrogen. As the TPD technique requires a thermal treatment at about 500 °C, to avoid further sintering, the catalyst was treated in a stream of H_2 for 2 hrs at 650 °C, and used in the chemisorption measurements after this procedure (specific surface area 0.1 m^2/g). For comparison, chemisorption measurements — after a similar pretreatment — on commercial "Adams" and "Platinschwarz" catalysts were also carried out. So-called "lamp nitrogen" was used as an inert gas. In order to remove oxygen, the nitrogen was passed through a copper contact at 200 °C, and then, for removal of condensable impurities and water, it was passed through a trap cooled with a dry ice-acetone bath, followed by a 4A molecule sieve. H_2 was admitted into the TPD apparatus after passing through a solution containing the Cr^{II}–Cr^{III} redox system, a liquid N_2 trap and an adsorption column filled with 4A molecule sieve.

For the activation of Al_2O_3, the following procedure was performed.

(1) Thermal treatment in a H_2 stream.
   a) Gradual increase of the temperature from 25 to 450 °C in 2 hrs.
   b) Heating for 30 min at 450 °C.
   c) Raising the temperature to 550 °C in 30 min.
   d) Heating for 1 hr at 550 °C.

(2) The catalyst was evacuated with a diffusion pump at 550 °C until the pressure reached 10^{-4} Torr.

(3) The sample was cooled down to room temperature in a N_2 stream and stored in N_2 atmosphere.

The experiments to be described were concerned only with desorption above 0 °C.

Results

(A) *The system involving Al_2O_3 and H_2*

The amount of chemisorbed H_2 is maximal (Fig. 1) if the adsorption is carried out according to the following program.

(1a) Sample stored under N_2 is warmed up to 500 °C and at this temperature N_2 is replaced by H_2,

(1b) the sample is kept for 30 min at 500 °C in a H_2 stream of 1 atm pressure, then

(1c) in about 15 min, the temperature is decreased to 350 °C, and

(1d) the sample is left for 1 hr at this temperature and subsequently

(1e) the adsorbent is slowly cooled down to 100 °C in about 90 min,

(1f) the catalyst is kept for 1 hr at 100 °C, and

(1g) also in a H_2 stream, the catalyst is allowed to cool down to room temperature and it is stored in a H_2 atmosphere until starting TPD.

Before recording the thermodesorptograms, nitrogen was replaced by hydrogen at 0 °C and, subsequently, the temperature program was initiated.

Figure 1 shows that the thermodesorptogram obtained is in fair agreement — except for the small peak maximum appearing at 30 °C — with that obtained by AMENOMIYA [3]. Thus, the Al_2O_3 studied by us contains chemisorbed H_2 of types H(III), H(IV) and H(V), in terms of his nomenclature (numbered

in the order of peak maxima of increasing temperature). Thermodesorptograms obtained in this manner were reproducible, regarding both the positions and the heights of peak maxima.

In order to study the stability of adsorbed hydrogen, the above set of measurements was repeated so that prior to TPD, nitrogen was passed for 70 hrs through the Al_2O_3 catalyst saturated with hydrogen. After this pretreatment the thermodesorptogram was recorded, and again the curve shown in Fig. 1 was obtained within the range of experimental error.

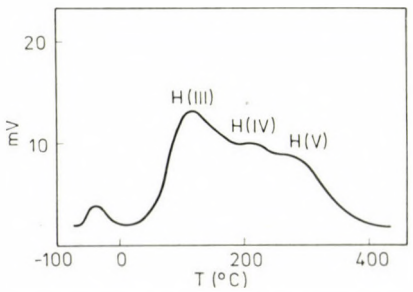

Fig. 1. Thermodesorptogram of Al_2O_3 covered maximally with hydrogen

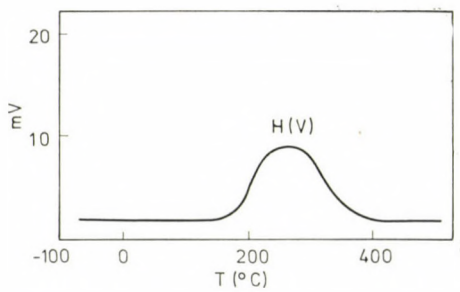

Fig. 2. Thermodesorptogram of Al_2O_3 containing chemisorbed hydrogen of type H(V)

The Al_2O_3 catalyst contains only hydrogen of type H(V) if saturation with hydrogen is carried out according to the following program.

(2a)—(2d) same as (1a)—(1d)

(2e) In ca. 10 mint the catalyst was slowly cooled down to 150 °C in a stream of hydrogen, then

(2f) after evacuation, the adsorbent was washed with nitrogen for about 30 min,

(2g) also in a N_2 stream, the catalyst was cooled down to room temperature.

On recording the thermodesorptogram after the above procedure, the curve shown in Fig. 2 is observed. Only a single peak appears on the curve

whose maximum ($\sim$ 280 °C) corresponds to that of a third peak obtainable in the case of full hydrogen coverage (*cf.* Fig. 1), which — as already mentioned — was considered to be of type H(V). By means of the adsorption program described, it can be accomplished that the Al_2O_3 should contain chemisorbed hydrogen which desorbs only at the highest temperature, and this type H(V) is not converted into hydrogen of types H(III) and/or H(IV).

The greatest part of the hydrogen is of type H(III), if the adsorption of hydrogen on Al_2O_3 is as follows.

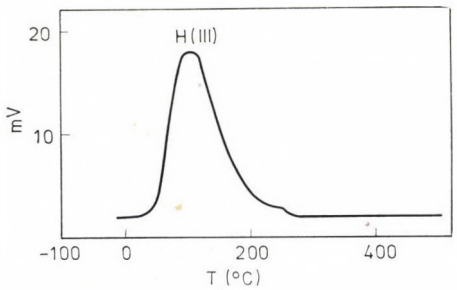

Fig. 3. Thermodesorptogram of Al_2O_3 containing mainly type H(III) of chemisorbed hydrogen

(3a) H_2-free catalyst stored under N_2 is warmed up to 100 °C and after evacuation the hydrogen stream is started,

(3b) the catalyst is kept in a stream of H_2 for 2 hrs at 100 °C, afterwards cooled down to 25 °C also in a H_2 stream,

(3c) the catalyst is left in a H_2 stream at 25 °C for 10—15 hrs, then, decreasing the temperature to 0 °C, the hydrogen is flushed out with nitrogen.

When recording the thermodesorptogram after the above pretreatment, the curve in Fig. 3 is obtained. As can be seen in Fig. 1, the catalyst contains only hydrogen of type H(III), which has a thermodesorption peak maximum at $\sim$ 110 °C.

It is also possible to obtain an Al_2O_3 catalyst that contains chemisorbed hydrogen of types H(III) and H(IV), but not type H(V). In this case, the treatment with hydrogen is as follows.

(4a) The hydrogen-free catalyst kept under N_2 is warmed up to 160 °C, then, after evacuation, the hydrogen stream is started, and the adsorbent is left for 1 hr at this temperature,

(4b) also in a H_2 stream, the catalyst is allowed to cool down to 25 °C in 1 hr,

(4c) the adsorbent is further kept in a stream of H_2 for 10—15 hrs at 25 °C, then, while decreasing the temperature to 0 °C, hydrogen is replaced by nitrogen.

If the thermodesorptogram is recorded after applying the adsorption conditions given, the curve shown in Fig. 4 is obtained. It is to be seen that both H(III) and H(IV) types of chemisorbed hydrogen can be observed; however, hydrogen of type H(V) does not appear.

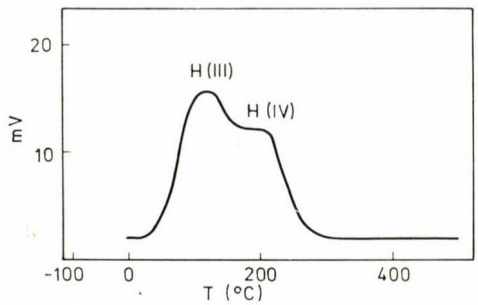

Fig. 4. Thermodesorptogram of Al_2O_3 containing chemisorbed hydrogen of types H(III) and H(IV)

(B) *The Pt–H_2 system*

In the case of a Pt catalyst maximum hydrogen coverage is found when adsorption is executed according to the following program.

(5a) The Pt powder is warmed up to 350 °C in a stream of nitrogen

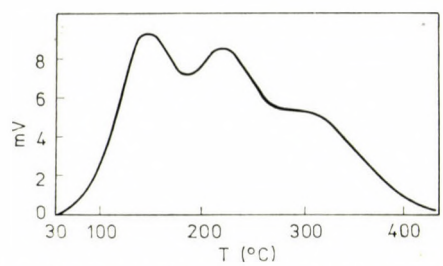

Fig. 5. Thermodesorptogram of the Pt catalyst prepared in this work, containing a maximal amount of chemisorbed hydrogen

After evacuation, the nitrogen is exchanged for H_2 and the catalyst is kept at this temperature for 1 hr, then

(5b) the adsorbent is cooled to 200 °C in a H_2 stream and this temperature is maintained for 40 min,

(5c) the system is slowly cooled down to 100 °C in about 40 min and the catalyst is kept for 20 min at this temperature,

(5d) also in a stream of H_2, the catalyst is cooled down to 0 °C in 1.5 hr, and then after evacuation, H_2 is replaced with nitrogen.

On recording the thermodesorptogram of the Pt catalyst after the above pretreatment, the curve shown in Fig. 5 is obtained. As described in the liter-

ature [6, 7], only two maxima in the thermodesorption curve of the Pt–H_2 system can be observed above 0 °C, referred to by CVETANOVIČ as γ and δ types of chemisorbed hydrogen.

In contrast to this, we have found 3 desorption peaks above 0 °C in the thermodesorptogram recorded. In order to examine to what extent this phenomenon is general, studies on "Adams" and "Platinschwarz" catalysts were also carried out. Figure 6 shows that in the case of both catalysts 3 desorption

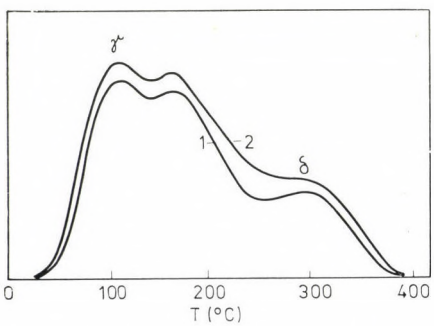

Fig. 6. Thermodesorptogram recorded in the case of maximal hydrogen coverage. (1) Adams, (2) Platinschwarz

peaks occur in the thermodesorptogram. The temperature for the new peak is ca. 220 °C which is between the temperatures (150 and 300 °C, respectively) corresponding to the γ and δ types of chemisorbed hydrogen.

Similarly as in the study of H_2 chemisorption on Al_2O_3, we searched for the sorption conditions under which only one peak for the hydrogen adsorbed on the catalyst appears.

There is a single desorption peak in the thermodesorptogram at 300 °C if the treatment with hydrogen is modified as follows.

(6a)—(6b) same as (5a)—(5b)

(6c) The system is evacuated at 200 °C (10^{-4} Torr) and, in about 10 min, the catalyst is cooled down to 0 °C. Subsequently, the apparatus is filled with nitrogen of ca. 1 atm pressure.

After the above pretreatment the thermodesorptogram shown in Fig. 7 is obtained. Only a single peak at about 300 °C can be observed in the TPD.

In order to check the "stability" of hydrogen, the measurement was repeated so that, before TPD, the catalyst was left for about 10—15 hrs in a stream of N_2 at 180 °C. This pretreatment did not cause any observable change in the thermodesorptogram.

Two desorption peaks are found in the thermodesorptogram (at 220 and 300 °C) if the pretreatment with hydrogen is carried out as follows.

(7a)—(7b) same as (5a)—(5b)

(7c) In about 1 hr the catalyst is cooled to 130 °C in a stream of H_2, then, after evacuation, the temperature is decreased to 0 °C. Afterwards the system is charged with N_2.

After application of these adsorption conditions, the thermodesorptogram shown in Fig. 8 is obtained. As can be seen from the figure, only two peaks occur in the curve, *viz.* at 220 and 300 °C.

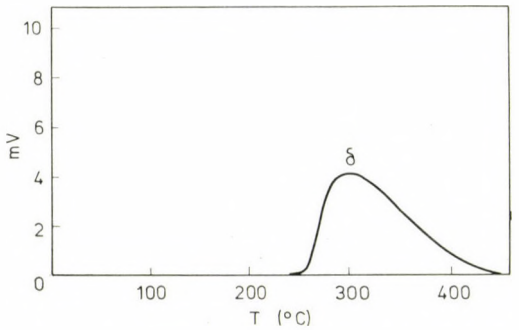

Fig. 7. Thermodesorptogram of hydrogen chemisorbed on Pt catalyst giving only one peak maximum at 300 °C

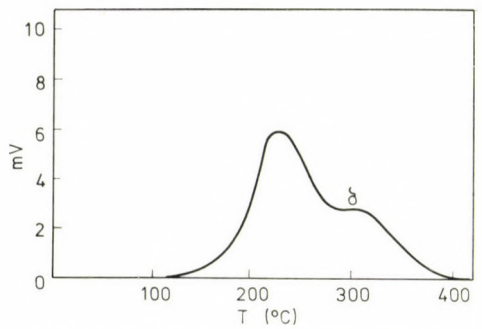

Fig. 8. Thermodesorptogram of Pt catalyst containing chemisorbed hydrogen resulting in peak maxima at 220 and 300 °C

It is also possible to prepare a Pt catalyst whose thermodesorptogram shows practically only one peak at 150 °C. To obtain this, the following treatment is required.

(8a) In a stream of N_2, the Pt is warmed up to 60 °C and, after evacuation, hydrogen of about 1 atm pressure is passed through the system for 2—3 hrs,

(8b) after cooling the catalyst to 0 °C in a H_2 stream, the system is pumped off and then filled up with N_2.

Figure 9 represents the thermodesorptogram determined after the above pretreatment. In this case, as can be seen, the catalyst practically contains only one type of chemisorbed hydrogen, with a desorption peak at 150 °C. The figure also shows that a small amount of hydrogen possessing a desorption peak maximum at 220 °C can also be found on the catalyst.

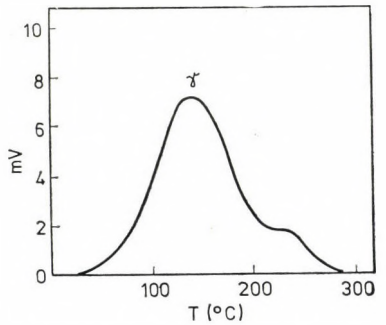

Fig. 9. Thermodesorptogram of hydrogen chemisorbed on Pt catalyst, giving practically only one peak maximum at 150 °C

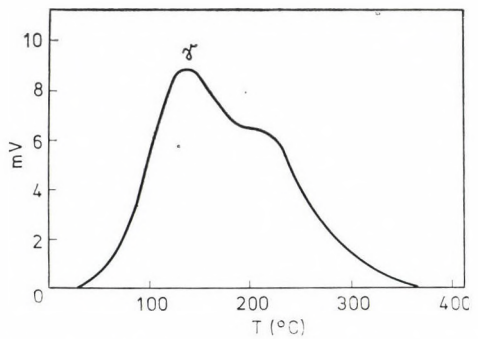

Fig. 10. Thermodesorptogram of hydrogen chemisorbed on Pt catalyst with peak maxima at 150 and 220 °C

The following treatment may also be performed but in this case two peaks at 150 and 200 °C can be observed.

(9a) The catalyst is warmed up to 100 °C in a N_2 stream, then, after evacuation, H_2 is passed through the apparatus for 40 min,

(9b) still in a stream of H_2, the catalyst is cooled to 0 °C in about 30 min and the system is filled up with N_2.

With the above adsorption conditions, the thermodesorptogram shown in Fig. 10 is obtained: two peaks appear, at 150 and 220 °C. The hydrogen type which has a desorption peak maximum at about 300 °C practically does not occur.

If the catalyst is warmed up to 160 °C after pretreatments (9a) and (9b), and is kept at this temperature until the H_2 detector returns to its normal position, then, after cooling the system to 0 °C, a repeated recording of the thermodesorptogram (between 0—400 °C) indicates that the catalyst is covered only with hydrogen giving a thermodesorption peak at 220 °C (*cf.* Fig. 11).

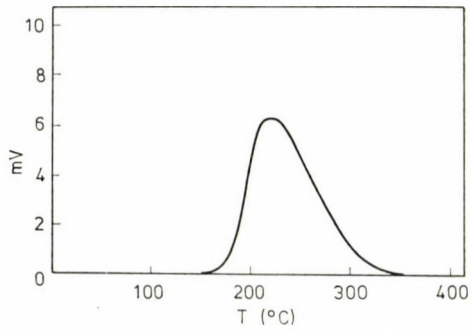

Fig. 11. Thermodesorptogram of a Pt catalyst containing chemisorbed H_2 with a peak maximum at 220 °C

In the case of both Pt and Al_2O_3, our only purpose was to examine if the types of chemisorbed hydrogen with desorption peaks at different temperatures may be separated from one another. Accordingly, in the present paper we are not concerned with the quantitative features of hydrogen chemisorption.

Discussion

The appearance of peaks in the thermodesorptograms is equivalent to the inhomogeneity of activation energies ($E_d^{\ddagger}$). There may be different interpretations of this phenomenon. The simplest is to assume that, if the activation energy of desorption is regarded as equal to the adsorption energy, there exist adsorption sites of different strength. This simple model is at variance with our observation supported also by CVETANOVIČ's measurements concerning the activation energy of adsorption, according to which the desorption of higher-temperature, *i.e.* stronger adsorption states can be observed only at higher temperatures. Hence, adsorption itself requires a considerable activation energy. In accordance with POLÁNYI's rule, however, if no structural differences among the adsorbed molecules are assumed, it is expected that the higher the bond energy, the smaller the activation energy of the bond-forming process, in this case adsorption. This difficulty seems to be resolvable if different structures or bonding forms are attributed to the adsorbed hydrogens resulting in desorption peaks at different temperatures. Essentially, this

has also been done by CVETANOVIČ when he has assigned the 4 desorption peaks (α, β, γ, δ) found in the case of Pt to H_2 molecules adsorbed on one site (α) and on two sites (β) as well as to hydrogen atoms adsorbed on one site (γ) and on two sites (δ), respectively. In terms of this model, the possible combinations are exhausted. Thus, if we want to model the adsorption state corresponding to the new peak found (it appears between the γ and δ peaks), we meet with difficulties. On the other hand, it would be highly speculative to give any model for adsorbed hydrogen, based only upon TPD measurements.

In the Al_2O_3 and Pt systems, comparison of the sums of the peak areas for hydrogens of types (III), (IV) and (V) (under identical experimental conditions, the area is proportional to the amount adsorbed) shows that if these adsorption states are prepared one by one, a larger value is obtained than in the case they are produced simultaneously. This seems to confirm that all three kinds of adsorbed hydrogen may be formed on the same surface.

The above observation may, however, be explained also by the assumption that the active sites of the adsorbent change owing to the effect of temperature, and this otherwise reversible process is stabilized by hydrogen adsorption.

In the case of platinum no similar phenomenon has been observed, so the assumption that the different activation energies of desorption are due to differences in the adsorption energies of the active sites is not inconsistent with the results. In the case of a Pt catalyst, we start from this supposition, though the possibility that hydrogen adsorption on active centers of different adsorption energies corresponds to various molecular states of hydrogen (*i.e.* H, H_2) cannot be precluded. Our observation that the different "active centers" may also be "filled up" selectively with hydrogen and, depending on the temperature, this state may persist for a long time (the transport of adsorbed hydrogen between different active sites requires an activation) permits to study the role of these active centers in hydrogenation reactions. We shall report on these studies in a forthcoming paper.

It should be noted that the generalization of our results concerning the Pt catalyst — although we undertook measurements on three sorts of catalysts — requires further studies, especially in the case of supported catalysts. These results as well as those in the literature indicate that the conditions of treatment, the chemical nature of the support and the Pt to support ratio affect very strongly the catalytic activity of Pt, consequently, the adsorption (desorption) properties of hydrogen probably depend on the above parameters, too.

REFERENCES

[1] CVETANOVIČ, R. J., AMENOMIYA, Y.: Adv. Catal., **17,** 103 (1967)
[2] SOKOLSKII, D. V.: Catalytic hydrogenation and oxidation (in Russian). Nauka, Kazakh SSR, Alma-Ata 1974
[3] AMENOMIYA, Y.: J. Catal., **22,** 109 (1971)
[4] TSUCHIYA, S., AMENOMIYA, Y., CVETANOVIČ, R. J.: J. Catal., **19,** 245 (1970)
[5] POPOVA, N. M., SOKOLSKII, D. V.: Conference on the mechanisms of heterogeneous catalytic reactions, Moscow 1974
[6] TSUCHIYA, S., AMENOMIYA, Y., CVETANOVIČ, R. J.: J. Catal., **20,** 1 (1971)
[7] MÓGER, D., KOVÁCS, G.: Magy. Kém. Foly., **81,** 123 (1975)

Dezső MÓGER
Gábor BESENYEI
Gizella KOVÁCS
Ferenc NAGY

H-1525 Budapest, Pf. 17.

Acta Chimica Academiae Scientiarum Hungaricae, Tomus 92 (3), pp. 249—262 (1977)

UNTERSUCHUNG DER SÄUERSTOFFÜBERSPANNUNG AN PLATINELEKTRODEN

ÜBER DIE DEUTUNG DER DURCH ε-CAPROLACTAM HERVORGERUFENEN ÜBERSPANNUNGSÄNDERUNGEN

T. ERDEY-GRÚZ†, GY. HORÁNYI* und É. SZETEY

(Lehrstuhl für physikalische Chemie und Radiologie, L. Eötvös-Universität, Budapest)

Eingegangen am 8. Januar 1976

Aufgrund unserer früheren Arbeiten wurde die Wirkung jener Faktoren untersucht, die bei der durch ε-Caprolactam hervorgerufenen Änderung der Sauerstoffüberspannung eine Rolle spielen.

Aus den kinetischen Gleichungen folgt, daß ein wesentlicher Teil der Überspannungsänderung die Folge der Abnahme der Wasserkonzentration und Elektrolytkonzentration ist.

Als Ergänzung der früheren experimentellen Arbeiten wurde die Dichte von Caprolactamlösungen in Wasser bzw. Elektrolytlösung gemessen und das Verhalten der Wasserstoffelektrode in konzentrierten Caprolactamlösungen untersucht. Diese Ergebnisse wurden zur Deutung der Überspannungserscheinungen herangezogen.

Unsere früheren Untersuchungen [1—5] bestätigten, daß die Änderung der Aktivität des Wassers durch Zugabe eines Nichtelektrolyts (ε-Caprolactam) eine Änderung der Sauerstoffüberspannung hervorruft. Im allgemeinen nimmt die Überspannung — in Abhängigkeit von der Natur der anwesenden Ionen — mit abnehmender Aktivität des Wassers zu. Dies steht vermutlich mit den Änderungen der Lösungsstruktur sowie mit Änderungen in der Doppelschicht und der Adsorption im Zusammenhang.

Aus der Literatur [6] geht hervor, daß in sauren Lösungen — um solche handelte es sich in unseren Versuchen — das Wasser als primär und geschwindigkeitbestimmend reagierende Komponente zu betrachten ist. Von dieser Annahme ausgehend besteht die Wirkung des Caprolactams darin, daß es die Konzentration der reagierenden Komponente verändert, wodurch die Überspannung beeinflußt wird. Darauf superponieren sich die sich in der Änderung der Aktivität des Wassers widerspiegelnden Strukturänderungen der Lösung sowie die Überspannungsänderungen infolge der Veränderung der Doppelschicht. Um also die sich aus den in der Lösungsstruktur und in der Doppelschicht vor sich gehenden Veränderungen ergebende Überspannungszunahme von jener trennen zu können, die auf die Änderung der Wasserkonzentration infolge der Gegenwart von Caprolactam zurückzuführen ist, muß geprüft werden, mit welchen Effekten im Idealfall — d. h. ohne wesent-

* Zentralforschungsinstitut für Chemie der Ungarischen Akademie der Wissenschaften. H-1525 Budapest.

liche Wechselwirkung der gelösten Komponenten und ohne Berücksichtigung der eventuellen Adsorption — gerechnet werden muß. Im weiteren behandeln wir diese Frage.

Kinetische Gleichungen bezüglich der Überspannung und der Geschwindigkeit der Sauerstoffabscheidung in caprolactamhaltigen Lösungen

In unseren früheren Mitteilungen berechneten wir die Überspannung η aus dem Zusammenhang

$$\eta = \varphi - E_{\text{rev}} = \varphi + \frac{RT}{4F} \ln \frac{\alpha p_0 a_v}{2} ,$$

wo E_{rev} die elektromotorische Kraft der Knallgaszelle, φ das Elektrodenpotential, gemessen gegen eine 1-Atm-Wasserstoffelektrode, die in eine Lösung gleicher Zusammensetzung wie die Prüflösung taucht, α der Dissoziationsgrad des Wasserdampfes, p_0 der Dampfdruck des reinen Wassers bei der Prüftemperatur und a_v die Aktivität des Wassers in der Prüflösung ist.

E_{rev} ist unabhängig davon, auf welche Weise die Aktivität des Wassers verändert wird; allein der Wert von a_v spielt eine Rolle. (Auch ist E_{rev} selbstverständlich eine Größe, die durch die in eine Lösung gleicher Zusammensetzung wie die Prüflösung tauchende 1-Atm-Wasserstoffelektrode und Sauerstoffelektrode bestimmt ist.)

Für eine gegebene Lösung ist also η ein eindeutig definierter, aus gut meßbaren bzw. berechenbaren Größen ableitbarer Wert.

Fraglich ist dagegen, inwiefern η-Werte, die in Lösungen mit verschiedenen Caprolactam-Konzentrationen bestimmt wurden, miteinander vergleichbar sind. Der Zusammenhang für E_{rev} zeigt nämlich nur an, wie sich — bei Veränderung der Aktivität des Wassers — der Potentialunterschied zwischen einer Sauerstoff- und einer Wasserstoffelektrode verändert, die in dieselbe Lösung tauchen. Dieser Zusammenhang sagt jedoch gar nichts darüber aus, wie groß der Potentialunterschied zwischen Wasserstoffelektroden oder Sauerstoffelektroden ist, die in zwei Lösungen mit unterschiedlicher Wasseraktivität oder in zwei verschiedene Lösungsmittel tauchen. Bekanntlich kann dieser Potentialunterschied nicht exakt bestimmt werden. Folglich ist ein derartiger Vergleich nur beschränkt gültig (siehe weiter unten).

In unseren früheren Versuchen wurde der Molenbruch des Wassers durch Auflösen von ε-Caprolactam im Bereich von 1,0—0,6 verändert. Unter solchen Bedingungen ergab sich — wie aus der angeführten Gleichung ersichtlich ist — keine wesentliche Änderung von η als Folge der Veränderung von E_{rev}, zumindest war die Änderung im Vergleich zu anderen Änderungen unwesentlich (die Verschiebung bei 20 °C betrug für eine Lösung mit $a_v = 0{,}5$ gegenüber

einer kein Caprolactam enthaltenden Lösung nur 13,5 mV). Die Überspannungsänderung gegenüber der reinen wäßrigen Lösung (für galvanostatische Messungen, auf die gleiche Stromdichte bezogen) ergibt sich, unter Berücksichtigung der folgenden Gleichung, in der alle invarianten Größen in K zusammengefaßt sind:

$$\eta = \varphi + \frac{3RT}{4F} \ln a_v + K = \varphi + \frac{3RT}{4F} \ln \gamma_v x_v + K ,$$

aus dem Zusammenhang

$$\Delta\eta = \eta_k - \eta_v = \varphi - \varphi_v + \frac{3RT}{4F} \ln \gamma_v x_v .$$

Hier ist η_k bzw. η_v die in der caprolactamhaltigen bzw. caprolactamfreien Lösung sonst gleicher Zusammensetzung gemessene Überspannung. Zwischen der Aktivität und dem Molenbruch des Wassers besteht, besonders bei 0,1 mol/l $HClO_4$ enthaltenden Lösungen, bei 25 °C kein nennenswerter Unterschied, der Aktivitätskoeffizient kann praktisch mit 1 angesetzt werden. (Im Molenbruchbereich von 0,908—0,653 liegt der Aktivitätskoeffizient zwischen 0,993 und 1,006.) Also ergibt sich mit guter Näherung

$$\Delta\eta \sim \varphi_k - \varphi_v + \frac{3RT}{4F} \ln x_v .$$

In schwefelsauren Lösungen weicht γ_v zwar stärker von 1 ab, jedoch ergibt sich auch bei diesen Lösungen kein nennenswerter Fehler, wenn man statt den Aktivitäten mit den Molenbrüchen rechnet.

In unseren vorangegangenen Mitteilungen wurde die Veränderung der Überspannung in Abhängigkeit von der Aktivität bzw. vom Molenbruch des Wassers angegeben. In den kinetischen Gleichungen wird jedoch die Konzentration im allgemeinen als mol/l angeführt. Es ist der Mühe wert, die Folgen dieses Unterschiedes eingehender zu überblicken.

Untersuchen wir zunächst, welche Form die kinetischen Gleichungen annehmen, wenn man die Konzentration in Molenbrüchen ausdrückt. Die Konzentration des Wassers c_v ist

$$c_v = \frac{1000\varrho x_v}{M_v x_v + M_k x_k + M_e x_e} ,$$

wo M_v, M_k bzw. M_e die Molekularmasse des Wassers, des Caprolactams bzw. des Elektrolyten und ϱ die Dichte der Lösung sind. Da die verschiedenen caprolactamhaltigen Lösungen so hergestellt wurden, daß das Caprolactam zu einer

gegebenen Masse der 0,1 mol/l $HClO_4$ enthaltenden Lösung zugegeben wurde, war das Verhältnis der Molenbrüche des Wassers und des Elektrolyten bei beliebiger Konzentration des Caprolactams stets gleich und identisch mit dem Molenbruchverhältnis der Grundlösung. Dieses Verhältnis, q, ist:

$$q = \frac{c_e^0 M_v}{1000\varrho_e - M_e c_e^0} = \frac{x_e}{x_v},$$

wo ϱ_e die Dichte der caprolactamfreien Elektrolytlösung und c_e^0 die Elektrolytkonzentration in dieser Lösung sind. Für 0,1 mol/l $HClO_4$ ist $q = 1{,}8 \cdot 10^{-3}$, d. h. ein ziemlich kleiner Wert.

Aufgrund der vorangegangenen Gleichung sowie unter Berücksichtigung dessen, daß die Summe der drei Molenbrüche zwangsläufig gleich eins ist, ergibt sich folgender Zusammenhang:

$$c_v = \frac{1000\varrho x_v}{M_k + x_v[M_v - M_k + q(M_e - M_k)]}.$$

Durch Umformung dieser Gleichung erhält man

$$c_v = \frac{1000\varrho}{M_k} \frac{x_v}{1 - x_v\delta}$$

mit $\delta = \beta + \gamma$ und

$$\beta = \frac{M_k - M_v}{M_k} \quad \text{bzw.} \quad \gamma = q\frac{M_k - M_e}{M_k}.$$

Für eine 0,1 M $HClO_4$-Lösung ist $\beta \gg \gamma$, folglich ist δ mit recht guter Näherung gleich β.

Wird vom einfachsten Modell des Mechanismus der Sauerstoffüberspannung ausgegangen, worin der mit Wasser verlaufende Ladungsübertritt als geschwindigkeitbestimmender Schritt betrachtet wird, so ist der bekannte Zusammenhang

$$i = z F k c_v \exp\left[-\frac{U_a^0 - \alpha z F \varepsilon}{RT}\right]$$

gültig, wo ε der Galvani-Potentialunterschied zwischen dem Elektrolyten und der Elektrode und c_v, die Konzentration des Wassers, in mol/l ausgedrückt sind (bezüglich der übrigen Zeichen s. [6]). Bekanntlich kann ε nicht bestimmt werden. Zwischen ε und dem gemessenen Potential φ besteht der Zusammenhang

$$\varphi = \varepsilon - \varepsilon_r,$$

wo ε_r der Galvani-Potentialunterschied der Referenzelektrode ist. Gemäß dem bereits bekannten Zusammenhang zwischen φ und η ist

$$i = z F k c_v \exp\left[- \frac{U_a^0 - \alpha z F \left(\eta - \frac{RT}{4F} \ln \frac{(\alpha p_0 a_v)^3}{2} + \varepsilon_r \right)}{RT} \right].$$

Die Referenzelektrode ist — wie bereits erwähnt wurde — die Wasserstoffelektrode, für die der Zusammenhang

$$\varepsilon_r = \varepsilon_r^0 + \frac{RT}{F} \ln a_{H+}$$

gilt.

Beim Vergleich der Daten der galvanostatischen Messungen stellen wir eigentlich die Frage, wie groß die Veränderung der Überspannung bei einer gegebenen Stromdichte infolge der Wirkung des Caprolactams ist. Dabei kann für den Unterschied zwischen der Überspannung η_k, gemessen in der caprolactamhaltigen Lösung mit der Wasserkonzentration c_v und der Überspannung η_v, gemessen in der caprolactamfreien Lösung mit der Wasserkonzentration c_v^0 ($\Delta\eta = \eta_k - \eta_v$), folgender Zusammenhang angegeben werden:

$$\Delta\eta = \frac{RT}{\alpha z F} \ln \frac{c_v^0}{c_v} + \frac{3RT}{4F} \ln \frac{a_v}{a_v^0} - \Delta\varepsilon_r ,$$

wo $\Delta\varepsilon_r$ die Differenz zwischen den Galvani-Potentialunterschieden der beiden Referenzelektroden ist:

$$\Delta\varepsilon_r = \varepsilon_r^k - \varepsilon_r^v .$$

Bei identischen Wasserstoffionenkonzentrationen bzw. -aktivitäten ist

$$\Delta\varepsilon_r = \Delta\varepsilon_r^0 .$$

Im vorangegangenen wurde bereits gezeigt, daß auch die Konzentration des Elektrolyten (der Wasserstoffionen) durch die Wirkung des Caprolactams verändert wird. Demgemäß taucht die Referenzelektrode in Abhängigkeit von der Caprolactamkonzentration jeweils in Lösungen mit unterschiedlichen Wasserstoffionenkonzentrationen. Folglich ist

$$\Delta\varepsilon_r = \Delta\varepsilon_r^0 + \frac{RT}{F} \ln \frac{a_{H+}^k}{a_{H+}^0} ,$$

bzw. unter Verwendung der Konzentration anstelle der Aktivitäten:

$$\Delta\varepsilon_r = \Delta\varepsilon_r^0 + \frac{RT}{F} \ln \frac{c_{H+}^k}{c_{H+}^0} .$$

(Um zu zeigen, daß diese Approximation berechtigt ist, werden im weiteren einige Versuchsergebnisse angeführt.)

Bei Annahme völliger Dissoziation ist

$$\frac{c_{H+}^{k}}{c_{H+}^{0}} = \frac{c_e}{c_e^0} .$$

$$\text{Da } \frac{c_e}{c_v} = \frac{c_e^0}{c_v^0} \text{, ist}$$

$$\frac{c_e}{c_e^0} = \frac{c_v}{c_v^0} .$$

Es ergibt sich also der Zusammenhang

$$\Delta\varepsilon_r = \Delta\varepsilon_r^0 + \frac{RT}{F} \ln \frac{c_v}{c_v^0} .$$

Die Berücksichtigung dieses Ausdruckes ergibt

$$\Delta\eta = \frac{RT}{\alpha z F} \ln \frac{c_v^0}{c_v} + \frac{3RT}{4F} \ln \frac{a_v}{a_v^0} + \frac{RT}{F} \ln \frac{c_v^0}{c_v} - \Delta\varepsilon_r^0$$

bzw. nach einer einfachen Umformung für den Fall $z = 1$:

$$\Delta\eta = \frac{RT}{F} \frac{\alpha + 1}{\alpha} \left[\ln \frac{c_v^0}{c_v} + \frac{\alpha}{1 + \alpha} \frac{3}{4} \ln \frac{a_v}{a_v^0} \right] - \Delta\varepsilon_r^0 .$$

Das erste Glied der rechten Seite der obigen Gleichung kann aus Versuchsdaten errechnet werden. Dasselbe gilt jedoch nicht für $\Delta\varepsilon_r^0$. Wasser bzw. Wasser und wesentliche Mengen an Caprolactam enthaltende Lösungen können im wesentlichen als verschiedene Lösungsmittel betrachtet werden, und in solchen Fällen kann $\Delta\varepsilon^0$ zur Zeit nicht exakt bestimmt werden. Aufgrund der Versuchsergebnisse könnten zwar bestimmte Annäherungen verwendet werden, doch würden diese den Rahmen der vorliegenden Arbeit weit überschreiten. In der Größe von $\Delta\varepsilon^0$ widerspiegeln sich alle Effekte, die Folgen der Strukturänderungen der Lösung sind.

Demgemäß liefert das erste Glied der obigen Gleichung, das im weiteren mit $\Delta\eta_I$ bezeichnet wird, eine Erklärung für nur einen Teil der Überspannungsänderung. Verwenden wir die Approximation $a_v/a_v^0 \approx x_v/x_v^0 \approx x_v$ und als Konzentrationsvariable den Molenbruch und berücksichtigen wir, daß

$$\frac{1000\varrho_e - M_e c_e^0}{M_v} = c_v^0 \text{ ist ,}$$

so erhalten wir folgenden Zusammenhang:

$$\Delta\eta_I = \frac{RT}{F}\frac{\alpha+1}{\alpha}\left[\ln\frac{M_k}{M_v} + \ln j - \ln\varrho + \ln\left(\frac{1}{x_v} - \delta\right) + \frac{\alpha}{1+\alpha}\frac{3}{4}\ln x_v\right],$$

mit

$$j = \left(\varrho_e - \frac{M_e c_e^0}{1000}\right).$$

Wie im folgenden gezeigt wird, sind die Dichten ebenfalls von den Molenbrüchen abhängig, da aber ihre Änderung sehr gering ist und ihr Wert nahe zu 1 liegt, ferner weil die Gleichung ihren Logarithmus enthält, können die Glieder $\ln j$ und $\ln \varrho$ in erster Näherung vernachlässigt werden. So ergibt sich

$$\Delta\eta_I = \frac{RT}{F}\frac{\alpha+1}{\alpha}\left[\ln\frac{M_k}{M_v} + \ln\left(\frac{1}{x_v} - \delta\right) + \frac{\alpha}{1+\alpha}\frac{3}{4}\ln x_v\right].$$

Der durch diese Gleichung beschriebene Zusammenhang besitzt Inflexionspunkte. Die erste Derivierte ist

$$\frac{\mathrm{d}\Delta\eta_k}{\mathrm{d}x_v} = \frac{RT}{F}\frac{1+\alpha}{\alpha}\left[-\frac{1}{(1-\delta x)\,x} + \frac{3}{4}\frac{\alpha}{1+\alpha}\frac{1}{x}\right].$$

Diese hat bei $1 > x_v > 0$ keine Nullstelle. Die zweite Derivierte kann in folgender Form angegeben werden:

$$\frac{\mathrm{d}^2\Delta\eta_k}{\mathrm{d}x^2} = \frac{RT}{F}\frac{1}{\alpha}\left[\frac{-4(1+\alpha)(1-2\delta x_v) - 3\alpha(1-\delta x_v)^2}{4(1-\delta x_v)^2 x_v^2}\right].$$

Diese Funktion nimmt im Intervall $0 < x < 1$ im Punkt

$$x = \frac{4+\alpha}{2\alpha\delta}\left(-1 + \sqrt{1 + \frac{3\alpha}{4+\alpha}}\right)$$

den Wert Null an. Für $\alpha = 1/2$ liegt dies bei $x_v = 0{,}54$.

Die aufgrund obiger Gleichung errechneten $\Delta\eta_I$-Werte sind als Funktion des Molenbruchs des Wassers — unter Annahme von $\alpha = 0{,}5$ — in Abb. 1 dargestellt.

Damit ist jener Teil der Überspannungsänderung festgelegt, der aus der Veränderung der Wasserkonzentration infolge der Gegenwart von Caprolactam herrührt. Die auf andere Ursachen zurückführbare Überspannungsänderung wird demgemäß durch Subtraktion dieser Größe aus den experimentell bestimmten Überspannungen erhalten.

Unsere bisherigen Überlegungen bezogen sich auf 0,1 *M* $HClO_4$-Lösung als Grundelektrolyt. Doch wird kein wesentlicher Fehler begangen, wenn man sie auch auf die experimentell untersuchten Systeme mit 0,1 Val/l H_2SO_4 als Grundelektrolyt ausdehnt. Zwar erscheint bei Schwefelsäure zunächst das Problem, daß das in der ersten Dissoziationsstufe gebildete HSO_4^--Ion sich

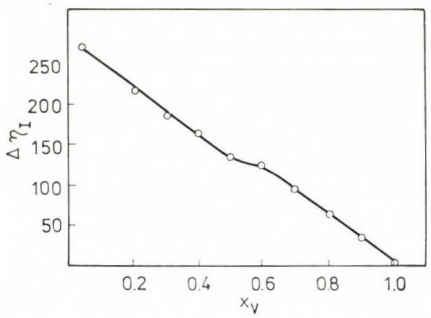

Abb. 1. Berechnete Werte von $\Delta\eta$ als Funktion des Molenbruchs des Wassers bei 0,1 mol/l $HClO_4$, unter der Annahme $\alpha = 1/2$

als schwache Säure verhält, so daß die Möglichkeit besteht, daß die Abnahme der Elektrolytkonzentration (bedingt durch die Zunahme der Caprolactamkonzentration) den Dissoziationsgrad, d. h. die Wasserstoffionenkonzentration ändert. Dies ist jedoch nicht der Fall. Schreibt man nämlich das Gleichgewicht für die Dissoziation des HSO_4^--Ions ($HSO_4^- + H_2O \rightleftharpoons H_3O^+ + SO_4^{2-}$) auf, so ergibt sich die Gleichgewichtskonstante

$$K = \frac{(1+\beta)\,\beta}{1-\beta}\,\frac{c_e^0}{c_v^0}$$

(statt Aktivitäten werden als Approximation die Konzentrationen verwendet; β ist der Dissoziationsgrad). In Gegenwart des als indifferent betrachteten Caprolactams gilt für das Gleichgewicht der Ausdruck

$$K = (1+\beta')\,\frac{\beta'}{1-\beta'}\,\frac{c_e}{c_v}\,.$$

Das Glied $(1 + \beta)$ stammt daraus, daß die erste Dissoziationsstufe der Schwefelsäure als vollständig betrachtet werden kann; c_e^0 bzw. c_e sind sinngemäß die Konzentration der Schwefelsäure. Da — wie früher gezeigt wurde — $c_e^0/c_v^0 = c_e/c_v$ ist, sind β und β' gleich, zumindest wenn sich die Aktivitäten nicht wesentlich von den Konzentrationen unterscheiden.

Bei schwefelsauren Caprolactamlösungen ist dies jedoch nur in erster Näherung annehmbar. Auch die Anwendung der oben abgeleiteten Gleichung für $\Delta\eta_I$ bei Schwefelsäure ist eine gröbere Approximation als bei Perchlorsäure, doch wird auch so kein großer Fehler gemacht (in der Gleichung würde der Logarithmus der Aktivitätskoeffizienten stehen). Bisher rechneten wir mit

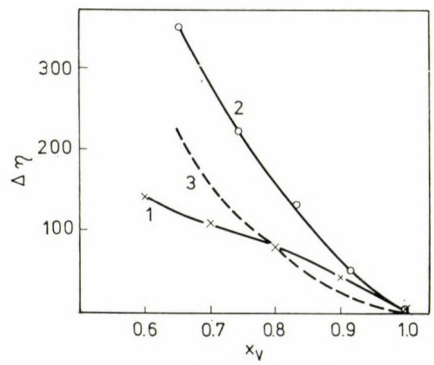

Abb. 2. Vergleich berechneter $\Delta\eta_I$ und gemessener $\Delta\eta$ Werte bei 0,1 val/l H_2SO_4
1 — berechnete Werte; 2 — gemessene Werte; 3 — $(\Delta\eta - \Delta\eta_I)$

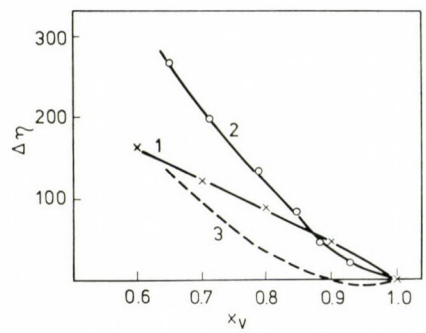

Abb. 3. Vergleich berechneter $\Delta\eta_I$ und gemessener $\Delta\eta$ Werte bei 0,1 mol/l $HClO_4$
1 — berechnete Werte; 2 — gemessene Werte; 3 — $(\Delta\eta - \Delta\eta_I)$

$\alpha = 1/2$; dies entspricht bei 25 °C einem Wert von 116 mV des Koeffizienten b der Tafelschen Geraden. Die Versuchsergebnisse zeigen, daß dieser Wert in perchlorsauren Lösungen $b = 130$ mV, in schwefelsauren Lösungen (abgesehen von den niedrigen Stromdichten) $b = 170$ mV ist. Dies entspricht α-Werten von 0,45 bzw. 0,34. Diese Werte müssen also in die Gleichungen eingesetzt werden. In Abb. 2 und 3 sind die auf diese Weise berechneten sowie die experimentell bestimmten Werte dargestellt.

Wie ersichtlicht, ist der Unterschied zwischen den berechneten $\Delta\eta_I$-Werten und den gemessenen $\Delta\eta$-Werten in perchlorsauren Lösungen wesent-

lich größer als in schwefelsauren Lösungen. Die zum Molenbruch 0,9 gehörenden Werte stimmen innerhalb der Versuchsfehlergrenze überein, hier ist also die Überspannungsänderung ausschließlich durch die Änderung der Wasserkonzentration bedingt. Wie aus der Abbildung ersichtlich ist, steigt der Unterschied $\Delta\eta - \Delta\eta_I$ besonders in den perchlorsauren Lösungen steil mit der Überspannung an. Eine quantitative Erklärung dieser Erscheinung läßt noch auf sich warten. Bezüglich der qualitativen Überlegungen hinsichtlich der Tendenzen verweisen wir auf unsere früheren Mitteilungen [1—5]. Jedenfalls bewiesen die obigen Ausführungen, daß die Änderung der Wasserkonzentration die Überspannung wesentlich beeinflußt. Damit wird die Annahme unterstützt, daß der Anodenvorgang von den Wassermolekülen ausgeht.

Anhang

Die Dichte der Lösungen

Um die in Molenbrüchen angegebene Zusammensetzung in mol/l auszudrücken, wurden — als Ergänzung unserer früheren experimentellen Arbeit — die Dichten der Lösungen bestimmt. Dabei kam eine interessante Eigenheit des Systems zum Vorschein.

Tabelle I

Dichte von Caprolactamlösungen

Konzentration Mol Caprolactam in 1000 g Lösungsmittel	Dichte g/cm³		
	Lösungsmittel		
	Wasser	0,1 mol/l $HClO_4$	0,1 val/l H_2SO_4
0	0,9970	1,0019	1,0016
5	1,0272	1,0312	1,0300
10	1,0413	1,0465	1,0417
15	1,0460	1,0488	1,0475
20	1,0499	1,0510	1,0515
25	1,0520	1,0547	1,0530
30	1,0525	1,0543	1,0533

In Tabelle I sind die bei 25 °C gemessenen Dichten von Caprolactamlösungen in elektrolytfreiem Wasser, in 0,1 mol/l $HClO_4$ und in 0,1 val/l H_2SO_4 angeführt. Diese Dichten sind in Abb. 4 gegen den Molenbruch des Wassers dargestellt. In der Abbildung sind außerdem noch einige Werte dargestellt, die in 1 mol/l $HClO_4$ gemessen wurden.

Aus der Tabelle und der Abbildung geht hervor, daß die Dichte mit steigender Konzentration der Lösungen in dauernd abnehmendem Maße

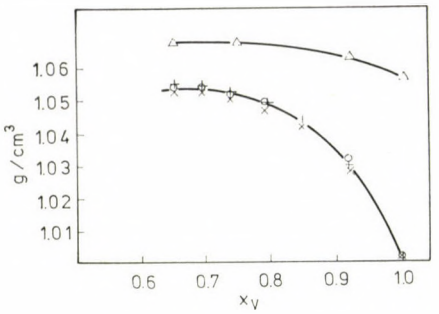

Abb. 4. Dichte von Caprolactamlösungen bei 25 °C; x — Wasser; + — 0,1 mol/l $HClO_4$; o — 0,1 val/l H_2SO_4; Δ — 1 mol/l $HClO_4$

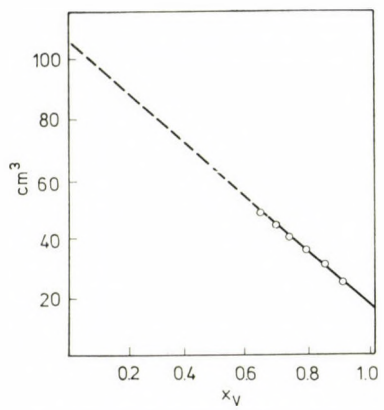

Abb. 5. Änderung des Molvolumens des Gemisches als Fuktion des Molenbruches des Wassers für 0,1 mol/l $HClO_4$

zunimmt; ihr Wert ist selbst in ungefähr 80 Gew.-% Caprolactam enthaltenden Lösungen ($x_v = 0{,}6$) auffallend gering ($\approx 1{,}060$).

Das Molvolumen der elektrolytfreien Lösungen V_M, berechnet aus dem Zusammenhang

$$V_M = \frac{M_k x_k + M_v x_v}{\varrho} = \frac{M_k - x_v(M_k - M_v)}{\varrho}$$

ändert sich nahezu linear mit dem Molenbruch des Wassers (Abb. 5). (M_k und M_v sind die Molekularmassen des Caprolactams bzw. des Wassers, x_k und x_v die Molenbrüche, ϱ die Dichte der Lösung.)

Für das Molvolumen kann also in erster Näherung der empirische Zusammenhang

$$V_M \approx A + Bx_v$$

angegeben werden, woraus — unter Berücksichtigung der Grenzfälle $x_v = 0$ und $x_v = 1$ — der Zusammenhang

$$V_M \approx V_k - (V_k - V_v)\, x_v$$

folgt. Hier sind V_k bzw. V_v das Molvolumen des Caprolactams bzw. des Wassers. Aus dem Gesagten folgt, daß das Molvolumen des Gemisches in erster Näherung als additiv aus den Molvolumina der Komponenten zusammengesetzt betrachtet werden kann.

Der Wert von V_k kann durch Extrapolation des empirischen Zusammenhanges bis $x_v = 0$ bestimmt werden und ergibt sich zu 105,6 cm^3/mol.

Für die Dichte kann demgemäß die Approximation

$$\varrho = \frac{M_k - x_v(M_k - M_v)}{V_k - x_v(V_k - V_v)} = \frac{M_v + x_k(M_k - M_v)}{V_v + x_k(V_k - V_v)}$$

angegeben werden. Zwischen den mit dieser Gleichung berechneten und den gemessenen Dichtewerten besteht kein nennenswerter Unterschied; dies ist ebenfalls ein Beweis dessen, daß das Molvolumen des Gemisches sich annähernd additiv aus den Molvolumina der Komponenten zusammensetzt.

Auch in den elektrolythaltigen Systemen ist dies praktisch der Fall, wenn wir die Grundlösung als eine einzige Komponente betrachten. Dies ist bei der 1 mol/l $HClO_4$-Grundlösung gut zu beobachten. Die Dichte der Grundlösung (1,0570) weicht nur geringfügig von der Dichte des Caprolactams (1,070) ab; demgemäß nimmt die Dichte nur wenig mit zunehmender Caprolactamkonzentration zu, wie aus Abb. 4 hervorgeht. Der Unterschied zwischen der additiv berechneten und der gemessenen Dichte ist auch in diesem Fall gering.

All diese Beobachtungen bezeugen, daß keine starken Wechselwirkungen zwischen dem Wasser und dem Caprolactam sowie zwischen dem Caprolactam und der Perchlorsäure bestehen. Mit der Feststellung, daß die Wechselwirkungen zwischen den Komponenten keine großen Effekte bezüglich der Aktivitäten und Volumenänderungen hervorrufen, es soll jedoch keineswegs behauptet werden, daß diese Wechselwirkungen keine Rolle in der Gestaltung bestimmter Eigenheiten des Systems, z. B. der Anzahl der in der Sauerstoffabscheidung teilnehmenden Wassermoleküle spielen könnten.

Abhängigkeit des Potentials der Wasserstoffelektrode von der Wasserstoffionenkonzentration in caprolactamhaltigen Lösungen

In Verbindung mit unseren früheren Untersuchungen tauchte die Frage auf, in welchem Maße das Caprolactam das Verhalten des Elektrolyts beeinflußt. Dies ist besonders hinsichtlich der Dissoziation der Säure, der Aktivität der Wasserstoffionen interessant. Da eine eingehende Prüfung dieser Frage schon zu weit von unserer ursprünglichen Zielsetzung liegt, führten wir nur einige Orientierungsversuche durch. Ausgehend aus einer Grund-Lösung der Molarität 20 Mol Caprolactam pro 1000 g Wasser, bereiteten wir Perchlorsäurelösungen folgender Konzentrationen: 1; 0,5; 0,1; 0,05; 0,01 mol/l. Dann wurde die elektromotorische Kraft einer Reihe von Konzentrationselementen ge-

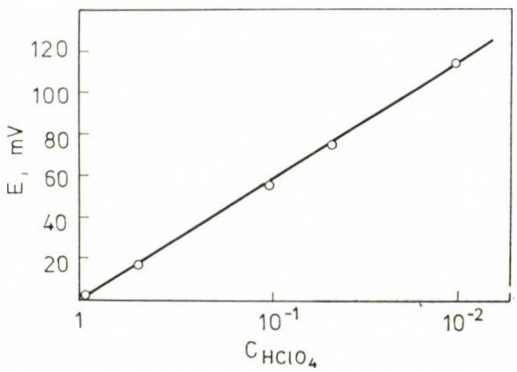

Abb. 6. Abhängigkeit des Potentials der Wasserstoffelektrode von der Perchlorsäurekonzentration in Gegenwart von 20 mol Caprolactam/1000 g Wasser

messen, wobei die eine Wasserstoffelektrode in die 1 mol/l $HClO_4$-Lösung tauchte, die andere in jeweils eine der obengenannten Lösungen. Die gemessenen Potentialunterschiede wurden gegen den Logarithmus der Perchlorsäurekonzentration in der zweiten Halbzelle aufgetragen (Abb. 6). Wie ersichtlich, ändert sich das Potential linear mit der Konzentration der Perchlorsäure, und die Richtungstangente der Geraden entspricht ungefähr 60 mV (die Messungen wurden bei Raumtemperatur durchgeführt). Daraus konnte gefolgert werden, daß das Nernstsche Gesetz auch in einer auf Caprolactam bezogen ziemlich konzentrierten Lösung mit guter Näherung gültig ist, daß die Aktivität der Wasserstoffionen (bzw. der Perchlorsäure) nicht wesentlich von der Konzentration abweicht, und die Dissoziation der Perchlorsäure auch unter diesen Bedingungen praktisch vollständig ist.

LITERATUR

[1] ERDEY-GRÚZ, T., GALLYAS, M., SZETEY, É.: Acta Chim. (Budapest) **69**, 203 (1971)
[2] ERDEY-GRÚZ, T., GALLYAS, M., SZETEY, É.: Acta Chim. (Budapest) **73**, 225 (1972)
[3] ERDEY-GRÚZ, T., GOLOPENCZA-BAJOR, O., GALLYAS, M.: Acta Chim. Acad. Sci. Hung., **50**, 179 (1966)
[4] ERDEY-GRÚZ, T., GALLYAS, M., SZETEY, É.: Acta Chim. (Budapest) **69**. 433 (1971)
[5] ERDEY-GRÚZ, T., SZETEY, É., HORÁNYI, G.: J. Electroanal. Chem., **65**, 177 (1975)
[6] ERDEY-GRÚZ T.: Elektródfolyamatok kinetikája. Akadémiai Kiadó, Budapest 1969

György HORÁNYI H-1025 Budapest, Pusztaszeri út 59—67.
Tibor ERDEY-GRÚZ†
Éva SZETEY H-1088 Budapest, Puskin u. 11—13.

Acta Chimica Academiae Scientiarum Hungaricae, Tomus 92 (3), pp. 263–270 (1977)

PREPARATION AND IR SPECTROPHOTOMETRIC STUDY OF CHARGE–TRANSFER COMPLEXES OF 3,5-DINITROBENZOIC ACID WITH AROMATIC COMPOUNDS

A. M. HINDAWEY, A. M. G. NASSAR and R. M. ISSA*

(Chemistry Department, Faculty of Science, Alexandria University, Alexandria, Egypt
** Tanta University)*

Received September 5, 1975
In revised form February 12, 1976

The IR spectra of the addition compounds of 3,5-dinitrobenzoic acid and aromatic molecules are analyzed in order to elucidate the type of interaction. The shifts in ν_{OH}, ν_{NO_2} asym. and $\nu_{C=O}$ bands of the acid are considered to differentiate between CT complexes, proton transfer interaction and molecular complexes.

Introduction

The formation of molecular complexes of charge transfer (CT) type ($D + A \rightleftharpoons D \ldots A$) is generally facilitated when the donor molecule has electron releasing substituents, *e.g.* fused aromatic hydrocarbons or some aromatic amines, while the acceptors carry electron attracting substituents such as aromatic polynitro compounds and also when both the donor and the acceptor molecule are planar.

Previous workers [1—4] investigating charge transfer complexes of picric acid with aromatic compounds suggested that the changes in the bands due to ν_{OH}, ν_{NO_2} asym., ν_{C-N} and γ_{CH} of picric acid, as well as ν_{NH_2} of the aromatic amine can be used to differentiate between CT complexes (π–π^*), proton transfer interaction (salt type), and molecular complexes (involving $n \rightarrow \pi^*$ or H-bonds besides $\pi \rightarrow \pi^*$ interaction [5]).

$HOPi \ldots ArNH_2$	$PiO^- \ldots H\text{–}NH_2\text{–}Ar$	$PiOH \ldots NH_2Ar$
CT complex	Proton transfer	Molecular complex

In the present work some addition products of 3,5-dinitrobenzoic acid with aromatic amines have been prepared and their IR spectra studied. This acid, though containing two NO_2 groups, does not act as a good electron acceptor owing to the presence of the electron attracting carboxyl group.

This study may help the elucidation of the nature of bonding in the complexes formed. Since the number of the NO_2 groups would affect the acceptor character of the molecule, it is intended to investigate this point in relation to the behaviour of acidic trinitrobenzene derivatives.

Experimental

The addition compounds were prepared by mixing a hot saturated alcoholic solution of 3,5-dinitrobenzoic acid with a similar one containing an equivalent quantity of the aromatic compound. From the hot saturated solution, the addition products separated as fine crystals of pale yellow (or even white) to reddish colour. The products were recrystallized from ethanol and their m.p.'s determined. The compounds prepared are listed in Tables I and II.

The IR spectra of the addition products were recorded in KBr discs on a UNICAM SP 200 spectrophotometer.

Table I

Some IR bands of 3,5-dinitrobenzoic acid and its CT complex with naphthalene

3,5-dinitrobenzoic acid	Naphthalene-3,5-dinitro-benzoic acid	Assignment
3110	3100	ν_{OH}
1707	1702	$\nu_{C=O}$
1556 1540	1558 1542	} $-NO_2$ sym.
1363	1365	$-NO_2$ sym.
1182	1180	ν_{C-N}
	790(1) 797(2)	γ_{CH}(donor)
733	730 Y	γ_{CH}(acid) colour

(1) Values of the free donor molecule
(2) Values of the donor in CT complex
Y = yellow

Results and discussion

The interaction between the donor and the acceptors in solution is very weak as shown by the spectra in the UV and visible regions, thus it is not possible to study the reaction under the prevailing experimental conditions [6]. Accordingly, the investigation was confined to the solid compounds using IR spectrometry.

A detailed analysis of the different parts of the spectrum is attempted especially for those bands expected to show drastic changes upon formation of the addition compound. For this purpose, the characteristic bands in the spectrum of the parent compound (3,5-dinitrobenzoic acid) are pointed out. The different types of complexes formed are discussed in the following:

(A) *Simple CT compounds formed through intermolecular charge—transfer interaction*

The interaction between a condensed ring system, as naphthalene and the acid would lead to the formation of a CT complex characterized by an intense colour and a low melting point [7]. The bonding in such a compound is due to an overlap of the π-orbitals of the acid and the aromatic ring, leading to $\pi - \pi^*$ interaction:

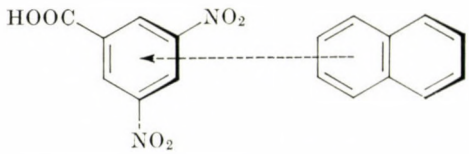

Charge—transfer is facilitated by the influence of electron attracting groups of the acceptor molecule.

The number of NO_2 bands in the spectrum of the acid is not changed but the bands are shifted to higher frequencies, which is more apparent with the asym. bands. This may be attributed to the increased charge migration from the aromatic ring to the NO_2 groups [8].

The band due to the C=O group retains its clear appearance with a slight shift to a lower frequency, indicating increased polarization of this group in the molecular complex.

The γ_{CH} band of the acid is shifted to a lower frequency while that of the donor system is shifted to a higher value. This may be explained by the increased attraction of the hydrogens towards the ring of the acceptor whereby the C–H bond length diminishes. The reverse would be true for the donor system. This behaviour resembles that observed with the addition compounds of naphthalene and picric acid [5] and trinitrobenzoic acid [9].

(B) *Compounds formed from slightly basic amines*

In the case of aromatic amines, including aniline and some of its substituted derivatives, containing not only acceptor but also donor groups, *viz.*

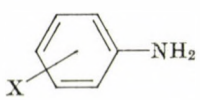

X = H, 2-Cl, 4-Cl, 4-Br, 2-COOH, 4-COOH, 2-NO_2, 3-NO_2 and 4-NO_2.

The basicity of the amino group is lowered through its mesomeric interaction with the aromatic ring and the acceptor substituent or the blocking of the lone pair through intermolecular H-bonding.

Table II

Some IR-bands of 3,5-dinitrobenzoic acid and its addition products with aromatic amines

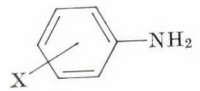

A \ X	*o*-OCH_3	*p*-OCH_3	*o*-CH_3	*m*-CH_3	*p*-CH_3	H	*o*-Cl	*m*-Cl	*p*-Cl	*p*-Br	*p*-COOH	*o*-COOH	*m*-NO_2	*o*-NO_2	*p*-NO_2	Assignment
3110	3100	3100	3110	3100	3110	3260	3400	3250	3130	3100	3420	3350	3300	3350	3410	ν_{OH}
	2670	2950	2940	2900	—	2930	3510	3375	3400	3310	3500	3400	3500	—	—	NH(as)
	2600	2650	2600	2700	2640	2620	2670	2900	2650	2950	2670	2800	2680	2800	2900	NH(s)
1707	—	—	—	—	—	—	1720	1720	1700	1705	1703	1710	1713	1700	1710	$\nu_{C=O}$
	1415	1405	1400	1402	1410	1404	—	—	—	—	—	—	—	—	—	$-COO^-$
1556	1558	1557	1560	1555	1558	1558	1567	1560	1560	1560	1554	1560	1560	1550	1570	NO_2-asym.
1540	1540	1540	1538	1540	1540	1540	1539	1540	1550	1540	1540	1550	1540	—	1558	
1363	1355	1360	1360	1358	1355	1358	1362	1360	1364	1355	1355	1352	1350	1363	1361	NO_2-sym.
1182	1185	1180	1188	1170	1185	1183	1181	1182	1190	1190	1180	1175	1190	1175	1180	$\nu_{C-N(acid)}$
733	732	738	735	732	728	738	736	730	735	739	739	732	740	730	?	$\gamma_{CH(acid)}$
	4.49	5.29	3.48	4.67	5.07	4.62	2.62	3.32	3.81	3.94	2.32	2.04	2.45	2.32	0.06	pK_a*
	W	W	W	W	W	W	O.Y.	W	Y	W	Y	Y	O.Y.	Y	Y	Colour
204	130	140	155	130	139	145	134	145	133	123	200	—	93	120	77	m.p. °C
A	P.T.	P.T.	P.T.	P.T.	P.T.	P.T.	M.C.	M.C.	M.C.	M.C.	M.C.	M.C.	M.C.	M.C.	M.C.	compound formed
A′	P.T.	P.T.	P.T.	P.T.	P.T.	P.T.	P.T.	P.T.	P.T.	P.T.	P.T.	P.T.	?	M.C.	M.C.	compound formed
A″	P.T.	P.T.	P.T.	P.T.	P.T.	P.T.	P.T.	P.T.	P.T.	P.T.	P.T.	P.T.	P.T.	P.T.	M.C.	compound formed

— = not recorded, ? = not readily identified, Y = yellow, O = orange, W = white; A = 3,5-dinitrobenzoic acid, A′ = Picric acid[5]
A″ = sym.-trinitrobenzoic acid[9]; P.T. = Proton transfer type, M.C. = molecular complex
* Values from Ref. [11]

The formation of the addition compound occurs through the usual $\pi—\pi^*$ interaction, which is, however, weaker than that with naphthalene. Another type of interaction is possible with this class of compounds, namely the $n - \pi^*$ interaction, due to the transfer of charge from the amino group to vacant antibonding levels of the NO_2 group, besides intermolecular H-bond formation, which would take place if the NH_2 group faces one of the two NO_2 groups.

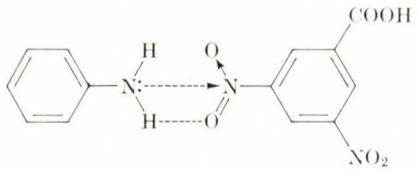

This type of interaction leads to lowering of the NH_2 frequencies, while the bands of the NO_2 groups are shifted to higher energies. On the other hand, lowering of the frequencies of both groups is observed when the NH_2 group is positioned between two NO_2-groups [5]. In this case, the $n - \pi^*$ interaction is not favoured and the H-bond predominates.

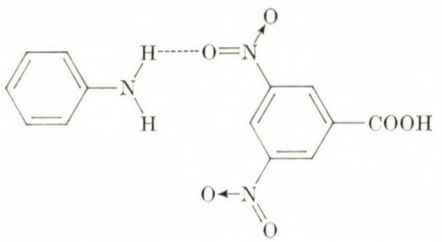

The case of *o*-NO_2-aniline is a typical example illustrating the following points.

(1) Bands due to $\nu_{C=O}$, ν_{OH} and ν_{NH} are still apparent, though ν_{OH} is shifted to higher frequencies, while the NH_2 bands are shifted to lower frequencies.

(2) Bands due to asym. NO_2 vibrations are shifted to higher or lower frequencies. The band of sym. NO_2 is still as broad as in the free acid.

(3) The $\nu_{C—N}$ band is slightly affected, indicating a weak interaction between the components of the addition products.

Compounds related to this class are known as molecular complexes and they are usually coloured due to $n - \pi^*$ interaction which requires absorption in the visible region and have low melting points. Low-polarity solvents and high temperatures favour the formation of molecular complexes since the existence of the ionic species is largely hindered and thus the formation of proton transfer compounds is not favoured.

(C) *Proton transfer compounds involving electrostatic bonding beside $n - \pi^*$ interaction*

This type of interaction occurs with amines of moderate or high basicity such as *o* and *p*-anisidine or *o*-, *m*- and *p*-toluidine, in which the nitrogen atom of the amino group can act as good proton acceptor from the carboxyl group of 3,5-dinitrobenzoic acid. The interaction between the two components of the complex molecule can be represented as follows:

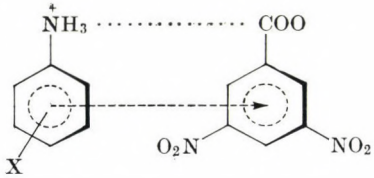

X = 2-OCH_3, 4-OCH_3, 2-CH_3, 3-CH_3 and 4-CH_3

The negative charge on the carboxylate anion acts as an electron donor center to the deficient aromatic ring and hence lowers its tendency to accept electrons from the aminophenyl ring. The blocking of the lone pair on the nitrogen atom of the amino group decreases the charge migration from it to the donor phenyl group and hence to the acceptor molecule. Accordingly, the ($n - \pi^*$) type of interaction would be of low contribution in the formation of the addition compounds of this class.

The main changes in the spectra of the addition compounds resulted are:

(1) Bands due to C=O disappear completely and are replaced by the bands characteristic of the carboxylate ion within the 1420—1400 cm^{-1} region. Also bands due to the NH_3 group make their appearance within the 2900—2500 cm^{-1} region, characteristic of this grouping [8].

(2) The NO_2 bands retain their appearance but are shifted to higher frequencies due to CT interaction.

Compounds belonging to this class have a pale colour and high m.p. Other spectral changes are similar to those for trinitrobenzoic acid [9].

From the results obtained in the present work in comparison with those of the previous investigations of picric acid [5] and sym.-trinitrobenzoic acid [9] CT complexes, it is concluded that the tendency to molecular complex formation with aromatic amines starts with *o*-NO_2 aniline ($pK_b = 3.32$) for sym.-trinitro- benzoic acid ($pK = 0.65$) [10], 3-NO_2 aniline ($pK_b = 4.57$) for picric acid ($pK_a = 0.7$) [10] and 2-Cl-aniline ($pK_b = 10.54$) for 3,5-dinitrobenzoic acid ($pK_a = 2.8$) [10]. This reveals that the formation of a salt type complexes occurs with amines of lower basicity as the acidic character of the acceptor

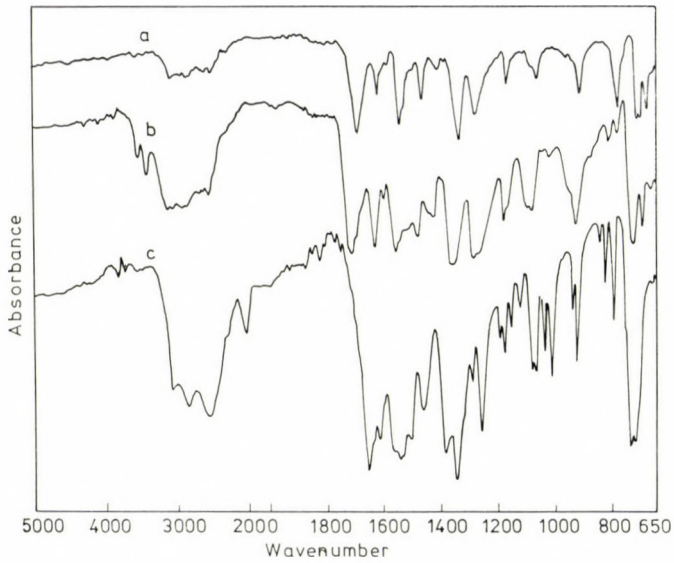

Fig. 1. The IR spectra of some addition compounds of 3,5-dinitrobenzoic acid with (a)-naphthalene, (b) *o*-nitroaniline and (c) *o*-anisidine.

molecule increases. Thus it can be concluded that the ability to CT complex formation is in accordance with the decreasing possibility of proton transfer from the acceptor molecule to the donor, *i.e.* decreases in the order 3,5-dinitrobenzoic acid > picric acid > 2, 4, 6-trinitrobenzoic acid.

The foregoing discussion reveals that the type of bonding between 3,5-dinitrobenzoic acid and aromatic compounds can be classified into different groups readily differentiated from each other if the behaviour of the $\nu_{C=O}$ and NO_2 asym. band is considered.

(1) $\pi - \pi^*$ complexes: ν_{OH}, $\nu_{C=O}$ retain their appearance and both are shifted to lower frequencies; NO_2 asym. are shifted to higher values.

(2) Proton transfer complexes (salt type): $\nu_{C=O}$ disappears more or less completely while the NO_2 asym. bands are shifted to higher or lower frequencies.

(3) $n - \pi^*$ complexes: $\nu_{C=O}$ and NO_2 asym. are shifted to higher frequencies.

REFERENCES

[1] Ross, S., Labes, M.: J. Amer. Chem. Soc., **77,** 4916 (1955)
[2] Kross, R. D., Fassel, V. A.: J. Amer. Chem. Soc., **79,** 38, (1957)
[3] Kross, R. D., Nakamoto, K., Fassel, V. A.: Spectrochim. Acta, **8,** 142 (1958)
[4] Mullikan, R. S.: J. Amer. Chem. Soc., **74,** 811 (1952)
[5] Issa, R. M., El Essawey, M. M.: Z. Phys. Chem. (Leipzig) **253,** 96 (1973)
[6] El-Essawey, M.: M. Sc. Thesis, Assiut Univ.; Issa, R. M.: Dissertation, Freiburg 1962
[7] Briegleb, G.: Elektronen — Donator Komplexe. Springer-Verlag 1961

[8] Bunsengesell, Phys. Chem. **64** 347 (1960); Z. Phys. Chem. (Frankfurt), **24**, 359 (1960)
[9] NASSAR, A. M. G., HINDAWEY, A. M.: Egypt. J. Chem. (In press)
[10] DIPPY, J. F., HUGHES, S. R. C., LAXTON, J. W.: J. Chem. Soc., **2995** (1956)
[11] BRAUDE, E. A., NACHOD, F. C.: Determination of Organic Structure by Physical Methods p. 590. Academic Press, New York (1955).

A. M. HINDAWEY, A. M. G. NASSAR — Chemistry Department, Faculty of Science, Alexandria University, Alexandria, Egypt.
R. M. ISSA — Tanta University, Egypt.

Acta Chimica Academiae Scientiarum Hungaricae, Tomus 92 (3), pp. 271–280 (1977)

THERMOLYSE VON CYANOKOMPLEXEN, X*

DARSTELLUNG UND THERMISCHER ABBAU VON QUARTÄREN AMMONIUM-CYANOMETALLATEN (NORMALSALZE)

B. MOHAI and L. BAGYIN

(Lehrstuhl für Allgemeine und Anorganische Chemie der Universität für Chemische Industrie Veszprém)

Eingegangen am 1. März 1976

Zur Gewinnung der Komplexe wurden auf Neutralisierung von Cyanometallat-Säuren mit quartären Ammoniumhydroxiden bzw. auf Austauschreaktion zwichen Silber-Cyanometallaten und quartären Ammoniumjodiden beruhende Methoden angewandt. Bei der Thermolyse entweicht zuerst das Kristallwasser, dann zwischen 220 und 280 °C Dicyan und Stickoxid, endlich zwischen 200 und 500 °C das entsprechende tertiäre Amin und Alkylcyanid. In den untersuchten 14 Komplexen war das Cyanometallat-Anion $[Fe(CN)_6]^{4-}$, $[Fe(CN)_6]^{3-}$, $[Fe(CN)_5NO]^{2-}$ und $[Co(CN)_6]^{3-}$, das quartäre Ammoniumkation $[(CH_3)_4N]^+$, $[(C_2H_5)_4N]^+$, $[(C_4H_9)_4N]^+$ und $[(CH_3)_3C_6H_5N]^+$.

Einleitung

Im Rahmen dieser Publikationsreihe wurde früher die thermische Zersetzung einiger Cyanometallat-Säuren [1] und ihrer Ammoniumsalze [2] beschrieben. Aus den flüchtige Kationen enthaltenden Cyanometallaten bilden sich gasförmige Zersetzungsprodukte: von den freien Säuren wird HCN, von den Ammoniumverbindungen NH_4CN ($NH_3 + HCN$) abgespalten, die infolge ihrer Flüchtigkeit sofort entweichen. Das bei den intramolekularen Redoxvorgängen der Cyanometallat(III)-Komplexe entstandene Dicyan oder das aus den Nitroprussiaten freigesetzte Stickoxid, sind ebenfalls gasförmig. Deshalb erhält man in den Derivatogrammen dieser Verbindungen gut auswertbare steile TG-Stufen und scharfe DTA-Spitzen.

Auch beim thermischen Abbau der quartären Ammonium-Cyanometallate sind flüchtige Zersetzungsprodukte zu erwarten. Das Ziel dieser Untersuchungen war die Gegenüberstellung der Zersetzungsvorgänge einerseits der *einfachen* und *quartären* Ammonium- [3], andererseits der quartären *Ammonium-* und quartären *Phosphonium*-Cyanometallate [4, 5]. Im Laufe dieser Arbeit wurden Komplexe der allgemeinen Formel $Q_4[Fe^{II}(CN)_6]$, $Q_3[Fe^{III}(CN)_6]$, $Q_2[Fe^{III}(CN)_5NO]$ und $Q_3[Co^{III}(CN)_6]$ untersucht, wo Q die folgenden Kationen bedeutet: $[(CH_3)_4N]^+$, $[(C_2H_5)_4N]^+$, $[(C_4H_9)_4N]^+$ und $[(CH_3)_3C_6H_5N]^+$. (Im weiteren: *Me* = CH_3, *Ät* = C_2H_5, *Bu* = C_4H_9 und *Ph* = C_6H_5.) Es soll

* IX. Mitteilung, PORZSOLT, Cs. É., MOHAI, B., BECK, M. T.: Magy. Kém. Folyóirat **80**, 254 (1974)

gleich erwähnt werden, daß von den [Hexacyanoferrat(II)]-Verbindungen nur das Tetrakis (tetramethyl)- und das Tetrakis (trimethyl-phenyl)-*ferrocyanid* in Form des Neutralsalzes hergestellt werden konnte; beim Äthyl- und Butylderivat enstanden jedesmal protonierte Komplexe (s. nachstehende Mitteilung).

Thermische Untersuchungen: Zersetzungsreaktionen, Zersetzungsprodukte

Die thermischen und stöchiometrischen Daten der Thermolysevorgänge sind in den Tabellen I—III zusammengefaßt.

In der ersten Spalte der Tabellen ist die Zusammensetzung der untersuchten Verbindungen angegeben. Die zweite Spalte enthält die von den DTA-Kurven abgelesenen Zersetzungstemperaturen. Mehr Temperaturangaben in derselben Reihe bedeutet, daß die bei verschiedenen Temperaturen ablaufenden Teilreaktionen zusammenfließen (Mehrfachstufen), stöchiometrisch kann deshalb nur der Gesamtprozeß interpretiert werden. In solchen Fällen ist die stärkste DTA-Spitze, die meist mit der Temperaturstelle der maximalen Zersetzungsgeschwindigkeit (DTG-Kurve) zusammenfällt, *kursiv* gedruckt.

Die von den TG-Kurven abgelesenen Gewichtsverluste, bezogen auf 1 Mol des Ausgansgkomplexes, sind in der dritten Spalte zu sehen. Spalte vier zeigt die entweichenden flüchtigen Zersetzungsprodukte. Da ihre Menge mit guter Näherung stöchiometrisch ist, wurde ihre Molzahl, weiterhin — zwecks unmittelbarer Vergleichbarkeit mit Spalte drei — auch ihr Molekulargewicht (in Klammern), d. h. die »theoretische« Gewichtsabnahme angegeben. In der letzten Spalte wird die Form der DTA-Spitzen kurz charakterisiert. Obwohl die Bemerkung sich in erster Reihe auf Größe und Richtung der die Zersetzungsvorgänge begleitenden Wärmeeffekte bezieht, kann man indirekt auch auf die relativen Reaktionsgeschwindigkeiten schließen (vgl. DTG-Spitzen).

In Abbildung 1 sind die Derivatogramme von vier Komplexen dargestellt, die aus der Reihe der 14 untersuchten Verbindungen so gewählt wurden, daß sämtliche quartäre Ammoniumkationen sowie Cyanometallat-Anionen in Form je eines Komplexes vertreten sind. Dies ermöglichte die Tatsache, daß — sowohl die Kationen als auch die Anionen betreffend — analoge Zersetzungsreaktionen verlaufen.

Enthalten die Verbindungen auch Kristallwasser, so findet in der ersten Zersetzungsstufe (100—200 °C) eine *Entwässerung* statt. Obzwar die Komplexe wohldefinierte Hydrate bilden, ist ihre thermische Stabilität dennoch verhältnismäßig gering: die meist einstufige Wasserabgabe ruft an den DTA-Kurven nur schwache endotherme Effekte hervor.

Die Zersetzung der wasserfreien Komplexe beginnt im allgemeinen zwischen 200—250 °C: nach mehrstufigen Zersetzungsvorgängen wird der feste Rückstand erst um 450—500 °C gewichtskonstant. Vergleicht man diese Reaktionen mit den entsprechenden Prozessen der *einfachen* Ammonium-Cyanometallate [2], so ist eine vollkommene Analogie zu finden. Z. B. bildet sich im Laufe der Thermolyse des $(NH_4)_4[Fe^{II}(CN)_6]$ 4 Mol NH_4CN/Mol Komplex, das sich sofort in NH_3 und HCN spaltet. In derselben Zersetzungsphase entspricht der Gewichtsverlust im Falle des $[Me_4N]_4[Fe^{II}(CN)_6]$ dem Ent-

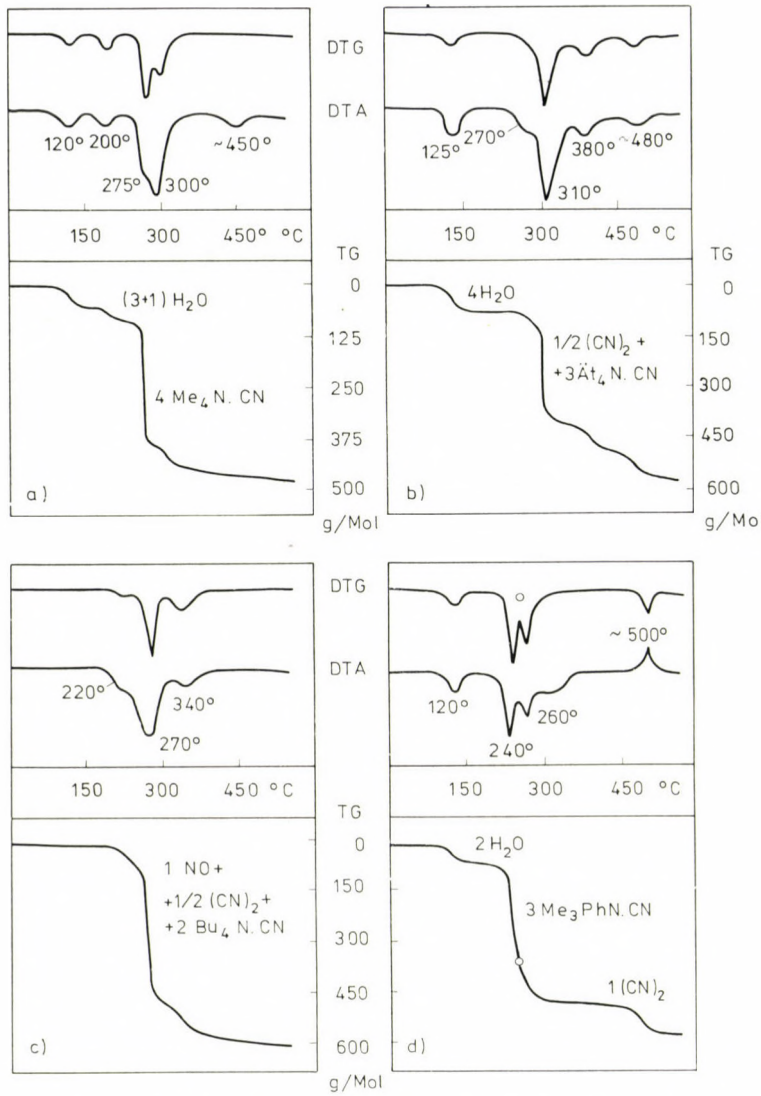

Abb. 1. Derivatogramme (TG-, DTA- u. DTG-Kurven) von quartären Ammonium-Cyanometallaten (Normalsalze). a) $[Me_4N]_4[Fe^{II}(CN)_6] \cdot 4H_2O$, b) $[Ät_4N]_3[Fe^{III}(CN)_6] \cdot 4H_2O$, c) $[Bu_4N]_2[Fe^{III}(CN)_5NO]$, d) $[Me_3PhN]_3[Co^{III}(CN)_6] \cdot 2H_2O$

weichen von 4 Mol $Me_4N \cdot CN$ (Tabelle I, Abb. 1-a). Im gasförmigen Zersetzungsprodukt sind Trimethylamin und Methylcyanid (d. h. die Methylderivate von NH_3 und HCN) vorhanden:

$$[Me_4N]_4\,[Fe^{II}(CN)_6] \xrightarrow[\text{endo.}]{275-450^\circ} 1/3\ Fe_2^{II}[Fe^{II}(CN)_6] + \\ + 4Me_4N \cdot CN \longrightarrow 4Me_3N + 4Me{-}CN. \qquad (1)$$

Acta Chim. (Budapest) 92, 1977

Tabelle I

Zersetzungsvorgänge von quartären Ammonium-[Hexacyanoferraten(II)] und -[Hexacyanoferraten(III)]

Verbindung	Zersetzungstemperatur (°C)	Gewichtsabnahme (g/Mol)	Zersetzungsprodukt (Mol/Mol Komplex)	Bemerkung
$[Me_4N]_4\,[Fe(CN)_6] \cdot 4\,H_2O$	120, 200	72,3	(3+1) H_2O (72,1)	schwach, flach: endo.
	275, *300*, ~450	402	4 $Me_4N \cdot CN$ (400,8)	stark, breit: endo.
$[Me_3PhN]_4\,[Fe(CN)_6] \cdot H_2O$	95	18,1	1 H_2O (18,0)	schwach, flach: endo.
	180, *225*, ~450	648	4 $Me_3PhN \cdot CN$ (648,8)	stark, breit: endo.
$[Me_4N]_3\,[Fe(CN)_6] \cdot 3\,H_2O$	105	53,7	3 H_2O (54,0)	mittelm., flach: endo.
	280, *330*, ~450	330	1/2 $(CN)_2$ + 3 $Me_4N \cdot CN$ (326,6)	stark, scharf: endo.
$[Ät_4N]_3[Fe(CN)_6] \cdot 4\,H_2O$	125	71,8	4 H_2O (72,1)	mittelm., breit: endo.
	270, *310* } 380, ~480 }	494	1/2 $(CN)_2$ + 3 $Ät_4N \cdot CN$ (494,9)	stark, breit: endo.
$[Bu_4N]_3\,[Fe(CN)_6]$	220, *270* } 320, ~450 }	836	1/2 $(CN)_2$ + 3 $Bu_4N \cdot CN$ (831,5)	stark, scharf: endo.
$[Me_3PhN]_3[Fe(CN)_6] \cdot 2\,H_2O$	130	36,6	2 H_2O (36,0)	mittelm., scharf: endo.
	240, 310, ~450	512	1/2 $(CN)_2$ + 3 $Me_3PhN \cdot CN$ (512,6)	stark, scharf: endo.

Tabelle II

Zersetzungsvorgänge von quartären Ammonium-[Pentacyano-nitrosylferraten(III)]

Verbindung	Zersetzungstemperatur (°C)	Gewichtsabnahme (g/Mol)	Zersetzungsprodukt (Mol/Mol Komplex)	Bemerkung
$[Me_4N]_2[Fe(CN)_5NO]$	260, *300*, ~450	257	1 NO+1/2 $(CN)_2$+2 $Me_4N \cdot CN$ (256,4)	stark, scharf: endo.
$[Ät_4N]_2[Fe(CN)_5NO]$	220, *290*, } 380, ~450 }	366	1 NO+1/2 $(CN)_2$+2 $Ät_4N \cdot CN$ (368,6)	mittelm., breit: endo.
$[Bu_4N]_2[Fe(CN)_5NO]$	220, *270*, 340	587	1 NO+1/2 $(CN)_2$+2 $Bu_4N \cdot CN$ (593,0)	mittelm., breit: endo.
$[Me_3PhN]_2[Fe(CN)_5NO]$	210, *240* } 380, ~500 }	380	1 NO+1/2 $(CN)_2$+2 $Me_3PhN \cdot CN$ (380,4)	stark, scharf: endo.

Eine ähnliche Analogie zeigen auch die Zersetzungsreaktionen der einfachen und quartären Ammonium-ferricyanide (Tabelle I). Bei der Thermolyse der *paramagnetischen* [Hexacyanoferrat(III)]-Komplexe werden gleichzeitig Dicyan und quartäres Ammoniumcyanid frei; der resultierende Wärmeeffekt des Gesamtpprozesses ist endotherm. Der Knickpunkt bei 270 °C an der DTA-Kurve (Abb. 1-b) bezeichnet den Endpunkt der $Fe^{III} \rightarrow Fe^{II}$ Reduktion, d. h. die Beendigung der *exothermen** Dicyanbildung; von hier angefangen ist nur der endotherme Effekt der Abspaltung von $Ät_4N \cdot CN$ wahrzunehmen. Die thermische Zersetzung des Äthylderivats geht also nach folgender Bruttogleichung vor sich:

$$[Ät_4N]_3\,[Fe^{III}(CN)_6] \xrightarrow[(endo.)]{270-480^\circ} 1/3\,Fe_2^{II}[Fe^{II}(CN)_6] + \\ + 1/2\,(CN)_2 + 3\,Ät_3N + 3\,Ät{-}CN\,. \qquad (2)$$

Beim thermischen Abbau der [Pentacyano-nitrosylferrat(III)]-Komplexe (Tabelle II, Abb. 1-c) läuft die Abspaltung des Heteroliganden (endotherm) und der intramolekulare Redoxvorgang (exotherm) parallel ab. Der bei 220 °C and der DTA-Kurve sichtbare Knickpunkt weist auch hier auf das Ausbleiben der Dicyanentwicklung hin. Unmittelbar an diese Prozesse schließt sich die endotherme Bildung von $Bu_4N \cdot CN$ an:

$$[Bu_4N]_2\,[Fe^{III}(CN)_5NO] \xrightarrow[(endo.)]{220-340^\circ} 1/3\,Fe_2^{II}[Fe^{II}(CN)_6] + \\ + NO + 1/2\,(CN)_2 + 2Bu_3N + 2Bu{-}CN\,. \qquad (3)$$

Im Falle der quartären Phosphonium-[Cyanonitrosylferrate] enthält das Gasprodukt — infolge der reduzierenden Wirkung des gebildeten tertiären Phosphins — hauptsächlich N_2O [4]. Ähnliche intramolekulare Redoxvorgänge finden auch im Laufe der Thermolyse von Molybdän- und Wolframkomplexen mit der allgemeinen Zusammensetzung $M(NO)_2Cl_2(PPh_3)_2$ statt, während neben $OP \cdot Ph_3$ vorwiegend N_2 entsteht [6].

Im Prinzip stimmt die Bruttoreaktion (3) mit der Gleichung (1) und (2) überein, unterscheidet sich aber grundsätzlich von den Zersetzungsvorgängen des $(NH_4)_2[Fe^{III}(CN)_5NO]$. Bei der Thermolyse des letzteren findet nämlich zwischen dem abgespaltenen NH_3 und NO eine *Sekundärreaktion* statt, wobei sich N_2 und H_2O bildet [7]. Eine ähnliche Konproportionierung der Stickstoffatome ist bei den quartären Ammonium-Nitroprussiaten, wegen der die Oxydationszahl stabilisierenden Wirkung der Substituenten, nicht zu erwarten.

Die Analogie ist zwischen den thermischen Zersetzungsreaktionen einfacher und quartärer Ammonium-[Hexacyanokobaltate(III)] wiederum vollständig (Tabelle III, Abb. 1-d). Da diese Verbindungen gegenüber den entsprechenden Eisen(III)-Verbindungen *diamagnetisch* sind, tritt die Dicyanbildung — die anfangs endotherm ($Co^{III} \rightarrow Co^{II}$), dann exotherm ($Co^{II} \rightarrow Co^{I}$)

* Anhand früherer Untersuchungen [2] wurde festgestellt, daß die paramagnetischen Eisen(III)-Komplexe in exothermer, die diamagnetischen Kobalt(III)-Komplexe in endothermer Reaktion Dicyan abgeben.

Tabelle III

Zersetzungsvorgänge von quartären Ammonium-[Hexacyanokobaltaten (III)]

Verbindung	Zersetzungstemperatur (°C)	Gewichtsabnahme (g/Mol)	Zersetzungsprodukt (Mol/Mol Komplex)		Bemerkung
$[Me_4N]_3[Co(CN)_6] \cdot 4\ H_2O$	110	~70	$4\ H_2O$	(72,1)	schwach, flach: endo.
	370	309	$3\ Me_4N \cdot CN$	(300,6)	stark, scharf: endo.
	530	50,4	$1\ (CN)_2$	(52,0)	schwach: endo. scharf: exo.
$[Ät_4N]_3[Co(CN)_6] \cdot 3\ H_2O$	135	56,9	$3\ H_2O$	(54,0)	schwach, flach: endo.
	305	467	$3\ Ät_4N \cdot CN$	(468,9)	stark, breit: endo.
	510	52,3	$1\ (CN)_2$	(52,0)	schwach: endo. scharf: exo.
$[Bu_4N]_3[Co(CN)_6]$	*280*, 330 ~500	857	$3\ Bu_4N \cdot CN +$ $+1\ (CN)_2$	(857,6)	stark, scharf: endo. schwach: endo. scharf: exo.
$[Me_3PhN]_3[Co(CN)_6] \cdot 2\ H_2O$	120	36,7	$2\ H_2O$	(36,0)	schwach, flach: endo.
	240, 260	~480	$3\ Me_3PhN \cdot CN$	(486,6)	mittelm., breit: endo.
	~500	~55	$1\ (CN)_2$	(52,0)	schwach: endo. scharf: exo.

verläuft — nur in der zweiten Zersetzungsstufe ein [1, 2]. Zuerst wird das quartäre Ammoniumcyanid abgespalten:

$$[Me_3PhN]_3\,[Co^{III}(CN)_6] \xrightarrow[\text{endo.}]{240-400^\circ} 1/2\,Co^{III}[Co^{III}(CN)_6] + \\ + 3Me_3PhN \cdot CN\,. \qquad (4)$$

Darauf folgt die intramolekulare Redoxreaktion:

$$1/2\,Co^{III}[Co^{III}(CN)_6] \xrightarrow[\text{endo., exo.}]{400-500^\circ} Co^{I}CN + (CN)_2\,, \qquad (5)$$

die im Laufe der Thermolyse des $(NH_4)_3[Co^{III}(CN)_6]$ und auch beim $[Co^{III}(NH_3)_6]\,[Co^{III}(CN)_6]$ auf wohldefinierte Teilreaktionen getrennt werden konnte [8]. Übrigens unterscheidet sich die Zersetzung des als Beispiel vorgeführten Trimethyl-phenyl-Derivats von der der vorigen nur darin, daß sich neben Methylcyanid N,N-dimethylanilin (tertiäres Amin mit gemischten Substituenten) bildet:

$$[(CH_3)_3C_6H_5 \cdot N]\,CN \longrightarrow C_6H_5N(CH_3)_2 + CH_3{-}CN\,. \qquad (6)$$

Es fehlt nun noch die Untersuchung dessen, ob die gebildeten Alkylcyanide *normale-* oder *iso*-Verbindungen sind. SONGSTAD und Mitarbeiter [9] erhielten nämlich aus einer nitrobenzolischen Lösung von [Triphenyl-methyl-*Phosphonium*]-[Dicyano-argentat], — die in Gegenwart von CH_3I unter Rückfluß gekocht wurde —, in einer Ausbeute von etwa 80% Methyl-isocyanid. Dagegen entstanden bei den von uns untersuchten Komplexen jedesmal die Normalverbindungen (s. auch »Experimentelles«). Für den Grund des abweichenden Verhaltens der quartären Kationen hielten wir zuerst die Gemischtheit der Liganden und dann den Ammonium—Phosphonium-Unterschied. Da aber die Thermolyse des [Tetrabutyl-*Ammonium*]-[Dicyano-argentats] ebenfalls vorwiegend Isocyanid (60—70%) lieferte und sich auch die analoge Goldverbindung, das $[Bu_4N]\,[Au^{I}(CN)_2]$ auf die gleiche Weise verhielt, mußte die Bildung von Isonitrilen den Zentralatomen bzw. der individuellen (linearen) Struktur der Cyano-*argentate* und *-aurate* zugeschrieben werden.

Auf die Zersetzungsreaktionen der quartären Ammonium-Cyanometallate *über 500 °C* wollen wir an dieser Stelle nicht eingehen: die in den Gleichungen (1)—(4) vorkommenden festen Rückstände sind nämlich mit den Zwischenprodukten der einfachen Ammonium-Cyanometallate identisch, deren weitere Zersetzung in den zitierten Publikationen [1, 2, 7, 8] schon eingehend diskutiert wurde.

Experimentelles

Darstellung und Identifizierung der Substanzen

Da die Mehrheit der untersuchten Komplexe aus der Literatur nicht bekannt war, wurde den präparativen Arbeiten auch diesmal besondere Bedeutung beigemessen. Zur Darstellung der Normalsalze wurden die folgenden Methoden angewandt.

a) Bei Verwendung der auf *Neutralisation* beruhenden Methode wurde die gewünschte Cyanometallat-Säure [1] und das entsprechende quartäre Ammoniumhydroxid getrennt hergestellt. Letztere gewann man aus quartären Ammoniumhalogeniden (meist aus Jodiden) mit Silberoxid. Nach dem Vermischen wurde die Lösung bei Zimmertemperatur mit einem Luftstrom eingedampft und das ausgeschiedene Rohprodukt aus dest. Wasser umkristallisiert. (Auf die gewöhnliche Fällung durch Alkohol wurde diesmal verzichtet, da unbestimmte Hydrate entstehen können.)

b) Im Falle der anderen Methode wurden aus den Alkali-Cyanometallaten erst die *Silbersalze* gefällt. Nach Filtrieren wurde der gewaschene Niederschlag in der Lösung des quartären Ammonium-jodids suspendiert (der erstere muß immer im Überschuß vorhanden sein). Die das Produkt enthaltende Lösung wurde vom Silberjodid getrennt und wie oben aufgearbeitet.

Die auf zweierlei Art verfertigten Präparate zeigten weder äußerlich, noch in ihren Derivatogrammen Unterschiede. Übrigens sind die Ferrocyanide blaßgelbe, die Ferricyanide goldgelbe, die Prussiate rotbraune und die Cyanokobaltate weiße, pulverförmige Substanzen.

Die Zusammensetzung der Präparate wurde einerseits durch Bestimmung des Zentralatoms (Tabelle IV), andererseits auf Grund der von den TG-Kurven abgelesenen Gewichtsverluste (Tabellen I—III) kontrolliert. Die Komplexe wurden mit einem 1 : 1-Gemisch von halbkonzentrierter HNO_3 — $HClO_4$ aufgeschlossen: der Eisengehalt wurde nach ZIMMERMANN-REINHARDT titrimetrisch, der Kobaltgehalt mit α-Nitroso-β-Naphthol gravimetrisch bestimmt

Tabelle IV

Analysenwerte und CN- bzw. NO-Valenzschwingungen von quartären Ammonium-Cyanometallaten

Verbindung	Molgewicht	Fe bzw. Co (Gew.-%)		Wellenzahl (cm^{-1})	
		ber.	gef.	ν_{CN}	ν_{NO}
$[Me_4N]_4[Fe(CN)_6] \cdot 4\ H_2O$	580,7	9,62	**9,63**	2030—40	
$[Me_3PhN]_4[Fe(CN)_6] \cdot H_2O$	774,8	7,21	6,98	2045	
$[Me_4N]_3[Fe(CN)_6] \cdot 3\ H_2O$	488,5	11,43	11,53	2105—10	
$[Ät_4N]_3[Fe(CN)_6] \cdot 4\ H_2O$	674,9	8,28	8,26	2105	
$[Bu_4N]_3[Fe(CN)_6]$	939,4	5,95	6,03	2100	
$[Me_3PhN]_3[Fe(CN)_6] \cdot 2\ H_2O$	656,7	8,51	8,81	2110	
$[Me_4N]_2[Fe(CN)_5NO]$	364,3	15,33	15,35	2135	1920
$[Ät_4N]_2[Fe(CN)_5NO]$	476,5	11,72	11,73	2135	1890
$[Bu_4N]_2[Fe(CN)_5NO]$	700,9	7,97	7,97	2135	1885
$[Me_3PhN]_2[Fe(CN)_5NO]$	488,4	11,44	11,50	2135	1920
$[Me_4N]_3[Co(CN)_6] \cdot 4\ H_2O$	509,7	11,56	11,68	2120	
$[Ät_4N]_3[Co(CN)_6] \cdot 3\ H_2O$	659,9	8,93	8,75	2115	
$[Bu_4N]_3[Co(CN)_6]$	942,5	6,25	6,27	2110	
$[Me_3PhN]_3[Co(CN)_6] \cdot 2\ H_2O$	659,8	8,93	8,88	2115—25	

UR-spektrophotometrische Untersuchung der Substanzen

Die Wellenzahl der CN-Valenzschwingungen ist in den Übergangsmetall-Cyanokomplexen vom Oxydationszustand des Zentralatoms und von der Qualität des Kations bekanntlich stark abhängig. Bei gleichem Metallatom werden die CN-Frequenzen mit zunehmender Oxydationszahl in Richtung der höheren Werte verschoben. Die gleiche Tendenz gelangt zur Geltung, wenn man die Alkaliionen gegen Wasserstoffionen austauscht [10]. Die höchsten CN-Frequenzen sind also in den ein dreiwertiges Zentralatom enthaltenden freien Säuren wahrzunehmen.

In den letzten Spalten der Tabelle IV sind die Wellenzahlen der CN-, bei den Nitroprussiaten auch die der NO-Valenzschwingungen angeführt. Da die UR-Spektren hauptsächlich zur Kontrolle der Zusammensetzung der Komplexe dienten (Fe^{II}- oder Fe^{III}-Verbindung bzw. neutrales oder saures Salz), wurde nur die Wellenzahl der zur Identifizierung geeignetsten Bande angegeben. Aus den Daten geht deutlich hervor, daß sowohl die CN- als auch die NO-Frequenzen mit der Erhöhung des Molekulargewichtes der quartären Kations abnehmen; übrigens sind sie in jedem Fall beteudend kleiner als die der einfachen Ammonium-Cyanometallate [7].

Identifizierung der Zersetzungsprodukte

Die bei der Thermolyse der quartären Ammonium-Cyanometallate entweichenden Zersetzungsprodukte wurden nicht nur als »stöchiometrische Gewichtsabnahmen«, sondern auch analytisch identifiziert. Zu diesem Zweck wurden die Einzelproben in einem DENNSTEDTschen Ofen bis zur gewünschten Temperatur (Derivatogramm) erhitzt und die flüchtigen Produkte im Stickstoffstrom ausgetrieben.

Die organischen Komponenten sollten nur qualitativ bestimmt werden (ihre Menge ist schon aus den TG-Stufen bekannt). Die aus dem Ofen entweichenden Produkte wurden in einem Absorbentengemisch mit der Zusammensetzung

1 Volum 1%ige	$Na_2[Fe(CN)_5NO]$-Lösung,
1 Volum 5%ige	Acetaldehyd-Lösung,
2 Volum 5%ige	Na_2CO_3-Lösung

aufgefangen. Auf Wirkung von *tertiären Aminen* ändert sich die rote Farbe des Reagens erst nach Blauviolett, dann nach Grün. Die Identifizierung der *Alkylcyanide* erfolgte aus einer getrennten Probe: die flüchtigen Produkte wurden in Chloroform gelöst und ihre UR-Spektren aufgenommen. Neben den tertiären Aminen fand man — unabhängig davon, ob das quartäre Kation

aromatische Liganden enthielt oder nicht — jedesmal *aliphatische* Nitrile (2250—60 cm^{-1}). Die Gegenwart von Isonitrilen konnte in keinem der Fälle nachgewiesen werden.

Der *Dicyan*gehalt des gasförmigen Produktes wurde in 0,1 *m* NaOH-Lösung aufgefangen und nach LIEBIG argentometrisch bestimmt. Die *Stickoxid*-Komponente wurde gaschromatographisch identifiziert.

Zu den Untersuchungen verwendete Instrumente

Die thermischen Untersuchungen wurden mit einem in Ungarn gebauten Derivatographen, Typ MOM G-425 durchgeführt. Der große Vorteil dieser Einrichtung liegt darin, daß die TG-, DTA- und DTG-Kurven aus derselben Probe gleichzeitig aufgenommen werden können. Abhängig von der Größe des Molekulargewichtes der untersuchten Komplexe bzw. von der des zu erwartenden Gewichtsverlustes, wurden Proben von 200—500 mg (etwa 1/3—1/2 mMol) eingewogen. Die Untersuchungen wurden in Stickstoffatmosphäre im Platintiegel durchgeführt, als Vergleichsmaterial diente bei 1200 °C geglühtes α-Al_2O_3. Die Versuchsparameter waren die folgenden:

T_{max}: 900 °C,
Aufheizgeschwindigkeit: 5°/Min.,
TG-Empfindlichkeit: 200 (100, 500) mg,
DTA-Empfindlichkeit: 1/10,
DTG-Empfindlichkeit: 1/15.

Die UR-Spektren (die der festen Substanzen in KBr-Preßlingen) wurden mit einem UR-10 Spektrophotometer der Firma Carl Zeiss Jena aufgenommen. Zu den gaschromatographischen Untersuchungen wurde eine Einrichtung vom Typ Fractovap 2400 T (Carlo Erba) angewandt.

LITERATUR

[1] MOHAI, B.: Acta Chim. Acad. Sci. Hung. **62,** 217 (1969)
[2] MOHAI, B.: *ibid.* **62,** 229 (1969)
[3] BAGYIN, L.: Doktorarbeit. Univ. f. Chem. Ind. Veszprém, 1971
[4] PAPP, S., KOVÁCS, S., LISZI, I.: J. Inorg. Nucl. Chem. **34,** 3111 (1972)
[5] PAPP, S., DOMBI, A.: Monatshefte Chem. **104,** 885 (1973)
[6] BENCZE, L., MOHAI, B.: Inorg. Chim. Acta **12,** 5 (1975)
[7] MOHAI, B., BAGYIN, L.: J. Inorg. Nucl. Chem. **33,** 3311 (1971)
[8] MOHAI, B.: Z. anorg. allg. Chem. **392,** 287 (1972)
[9] SONGSTAD, J. et al.: Acta Chim. Scand. **24,** 355 (1970)
[10] BECK, W., SMEDAL, H. S.: Z. Naturforsch. **20b,** 109 (1965)

Béla MOHAI; H-8201 Veszprém, Pf. 28.
László BAGYIN; H-2600 Vác, Csokonai u. 3.

Acta Chimica Academiae Scientiarum Hungaricae, Tomus 92 (3), pp. 281–287 (1977)

THERMOLYSE VON CAYNOKOMPLEXEN, XI*

HERSTELLUNG UND THERMISCHE ZERSETZUNG VON QUARTÄREN AMMONIUM-WASSERSTOFF-CYANOMETALLATEN (PROTONIERTE KOMPLEXE)

B. MOHAI und L. BAGYIN

(Lehrstuhl für Allgemeine und Anorganische Chemie der Universitat für Chemische Industrie, Veszprém)

Eingegangen am 1. März 1976

Aus den gemeinsamen salzsauren Lösungen von Kalium-[Hexacyano-ferrat(II)] und verschiedenen quartären Ammoniumsalzen (Tetramethyl-, Tetraäthyl-, Tetrabutyl-, Triphenyl-methyl-Ammoniumchlorid) scheiden sich wohldefinierte ein-, zwei- bzw. dreimalsaure Salze aus. [Hexacyano-ferrat(III)] und [-kobaltat(III)] bilden nur einmalsaures Salz. In den TG-Kurven dieser Verbindungen erscheinen wohldefinierte HCN-Stufen, und das Maß der Protonierung kann auch azidimetrisch unmittelbar bestimmt werden. Ihre Zersetzungsprozesse erinnern, abgesehen von der geringeren thermischen Stabilität, an die der entsprechenden Normalsalze.

Bildung und Darstellung von protonierten Komplexen

In unserer vorangegangenen Mitteilung [1] wurde bereits erwähnt, daß im Falle der vierbasigen [Hexacyano-ferrat(II)]-Säure die blaßgelben Normalsalze nur mit Tetramethyl- und Trimethyl-phenyl-Ammoniumkationen hergestellt werden konnten. Mit Tetraäthyl- und Tetrabutyl-Ammoniumkationen erhielt man jedesmal goldgelbe Produkte, bei denen die hohe Wellenzahl der CN-Valenzschwingungen eher auf die Bildung von *Ferri*cyaniden deutete. Die Verschiedenheit der Produkte konnte selbst bei sorgfältigstem Ausschluß der Oxydation nicht beseitigt werden, dagegen bildeten die »kleineren« Kationen auch an der Luft *Ferro*verbindungen.

Zur Klärung dieser Widersprüche wurde die Elementar- und Thermoanalyse der fraglichen Substanzen durchgeführt, ferner wurden ihre IR-Spektren und magnetischen Eigenschaften untersucht [2]. Die Analysendaten zeigten eindeutig, daß die Zusammensetzung des Äthyl- und Butylderivats den Formeln $[Ät_4N]_3H[Fe^{II}(CN)_6]$ bzw. $[Bu_4N]_3H[Fe^{II}(CN)_6]$ entspricht, d. h. man erhielt *protonierte Ferrocyanide*. Die Verschiebung der CN-Frequenzen nach größeren Werten ist also die Folge der Protonierung [3] und nicht der höheren Oxydationszahl des Zentralatoms. Obwohl an der TG-Kurve beider Komplexe — ähnlich den freien Säuren [4] — wohlseparierte HCN-Stufen erscheinen, erwiesen sich ihre wäßrigen Lösungen als *neutral*.

* XI. Mitteilung, MOHAI, B., BAGYIN, L.: vorangehende Mitteilung in dieser Zeitschrift.

Zum protonierten Äthyl- bzw. Butylderivat des [Hexacyano-ferrat(II)] gelangten wir übrigens durch Anwendung der selben Methoden [1], mit denen im allgemeinen die Normalsalze hergestellt wurden. Ihre anomale Bildung kann mit der Größe der Tetraäthyl- und Tetrabutyl-Ammoniumkationen (sterische Hemmung) erklärt werden: bei den [Hexacyano-ferrat(III)]- und [-kobaltat(III)]-Komplexen kamen nämlich solche Unregelmäßigkeiten nicht vor (die Normalsalze der letzteren enthalten nur drei quartäre Kationen).

Die zufällige Gewinnung der protonierten, doch neutralen Ferrocyanide legte den Gedanken nahe, die Herstellung der protonierten Verbindungen — mit den quartären Kationen $[Me_4N]^+$, $[Ät_4N]^+$, $[Bu_4N]^+$ und $[Me_3PhN]^+$ bzw. mit den Cyanometallat-Anionen $[Fe(CN)_6]^{4-}$, $[Fe(CN)_6]^{3-}$, $[Fe(CN)_5NO]^{2-}$ und $[Co(CN)_6]^{3-}$ — auch systematisch zu untersuchen. Die stufenweise Dissoziation der mehrbasigen Cyanometallat-Säuren [5, 6] versprach dazu gute Chancen.

Die in Tabelle I angeführten protonierten Komplexe (ausgenommen die neutralen Verbindungen) wurden nach der folgenden einfachen Methode hergestellt: zur wäßrigen Lösung des gewünschten Alkali-Cyanometallats wurde die Lösung des entsprechenden quartären Ammoniumhalogenids zugegeben, dann wurde mit 10%iger Salzsäure versetzt. Unabhängig von der Säuremenge scheidet sich immer das stöchiometrisch mögliche saure Salz ab. Die Zusammensetzung derselben (nach Filtrieren, Waschen und Trocknen) ist in der ersten Spalte der Tabelle angegeben. Mit dem Nitroprussiatanion bildet sich kein saures Salz, was im Falle einer zweibasigen starken Säure auch nicht zu erwarten war.

Tabelle I

Analysenwerte und CN-Valenzschwingungen von quartären Ammonium-Wasserstoff-Cyanometallaten

Verbindung	Molgewicht	Fe bzw. Co (Gew.-%)		HCN/Mol (thermisch)	H^+/Mol (azidimetr.)	ν_{CN} (cm^{-1})
		ber.	gef.			
$[Me_4N]_2H_2[Fe(CN)_6]$	362,3	15,42	15,28	1,93	2,02	2075
$[Ät_4N]_3H[Fe(CN)_6] \cdot 4\,H_2O$	675,9	8,26	8,20	0,99	(neutral)	2115
$[Bu_4N]_3H[Fe(CN)_6]$	940,4	5,94	5,52	0,93	(neutral)	2105
$[Bu_4N]H_3[Fe(CN)_6]$	457,5	12,21	12,45	2,97	3,06	2090
$[Me_3PhN]_2H_2[Fe(CN)_6]$	486,4	11,48	11,45	1,96	1,96	2075
$[Me_4N]_2H[Fe(CN)_6]$	361,3	15,49	15,31	0,99	1,03	2135
$[Me_3PhN]_2H[Fe(CN)_6] \cdot 2\,H_2O$	521,4	10,71	10,60	1,01	1,02	2130
$[Me_4N]_2H[Co(CN)_6] \cdot H_2O$	382,4	15,41	15,37	0,97	0,99	2145
$[Me_3PhN]_2H[Co(CN)_6] \cdot 3\,H_2O$	542,5	10,87	10,95	0,95	0,98	2140

Zur Identifizierung der protonierten Komplexe benutzten wir die bei den Normalsalzen angewandten Methoden [1]. Analytisch wurde der Zentralatom- und Cyanwasserstoff-Gehalt bestimmt. Die in einem DENNSTEDTschen Ofen aus einer getrennten Probe freigesetzten flüchtigen Produkte wurden mit einem Stickstoffstrom durch 0,1 m NaOH-Lösung getrieben. Die gebundenen Cyanidionen können nach LIEBIG argentometrisch bestimmt werden.

Zur Messung des Protonierungsgrades stand uns im Falle der tatsächlich sauren Salze auch eine von der Thermolyse unabhängige Methode zur Verfügung. Da die Verbindungen wasserlöslich sind (unlöslich nur in Säuren), konnten sie mit 0,1 *n* NaOH direkt titriert werden. Aus der Tabelle ist ersichtlich, daß die auf thermischem bzw. azidimetrischem Wege erhaltenen Ergebnisse gut übereinstimmen.

In der letzten Spalte der Tabelle I sind die Wellenzahlen der CN-Valenzschwingungen angeführt. Vergleicht man diese mit den auf die entsprechenden Normalsalze bezüglichen Werten [1], so ist die größere Wellenzahl immer beim protonierten Komplex zu beobachten. Beachtenswert ist die Tatsache, daß von den protonierten *Ferro*cyaniden gerade die neutralen Verbindungen die höchsten Wellenzahlwerte zeigen: etwas größere als die normalen, aber bedeutend kleinere als die sauren *Ferric*yanide. Mit dieser Reihenfolge der CN-Frequenzen wurde die anfängliche Unsicherheit in den Oxydationszuständen der *protonierten Ferrocyanidkomplexe* beseitigt, und es wurde auch mit den *diamagnetischen* Eigenschaften dieser Verbindungen Einklang geschaffen.

Ergenisse der thermischen Untersuchungen: Zerzetzungsreaktionen

Bei der Untersuchung des thermischen Abbaus der protonierten Verbindungen gingen wir wie bei den Normalsalzen vor [1]; auch die thermischen und stöchiometrischen Daten (Tabelle II und III) wurden auf ähnliche Weise zusammengestellt. In Abbildung 1 sind die Derivatogramme von vier Komplexen vorgeführt, die von den neun untersuchten Verbindungen so ausgewählt wurden, daß einerseits alle drei Anionen in Form eines Komplexen vertreten sind und andererseits auch das Verhalten der verschiedenen sauren Salze sowie das der Komplexe von gleiche und gemischte Liganden enthaltenden Kationen verglichen werden kann.

Die Verbindung $[Me_4N]_2H_2[Fe^{II}(CN)_6]$ gibt in der ersten Zersetzungsstufe unter endothermen Verhältnissen 2 Mol HCN ab (Tabelle II, Abb. 1-a). Die Abspaltungstemperatur von HCN (185°) ist annähernd der der freien Säure [4] gleich (190°), was — unter Berücksichtigung der Identität der freiwerdenden Komponenten — gar nicht überraschend ist. Die Zersetzung verläuft nach folgenden Gleichungen:

$$[Me_4N]_2\,H_2[Fe^{II}(CN)_6] \xrightarrow[\text{endo.}]{185^\circ} 1/6\ Fe_2{}^{II}[Fe^{II}(CN)_6] + \\ + 1/2\ [Me_4N]_4\,[Fe^{II}(CN)_6] + 2\ HCN\,. \qquad (1)$$

Der in der ersten Stufe gebildete Normalkomplex zersetzt sich in schon bekannter Weise weiter:

$$1/2\ [Me_4N]_4\,[Fe^{II}(CN)_6] \xrightarrow[\text{endo.}]{300-450^\circ} 1/6\ Fe_2{}^{II}[Fe^{II}(CN)_6] + \\ + 2\ Me_4N\cdot CN \longrightarrow 2\ Me_3N + 2\ Me-CN\,. \qquad (2)$$

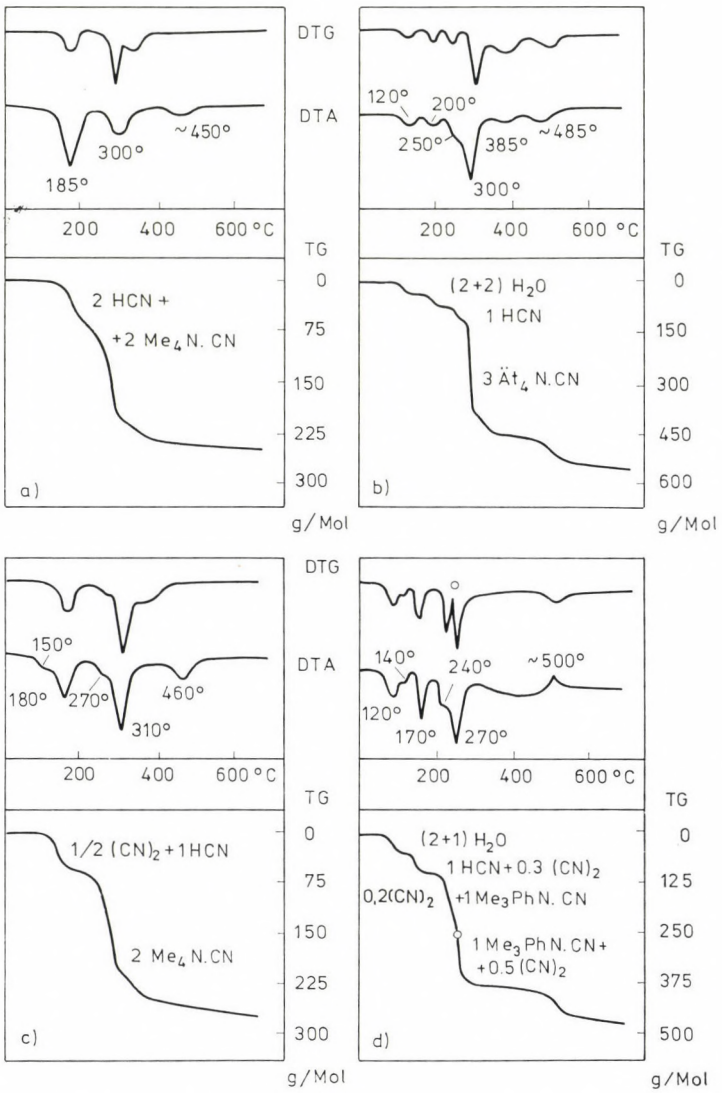

Abb. 1. Derivatogramme (TG-, DTA- u. DTG-Kurven) von quartären Ammonium-Wasserstoff-Cyanometallaten (protonierte Komplexe): a) $[Me_4N]_2H_2[Fe^{II}(CN)_6]$, b) $[Ät_4N]_3H[Fe^{II}(CN)_6] \cdot 4H_2O$, c) $[Me_4N]_2H[Fe^{III}(CN)_6]$, d) $[Me_3PhN]_2H[Co^{III}(CN)_6] \cdot 3H_2O$

Das in der Endphase gebildete tertiäre Amin und das Alkylcyanid wurde spektrophotometrisch identifiziert [1].

Der Typ der protonierten »neutralen« Komplexe wird am Beispiel des $[Ät_4N]_3H[Fe^{II}(CN)_6] \cdot 4H_2O$ dargestellt (Tabelle II, Abb. 1-b). Nach symmetrischer zweistufiger Wasserabgabe (120, 200°) beginnt die Zersetzung des

Tabelle II

Zersetzungsvorgänge von quartären Ammonium-Wasserstoff-[Hexacyanoferraten(II)]

Verbindung	Zersetzungstemperatur (°C)	Gewichtsabnahme (g/Mol)	Zersetzungsprodukt (Mol/Mol Komplex)		Bemerkung
$[Me_4N]_2H_2[Fe(CN)_6]$	185				stark, scharf: endo.
	300, 450	255	2 HCN + 2 $Me_4N \cdot CN$	(254,4)	mittelm., breit: endo.
$[Ät_4N]_3H[Fe(CN)_6] \cdot 4\ H_2O$	120, 200	72,4	(2+2) H_2O	(72,1)	schwach, flach: endo.
	230—250	27,7	1 HCN	(27,0)	Schulter: endo.
	300, 385, ~485	471	3 $Ät_4N \cdot CN$	(468,9)	mittelm., scharf: endo.
$[Bu_4N]_3H[Fe(CN)_6]$	200—220	27,6	1 HCN	(27,0)	Schulter: endo.
	275, 340, 410	803	3 $Bu_4N \cdot CN$	(805,5)	stark, scharf: endo.
$[Bu_4N]H_3[Fe(CN)_6]$	205	82,4	3 HCN	(81,0)	mittelm., scharf: endo.
	260, *320*, 420	269	1 $Bu_4N \cdot CN$	(268,5)	schwach, breit: endo.
$[Me_3PhN]_2H_2[Fe(CN)_6]$	*180*, 360 ~450	381	2 HCN + 2 $Me_3PhN \cdot CN$	(378,4)	stark, breit: endo.

Tabelle III

Zersetzungsvorgänge von quartären Ammonium-Wasserstoff-[Hexacyanoferraten(III)] und -[Hexacyanokobaltaten(III)]

Verbindung	Zersetzungstemperatur (°C)	Gewichtsabnahme (g/Mol)	Zersetzungsprodukt (Mol/Mol Komplex)		Bemerkung
$[Me_4N]_2H[Fe(CN)_6]$	150—*180*	53,6	1/2 $(CN)_2$ + 1HCN	(53,0)	mittelm., breit: endo.
	270, *310*, 460	205	2 $Me_4N \cdot CN$	(200,4)	stark, scharf: endo.
$[Me_3PhN]_2H[Fe(CN)_6] \cdot 2\ H_2O$	120, *155*	91,2	2 H_2O + 1/2 $(CN)_2$ + 1 HCN	(89,0)	stark, breit: endo.
	230, 380, 480	325	2 $Me_3PhN \cdot CN$	(324,4)	mittelm., scharf: endo.
$[Me_4N]_2H[Co(CN)_6] \cdot H_2O$	125	18,2	1 H_2O	(18,0)	schwach, flach: endo.
	200	27,3	1 HCN	(27,0)	mittelm., scharf: endo.
	305, *330*	199	2 $Me_4N \cdot CN$	(200,4)	stark, scharf: endo.
	~500	51,8	1 $(CN)_2$	(52,0)	schwach, scharf: exo.
$[Me_3PhN]_2H[Co(CN)_6] \cdot 3\ H_2O$	*120*, 140	54,7	(2+1) H_2O	(54,0)	mittelm., breit: endo.
	170	41,5	1 HCN + 0,3 $(CN)_2$	(42,6)	mittelm., scharf: endo.
	240, *270*	173	0,2 $(CN)_2$ + 1 $Me_3PhN \cdot CN$	(172,6)	stark, breit: endo.
	300—450	185	1 $Me_3PhN \cdot CN$ +	188,2	schwach, breit: endo.
	~500		+ 0,5 $(CN)_2$		schwach, scharf: exo.

eigentlichen Komplexes auch hier mit HCN-Entwicklung, findet aber bei höherer Temperatur statt (250°) als beim vorigen Komplex. Daher ist die HCN-Stufe weniger getrennt und zum Teil mit dem Effekt des quartären Ammoniumcyanids verschmolzen (300°). Die Bruttogleichung der Zersetzung ist:

$$[\text{Ät}_4\text{N}]_3\,\text{H}[\text{Fe}^{\text{II}}(\text{CN})_6] \xrightarrow[\text{endo.}]{250,\,300-485^\circ} 1/3\,\text{Fe}_2^{\text{II}}[\text{Fe}^{\text{II}}(\text{CN})_6] + \\ + \text{HCN} + 3\,\text{Ät}_3\text{N} + 3\,\text{Ät—CN}\,. \qquad (3)$$

Der thermische Abbau des *paramagnetischen* $[\text{Me}_4\text{N}]_2\text{H}[\text{Fe}^{\text{III}}(\text{CN})_6]$ unterscheidet sich von dem der vorherigen in erster Reihe darin, daß infolge des intramolekularen $\text{Fe}^{\text{III}} \rightarrow \text{Fe}^{\text{II}}$ Redoxvorganges neben Cyanwasserstoff (endotherm) auch Dicyan (exotherm) entsteht. Die zwei Reaktionen verlaufen parallel (Tabelle III, Abb. 1-c). Der in der DTA-Kurve bei 150° sichtbare Knickpunkt bezeichnet den Endpunkt der exothermen Reaktion, d. h. die Beendigung der Dicyanbildung; von hier angefangen ist nur der endotherme Effekt der HCN-Abspaltung (180°) zu beobachten. Die endothermen Effekte unter 270 und 310° sind schon der Abspaltung von 2 Mol $\text{Me}_4\text{N} \cdot \text{CN}$ zuzuschreiben. Demnach geht die Zersetzung nach der Gleichung

$$[\text{Me}_4\text{N}]_2\,\text{H}[\text{Fe}^{\text{III}}(\text{CN})_6] \xrightarrow[(\text{endo.})]{150,\,180^\circ} 1/6\,\text{Fe}_2^{\text{II}}[\text{Fe}^{\text{II}}(\text{CN})_6] + \\ + 1/2\,(\text{CN})_2 + \text{HCN} + 1/2\,[\text{Me}_4\text{N}]_4\,[\text{Fe}^{\text{II}}(\text{CN})_6] \qquad (4)$$

vor sich. Das Tetrakis (tetramethyl)-Ferrocyanid zerfällt wieder nach Gleichung (2).

Die Zersetzungsprozesse von $[\text{Me}_3\text{PhN}]_2\text{H}[\text{Co}^{\text{III}}(\text{CN})_6] \cdot 3\text{H}_2\text{O}$ scheinen ziemlich verwickelt zu sein, doch wird der Ablauf der in Abbildung 1-d angedeuteten Teilreaktionen einerseits von der guten Übereinstimmung der gemessenen und berechneten Daten der Tabelle III, andererseits auch von den schon früher geklärten Zersetzungsvorgängen des einfachen $(\text{NH}_4)_3[\text{Co}^{\text{III}}(\text{CN})_6]$ unterstüzt [7]. Die Zersetzung beginnt in 2 + 1 Molverteilung mit Wasserabgabe (120, 140°). Anschließend entweicht HCN, aber gleichzeitig tritt auch die mit Dicyanbildung verlaufende Redoxreaktion ein (170°). Da der Kobalt-(III)-Komplex *diamagnetisch* ist, spaltet sich das Dicyan anfangs *endotherm* ab. Die Verteilung des freigesetzten Dicyans (0,3 + 0,2 + 0,5 Mol/Mol Komplex) zeigt, daß die Reduktion des Cyanokobaltats(III) stufenweise vor sich geht: zu erst bildet sich ein gemischter $\text{Co}^{\text{III}}—\text{Co}^{\text{II}}$, dann ein nur Co^{II} enthaltender Komplex bzw. einfaches $\text{Co}^{\text{II}}(\text{CN})_2$. Letzteres ist schon *paramagnetisch*, deshalb reduziert es sich unter *exothermen* Verhältnissen zu Co^{I} ($\sim$ 500°). Die einzelnen Teilvorgänge sind also die folgenden:

$$[\text{Me}_3\text{PhN}]_2\,\text{H}[\text{Co}^{\text{III}}(\text{CN})_6] \xrightarrow[\text{endo.}]{170^\circ} 1/5\,\text{Co}_3^{\text{II}}[\text{Co}^{\text{III}}(\text{CN})_6]_2 + \\ + 2\,\text{Me}_3\text{PhN} \cdot \text{CN} + \text{HCN} + 0{,}3(\text{CN})_2\,, \qquad (5)$$

dann:

$$1/5\ Co_3^{II}[Co^{III}(CN)_6]_2 \xrightarrow[\text{endo.}]{240^\circ} 1/5\ Co_3^{II}[Co_2^{II}(CN)_{10}] + 0{,}2(CN)_2\,, \qquad (6)$$

schließlich:

$$1/5\ Co_3^{II}[Co_2^{II}(CN)_{10}] \xrightarrow[\text{endo.}]{270^\circ} Co^{II}(CN)_2 \xrightarrow[\text{exo.}]{500^\circ} Co^{I}CN + 0{,}5\,(CN)_2\,. \qquad (7)$$

Der komplizierte Redoxvorgang wird noch von der stufenweisen Abspaltung des 2 Mol $Me_3PhN \cdot CN$ überlagert, das sich sofort — ähnlich dem entsprechenden Neutralsalz — zu N,N-dimethylanilin und Methylcyanid zersetzt [1].

Die weitere Zersetzung der in den Gleichungen (1)—(4) bzw. (7) vorkommenden festen Rückstände ist schon aus früheren Arbeiten [4, 7] bekannt. Die Identifizierung der Präparate und ihrer thermischen Zersetzungsprodukte sowie Methoden und Geräte dieser Untersuchungen wurden in der vorangehenden Mitteilung bereits ausführlich beschrieben.

*

Für die Herstellung der Präparate bzw. für die Anfertigung der derivatographischen und spektrophotometrischen Aufnahmen sprechen die Verfasser Frau É. Csukás, E. Csiszár und H. Haeffner auch an dieser Stelle ihren Dank aus.

LITERATUR

[1] Mohai, B., Bagyin, L.: Acta Chim. (Budapest) **92,** 279 (1977)
[2] Bagyin, L.: Doktorarbeit. Univ. f. Chem. Ind. Veszprém, 1971
[3] Beck, W., Smedal, H. S.: Z. Naturforsch. **20b,** 109 (1965)
[4] Mohai, B.: Acta Chim. Acad. Sci. Hung. **62,** 217 u. 229 (1969)
[5] Kolthoff, I. M., Tomsiček, W. J.: J. Physic. Chem. **39,** 355 (1935)
[6] Jordan, J., Ewing, G. J.: Inorg. Chem. **1,** 587 (1962)
[7] Mohai, B.: Z. anorg. allg. Chem. **392,** 287 (1972)

Béla Mohai; H-8201 Veszprém, Pf. 28.
László Bagyin; H-2600 Vác, Csokonai u. 3.

Acta Chimica Academiae Scientiarum Hungaricae, Tomus 92 (3), pp. 289—292 (1977)

ANODIC OXIDATION OF POTASSIUM OXALATE IN SULFURIC ACID ON A GERMANIUM SEMICONDUCTOR-ELECTROLYTE INTERFACE

M. M. SINGH* and C. S. SINGH**

*(*Applied Chemistry Section, Institute of Technology Banaras Hindu University, India and **Chemistry Department, Udai Pratap College)*

Received May 26, 1976

The anodic oxidation of potassium oxalate on the surface of *n*- and *p*-Ge electrodes has been studied in 0.1 *N* sulfuric acid. Tafel curves are plotted and the nature of the current carriers involved in the process is ascertained from the comparison of polarization curves of *n*- and *p*-Ge anodes. The tafel relation, $\eta = a + b \log i$, is valid in a very narrow range of current density. A saturation current density is observed only on the polarization curves of the *n*-Ge anode; its magnitude increases on the addition of oxalate to the sulfuric acid solution. On the *p*-Ge anode the overvoltage increases steadily with increase in the current density. Illumination of the electrode surface does not alter the nature of the polarization curve on the *p*-Ge anode, whereas the anodic saturation current density on *n*-Ge is increased on illumination. Our results show that the process of oxidation of oxalate ions involves electron transfer from ions to the conductance band of germanium.

The anodic oxidation of ions in an electrolyte at the surface of a germanium electrode occurs with the simultaneous dissolution of the electrode material. The process of dissolution occurs with the participation of holes [1], whereas the process of oxidation may involve the depletion of holes in the valence band or the injection of electrons into the conduction band of the semiconductor electrode. The nature of current carriers involved has a marked influence on the anodic polarization behaviour of the electrode under study and, consequently, the natures of the polarization curves on *n*- and *p*-Ge differ considerably. Moreover, the processes occurring at the surface of a semiconductor may lead to a typical saturation current which is light sensitive [1—3] and whose magnitude depends upon the redox potential [4] and concentration of the redox reagents.

In the present work the anodic polarization behaviour of *n*- and *p*-Ge electrodes in the oxidation of potassium oxalate in the presence of sulfuric acid has been studied so as to ascertain the nature of current carriers involved during the oxidation of oxalate ions.

Experimental

The results of anodic polarization measurements have been recorded galvanostatically in stirred solutions. The details of the procedure and apparatus used have been described [5].

The chemicals used were of B. D. H. Analar grade, recrystallized from conductivity water before use. Sulfuric acid used as supporting electrolyte was purified by pre-electrolysis.

A stock solution of sulfuric acid was prepared in conductivity water and stored in a Jena glass reagent bottle. The solutions of desired concentrations were prepared by the volumetric method followed by accurate and appropriate dilutions.

Results and discussion

The comparison of the curves obtained upon anodic polarization of *n*-Ge (Fig. 1) and *p*-Ge (Fig. 2) electrodes reveals that the saturation current density is exhibited only on *n*-Ge whereas on *p*-Ge there is a steady increase in the overpotential with increasing current density. The addition of oxalate

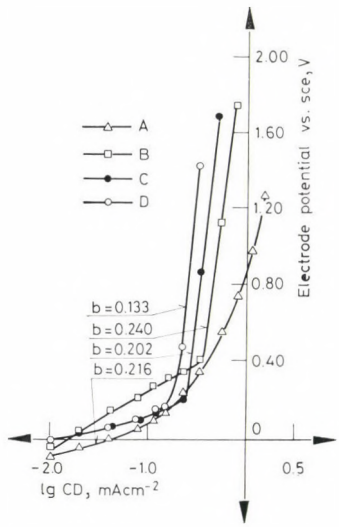

Fig. 1. Anodic polarization curves for the oxidation of potassium oxalate in 0.1 *N* H_2SO_4 on an *n*-Ge electrode. A — 0.10 *M* $K_2C_2O_4$; B — 0.05 *M* $K_2C_2O_4$; C — 0.02 *M* $K_2C_2O_4$; D — 0.1 *N* H_2SO_4

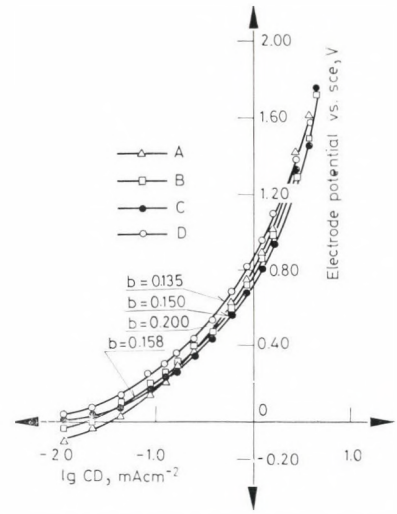

Fig. 2. Anodic polarization curves for the oxidation of potassium oxalate in 0.1 *N* H_2SO_4 on a *p*-Ge electrode. A — 0.10 *M* $K_2C_2O_4$; B — 0.05 *M* $K_2C_2O_4$; C — 0.02 *M* $K_2C_2O_4$; D — 0.1 *N* H_2SO_4

ions to the sulfuric acid solution does not affect the anodic polarization behaviour of *p*-Ge but the magnitude of saturation current density observed on *n*-Ge for the dissolution of germanium is increased. The increase in saturation current density on addition of oxalate ions has also been reported by Efimov and Erusalimchik [6]. The change in overpotential upon the addition of oxalate ions in both cases is very small and may be attributed to the change in pH of the electrolyte solution [7] resulting from the addition of potassium oxalate.

The curves obey the Tafel relation in a very narrow range of current density. The slope of the curve increases with the addition of the reductant,

both on *n*- and *p*-Ge anodes. (The slopes were calculated by plotting typical curves for Tafel regions on a highly sensitive scale.) The value of the Tafel slope *b* decreases as the amount of potassium oxalate added is decreased, however, for the same concentrations of oxalate ion the respective value of *b* on *n*-Ge is always greater than that on *p*-Ge. Taking the *b* value as a measure of the overall reaction rate it may be easily suggested that the rate of dissolution is appreciably influenced during the oxidation of oxalate ions. The extent of this influence depends upon the type of conductivity.

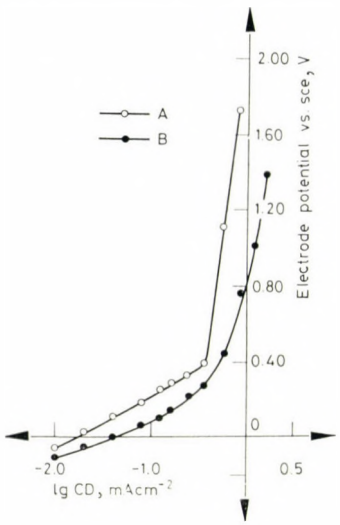

Fig. 3. Influence of illumination on the anodic polarization of an *n*-Ge electrode. A — Not illuminated; B — illuminated

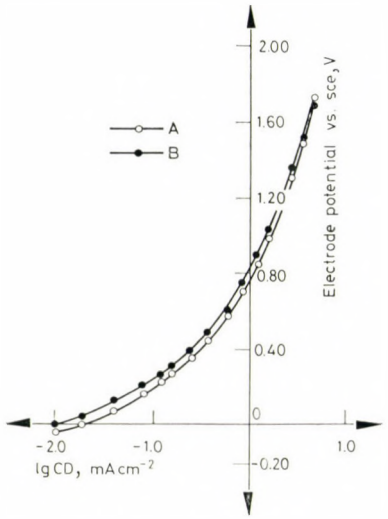

Fig. 4. Influence of illumination on the anodic polarization of a *p*-Ge electrode. A — Not illuminated; B — illuminated

The oxidation of oxalate ions may involve either the transfer of electrons from oxalate ions to the valence band or to the conduction band of germanium. If electron transfer occurs from oxalate to the valence band of the semiconductor, the saturation current density observed on *n*-Ge in sulfuric acid should decrease [8] on the addition of the reductant. In this case two processes, namely, dissolution of germanium and oxidation of oxalate ions will compete for holes, resulting in faster consumption of holes. Therefore, the participation of holes in the oxidation process is unlikely. On the other hand, if conductance band electrons were to participate, electrons should be injected into the conductance band during oxidation of the reductant. As a result of injection of electrons and increase in their concentration at the surface of germanium a strong electric field is produced which in its turn promotes the appearance of a large number of holes at the surface, largely due to drift. These extra

holes produced may be simultaneously utilized during the process of dissolution, which results in an increase in the saturation current density. Our finding that no change is observed in the nature of the polarization curve on *p*-Ge is obvious in the light of the proposed mechanism. In this case injection of electrons into the conductance band simply increases the number of electrons. EFIMOV and ERUSALIMCHIK [9, 10] have also proposed participation of the conductance band in the oxidation of oxalate ions.

Our mechanism has been further confirmed by studying the photosensitivity of the saturation current density. The influence of illumination on the polarizations of an *n*-Ge anode is shown in Fig. 3. The electrolyte consisted of 0.05 *M* potassium oxalate in 0.1 *N* sulfuric acid. In dark a well-defined saturation current density is obtained, which increases on illumination. A simultaneous distortion of the curve is observed and the saturation current ceases to be well-defined. This can be easily explained assuming the conductance band mechanism to be completely valid. The quanta absorbed on illumination promote electrons from the valence to the conductance band. Thus, whereas holes are produced both during oxidation of oxalate ions and illumination, their consumption occurs only during anodic dissolution. Since there are two sources of extra holes, the saturation current density observed for the oxidation of oxalate ions on *n*-Ge is further increased, the polarization behaviour of *p*-Ge being assumed. On *p*-Ge the anodic polarization curves remain unaffected in accordance with the theory. Any increase in the number of holes in *p*-Ge should not have any influence on the polarization behaviour.

*

The authors express their gratefulness to late Dr. D. SINGH, Ex-Reader in Chemistry, B. H. U., for the initiation of work and thank Professor C. V. AGARWAL, In charge of Applied Chemistry Section, Institute of Technology, B. H. U., for encouragement.

REFERENCES

[1] BRATTAIN, W. H., GARRETT, C. G. B.: Bell Syst. Tech. J., **34,** 29 (1955)
[2] EFIMOV, E. A., ERUSALIMCHICK, I. G.: Zh. Fiz. Khim., **32,** 1103 (1958)
[3] GREEN, M.: J. Chem. Phys., **31,** 200 (1959)
[4] TURNER, D. R.: J. Electrochem. Soc., **103,** 252 (1956)
[5] SINGH, M. M., SINGH, D.: Acta Chim. (Budapest), **87,** 51 (1975)
[6] EFIMOV, E. A., ERUSALIMCHIK, I. G.: Dokl. Akad. Nauk. SSSR, **128,** 124 (1959)
[7] SINGH, D., SHARMA, S., SINGH, M. M.: J. Sci. Res. (B. H. U.), **22,** 171 (1971—72)
[8] GERISCHER, H., BECK, F.: Z. Physik. Chem. NF., **13,** 389 (1957)
[9] EFIMOV, E. A., ERUSALIMCHIK, I. G.: Zh. Fiz. Khim., **35,** 543 (1961)
[10] EFIMOV, E. A., ERUSALIMCHIK, I. G.: Zh. Fiz. Khim., **36,** 1791 (1962)

*

M. M. SINGH; Banaras Hindu University, Applied Chemistry Section, Institute of Technology, Varanasi-221005 India

C. S. SINGH; Chemistry Department, Udai Pratap College, Varanasi-221002 India

Acta Chimica Academiae Scientiarum Hungaricae, Tomus 92 (3), pp. 293–309 (1977)

UNTERSUCHUNGEN ÜBER DIE SYNTHESE VON 1,5-BENZODIAZEPINEN

Z. Zubovics, G. Fehér und L. Toldy

(Institut für Arzneimittelforschung, Budapest)

Eingegangen am 12. Dezember, 1975

Es wird über die Synthese von neuen 1,5-Benzodiazepin-2-onen durch Reaktion von 1,3-Diphenyl-2-hydroxy-2-cyclobuten-1-on (Phenylketen-Dimer) mit ringsubstituierten *o*-Phenylendiaminen berichtet, wobei die Amidgruppe im Siebenring aus der nukleofileren Aminogruppe des Ausgangsdiamins gebildet wird. Die Struktur bzw. Stellung des Substituenten wurde durch unabhängige Synthese bewiesen.

Die Reaktion von α, γ-Diphenyl-acetessigester mit *o*-Phenylendiamin führte nicht zum erwarteten Benzodiazepin, sondern zu mehreren anderen Verbindungen, deren Strukturaufklärung auf den Mechanismus der Reaktion schließen ließ.

A synthesis of 1.5-benzodiazepin-2-ones by reaction of 1.3-diphenyl-2-hydroxy-2-cyclobuten-1-one (phenylketene dimer) with *o*-phenylene diamines is described, during which the amide group in the seven membered ring is formed from the more nucleofilic amino group in the starting diamine. The structure and position of the substituents were proved by an independent synthesis.

The reaction of ethyl α, γ-diphenyl-acetoacetate with *o*-phenylene diamine did not afford the expected benzodiazepine, but several other products, the structure elucidation of which gave informations about the reaction mechanism.

Einleitung

Ketene und Keten-Dimere stellen bekanntlich reaktive Ausgangsmaterialien für vielerlei Synthesen dar [1]. Unter anderen kann der Vierring eines Keten-Dimers mit Aminen aufgespalten werden [2]. Verwendet man nun Diamine, so können beide Aminogruppen in Reaktion treten, wobei Heterocyclen gebildet werden; so entstehen z. B. aus 1,1,3,3-Tetramethylcyclobutan-2,4-dion (Dimethylketen-Dimer) (**I**) und Äthylendiamin (**II**), das lineare Amid **III** und oder der Fünfring **IV** [3].

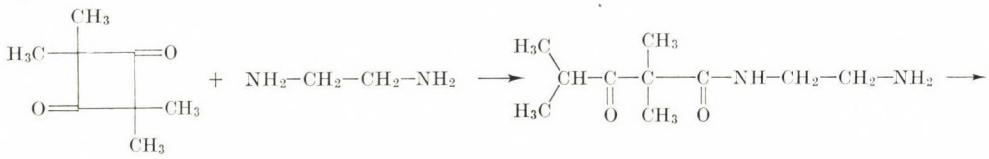

I II III

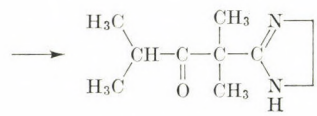

IV

Die Reaktion von Diketen (**V**) mit *o*-Phenylendiamin (**VI**) führt dagegen zu einem Siebenringsystem (**VII**) [4].

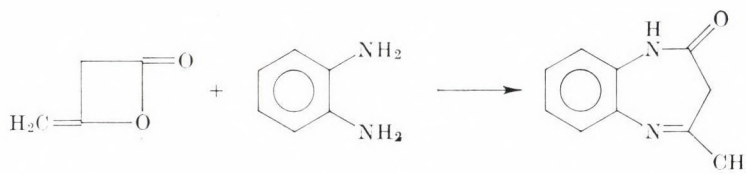

V VI VII

Unser Ziel war, die Reaktionen einer in weniger breitem Kreis erforschten Keten-Dimer-Gruppe, u. w. der Aryl-aldoketen-Dimere mit Diaminen, zu untersuchen. Als Modellverbindung wurde der Phenylketen-Dimer (**VIII**) [5] gewählt.

Ergebnisse und Diskussion

Bei der Umsetzung von **VIII** mit einem primären aliphatischen Amin entstand das erwartete Amid **X**, welches auch durch eine von α, γ-Diphenylacetessigester (**IX**) ausgehende, unabhängige Synthese hergestellt wurde.

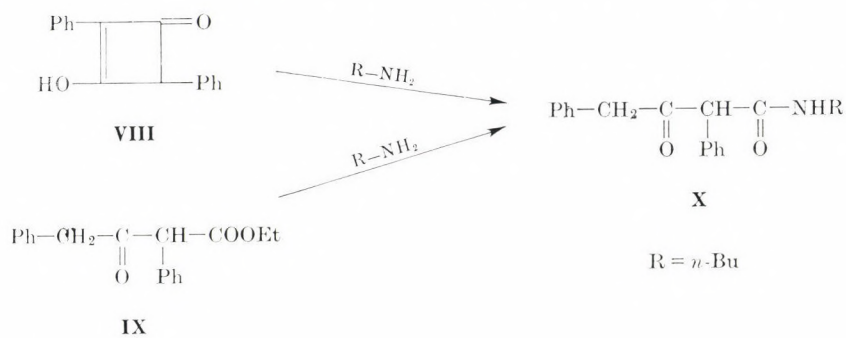

VIII X IX

R = *n*-Bu

Im Gegensatz zu der Reaktion von **I** mit **II**, wurde **VIII** bei der Umsetzung mit **II** selbst unter relativ milden Bedingungen zum Monomer gespalten, und es wurden nur einfach bzw. zweifach phenacylierte Äthylendiamin-Derivate isoliert.

Mit *o*-Phenylendiamin und seinen ringsubstitutierten Derivaten reagierte **VIII** unter Rückfluß in Benzol glatt, und ergab neuartig substituierte 1,5-Benzodiazepin-2-one der allgemeinen Formel **XI*** (Methode A zur Synthese von **XI**).

Die Struktur dieser neuen Verbindungen wurde mittels der gewöhnlichen analitischen und spektroskopischen Methoden sichergestellt, **XIa** wurde ferner mit seinem 4,5-hydrierten Derivat (**XIIa**) charakterisiert.

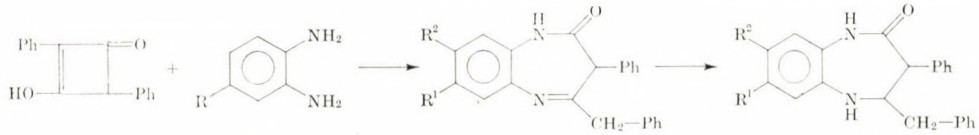

VIII VI XI XII

R	R^1	R^2
a H	a H	H
b Cl	b Cl	H
c OCH_3	c OCH_3	H
d CH_3	d CH_3	H
	e H	CH_3
	f H	Cl

a $R^1 = R^2 = H$

Mit Rücksicht darauf, daß in **VI** beide Aminogruppen im ersten Reaktionsschritt angegriffen werden können, ergibt sich für R die Stellung 7 oder 8 in **XI**. Dieses Problem wurde zuerst mit NMR untersucht.

Nach der Literatur wurden 1,5-Benzodiazepine aus 4-substituierten *o*-Phenylendiaminen auf anderen Synthesewegen hergestellt, und die Stellung von R im Endprodukt wurde diskutiert [6, 7, 8].

Kost und Mitarb. haben gefunden, daß aus 4-Methyl-*o*-phenylendiamin und Acetessigester nur ein einziges Produkt entsteht, u. zw. das entsprechende 7-Methyl-1,5-benzodiazepin-Derivat, dessen Struktur durch eine unabhängige Synthese bewiesen wurde [6a]. Gleichzeitig traten aber die CH_3-Signale des aus 4,5-Dimethyl-*o*-phenylendiamin und Acrylamid hergestellten 7,8-Dimethyl-1,3,4,5-tetrahydro-2H-1,5-benzodiazepin-2-ons im NMR nicht getrennt auf [6e]. Israel und Mitarb. haben sogar beide Isomere aus der Reaktion von

* Im voraus konnte mit Sicherheit nicht beurteilt werden, ob **VIII** analog zu **V** reagieren wird. Diketen (**V**) stellt nähmlich einen Vertreter der »Kopf-Kopf« geknüpften Keten-Dimere mit β-Lacton-Struktur dar, während **VIII** ein »Kopf-Schwanz«-Dimer — mit einem, aus der Cyclobutandion-Struktur abgeleiteten, tautomeren Cyclobutenolon-Skelett — repräsentiert. Dieser Unterschied scheint wichtig zu sein, da diese beiden Typen selbst im Falle derselben Substituenten im Monomer gegebenenfalls verschiedenartig reagieren können (s. z. B. 1a, 1b).

4-Methyl-*o*-phenylendiamin mit γ, γ, γ-Trifluoro-acetessigester isoliert, die Methylsignale erschienen aber auch in diesem Fall bei demselben Wert [8].

In unseren Versuchen entstand aus 4-Methyl-*o*-phenylendiamin und **VIII** ein Gemisch, das offensichtlich aus dem 7-Methyl- und dem 8-Methyl-benzodiazepin-Derivat bestand. (Im NMR erschienen zwei Methylsingulette bei $\delta = 2{,}21$ und $\delta = 2{,}25$ ppm, die Summe der Integralwerte dieser zwei Banden entsprach 3 Protonen.)

Nachdem die Zuordnung der Methyl-Banden im NMR zu dem 7- bzw. 8-Methyl-Derivat nicht möglich war, und ferner auch die spektroskopischen Untersuchungen der anderen Derivate keine genügende Information über die Stellung der Substitution ergaben, wurden 7- bzw. 8-substituierte 1,5-Benzodiazepin-Derivate mit zweifelloser Struktur auf folgende Weise synthetisiert:

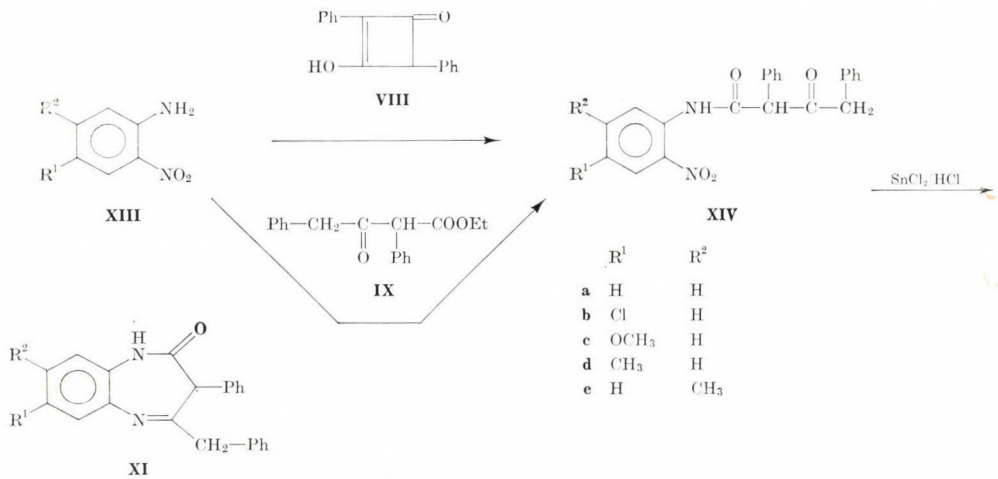

Sowohl die Synthese von N-acetoacetylierten *o*-Nitranilin-Derivaten des Typs **XIV**, als auch ihre Umwandlung in die Benzodiazepine des Typs **XI** mit anderen Substituenten sind schon früher, auf anderen Synthesewegen (Reaktion von *o*-Nitranilin mit Diketen bzw. Reduktion durch katalytische Hydrierung), beschrieben worden [9, 10]. Die hier beschriebene Herstellung von **XI** ist aber vom Gesichtspunkt der praktischen Ausführung eine modifizierte, milde Methode.

VIII wurde mit dem entsprechenden Nitranilin (**XIII**) in Benzol oder Toluol umgesetzt. Diese Acylierung verläuft bei 80 °C recht langsam, die Reaktionstemperatur kann aber nicht beliebig erhöht werden, denn **VIII** wird thermisch leicht (eine Stunde in siedendem Xylol) in das isomere Phenyl-naphthalin-diol (**XV**) umgewandelt [11, 12].

Um diese Schwierigkeit zu umgehen, wurde die Reaktion am besten durch kurzdauerndes Kochen der Reaktanten in Toluol durchgeführt.

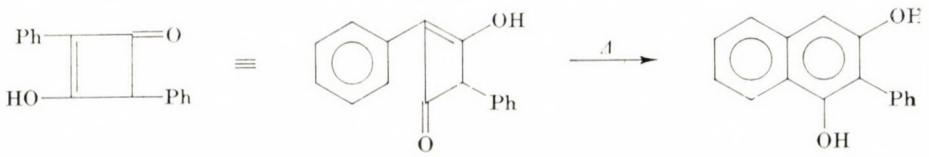

VIII XV

Die Verbindungen **XIV** wurden auch auf einem anderen Weg hergestellt: die Nitraniline **XIII** wurden mit α, γ-Diphenyl-acetessigester (**IX**) in siedendem Xylol oder vorteilhafter in Chlorbenzol acyliert, dadurch konnte die mühsame Herstellung von **VIII** vermieden werden. Es ist bemerkenswert, daß α, γ-Diphenyl-acetessigester, im Gegensatz zu einer Anzahl anderer Acetessigester-Derivate, nicht mit seinem Keto-, sondern mit der Esterfunktion in Reaktion tritt (s. z. B. 6, 7, und die dort zitierte Literatur). Dieser Befund kann mit der durch die α-Phenylgruppe erhöhten Reaktionsfähigkeit der Estergruppe erklärt werden.

Die Reduktion der acylierten Nitraniline **XIV** wurde durch eine an und für sich bekannte Methode [13], u. zw. mittels einer essigsauren-salzsauren Lösung von $SnCl_2$ bei 0— +5 °C, durchgeführt, die entstandenen Amine cyclisierten unter diesen Reaktionsbedingungen spontan (Methode B zur Herstellung von **XI**).

Die erwähnte Reduktionsmethode ist zur Herstellung von aromatischen und heterocyclischen Aminen ausgedehnt verwendet, über ihre Anwendung in der Synthese von Benzodiazepinen auf diesem Weg ist aber noch nicht berichtet worden.

Reduktionsversuche mit anderen bekannten Methoden [14] führten nicht zu den gewünschten Produkten. $SnCl_2$/cc. HCl in Äthanol bei 80 °C, wie auch H_2S/NH_3 in Methanol, ergaben heterogene Gemische, durch katalytische Hydrierung konnte aber das 4,5-Dihydro-Derivat der Grundverbindung (**XIIa**) erhalten werden. Eine mit Zn/H_3PO_4 in Dioxan bei Siedetemperatur durchgeführte Reduktion von **XIVa** ergab dagegen nicht **XIa**, sondern das isomere Benzimidazolon-Derivat **XVI**, s. später.

Durch Vergleich der mit Methode B erhaltenen Verbindungen **XI** mit zweifelloser Struktur mit den durch Methode A gewonnenen konnte die folgende Richtung der Reaktion von **VIII** mit **VIa—d** festgestellt werden:

Aus 4-Methoxy-o-phenylendiamin entsteht in der Reaktion mit dem Phenylketen-Dimer (Methode A) das entsprechende 7-Methoxy-1,5-benzodiazepin-Derivat (**XIc**). Aus 4-Methyl-*o*-phenylendiamin wird ein 6 : 4 Gemisch der 7- und 8-Isomere (**XId** und **XIe**) erhalten. Der Vergleich des nach Methode B erhaltenen Verbindungspaares **XId—XIe** mit ihrem gemäß Methode A gewonnenen Gemisch entspricht der Erwartung, die Methylsignale im NMR der beiden Isomeren können wie folgt zugeordnet werden: 7-Methyl-Derivat (**XId**): δ CH_3 = 2,28 ppm; 8-Methyl-Derivat (**XIe**): δ CH_3 = 2,23 ppm. 4-

Chlor-*o*-phenylendiamin liefert dagegen eine mit **XIb** (Methode B) isomere Verbindung, u. zw. das 8-Chlor-Derivat (**XIf**).

Eine derartige Richtung der Reaktion konnte angesichts der elektronenanziehenden bzw. -sendenden Eigenschaften des Substituenten wohl erwartet werden, denn der Vierring von **VIII** wird von dem nukleofileren N-Atom des Diamins angegriffen und geöffnet. Dementsprechend führt die Reaktion des 4-Chlor-*o*-phenylendiamins zum 8-Chlor-benzodiazepin (**XIf**), während das 4-Methoxy-diamin das 7-Methoxy-benzodiazepin (**XIe**) liefert. Ferner kann, nachdem die Nukleofilität der N-Atome in **VId** von der 4-Methylgruppe nur wenig beeinflußt wird, in diesem Fall ein Gemisch des 7- und des 8-Isomers gewonnen werden.

Die Reaktion von x,y-Diphenyl-acetessigester mit o-Phenylendiamin

Die meistverwendete Synthese zur Herstellung von 1,5-Benzodiazepin-2-onen ist die Reaktion von *o*-Phenylendiamin mit Acetessigester-Derivaten. Nach zahlreichen Literaturangaben liefert diese Reaktion, abhängig vom pH des Mediums und den Substituenten in α- bzw. γ-Stellung zur Estergruppe, verschiedene Produkte. Die durch primäre Reaktion der Keto- oder der Estergruppe entstehenden Zwischenprodukte können durch nachfolgende Cyclisierung in fünf- bzw. siebengliedrige Heterocyclen überführt werden [5, 9, 14—20].

Zur Herstellung unserer Grundverbindung **XIa** wurde *o*-Phenylendiamin in siedendem Xylol, unter Entfernung des entstandenen Wassers und Alkohols durch azeotrope Destillation, mit α, γ-Diphenyl-acetessigester umgesetzt. Im Anwesenheit katalytischer Mengen wasserfreier Salzsäure, wie auch einer organischen Base (Pyridin) erhielt man das 1-[(1', 3'-Diphenyl)-1'-propen-2'-yl]-2,3-dihydro-2-benzimidazolon (**XVI**) in einer Ausbeute von 73,5% bzw. 62%. Verwendete man eine anorganische Base (K_2CO_3, $NaHCO_3$) als Katalysator, so entstanden N,N'-Bis-phenacyl-*o*-phenylendiamin (**XVII**) und 2,3-Dihydro-2-benzimidazolon (**XVIII**) in einem Verhältnis von etwa 10 : 1, die Gesamtausbeute betrug 90%.

In neutralem Medium entstanden unter den gleichen Bedingungen 3 Hauptprodukte, welche durch Säulenchromatographie getrennt wurden, und deren Struktur durch Elementaranalyse, IR-, NMR- und Massenspektrum sichergestellt wurde. Demgemäß waren die drei Verbindungen 1-[(1', 3'-Diphenyl)-1'-propen-2'-yl]-2,3-dihydro-2-benzimidazolon (**XVI**) (Ausbeute: 36,1%), N-(α, γ-Diphenyl-acetoacetyl)-*o*-phenylendiamin (**XIX**) (14,3%) und 3-Phenyl-4-benzoyl-1,3-dihydro-2H-1,5-benzodiazepin-2-on (**XX**) (23%).

Wie ersichtlich, konnte in dieser Reaktion unabhängig vom pH des Mediums kein **XIa** isoliert werden. Das Entstehen von **XX** weist darauf hin,

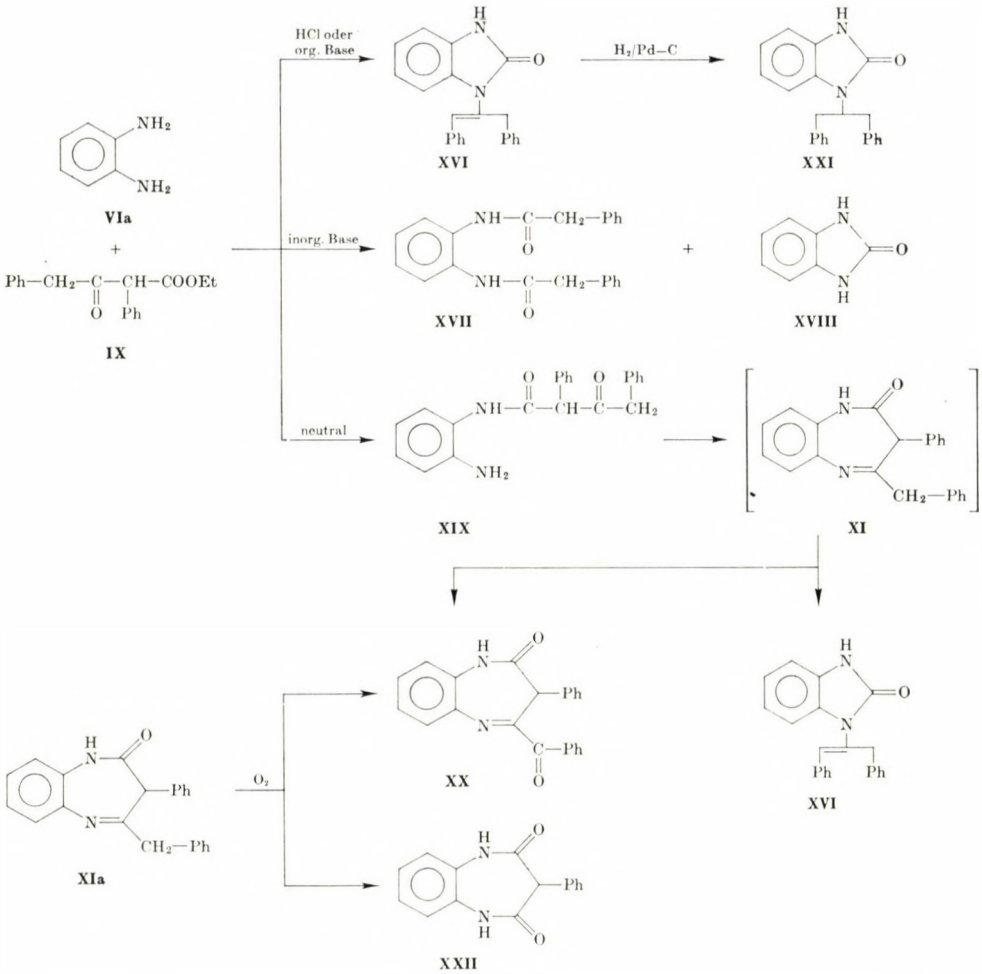

daß sich **XIX**, das vermutliche Zwischenprodukt der Reaktion, zuerst in **XIa** umwandelt, welches aber gleich weiterneagiers **XX** entstekt auf den binfluß von Luft sauerstoff, wie das in einem aus **XIa** ausgehenden Oxydationsversuch bewiesen werden konnte (als Nebenprodukt dieser Oxidation entstand das Benzodiazepin-dion **XXII**). Bei der Wiederholung dieser, in neutralem Medium durchgeführten, Reaktion in Abwesenheit von Luft entstand kein **XX**, der Anteil an **XVI** war aber wesentlich höher.

XVI entsteht ebenfalls aus **XIa**, u. zw. durch Isomerisation, derartige Umlagerungen von analogen Benzodiazepinen sind aus der Literatur bekannt [14]. In unserem Fall ist **XIa** wegen der elektronenanziehenden Phenylgruppe am C_3 mäßig stabil und wird schon bei der Siedetemperatur des Xylols umgelagert, während andere Acetessigester-Derivate und *o*-Phenylendiamine nach

Literaturangaben [14] meistens in siedendem Xylol zu den entsprechenden Benzodiazepinen kondensiert, und bei 180—220 °C in die isomeren 2-Benzimidazolone umgelagert werden können. (In Versuchen zur Herstellung von **XIa** in der gleichen Reaktion bei niedrigerer Temperatur, z. B. in Toluol gekocht, war die Konversion selbst nach verlängertem Kochen sehr gering.) Der Einfluß des Substituenten am C_3 wird auch dadurch unterstützt, daß sich das aus α, γ-Bis-(*p*-methoxyphenyl)-acetessigester hergestellte Analogon von **XIa** beim Erhitzen als wesentlich stabiler erwies.

Die Reaktionsgeschwindigkeit der Umlagerung **XIa** → **XVI** hängt stark von der Polarität des Lösungsmittels ab, so verläuft z. B. die Reaktion beim Erhitzen von **XIa** in *n*-Butanol bei 100 °C innerhalb von 3 Stunden. Arbeitet man in Xylol, so ist die Siedetemperatur zur Vollendung der Reaktion innerhalb von 3 Stunden notwendig.

α, γ-Diphenyl-acetessigester und *o*-Phenylendiamin wurden noch unter anderen, in der Literatur für die Kondensation von β-Diketo-Verbindungen mit diesem Amin beschriebenen Bedingungen (**XIVa**) umgesetzt, das erwartete Benzodiazepin **XI** konnte jedoch nicht erhalten werden.

Für die Elementaranalysen sind wir Frau Judit HEGEDÜS, für die Aufnahme und Auswertung der IR-, NMR- und Massenspektren sowie für wertvolle Vorschläge und Diskussionen den Herren Gábor TÓTH und Gyula HORVÁTH zu Dank verflichtet.

Experimenteller Teil

Die Schmelzpunkte sind nicht korrigiert und wurden auf einem Kofler-Boetius-Mikroheiztisch bestimmt.

Die IR-Spektren wurden mit einem Perkin-Elmer 457 Spektrophotometer in KBr-Pastillen, die NMR-Spektren mit einem JEOL C-60 (23 °C) bzw. mit einem Varian A-60D (36 °C) Apparat, mit TMS als inneren Standard und die Massenspektren mit einem Varian MAT SM-1 Spektrometer aufgenommen. Die Werte der chemischen Verschiebung in den NMR-Spektren sind in δ (ppm) angegeben.

2,4-Diphenyl-3-hydroxy-2-cyclobuten-1-on (Phenylketen-Dimer, VIII)

wurde nach der Methode von FARNUM und Mitarb. [5] hergestellt.

α, γ-Diphenyl-N-(n-butyl)-acetessigsäure-amid (X)

A. Aus Phenylketen-Dime (VIII) und prim.-n-Butylamin

0,1 cm^2 (0,0015 Mol) prim.-*n*-Butylamin und 0,25 g (0,001 Mol) Phenylketen-Dimer (**VIII**) wurden in absol. Benzol 30 Minuten lang gekocht. Die erhaltene klare Lösung wurde partiell eingedampft und das Produkt mit Petroläther ausgefällt. Ausbeute: 0,10 g (29%), Schmp. 109—111 °C.

Analyse für $C_{20}H_{23}NO_2$ (309,41)		Ber.	Gef.
		C 77,64	76,92
		H 7,49	7,77
		N 4,53	4,47
IR-Spektrum	NH	3300 cm^{-1}	
	ww	1720 cm^{-1}	
	Amid I.	1640 cm^{-1}	

NMR-Spektrum (in $CDCl_3$)

Ph-CH_2	3,82 s (2H)
Ph-CH	4,8 s (1H)
$CH_3(CH_2)_3$	0,8—1,8 m (9H)

Massenspektrum

	m/e	relative Intensität (%)
M^+	309	95
$M-C_6H_5CH_2$	218	100
$M-C_6H_5CHCO$	191	80

B. Aus α, γ-Diphenyl-acetessigester (**IX**) *und prim.-n-Butilamin*

Zu einer Lösung von 1,4 g (0,005 Mol) α, γ-Diphenyl-acetessigester (**IX**) [23] in 50 cm^3 absol. Xylol wurde 0,5 cm^3 (0,005 Mol) prim.-n-Butilamin, in 20 cm^3 absol. Xylol gelöst, innerhalb einer Stunde, unter ständigem langsamem Destillieren, zugetropft. Nach einer weiteren Stunde Destillieren (das Volumen des Reaktionsgemisches wurde durch langsames Zutropfen von reinem Xylol konstant gehalten) wurde die Lösung zur Trockne eingedampft, und der Rückstand aus Benzol/Petroläther umkristallisiert. Ausbeute: 0,65 g (21%), Schmp. 108—109 °C, keine Depression mit dem Produkt nach Methode A. Die IR-Spektren waren ebenfalls identisch.

Reaktion von Phenylketen-Dimer (VIII) mit Äthylendiamin (II)

2,35 g (0,01 Mol) Phenylketen-Dimer (**VIII**) wurden portionsweise zu einer siedenden Lösung von 0,7 cm^3 (0,63 g — (0,0105 Mol) Äthylendiamin und 0,5 cm^3 HCl/Isopropanol (ca. 10 g HCl/100 ml Lösung) in 200 cm^3 trockenem Benzol zugefügt. Das Gemisch wurde 20 Stunden lang gekocht, und nach Zugabe von weiteren 1,4 cm^3 Äthylendiamin wieder 7 Stunden lang zum Sieden erhitzt. Nach Abkühlen wurden die ausgeschiedenen Krystalle filtriert und getrocknet. Das fast farblose Rohprodukt (1,0 g, Schmp. 200—205 °C) wurde aus Isopropanol umkristallisiert, Schmp. 204—206 °C. Die Verbindung war laut Mischschmp. und IR-Spektrum mit einer authentischen Probe von *N,N'-Bis-phenacyl-äthylendiamin* [*21*] identisch.

Die benzolische Mutterlauge wurde 3 mal mit je 50 cm^3 Wasser extrahiert, und die wäßrigen Extrakte 10mal mit je 50 cm^3 Chloroform ausgeschüttelt. Nach Trocken über wasserfreiem Na_2SO_4 wurde das Chloroform abgedampft und das zurückgebliebene gelbliche Öl durch Verreiben mit kaltem Essigester kristallisiert. 0,15 g farblose Kristalle mit dem Schmp. 94—96 °C wurden erhalten, welche sich laut IR-, NMR- und Massenspektrum als Monophenacetyl-äthylendiamin erwiesen Lit. [22] Schmp. 97—100 °C.

IR-Spektrum

ν_{NH}	3290 cm^{-1}
Amid I	1635 cm^{-1}
Amid II	1555 cm^{-1}
β_{NH}	750 cm^{-1}

NMR-Spektrum (in $CDCl_3$)

CH_2	2,87 m (2H)
	3,08 t (2H)
$ArCH_2$	3,43 s (2H)
ArH	7,25 s (5H)
NH	8,17 s (1H)

Massenspektrum

	m/e	%
M^+	178	23
$M\text{-}CHNH_2$	149	100
$M\text{-}CH_2NH_2$	148	34
$C_6H_5CH_2NH$	106	13
$C_6H_5CH_2$	91	45

Allgemeine Vorschrift zur Herstellung von 7- (bzw. 8-) substituierten 3-Phenyl-4-benzyl-1,3,dihydro-2H-1,5-benzodiazepin-2-onen

A) *Aus Phenylketen-Dimer* (**VIII**) *und 4-R-o-phenylendiamin* (**VIa—d**), *Herstellung von* **XIa**, *c, d+e und f Methode A.*

0,002 Mol 4-R-o-phenylendiamin (**VIa—d**) wurden in 15 cm^3 absol. Benzol gelöst und in Stickstoffatmosphäre mit 0,002 Mol Phenylketen-Dimer (**VIII**) bis zum Verschwinden des Unlös-

Tabelle I

Die Angaben der 1,5-Benzodiazepin-2-one

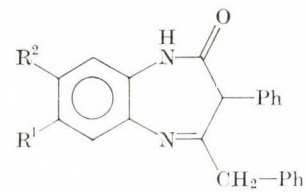

Verbindung	R¹	R²	Methode der Herstellung	Reaktionszeit	Schmp. (°C)	Ausbeute (%) Rohprodukt	Ausbeute (%) Gereinigtes Produkt	Formel/Mol.-Gew.
XIa*	H	H	A	120 Min	124—125 aus Isopropanol	81	43	$C_{22}H_{18}N_2O$ 326,40
			B	48 Stunden	128—130	72	42	
		HCl-Salz			140—142 aus Isopropanol/Äther			
XIb	Cl	H	B	24 Stunden	174—176 aus Isopropanol	83	48	$C_{22}H_{17}ClN_2O$ 360,93
XIc	OCH_3	H	A	25 Min	152—154 aus Acetonitril	42	35	$C_{23}H_{20}N_2O_2$ 356,41
			B	72 Stunden		60	30	
XId	CH_3	H	B	48 Stunden	158—160 aus Acetonitril	67	48	$C_{23}H_{20}N_2O$ 340,41
XIe	H	CH_3	B	48 Stunden	188—192 aus Acetonitril	78	35	$C_{23}H_{20}N_2O$ 340,41
Gemisch von **XIe** und **XId**			A	35 Min	149—153 aus Acetonitril	55	34	$C_{23}H_{20}N_2O$ 340,41
XIf	H	Cl	A	180 Min	148—151 aus Isopropanol	29	22	$C_{22}H_{17}ClN_2O$ 360,93

s = Singulett
m = Multiplett
* MS-Angaben von **XIa**: M^+ m/e: 326 Rel. Int.: 61%
$M-C_6H_5CH_2$ 235 5,6%
$M-C_6H_5-C\equiv C=O$ 209 100%
** in $CDCl_3$ aufgenommen

(XIa—f)

Analyse				Spektroskopische Angaben						
				IR-Banden (cm^{-1})			NMR-Banden δ(in ppm)**			
C	H	N	Cl	ν_{NH}	Amid I.	ν_{CN}	CH_2	CH	NH	ArH
Ber. 80,96 Gef. 80,52	5,56 5,72	8,58 9,04	— —	3185— 2800	1662	1633	3,98*s*	4,83*s*	9,35*s*	6,7—7,4*m*
				3200— 2500	1715	1660				
Ber. 73,22 Gef. 72,58	4,75 4,74	7,77 7,43	9,83 10,35	3320— 2800	1670	1635	4,01*s*	4,80*s*	8,3*s*	6,6—7,5*m*
Ber. 77,50 Gef. 77,77	5,66 5,76	7,86 8,16	— —	3200— 2800	1670	1640	3,94*s*	4,80*s* OCH_3 = 3,70*s*	8,9*s*	6,6—7,4*m*
Ber. 81,15 Gef. 80,44	5,92 6,13	8,23 8,05	— —	3250— 2700	1660	1625	3,95*s*	4,80*s* CH_3 = 2,28*s*	9,20*s*	6,6—7,4*m*
Ber. 81,15 Gef. 81,00	5,92 5,74	8,23 8,40	— —	3250— 2700	1673	1638	3,96*s*	4,82*s* CH_3 = 2,23*s*	9,0*s*	6,5—7,4*m*
Ber. 81,15 Gef. 81,31	5,92 5,95	8,23 8,40	— —	3250— 2700	1668	1630	3,94*s*	4,79*s* CH_3 = 2,21 und 2,25; beide *s*		6,2—7,4*m*
Ber. 73,22 Gef. 73,50	4 75 4,71	7 77 7,70	9,83 9,53	3180— 2800	1670	1630	3,96*s*	4,86*s*	9,8*s*	6,7—7,4*m*

Tabelle II

Die Angaben der N-(α, γ-diphenyl-acetoacetyl)-2-nitro-4-R¹-5-R²-aniline

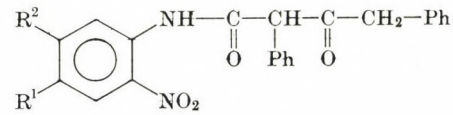

Verbindung	R^1	R^2	Methode der Herstellung	Reaktionszeit	Schmp. (°C)	Ausbeute (%)		Formel/ Mol.-Gew.
						Rohprodukt	Gereinigtes Produkt	
XIVa	H	H	A	15 Min$^{\tau}$	110—112 aus Isopropanol	75	27	$C_{22}H_{18}N_2O_4$ 374,40
			B	20 Stunden^{C}		77	62	
XIVb	Cl	H	A	180 Min^{B}	98—101 aus Isopropanol	64	23	$C_{22}H_{17}ClN_2O_4$ 409,84
				15 Min$^{\tau}$		70	26	
			B	20 Stunden^{C}			48	
XIVc	OCH_3	H	A	180 Min^{B}	139—141 aus Acetonitril	83	34	$C_{23}H_{20}N_2O_5$ 404,41
				25 Min$^{\tau}$		92	39	
			B	20 Stunden^{C}			63	
XIVd	CH_3	H	A	300 Min^{B}	96—97 aus Acetonitril	60	40	$C_{23}H_{20}N_2O_4$ 388,41
XIVe	H	CH_3	A	180 Min^{B}	100—101 aus Isopropanol	59	23	$C_{23}H_{20}N_2O_4$ 388,41
				15 Min$^{\tau}$			39	

B = in Benzol
T = in Toluol
C = in Chlorbenzol
s = Singulett
* in DMSO aufgenommen

lichen unter Rühren gekocht. Nach Abkühlen und Abdampfen des Lösungsmittels wurde der Rückstand kristallisiert. Die ausführlichen Angaben der Produkte sind in Tabelle I enthalten.

(XIVa—e)

Analyse				Spektroskopische Angaben						
				IR-Banden (cm^{-1})			NMR-Banden δ(in ppm)*			
C	H	N	Cl	ν_{NH}	ν_{OH}	Amid I.	CH_3	CH_2	NH	OH
Ber. 70,58 Gef. 71,28	4,85 5,14	7,48 7,05	— —	3280	3000— 2300	1630	—	3,40*s*	9,3*s*	
Ber. 64,63 Gef. 64,78	4,19 4,22	6,85 6,85	8,67 8,67	3300	3000— 2300	1633	—	3,42*s*	9,85*s*	14,15*s*
Ber. 68,31 Gef. 68,62	4,99 5,01	6,93 7,03	— —	3280	3000— 2300	1630	—	3,51*s* OCH_3 : 3,90*s*	9,88*s*	14,00*s*
Ber. 71,12 Gef. 71,01	5,19 5,19	7,21 7,21	— —	3300	3000— 2100	1637	2,26*s*	3,33*s*	9,14*s*	13,94*s*
Ber. 71,12 Gef. 70,92	5,19 5,33	7,21 7,35	— —	3290	3000— 2100	1635	2,47*s*	3,47*s*	9,85*s*	14,31*s*

B) *Durch Reduktion von N-(α, γ-Diphenyl-)-acetoacetyl-4-R^1-5-R^2-2-nitroanilinen* (**XIVa—e**), *Herstellung von* **XIa—e**, *Methode B.*

0,5 g **XIV** wurde mit 10 cm^3 einer essigsauren-salzsauren Lösung von $SnCl_2$ im Kühlschrank stehen gelassen, wobei das unlösliche Ausgangsmaterial allmählich aufgelöst wurde (1—3 Tage). Nach vollkommenem Auflösen wurde das Gemisch auf Eiswasser gegossen, und ein Überschuß an 10 *N* Natronlauge zugefügt. Das Produkt wurde mit Chloroform extrahiert, die Extrakte mit Wasser gewaschen, über wasserfreiem K_2CO_3 getrocknet, im Vakuum zur Trockne eingedampft und der Rückstand kristallisiert. Die ausführlichen Angaben sind in Tabelle I enthalten.

3-Phenyl-4-benzyl-2,3,4,5-tetrahydro-1H-1,5-benzodiazepin-2-on (XIIa)

A) *Durch Hydrierung von* **XIa**

2,0 g (0,0061 Mol) 3-Phenyl-4-benzyl-2,3-dihydro--1H-1,5-benzodiazepin-2-on (**XIa**) wurden in 50 cm^3 Methanol mit Pd/C als Katalysator hydriert und das Produkt auf gewöhnliche Weise isoliert. Ausbeute: 1,1 g (54,8%), Schmp. 186—188 °C (aus Äthanol).

Analyse : $C_{22}H_{20}N_2O$ (328,42)

	Ber.	Gef.
C	80,46	80,33
H	6,14	6,58
N	8,53	8,32

IR-Spektrum

ν_{NH}	3360 und 3200 cm^{-1}	
Amid I	1650 cm^{-1}	

NMR-Spektrum (in DMSO)

CH_2	2,8 d	(2H)
C_3-H+C_4—H	4,05 m	(2H)
NH	5,4 m	(1H) und
	8,6 s (breit)	(1H)

B) *Durch Hydrierung von* **XIVa**

2,0 g (0,0053 Mol) N-(α, γ-Diphenyl)-acetoacetyl-2-nitro-anilin (**XIVa**) wurden in 50 cm^3 Methanol mit Pd/C als Katalysator hydriert und das Produkt auf gewöhnliche Weise isoliert. Ausbeute: 1,2 g (60%), Schmp. 183—185 °C (aus Aceton). Die mit der Methode A und B erhaltenen Produkte waren laut Mischschmelzpunkt und IR-Spektrum identisch.

Allgemeine Vorschrift zur Herstellung von N-(α, γ-Diphenyl)-acetoacetyl-2-nitro-4-R^1-5-R^2-anilinen (XIVa—e)

A) *Aus Phenylketen-Dimer* (**VIII**) *und 2-nitro-4-R^1-5-R^2-anilin* (**XIIIa—e**)

0,002 Mol 2-Nitro-4-R^1-5-R^2-anilin (**XIIIa—e**) wurden in 20 cm^3 absol. Benzol oder Toluol aufgelöst, und nach Zugabe von 0,002 Mol Phenylketen-Dimer (**VIII**) unter Rühren, in Stickstoff-Atmosphäre so lange gekocht, bis eine homogene Lösung entstand. Nach Abkühlen und Eindampfen der Lösung wurde der Rückstand kristallisiert. Angaben der einzelnen Verbindungen s. in Tabelle II. enthalten

B) *Aus α, γ-Diphenyl-acetessigester* (**IX**) *und 2-Nitro-4-R^1-5-R^2-anilin* (**XIIIa—e**)

0,02 Mol α, γ-Diphenyl-acetessigester (**IX**) [23] und 0,02 Mol 2-Nitro-4-R^1-5-R^2-anilin (**XIII*a—e***) wurden in 60 cm^3 Chlorbenzol unter ständiger Entfernung des entstandenen Alkohols durch azeotrope Destillation, bis zum Verschwinden der Ausgangsmaterialien laut DS-Chromatographie gekocht. Nach Eindampfen der Lösung wurde der Rückstand kristallisiert, s. Tabelle II.

Umsetzung von α, γ-Diphenyl-acetessigester (IX) mit o-Phenylendiamin (VIa)

1. *In Anwesenheit von wasserfreiem HCl als Katalysator: Herstellung von 1-[(1',3'-Diphenyl)-propen-2'-il]-2,3,-dihydro-benzimidazol-2-on* (**XVI**)

0,54 g (0,005 Mol) o-Phenylendiamin (**VIa**) und 0,2 ml einer 18%igen isopropanolischen Lösung von wasserfreiem HCl in 50 cm^3 absol. Xylol wurden zum Sieden erhitzt, und die Lösung von 1,4 g (0,005 Mol) α, γ-Diphenyl-acetessigester (**IX**) in 30 cm^3 absol. Xylol wurde innerhalb von einer Stunde bei dieser Temperatur zugetropft, wobei das entstandene Wasser und Alkohol ständig durch azeotrope Destillation entfernt wurden. Beim Abkühlen fiel das Produkt in Form von farblosen Kristallen aus. Ausbeute: 1,2 g (73,5%), Schmp. 185—192 °C. Durch einmaliges Umkristallisieren wurde der Schmelzpunkt auf 190—192 °C erhöht.

Analyse: $C_{22}H_{18}N_2O$ (326,40)

	Ber.	Gef.
C	80,96	80,53
H	5,56	5,73
N	8,58	9,06

IR-Spektrum

ν_{NH}	3200—2700 cm^{-1}
Amid I	1680 cm^{-1}

NMR-Spektrum (in Trifluoressigsäure)

CH_2	4,38 s (2H)
ArH + Ph—CH=	7,0—7,7 m (15H)
NH	10,83 s (1H)

Massenspektrum

	m/e	%
M^+	326	100
Ph—CH, Ph—C ⟩ C	192	69
H, H ⟩ C	191	41
Ph—C		
M-191	135	40

Zur weiteren Charakterisierung wurde auch das Dihydro-Derivat von **XVI** hergestellt:

1-[(1',3'-Diphenyl)-prop-2'-yl]-2,3-dihydro-benzimidazol-2-on (XXI)

1,5 g (0,0046 Mol) **XVI** wurden in 50 cm^3 Methanol über Pd/C als Katalysator hydriert und das Produkt auf die gewohnte Weise isoliert. Man erhielt 0,65 g farbloses Produkt vom Schmp. 154—156 °C (aus Äthanol), Ausbeute: 43,3%.

Analyse: $C_{22}H_{20}N_2O$ (328,42)

	Ber.	Gef.
C	80,46	80,40
H	6,14	6,24
N	8,53	8,48

IR-Spektrum

ν_{NH}	3300—2700 cm^{-1}
Amid I	1685 cm^{-1}

NMR-Spektrum (in $CDCl_3$)

CH_2	3,3 (4H)	8 Linien eines A_2B_2X Systems
CH	4,81 (1H)	Triplett von Tripletten
NH	8,6 s (1H)	
ArH	7,12 s (14H)	

2. *Mit Pyridin als Katalysator*

Die Reaktion wurde wie unter 1. beschrieben durchgeführt, anstatt HCl/Isopropanol aber unter Verwendung von 10 Mol% Pyridin als Katalysator. Man erhielt gereinigtes **XVI** mit einer Ausbeute von 61,5%.

3. *Mit Wasserfreier anorganischer Base als Katalysator*

Anstelle von HCl/Isopropanol wurden hier 0,2 g (0,0015 Mol) wasserfreies Kaliumcarbonat oder 0,12 g wasserfreies Natriumbicarbonat für die unter 1. angegebenen Mengen der Ausgangsmaterialien verwendet. Nach Beendigung der Reaktion wurde der anorganische Teil noch heiß filtriert, und beim Abkühlen fielen 1,4 g farblose Kristalle vom Schmp. 167—170 °C aus. Nach Umkristallisieren aus Äthanol Schmp. 172—173 °C. Lit. [24] Schmp. von N,N'-Bisphenacetyl-*o*-phenylendiamin (**XVII**): 168 °C.

Die Elementaranalyse und die spektroskopischen Angaben entsprachen der Erwartung. Durch partielles Einengen der Mutterlauge wurden 0,05 g eines weiteren Produktes, des 2,3-Dihydro-2-benzimidazol-2-ons (**XVIII**) isoliert, Schmp. 320—322 °C (aus Dioxan), Lit. [25] Schmp. 310—312 °C.

4. a) *Ohne Katalysator, in neutralem Medium*

Zu einer Lösung von 1,65 g (0,0153 Mol) *o*-Phenylendiamin (**VI***a*) in 100 cm^3 absol. Xylol wurde eine Lösung von 4,35 g (0,0153 Mol) α,γ-Diphenyl-acetessigester (**IX**) in 50 cm^3 absol. Xylol, unter azeotroper Destillation, innerhalb einer Stunde zugetropft, und weitere 2 Stunden lang unter Konstanthalten des Volumens destilliert. Die erhaltene Lösung wurde nach Eneit-

färbung mit Aktivkohle zur Trockne eingedampft und das gewonnene rötliche Öl der Säulenchromatographie an Kieselgel G, Merck (Eluent: Benzol–Esstigester 3 : 1) unterworfen. Die folgenden drei Verbindungen wurden isoliert.

N-(α, γ-Diphenyl)-acetoacetyl-o-phenylendiamin (**XIX**), *rf = 0,95*

Schmp. 145—147 °C (dimorphe Kristalle, die zum Teil bei 135 °C schmelzen, dann wieder erstarren und endlich bei dem angegebenen Wert restlos schmelzen), farblose Kristalle, Ausbeute: 0,75 g (14,3%)

Analyse: $C_{22}H_{20}N_2O_2$ (344,42)

	Ber.	Gef.
C	76,72	77,19
H	5,85	5,91
N	8,13	8,34

IR-Spektrum

ν_{NH}	3380 und 3280 cm^{-1}
ν_{OH}	2800—2500 cm^{-1}
Amid I	1623 cm^{-1}

NMR-Spektrum (in $CDCl_3$)

CH_2	2,84 s	(2H)
ArH	6,8 s (breit)	(14H)
OH	6,55 s	(1H)
NH_2	12,05 s (breit)	(2H)

Massenspektrum

	m/e	%
M^+	344	44
$C_6H_5CH_2$	91	100
$C_6H_4(NH_2)_2$	108	64

3-Phenyl-4-benzoyl-1,3-dihydro-2H-1,5-benzodiazepin-2-on (**XX**), *rf = 0,65*

Schmp. 192—194 °C, zitronengelbe Nadeln, Ausbeute: 1,2 g (23%) (aus Isopropanol)

Analyse: $C_{22}H_{16}N_2O_2$ (340,39)

	Ber.	Gef.
C	77,63	77,60
H	4,74	5,15
N	8,23	8,29

IR-Spektrum

ν_{NH}	3200—2800 cm^{-1}
Amid I + ν_{CO}	1670 cm^{-1}, breit

NMR-Spektrum (in DMSO)

CH	5,46 s	(1H)
ArH	7,0—8,2 m	(14H)
NH	10,9 s	(1H)

Massenspektrum

	m/e	%
M^+	340	52,5
$M-C_6H_5CO$	235	34
C_6H_5CO	105	100

1-[(1',3'-Diphenyl)-1'-propen-2'-yl]-2,3-dihydro-benzimidazol-2-on (**XVI**), *0,55rf =*

Nach Umkristallisieren aus Isopropanol, unter Entfärbung mit Aktivkohle wurden 1,8 g (36,1%) **XVI** erhalten, Schmp. 192—194 °C; gibt keine Depression mit dem in saurem Medium hergestellten Produkt (s. unter 1.), die IR-Spektren sind ebenfalls identisch.

b) Bei der Wiederholung der Reaktion in Stickstoff-Atmosphäre konnte kein **XX** isoliert werden, die Ausbeuten an **XVI** und **XIX** betrugen 44 bzw. 17%.

Herstellung von 3-Phenyl-4-benzoyl-1,3-dihydro-2H-1,5-benzodiazepin-2-on (XX) durch Oxidierung von XIa

5,0 g (0,0153 Mol) **XI***a* wurden in 250 cm^3 absol. Benzol 5 Stunden lang unter Durchleiten von Luft am Rückfluß gekocht und über Nacht stehen gelassen. Die abgeschiedenen Kristalle wurden filtriert und aus Acetonitril-Dimethylformamid 4 : 1 umkristallisiert. Man erhielt 0,1 g 3-Phenyl-1,3,4,5-tetrahydro-2H-1,5-benzodiazepin-2,4-dion (**XXII**) vom Schmp. 270—273 °C.

Analyse: $C_{15}H_{12}N_2O_2$ (252,28)	Ber.	Gef.
	C 71,42	71,08
	H 4,79	5,08
	N 11,10	11,02

IR-Spektrum

ν_{NH}	3300—2700 cm^{-1}
Amid I	1680 und 1660 cm^{-1}

NMR-Spektrum (in DMSO)

CH	4,52 s	(1H)
NH	10,62 s	(1H)
C_6H_4	7,34 s	(4H)
C_6H_5	7,25 s	(5H)

Durch Eindampfen der Mutterlauge und Kristallisieren des Rückstandes aus Isopropanol erhieltman 2,6 g (50,1%) **XX** als zitronengelbe Kristalle, Schmp. 187—190 °C, die Substanz war laut Mischschmp. und IR-Spektrum mit der oben beschriebenen identisch.

LITERATUR

[1] *a)* Bormann, D. in Houben-Weyl: Methoden der organischen Chemie, Bd. 7/4, ab S. 259, Georg Thieme Verlag, Stuttgart, 1968.
b) ibid. Bd. 7/4, S. 279
c) ibid. Bd. 7/4, S. 274
[2] Staudinger, H.: Ber. **44,** 533 (1911)
[3] *a)* Hansen, G. R., De Marco, R. A.: J. Het. Chem. **6,** 291 (1969)
b) Elam, E. U.: Org. Chem. Bull. **36,** 1 (1964)
[4] Ried, W., Stahlhofen: Ber. **90,** 825 (1957)
[5] Farnum, G. A. *et al.:* J. Am. Chem. Soc. **87,** 5191 (1965)
[6] *a)* Kost, A. N. *et al.:* Khim. Geterocikl. Soedin. **1971**, 1556
b) Kost, A. N. *et al.: ibid.* **1971,** 428
c) Kost, A. N. *et al.: ibid.* **1971,** 698
d) Kost, A. N. *et al.: ibid.* **1971,** 721
e) Solomko, Z. F. *et al.: ibid.* **1971,** 987
f) Stolartschuk, A. A. *et al.:* Khim. Pharm. Zh. **1975,** 19
[7] Acheson, R. M., Tully, W. R.: J. Chem. Soc. C. **1970,** 1117
[8] Israel, M., Jones, L. C., Joullié, M. M.: J. Het. Chem. **8,** 1015 (1971)
[9] Sexton, W. A.: J. Chem. Soc. **1942,** 303
[10] *a)* Davoll, J.: J. Chem. Soc. **1960,** 308
b) Czech Patent 113, 422; C. A. **63,** 18129d (1965)
[11] Zubovics, Z., Wittmann, H.: Ann. **760,** 171 (1972)
[12] Zubovics, H., Wittmann, H.: Ann. **765,** 15 (1972)
[13] Schröter, R. in Houben-Weyl: Methoden der organischen Chemie, Bd. 11/1, S. 422, Georg Thieme Verlag, Stuttgart, 1957
[14] *a)* Archer, G. A., Sternbach, L. H.: Chem. Rev. **68,** 747 (1968), und dort zitierte Literatur
b) Moore, J. A., Mitchell, E. in Heterocyclic Compounds, ed. Elderfield, R. C., Bd. 9, S. 313—331, John Wiley and Sons, Inc., New York, 1967.
[15] Rossi, A., Hunger, A., Kebrle, J., Hoffmann, K.: Helv. **43,** 1268 (1960)
[16] Israel, M., Jones, L. C., Modest, E. J.: Tetrahedron Letters, **1968,** 4811
[17] Wigton, F. B., Joullié, M. M., J. Am. Chem. Soc. **81,** 5212 (1959)
[18] Barchet, R., Merz, K. W.: Tetrahedron Letters, **33,** 2239 (1964)
[19] Ried, W., Stahlhofen, P.: Ber. **90,** 828 (1957)
[20] Rossi, A., Hunger, A., Kebrle, J., Hoffmann, K.: Helv. **43,** 1046 (1960)
[21] Grudzinski, S., Misiak, M.: Lodz. Towarz. Nauk Wydzial. III. Acta Chim. **8,** 119 (1962); C. A. **59,** 7476e (1963)
[22] Behrens, O. K. *et al.:* J. Biol. Chem. **175,** 751 (1948)
[23] Zaugg, H. E., Rapala, R. T., Lefler, M. T.: J. Am. Chem. Soc. **70,** 3224 (1948)
[24] Walther, A., Paulawski, V.: J. prakt. Chem. (2) **59,** 252; Blst. **13** H 21
[25] Hartmann, H.: Ber. **23,** 1047 (1890)

Zoltán Zubovics
G. Fehér
Lajos Toldy
H-1325 Budapest, Pf. 82.

Acta Chimica Academiae Scientiarum Hungaricae, Tomus 92 (3), pp. 311–315 (1977)

HERSTELLUNG UND STRUKTURUNTERSUCHUNG EINIGER 6-SUBSTITUIERTER DIHYDROCODEINE BZW. DIHYDROISOCODEINE

G. Horváth, Gy. Gaál, P. Kerekes und R. Bognár

(Lehrstuhl für organische Chemie, L. Kossuth Universität, Debrecen)

Eingegangen am 28. Dezember 1975

Als Ergebnis der Reaktion von Dihydrocodeinon und Dimethylsulfoniummethylid wurde 6-Desoxy-6,6-methylenoxydihydrocodein erhalten, worin die neue Kohlenstoff-Kohlenstoff-Bindung in äquatorialer Lage ist. Durch Reduktion des Epoxydringes der Verbindung mit Lithiumaluminiumhydrid wurde das aus dem Keton mit Methyllithium gewonnene 6-Methyldihydrocodein erhalten.

Die Ringöffnung wurde auch mit anderen nukleophilen Reagentien durchgeführt, wobei 6-Chlormethyl-, 6-Azidomethyl-, 6-Aminomethyl- und 6-Hydroxymethyl-dihydrocodein erhalten wurde.

Diese neuen Verbindungen sind die C_6-Epimeren jener Verbindungen, die durch unter gleichen Bedingungen durchgeführte Reaktionen aus dem von den Verfassern aus Dihydrocodeinon mit Dimethyloxosulfoniummethylid bereits früher hergestellten 6-Desoxy-6,6-methylenoxydihydroisocodein gewonnen wurden.

In unserer früheren Mitteilung [1] wurde festgestellt, daß die Reduktion des nach dem Verfahren von Corey und Chaykovsky [2] aus Dihydrocodeinon (**I**) mit Dimethyl-oxosulfoniummethylid gewonnenen Epoxyds (**II**, 6-Desoxy-6,6-methylenoxydihydroisocodein) mit Lithiumaluminiumhydrid zum 6-Methyldihydroisocodein (**III**) führt, in dem — auf Grund des IR-Spektrums der Verbindung — die neuenstandene C_6-C-Bindung in axialer Lage vorliegt, während die neuentstandene C_6-C-Bindung in dem aus demselben Keton (**I**) mit Methyllithium gewonnenen 6-Methyldihydrocodein [3] äquatorialer Lage einnimmt.

In der vorliegenden Mitteilung berichten wir über die Reaktion des Dihydrocodeinons mit Dimethylsulfoniummethylid sowie über die Verbindungen, die durch Ringspaltung der C_6-epimeren Oxirane erhalten wurden.

Die Reaktion des aus Trimethylsulfoniumjodid mit Natriumhydrid im Gemisch von Dimethylsulfoxid und Tetrahydrofuran gewonnenen Ylids [2] und des Dihydrocodeinons (**I**) wurde bei — 20. . . —10 °C durchgeführt, das Reagens wurde im Überschuß von 1 Mol angewendet. Das C_6-Epimere von (**II**), das 6-Desoxy-6,6-methylenoxydihydrocodein (**V**) wurde mit einer Ausbeute von 90% gewonnen.

Durch die Reduktion des Epoxydringes mit Lithiumaluminiumhydrid gelangten wir zu 6-Methyldihydrocodein (**IV**), was den Angriff des Ylids aus äquatorialer Richtung beweist, in Übereinstimmung mit der Feststellung von Johnson und Schroeck [4], wonach die Addition dieses nukleophilen Reagens eine kinetisch kontrollierte, irreversible Reaktion ist.

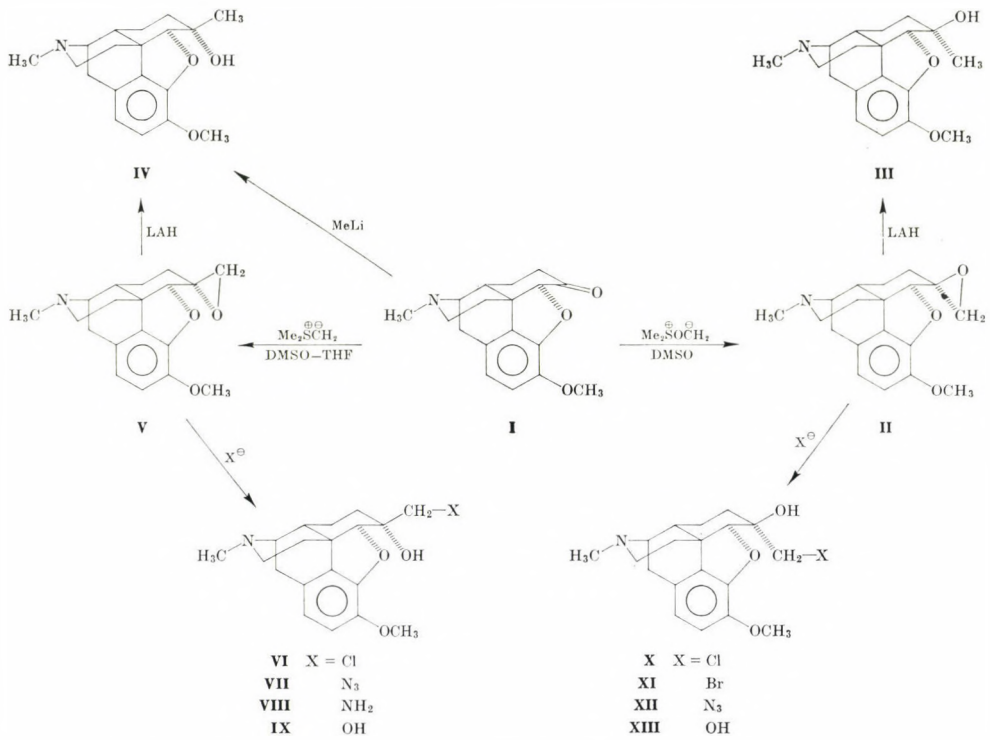

Die Ringöffnung der epimeren Oxirane (**II** bzw. **V**) mit anderen nukleophilen Reagentien führte nicht zur Bildung isomerer Produkte, obwohl hierzu theoretisch die Möglichkeit besteht; es wurden in stereoselektiven Reaktionen nur 6-(subst. Methyl)-dihydrocodein bzw. -dihydroisocodein-Derivate erhalten.

Bei der Öffnung des Oxiranringes des 6-Desoxy-6,6-methylenoxydihydrocodeins (**V**) mit 10%iger Salzsäure wurde 6-Chlormethyl- (**VI**) und durch Reduktion des letzteren mit $LiAlH_4$ 6-Methyldihydrocodein (**IV**) hergestellt. Das 6-Azidomethyldihydrocodein (**VII**) wurde entweder unmittelbar aus dem Epoxyd oder durch Azidolyse des Chlorhydrins (**VI**) gewonnen. Zum 6-Hydroxymethyl-dihydrocodein (**IX**) gelangten wir durch die Behandlung des dreigliedrigen Ringes mit Ameisensäure und Alkali bzw. durch Spaltung mit Schwefelsäure. Das 6-Aminomethyldihydrocodein (**VIII**) wurde durch Reduktion des Azidoalkohols (**VII**) erhalten.

Unter ähnlichen Reaktionsbedingungen erhielten wir aus dem 6-Desoxy-6,6-methylenoxydihydroisocodein (**II**) das 6-Chlormethyl-(**X**) bzw. mit Bromwasserstoff das 6-Brommethyldihydroisocodein (**XI**). Diese Verbindungen sind die optischen Antipoden der von Goto [5] beschriebenen Halogenhydrine. Durch Azidolyse des Chlorhydrins (**X**) wurde das 6-Azidomethyldihydroisocodein (**XIII**) bzw. bei der Ringöffnung mit Ameisensäure das 6-Hydroxy-

methyldihydroisocodein erhalten. Die letztere Verbindung ist mit der durch RAPOPORT und CHADHA [6] aus 6-Desoxy-6-methylendihydrocodein durch Oxydation mit OsO_4 erhaltenen Verbindung identisch.

Experimenteller Teil

Die Schmelzpunkte sind unkorrigiert. Die Reinheit der Verbindungen wurde dünnschichtchromatographisch geprüft (Adsorbent: Silicagel G; Laufmittel: Benzol/Methanol = = 4 : 1, Chloroform/Aceton/Diäthylamin = 5 : 4 : 1; Entwickler: Draggendorf-Reagens). Das spezifische Drehungsvermögen wurde mit einem automatischen Polarimeter, Bendix NPL 143 D, gemessen (c = 0,5; 1 = 0,2004). Die IR-Spektren wurden mit einem UNICAM SP 200 G Gerät in KBr-Tabletten aufgenommen.

6-Desoxy-6,6-methylenoxydihydrocodein (V)

1,92 g (50 mmol) Natriumhydrid (50%ig in Öl) wurden unter kräftigem Rühren in Argon-Atmosphäre bei 75 °C in 25 cm³ abs. DMSO gelöst (ungefähr 1 Stunde). Die Lösung wurde auf Raumtemperatur gekühlt, 25 cm³ abs. THF wurden zugegeben, anschließend wurde auf −20 °C abgekühlt und tropfenweise mit einer Lösung von 8,20 g (40 mmol) Trimethylsulfoniumjodid in 35 cm³ abs. DMSO versetzt. Nach weiterem Rühren (3 Minuten) wurden 6 g (20 mmol) Dihydrocodeinon und 20 cm³ THF auf einmal zugegeben. Danach wurde 1 Stunde lang bei −20 ...−10 °C und anschließend 2 Stunden lang bei Raumtemperatur gerührt. Das Reaktionsgemisch samt Niederschlag wurde dann in 200 cm³ eiskalte gesättigte Na_2SO_4-Lösung gegossen. Die wäßrige Lösung wurde mit 5 × 30 cm³ Chloroform extrahiert, die vereinigte organische Phase mit 2 × 50 cm³ Na_2SO_4-Lösung, mit 2 × 100 cm³ Sulfit–Bisulfit–Puffer-lösung (pH 7) und anschließend mit Wasser gewaschen, über Na_2SO_4 getrocknet und eingedampft. Der ölige Rückstand wurde mit 20 cm³ n-Hexan verrieben. Man erhielt 6,0 g (95,5%) Rohprodukt.

Eine kleine Probe davon wurde aus Äther umkristallisiert: Schmp. 103—4 °C; $[\alpha]_D^{28}$ = = −113° ($CHCl_3$).

Analyse: $C_{19}H_{23}NO_3$, 313,4					
Ber.	C	73,47%	H	7,51%	N 4,50%
Gef.	C	72,84%	H	7,39%	N 4,47%

0,8 g der Verbindung wurde in abs. THF mit Lithiumaluminiumhydrid (0,1 g) reduziert, wobei 0,8 g (~100%) 6-Methyldihydrocodein (**IV**) gewonnen wurden. Der Schmelzpunkt der in Vakuum getrockneten Verbindung war 113—5 °C, deren Gemisch mit einer auf anderem Wege erhaltenen Probe [3] keine Schmelzpunktdepression zeigte.

6-Chlormethyldihydrocodein (VI)

2 g (6,3 mmol) der Verbindung (**V**) wurden in 20 cm³ 10%iger Salzsäure gelöst und 1 Stunde lang auf siedendem Wasserbad gehalten, das Reaktionsgemisch wurde auf Eis gegossen, mit NH_4OH (Verdünnung 1 : 1) alkalisch gemacht und mit 3 × 30 cm³ Chloroform extrahiert. Der Extrakt wurde mit Wasser neutral gewaschen, über Na_2SO_4 getrocknet und eingedampft. Man erhielt einen Sirup, der aus einem Gemisch von Benzol und Äther umkristallisiert, 1,60 g (71,8%) eines festen Produkts lieferte, das bei 117—9 °C unter Zersetzung schmilzt. $[\alpha]_D^{27.5}$ = = −115,6° ($CHCl_3$).

Analyse: $C_{19}H_{27}NO_3Cl$, 349,8		
Ber.	Cl	10,14%
Gef.	Cl	10,50%

Die Reduktion von 0,5 g der Verbindung (**VI**) in abs. THF mit $LiAlH_4$ (0,30 g) ergab 0,40 g (88,9%) 6-Methyldihydrocodein (**IV**). Schmp. 114—6 °C; mit (**IV**), erhalten aus (**V**), ergibt sich keine Schmelzpunktdepression.

6-Azidomethyldihydrocodein (VII)

a) Die Lösung von 1 g (3,2 mmol) Epoxyd (**V**), 2 g NH_4Cl und 2,5 g Natriumazid in 6 cm^3 Wasser und 25 cm^3 Methanol wurde 48 Stunden lang auf dem Wasserbad unter Rückfluß erhitzt. Das heiße Reaktionsgemisch wurde vom unlöslichen Rückstand filtriert, das Filtrat in Wasser gegossen und mit 3×30 cm^3 Chloroform extrahiert. Die Verarbeitung der organischen Phase ergab 0,97 g eines beim Stehen kristallisierenden Harzes. Aus einem Gemisch von Äther und Hexan umkristallisiert, wurden 0,75 g (65%) eines bei 116—8 °C schmelzenden Stoffes erhalten.

b) Zu einer Lösung von 1 g (2,7 mmol) des Chlorhydrins (**VI**) in 25 cm^3 Methanol wurde die Lösung von 1 g Natriumazid in 3 cm^3 Wasser zugegeben. Die Lösung wurde 48 Stunden lang gekocht, mit 20 cm^3 Wasser verdünnt und mit 3×25 cm^3 Chloroform extrahiert. Der Extrakt ergab nach Extraktion mit Wasser, Trocknen, Eindampfen und Kristallisieren 0,65 g (63,7%) Produkt (Schmp. 116—8 °C).
$[\alpha]_D^{27,5} = -155,5°$ ($CHCl_3$)

Analyse: $C_{19}H_{27}N_4O_3$, 356,4
Ber. N 15,72%
Gef. N 16,80%
IR: $\nu_{N_3} = 2108$ cm^{-1}

6-Aminomethyldihydrocodein (VIII)

0,5 g $LiAlH_4$ wurden in 30 cm^3 abs. Äther suspendiert und tropfenweise wurde 1 g (2,8 mmol) Azidoalkohol (**VII**), in 30 cm^3 abs. Benzol gelöst, zugegeben. Das Reaktionsgemisch wurde 5 Stunden lang gekocht und anschließend — nach Zersetzung des Überschusses an Reduktionsmittel — mit 10%iger Salzsäure behandelt. Nach dem Abtrennen der organischen Phase wurde die saure Lösung mit Signette-Salz versetzt und mit 10%iger NaOH-Lösung alkalisch gemacht. Die durch Extraktion isolierte Substanz wurde aus Benzol-Äther kristallisiert. Es wurden 0,75 g (80,9%) erhalten. Schmp. 184—7 °C; $[\alpha]_D^{28} = -137°$ ($CHCl_3$)
$-138°$ (EtOH)

Analyse: $C_{19}H_{26}N_2O_3$, 330,4
Ber. N 8,78%
Gef. N 8,81%

6-Hydroxymethyldihydrocodein (IX)

a) 1 g (3,2 mmol) der Verbindung (**V**) wurde mit 6 cm^3 Ameisensäure 3 Stunden lang unter Rückfluß erhitzt. Die Lösung wurde eingedampft, der Rückstand in 5 cm^3 Wasser gelöst und mit 10%iger NaOH-Lösung alkalisch gemacht. Das erhaltene Rohprodukt (1,0 g, 94,7%) wurde aus 20%igem Methanol umkristallisiert, wobei 0,68 g der Verbindung erhalten wurden. Schmp. 141—2 °C, unter Zersetzung.
$[\alpha]_D^{25} = -133,5°$ (EtOH)

Analyse: $C_{19}H_{25}NO_4$, 331,4
Ber. N 4,23%
Gef. N 4,73%

b) 0,50 g Oxiran wurden in 6,0 g 50 gew.%iger Schwefelsäure gelöst. Das Reaktionsgemisch wurde nach 6 Stunden auf Eis gegossen und mit Na_2CO_3 neutralisiert. Die Extraktion mit Chloroform ergab 0,42 g eines Öles, das aus 20%igem Methanol kristallisiert, 0,42 g (74%) der Verbindung (**IX**) lieferte: Schmp. 140—2 °C. Mit der Verbindung (**IX**) nach *a)* zeigte sich keine Schmelzpunktdepression.

6-Chlormethyldihydroisocodein (X)

Aus 3,1 g (10 mmol) 6-Desoxy-6,6-methylenoxydihydroisocodein (**II**) wurden durch Öffnung des Epoxydringes mit 10%iger Salzsäure (wie bei [**VI**] beschrieben) und Umkristallisieren des Rohproduktes aus Benzol–Petroläther 2,33 g (65,6%) des Produktes erhalten. Schmp. 167—8 °C. $[\alpha]_D^{27,5} = -160,5°$ ($CHCl_3$).

(Literaturangaben [5]: Schmp. 168 °C, $[\alpha]_D^{23} - 161{,}7°$ ($c = 1{,}216$ $CHCl_3$)).

Analyse: $C_{19}H_{27}NO_3Cl$, 349,8
Ber. Cl 10,19%
Gef. Cl 10,32%

6-Brommethyldihydroisocodein (XI)

3,1 g (10 mmol) des Epoxyds (**II**) wurden mit 30 cm³ 10%igem Bromwasserstoff 1 Stunde lang auf dem Dampfbad gehalten und anschließend wie bei (**VI**) beschrieben verarbeitet. Es wurden 2,15 g (55%) der Verbindung (**XI**) erhalten. Schmp. 164—5° ($CHCl_3$). (Literaturangaben [5]: Schmp. 168 °C, $[\alpha]_D^{28} = -169{,}4°$ ($c = 2{,}011$; $CHCl_3$)).

Analyse: $C_{19}H_{24}NO_3Br$, 394,3
Ber. Br 20,22%
Gef. Br 21,60%

6-Azidomethyldihydroisocodein (XII)

Das Rohprodukt wurde aus 1,8 g (5,1 mmol) der Verbindung (**X**) nach (**VIIb**) hergestellt. Nach Umkristallisieren aus Äther–Petroläther wurden 1,11 g (57,5%) der Verbindung erhalten, die sich ab 96 °C unter Gasentwicklung zersetzt. $[\alpha]_D^{27,5} = -181°$ ($CHCl_3$).

Analyse: $C_{19}H_{24}N_4O_3$, 356,4
Ber. N 15,72%
Gef. N 15,71%
IR $\nu_{N_3} = 2102$ cm^{-1}

6-Hydroxymethyldihydroisocodein (XIII)

3 g (9,6 mmol) der Verbindung (**II**) wurden 6 Stunden lang unter Rückfluß mit 18 cm³ Ameisensäure erhitzt. Danach wurde die Lösung eingedampft, der Rückstand in Wasser gelöst, mit $NaHCO_3$ neutralisiert, mit 5×30 cm³ Chloroform/Äthanol = 2 : 1 extrahiert, mit gesättigter NaCl-Lösung gewaschen und über Na_2SO_4 getrocknet. Nach dem Eindampfen wurde der feste Rückstand in 70 cm³ heißem Chloroform gelöst, mit Kohle behandelt, bis zum Beginn der Kristallisation eingedampft und Petroläther zugegeben.

2,05 g (68,3%), Schmp. 206—8 °C (Literaturangabe [6] Schmp. 202—3 °C).

Analyse: $C_{19}H_{23}NO_4$, 331,7
Ber. N 4,23%
Gef. N 4,26%

0,5 g der Verbindung wurden mit Hilfe von 0,5 g *p*-Toluolsulfonsäure, 10 cm³ Essigsäureanhydrid und 20 cm³ Essigsäure über Nacht acetyliert, wobei 0,35 g (60,5%) 6-Acetyl-6-acetoxymethyldihydroisocodein erhalten wurden. Schmp. 146—8 °C.

Analyse: $C_{23}H_{29}NO_6$, 383,6
Ber. Ac 27,26%
Gef. Ac 27,80%

LITERATUR

[1] Horváth, G., Kerekes, P., Gaál, Gy., Bognár, R.: Acta Chim. (Budapest) **82,** 217 (1974)
[2] Corey, E. J., Chaykovsky, M.: J. Am. Chem. Soc., **87,** 1353 (1965)
[3] Small, L. F., Rapoport, H.: J. Org. Chem., **12,** 284 (1974)
[4] Johnson, C. R., Schroeck, C. W., Shanklin, J. R.: J. Am. Chem. Soc., **95,** 7424, (1973)
[5] Goto, K., Yamamoto, J.: Proc. Japan Acad., **34,** 172 (1958)
[6] Chadha, M. S., Rapoport, H.: J. Am. Chem. Soc., **79,** 5730 (1957)

Géza Horváth
György Gaál
Péter Kerekes
Rezső Bognár

H-4010 Debrecen, Pf. 20.

Acta Chimica Academiae Scientiarum Hungaricae, Tomus 92 (3), pp. 317–322 (1977)

SYNTHESIS OF 2*H*-1,3-BENZOTHIAZINE DERIVATIVES, II

J. Szabó, L. Fodor, I. Varga, E. Vinkler and P. Sohár*

*(Department for Pharmaceutical Chemistry, Medical University, Szeged, and *Pharmaceutical Research Institute, Budapest)*

Received February 20, 1976

In the course of studies on the ring closure reaction developed earlier [1] for the preparation of 2*H*-1,3-benzothiazine derivatives, acid amides were found to form N-(hydroxymethyl) acid amides with formaldehyde in pyridine solution, which products are converted with 3,4-dimethoxythiophenol, in the presence of phosphorus oxychloride, into N-(3,4-dimethoxyphenylthiomethyl) acid amides. In pyridine solution these compounds undergo 2*H*-1,3-benzothiazine ring closure when heated with phosphorus oxychloride. This reaction represents a new route for the synthesis of 2*H*-1,3-benzothiazine and its derivatives carrying substituent in the 4 position.

In our earlier paper [1] the preparation of 2H-1,3-benzothiazine derivatives (**IIIa—c**) was reported which were formed by cyclization of 3,4-dimethoxythiophenol, acid amides and formaldehyde in pyridine solution.

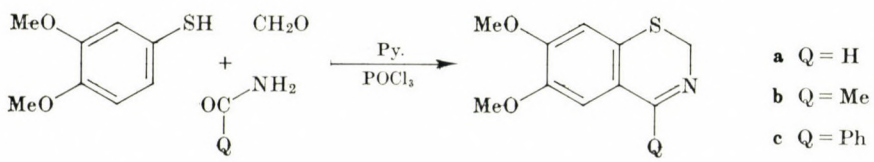

I **II** **III**

Further studies of the reaction revealed that the benzamide (**IIc**) with formaldehyde forms the N-(hydroxymethyl)-derivative **IV** under the experimental conditions given in [1a] (that is in basic solution), and the product undergoes condensation with 3,4-dimethoxythiophenol (**I**) in pyridine solution in the presence of phosphorus oxychloride, to yield N-(3,4-dimethoxyphenylthiomethyl)-benzamide (**Vc**). Bis(3,4-dimethoxyphenylthio)methane (**VI**) formed by condensation of compound **I** and formaldehyde, was also isolated as by-product from the reaction mixture.

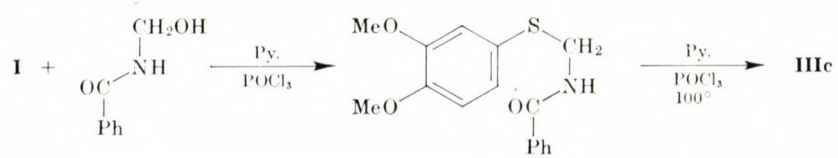

IV **V**

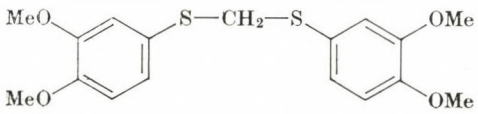

VI

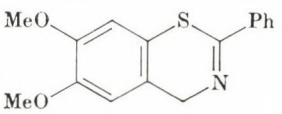

VII

Compound **Vc**, heated with phosphorus oxychloride in pyridine solution, undergoes cyclization yielding 4-phenyl-6,7-dimethoxy-2*H*-1,3-benzothiazine (**IIIc**). In this reaction, no 2-phenyl-6,7-dimethoxy-4*H*-1,3-benzothiazine (**VII**) is formed, contrary to the ring closure reaction conducted in the absence of pyridine [2]. This shows that, a properly chosen solvent (that is, pyridine) acting as a proton-acceptor agent can prevent the intermolecular proton-catalyzed rearrangement reaction of compound **V** [3] and, indirectly, the formation of the 4*H*-1,3-benzothiazine derivative (**VII**), too.

In the analogous reactions of several acid amides (**Vb—i**) only the 2*H*-1,3-benzothiazine derivatives (**IIIb—i**) were formed, in each case by electrophilic substitution, on the analogy of the Bischler-Napieralski synthesis of 3,4-dihydroisoquinoline.

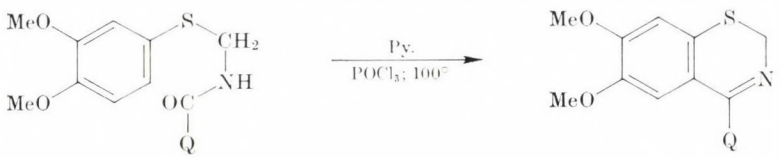

V **III**

a	Q = H	**d**	Q = 4-(MeO)C_6H_4	**g**	Q = $PhCH_2$
b	Q = Me	**e**	Q = 4-ClC_6H_4	**h**	Q = 3,4-$(MeO)_2C_6H_2CH_2$
c	Q = Ph	**f**	Q = 3,4-$(MeO)_2C_6H_3$	**i**	Q = Et

Numerous well-known procedures for the preparation of the acid amide thioether **Va** were failed. Therefore the condensation of N-(hydroxymethyl)-formamide and 3,4-dimethoxythiophenol by dehydration in pyridine solution with phosphorus oxychloride was attempted. We found that, this reaction proceeded through the intermediate **Va** can not be isolated, resulting in the 6,7-dimethoxy-2*H*-1,3-benzothiazine (**IIIa**).

The structures of 2*H*-1,3-benzothiazine derivatives were verified on the basis of elemental analyses and partly of their IR and NMR spectra. (Spectroscopic data are shown in Table I.)

Experimental

M. ps. are uncorrected.

IR spectra were recorded with a Perkin—Elmer 457 instrument. NMR spectra were obtained at room temperature with a JEOL 60-HL (60MHz) spectrometer, using TMS internal standard.

Table I

Compound	IR data, cm^{-1} (KBr)		NMR data ($CDCl_3$), $\delta_{TMS} = 0$ ppm				
	νOCH_3	$\nu C{=}N^*$	δCH_2 $s(2H)$	δOCH_3	δH-5	δH-8	Signals for substituent Q
IIId	2835	1555 1545	4.67	3.70 3.83 3.92 $3\times s(3\times 3H)$	6.85 $s(2H)$		δH-3',5' = 6.95· (2H) δH-2',6' = 7.50· (2H) $J_{2',3'} \equiv J_{5',6'} = 9$ Hz·
IIIe	2830	1545	4.62	3.67 3.90 $2\times s(2\times 3H)$	6.80 $s(1H)$	6.66 $s(1H)$	δArH ~ 7.34 $s(4H)$
IIIf	2830	1550	4.75	3.80 3.95 3.98 4.00 $4\times s(4\times 3H)$	7.30 $s(1H)$	7.00 $s(1H)$	δH-5'~6.98 ppm, d·· (1H) δH-2'~7.00 ppm, d·· (1H) δH-6'~7.20 ppm, $2\times d$·· (1H) $J_{5',6'} = 9$Hz·· $J_{2',6'} = 2$Hz··
IIIi. HCl**	2830	1580	4.83	4.02 4.06 $2\times s(2\times 3H)$	7.41 $s(1H)$	7.07 $s(1H)$	$\delta CH_3 = 1.42$ ppm, $t^{\blacktriangleright}$ (3H) $\delta CH_2 = 3.42$ ppm, $ga^{\blacktriangleright}$ (2H) $J_{AX} \equiv 7.5$Hz$^{\blacktriangleright}$

· Data calculated from the AA'BB' multiplet by the AB approximation
·· Data calculated from the AMX multiplet, $J_{2',5'} \equiv J^{para} \approx 0$
* Band due to a group vibration of $\nu C{=}N$ character, coupled with the aromatic skeletal vibration appearing at 1600 cm^{-1}
** $\nu(=N^+H)$ bands appear at 2800—2100 and 1865 cm^{-1}
$^{\blacktriangleright}$ Data calculated from the multiplet A_2X_3

1. Formation of N-(hydroxymethyl)benzamide in pyridine solution

Benzamide (0.12 g; 0.001 mole) was dissolved, with heating, a mixture of formaldehyde (35%; 0.1 ml), potassium carbonate (0.005 g) and pyridine (1 ml). The mixture was allowed to stand for 15 min and the solvent was removed at reduced pressure. The residue was crystallized from benzene to obtain colourless crystals (0.11 g), m.p. 82—84 °C. Recrystallization from water gave colourless crystals, m.p. 104—106 °C; no melting point depression was observed with an authentic sample [4].

2. Formation of N-(3,4-dimethoxyphenylthiomethyl)-benzamide (Vc) in pyridine solution

Benzamide (1.21 g; 0.01 mole) was dissolved, with heating, in a solution of potassium carbonate (0.01 g) in 35% formaldehyde (1 ml) and pyridine (5 ml), and the reaction mixture was allowed to cool to room temperature. 3,4-Dimethoxythiophenol (1.7 g; 0.01 mole) was added, followed by the addition of phosphorus oxychloride (2 ml) with cooling and stirring; then the mixture was allowed to stand. Icy-water was added and the crystalline substance which separated was subjected to fractional crystallization from ethanol, to yield bis(3,4-dimethoxyphenylthio)methane (**VI**) (0.45 g), m.p. 123—124 °C, and N-(3,4-dimethoxyphenylthiomethyl)-benzamide (**Vc**) (0.45 g), m.p. 118—120 °C; the products showed no melting point depression with the authentic samples ([1] and [2]).

3. 4-Phenyl-6,7-dimethoxy-2*H*-1,3-benzothiazine (IIIc)

N-(3,4-Dimethoxyphenylthiomethyl)benzamide (6.06 g; 0.02 mole) was dissolved in pyridine (30 ml) and mixed cautionally with phosphorus oxychloride (6 ml), then heated on a hot water-bath for 30 min. After cooling, the reaction mixture was poured into icy-water, made alkaline with sodium carbonate and extracted with benzene. The benzene solution was dried over anhydrous sodium sulfate and the solvent was evaporated. The residue was dissolved in benzene and extracted with 10% hydrochloric acid (50 ml). The hydrochloric acid solution was neutralized with sodium carbonate and the crude product was extracted with benzene. The residue obtained after evaporation of the solvent was dissolved in hot ethanol (10 ml) and the picrate was precipitated (1.14 g) by the addition of ethanolic picric acid solution. Yellow crystals from ethanol, m.p. 222—223 °C (d.), no melting point depression was observed with an authentic sample [1]. The base from picrate pale yellow prisms from ethanol, m.p. 142—143 °C; no melting point depression was observed with an authentic sample [1].

4. 4-Methyl-6,7-dimethoxy-2*H*-1,3-benzothiazine (IIIb)

According to the procedure described in Experiment 3, N-(3,4-dimethoxyphenylthiomethyl)-acetamide (4.83 g; 0.02 mole) was convert to obtained the crude base (0.85 g): pale yellow prisms from anhydrous ethanol, m.p. 110—111 °C. No melting point depression was observed with an authentic sample [1].

5. 4-(4'-Methoxyphenyl)-6,7-dimethoxy-2*H*-1,3-benzothiazine (IIId)

N-(3,4-Dimethoxyphenylthiomethyl)anisic acid amide [2] (3.29 g; 0.01 mole) was converted into the base (0.16 g) according to the procedure described in Experiment 3, to obtain pale yellow needles m.p. 144—145 °C (from ethanol).

$C_{17}H_{17}NO_3S$ (315.38). Calcd. C 64.74; H 5.43; N 4.44; S 10.15. Found C 64.90; H 5.56; N 4.48; S 9.97%.

The hydrochloride was precipitated from an ethanolic solution with ether; yellow crystals, m.p. 178—179 °C (d.).

$C_{17}H_{18}ClNO_3S$ (351.85). Calcd. C 58.04; H 5.16; Cl 10.08. Found C 58.40; H 5.28; Cl 10.30%.

6. N-(3,4-Dimethoxyphenylthiomethyl)-4-chlorobenzamide (Ve)

3,4-Dimethoxythiophenol (1.70 g; 0.01 mole) and N-(hydroxymethyl)-4-chlorobenzamide (1.85 g; 0.01 mole) were dissolved in ethanol (25 ml). Saturated ethanolic hydrochloric

acid solution (5 ml) was added and the mixture was allowed to stand for 2 hrs. The crystals which precipitated were filtered off (3.0 g). Colourless needles, m.p. 139—140 °C (from ethanol).

$C_{16}H_{16}ClNO_3S$ (337.83). Calcd. C 56.89; H 4.77; Cl 10.50; N 4.14; S 9.49. Found C 56.54; H 4.64; Cl 10.30; N 4.12; S 9.20%.

7. 4-(4'-Chlorophenyl)-6,7-dimethoxy-2*H*-1,3-benzothiazine (IIIe)

N-(3,4-Dimethoxyphenylthiomethyl)-4'-chlorobenzamide (3.38 g; 0.01 mole) was converted into compound **IIIe** (0.17 g) according to the procedure given in Experiment 3, to obtain colourless needles, m.p. 139—140 °C (from ethanol).

$C_{16}H_{14}ClNO_2S$ (319.81). Calcd. C 60.08; H 4.41; S 10.03. Found C 59.75; H 4.54; S 10.15%.

The picrate was prepared as yellow crystals, m.p. 216—217 °C (d.).

$C_{22}H_{17}ClN_4O_9S$ (516.85). Calcd. C 48.09; H 3.12; N 10.21. Found C 47.90; H 3.28; N 10.25%.

8. 4-(3',4'-Dimethoxyphenyl)-6,7-dimethoxy-2*H*-1,3-benzothiazine (IIIf)

Cyclization of N-(3,4-dimethoxyphenylthiomethyl)veratric acid amide [2] (3.63 g; 0.01 mole), was effected as described in Experiment 3, yielded compound **IIIf** (0.20 g) pale yellow prisms, m.p. 152—153 °C (from benzene).

$C_{18}H_{19}NO_4S$ (345.42). Calcd. C 62.60; H 5.55; S 9.29. Found C 62.20; H 5.75; S 9.00%.

The picrate orange yellow crystals from ethanol, m.p. 175—176 °C (d.).

$C_{24}H_{22}N_4O_{11}S$ (574.52). Calcd. C 50.18; H 3.86; N 9.75. Found 50.00; H 3.90; N 9.81%.

9. 4-Benzyl-6,7-dimethoxy-2*H*-1,3-benzothiazine (IIIg)

Cyclization of N-(3,4-dimethoxyphenylthiomethyl)phenylacetamide [2] (3.17 g; 0.01 mole) was effected according to the procedure described in Experiment 3. The crude product was purified by chromatography on a preparative silica gel layer (benzene : ethanol, 9 : 1) to obtain pale yellow crystals (0.09 g) m.p. 80—82 °C (from ether).

$C_{17}H_{17}NO_2S$ (299.39). Calcd. C 68.20; H 5.73. Found C 67.90; H 5.75%.

The picrate yellow needles, m.p. 169—171 °C (d.) (from ethanol).

$C_{23}H_{20}N_4O_9S$ (528.90). Calcd. C 52.23; H 3.82; N 10.60. Found C 52.09; H 3.91; N 10.47%.

The hydrochloride was precipitated from ethanolic solution with ether. Yellow crystals, m.p. 174—175 °C (d.).

$C_{17}H_{18}ClNO_2S$ (335.85). Calcd. C 60.80; H 5.40; Cl 10.62; S 9.55. Found C 60.60; H 5.50; Cl 10.61; S 9.72%.

10. 4-(3',4'-Dimethoxybenzyl)-6,7-dimethoxy-2*H*-1,3-benzothiazine (IIIh)

N-(3,4-Dimethoxyphenylthiomethyl)homoveratric acid amide [2] (3.77 g; 0.01 mole) was converted into compound **IIIh** (0.04 g) according to the procedure given in Experiment 9, to obtain yellow crystals, m.p. 143—145 °C (from ether).

$C_{19}H_{21}NO_4S$ (359.45). Calcd. C 63.50; H 5.89; S 9.56. Found C 63.20; H 5.92; S 9.70%.

The picrate yellow crystals, m.p. 160—161 °C (d.) (from ethanol).

$C_{25}H_{24}N_4O_{11}S$ (588.55). Calcd. C 51.02; H 4.11; N 9.52. Found C 50.67; H 4.10; N 9.63%.

11. N-(3,4-Dimethoxyphenylthiomethyl)propionic acid amide (Vi)

3,4-Dimethoxythiophenol (17.0 g; 0.1 mole) and N-(hydroxymethyl)propionic acid amide (10.3 g) were dissolved in ethanol (20 ml), and ethanol saturated with hydrogen chloride (10 ml) was added to the solution. The reaction mixture was allowed to stand for 6 hrs. After mixing with ice (100 g), the reaction product was obtained in crystalline form. Recrystallization from benzene gave colourless radial needles (14.4 g), m.p. 91—93 °C.

$C_{12}H_{17}NO_3S$ (255.34). Calcd. C 56.46; H 6.71; N 5.49; S 12.56. Found C 56.59; H 6.90; N 5.54; S 12.45%.

12. 4-Ethyl-6,7-dimethoxy-2*H*-1,3-benzothiazine (IIIi)

Compound **IIIi** (0.26 g) was obtained from N-(3,4-dimethoxyphenylthiomethyl)propionic acid amide (2.55 g; 0.01 mole) according to the procedure given in Experiment 9. The product was a chromatographically homogeneous pale yellow oil.

$C_{12}H_{15}NO_2S$ (237.32). Calcd. C 60.74; H 6.37. Found C 60.41; H 6.40%.

The hydrochloride was obtained as yellow crystals, m.p. 184—185 °C (d.) (from ethanol).

$C_{12}H_{16}ClNO_2S$ (273.78). Calcd. C 52.66; H 5.89; S 11.70. Found C 52.20; H 5.90; S 11.45%.

The picrate was obtained in the form of yellow crystals m.p. 180—182 °C (d.) (from ethanol).

$C_{18}H_{18}N_4O_9S$ (466.43). Calcd. C 46.36; H 3.89; N 12.01; S 6.87. Found C 46.50; H 3.90; N 11.90; S 6.69%.

13. 6,7-Dimethoxy-2*H*-1,3-benzothiazine (IIIa)

3,4-Dimethoxythiophenol (1.7 g; 0.01 mole) and N-(hydroxymethyl)formamide (0.75 g) were dissolved in pyridine (5 ml), and phosphorus oxychloride (1 ml) was added dropwise, then the mixture was allowed to stand for 12 hrs. The mixture was processed as described in Experiment 3 to obtain compound **IIIa** (0.06 g) as a chromatographically homogeneous colourless oil.

$C_{10}H_{11}NO_2S$ (209.27). Calcd. C 57.42; H 5.30; S 15.32. Found C 57.01; H 5.35; S 15.25%.

The picrate yellow crystals, m.p. 195—196 °C (d.) (from ethanol); no melting point depression was observed with an authentic sample [1].

*

The authors are grateful to (Mrs.) Dr. J. SZABÓ (Pharmaceutical Chemical Institute) for the microanalyses, and to (Mrs.) Dr. B. CSÁKVÁRI and Mr. A. FÜRJES (Pharmaceutical Research Institute) for their assistances in recording the spectra.

REFERENCES

[1] SZABÓ J., FODOR, L., VARGA, I., SOHÁR, P.: Acta Chim. (Budapest) **88,** 145 (1976)
[2] VINKLER, E., SZABÓ, J.: Acta Chim. Acad. Sci. Hung. **6,** 323 (1955)
[3] SZABÓ, J., VINKLER, E.: Acta Chim. Acad. Sci. Hung. **34,** 447 (1962)
[4] EINHORN, A. *et al.:* Ann. **343,** 223 (1905)

János SZABÓ
Lajos FODOR
István VARGA
Elemér VINKLER
H-6720, Szeged, Eötvös u. 6.

Pál SOHÁR
H-1045, Budapest, Szabadságharcosok u. 47.

Acta Chimica Academiae Scientiarum Hungaricae, Tomus 92 (3), pp. 323–326 (1977)

1,2,4-TRIAZINES AND CONDENSED DERIVATIVES, XVII*

ETHANOLYSIS OF 3-METHYLTHIO-1,2,4-TRIAZIN-5(2*H*)-ONE AND A NOVEL SYNTHESIS OF 6-AZA-2-THIOURACIL**

G. DOLESCHALL and G. VÁNKAI

(Department of Organic Chemistry, Technical University, Budapest)

Received May 24, 1976

5-Ethoxy-3-methylthio-1,2,4-triazine (**2b**) is shown to be a possible intermediate of the two-step aminolysis of 3-methylthio-1,2,4-triazin-5(2*H*)-one (**1b**) leading, with benzylamine to 5-benzylamino-3-methylthio-1,2,4-triazine (**3b**). A novel synthesis of 6-aza-2-thiouracil (**6a**) starting with isonitrosoacetanilide (**7a**) has been devised.

In Part I [1] the novel aminolysis of the carbonyl group of 6-methyl-3-methylthio-1,2,4-triazin-5(2*H*)-one (**1a**) by successive treatment with boron trifluoride etherate in ethanol, and primary amines to yield the corresponding 5-(subst.-amino)-6-methyl-3-methylthio-1,2,4-triazines (**3a**) has been described. 5-Ethoxy-6-methyl-3-methylthio-1,2,4-triazines (**2a**) and or 5-ethoxy-6-methyl-3-methylthio-2,5-dihydro-1,2,4-triazin-5-ol (**4**) — both complexed with BF_3 — have been assumed as the intermediates of the aminolyses. In order to substantiate this assumption, aminolyses of the bicyclic analogue **5** [2] of **2a** · BF_3 were attempted. However, although compound **5** did react with amines, the expected type **3c** amines could in no case be isolated [2].

We have now found [1] that the transformation of **1b** into **3b** may be brought about by similar treatment as applied for the conversion of **1a** into the amines **3a**, (2) that compound **2b** may be isolated from the reaction mixture obtained after boron trifluoride dimethyl etherate treatment of **1b** in ethanolic solution, and (3) that **2b** may be aminolyzed in a separate step to give **3b**. These observations are consistent with the assumption of the intermediacy of the type **2** ethoxy derivatives in the aminolysis reactions of the triazinones **1**.

1b is easily accessible by methylation of 6-aza-2-thiouracil **6a**. The latter, in turn, has hitherto been obtained by ring closure of the thiosemicarbazones of glyoxylic acid or its esters [3, 4]. By appropriate modification of the reaction conditions these syntheses may be directed towards the formation of 6-azauracil (**6b**) [5]. Since glyoxylic acid and its esters are rather expensive starting substances, a new method for the synthesis of **6a** was desirable. We have

* For Part XVI, see. Ref. [11]

** Based on the Thesis of G. VÁNKAI, submitted to the Faculty of Chemical Engineering of the Technical University, Budapest, 1974.

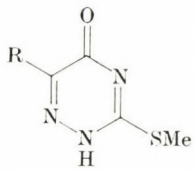

1

a: R = Me
b: R = H

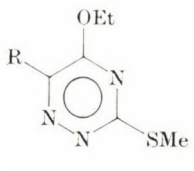

2

a: R = Me
b: R = H

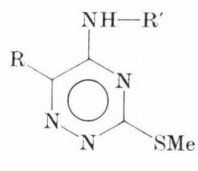

3

a: R = Me; R′ = Pr, Bu, $PhCH_2$
b: R = H; R′ = $PhCH_2$
c: R = HO—(CH_2)—

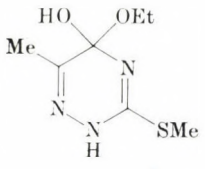

4

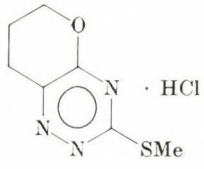

5

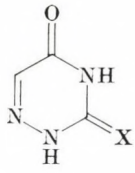

6

a: X = S
b: X = O

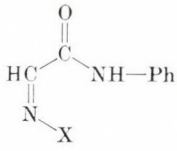

7

a: X = OH
b: X = NH—CS—NH_2

found that the readily accessible oxime of glyoxylanilide (**7a**) [6] is converted by treatment with thiosemicarbazide in the presence of hydrochloric acid into the corresponding thiosemicarbazone **7b** (90% yield), and that the latter is cyclized by alkaline treatment to give 6-aza-2-thiouracil (**6a**) in 56% yield. The latter may be directly *S*-methylated without isolation, to yield **1b**. **6a** is a convenient starting substance also for the synthesis of other 1,2,4-triazine derivatives including **6b** [3] and 6-azacytosine [7, 8]. A synthesis of **6b**, related to our synthesis of **6a** has been described by CHANG and ULBRICHT [9].

Experimental

Thiosemicarbazonoacetanilide (7b)

A suspension of thiosemicarbazide (36 g; 396 mmoles) in the mixture of conc. HCl (88 ml) and water (40 ml) was added to a solution of **7a** [6] (65 g; 396 mmoles) in warm ethanol (325 ml). The mixture was refluxed for 3 min and the resulting clear solution was diluted with water (100 ml) and allowed to cool to yield 80 g (90%) of the yellow crystals of **7b**, m.p. 213 °C (from aqueous DMF) (lit. [10] m.p. 210 °C).

6-Aza-2-thiouracil (6a)

The above compound (75 g; 337 mmoles) was refluxed for 1/2 hr with the aqueous (375 ml) solution of NaOH (15 g; 375 mmoles). The mixture was allowed to cool and the aniline formed was removed by extraction with ether (one 100-ml and two 50-ml portions. The aqueous solution was treated with charcoal and acidified (caution vigorous foaming) with acetic acid (30 ml). The resulting mixture was kept overnight at 0 °C to yield 24.5 g (56%) of **6a**, m.p. 264—265 °C (d.), lit. [3] m.p. 250 °C (d.). Recrystallization from water raised the m.p. to 269—270 °C (d.), but the non-recrystallized product was already pure as shown by the identity of its IR spectrum with that of a product obtained as described in the literature [3].

3-Methylthio-1,2,4-triazin-5(2H)-one (1b)

(a) Alkaline ring closure of compound **7b** (64 g; 288 mmoles) was effected as described above. The aniline formed was removed, and methyl iodide (18.1 ml; 290 mmoles) was added to the decolorized aqueous solution. The mixture was vigorously stirred for 2 hrs at room temperature and subsequently kept for 1 hr at 0 °C to yield 22 g (53%) of **1b**, m.p. 219—220 °C, which was raised by recrystallization from aqueous ethanol (1 : 4, v/v) to 223—224 °C, lit. [8] m.p. 214—216 °C. The IR spectrum (KBr) was identical with that of an authentic product obtained as described in the literature [8].

(b) The same product was obtained in 76% yield by similar treatment of a mixture of isolated **6a** (12 g; 93 mmoles), NaOH (4.0 g; 100 mmoles) and water (100 ml) with methyl iodide (7 ml; 112 mmoles).

5-Ethoxy-3-methylthio-1,2,4-triazine (2b)

A mixture of **1b** (5.0 g; 35 mmoles), anhydrous ethanol (50 ml) and $BF_3 \cdot Me_2O$, (9.0 g; 79 mmoles) was refluxed for 1 hr in a hood (slight evolution of methanethiol) and cooled to 0 °C. The cold mixture was cautiously poured into a vigorously stirred mixture of $NaHCO_3$ (10 g), water (200 ml) and ice (100 g). The product was extracted with pentane (one 150-ml and two 50-ml portions). The combined pentane solutions were washed with water, dried ($MgSO_4$) and concentrated to about 20 ml by evaporation of the solvent below 30 °C in vacuum. The solution was chilled to —40 °C to yield 0.8 g (13%) of **2b**, m.p. 42—43 °C (from pentane).

$C_6H_9N_3OS$ (171.22). Calcd. N 24.54; S 18.73. Found N 23.72; S 18.64%.

NMR ($CDCl_3$; reference: TMS): δ 8.6, s 1H, 5-H; 4.55, q, 2H + 1.5, t, 3H, OEt; 2.7, s, 3H, SMe.

5-Benzylamino-3-methylthio-1,2,4-triazine (3b)

(a) The above product (0.3 g; 1.4 mmole) was refluxed for 1/2 hr with benzylamine (0.6 ml; 5.5 mmoles) in EtOH (10 ml). The mixture was concentrated to about 2 ml by evaporation of the solvent in vacuum. Water was added to obtain 0.17 g (53%) of **3b**, faint yellow crystals, m.p. 188—190 °C (from 2-propanol).

$C_{11}H_{12}N_4S$ (232.31). Calcd. N 24.12; S 13.80. Found N 24.10; S 13.62%.

(b) A mixture of **1b** (1.82 g; 12.7 mmoles), anhydrous EtOH (25 ml) and $BF_3 \cdot Et_2O$ (3.0 g; 21 mmoles) was refluxed for 1 hr and allowed to cool. Benzylamine (6.6 ml; 60 mmoles)

was added. The mixture was refluxed for 1/2 hr and concentrated to about 15 ml. Water (100 ml) was added to obtain 1.0 g (34%) of **3b**, m.p. 188—190 °C (from 2-propanol), which proved identical with the product synthesized as described under *(a)*.

*

The authors are indebted to Mrs. M. Szirányi-Kiss for the NMR spectrum and to Mrs. I. Balogh-Batta and staff for the microanalyses.

REFERENCES

[1] Doleschall, G.: Acta Chim. Acad Sci. Hung. **53,** 305 (1967)
[2] Doleschall, G., Hornyák-Hámori, M., Lempert, K.: Acta Chim. Acad. Sci. Hung. **55,** 319 (1968)
[3] Gut, J.: Collection Czechoslov. Chem. Commun. **23,** 1588 (1958)
[4] Chung-Li, Li-Ho Chang, Chen-Fuan Tung, Hsiu Wang: Hua Hsueh Hsueh Pao **28,** No. 3, 167 (1962); Chem. Abstr. **59,** 3925h (1963)
[5] Revlon Inc., Netherlands Pat. 7.312.239 (1975); Current Highlights in Heterocyclic Chem. **2,** 353 (1975)
[6] Marvel, C. S., Hiers, G. S.: Organic Syntheses, Coll. Vol. I, John Wiley and Sons, New-York, London, 1961, p. 327.
[7] Falco, A. E., Pappas, E., Hitchings, G. H.: J. Am. Chem. Soc. **78,** 1938 (1956)
[8] Gut, J., Prystás, M., Jonas, J.: Collection Czechoslov. Chem. Commun. **26,** 986 (1961)
[9] Chang, P. K., Ulbricht, T. L. V.: J. Am. Chem. Soc. **80,** 976 (1958)
[10] Wolf, M., Szabó, J. H., Diebold, J. L. (to American Home Products Corp.) U.S. Pat. 3.299.133 (Jan. 17. 1967); Chem. Abstr. **67,** 2913 (1967)
[11] Doleschall, G., Lempert, K.: Tetrahedron, accepted for publication

Gábor Doleschall; H-1521 Budapest, Gellért-tér 4.
Gábor Vánkai; H-1045 Budapest, Tó u. 1—5.

RECENSIONES

R. J. STOODLEY: *Rearrangements of Penicillanic Acid Derivatives.* Tetrahedron Report No. 2

Pergamon Press, Oxford—New York—Toronto—Sydney—Paris—Frankfurt
1976, 25 pages

This comprehensive survey is the second member of the Tetrahedron Report series edited by Sir D. BARTON, and was published earlier by R. J. STOODLEY in the Tetrahedron [**31**, 2321 (1975)].

After the introductory part, the structural units of β-lactam antibiotics, the *penam* and *cepham* skeletons, are described and the nomenclature of the most important derivatives is given.

The mechanism of the formation of *secoceph-2-ems* and *secoceph-3-ems* obtainable from penicillin sulfoxides by the cleavage of the 1—2 bond is discussed and their rearrangements and other reactions (cycloaddition, electrophilic, nucleophilic, ring cleavage and intramolecular reactions) are dealt with in detail. The literature data are reviewed in a concise and theoretically thorough way. Reactions and rearrangements involving the cleavage of other bonds are also discussed in accordance with the numbering of the thiazolidine–azetidione ring system. The conversion of the azetidinyl cation and the intermediates of azetinone formed through heterolysis of the 1—5 bond are treated separately. This is followed by a thorough discussion of the thermodynamic and kinetic aspects of the C-6 epimerization.

This method of treatment is very advantageous, as it affords the possibility of rapid orientation for the reader in the literature listing 166 references.

The survey, also containing the papers of the author, gives a clear picture of the results in this group of compounds which have great theoretical and practical importance and are examined very intensely all over the world.

The present volume will be useful not only to research workers dealing with β-lactam antibiotics, but also to those interested in heterocyclics.

F. SZTARICSKAI

J. A. MOORE, D. L. DALRYMPLE: *Experimental Methods in Organic Chemistry*

Second Edition. W. B. Saunders Company, Philadelphia—London—Toronto
1976, pp. 334

Organic chemistry is perhaps the branch of chemistry requiring the greatest skill and experimental knowledge. It is therefore quite evident that the various text-books of preparations and practical guides have always been very important in organic chemical education. Advancement in chemistry was necessarily accompanied by the requirement of modernizing the teaching of experimental methods and this has been reflected by changes in the corresponding text-books, by the increase of their scope. Practical organic chemistry was fundamentally changed by the introduction of the modern separation and spectroscopic techniques. In the last century it has become evident that these techniques must gain an increased importance in practical organic chemical education, too.

Therefore, all attempts must be welcome which endeavour at the alteration of the teaching of experimental methods in this direction. The present book has solved this task successfully: while taking into account the temporal and financial limits of laboratory education, the discussion of the art, the high-level preparative work is combined with the practical description of modern separation techniques and spectroscopic methods and their scope of applications.

The size and composition of the book make it suitable for use in teaching organic chemical laboratory practice for one or more semesters. There are three main parts: in the first (Chapters 1—10) the basic laboratory techniques and methods (crystallization, extraction, distillation, chromatographic methods, etc.) are thoroughly and clearly treated. In accordance with their importance, this part deals with the IR (Chapter 8) and ^{1}H and ^{13}C spectroscopic techniques (Chapter 9). The relatively detailed discussion of ^{13}C-NMR spectroscopy finding more and more increasing use in organic chemistry, is one of the greatest merits of the book. However, purely practical aspects are not absent either, *e.g.* Chapter 6 (Liquid phase chromatography) describes in detail the preparation of thin-layers and the packing of chromatographic columns.

In Chapters 11—41, the sequence of treatment usual in modern organic chemical books has been followed. Some of the experiments are purely synthetic in character, whereas others point out the thermodynamic and kinetic aspects of organic chemical reactions (*e.g.*, Chapter 19: Determination of the equilibrium constants of esterification; Chapter 13: Nucleophilic substitution of alkyl halides; Chapter 21: Effects of substituents on reactivity).

The authors of the book, taking into account the increasing importance of special fields of organic chemistry (*e.g.*, biochemistry, polymer chemistry), devoted several chapters to the introduction of special laboratory techniques employed in these fields. In Chapter 29, the synthesis of a bioregulator is described, while Chapter 38 deals with the comparison of enzymic and acid-catalyzed reactions from the kinetic point of view; two chapters treat the synthesis of drugs (lidocaine, sulfonamides). Chapters 40 and 41 review synthetic polymers and dyes and dying procedures, respectively.

The last chapter of the book discusses methods for identification of compounds. It relies primarily on IR and NMR spectroscopic techniques, but qualitative elemental analysis, simple functional group tests and methods of derivative preparation are also discussed. The list of "unknown compounds" suggested comprises 250 compounds, the spectra of which are shown in the manual for teachers.

At the end of the chapters, checking questions, as well as references are given. This laboratory book, composed very successfully from both the theoretical and practical points of view, is printed excellently and the clear pictures and tables greatly increase its practical value.

Á. KUCSMAN

Proceedings of the International Conference on Colloid and Surface Science. Vol. 2. Discussion and Free Communications. Edited by E. WOLFRAM and T. SZEKRÉNYESSY

Akadémiai Kiadó, Budapest 1976, 219 pages

Two volumes have appeared on the subject of the 6-day International Conference on Colloid and Surface Chemistry organized under the auspices of IUPAC, September 1975, Budapest. The first volume, published in 1975 comprises the papers read at the sessions. The second volume recently published is divided into three parts and complements the previously published material of the conference from several aspects.

The first chapter of the volume covers the large and valuable material of the discussions in conjunction with the main lectures contained in the Abstract of Papers.

In the second chapter, the discussion of the contributed papers is organized in groups according to the four sections of the conference:

I. Surface chemistry,
II. Disperse systems,
III. Surfactants, monolayers and foams,
IV. Applications and methods.

A third chapter increases the value of the publication by giving the full text, together with discussions, of the 7 free communications presented at the Conference.

The Author Index closing the volume helps orientation in both volumes.

The typography and the nice make-up, similarly to the first volume, testify of careful work.

K. UDVARHELYI

INDEX

PHYSICAL AND INORGANIC CHEMISTRY

Electronic Absorption Spectra of Substituted Carbazoloquinones, R. M. Issa, A. A. El-Samahy, I. M. Issa, S. H. Etaiw 211

Study of the Mechanism of Hexene Radiolysis, II. Investigation of *n*-Hexene Isomers with Additives, A. Kovács, Gy. Cserép, G. Földiák 223

TPD Study of the "Stability" of H_2 Chemisorbed on Al_2O_3 and Pt, D. Móger, G. Besenyei, G. Kovács, F. Nagy 237

Studies of Oxygen Overvoltage on Platinum Electrodes. The Interpretation of the Changes in Overvoltage under the Effect of ε-Caprolactam (in German), T. Erdey-Grúz†, Gy. Horányi, É. Szetey 249

Preparation and IR Spectrophotometric Study of Charge-Transfer Complexes of 3,5-Dinitrobenzoic Acid with Aromatic Compounds, A. M. Hindawey, A. M. G. Nassar, R. M. Issa 263

Thermolysis of Cyano Complexes, X. Synthesis and Thermal Decomposition of Quaternary Ammonium Cyanometallates (Regular Salts), B. Mohai, L. Bagyin (in German) . 271

Thermolysis of Cyano Complexes, XI. Synthesis and Thermal Decomposition of Quaternary Ammonium Hydrogen Cyanometallates (Protonisation Complexes) (in German) B. Mohai, L. Bagyin 281

Anodic Oxidation of Potassium Oxalate in Sulfuric Acid on a Germanium Semiconductor-Electrolyte Interface, M. M. Singh, C. S. Singh 289

ORGANIC CHEMISTRY

Investigations on the Synthesis of 1,5-Benzodiazepines (in German), Z. Zubovics, G. Fehér, L. Toldy 293

Synthesis and Structure Investigations of some 6-Substituted Dihydrocodeins and Dihydro-iso-codeins, (in German), G. Horváth, Gy. Gaál, P. Kerekes, R. Bognár 311

Synthesis of 2*H*-1,3-benzothiazine Derivatives, II. J. Szabó, L. Fodor, I. Varga, E. Vinkler, P. Sohár 317

1,2,4-Triazines and Condensed Derivatives, XVII. Ethanolysis of 3-methylthio-1,2,4-triazin-5 (2*H*)-one and a Novel Synthesis of 6-aza-2-thiouracil, G. Doleschall, G. Vánkai 323

RECENSIONES 327

Printed in Hungary

A kiadásért felel az Akadémiai Kiadó igazgatója — Műszaki szerkesztő: Zacsik Annamária

A kézirat nyomdába érkezett: 1976. XI. 24. — Terjedelem: 10,5 (A/5) ív, 64 ábra

77.3864 Akadémiai Nyomda, Budapest — Felelős vezető: Bernát György

ACTA CHIMICA

ТОМ 92 – ВЫП. 3

РЕЗЮМЕ

Электронные спектры поглощения замещенных карбазолохинонов

Р. М. ИССА, А. А. ЭЛЬ-САМАБИ, И. М. ИССА и С. Б. ЭТАИВ

Были сняты УФ и видимые спектры карбазолохинонов в органических растворителях и водных буферных растворах. Электронные переходы были идентифицированы либо как локально возбужденные либо преимущественно как состояния с переносом заряда. Спектральные сдвиги обсуждаются с точки зрения эффекта среды и молекулярной структуры. Изменение поглощения с pH использовано для определения pK_a. Важные полосы ИК спектров были отнесены и обсуждены в отношении молекулярной структуры.

Исследование механизма реакции радиолиза гексена, II

Исследование изомеров н-гексана с добавками

А. КОВАЧ, ДЬ. ЧЕРЕП и Г. ФЁЛЬДИАК

Экспериментально были подтверждены, а также распространены на изомеры н-гексена те заключения относительно образования водорода и сопряженных диенов, а также относительно совокупности отдельных реакций, которые были сделаны ранее, исходя из данных радиолиза циклогексена в присутствии ловушек.

На основе исследований, проводенных в присутствии ловушек радикалов и электронов, были подтверждены уже ранее предполагаемые процессы радикально-ионного разложения и внутренней перегруппировки, приводящие к образованию этилена и пропена.

При образовании димеров важное значение имеют как радикальные, так и ионные реакции. Однако, при радиолиза гексенов, содержащих внутреннюю двойную связь, в образовании этих продуктов радикальные процессы приобретают большую роль, нежели ранее предполагалось.

Было обнаружено, что в процессе радиолиза н-гексенов протекает также и изомеризация.

Исследование «стабилизации», H_2, хемисорбированного на Al_2O_3 и Pt, с помощью метода ТПД

Д. МОГЕР, Г. БЕШЕН ЕИ, Г. КОВАЧ и Ф. НАДЬ

Исследуя хемисорбцию водорода на катализаторах Al_2O_3 и Pt при температурах, выше комнатной с помощью термодесорбционной методики, было установлено следующее.

1) В случае Pt, если адсорбция проводится с помощью соответствующей программы, то на термодесорбтограмме, в противоположность литературным данным, наблюдается не два, а три пика. Новый пик расположен между пиками, соответствующими γ и δ водородам.

2) Как для случая Al_2O_3, так и для Pt были разработаны такие адсорбционные программы, с помощью которых осуществляется то, что на термодесорбтограмме наблюдается всего один пик, что свидетельствует о существовании лишь одного типа адсорбированного водорода.

3) «Стабилизация» этих катализаторов и адсорбированных состояний (постояность во времени) позволяет исследование роли адсорбированного водорода, характеризуемого различными десорбционными максимумами, в каталитических реакциях.

Исследование перенапряжения кислорода на платиновом электроде

Интерпретация изменения перенапряжения, проявляющегося под влиянием ε-капролактама

Т. ЭРДЕИ-ГРУЗ, ДЬ. ХОРАНИ и З-НЕ СЕТЕИ

Опираясь на более ранние экспериментальные результаты, были проанализированы те факторы, которые могут играть роль в изменении перенапряжения при выделении кислорода на платиновом электроде под влиянием ε-капролактама. На основе исследований кинетических зависимостей вытекает, что значительная часть изменения перенапряжения вызвана уменьшением концентраций как воды, так и электролита в присутствии капролактама. С целью дополнения более ранних исследований и для получения вспомогательных данных кинетического анализа, были измерены плотности растворов капролактама в зависимости от концентрации последенего. Было установлено, что зависимость между молярным объемом растворов и молярной долью воды является линейной в первом приближении. Был исследован потенциал водородного электрода в зависимости от концентрации водородного иона в концентрированных капролактамовых растворах. Было установлено, что в интервале концентраций HCl_4 0,001—1М закон Нернста приближенно соблюдается.

Проготовление и ИК спектрометрическое исследование КПЗ 3,5-динитробензойной кислоты с ароматическими соединениями

А. М. ХИНДЭВЭЙ, А. М. Г. НАССАР и Р. М. ИССА

Были сняты ИК спектри аддиционных соединений 3,5-динитробензойной куслоты с ароматическими молекулами. Их анализировали с целью определения типа взаимодействий. Сдвиги полос ν_{OH}, асим. ν_{NO_2} и $\nu_{C=O}$ кислоты были рассмотрены с целью различия КПЗ, взаимодействий с переносом протона и молекулярных комплексов.

Термолиз циановых комплексов, X

Получение четвертичных аммонийных цианометаллатов (регулярных солей) и их терморазложение

Б. МОХАИ и Л. БАДИН

Для получения комплексов была использована нейтрализация цианометаллатной кислоты четвертичной гироокисью аммония, а также реакция замещения между серебрянным цианометаллатом и четвертичным иодистым аммонием. При термолизе вначале удаляется кристаллизационная вода, далее в интервале температур 220—280°С —дициан и монооκись азота, и конечно при 200—500°С удаляются соответствующие третичные амины и алкильные цианиды. В 14 изученных комплексах цианометаллатным анионом были: $[Fe(CN)_6]^{4-}$, $[Fe(CN_6)^{3-}$, $[Fe(CN)_5NO]^{2-}$ и $[CO(CN_6)^{3-}$, а с четвертичными катионами: $[(CH_3)_4N]^+$, $[(C_2H_5)_4N)^+$, $[(C_4H_9)_4N]^+$ и $[(CH_3)_3C_6H_5N]^+$.

Термолиз цианокомплексов, XI

Получение и термическое разложение четвертичных бицианометаллатов аммония (протонированные комплексы)

Б. МОХАИ и Л. БАДИН

Из солянокислых растворов, содержащих четвертичные амонные соли (тетраметил-, тетраэтил-, тетрабутил-, триметилфениламмонийхлорид) и калий- [гексацианоферрат(II)], выделяются соли, содержащие одино, два и три водородных иона. [Гексацианоферрат(III)] и — [кобальтат(III)] образует лишь однокислые соли. В ходе термолиза комплексов на кривых ТГ появляются самостоятельные ступени HCN, и степень протониро-

вания непосредственно была измерена ацидометрически. Процессы разложения этих соединений, подобны разложению соответствующих средних солей пренебрегая их небольшой термостабильностью.

Анодное окисление оксалата калия в присутствии серной кислоты на поверхности раздела германиевый полупроводник - электролит

М. М. СИНГ и Ц. С. СИНГ

Анодные окисление оксалата калия на поверхности *n*-и p—Ge электродов было исследовано в присутствии 0,1N растворов серой кислоты. Кривые Тафеля были построены и природа носителя тока, играющего роль в процессе, была определена из сравнения кривых поляризации анодов *n*- и p—Ge. Зависимость Тафеля $\eta + a + b \log i$ действительна в очень узком интервале плотности тока. Плотность тока насыщения, наблюдаемого на поляризационных кривых анода *n*—Ge, увеличивается при добавлении оксалата к раствору серной кислоты. На аноде p—Ge перенапряжение постоянно увеличивается с увеличением применяемой силы тока. Освещение поверхности электрода не влияет на характер поляризационных кривых p—Ge, в то время как плотность тока насыщения на *n*—Ge увеличивается. Результаты указывают на то, что процесс окисления ионов оксалата включает передачу электрона от иона на уровень проводимости германия.

Исследование синтеза 1,5-бензодиазепинов

З. ЗУБОВИЧ, Г. ФЕХЕР и Л. ТОЛЬДИ

Описывается синтез 1,5-бензодиазепин-2-онов взаимодействием 1,3-дифенил-2-гидрокси-2-циклобутен-1-она (димер фенилкетена) с о-фенилендиаминами; при этом образуется амидная группа в семичленном цикле из более нуклеофильной аминогруппы в исходном диамине. Структура и положение заместителей были доказаны независимыми синтезами.

Реакция этил-α, γ-дифенилацетоацетата с о-фенилендиамином не приводит к ожидаемому бензодиазепину, а к некоторым другим продуктам, выяснение структуры которых дает сведения относительно механизма реакции.

Получение и исследование структуры некоторых 6-замещенных дигидрокодеина и дигидроизокодеина

Г. ХОРВАТ, ДЬ. ГААЛ, П. КЕРЕКЕШ и Р. БОГНАР

При взаимодействии дигидрокодеинона с метилидом диметилсульфония образуется 6-дезокси-6,6-метиленоксидигидрокодеин, вновь образующаяся углерод-углеродная связь которого является экваториальной. Восстанавливая эпоксидное кольцо с помощью алюмогидрида лития, из кетона с помощью метиллития был выделен 6-метилдигидрокодеин.

Производя раскрытие кольца с помощью других нуклеофильных реагентов, были получены 6-гидроксиметилдигидрокодеины.

Эти новые соединения представляют собой C_6-эпимеры соединений, уже ранее полученных из дигидрокодеинона и метилида диметилоксосульфония, с той лишь разницей, что исходным веществом реакции, проведенной в тех же самых условиях, был 6-дезокси-6,6-метиленокси-дигидроизокодеин.

Получение производных 2*H*-1,3-бентиазина, II

Я. САДО, Л. ФОДОР. И. ВАРГА, Е. ВИНКЛЕР и П, ШОХАР

Исследуя реакцию циклизации, разработанную ранее для получения производных 2*H*-1,3-бентиазинов [1], было показано, что в приидиновом растворе амиды кислот, взаимодействуя с формальдегидом, дают амиды N-(гидроксиметил)-кислот, которые под влиянием хлористой окиси фосфора присоединяют 3,4-диметокситиофенол, давая амиды

N-(3,4-диметоксифенилтиометил)-кислот. Последние в пиридиновом растворе при нагреве циклизуются с образованием 2*H*-1,3-бензтиазинового кольца. Эта реакция представляет собой новый метод получения 2*H*-1,3-бензтиазина и его 4-замещенных производных.

1,2,4-Триазины и их конденсированные производные, XVII

Этанолиз 3-метилтио-1,2,4-триазин-5(2*H*)-она и новый синтез 6-аза-2-тиоурацила

Г. ДОЛЕШАЛЛ и Г. ВАНЬКАИ

5-Этокси-3-метилтио-1,2,4-триазин (*2b*) является вероятным промежуточным продуктом двухступенчатого бензиламинолиза 3-метилтио-1,2,4-триазин-5(2*H*)-она (*1b*), приводящего к образованию 5-бензиламино-3-метилтио-1,2,4-триазина (*3b*). Предлагается новый синтез 6-аза-2-тиоурацила (*6a*), исходя из изонитрозоацетанилида (*7a*).

Les Acta Chimica paraissent en français, allemand, anglais et russe et publient des mémoires du domaine des sciences chimiques.

Les Acta Chimica sont publiés sous forme de fascicules. Quatre fascicules seront réunis en un volume (4 volumes par an).

On est prié d'envoyer les manuscrits destinés à la rédaction à l'adresse suivante:

Acta Chimica
H-1521 Budapest, Hongrie

Toute correspondance doit être envoyée à cette même adresse.

La rédaction ne rend pas de manuscript.

Le prix de l'abonnement est de $ 32,00 par volume.

Abonnement — en Hongrie à l'Akadémiai Kiadó (1363 Budapest, P.O.B. 24. C.C.B. Bankszámla 215 11488), à l'étranger à l'Entreprise pour le Commerce Extérieur «Kultúra» (H-1389 Budapest 62, P.O.B. 149 Compte-courant No. 218 10990) ou l'étranger chez tous les représentants ou dépositaires.

Die Acta Chimica veröffentlichen Abhandlungen aus dem Bereich der chemischen Wissenschaften in deutscher, englischer, französischer und russischer Sprache.

Die Acta Chimica erscheinen in Heften wechselnden Umfanges. Vier Hefte bilden einen Band. Jährlich erscheinen 4 Bände.

Die zur Veröffentlichung bestimmten Manuskripte sind an folgende Adresse zu senden:

Acta Chimica
H-1521 Budapest, Ungarn

An die gleiche Anschrift ist auch jede für die Redaktion bestimmte Korrespondenz zu richten.

Manuskripte werden nicht zurückerstattet.

Abonnementpreis pro Band: $ 32,00.

Bestellbar für das Inland bei Akadémiai Kiadó (1363 Budapest, Postfach 24, Bankkonto Nr. 215 11488), für das Ausland bei dem Außenhandels-Unternehmen „Kultúra" (H-1389 Budapest 62, P.O.B. 149. Bankkonto Nr. 218 10990) oder bei seinen Auslandsvertretungen und Kommissionären.

«Acta Chimica» издают статьи по химии на русском, английском, французском и немецком языках.

«Acta Chimica» выходит отдельными выпусками разного объема, 4 выпуска составляют один том и за год выходят 4 тома.

Предназначенные для публикации рукописи следует направлять по адресу:

Acta Chimica
H-1521 Budapest, ВНР

Всякую корреспонденцию в редакцию направляйте по этому же адресу.

Редакция рукописей не возвращает.

Подписная цена — $ 32,00 за том.

Отечественные подписчики направляйте свои заявки по адресу Издательства Академии Наук (1363 Budapest, P.O.B. 24, Текущий счет 215 11488), а иностранные подписчики через организацию по внешиней торговле «Kultúra» (H-1389 Budapest 62, P.O.B. 149. Текущий счет 218 10990) или через ее заграничные представительства и уполномоченных.

Reviews of the Hungarian Academy of Sciences are obtainable at the following addresses:

AUSTRALIA
C.B.D. LIBRARY AND SUBSCRIPTION SERVICE, Box 4886, G.P.O., *Sydney N.S.W.2001*
COSMOS BOOKSHOP, 145 Ackland Street, *St. Kilda (Melbourne), Victoria 3182*

AUSTRIA
GLOBUS, Höchstädtplatz 3, *1200 Wien XX*

BELGIUM
OFFICE INTERNATIONAL DE LIBRAIRIE, 30 Avenue Marnix, *1050 Bruxelles*
LIBRAIRIE DU MONDE ENTIER, 162 Rue du Midi, *1000 Bruxelles*

BULGARIA
HEMUS, Bulvar Ruszki 6, *Sofia*

CANADA
PANNONIA BOOKS, P.O.Box 1017, Postal Station "B", *Toronto, Ontario M5T 2T8*

CHINA
CNPICOR, Periodical Department, P.O.Box 50, *Peking*

CZECHOSLOVAKIA
MAD'ARSKÁ KULTURA, Národní třida 22, *115 66 Praha*
PNS DOVOZ TISKU, Vinohradská 46, *Praha 2*
PNS DOVOZ TLAČE, *Bratislava 2*

DENMARK
EJNAR MUNKSGAARD, Norregade 6, *1165 Copenhagen*

FINLAND
AKATEEMINEN KIRJAKAUPPA, P.O.Box 128, *SF-00101 Helsinki 10*

FRANCE
EUROPÉRIODIQUES S. A., 31 Avenue de Versailles, *78170 La Celle St.-Cloud*
LIBRAIRIE LAVOISIER, 11 rue Lavoisier, *75008 Paris*
OFFICE INTERNATIONAL DE DOCUMENTATION ET LIBRAIRIE, 48 rue Gay Lussac, *75240 Paris Cedex 05*

GERMAN DEMOCRATIC REPUBLIC
HAUS DER UNGARISCHEN KULTUR, Karl-Liebknecht-Strasse 9, *DDR-102 Berlin*
DEUTSCHE POST, ZEITUNGSVERTRIEBSAMT, Strasse der Pariser Kommüne 3—4, *DDR-104 Berlin*

GERMAN FEDERAL REPUBLIC
KUNST UND WISSEN, ERICH BIEBER, Postfach 46, *7000 Stuttgart 1*

GREAT BRITAIN
BLACKWELL'S PERIODICALS DIVISION, Hythe Bridge Street, *Oxford OX1 2ET*
BUMPUS, HALDANE AND MAXWELL LTD., Cowper Works, *Olney, Bucks MK46 4BN*
COLLET'S HOLDINGS LTD., Denington Estate, *Wellingborough, Northants NN8 2QT*
WM. DAWSON AND SONS LTD., Cannon House, *Folkestone, Kent CT19 5EE*
H. K. LEWIS AND CO., 136 Gower Street, *London WC1E 6BS*

GREECE
KOSTARAKIS BROTHERS, International Booksellers, 2 Hippokratous Street, *Athens-143*

HOLLAND
MEULENHOFF-BRUNA B.V., Beulingstraat 2, *Amsterdam*
MARTINUS NIJHOFF B.V., Lange Voorhout 9—11, *Den Haag*
SWETS SUBSCRIPTION SERVICE, 347b Heereweg, *Lisse*

INDIA
ALLIED PUBLISHING PRIVATE LTD., 13/14 Asaf Ali Road, *New Delhi 110001*
150 B-6 Mount Road, *Madras 600002*
INTERNATIONAL BOOK HOUSE PVT. LTD., Madame Cama Road, *Bombay 400039*
THE STATE TRADING CORPORATION OF INDIA LTS., Books Import Division, Chandralok, 36 Janpath, *New Delhi 110001*

ITALY
EUGENIO CARLUCCI, P.O.Box 252, *70100 Bari*
INTERSCIENTIA, Via Mazzè 28, *10149 Torino*
LIBRERIA COMMISSIONARIA SANSONI, Via Lamarmora 45, *50121 Firenze*
SANTO VANASIA, Via M. Macchi 58, *20124 Milano*
D. E. A., Via Lima 28, *00198 Roma*

JAPAN
KINOKUNIYA BOOK-STORE CO. LTD., 17-7 Shinjuku 3 chome, Shinjuku-ku, *Tokyo 160-91*
MARUZEN COMPANY LTD., Book Department, P.O.Box 5050 Tokyo International, *Tokyo 100-31*
NAUKA LTD. IMPORT DEPARTMENT, 2-30-19 Minami Ikebukuro, Toshima-ku, *Tokyo 171*

KOREA
CHULPANMUL, *Phenjan*

NORWAY
TANUM-CAMMERMEYER, Karl Johansgatan 41—43, *1000 Oslo*

POLAND
WĘGIERSKI INSTYTUT KULTURY, Marszałkowska 80, *Warszawa*
CKP I W ul. Towarowa 28 *00-958 Warsaw*

ROUMANIA
D. E. P., *Bucureşti*
ROMLIBRI, Str. Biserica Amzei 7, *Bucureşti*

SOVIET UNION
SOJUZPETCHATJ — IMPORT, *Moscow*
and the post offices in each town
MEZHDUNARODNAYA KNIGA, *Moscow G-200*

SPAIN
DIAZ DE SANTOS, Lagasca 95, *Madrid 6*

SWEDEN
ALMQVIST AND WIKSELL, Gamla Brogatan 26, *101 20 Stockholm*
GUMPERTS UNIVERSITETSBOKHANDEL AB, Box 346, *401 25 Göteborg 1*

SWITZERLAND
KARGER LIBRI AG, Petersgraben 31, *4011 Base*

USA
EBSCO SUBSCRIPTION SERVICES, P.O.Box 1943, *Birmingham, Alabama 35201*
F. W. FAXON COMPANY, INC., 15 Southwest Park, *Westwood, Mass, 02090*
THE MOORE-COTTRELL SUBSCRIPTION AGENCIES, *North Cohocton, N. Y. 14868*
READ-MORE PUBLICATIONS, INC., 140 Cedar Street, *New York, N. Y. 10006*
STECHERT-MACMILLAN, INC., 7250 Westfield Avenue, *Pennsauken N. J. 08110*

VIETNAM
XUNHASABA, 32, Hai Ba Trung, *Hanoi*

YUGOSLAVIA
JUGOSLAVENSKA KNJIGA, Terazije 27, *Beograd*
FORUM, Vojvode Mišiča 1, *21000 Novi Sad*

ACTA CHIMICA

ACADEMIAE SCIENTIARUM HUNGARICAE

ADIUVANTIBUS

M. BECK, R. BOGNÁR, V. BRUCKNER,
GY. HARDY, K. LEMPERT, F. MÁRTA,
K. POLINSZKY, E. PUNGOR,
G. SCHAY, Z. G. SZABÓ, P. TÉTÉNYI

REDIGUNT

B. LENGYEL et GY. DEÁK

TOMUS 92 FASCICULUS 4

AKADÉMIAI KIADÓ, BUDAPEST

1977

ACTA CHIM. (BUDAPEST) ACASA2 92 (4) 329–433 (1977)

ACTA CHIMICA

A MAGYAR TUDOMÁNYOS AKADÉMIA KÉMIAI TUDOMÁNYOK OSZTÁLYÁNAK IDEGEN NYELVŰ KÖZLEMÉNYEI

FŐSZERKESZTŐ

LENGYEL BÉLA

SZERKESZTŐ

DEÁK GYULA

TECHNIKAI SZERKESZTŐ

HARASZTHY-PAPP MELINDA

SZERKESZTŐ BIZOTTSÁG

BECK MIHÁLY, BOGNÁR REZSŐ, BRUCKNER GYŐZŐ, HARDY GYULA, LEMPERT KÁROLY, MÁRTA FERENC, POLINSZKY KÁROLY, PUNGOR ERNŐ, SCHAY GÉZA, SZABÓ ZOLTÁN, TÉTÉNYI PÁL

Acta Chimica is a journal for the publication of papers on all aspects of chemistry, in the English, French, German and Russian languages.

Acta Chimica are published in 4 volumes per year. Each volume consists of 4 issues of varying size.

Manuscripts should be sent to

Acta Chimica
H-1521 Budapest, Hungary

Correspondence with the Editors should be sent to the same address. Manuscripts are not returned to the Authors.

Subscription rate $ 32.00 per volume.

Hungarian subscribers should order from Akadémiai Kiadó, 1363 Budapest, P.O. Box 24. Account No. 215 11488.

Orders from other countries are to be sent to "Kultúra" Foreign Trade Company (H-1389 Budapest 62, P.O. Box 149. Account No. 218 10990) or to its representatives abroad.

Acta Chimica Academiae Scientiarum Hungaricae, Tomus 92 (4), pp. 329—349 (1977)

ON THE MECHANISM OF CYCLOPENTANE RADIOLYSIS

Cs. KESZEI, L. WOJNÁROVITS and G. FÖLDIÁK

(Institute of Isotopes of the Hungarian Academy of Sciences, Budapest)

Received Oct. 11, 1975

The radiolysis of cyclopentane has been studied by means of radical, electron and positive ion scavengers. The main components of the $G(H_2)$ value were determined (monomolecular hydrogen elimination: 1.5, thermal and hot hydrogen atom formation: 1.6 and 2.3 G-units, respectively), together with the yields of fragments and cyclopentyl radicals ($G \simeq 5.2$). The k_d/k_c value for the latter type of monoradicals has also been determined (1.0). The total ion yield generated by radiation is $G_{ti} = G_{fi} + G_{gi} = 4.4$; the yield of free ions is as low as 0.12, *i. e.* about 3% of the total yield. The considerable variation of yields of products involving C–H bond rupture indicates several ionic processes: about 60—80% of the monomolecular cyclopentene formation is a result of such reactions. It has been shown that about 90% of the ring fragments is produced in monomolecular reactions. A formula has been proposed to describe the charge scavenging without contradictions: using this, and our experimental data, the α efficiency value of the additive has been found to be equal to 3.9 M^{-1} for CCl_4 electron scavenger and 0.086 M^{-1} for cyclopropane positive ion scavenger.

Introduction

Although cyclopentane is the second most frequently investigated cycloalkane after cyclohexane, as for radiation chemical studies are concerned, the number of papers dealing with cyclohexane is about ten times higher.

1. Literature survey

The C_5 ring has a slightly strained structure; the yield of radiolysis products [1—8] involving C–C bond rupture is about twice as much as from cyclohexane having practically no strain [5, 6].

BUSI and FREEMAN have summarized reactions of cyclopentane leading to C–H bond rupture [8]:

$$\text{c-}C_5H_{10} \xrightarrow{\sim\sim\rightarrow} \text{c-}C_5H_{10}^{+} + e^{-} \qquad (1a)$$

$$\text{c-}C_5H_{10} \xrightarrow{\sim\sim\rightarrow} \text{c-}C_5H_{10}^{*} \qquad (1b)$$

$$\text{c-}C_5H_{10}^{+} + e^{-} \longrightarrow \text{c-}C_5H_{10}^{x} \qquad (2)$$

$$c\text{-}C_5H_{10}^{*} \begin{cases} \longrightarrow H + c\text{-}C_5H_9^{\cdot} & (3a) \\ \longrightarrow H_2 + c\text{-}C_5H_8 & (3b) \end{cases}$$

$$c\text{-}C_5H_{10}^{x} \begin{cases} \longrightarrow H + c\text{-}C_5H_9^{\cdot} & (4a) \\ \longrightarrow H_2 + c\text{-}C_5H_8 & (4b) \end{cases}$$

$$H + c\text{-}C_5H_{10} \longrightarrow H_2 + c\text{-}C_5H_9^{\cdot} \qquad (5)$$

where x denotes activated molecules where the excess energy comes from recombination, and * the directly excited ones.

Of products involving C–H bond rupture, the yield of cyclopentene is 2.9—3.1, that of bicyclopentane is 1.2—1.3 [1, 5, 9]. Cyclopentene may be formed either in monomolecular processes: (3b) and (4b) or *via* disproportionation, being a bimolecular reaction: (6a). Process (6b) gives explanation for bicyclopentane formation:

$$2c\text{-}C_5H_9^{\cdot} \begin{cases} \xrightarrow{k_d} c\text{-}C_5H_{10} + c\text{-}C_5H_8 & (6a) \\ \xrightarrow{k_c} (c\text{-}C_5H_9)_2 & (6b) \end{cases}$$

Most detailed study of C–C bond rupture processes of cyclopentane has been published by DOEPKER *et al.* [10].

The existence of monoradicals can be verified by chemical methods (*e.g.* by application of I_2 or O_2 radical scavengers), even if they are very short-living species [3, 4, 9]. By analyzing the C_n, C_{2n} etc. products formed in interactions with the scavenger, the mechanism of formation of hydrocarbon products from radicals can be established [12, 13]. For example, in the presence of I_2, the following processes occur with the participation of cycloalkyl radicals and hydrogen atoms formed in reactions involving C–H bond rupture from an irradiated $c\text{-}C_2H_{2n}$ cycloalkane:

$$c\text{-}C_nH_{2n-1}^{\cdot} + I_2 \longrightarrow c\text{-}C_nH_{2n-1}I + I \qquad (7)$$

$$c\text{-}C_nH_{2n-1}^{\cdot} + I \longrightarrow c\text{-}C_nH_{2n-1}I \qquad (8)$$

$$H + I_2 \longrightarrow HI + I \qquad (9)$$

Thus, as a result of scavenging processes, cycloalkyl iodides and hydrogen iodide are formed [9].

No direct experimental evidence is available for the existence of biradicals [11].

The reactions outlined give an approximately correct picture of the actual phenomena only for low doses and low scavenger concentrations since,

with higher values of these parameters, the secondary processes of scavengers and their products gain a larger importance. For example, hydrogen iodide produced from iodine scavenger in reaction (9) can behave also as a hydrogen-transferring agent:

$$HI + \text{c-}C_nH_{2n-1}^{\cdot} \longrightarrow \text{c-}C_nH_{2n} + I \tag{10}$$

If these side-processes were left out of consideration, the calculated yields in the case of higher doses — owing to the higher scavenger concentrations necessary to fix all the intermediates — would be considerably lower than their actual values.

Stabilization of H-atoms formed during irradiation of pure alkanes takes place in the following processes:

$$H + \text{c-}C_nH_{2n} \xrightarrow{k_a} H_2 + \text{c-}C_nH_{2n-1}^{\cdot} \tag{11}$$

$$H + H \longrightarrow H_2 \tag{12}$$

All 'hot' hydrogen atoms react according to (11) together with a fraction of the thermal H-atoms; the rest of the latter is stabilized in reaction (12) having smaller importance and being even negligible at room temperature. In the presence of radical scavenger (S), thermal hydrogen atoms disappear mainly in processes (11) and (13):

$$H + S \xrightarrow{k_b} SH \tag{13}$$

The rate of capturing of H-atoms can be described by Expression (14) [12, 14, 15]:

$$G(SH) = \frac{G(H_{therm})}{1 + \dfrac{k_a[\text{c-}C_nH_{2n}]}{k_b[S]}} \tag{14}$$

The ratio of rate constants of abstraction and radical capturing reactions k_a/k_b for thermal hydrogen atoms is equal to $4.75 \cdot 10^{-3}$ in the system cyclohexane–ethylene [14] and $0.022 \cdot 10^{-3}$ in the solution of iodine in cyclohexane [15].

There are considerably less possibilities to investigate ionic reactions in the liquid and solid states as compared with radical reactions. The yield of free electrons has been found to be $G_{fi} = 0.1-0.15$ as determined by means of conductivity measurements [16].

Due to its high electron capturing efficiency, CCl_4 electron scavenger has been used in the present study. Analogously to systems containing cyclo-

hexane and CCl_4 [17, 18], the following reactions can be proposed between cyclopentane and CCl_4:

$$e^- + CCl_4 \longrightarrow CCl_4^- \tag{15}$$

$$CCl_4^- \rightarrow CCl_3^{\cdot} + Cl^- \qquad \Delta H_0 = -52.7 \text{ kJ} \cdot \text{mol}^{-1} \tag{16}$$

$$c\text{-}C_5H_{10}^+ + CCl_4^- \longrightarrow c\text{-}C_5H_{10} + CCl_4 \tag{17}$$

$$CCl_3^{\cdot} + c\text{-}C_5H_9^{\cdot} \longrightarrow c\text{-}C_5H_9\text{-}CCl_3 \tag{18}$$

$$CCl_3^{\cdot} + c\text{-}C_5H_{10} \longrightarrow c\text{-}C_5H_9^{\cdot} + CHCl_3 \tag{19}$$

$$\Delta H_0 = -10.5 \text{ kJ} \cdot \text{mol}^{-1}$$

$$c\text{-}C_5H_{10}^+ + Cl^- \longrightarrow c\text{-}C_5H_{10} + Cl \tag{20}$$

$$Cl + c\text{-}C_5H_9^{\cdot} \longrightarrow c\text{-}C_5H_9Cl \tag{21}$$

$$Cl + c\text{-}C_5H_{10} \longrightarrow c\text{-}C_5H_9^{\cdot} + HCl \tag{22}$$

$$2CCl_3^{\cdot} \longrightarrow C_2Cl_6 \tag{23}$$

$$H + CCl_4 \longrightarrow HCl + CCl_3^{\cdot} \qquad \Delta H_0 = -121.4 \text{ kJ} \cdot \text{mol}^{-1} \tag{24}$$

$$Cl + c\text{-}C_5H_8 \longrightarrow c\text{-}C_5H_8Cl^{\cdot} \tag{25}$$

In addition to electron scavengers, positive ion scavengers can also be applied, *e. g.* NH_3 [19] and cyclopropane [20, 21].

With the latter, the ion yield is generally determined by measuring the propane yield [20, 21]:

$$c\text{-}C_6H_{12}^+ + c\text{-}C_3H_6 \longrightarrow c\text{-}C_6H_{12}^+ + C_3H_8 \tag{26}$$

The most widely used method for the mathemathical description of ion or electron capturing process by scavengers and the variation of H_2, C_n and C_{2n} yields under these conditions applies the formula derived theoretically by HUMMEL [22] and developed further on an empirical basis by WARMAN *et al.* [23, 24]. According to the literature, the equation represents a good approximation in the range of scavenger concentration between 10^{-5} and 10^{-1} M for both the decrease of the yields of T products formed in ionic reactions (ΔT) and for the yield of P product formed in the scavenging reaction:

$$G(\Delta T) \text{ or } G(P) = \left(G_{fi} + \frac{G_{gi}\sqrt{\alpha[S]}}{1 + \sqrt{\alpha[S]}}\right)\sigma \tag{27}$$

The value of $G_{fi} + G_{gi}$ is the total ion yield which can be approximated on the basis of the W value which means the average energy necessary to

generate one ion pair in the gas phase. G_{fi} is the yield of free ions and G_{gi} is that of the geminate ions. Higher concentrations of scavengers affect only the value of G_{gi} because electrons or positive ions representing G_{fi} react with scavengers at a very low concentration of the latter. [S] means the scavenger concentration expressed in M, and σ the frequency of formation of P product in the process of charge neutralization. The symbol α denotes the efficiency of the scavenger related to the process of ion recombination, its dimension is M^{-1}. Its value for diffusion-controlled processes can be given by the NERNST–EINSTEIN formula [16]:

$$\alpha_x = \frac{D_x + D_s}{D_e + D_+} \frac{4\pi R_x b^3 N}{3r_c \cdot 100} \tag{28}$$

where D_s, D_e and D_+ are the diffusion coefficients of the scavenger, electron and positive ion, respectively, R_x is the diffusion-controlled collision diameter, b is the characteristic distance in the function $F(r)$ describing electron thermalization, r_c is the critical distance after ONSAGER:

$$r_c = \frac{e^2}{\varepsilon kT} \tag{29}$$

which can be calculated if the dielectric constant (ε) is known.

Since the diffusion coefficient of unsolvated electrons is by nearly three orders of magnitude higher than that of positive ions, it is obvious from the formula that the α-value for positive ion scavenging is lower than that obtained for electron scavenging by one or two orders of magnitude (about $0.1-1.2\ M^{-1}$ as opposed to $3-30\ M^{-1}$) [25, 26].

2. Experimental

Non-radioactive cyclopentane supplied by FLUKA was shaken with concentrated sulphuric acid in order to remove unsaturated species then purified again by distillation and preparative gas chromatography. No impurities could be shown after this procedure if the hydrocarbons were chromatographed on 100-m capillary column coated with squalane.

Non-radioactive iodine purchased from REANAL was sublimed before use. Radioactive $^{131}I_2$ was prepared in our institute. The radioactive iodine was kept on the surface of a platinum needle and upon its immersing into the solution of inactive iodine, isotope exchange transferred radioactivity into the solution. The radioactive concentration was $40-100\ \mu Ci\ ml^{-1}$.

Carbon tetrachloride manufactured by BIOGAL served — after redistillation — as an electron scavenger.

Samples have been irradiated in the ^{60}Co γ-radiation source of the institute having a nominal activity of about 3.10^{15}Bq (80,000 Ci). The dose rate was $4.3 \cdot 10^{16}$ eV $g^{-1}s^{-1}$ (~ 2.5 Mrd h^{-1}). The irradiation temperature was about 25–30 °C.

Alkyl iodides produced with low G-values were determined by means of radioactive tracer technique. The alkyl iodides were separated by gas chromatography using columns

with silicon grease (length: 2—4 m, I. D. 4 mm, Q = 10—15 ml min^{-1}) and polyethylene glycol adipate (length 3—6 m, I. D. 4 mm, Q = 10—15 ml min^{-1}) as stationary phases.

Other details of the experimental technique have been described previously [27, 28].

3. Results and discussion

During the radiolysis of liquid cyclopentane hydrogen and various hydrocarbons are produced both in the presence and absence of scavengers. Our data are summarized in Table I together with those reported in papers [1] and [9]. Although literature data have been extrapolated to zero dose and our values are related to the actual irradiation dose of $\sim 3.1 \cdot 10^{20}$ eV g^{-1} (5 Mrd), the agreement of the numbers is, nevertheless, rather good. This, at the same time, indicates — in agreement with [9] — that in our case the dose dependence of yields is not considerable.

Table I

Products of the radiolysis of liquid cyclopentane

Product \ Additive	None			5 m*M* I_2	8.5m*M* I_2	78 m*M* CCl_4
	(a)	(b)	Present work			
Hydrogen	5.2	5.35	5.2	—	3.75	—
Methane	0.04	0.03	0.036	0.03	—	0.06
Ethane	0.08	0.03	0.034	0.03	—	0.068
Ethylene	0.40	0.45	0.45	0.39	—	0.45
Acetylene	—	0.05	—	—	—	—
Propane	0.08	0.08	0.065	0.041	—	0.12
Cyclopropane	0.1	0.12	0.06	0.22	—	0.18
Propene	0.16	0.28	0.18		—	
Allene		0.05	—	—	—	—
1-Pentene	0.62	0.74	0.74	—	—	—
n-Pentane	0.16	0.14	0.14	0.03	—	—
Cyclopentene	3.1	2.97	2.7	1.92	1.8	0.94
Ethylcyclopentane		0.05	—	—	—	—
Propylcyclopentane		0.05	—	—	—	—
n-Decane	0.005		0.028	—	—	—
Pentylcyclopentane	0.05	0.06	0.029	—	—	—
Bicyclopentane	1.22	1.29	1.23	0.46	0.32	0.57
Cyclopentylcyclopentene	0.05	0.11	0.13		0.06	0.077

(a) Data from Ref. [9]
(b) Data from Ref. [1]

3.1. Study of the mechanism of cyclopentane radiolysis by means of scavengers

3.1.1. *Effect of radical scavengers on product formation*

The $G(H_2)$-value of cyclopentane radiolysis is 5.2 in the case of a dose of $\sim 3.1 \cdot 10^{20}$ eV g^{-1} (5 Mrd) and with a lower dose ($\sim 3.1\ 10^{19}$ eV g^{-1} corresponding to 0.5 Mrd) a somewhat higher value is obtained: $G(H_2) = 5.4$. This latter value should be taken as a reasonable basis for scavenger studies since the dose dependence of the hydrogen yield is negligible in the presence of scavengers.

The next two products of highest yields after hydrogen are cyclopentene ($G = 2.7$) and bicyclopentane ($G = 1.23$) formed similarly to hydrogen, in dehydrogenation processes. The mechanism of hydrogen formation (or, in other words, of C–H bond rupture processes) can, therefore, be followed through these two products, too, considering reactions (3)—(6).

Investigations applying I_2 scavengers render it possible to determine the quantitative ratio of pathways (6a) and (6b) as well as to provide a better

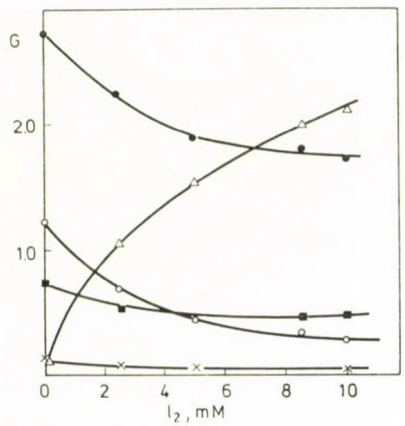

Fig. 1. Products of radiolysis of cyclopentane–iodine mixtures: ■ 1-pentene; ● cyclopentene; △ cyclopentyl iodide; ○ bicyclopentane; × cyclopentylcyclopentene.

understanding of parallel hydrogen formation reactions. As illustrated by Fig. 1, with increasing iodine concentration, the yields of C_5 and C_{10} products sharply decrease, that of cyclo-C_5H_9I increases.

G-values of cyclopentene product are plotted in Fig. 2 as a function of *G* (bicyclopentane) values, obtained without any additives and with a few I_2 and O_2 concentration values. The experimental points fall — as expected — roughly on a straight line with a slope of about 1.0. This value gives the ratio of reactions (6a) and (6b), *i. e.* the value of k_d/k_c. The intersection with

the ordinate is at about G(cyclopentene) = 1.5; this value gives the yield of cyclopentene formed in other than radical processes, according to the scheme, in reactions (3b) and (4b). Consequently, the G-values of both monomolecular H_2 and cyclopentene formation are similarly equal to $\simeq$ 1.5.

Our observation that the rate constants of disproportionation and combination of cyclopentyl radicals between each other are nearly equal is in agreement with the gas-phase studies of STOCK and GUNNING [29]. Recently, SÖYLEMEZ and SCHULER [30] have found a k_d/k_c value = 1.4 for aqueous

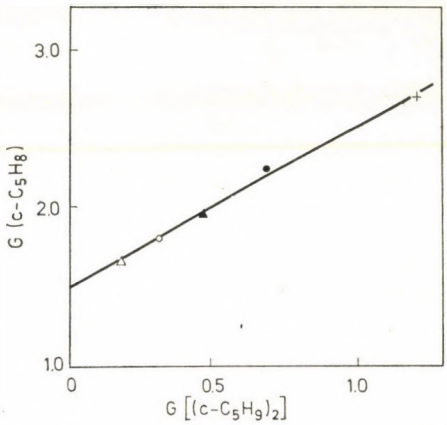

Fig. 2. The k_d/k_c value of cyclopentyl radicals: + without additive; ● with 2.5 mM I_2; ▲ with 5.0 mM I_2; ○ with 8.5 mM I_2; △ with 5 mM O_2.

solution of cyclopentane, using a pulse radiolysis method; for the time being, no explanation can be given for the difference as high as 40%.

Since earlier data from this laboratory [27] gave a value of $k_d/k_c \simeq 1$ for cycloalkyl radicals with 6–10 carbon atoms, it can be stated that — at least between five and ten carbon atoms — the ratio of rates of disproportionation and combination processes of cycloalkyl radicals is practically not influenced by the number of carbon atoms in the parent compound, *i. e.* by the ring size.

In addition to the determination of the yield of monomolecular H_2, the knowledge of G-values for 'thermal' and 'hot' hydrogen atoms is also important. Thermal H-atoms react with iodine according to Eq. (9). For example, the application of I_2 in a concentration of 8.5 mM decreases the $G(H_2)$ value by 1.65 G-units, as compared with G = 5.4 for pure cyclopentane. A fraction of this decrease can be attributed — as discussed in the literature survey — probably to the ionic interaction of iodine with the ionic intermediate of C–H bond decomposition. The G-value of the latter process can be estimated to be 0.2, analogously to the cyclohexane–I_2 system [15].

Using Eq. (14), $G \simeq 1.6$ is obtained for the yield of thermal hydrogen atoms, if the value of k_a/k_b measured for cyclohexane [15] is accepted in our case, too.

Two ways are possible to determine the total cyclo-$C_5H_9^{\cdot}$ radical yield: it is possible to calculate on the basis of the limiting yield of the scavenged product c-C_5H_9I or on the basis of the decrease of the cyclo-C_5H_8 and (c-$C_5H_9)_2$ produced in radical reactions. In principle, these two data should be equal to each other. In practice, however, the decrease of G(c-$C_5H_9^{\cdot}$) as calculated according to the latter method is much higher than the result obtained by the former calculation:

$$G(\text{c-}C_5H_9I) < 2[\Delta G(\text{c-}C_5H_8) + \Delta G(/\text{c-}C_5H_{9/2})] \tag{30}$$

Expression (30) can probably be attributed to the fact that a fraction of c-$C_5H_9^{\cdot}$ radicals react with HI produced under irradiation and give c-C_5H_{10} according to (10); *i. e.* the decrease of radical yield calculated from the right-hand side of Eq. (30) gives only partially cyclopentyl iodide. This assumption is supported also by the fact that — with a I_2 concentration of 8.5 mM — the value of G(HI) expected should be the same as measured for $\Delta G(H_2)_{\text{radical}} = 1.5$, as opposed with the actual G(HI) = 0.1.

Considering also this H-transferring role of HI, the apparent decrease of radical yield as observed on the basis of c-C_5H_8 and (c-$C_5H_9)_2$ yield is as follows:

$$\Delta G(\text{c-}C_5H_9^{\cdot}) = G(\text{c-}C_5H_9I) + 2[G(H_2)_{\text{radical}} - G(\text{HI})_{\text{meas.}}] + G(\text{HI})_{\text{meas.}} \tag{31}$$

where the value $[G(H_2)_{\text{radical}} - G(\text{HI})_{\text{meas.}}]$ is the decrease of $G(H_2)$ caused by reaction (10), which is a half of the c-$C_5H_9^{\cdot}$ decrease attributable to reactions (9) and (10). For example, with 8.5 mM I_2, G(c-$C_5H_9^{\cdot}$) = 4.0 as estimated from data of $\Delta G(H_2)_{\text{radical}}$ and $G(\text{HI})_{\text{meas.}}$; at the same time, on the basis of the change of (c-$C_5H_9)_2$ and c-C_5H_8 yields $G = 4.6$ is calculated. The difference of about 15% can be attributed to the summed experimental errors.

It is seen that, with high I_2 concentrations, the measurement of cyclopentyl iodide yields only cannot lead to the exact value of G(c-$C_5H_9^{\cdot}$). The simultaneous determination of the yields of iodides and H_2 can, however, provide a method for the determination of ΔG(c-$C_5H_9^{\cdot}$) value; this gives, as a limiting value for high iodine concentrations the total G-value of cyclopentyl radicals; the extrapolation can only be performed with the knowledge of the dependence of ΔG(c-$C_5H_9^{\cdot}$) on iodine concentration.

It seems to be more advantageous to measure the total c-$C_5H_9^{\cdot}$ yield on the basis of the changes of yields of c-C_5H_8 and (c-$C_5H_9)_2$, especially if the $k_d/k_c = 1$ value stated above is considered together with the fact that bicyclo-

pentane can be formed only with the coupling of two cyclopentyl radicals (at least, in first approximation). Then, knowing that G(bicyclopentane) = = 1.23, the total radical yield will be given by Eq. (32):

$$G(\text{c-}C_5H_9^{\cdot}) = 2[G(\text{c-}C_5H_9)_2 + k_d/k_c\, G(/\text{c-}C_5H_9/_2)] = 4G(/\text{c-}C_5H_9/_2) \qquad (32)$$

i. e. G (cyclopentyl) = 4.92. Since, however, during the high dose irradiation the secondary reaction of accumulated c-C_5H_8 gives also c-C_5H_9-c-C_5H_7 (G = = 0.13) equivalent to $G(\text{c-}C_5H_9^{\cdot}) \simeq 0.25$, the total radical yield is G = 4.92 + + 0.25 = 5.17 molecules per 100 eV. As seen before, the scavengeable amount under the effect of 8.5 mM iodine is about 4.6 G-unit (as calculated from cyclopentene and bicyclopentane yields), that is, the efficiency of scavenging is about 90% even for this low scavenger concentration; although this is not in agreement with the plot seen in Fig. 1.

As judged from the product spectrum, the most probable ring breakdown gives C_2 plus C_3 products, but also C_5 ring-opening products are formed with high yields. The hydrogen content of the total breakdown product is higher only by $G(H_2) = 0.2-0.3$ units than the amount which could have originated from the monomolecular decomposition of cyclopentane. Since the hydrogen excess of fragments must have its origin in bimolecular processes, and the total G(fragment) = 1.7, it can be regarded as verified that the fragments are formed mainly in monomolecular reactions.

Table II

Iodide products of the radiolysis of cyclopentane–iodide mixtures

Additive	0.65 mM I_2 [a]	8.5 mM I_2 [b]
HI	0.11	0.1
CH_3I	0.26	0.026
C_2H_5I	0.067	0.019
1-C_3H_7I	0.054	0.049
2-C_3H_7I	0.054	0.016
2-$C_5H_{11}I$	0.011	0.047
1-$C_5H_{11}I$	0.23	0.147
c-C_5H_9I	3.0	1.95

[a] DAUPHIN's data [3]

$D = 3.1 \cdot 10^{19}$ eV g^{-1} (0.5 Mrd), $\dot{D} = 5 \cdot 10^{13}$ eV g^{-1}s^{-1} (2.9 krd h^{-1})

[b] Present work:

$D = 3.1 \cdot 10^{20}$ eV g^{-1} (5 Mrd), $\dot{D} = 4.3 \cdot 10^{16}$ eV g^{-1}s^{1} (2.5 Mrd h^{-1})

The same result is given by studies applying $^{131}I_2$ radical scavenger (Tables I and II). The presence of iodine had but a little influence on the fragment yields, together with the formation of alkyl iodides. A noticeable change (80%) was observed only in the *G*-value of *n*-pentane; thus, this product is formed in bimolecular processes involving monoradical intermediates as opposed with the majority of other fragments (*e. g.* C_2H_4, C_3H_6) produced in monomolecular reactions involving biradical intermediates. As evidenced by the high yield of 1-pentyl iodide, pentane is formed *via* pentyl radicals.

AVDONINA [31] proposed the reaction

$$c\text{-}C_5H_{10} + H_{hot} \rightarrow n\text{-}C_5H_{11} \qquad (33)$$

for the explanation of pentyl monoradical formation; this, in turn, is stabilized in H-abstraction, disproportionation or combination processes, in the absence of radical scavenger. The presence of pentyl-cyclopentane ($G = 0.029$) indicates also the possibility of a combination process.

3.1.2. *Effect of ion scavengers on product formation*

Addition of carbon tetrachloride

The addition of CCl_4 electron scavenger causes a decrease in $G(H_2)$ and $G(c\text{-}C_5H_9)_2$ values together with an enhanced HCl formation (Fig. 3). The change can be attributed probably to the fact that the hindrance of electron–ion recombination process involves also the hindrance of C–H decomposition. The total difference, however, — as to be discussed later — cannot be attributed

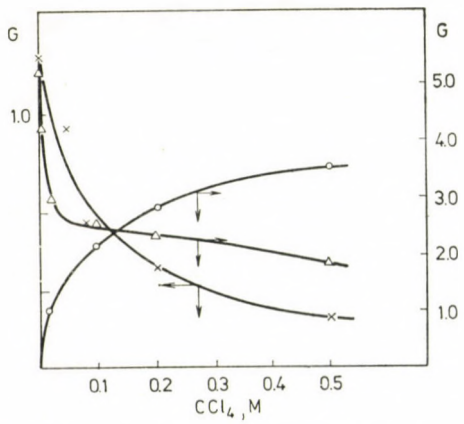

Fig. 3. Radiolysis products from cyclopentane–CCl_4 mixtures: △ hydrogen; ○ hydrogen chloride; × bicyclopentane.

exclusively to ionic processes. If the decrease of hydrogen yield is plotted as a function of $G(HCl)$ (Fig. 4), it is found that, for low scavenger concentrations, the $\Delta G(H_2)$ values are much higher than $G(HCl)$ values, though, if only ionic and hydrochloric acid producing radical processes took place, $\Delta G(H_2)$ should be lower than or equal to $G(HCl)$. The difference between expected and observed changes may be due to the excitation energy transfer between CCl_4 and cyclo-C_5H_{10}: this process lowers the probability of C–H bond rupture without altering

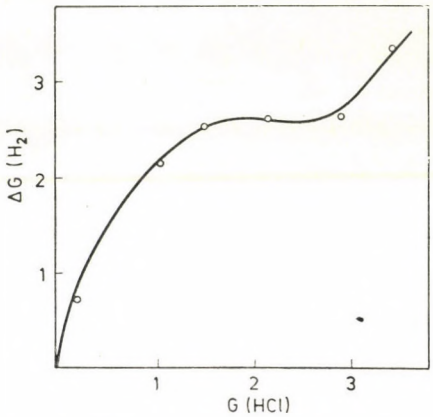

Fig. 4. Correlation between hydrogen chloride yield and the decrease of hydrogen yield in irradiated cyclopentane–CCl_4 mixtures

the extent of C–Cl bond dissociation. This is supported also by NAFISI-MOVAGHAR and HATANO who have found excitation energy transfer in the photolysis of cyclohexane–CCl_4 system [18].

The phenomenon can be explained alternatively by assuming the reaction

$$CCl_3^{\cdot} + H \rightarrow CHCl_3 \qquad (34)$$

but its influence has no experimental support.

The ratio $G(HCl)$: $\Delta G(H_2)$ measured in our experiments may also be attributed in principle to the capture of chlorine atoms or ions produced in the scavenging processes, by alkenes; thus, the yield of HCl would decrease without any alteration of $\Delta G(H_2)$.

This possibility has been checked by irradiating a ternary mixture of cyclopentane–cyclopentene–carbon tetrachloride (molar ratio: 12—12.5 : 0.1—0.3 : 0.1). Addition of cyclopentene caused a change of as little as ± 0.1 G-unit in the HCl yield (as compared with $G(HCl) = 2.1$ observed in a binary mixture of c-C_5H_{10}—CCl_4 with a mole ratio of 12.3 : 0.1), *i. e.* the effect of cyclopentene is within the limits of the experimental error.

Alkene addition does not influence the value of G(HCl), neither does the ratio between hydrogen chloride formation and decrease of hydrogen yield. This means also that — in spite of some earlier assumptions [32, 33] — alkenes are very weak electron traps and do not compete with CCl_4 electron scavenger. BUSI and FREEMAN [8] have drawn a similar conclusion with respect to the cyclopentane–alkene–N_2O system.

The yield of cyclopentene has also been determined in the presence of 0.078 M CCl_4; a value of $G = 0.94$ was found as opposed to the $G(c\text{-}C_5H_8) = 2.7$ for pure cyclopentane (Table I).

The value of G(bicyclopentane) in the presence of 0.5 M CCl_4 is about 20% of the original value. At this $c\text{-}C_5H_{10}$–CCl_4 ratio about 60% of the total ion yield has been scavenged (Fig. 6) — as shown by the calculation in Section 3.2.1. — and this could bring about a decrease of G(bicyclopentane) $= 0.6 \cdot 1.23 = 0.74$ units (considering the G(dimer) = 1.23 value for pure cyclopentane), assuming that the amount of $c\text{-}C_5H_9^+$ with an ionic precursor changed proportionally to the amount of scavengeable ions.

The difference between observed and calculated G(bicyclopentane) values can be explained by the energy transfer mentioned above or by the reaction between H atoms and CCl_3 radicals inhibiting reaction (5). The capture of $c\text{-}C_5H_9^+$ radicals in reaction (18) can also be proposed: its product could be observed on the chromatograms but the yield could not be determined due to experimental difficulties.

The decrease of cyclopentene yield in the presence of 0.078 M additive is $\Delta G(c\text{-}C_5H_8) = 2.7 - 0.94 = 1.76$ and the difference in the dimer yield is $\Delta G(/c\text{-}C_5H_9/_2) = 1.23 - 0.57 = 0.66$ (Table I). Considering the $k_d/k_c = 1$ value for cyclopentyl radicals as well as the actual value of the decrease of the dimer yield (0.66), we obtain that the decrease of yield of cyclopentene produced in monomolecular reaction (4b): $\Delta G(c\text{-}C_5H_8) = 1.76 - 0.66 = 1.1$; while the total 'monomolecular' cyclopentene yield is $G = 1.5$, as determined before. If the decrease of the amount of 'monomolecular" cyclopentene formation is due exclusively to ion capturing, then our data indicate that at least 70% of it has an ionic precursor.

Data in Table I show that the yields of methane, ethane and propane involving C–C bond rupture(s) increase by about 66, 100 and 84%, respectively; at the same time, those of propene plus cyclopropane and 1-pentene decreased by 30 and 50%, respectively, in the presence of CCl_4 scavenger.

The increased yield of alkane fragments, *i.e.* methane, ethane and propane in the presence of CCl_4 can be attributed to the prolongation of the lifetime of positive ions by electron capturing; thus, the probability of formation of radicals and/or ions being precursors of fragmentation products also increases. Analogous mass-spectrometric studies have shown the formation of $C_4H_7^+$,

$C_3H_5^+$ and $C_3H_6^+$ ions. The complementary products of these ions are $CH_3^\cdot$ and $C_2H_5^\cdot$ radicals and C_2H_4 molecule, respectively [9].

The decrease of the yield of 1-pentene under the effect of added CCl_4 can be due to the fact that such a fraction of this product is formed *via* recombination of c-$C_5H_{10}^+$ with electrons.

Addition of cyclopropane

Addition of cyclopropane leads to the increase of the yields of C_3-products and cyclopentyl-cyclopentene (c-C_5H_9-c-C_5H_7), and to the decrease of that of bicyclopentane (Fig. 5).

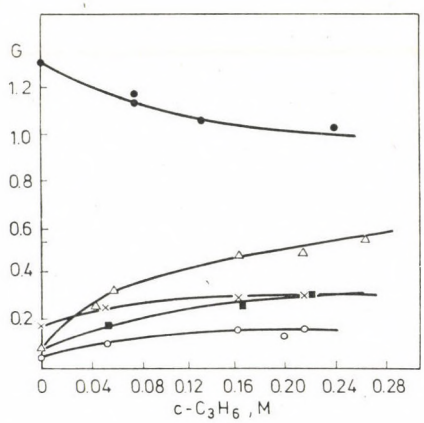

Fig. 5. Radiolysis products of cyclopentane–cyclopropane mixtures: ○ ethane; △ propane; × propene; ● bicyclopentane; ■ cyclopentylcyclopentene.

According to the literature reporting on the positive ion-scavenging effect of cyclopropane [20, 21], propyl radicals are also formed during reaction with alkane positive ions. The correctness of this suggestion has been checked by irradiating a ternary system consisting of cyclopentane, cyclopropane and $^{131}I_2$. The concentrations of the latter two substances were 300 and 11 mM, respectively. The yield of 1-propyl iodide was found to be $G(1 - C_3H_7I) = 0.14$, at the same time, this value was $G(1 - C_3H_7I) = 0.05$ in a binary mixture of cyclopentane–iodine (with a concentration of iodine of 11 mM).

Our measurements support the assumption of AUSLOOS *et al.* [20, 21, 34] as well as of KENNEDY and STONE [35] who suggested the following main reactions for positive ion scavenging by cyclopropane:

$$\text{c-}C_5H_{10}^+ + \text{c-}C_3H_6 \rightarrow \text{c-}C_5H_8^+ + C_3H_8 \qquad (35)$$

$$\text{c-}C_5H_{10}^+ + \text{c-}C_3H_6 \rightarrow \text{c-}C_5H_9^+ + C_3H_7 \qquad (36)$$

The high yield of propane formed in cyclopentane–cyclopropane mixtures is in favour of pathway (35) while the reality of reaction (36) is supported by the formation of 1-propyl iodide with a yield of $G \simeq 0.14$.

The effect of cyclopropane addition on dimer products has also been studied. It has been stated that positive ion scavenging decreases the yield of bicyclopentane by about 25% in the range studied with the simultaneous increase of the cyclopentylcyclopentene yield. The decrease can be attributed in cyclopentane–cyclopropane mixtures presumably to the formation of cyclopentene and cyclopentyl ion-radical from cyclopentane ion in reactions (35) and (36), respectively; their neutralization in ion–electron processes lead to cyclopentene and cyclopentylcyclopentene, inhibiting thus the decomposition of cyclopentane into c-C_5H_9, and this, in turn, hinders the formation of $(c\text{-}C_5H_9)_2$.

3.2. The characterization of the efficiency of ion scavengers

3.2.1. *Studies with carbon tetrachloride electron scavenger*

Our primary aim was the determination of the total ion yield by means of CCl_4 electron scavenger. The yields of HCl produced in reactions (15), (16), (20) and (22) have been used for determining the electron-scavenging reactions.

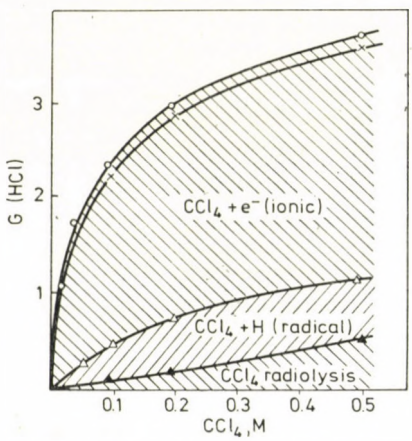

Fig. 6. Components of HCl yield from irradiated cyclopentane–CCl_4 mixtures: × measured values; ○ values corrected for the electron fraction

Since the HCl yield measured is not equal to the G-value of the electrons captured, the following corrections were considered:

— Addition of CCl_4 decreases somewhat the electron fraction of cyclopentane in the mixture. HCl values should therefore be extrapolated to undiluted cyclopentane. Figure 6 shows that this correction is relatively small in

the scavenger concentration range studied: it is not more than about 5% even for the highest CCl_4 concentration.

— HCl measured after irradiation can be formed in both ionic and radical reactions. Primary decomposition of CCl_4 gives a chlorine atom:

$$CCl_4^* \rightarrow CCl_3^{\cdot} + Cl \tag{37}$$

and this, colliding with cyclopentane, gives hydrogen chloride. Our experiments have shown that the yield of chlorine atoms during the decomposition of pure CCl_4 is $G(Cl) = 7.2$. Consequently, the value of $G(HCl)$ due to reaction (22) can be calculated according to the linear mixing rule (assuming no interaction between components):

$$G(-HCl)_{primary} = e_{CCl_4} G(Cl) \tag{38}$$

where e_{CCl_4} denotes the electron fraction of the scavenger, $G(-HCl)_{primary}$ the HCl yield of the primary decomposition of CCl_4. The HCl yield due to the primary decomposition of CCl_4 increases up to $G(HCl) = 0.5$ in the range studied (Fig. 6).

— Reaction (24) leads also to the formation of hydrogen chloride. Thermal hydrogen atoms abstract either hydrogen from cyclopentane according to reaction (11) or chlorine from CCl_4 in process (24).

The dependence of hydrogen chloride yield produced in reaction (24) on the scavenger concentration can be described by an expression analogous to Eq. (14) applied for radical scavengers:

$$G(HCl_{H\ abs}) = \frac{G(H_{therm})}{1 + \dfrac{k_a[c\text{-}C_5H_{10}]}{k_{a_1}[CCl_4]}} \tag{39}$$

where k_a and k_{a_1} are the rate constants for reactions (11) and (24), respectively. Their ratio has been estimated to be 0.017, on the basis of literature data [36] on absolute reaction rates in the gas phase. Since, as mentioned above, the yield of $G(H_{therm})$ for pure cyclopentane is ~ 1.6, it can be assumed analogously to cyclohexane radiolysis [14], that, of this value, $G = 0.6$ originates from directly excited molecules, $G = 1.0$ from ion–electron recombination.

The yield of thermal hydrogen atoms can be written formally as follows

$$G(H_{therm}) = 0.6 + 1.0\ \frac{G_{ti} - G(J)}{G_{ti}} \tag{40}$$

where G_{ti} denotes the total ion yield ($G_{fi} + G_{gi}$) and $G(J)$ is the value captured by a given CCl_4 concentration.

The values of G_{ti} and $G(J)$ in Eq. (40) are not known but the use of Eq. (27) leads us nearer to the solution of the problem since it gives the correlation between G_{ti} and $G(J)$ being the part of Eq. (27) in brackets.

The disadvantage of the original Eq. (27) is not only that the concentration dependence of $G(J)$ is described with a relatively large error but it gives a 'scavenged yield' also at zero concentration which indicates an intrinsic contradiction. In order to avoid these anomalies, the yield G_{fi} and G_{gi} have been amalgamated and the yield described by means of Eq. (41):

$$G(J) = \frac{(G_{fi} + G_{gi})\sqrt{\alpha[S]}}{1 + \sqrt{\alpha[S]}} = \frac{G_{ti}\sqrt{\alpha[S]}}{1 + \sqrt{\alpha[S]}} \tag{41}$$

where [S] is the CCl_4 concentration expressed in M, α is a number characteristic of the electron-scavenging efficiency of the substance having a dimension of M^{-1}.

BANSAL and RZAD have applied a formula analogous to (41) [37]. They were able to describe the H_2 and HD formation from 2,2,4-trimethylpentane containing ND_3 positive ion scavenger with relatively low error only if they left the term G_{fi} in Expression (27) out of consideration.

If $G(J)$ is expressed from (41) and this is substituted into (40), and this, in turn, into (39), the yield of HCl formed in reaction (24) — *i. e.* $G(HCl_{H\ abs})$ — will be obtained as a function of the scavenger concentration.

Since, however, the original purpose of Eqs (39)—(41) is to determine the values of G_{ti} and α defined in Section 1.2, we need an equation containing the components of hydrogen chloride yields separately:

$$G(HCl) = G(J) + G(HCl_{abs}) + G(HCl)_{primary} \tag{42}$$

where the symbols have the same meaning as before.

Analogously to RX-type electron-capturing reactions known from the literature (such as reactions (23) and (24)), it has been assumed that, in the electron-capturing process by CCl_4, the efficiency of HCl formation is 100%, that is $G(HCl_{ionic}) = G(J)$.

Substituting thus expression (41) into (42) for $G(J)$, an unambiguous correlation is obtained between the scavenger concentration and $G(HCl)$ value. Equation (42) contains two parameters to be fitted: α and G_{ti}; these were determined by means of a computer optimizing process. The results are:

$$G_{ti} = 4.4 \pm 0.3$$

$$\alpha = 3.9 \pm 0.3$$

Knowing these parameters, the HCl yield measured for any scavenger concentration can be divided into the components mentioned.

Figure 6 constructed on this basis illustrates that only about 2/3 of the hydrogen chloride formed in the presence of CCl_4 additive can be attributed to ionic reactions, consequently, the importance of reactions of other type is not negligible.

In scavenger studies G_{ti} is often regarded as a value known from gas-phase electric measurements while α is determined from Eq. (27). According to our measurements, the ion yields in the gas and liquid states are identical since electric conductivity measurements gave a total ion yield for alkanes $G_{ti} = 4.35 \pm 0.1$ ion per 100 eV [38] whereas $G_{ti} = 4.4 \pm 0.3$ for cyclopentane in the liquid phase, as shown by our present data.

If the determination of the value of α based on Eq. (41) and using this experimental G_{ti} value, had been carried out on the basis of the total HCl yield without consideration the radical processes of HCl formation, the resulting error would have been as high as nearly an order of magnitude since this calculation would have resulted in $\alpha = 20-22$ instead of the correct value of $\alpha = 3.9 \pm 0.3$.

It can be concluded that the α-value characteristic of the efficiency of various electron scavengers is correct only in the case if for 'disturbing' radical reactions appropriate corrections — which may be different for different scavengers (C_2H_5Br, SF_6 etc.) — are applied.

Having calculated the total ion yield, it is possible to distinguish between G_{fi} and G_{gi}, too. According to Eq. (43) derived for low scavenger concentrations [22—24]:

$$G(\mathrm{J}) = G_{fi} + G_{gi}\sqrt{\alpha\,[\mathrm{S}]} \tag{43}$$

Plotting $G(\mathrm{J})$ values as a function of $\sqrt{[\mathrm{S}]}$ (Fig. 7), the intersection of $G(\mathrm{J})$ with the axis will give G_{fi}, in our case: $G_{fi} = 0.12 \pm 0.03$. The same value ($G_{fi} = 0.15$) is determined by conductivity measurements [16].

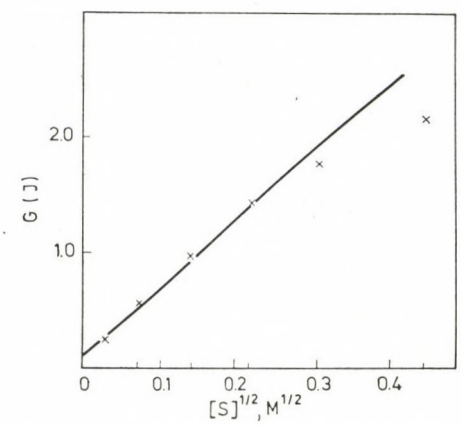

Fig. 7. Determination of G_{fi} from cyclopentane by means of CCl_4 additive

3.2.2. *Studies with cyclopropane positive ion scavenger*

Since propyl radicals formed in reaction (36) give propene and propane *via* disproportionation, the extent of ionic reactions (35) and (36) has been calculated on the basis of surplus propane and propene yield under the effect of cyclopropane addition.

There is a possibility, however, that propyl radicals can be stabilized partly as propylcyclopentane: leaving this out of consideration would lead

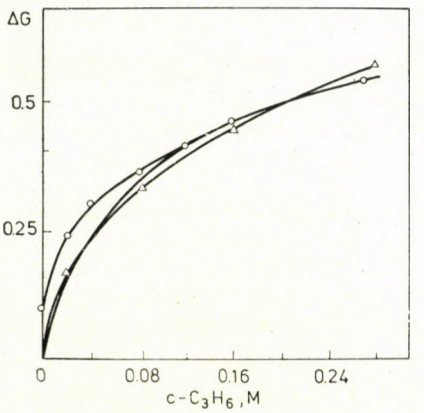

Fig. 8. The increase of G(propane + propene) during radiolysis of cyclopentane–cyclopropane mixtures, as a function of the cyclopropane concentration: — measured values; ○ calculated, using SCHULER's equation:

$$G_{fi} + \frac{G_{gi}\sqrt{\alpha\,[S]}}{1 + \sqrt{\alpha\,[S]}}$$

△ calculated, using our equation:

$$\frac{G_{ti}\sqrt{\alpha\,[S]}}{1 + \sqrt{\alpha\,[S]}}$$

us to an underestimated scavenged ion yield, the error being about 10—15% as compared with the work of KENNEDY and STONE [35]. Figure 8 illustrates the surplus propane and propene yield formed from cyclopropane additive (ΔG) as a function of the scavenger concentration.

The curve has been approximated both by Eqs (27) and (41). It has been stated that SCHULER's original equation cannot be used here, either, due to the reasons already mentioned in connection with CCl_4. When Eq. (41) has been used, the value of $G_{ti} = 4.4 \pm 0.3$ determined by electron scavengers has been applied and only α was fitted, the procedure resulting in the value of $\alpha = 0.086 \pm 0.008$. The experimental determination of G_{ti} was impossible because — as seen in Fig. 8 — with the highest concentration of the positive

ion scavenger having a low efficiency only as little as 15% of the total ion yield was scavenged; thus, the curve could have been extrapolated to 100% only with a very large error.

The α-values obtained for CCl_4 and cyclopropane (3.9 and 0.086, respectively) illustrate the different efficiencies of the two types of scavengers. These results are in good agreement with the NERNST—EINSTEIN equation (28): as discussed in Section 1, the rate determining for electron scavenging is the relatively rapid electron diffusion, whereas for positive ion scavenging, the diffusion of positive ions and scavenger molecules which are much slower. The rate constant of scavenging competing in the latter case with charge

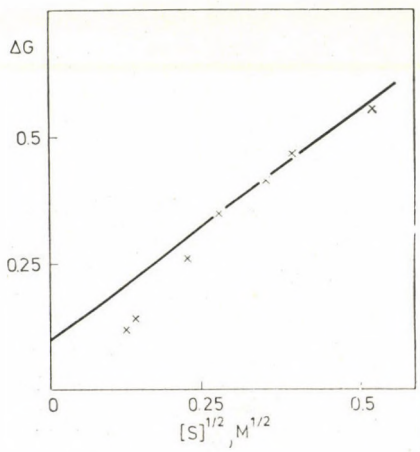

Fig. 9. Determination of G_{fi} for cyclopentane by means of cyclopropane additive

neutralization is much smaller. Another important difference between positive ion and electron scavenging is that with CCl_4 ($[S] < 1$ mM) the value of G(HCl) indicates a nearly 100% decomposition whereas the conversion of cyclopropane applied in similar concentration is not more than 2—3%.

With such a low scavenger concentration, the main reaction expected occurs between the scavenger and the free ion pairs with a relatively long lifetime, because, considering the value of $G_{ti} = 0.11 \pm 0.03$ calculated from Fig. 9 and the dose of $3.1 \cdot 10^{20}$ eV g^{-1} ($\sim$ 5 Mrd), an additive concentration of 0.4 mM is necessary to capture the free ions. If we accept that the rate-determining step of the scavenging reactions is diffusion, it can be stated that the lifetime of free ions is longer than the time necessary for electrons and the additive molecules to reach each other by diffusion at a concentration of 1 mM CCl_4 but shorter than that necessary for the encounter of cyclopropane with cyclopentane ion at the same cyclopropane concentration.

REFERENCES

[1] FREEMAN, G. R.: Radiation Res. Rev. **1,** 1 (1968)
[2] FREEMAN, G. R., STOVER, E. D.: Can. J. Chem. **46,** 3235 (1968)
[3] DAUPHIN, J.: J. Chim. Phys. **59,** 1207, 1223 (1962)
[4] TOMA, S. Z., HAMILL, W. H.: J. Am. Chem. Soc. **86,** 1478 (1964)
[5] WOJNÁROVITS, L.: Effect of cyclic structure on the radiolysis of cycloalkanes (in Hungarian). Ph. D. Thesis, Budapest, 1973
[6] WOJNÁROVITS, L., FÖLDIÁK, G.: Acta Chim. (Budapest) **82,** 285 (1974)
[7] HARDWICK, T. J.: J. Phys. Chem. **65,** 101 (1961)
[8] BUSI, F., FREEMAN, G. R.: J. Phys. Chem. **75,** 2560 (1971)
[9] HUGHES, B. M., HANRAHAN, R. J.: J. Phys. Chem. **69,** 2707 (1965); Radiation Res. **36,** 261 (1968)
[10] DOEPKER, R. D., LIAS, S. G., AUSLOOS, P.: J. Chem. Phys. **46,** 4340 (1967)
[11] SALEM, L., ROWLAND, C.: Angew. Chem., Internat. Edit. **11,** 92 (1972)
[12] ESSER, J., STONE, J. A.: Can. J. Chem. **51,** 192 (1973)
[13] HO, S. K., FREEMAN, G. R.: J. Phys. Chem. **68,** 2189 (1964)
[14] ASMUS, K.-D., WARMAN, J. M., SCHULER, R. H.: J. Phys. Chem. **74,** 246 (1970)
[15] BANSAL, K. M., SCHULER, R. H.: J. Phys. Chem. **74,** 3924 (1970)
[16] HUMMEL, A., SCHMIDT, W.: Radiation Res. Rev. **5,** 199 (1974)
[17] HENGLEIN, A., HECKEL, E., OJIMA, Y., MEISNER, G.: Ber. Bunsenges, Phys. Chem. **67,** 988 (1964)
[18] NAFISI-MOVAGHAR, J., HATANO, Y.: J. Phys. Chem. **78,** 1899 (1974)
[19] ASMUS, K.-D.: Int. J. Radiat. Phys. Chem. **3,** 419 (1971)
[20] DOEPKER, R. D., AUSLOOS, P.: J. Chem. Phys. **42,** 3746 (1965)
[21] AUSLOOS, P., SCALA, A. A., LIAS, S. G.: J. Am. Chem. Soc. **89,** 3677 (1967)
[22] HUMMEL, A.: J. Chem. Phys. **48,** 3268 (1968)
[23] WARMAN, J. M., ASMUS, K.-D., SCHULER, R. H.: J. Phys. Chem. **73,** 931 (1969)
[24] WARMAN, J. M., ASMUS, K.-D., SCHULER, R. H.: Advan. Chem. Ser. No. **82,** 25 (1968)
[25] KLEIN, G. W., SCHULER, R. H.: J. Phys. Chem. **77,** 978 (1973)
[26] SAGERT, N. H., REID, J. A., ROBINSON, R. W.: Can. J. Chem. **47,** 2655 (1969)
[27] FÖLDIÁK, G., WOJNÁROVITS, L.: Acta Chim. (Budapest) **82,** 269 (1974)
[28] KESZEI, Cs.: Izotóptechnika (Budapest) **17,** 361 (1974)
[29] STOCK, R. L., GUNNING, H. E.: Can. J. Chem. **28,** 2295 (1960)
[30] SÖYLEMEZ, T., SCHULER, R. H.: J. Phys. Chem. **78,** 1052 (1974)
[31] AVDONINA, E. N.: Khimiya vysokih energij **4,** 531 (1970)
[32] BURTON, M.: Proc. 2nd. Tihany Symp. on Rad. Chem. Akadémiai Kiadó, Budapest (1967)
[33] ROBINSON, M. G., FREEMAN, G. R.: J. Chem. Phys. **48,** 983 (1968)
[34] AUSLOOS, P., REBBERT, R. E., LIAS, S. G.: J. Phys. Chem. **72,** 3904 (1968)
[35] KENNEDY, M. G., STONE, J. A.: Can. J. Chem. **51,** 149 (1973)
[36] STEACIE, E. W. R.: Atomic and Free Radical Reactions. Reinhold Publishing Co., New York 1954
[37] BANSAL, K. M., RZAD, S. J.: J. Phys. Chem. **76,** 2381 (1972)
[38] STONEHAM, T. A., ETHRIDGE, D. R., MEISELS, G. G.: J. Chem. Phys. **54,** 4054 (1971)

Csaba KESZEI
László WOJNÁROVITS
Gábor FÖLDIÁK

H-1525 Budapest, P.O. Box 77.

Acta Chimica Academiae Scientiarum Hungaricae, Tomus 92 (4), pp. 351—365 (1977)

POSSIBILITY OF COUPLING POLARIZATION MEASUREMENTS AND TRACER ADSORPTION MEASUREMENTS FOR THE STUDY OF OXIDATION AND REDUCTION PROCESSES ON A PLATINUM ELECTRODE

GY. HORÁNYI

(Central Research Institute for Chemistry of the Hungarian Academy of Sciences)

Received February 14, 1976

Consideration is given to theoretical questions connected with the possibility of simultaneous application of polarization measurements and tracer adsorption measurements.

The applicability of these considerations is illustrated on a number of examples: electrohydrogenation of phenylacetic acid, oxidation of oxalic acid, reduction and oxidation of *p*-nitrophenol, and electrohydrogenation of acetone.

In earlier publications in connection with the study of the adsorption of various organic compounds, it was demonstrated that, if the adsorption is followed by some reaction, then in most cases the assumption of adsorption pre-equilibrium is not justified, primarily because of the low desorption rates [1—6, 10, 11].

It follows from this, however, that a kinetic treatment of the electrode processes in such cases encounters difficulties; in the literature these are generally skipped over by the assumption of an equilibrium describable by some isotherm. It is very frequently assumed that the adsorption processes preceding the reactions on the electrode surface are fast, and even that the rates of the corresponding desorption processes are high, so that an adsorption equilibrium is established as regards all or most of the components featuring in the reaction.

The assumption of the equilibrium is of theoretical importance, as in this way a reaction-independent forced connection is assumed between the concentrations of the reaction components in the homogeneous (liquid) phase and in the surface phase.

If the possibility of equilibrium is excluded, this connecting link in the utilization of the adsorption isotherms is eliminated, and it is no longer possible to set out simply only from the concentrations measured in the solution phase to describe the rates of the reactions. It appears necessary, therefore, to acquire information by some means on the concentration (coverage) conditions prevailing in the surface phase.

For a discussion of the reactions on the surface of the electrode, however, it is essential to conceive some model regarding the adsorption layer on the

surface. In the case of chemisorption, a monomolecular adsorption layer may generally be assumed, and hence we too shall use this model in the following. Let us examine what correlations exist between the coverages generally used in the monomolecular model and the relative surface excess concentrations of the corresponding components. The relative surface excess concentration (Γ'_i) of some i-th component referred to the solvent (water) is given by

$$\Gamma'_i = \frac{1}{A}\left(n_i + n_{\mathrm{w}}\frac{x_i}{x_{\mathrm{w}}}\right) \tag{1}$$

where n_i and n_{w} are the numbers of moles of the i-th component and of water, respectively, in the entire system, x_i and x_{w} are the corresponding equilibrium mole fractions in the liquid phase, and A is the surface area of the electrode.

At the same time, if an adsorption layer of some definite thickness is assumed, then

$$n_i = n_i^{\mathrm{a}} + n_i^{\mathrm{l}} \tag{2}$$

$$n_{\mathrm{w}} = n_{\mathrm{w}}^{\mathrm{a}} + n_{\mathrm{w}}^{\mathrm{l}}$$

where the indices a and l refer to the adsorption and liquid phase, respectively. Since

$$\frac{x_i}{x_{\mathrm{w}}} = \frac{n_i^{\mathrm{l}}}{n_{\mathrm{w}}^{\mathrm{l}}} \tag{3}$$

we obtain the relation

$$\Gamma'_i = \frac{1}{A}\left(n_i^{\mathrm{a}} - n_{\mathrm{w}}^{\mathrm{a}}\frac{x_i}{x_{\mathrm{w}}}\right) \tag{4}$$

If a monomolecular adsorption layer is assumed, for the total surface area A we have

$$\Sigma A_i\, n_i^{\mathrm{a}} = A \tag{5}$$

where A_i is the surface requirement of one mole of the i-th component. From this

$$n_{\mathrm{w}}^{\mathrm{a}} = \frac{A - \sum\limits_{i \neq \mathrm{w}} A_i n_i^{\mathrm{a}}}{A_{\mathrm{w}}} \tag{6}$$

and hence

$$\Gamma'_i = \frac{1}{A}\left(n_i^{\mathrm{a}} - \frac{A - \Sigma A_i\, n_i^{\mathrm{a}}}{A_{\mathrm{w}}}\frac{x_i}{x_{\mathrm{w}}}\right) \tag{7}$$

In dilute solutions $x_i \ll x_w$ and $x_w \approx 1$, and therefore

$$\Gamma'_i \approx \frac{1}{A} n_i^a \tag{8}$$

That is, the thermodynamically determinable relative surface excess amount is practically the same as the total amount of substance in the monomolecular layer, and on the above basis the coverage Θ_i relating to the i-th component is

$$A_i \Gamma'_i = \frac{A_i n_i^a}{A} = \Theta_i \tag{9}$$

In the sense of the outlined model, the surface is always completely covered, and thus the adsorption of some dissolved component S can in essence be regarded as an exchange process, characterized in the simplest case by the equation

$$S_l + H_2O_a \rightarrow S_a + H_2O_l^1$$

In a system consisting of solvent (water) and a single solute we have for this equilibrium

$$K = \frac{a_1^a a_w^l}{a_1^0 a_w^a} = \frac{f_1^a f_w^0}{f_1^0 f_w^a} \cdot \frac{x_1^a x_w^0}{x_1^0 x_w^a} \tag{10}$$

The a values are the activities referring to the adsorption and liquid phases, while the f values are the activity coefficients.

From the above relations it follows that

$$K \frac{x_1^0}{x_w^0} = \frac{f_1^a f_w^0}{f_w^a f_1^0} \cdot \frac{n_1^a}{n_w^a} = \frac{f_1^0 f_w^0}{f_1^0 f_w^a} \cdot \frac{A_w n_1^a}{A - A_1 n_1^a} = \frac{f_1^a f_w^0}{f_w^0 f_w^a} \cdot \frac{A_w}{A_1} \cdot \frac{\Theta_1}{1-\Theta_1} \tag{11}$$

In dilute solutions f_1^0/f_w^0 can be regarded as constant, and in ideal mixtures as unity. Further, $x_w \approx 1$, and thus

$$K x_1^0 = \frac{f_1^a}{f_w^a} \cdot \frac{A_w}{A_1} \frac{\Theta_1}{1-\Theta_1} \tag{12}$$

This is in effect the equation describing the adsorption isotherm. If the adsorption phase is also regarded as an ideal mixture, *i. e.* $f_1^a/f_w^a = 1$, an isotherm of Langmuir type is obtained.

In the event of heterogeneous surfaces, with the assumption $f_1^a/f_w^a \approx 1$ for the individual centre species, a logarithmic isotherm may be obtained by using the approximation method applied in gas adsorption.

Relations valid for the adsorption of gases are generally used in the treatment of kinetic measurements connected with the adsorption of liquid mixtures, although this may not be correct in principle, for, as already mentioned, we can only speak of exchange reactions on the liquid/solid interface, the surface always being completely covered. As demonstrated by SCHAY [12] in connection with the physical adsorption of liquid mixtures, the rate of adsorption of some component (assuming a monomolecular adsorption layer) depends on the number of holes forming in the layer in unit time; this is governed by the average residence time of the individual adsorbed molecular species on the surface.

Via the model employed in [12], with the notations used above and in [12], the rate of adsorption in a two-component system is

$$w_a = x_1^0 (n_w^a \tau_w^{-1} + n_1^a \tau_1^{-1}) \tag{13}$$

where τ is the average residence time of the individual components on the surface. By appropriate rearrangement we have

$$w_a = x_1 \frac{A}{A_w} \tau_w^{-1} \left[1 - \Theta_i \left(1 - \frac{\tau_1^{-1}}{\tau_w^{-1}} \frac{A_w}{A_1} \right) \right] \tag{14}$$

If the dissolved component is chemisorbed substantially more strongly than the solvent, we may apply the assumption

$$\frac{\tau_1^{-1}}{\tau_w^{-1}} \ll 1 \tag{15}$$

We thus obtain

$$w_a \approx x_1^0 \frac{A}{A_w} \tau_w^{-1} (1 - \Theta_1) \tag{16}$$

This agrees formally with the relation for the adsorption of gases, although its physical content is naturally quite different. For the rate of desorption of the dissolved component we have

$$w_d = n_1^a \tau_1^{-1} = \frac{A}{A_1} \tau_1^{-1} \Theta_1 \tag{17}$$

At equilibrium $w_a = w_d$, and hence we have the equality

$$x_1^0 \frac{\tau_w^{-1}}{\tau_1^{-1}} = \frac{A_w}{A_1} \cdot \frac{\Theta_1}{1 - \Theta_1} \tag{18}$$

If τ is independent of the coverage and is constant, then a relation coinciding with the Langmuir isotherm is again obtained. It can be seen that, in agreement with experience, relations of the same type are valid for adsorption from dilute solutions as for the case of gas/solid interfaces. It has also been seen that the physical meanings of the corresponding constants are naturally quite different. Only in the knowledge of this is it possible to apply the relations valid for gas adsorption to the adsorption of the dissolved component. For the sake of simplicity, we too shall proceed in accordance with this in the following.

Even if only to a limited extent, the earlier reported tracer method provides a certain possibility for simple study of the reaction and the adsorption.

Essentially, the procedure that may be followed is to examine the adsorption of some reacting, labelled component simultaneously with the customary electrochemical measurements (recording of polarization curves).

It must not be forgotten, however, that the tracer method provides information on the overall amount of every compound (intermediates and end-products) on the surface containing the labelled atom, and accordingly, the experimental results must be evaluated with great circumspection. Let us consider a few of the more simple cases from this aspect.

(1) Only a single reaction, but taking place in several steps, need be reckoned with on the surface of the electrode. Let us assume that all of the reactions are only first-order with respect to the intermediates containing the labelled atom. Let A be the labelled molecular species the reaction of which is under investigation. The reaction may be characterized by the following scheme:

$$A_l \rightarrow A_a \rightarrow B_a \rightarrow C_a \rightarrow \ldots \rightarrow X_a \rightarrow X_l$$

where the indexes l and a denote the liquid and adsorption phases.

In a stationary state, with the assumption of Langmuir conditions, *i. e.* rate constants independent of the coverage, the rate may be given as

$$w = k_A \Theta_A = k_B \Theta_B = k_C \Theta_C = \ldots = k_X \Theta_X \tag{19}$$

With the tracer technique we may acquire information on $\Sigma\Theta_i$. From Eq. (19), the following relation exists between $\sum_i \Theta_i$ and the coverage relating to any j-th molecular species

$$\Theta_j \left(1 + k_j \sum_{i \neq j} \frac{1}{k_i}\right) = \sum \Theta_i \tag{20}$$

It follows from Eq. (20) that if the conditions of Eq. (19) hold, then there is a connection between any optionally selected Θ_j and $\Sigma\Theta_i$. From

(19) and (20), the relation between the rate and the adsorption coverage $\Sigma\Theta_i$ determined by the tracer method is

$$w = \frac{k_j \sum \Theta_i}{1 + k_j \sum\limits_{i \neq j} \frac{1}{k_i}} \tag{21}$$

If $k_j \ll k_i$, then

$$\Theta_j \approx \sum \Theta_i \tag{22}$$

That is, in the adsorption phase on the surface the labelled atom is to be found almost exclusively as a constituent of the j-th component. This is understandable, as the labelled molecules accumulate before the rate-determining part process.

(2) If two parallel reactions are assumed, with the same conditions as above, then a number of schemes may be written, depending on where the reactions branch. As examples, let us consider two simple schemes:

$$\mathrm{A_l} \begin{cases} \longrightarrow \mathrm{A'_a} \rightarrow \mathrm{B'_a} \rightarrow \ldots \rightarrow \mathrm{X'_a} \rightarrow \mathrm{X'_l} \\ \longrightarrow \mathrm{A''_a} \rightarrow \mathrm{B''_a} \rightarrow \ldots \rightarrow \mathrm{X''_a} \rightarrow \mathrm{X''_l} \end{cases} \tag{a}$$

$$\mathrm{A_l} \rightarrow \mathrm{A_a} \begin{cases} \longrightarrow \mathrm{B'_a} \rightarrow \mathrm{C'_a} \rightarrow \ldots \rightarrow \mathrm{X'_a} \rightarrow \mathrm{X'_l} \\ \longrightarrow \mathrm{B''_a} \rightarrow \mathrm{C''_a} \rightarrow \ldots \rightarrow \mathrm{X''_a} \rightarrow \mathrm{X''_l} \end{cases} \tag{b}$$

For scheme (a) we have

$$\Theta'_j \left(1 + k'_j \sum_{i \neq j} \frac{1}{k'_i}\right) = \sum \Theta'_i \tag{23}$$

$$\Theta''_j \left(1 + k''_j \sum_{i \neq j} \frac{1}{k''_i}\right) = \sum \Theta''_i \tag{24}$$

The surface coverage measured by the tracer method is given by

$$\sum \Theta'_i + \sum \Theta''_i = \sum \Theta_i = \Theta'_j \left(1 + k'_j \sum_{i \neq j} \frac{1}{k'_i}\right) + \\ + \Theta''_j \left(1 + k''_j \sum_{i \neq j} \frac{1}{k''_1}\right) \tag{25}$$

It can readily be seen that a similar relation is obtained for scheme (b).

(3) In Eqs (19) and (20) it was assumed that the rate constants do not depend on the coverages. In the case of heterogeneous surfaces or the occurrence of an interaction between the adsorbed molecules, the rate constant

must be regarded as a function of the complete coverage even in the simplest case, *e. g.*

$$w = k_j^0 \Theta_j \exp\ [b_j \Sigma \Theta_i] \tag{26}$$

In place of Eq. (20) we then have

$$\sum \Theta_i = \Theta_j \left\{ 1 + k_j^0 \sum_{i \neq j} \frac{1}{k_i^0} \exp\left[(b_j - b_i) \sum \Theta_i \right] \right\} \tag{27}$$

Correspondingly, the rate relation too will be appreciably more complex than previously:

$$w = \frac{k_j^0 \left(\sum \Theta_i \right) \exp\left[b_j \sum \Theta_i \right]}{1 + k_j^0 \sum_{i \neq j} \frac{1}{k_i^0} \exp\left[(b_j - b_i) \sum \Theta_i \right]} \tag{28}$$

In this case too the situation is comparatively simple only if $k_j^0 \ll k_i^0$. The relation between the rate and the coverage measurable by the tracer method is then

$$\ln w = \ln k_j^0 + \ln \Sigma \Theta_i + b_j \Sigma \Theta_i \tag{29}$$

(4) As we shall see later, the difference between the active-centre species on the electrode surface is often manifested in the reaction at certain sites giving rise to products which remain permanently bound to the surface, and thus the surface elements in question can no longer come into consideration as regards further reactions. The actual chemical transformation takes place on the residual other (possibly only one) active-site species, and after removal of the end-product these sites are again available for the reaction.

If the connection between the reaction rate and the adsorption is sought in such a case, then the total coverage measured with the tracer method must be corrected for the adsorbed amount corresponding to the components bound to the surface and not taking part in the reaction. An extra measurement is required to determine this.

In the following, we make a concrete examination of the possibilities and limits of the interconnection of adsorption and kinetic measurements in the case of several reactions which were treated in some detail previously.

(a) Electrohydrogenation of phenylacetic acid [3]

The hydrogenation or electrohydrogenation of phenylacetic acid is accompanied by the uptake of 3 moles H_2, *i. e.* the aromatic ring is saturated. It is obvious that the process involved takes place in several steps. It is found

experimentally that an appreciable reaction rate may be reckoned with only at potentials more negative than 150 mV. Both here and subsequently, the potentials are referred to an equilibrium hydrogen electrode immersed in the base solution. As illustrated in Fig. 1, at constant potential a linear connection exists between the current and the amount of labelled adsorbed phenylacetic

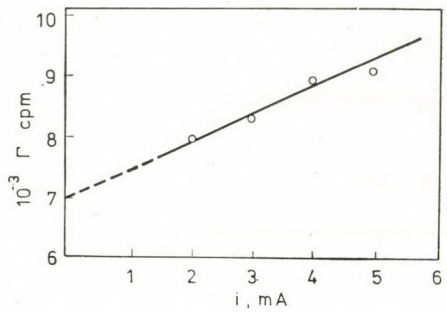

Fig. 1. Relation between the count rate (proportional to the adsorbed amount) and the current in the case of phenylacetic acid ($E = 50$ mV)

acid (or the number of counts per minute). From the Figure it follows that the relation between the current and the coverage is

$$i = k(\Sigma\Theta_i - \Theta') \tag{30}$$

Θ' is that part of the adsorbed amount which does not participate in the reaction under the given conditions; it is known as the residual adsorption. Its magnitude can be determined by the addition of inactive phenylacetic acid to the system, for in such a case too this part remains on the surface, or its departure is a very slow process. If only the adsorbed part actually participating in the reaction is considered in the following, we obtain the relation

$$i = k\,\Sigma\Theta_R \tag{31}$$

By plotting $\Sigma\Theta_R = (\Sigma\Theta_i - \Theta')\dfrac{i}{\Sigma\Theta_R}$ as a function of the electrode potential, we obtain the potential-dependence of k. This is shown in Fig. 2. The plot of $\lg \dfrac{i}{\Sigma\Theta_R}$ *vs.* E is linear, with a slope of about 1/60 mV^{-1}. This corresponds approximately to the quantity $F/2.3\ RT$; *i. e.*

$$k = k_0\, 10^{-\frac{F}{2.3\,RT}E} \tag{32}$$

and thus Eq. (31) assumes the form

$$i = k_0 10^{-\frac{FE}{2.3RT}} \Sigma\Theta_R \tag{33}$$

From investigations connected with the electrohydrogenation it is known [4] that a relation of such a type is obtained in hydrogenations proceeding by a radical mechanism, if the rate-determining part-process can be given by

$$S_a + H_a \rightarrow (SH)_a \tag{34}$$

Based on what was said in the preceding section, it may be assumed that our measured $\Sigma\Theta_R$ agrees practically completely with the amount Θ_j of the adsorbed component taking part in the rate-determining process: $\Sigma\Theta_R \approx \Theta_j$. This leads to the rate equation

$$i = k_0 10^{-\frac{FE}{2.3RT}} \Theta_j \tag{35}$$

Simultaneous measurement of the reaction rate and the adsorption therefore strongly suggests the rate-determining part-process characterized by Eq. (34). Naturally, nothing can be said as to which step in the multistep reaction is the rate-determining one.

It is of definite interest that the rate constant k_0 does not depend on the coverage referred to the mobile part. It thus appears that the reaction

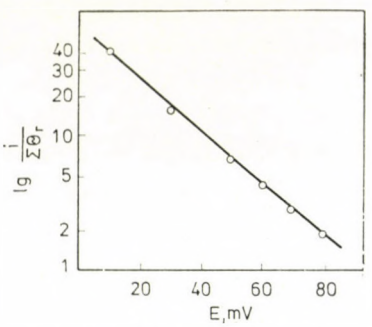

Fig. 2. lg $i/\Sigma\Theta_R$ *vs.* E for phenylacetic acid (c = 10^{-3} mole dm^{-3})

takes place on energetically homogeneous sites, or that there is no appreciable interaction between the adsorbed molecules participating in the reaction. This may perhaps be explained in that the heterogeneity of the platinum surface is decreased by the residually adsorbed molecules in such a way that they completely occupy many (possibly all but one) of the active-site species,

and thus the remaining functional surface sites are practically identical energetically. The reason why the interaction between the adsorbed molecules taking part in the reaction is small, may then clearly be the relatively large separation of the functional centres because of the residually adsorbed molecules.

(b) Oxidation of oxalic acid [5]

A somewhat different case is the oxidation of oxalic acid, described by the overall equation $(COOH)_2 \rightarrow 2CO_2 + 2H^+ + 2e$. At those potentials where the oxidation proceeds, the adsorption of oxalic acid is a reversible

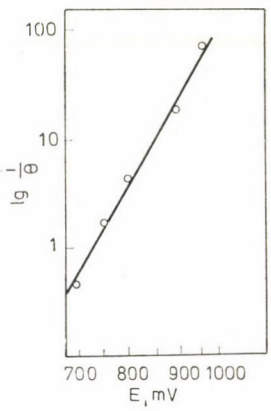

Fig. 3. lg i/Θ *vs.* E for oxalic acid ($c = 4 \times 10^{-3}$ mole dm^{-3}) [5]

process. Residual adsorption is very slight and thus, in contrast with phenylacetic acid, calculations here may be made with the total adsorbed amount. As Fig. 3 shows, in this case a plot of lg $i/\Sigma\Theta_i$ *vs.* potential is linear, with a slope of $1/120 - 1/130$ mV^{-1}. Since $\alpha F/2.3RT \sim 1/120$ mV^{-1} if $\alpha = 0.5$, the following relation can be given for the potential-dependence of the rate (current):

$$i = k_0 10^{-\frac{\alpha FE}{2.3RT}} \Sigma\Theta_i \tag{36}$$

On the above basis, assuming a single rate-determining process, Θ_j may be written in place of $\Sigma\Theta_i$.

The coverage-independent rate constant k_0 is not in agreement with the energetic heterogeneity of the platinum surface in this case either, and thus not with the result to be expected on the basis of interaction between the adsorbed molecules.

This experimental result might be explained by assuming that only one active-site species can come into consideration as regards the reaction. Although the other centre species are accessible from the aspect of adsorption, they do not play a role in the reaction. This assumption is strongly indicated by, for example, phenomena observed in the case of oxygen-covered surfaces [5].

(c) Adsorption phenomena accompanying the electrohydrogenation and electro-oxidation of p-nitrophenol [6]

Due to the presence of the nitro group, *p*-nitrophenol undergoes hydrogenation *via* an ionic mechanism, to yield *p*-aminophenol. At the same time, on a platinum catalyst or electrode the aromatic ring too may be hydrogenated. However, the two processes occur at different potentials. Reduction of the nitro group proceeds at an appreciable rate at potentials of 200—300 mV, whereas that of the aromatic nucleus (as seen in the case of phenylacetic acid, for instance) takes place only at potentials more negative than 100—150 mV. In hydrogenations with an ionic mechanism it was earlier assumed that there

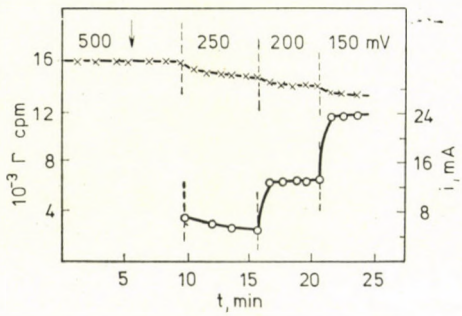

Fig. 4. Reaction rates observed for labelled *p*-nitrophenol adsorbed on the surface, in the presence of inactive *p*-nitrophenol ($c = 5 \times 10^{-2}$ mole dm^{-3}). The arrow indicates the time when the inactive *p*-nitrophenol was added to the system

is no need for the compound to be chemisorbed. This appears to be confirmed by the fact that preliminarily-adsorbed labelled *p*-nitrophenol remains on the surface if inactive *p*-nitrophenol is added to the system, even at potentials (150—300 mV) at which electrohydrogenation already proceeds at an appreciable rate (Fig. 4).

In the case of *p*-nitrophenol it is also possible to demonstrate another interesting facet of the connection between the adsorption and the reaction. Self-inhibitory phenomena during electro-oxidation of the phenols in acidic medium, together with the observation that the rates of certain oxidation

reactions are reduced considerably in the presence of a small amount of phenol or phenol derivative, served as the basis of more recent experimental confirmation of theoretical considerations relating to the adsorption of the phenols, and also of the DEVANATHAN—BOCKRIS—MÜLLER theory [7].

Measurements by the tracer technique on *p*-nitrophenol as model compound [6] revealed that at those potentials where the phenols undergo oxidation ($E > 1300$ mV), the labelled substance is accumulated to such an extent

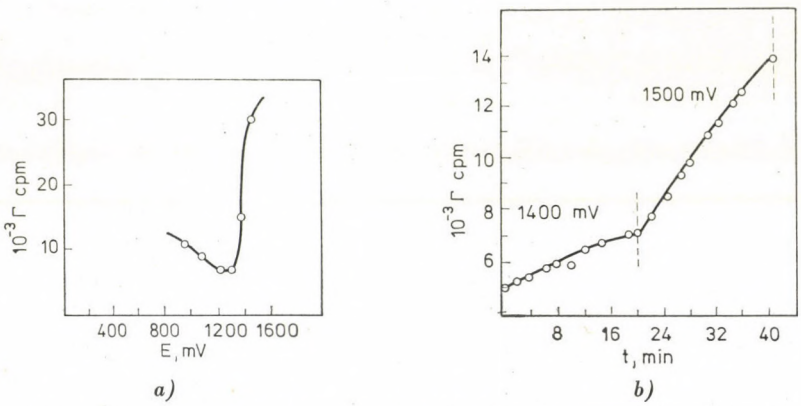

Fig. 5. (a) Increase in apparent adsorption of *p*-nitrophenol above 1300 mV ($c = 10^{-3}$ mole dm^{-3}) [6]; (b) change in time of apparent adsorption of *p*-nitrophenol

on the surface that it can by no means be regarded as a monomolecular adsorption layer.

The 'adsorption' increase occurring above 1300 mV is well-illustrated in Fig. 5a. The phenomenon is extremely striking if it is examined in the case of a preliminarily oxidized platinum surface. The adsorption in the potential interval 800—1300 mV is then slight, for the *p*-nitrophenol is adsorbed only on the free metal surface. Beginning from 1400 mV, the 'adsorption' increases and, as shown in Fig. 5b, is a very protracted process.

It has been found that the material accumulated on the surface can not be removed by either cathodic or anodic polarization, whereas if the electrode is washed with aqueous alkali (1 *M* NaOH), the surface can be cleaned. Treatment with various organic solvents leads to a similar result.

This gives a possibility for the amount of the material accumulated on the surface to be determined, *e. g.* in the alkaline washing solution. It turned out that the amount of material accumulating on the surface at high positive potentials may exceed even ten times the value corresponding to a *p*-nitrophenol monolayer, and is chemically no longer identical with *p*-nitrophenol (oxidation products, phenol ethers, etc.). From all this it must be concluded that, in the inhibitory processes during the oxidation of the phenols, the decisive role is played not by the adsorption phenomena, but by the poly-

molecular film formed from the oxidation products. Among others, these observations were utilized by DAMASKIN and FRUMKIN [13] in their criticism of certain work of GILEADI and BARRADAS.

(d) Study of adsorption phenomena in the propane-yielding electrohydrogenation of acetone [10]

In acidic medium the electrohydrogenation of acetone yields propane according to the overall equation

$$CH_3COCH_3 + 4H^+ + 4e \rightarrow CH_3CH_2CH_3 + H_2O$$

Simultaneous kinetic measurements and adsorption measurements with the tracer technique did not prove effective in this case, but they led to one extremely important finding: insofar as gas-phase products may be formed in some reaction, these exert a significant influence on the evaluability of adsorption measurements with the tracer technique.

Figures 6a and 6b show the result of polarization measurements with a galvanostatic or potentiostatic method, and simultaneous adsorption measure-

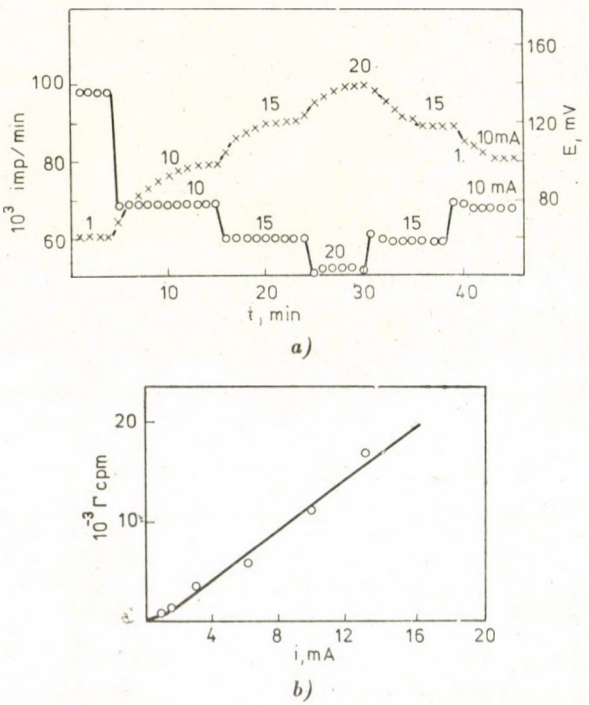

Fig. 6. (a) Changes in time of the count rate (1) and the potential (2) in galvanostatic measurements ($c = 5 \times 10^{-2}$ mole dm^{-3}) [10]. (b) Count rate *vs.* current for potentiostatic measurements (acetone concentration $= 2 \times 10^{-2}$ mole dm^{-3})

ments. It can be seen that increase of the current is accompanied by an increase in the count rate, *i. e.* the adsorption apparently increases.

It must be noted that this apparent increase in adsorption can be observed above a certain current value or acetone concentration. Thus, at low acetone concentrations, and hence at low electrohydrogenation rates, the adsorption is observed to decrease with increasing currents. At higher acetone concentrations, and thus at higher currents (current densities) at given potentials, gas bubbles are observed to accumulate on and leave the electrode surface, and this is naturally the more significant, the higher the strength of the current passing through the system.

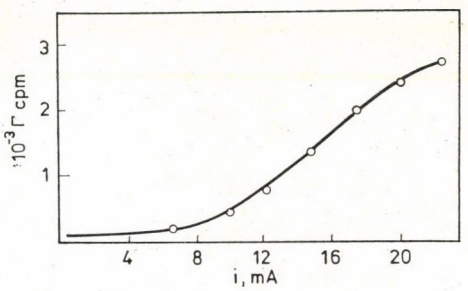

Fig. 7. Count rate *vs.* current for potentiostatic measurements (oxalic acid concentration = 6×10^{-3} mole dm^{-3})

This observation provides an explanation why the count rate increases in parallel with an increase in the current strength. In the measurement of the radioactive radiation originating from the electrode, the radiation from the bubbles containing labelled propane, accumulating on the surface or in the pores of the platinum black electrode, is also measured. At low reaction rates no bubbles are formed (the gas-phase product is lost by diffusion), or the relatively low number of bubbles have a negligible effect.

The question arises as to why the phenomenon induced by the gas bubbles could not be observed in the earlier discussed oxidation of oxalic acid, even though the oxidation product (CO_2) is gaseous in this case too.

The fact is that the phenomenon does occur with oxalic acid too, but only at higher current densities than in the case of acetone. This can probably be explained by the differences between the solubilities and diffusion constants of CO_2 and propane, and possibly by the fact that the two reactions proceed at very different electrode potentials, and thus the bubbles may have different adhesions too. Figure 7 shows the connection between the current and the count rate increase due to bubble formation on a preliminarily-oxidized platinum surface, where the adsorption of oxalic acid is negligible.

At any event, the phenomena discussed draw attention to the fact that careful consideration must be devoted in adsorption measurements to whether or not a gaseous product may be formed from the labelled component, even transitionally.

REFERENCES

[1] HORÁNYI, G.: J. Electroanal. Chem. **51,** 163 (1974)
[2] HORÁNYI, G., NAGY, F.: J. Electroanal. Chem. **32,** 275 (1971)
[3] HORÁNYI, G., NAGY, F.: Electroanal. Chem. **34,** 240 (1972)
[4] NAGY, F., HORÁNYI, G.: A vizesfázisú kontakt katalitikus hidrogénezis mechanizmusa (Mechanizm of aqueous-phase heterogeneous catalytic hydrogenation). A kémia újabb eredményei (Recent Results in Chemistry), Vol. 6, p. 75, 1971. Akadémiai Kiadó, Budapest
[5] HORÁNYI, G., HEGEDŰS, D., RIZMAYER, E. M.: J. Electroanal Chem. **40,** 393 (1972)
HORÁNYI, G., VÉRTES, G.: J. Electroanal. Chem. **43,** 225 (1973)
[6] HORÁNYI, G., VÉRTES, G.: J. Electroanal. Chem. **43,** 441 (1973)
[7] BEJERANO, T., FORGACH, C., GILEADI, E.: J. Electroanal. Chem. **27,** 69 (1970)
[8] ZEIGERSON, E., GILEADI, E.: J. Electroanal. Chem. **28,** 421 (1970)
[9] BEJERANO, T., GILEADI, E.: J. Electroanal. Chem. **38,** 137 (1972)
[10] HORÁNYI, G., NAGY, F.: Acta Chim. (Budapest) **72,** 261 (1972)
[11] HORÁNYI, G., SZABÓ, S., SOLT, J., NAGY, F.: Acta Chim. Acad. Sci. Hung. **68,** 206 (1971)
[12] SCHAY, G.: Acta Chim. Acad. Sci. Hung. **60,** 237 (1969)
SCHAY, G.: Ber. Bunsenges. **7,** 184 (1973)
[13] DAMASKIN, B. B., FRUMKIN, A. N.: Electrochim. Acta **18,** 925 (1973)

György HORÁNYI; H-1025 Budapest, Pusztaszeri út 57—69.

Acta Chimica Academiae Scientiarum Hungaricae, Tomus 92 (4), pp. 367—378 (1977)

ITERATIVE RECALCULATION OF BETA INTEGRALS

J. SZŐKE and Á. I. KISS

(Department of Optical Spectroscopy, Central Research Institute for Physics, Budapest, and Department of Physical Chemistry, Technical University, Budapest)

Received April 20, 1976

Exact values of β-integrals have been recalculated from the singlet transition energies for mono- and homo-disubstituted benzene derivatives with the following donor groups: $-CH_3$, $-OH$, $-OMe$, $-NH_2$, $-F$, $-Cl$. Using the weighted averages of the β-integrals of the same bond types, the first experimental and calculated singlet transition energies are in good agreement (the values vary between 0.7 and 1.5%). The large variance (about 15%) of the recalculated β-integrals can be explained by the unreliability of the experimental data and the fixed atomic parameters, and the approximate character of the Coulomb integral calculation and the PPP algorithm, respectively.

Introduction

Among the numerous approximations developed so far, the Pariser–Parr–Pople (PPP) method [1] proved to be the most successful for the calculation of π-electronic spectra. Different versions have been reported in the literature, for reviews see *e. g.* [2, 3]. Nowadays, the PPP method is employed by organic chemists as a standard tool, the reliable use of which requires a general scheme of parameterization. General parameter systems have been suggested recently *e. g.* by BEVERIDGE and HINZE [4], and by PANCIR *et al.* [5]. In the usual PPP treatment the atomic parameters and the bond distances and angles are experimentally fixed values (*e. g.* [6, 7]), for the evaluation of two-center repulsion integrals many different approximations have been published [2, 3]. The resonance integrals are treated both as fixed [8, 4, 5] and as adjustable parameters [9, 10, 11, 12, 13, 14]. It seems to be appropriate in a semiempirical treatment to have one variable parameter which is adjusted to experimental data. The resonance integral seems to be the most suitable for this purpose because of its important role in the PPP method for the characterization of bonds, and because of its relatively poor theoretical justification. It is an essential requirement that a given value of resonance integral should be applicable for a wide range of compounds. The simplest way is to adjust the resonance integrals to the experimental singlet transition energies [9—14] which can be obtained with the highest accuracy among the spectral characteristics.

The purpose of the present work is to obtain transferable resonance integrals. A computer method has been developed which uses the experimental first singlet transition energy for the evaluation of a given resonance integral. In this paper the results for mono- and homo-disubstituted benzenes containing methyl, fluoro, chloro, hydroxy and amino groups are considered.

Data and method

Transition energies

The method requires the experimental transition energy of the first $\pi \rightarrow \pi^*$ band.

The most appropriate calculation procedure is based on the 0,0-transition. Except for the simplest derivatives [15], however, the position of the 0,0-band is not available (symmetry forbidden transitions) and the experimental band maximum is considered as transition energy. This maximum can be assigned to $\nu_{0,0} + \nu_2 + \nu_{18}$, where ν_2 and ν_{18} are the appropriate benzene normal vibrations [16]. With substituted benzene derivatives the substituent can perturb the symmetry of the π-electron system and, as a consequence, the 0,0-transition will be partially allowed. In this case the $\nu_{0,0} + n\nu_2$ combination will produce a long progression completely overlapping each other. The highest intensity is in both types of progression at the first ν_{18} combination. With mixed systems, therefore, the fine structure is destroyed.

Particular care was taken to check the reliability of the data used. In the 5th column of Table 3 data references are listed.

Atomic and bond parameters. The I_μ atomic ionization potentials and the $\gamma_{\mu\mu}$ one-center repulsion integrals were considered as fixed. They were taken from the tables by HINZE and JAFFÉ [6] for atoms contributing one electron. The KVIATKOWSKI approximation [14]

$$I_\mu = I_{Me-X} + \gamma_{\mu\mu} \tag{1}$$

was used for the evaluation of the I_μ values of atoms contributing two electrons to the π-electron system. The $\gamma_{\mu\mu}$ values for N and O atoms were the same as in BAILEY's work [10], those for F and Cl the same as in FORD's paper [9]. The fixed parameters used are listed in Table I.

Table I

The atomic parameters applied

	Ċ	C̈	N̈	Ö	F̈	C̈l
I	11.16	29.00	25.73	30.07	34.00	24.37
A	0.03	19.00	8.97	10.83	12.61	11.34

The geometry of olecules was calculated from the accepted average bond length [24] of ea bond type given in Table II. All bond angles were set to 120°. For the C– onds in the benzene ring β_{CC} was set equal to −2.39 eV, the generally used value [23]. The resonance integrals of the substituent–ring bonds were calculated with the aid of the experimental energy.

Table II

The bond lengths used in the calculations Å

Bond type	Bond length	Bond type	Bond length
C = C	1.397	C — Cl	1.69
C — C	1.50	C — O	1.36
C — F	1.30	C — N	1.38

Method of calculation. The calculation procedure was based on the original PPP approximation. The block diagram of the program calculating the singlet–singlet transition energies is represented in Fig. 1. The task of

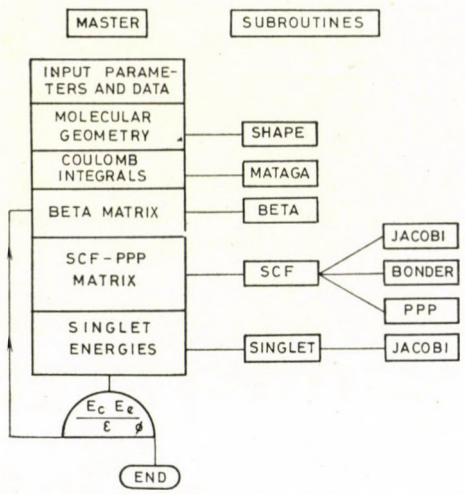

Fig. 1. Block diagram of the recalculation program

each subroutine is determined unambiguously. The complete program is available as a KFKI Report.

The speciality of the calculation procedure is the recalculation algorithm in subroutine BETA for the β_{C-X} resonance integrals of the bonds between an aromatic ring C atom and the adjoining atom X of a distinct substituent.

This subroutine builds up the BETA matrix from the calculated β^{c}_{c-x}, and the fixed β-integrals.

The atomic parameters, the bond length and bond angle of the C–X bond, the starting β_{c-x} (denoted as β_1), the starting and maximum values of D (the change of β) and the lowest singlet transition energy ($^1E^e_1$) are required as input data. In the first and second cycles the starting β_1 and $\beta_2 = (\beta_1 + D)$ are used for the C–X bonds, respectively, as matrix elements in the BETA matrix. The usual PPP calculation with complete CI gives, in the two cycles, two series of singlet–singlet transition energies from which the lower value ($^1E^c_1$) is taken as ε_1 and ε_2 where the indices represent the cycle 'before' and 'after', respectively. From these data in the third cycle δ is calculated as

$$\delta = (\varepsilon_2 - \varepsilon_1)/(\beta_2 - \beta_1) \tag{2}$$

followed by $\beta_1 = \beta_2$; $\varepsilon_1 = \varepsilon_2$; $F = \varepsilon_1 - {}^1E^e_1$; $c = F/\delta$;

$$\beta_2 = \beta_1 + c \tag{3}$$

where our previous result was applied, namely that the first singlet–singlet transition energy varies quasi-linearly with the β-integral for most compounds investigated [24]. Using this new $\beta_{c-x} = \beta_2$, the repeated PPP calculation gives a new set of singlet energies and the new $^1E^c_1$ overwrites the value of ε_2. This cyclic operation is repeated until

$$[{}^1E^c_1 - {}^1E^e_1] < \varrho \tag{4}$$

where ϱ is a given small number (usually 0.001 eV).

Results and discussion

The lowest calculated ($^1E^c_1$) and experimental ($^1E^e_1$) singlet–singlet transition energies are given in Table IV and Fig. 2. Condition (4) is valid in the last iterational cycle for all compounds except *m*-diaminobenzene. The slope of the $^1E^c_1(\beta_{c-x})$ function is quasi-linear in the investigated range of β_{c-x}. A higher deviation from linearity was observed in the case of *m*-xylene (Fig. 3) where $^1E^c_1$ approaches $^1E^e_1$ asymptotically. The task is insoluble in the case of *m*-diaminobenzene, (Fig. 4) because the $^1E^c_1(\beta_{c-x})$ function has a minimum at $\beta_{c-x} = -2.4$ but the $^1E^c_1$ is in this point higher by 0.037 eV than $^1E^e_1$.

The code numbers of the compounds investigated are identical in Tables III and IV and Fig. 2.

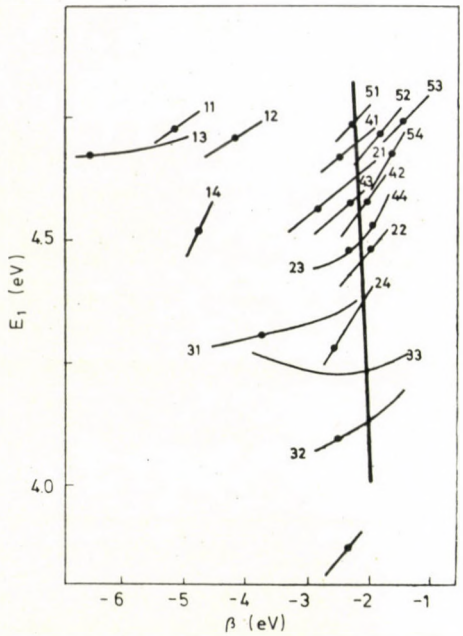

Fig. 2. The first singlet transition energies of the different benzene derivatives as a function of the β-integral

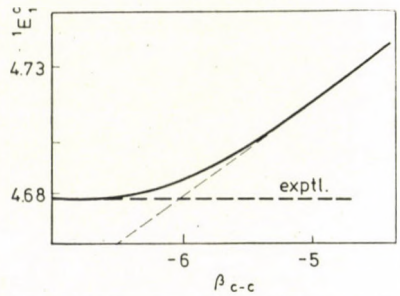

Fig. 3. The first singlet transition energy of *m*-xylene as a function of the β-integral

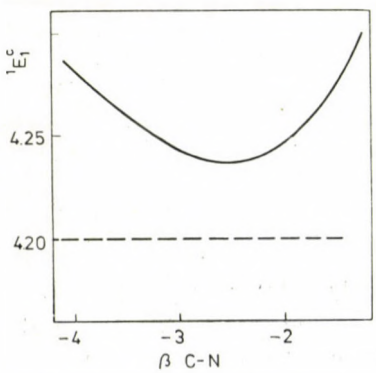

Fig. 4. The first singlet transition energies of *m*-diaminobenzene as a function of the β-integral

Table III

The compounds investigated, and the experimental and calculated results

Code	Name of compound	Bond type	$^1E_1^e$	Ref.	β_{C-X}^C	δ
1	Benzene	C = C	4.8811	[17]	−2.3768	
11	Me-benzene	C — C	4.7321	[17]	−5.4000	0.060850
12	*o*-di-Me-benzene		4.7141	[17]	−4.2407	0.079960
13	*m*-di-Me-benzene		4.6785	[17]	−6.5302	0.010599
14	*p*-di-Me-benzene		4.5248	[17]	−4.7678	0.173495
21	F-benzene	C — F	4.7502	[17]	−2.2710	0.090192
22	*o*-F_2-benzene		4.7357	[17]	−1.8682	0.152101
23	*m*-F_2-benzene		4.7680	[18]	−1.4336	0.139399
24	*p*-F_2-benzene		4.6430	[18]	−1.9045	0.220000
31	Cl-benzene	C — Cl	4.6784	[17]	−2.5255	0.118067
32	*o*-Cl_2-benzene		4.5920	[19]	−2.1112	0.234609
33	*m*-Cl_2-benzene		4.5920	[19]	−2.3363	0.134278
34	*p*-Cl_2-benzene		4.5410	[19]	−2.0657	0.271531
41	Hydroxybenzene	C — OH	4.6089	[20]	−2.5376	0.109983
42	*o*-dihydroxybenzene		4.4920	[20]	−2.0282	0.209482
43	*m*-dihydroxybenzene		4.5000	[20]	−2.3459	0.120651
44	*p*-dihydroxybenzene		4.2610	[20]	−2.5485	0.275041
51	Metoxybenzene	C — OMe	4.6089	[21]	−2.5376	0.109983
52	*o*-dimethoxybenzene		4.5084	[21]	−1.9401	0.167597
53	*m*-dimethoxybenzene		4.5000	[21]	−2.3905	0.136920
54	*p*-dimethoxybenzene		4.2751	[21]	−2.4971	0.258600
61	Aminobenzene	C — NH_2	4.3049	[22]	−3.7404	0.039260
62	*o*-diaminobenzene		4.2610	[22]	−1.0849	0.048718
63	*m*-diaminobenzene		4.2030	[22]	(−2.60)	0.000000
64	*p*-diaminobenzene		3.9110	[22]	−2.2719	0.530095

The calculated β_{C-X}^C and δ in the range of the experimental energies are listed in Table IV. The latter data can be used for rapid approximate calculations. Energies obtained by the different 'transferable' β_{C-X} values and their deviations from the experimental energies are listed in Table V.

Table IV

The calculated energy values and their evaluation

Code of comp.	β^{av}_{c-x}				β^{a}_{c-x}			β^{w}_{c-x}			$(\Sigma \Delta_w^2/N)^{1/2}$
	$^1E_1^{av}$	$^1E_1^{\sigma *}$	Δ_{av}	S_{av}	$^1E_1^{a}$	Δ_a	S_a	$^1E_1^{w}$	Δ_w	S_w	
11	4.7422	0.0519	+0.213		4.7576	+0.514		4.7648	+0.691		
12	4.6346	0.0682	−1.686		4.6534	−1.288		4.6644	−1.054		
13	4.6922	0.0090	+0.294		4.6947	+0.347		4.6962	+0.378		
14	4.4438	0.2848	−1.790	−2.969	4.4845	−0.890	−1.317	4.5048	−0.362	−0.347	0.682
21	4.7865	0.0271	+0.764		4.7567	+0.137		4.7844	+0.719		
22	4.7358	0.0458	−0.003		4.6852	−1.066		4.7321	−0.077		
23	4.7073	0.0418	−1.273		4.6612	−2.239		4.7041	−1.340		
24	4.6352	0.0539	−1.168	−0.680	4.5780	−1.400	−4.568	4.6451	+0.058	−0.640	0.761
31	4.7098	0.0218	+0.671		4.7168	+0.821		4.7169	+0.823		
32	4.5572	0.0262	−0.758		4.5712	−0.454		4.5714	−0.450		
33	4.6023	0.0249	+0.224		4.6103	+0.399		4.6104	+0.400		
34	4.4883	0.0502	−1.160	−1.023	4.5045	−0.803	−0.037	4.5048	−0.798	−0.025	0.648
41	4.6192	0.1306	+0.967		4.6143	+0.858		4.6256	+0.362		
42	4.4033	0.0754	−1.974		4.3932	−2.200		4.4170	−1.670		
43	4.4872	0.0434	−0.028		4.4814	−0.413		4.4951	−0.109		
44	4.2876	0.0989	+0.626	−0.409	4.2743	−0.313	−2.068	4.3057	+1.049	+0.368	1.034
51					4.6130	+0.089		4.6305	+0.464		
52					4.4845	−2.082		4.4080	−2.227		
53					4.3453	−4.844		4.4904	−0.213		
54					4.2743	−0.017		4.2160	+1.381	+0.145	1.335
61	4.3657	0.0462	+1.200		4.3615	+1.314		4.3626	+1.340		
62	4.1957	0.0460	−1.531		4.2018	−1.389	−6.854	4.2032	−1.357		
63	4.2355	0.0003	+0.750		4.239	∼0.840		4.24	+0.880		
64	3.8302	0.5893	+2.066	+1.735	3.8961	−0.831	−0.456	3.9112	+0.004	−0.867	1.050

$^1E_1^{av} - {}^1E_1^{\sigma}$ by using Eq. (8)

Table V

Calculated energy values of hydroxy- and methoxybenzenes, using the common

$$\beta^{c}_{c-o} = -2.3520$$

Code of compd.	$^1E_1^e$	$^1E_1^w$	Δ_w
41	4.6089	4.6293	+0.443
42	4.4920	4.4242	−1.510
43	4.5000	4.4993	−0.016
44	4.2610	4.3150	+1.268
51	4.6089	4.6293	+0.443
52	4.5084	4.4394	−1.531
53	4.5000	4.5053	−0.117
54	4.2751	4.3126	+0.878

$$S_w = -0.142$$

$$(\Sigma\Delta_w^1/N)^{1/2} = 0.962$$

It is clear that the principle "all errors to be corrected by β" is not unconditionally approvable, because the fixed parameters may also contain errors; nevertheless, we think that this is a favourable first step for the systematic exploration of the sources of errors.

The complete list of computational results and their graphical representations are collected in a KFKI Report [26].

The value of $\beta_{c=c}$

The explicit form* of $^1E_1^c(\beta_{c-x})$ for benzene is

$$\beta_{c=c} = -(^1E_1^c/2) + 0.0636 \tag{5}$$

The most generally accepted $^1E_1^e$ for benzene measured in hexane solution is 4.8810 eV (= 254.0 nm). The exact β^c_{c-c} is −2.3768 eV, using Eq. (5).

In this work $\beta_{c=c} = -2.39$ eV was chosen since most of the early publication [23] applied this value, supplying comparable results. The calculated $^1E_1^c$ energy for benzene can be considered as within the experimental error (−2.39 eV = 252.65 nm).

* The higher PPP energies of benzene transitions can be calculated by the following simple equation:

$$^1E_1^c = -2 \cdot \beta + C_n \tag{5a}$$

where n = 1, 2, 3, 4 and $C_1 = 0.1273$; $C_2 = 1.4246$; $C_3 - C_4 = 2.2503$. The accuracy of the results is better than 0.001 eV in the useful range (between −2 and −3) of β-integrals.

Average value of β_{c-x}

The best transferable β_{c-x} was supposed to be the β_{c-x} average value of β^c_{c-x} recalculated from each adequate compound using ${}^1E^e_1$. If this idea had been fulfilled, the recalculated β^c_{c-x} would have been grouped around vertical lines in Fig. 5. The β^c_{c-x} show considerable deviations.

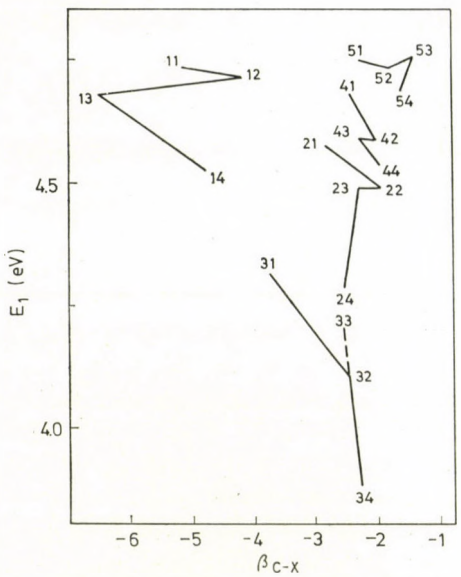

Fig. 5. The recalculated β-integrals for different compounds. The points belonging to the same substituent are connected with a solid line

The calculation of the averaged β^c_{c-x} integrals and their σ_β variance were performed by Eqs (6) and (7), respectively:

$$\beta^{av}_{c-x} = \left(\sum^{N} \beta_{c-x}\right) \Big/ N \tag{6}$$

$$\sigma_\beta = \left[\sum^{N} (\Delta\beta_{c-x})^2/N\right]^{1/2} \tag{7}$$

where

$$\Delta\beta_{c-x} = \beta^{av}_{c-x} - \beta^c_{c-x} \tag{7a}$$

The divisor N is used instead of N − 1 because of the small number of elements (N = 4).

The approximate ${}^1E^{av}_1$ energies can be obtained from Eq. (8) by using the average β_{c-x}:

$${}^1E^{av}_1 = \Delta\beta_{c-x} = \delta + {}^1E^e_1 \tag{8}$$

Similarly, ${}^1E_1^+$ and ${}^1E_1^-$ can be calculated from Eq. (8), where $\Delta\beta_{c-x} = \pm\sigma\beta$, respectively. The ${}^1E_1$ energies corresponding to the β-deviations can be obtained from

$${}^1E_1^\sigma = ({}^1E_1^+ + {}^1E_1^- - 2\,{}^1E_1^e)/2 \tag{9}$$

The ${}^1E_1^{av}$ and ${}^1E_1^\sigma$ energies may be found in the 2nd column of Table IV. In the 3rd column of this table are listed the Δ_{av} values defined by

$$\Delta_{av} = 100\,{}^1E_1^{av}/{}^1E_1^e \tag{10}$$

The 4th column of Table V contains the S_{av} values which are the sum of the percentual deviations of Δ_{av} according to

$$S_{av} = \sum^N \Delta_{av} \tag{11}$$

In this case we applied our β_{c-x}^a integrals accurate to 0.1; these results listed in columns 6–8 of Table IV were taken from earlier publications [24]. ${}^1E_1^{as}$, Δ_{as} and S_{as} were defined similarly to Eqs (8), (10) and (11).

The results obtained by using the two β-integral sets are sufficiently good; the recalculated average β-s give no better results than the assessed ones. The significant differences of S_{av} from zero show that the simple average β-integrals applied are 'not transferable' enough.

In the second approximation we attempted to utilize the weighted average β's. As the effect of a β_{c-x} for the ${}^1E_1^c$ depends on the slope of ${}^1E_1^c(\beta_{c-x})$, normalization factor f has been introduced

$$f = 1\Big/\sum_i \delta_i \tag{12}$$

which can be used for the calculation of the β_{c-x} weighted average β-integrals:

$$\beta_{c-x}^w = \sum_i (\beta_{c-x}^c)_i\, f\delta_i \tag{13}$$

where index i marks the elements in the compound groups having identical substituents. The product $f\delta_i = W_i$ is the weighting factor for each β_{c-x}^c. In the 5th and 6th columns of Table VI the β_{c-x}^w and W_i – s (f) are listed. The results of the calculation by using β_{c-x}^w integrals are in Table IV (columns 9–11). The calculated energies are in better agreement with the experimental one than in the case of the β_{c-x}^{as} and β_{c-x}^{as} integral sets. The averages of the per-cent deviations are less than 1.8%.

The transition energies for the hydroxy and methoxy derivatives are nearly the same, therefore, both compound groups were used for the calculation of the β_{C-O} integrals. The carbon atoms of the methyl group had been

Table VI

Resonance integrals of different bonds (eV)

Bond type	β^{av}_{c-x}	σ_β(eV)	σ_β(%)	β^{w}_{c-x}	f*	β^{a}_{c-x}
C=C	−2.3768	—	—	—	—	−2.39
C−Me	−5.23	0.85	16.3	4.86	3.0778	−5.00
C−F	−1.87	0.30	16.0	1.89	1.6620	−2.20
C−Cl	−2.26	0.18	8.2	2.20	1.3184	−2.20
C−OH	−2.37	0.31	14.7	2.39	1.4136	−2.50
C−OMe	−2.34	0.24	10.2	2.34	1.4884	−2.50
C−O≠	−2.35	0.19	8.0	2.35	0.7203	—
$C-NH_2$	−2.42	0.95	39.0	2.27	1.6179	−2.30

* calculated by Eq. (12)

≠ average values of the β-integrals of C–OH and C–OMe compounds

neglected as π-centers. A higher number of compounds gave better statistics: the energies calculated from the weighted average agree better with the experimental values than for only one compound group (see Table V).

Required precision of β-integrals

In the best case a $\pm 0.5\%$ accuracy can be expected from the calculation. We now wish to estimate the required accuracy of β-integrals to reach the maximum accuracy (0.1%) in the calculation.

We can see in Eq. (8) that $\Delta\beta_{c-x}$ depends on the absolute value of $^1E^e_1$, the slope of the $^1E^c_1(\beta_{c-x})$ function, and the required approximation of the $^1E^e_1$. At 4.6 eV and the required 0.1% accuracy, Eq. (14) is obtained

$$\Delta\beta_{c-x} = 0.0046/\delta \tag{14}$$

Figure 6 shows how $\Delta\beta_{c-x}$ depends on δ if $\Delta^1E^c_1$ equals 0.1% at 4.6 eV; the range of δ is from 0.01 to 0.6.

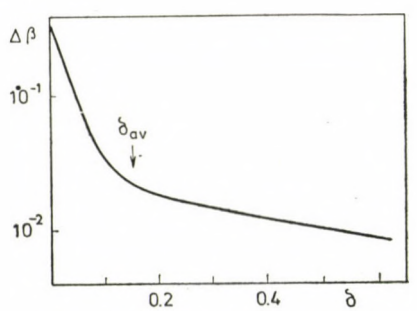

Fig. 6. The function $\Delta\beta$ *vs.* δ

It can be stated that 1×10^{-2} precision of β_{c-x} is required to cover the full range of δ for 0.1% accuracy of the experimental energies.

REFERENCES

[1] R. G. Parr: The Quantum Theory of Molecular Electronic Structure. W. A. Benjamin, New York 1964
[2] R. L. Flurry, Jr.: Molecular Orbital Theories of Bonding in Organic Molecules. Marcel Dekker, New York 1968
[3] Jug, K.: Theoret. Chim Acta, **1,** 91 (1969)
[4] Beveridge, D. L., Hinze, J.: J. Amer. Chem. Soc. **93,** 3107 (1971)
[5] Pančíř, I., Matovšek, I., Zahradnik, R.: Coll. Czech. Chem. Commun., **38,** 3039 (1973)
[6] Hinze, J., Jaffé, H. H.: J. Amer. Chem. Soc. **84**, 540 (1962)
[7] L. E. Sutton, Ed.: Tables of Interatomic Distances, Spec. Publ. No. 11, Chem. Soc. London 1958: Supplement, Spec. Publ. No. 18, Chem. Soc. London 1965
[8] Wolfsberg, M., Helmholz, L.: J. Chem. Phys., **20,** 837 (1952)
[9] Ford, B.: Theoret. Chim. Acta, **10,** 342 (1968)
[10] Bailey, M. L.: Theoret. Chim. Acta, **13,** 56 (1969)
[11] Chalvet, O., Leibovici, C.: Theoret. Chim. Acta, **13,** 297 (1969); **14,** 65 (1969)
[12] Billingsley, F. P., Bloor, J. E.: Theoret. Chim Acta, **11,** 325 (1969)
[13] Fabian, J., Mehlhorn, A., Zahradnik, R.: Theoret. Chim Acta, **12,** 247 (1968)
[14] Kwiatkowski, J. S.: Acta Phys. Polon., **29,** 477 (1966); **30,** 529 (1966)
[15] Petruska, J.: J. Chem. Phys. **34,** 1120 (1961)
[16] Latt, J. R.: J. Chem. Phys., **10,** 135 (1942)
[17] DMS UV Atlas of Organic Compounds, Butterworths, Verlag Chemie 1967—68
[18] Forbes, W. F.: Can. J. Chem., **37,** 1977 (1959)
[19] Forbes, W. F.: Can. J. Chem., **38,** 1104 (1960)
[20] Dearden, J. C., Forbes, W. F.: Can. J. Chem., **37,** 1294 (1959)
[21] Dearden, J. C., Forbes, W. F.: Can. J. Chem., **37,** 1305 (1959)
[22] Forbes, W. F., Leckie, I. R.: Can. J. Chem., **36,** 1371 (1958)
[23] Pariser, R., Parr, R. G.: J. Chem. Phys., **21,** 767 (1953)
[24] Kiss, A. I., Szőke, J.: Chem. Phys. Lett., **11,** 52 (1971); Acta Chim. Budapest **74,** 33, (1972); J. Mol. Struct., **18,** 457 (1973); KFKI Report 1974—92

József Szőke
Árpád István Kiss } H-1525 Budapest, P.O.B. 49.

Acta Chimica Academiae Scientiarum Hungaricae, Tomus 92 (4), pp. 379—386 (1977)

KINETICS OF THE COMPLEX FORMATION BETWEEN IRON(III) AND α-OXY-α-DIBUTYLPHOSPHINEOXIDO-PROPIONIC ACID

A. MIFTAHOVA,* L. DÓZSA and M. T. BECK**

*(*Ulyanov-Lenin University, Kazany, U. S. S. R.*

***Department of Physical Chemistry, Kossuth L. University)*

Received April 26, 1976

The kinetics of the reaction of α-oxy-α-dibutylphosphineoxido-propionic acid (ODFP) and iron(III) was studied by photometry, using the 'stopped flow' method in an aqueous solution at pH 1.4—2.2, at an ionic strength of 0.2, at 20, 25 and 30 °C. At constant pH the rate of the reaction showed first-order dependence on the concentration of both reactants:

$$w = k_H \, c_{Fe} \, c_{ODFP} \cdot$$

On increasing the hydrogen ion concentration, the apparent rate constant (k_H) decreased. Its value was 8.0×10^2 dm^3 mole^{-1} s^{-1} at pH 2.00 and 25 °C. At the same pH value the apparent activation energy was 12.3 kcal mole^{-1} (51.5 kJ mole^{-1}). As regards the mechanism of the reaction, it was presumed that both iron(III) and the ligand may react through various protonation and deprotonation pre-equilibria.

It has been shown earlier [1] by one of the authors (A. M.) that α-oxy-α-dibutylphosphineoxido-propionic acid (ODFP)

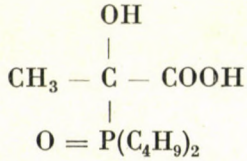

— an extraction reagent — can be well applied for the separation of metal ions in aqueous solutions, provided the pH value is chosen suitably. The extraction is based on the fact that ODFP forms complexes of adequate stability with the metal ions. A 1 : 1 complex is formed with iron(III) ion:

$$Fe^{3+} + H_2A \rightleftharpoons FeA^+ + 2H^+ \qquad (1)$$

where H_2A denotes the doubly protonated ODFP. After the determination of the equilibrium constant of the reaction ($\lg \beta_1 = 14.34$) (2) we set us the aim of studying the kinetics of complex formation which is important from the aspect of the application of ODFP in extractions. Owing to the high reaction rate 'stopped flow' technique was applied.

Experimental

Method, instruments

A "stopped flow" cell (of 0.188 cm optical pathway) constructed at our Department was used. A Hitachi-Perkin-Elmer UV-VIS-type spectrophotometer and a Tektronix Guernsey (Island) N. 5103-type oscilloscope (whose inertia is lower than 1 μs) were attached to the cell. Changes in time of the absorbance of the reaction mixture at 370 nm were measured, then the initial rates were determined as a function of the various initial concentrations. The half-time of the reaction varied between 50 and 200 ms (the dead time of the instrument was shorter then 5 ms). The pH value of reaction mixtures was measured with an accuracy of ± 0.01 pH, using a pH-meter of Radiometer 51 type. The temperature of reaction mixtures was kept by a thermostat within ± 0.2 °C.

Materials

The aqueous solution of iron(III) perchlorate was prepared by dissolving powdered iron (ferrum reductum of analytical grade) in an equivalent amount of perchloric acid by heating on a water bath and subsequently adding a 3% solution of hydrogen peroxide. Excess hydrogen peroxide was removed by boiling. The concentration of iron(III) was determined by EDTA titration, using sulphosalicylic acid as an indicator [2]. The aqueous solution of ODFP was prepared as described earlier [3], whereas the sodium perchlorate solution was made by dissolving anhydrous sodium carbonate in perchloric acid [4].

Experimental results and their evaluation

In Figs 1 and 2 the logarithmic values of the initial rates are plotted against the logarithmic values of the initial concentration of iron(III) and of ODFP, respectively. It can be seen that the reaction is of first order on both reactants (1.02, 1.0). In Fig. 3 the logarithmic values of the reaction rate are plotted against the pH values in the case of equivalent amounts of iron(III) and ODFP, and of a fivefold excess of the ligand. Thus, we obtain from the

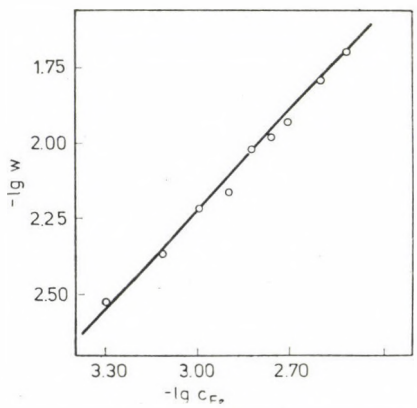

Fig. 1. Logarithmic values of reaction rates plotted against the logarithmic values of iron(III) concentration, $c_{ODFP} = 7.5 \times 10^{-3}$ mole dm^{-3}; pH = 2.0

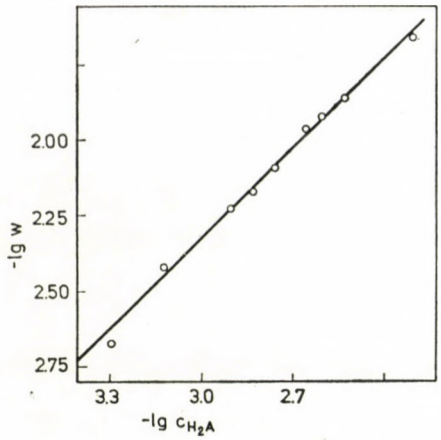

Fig. 2. Logarithmic values of reaction rates plotted against the logarithmic values of ODFP concentration $c_{Fe} = 5 \times 10^{-3}$ mole dm^{-3}; pH = 2.0

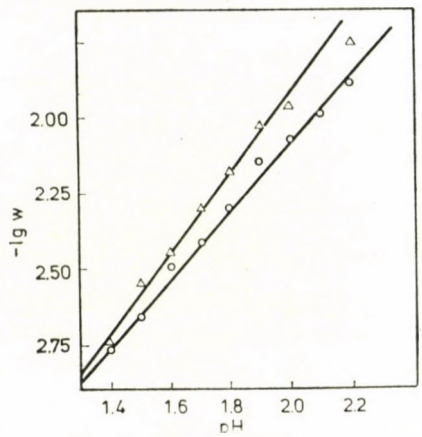

Fig. 3. Logarithmic values of reaction rates plotted against the pH values, ○ ○ ○ $c_{Fe} = c_{ODFP} = 3 \times 10^{3}$ mole dm^{-3}; △ △ △ $c_{Fe} = 1.5 \times 10^{-3}$ mole dm^{-3}; $c_{ODFP} = 7.5 \times 10^{-3}$ mole dm^{-3}

slope of the straights an order of −1.1, −1.3 for the activity of hydrogen ion. On this basis the following empirical rate equation can be described:

$$w = \frac{\mathrm{d}\,[\mathrm{Fe\,A}]}{\mathrm{d}t} = k\,\frac{c_{\mathrm{Fe}}\,c_{\mathrm{ODFP}}}{a_{\mathrm{H}^+}^{n}} \tag{2}$$

where $n = 1.1-1.3$ and a_{H^+} is the hydrogen ion activity. At constant pH, this equation can be written in the form

$$w = k_{\mathrm{H}}\,c_{\mathrm{Fe}}\,c_{\mathrm{ODFP}} \tag{3}$$

In Fig. 4 the logarithmic values of the apparent constants are plotted against the reciprocal values of temperature. The data of activation enthalpy and activation energy obtained by means of these functions are given in Table I.

On establishing the mechanism of the reaction it must be taken into account that various forms of both iron(III) and of the ligand are present in the reaction mixture. On the one hand, one must reckon with the hydrolysis

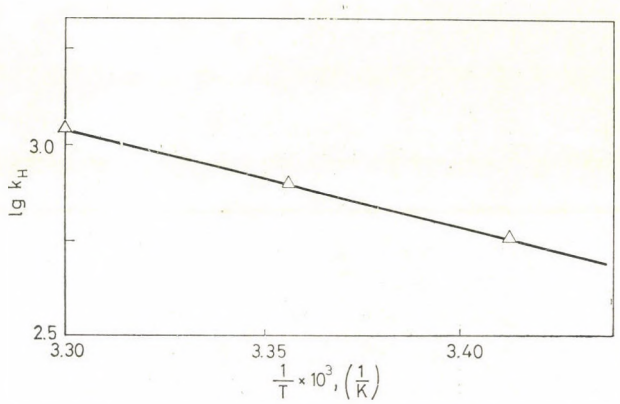

Fig. 4. Logarithmic values of reaction rates determined at constant pH value (= 2.0) plotted against the reciprocal values of temperature

Table I

Kinetic parameters of the complex formation between iron (III) and ODFP

t °C	$K_H \cdot 10^{-2}$ dm³mole⁻¹s⁻¹	$\Delta H^{\neq}$		$\Delta H^{\neq}$	
		kcal mole⁻¹	KJ mole⁻¹	cal moleγ_1K⁻¹	J mole K⁻¹
20	11.1				
25	8.0	12.3	51.5	−1.7	−7.1
30	5.84				

pH = 2.0

of iron(III):

$$Fe^{3+} + H_2O \underset{\leftarrow}{\overset{K'_{OH^-}}{\rightleftharpoons}} FeOH^{2+} + H^+ \qquad (4)$$

where $K'_{OH^-} \cdot a_{H_2O} = K' = 7.4 \times 10^{-3}$

$$FeOH^{2+} + H_2O \underset{\leftarrow}{\overset{K''_{OH^-}}{\rightleftharpoons}} Fe(OH)_2^+ + H^+ \qquad (5)$$

where $K''_{OH^-} \cdot a_{H_2O} = K'' = 8.9 \times 10^{-7}$

(it must be noted here that this value has been obtained in a concentration of 1 M $NaClO_4$, *i. e.* under different conditions [5]), and, on the other hand, with the dissociation [3] of ODFP (= H_2A) as a dibasic acid:

$$H_2A \overset{K_1}{\rightleftharpoons} HA^- + H^+ \; (K_1 = 1.096 \times 10^{-3}) \tag{6}$$

$$HA^- \overset{K_2}{\rightleftharpoons} A^{2-} + H^+ \; (K_2 = 10^{-12}) \tag{7}$$

According to recent measurements [6], the value of K_2 is lower than that given in the cited literature. These processes are faster by orders of magnitude than the complex formation. Therefore, they may be considered as pre-equilibria.

Thus, the reactants are present in the reaction mixture as Fe^{3+}, $FeOH^{2+}$, $Fe(OH)_2^+$ and H_2A, HA^- and A^{2-}, respectively. However, it can be detected by a simple consideration that A^{2-} cannot play an important role in the reaction. Let us denote by w_A the greatest rate component of the three components theoretically possible, and by k_A the rate constant of second order pertaining to it:

$$w_A = k_A [A^-] [Fe(OH)_x^{3-x}] \tag{8}$$

where $x = 0, 1, 2$, and $Fe(OH)_x^{3-x}$ denotes the most reactive form of iron(III). This term is detectable only when it amounts to more than 10% of the complete experimental rate:

$$w_A > w_{exp}/10 = 80 \, c_{ODFP} \, c_{Fe} \tag{9}$$

Since $[Fe(OH)_x^{3-x}] < c_{Fe}$,

$$w_A < k_a [A^-] \, c_{Fe} \tag{10}$$

From equations (6) and (7)

$$[A^-] = \frac{K_1 K_2 [H_2A]}{[H^+]^2} \tag{11}$$

where $[H^+] \approx 10^{-2}$, and on substituting the constants

$$[A^-] < 10^{-11} [H_2A] < 10^{-11} \, c_{OFDP} \tag{12}$$

and thus

$$w_A < k_A \, 10^{-11} \, c_{ODPF} \, c_{Fe} \, . \tag{13}$$

On combining (9) and (13)

$$10^{-11} \, k_A \, c_{ODFP} \, c_{Fe} > 80 \, c_{ODFP} \, c_{Fe} \tag{14}$$

wherefrom

$$k_A > 8.0 \times 10^{-2} \tag{15}$$

is obtained *i. e.* w_A would be higher than the rate of diffusion.

Consequently, the following reaction routes remain:

$$\begin{aligned}
&\text{I} && H_2A + Fe^{3+} \xrightarrow{k_1} \\
&\text{II} && HA^- + Fe^{3+} \xrightarrow{k_2} \\
&\text{III} && H_2A + FeOH^{2+} \xrightarrow{k_3} \\
&\text{IV} && HA^- + FeOH^{2+} \xrightarrow{k_4} \\
&\text{V} && H_2A + Fe(OH)_2^+ \xrightarrow{k_5} \\
&\text{VI} && HA^- + Fe(OH)_2^+ \xrightarrow{k_6}
\end{aligned} \tag{16}$$

$$\begin{aligned}
w = {} & k_1[Fe^{3+}][H_2A] + k_2[Fe^{3+}][HA^-] + k_3[FeOH^{2+}][H_2A] + \\
& + k_4[FeOH^{2+}][HA^-] + k_5[Fe(OH)_2^+][H_2A] + k_6[Fe(OH)_2^+][HA^-]
\end{aligned} \tag{17}$$

On taking into account the above presented equilibria and

$$c_{Fe} = [Fe^{3+}] + [FeOH^{2+}] \tag{18}$$

$$c_{ODFP} = [H_2A] + [HA^-] \tag{19}$$

we find that

$$\begin{aligned}
\frac{w\,N}{c_{Fe}\,c_{ODFP}} = {} & k_1[H^+]^2 + k_2 k_1[H^+] + k_3 K'[H^+] + k_4 K_1 K' + \\
& + k_5 K' K'' + k_6 K' K'' K_1[H^+]^{-1}
\end{aligned}$$

$$N = [H^+]^2 + K_1[H^+] + K'[H^+] + K_1K' \tag{20}$$

(It must be noted that the constants used in the calculations have been determined by measuring the pH values, and thus $[H^+]$ denotes in fact the hydrogen ion activity.)

On plotting the term on the left side against the hydrogen ion activity (Fig. 5), a straight is obtained, no deviation in a positive direction appears at low or high hydrogen ion concentrations. Thus, reaction routes I and VI cannot play any important role in the reaction. It is not possible to determine the constants of the individual processes from the obtained function. From the intercepts and the slopes only the following relationship could be derived:

$$k_2K_1 + k_3K' = 6.04 \tag{21}$$

$$k_4K_1K' + k_5K'K'' = 0.117, \tag{22}$$

since $K'K'' \ll K_1K'$ and, owing to electrostatic reasons, it is likely that $k_4 > k_5$, it can be presumed that the second term in (22) is negligible; thus, a value of 1.44×10^4 dm^3 mole^{-1}s^{-1} is obtained for k_4.

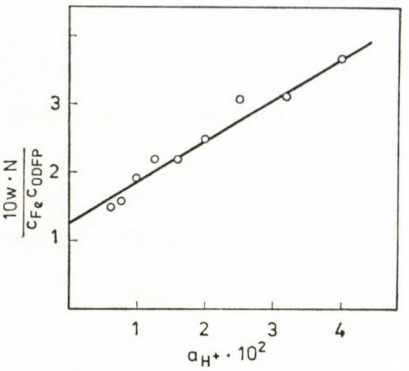

Fig. 5. Values of $w \cdot N/c_{Fe} \cdot c_{ODFP}$ (where $N = [H^+]^2 + K_1[H^+] + K'[H^+] + K_1K'$) plotted against the hydrogen ion activity. $c_{Fe} = c_{OFDP} = 3 \times 10^{-3}$ mole dm^{-3}

On the basis of the above relationships the functions of reaction rate *vs.* hydrogen ion concentration were back-calculated, and the result proved to fit well the experimental curves (Fig. 6).

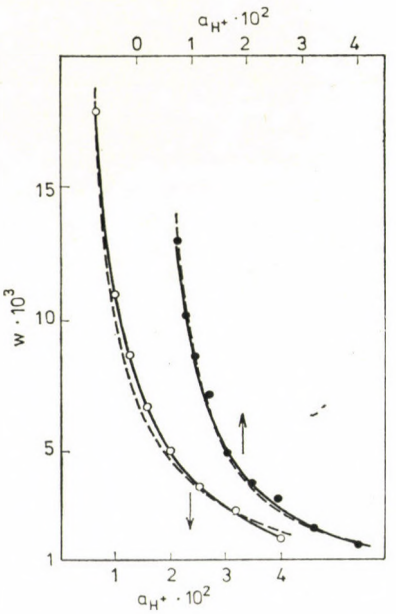

Fig. 6. Reaction rates plotted against the hydrogen ion activity. Continuous line denotes the calculated function, the points denoting the measured values. Concentrations were: ○ ○ ○ $c_{Fe} = 1.5 \times 10^{-3}$ mole dm^{-3}, $c_{ODFP} = 7.5 \times 10^{-3}$ mole dm^{-3}, ● ● ● $c_{Fe} = c_{ODFP} = 3 \times 10^{-3}$ mole dm^{-3}

However, the available data are unsatisfactory for establishing the ratios of the rate constants belonging to reaction routes II to V. Probably, it is not at all possible to determine them in the given system because the measurements can be carried out only in a relatively narrow pH range. Namely, in solutions more acid than that applied by us, the formation of the complex is incomplete, whereas at higher pH values the hydrolysis of iron(III) becomes predominant.

REFERENCES

[1] MIFTAHOVA, A. H., SABITOVA, Z. A., ZIMIN, M. G., TOROPOVA, V. F.: Zh. Anal. Khim. **27,** 1836 (1972)
[2] TOROPOVA, V. F., MIFTAHOVA, A. H., GURYANOVA, I. V., ZIMIN, M. G., PUDOVIK, A. N.: Zh. Obshch. Khim. **38,** 2177 (1970)
[3] TOROPOVA, V. F., MIFTAHOVA, A. H., GURYANOVA, I. V., ZIMIN, M. G., PUDOVIK, A. N.: Zh. Obshch. Khim. **40,** 2172 (1970)
[4] SILLÉN, L. G.: Some Laboratory Methods, KTH org. kemi 1959, 9
[5] SILLÉN, L. G., MARTELL, A. E.: Stability Constants of Metal–Ion Complexes. The Chemical Society, London 1964
[6] Data not yet published

Ad'ilya MIFTAHOVA, Ulyanov-Lenin University, Kazany.

László DÓZSA
Mihály T. BECK
H-4010 Debrecen KLTE

Acta Chimica Academiae Scientiarum Hungaricae, Tomus 92 (4), pp. 387—393)1977)

IDENTITY OF THE DONOR ATOMS IN N,N$^{|}$ DISUBSTITUTED THIOUREA COMPLEXES OF TIN(IV) HALIDES

S. A. A. ZAIDI, T. A. KHAN and K. S. SIDDIQI

(Inorganic Division, Department of Chemistry, Aligarh Muslim University)

Received May 26, 1976

The preparation and characterization of complexes of the type $SnX_4 \cdot 2L$ (X = Cl, Br, I; L = N,N$^{|}$-diallylthiourea, N,N$^{|}$-diethylthiourea, N,N$^{|}$-dibutylthiourea, N,N$^{|}$-diisopropylthiourea and N,N$^{|}$-diphenylthiourea is described. The molar conductances in nitrobenzene and nitromethane indicate that the complexes are covalent in nature. Infrared spectral data (4000—200 cm^{-1}) point to co-ordination through the imino nitrogen.

Introduction

The site of co-ordination in thioamides and thioureas has been a subject of controversy; both sulfur [1—2] and nitrogen [3—8] being claimed as the donor atom. Recent studies of the behaviour of thioureas in strong acids [9, 10] have shown that protonation occurs on the sulfur atom, however, in superacids diprotonation occurs, involving also the nitrogen atom. Thioureas have been reported to co-ordinate with the tetrahalides of group(IV) elements through nitrogen [11—13]. It was, therefore, of interest to synthesize tin(IV) halide complexes with various N,N$^{|}$-substituted thioureas, *viz.* N,N$^{|}$-diallylthiourea (datu), N,N$^{|}$-diethylthiourea (detu), N,N$^{|}$-dibuthylthiourea (dbtu), N,N$^{|}$-diisopropylthiourea (ditu) and N,N$^{|}$-diphenylthiourea (dptu), having varying degrees of electron densities on the nitrogen atoms, and to examine if nitrogen could supersede sulfur in its donor ability.

Experimental

Tin(IV) halides were prepared according to standard methods [14]. Thioureas (all commercial samples) were recrystallized from ethanol. All manipulations were done in a dry box.

The IR spectra were recorded on a Beckman IR-12 spectrophotometer in KBr discs, or in CCl_4 or $CHCl_3$ solution (in the 4000—650 cm^{-1} region) and (in the 650—200 cm^{-1} region) in nujol mull. Conductivity measurements were made on a Systronix-type 302 bridge.

Preparation of the complexes. All the complexes were prepared by mixing the chloroform solutions of the metal halides and the ligand in a 1 : 2 metal-to-ligand ratio. In the case of datu, ditu and dptu, crystalline products were obtained either immediately of after heating the reactant solution. Tin (IV) chloride and bromide complexes of detu and dbtu were obtained

by shaking the reactant solutions, separating the viscous layer thus formed, washing with chloroform and drying in vacuum. *Detu* however, yielded a crystalline product immediately with SnI_4.

Results and discussion

The analytical data (Table I) indicate that all the complexes are of the type $SnX_4 \cdot 2L$. The molar conductances of the complexes in nitrobenzene and nitromethane (Table II) show that they are covalent in nature [15].

Table I

Colours, melting points and analytical data of the complexes

Complex	Colour	M.P. (°C)	C (%) Found (Calcd.)	H (%) Found (Calcd.)	N (%) Found (Calcd.)	X (%) Found (Calcd.)	Sn (%) Found (Calcd.)
$SnCl_4$ *(datu)*$_2$	white	206	28.69 (29.34)	4.50 (4.22)	9 .50 (9.78)	25.20 (24.74)	21.01 (20.70)
$SnBr_4$ *(datu)*$_2$	white	200	22.12 (22.39)	3.56 (3.22)	6.71 (7.46)	41.46 (42.56)	16.66 (15.80)
$SnCl_4$ *(detu)*$_2$	light yellow	160	22.68 (22.89)	4.40 (4.61)	9.91 (10.68)	27.82 (27.01)	22.21 (22.60)
$SnBr_4$ *(detu)*$_2$	yellow	130	17.00 (17.09)	3.84 (3.44)	8.21 (7.97)	45.21 (45.48)	16.77 (16.89)
SnI_4 *(detu)*$_2$	dark brown	148	13.42 (13.48)	3.02 (2.71)	6.19 (6.29)	57.21 (56.99)	12.81 (13.32)
$SnCl_4$ *(dbtu)*$_2$	light yellow	85	33.30 (33.94)	6.59 (6.32)	8.48 (8.79)	22.84 (22.25)	18.92 (18.62)
$SnBr_4$ *(dbtu)*$_2$	yellow	90	27.68 (26.54)	5.56 (4.94)	6.80 (6.87)	38.99 (39.22)	13.97 (14.55)
$SnCl_4$ *(ditu)*$_2$	light yellow	202	29.02 (28.94)	5.51 (5.55)	9.93 (9.64)	23.23 (24.40)	20.24 (20.42)
$SnBr_4$ *(ditu)*$_2$	yellow	188	20.98 (22.15)	4.39 (4.25)	7.34 (7.38)	41.96 (42.11)	15.14 (15.63)
SnI_4 *(ditu)*$_2$	brown	180	18.08 (17.75)	3.68 (3.40)	5.92 (5.92)	52.89 (53.60)	12.41 (12.52)
$SnCl_4$ *(dptu)*$_2$	light yellow	132	43.11 (43.54)	3.69 (3.37)	7.62 (7.81)	19.02 (19.76)	16.02 (16.54)
$SnBr_4$ *(dptu)*$_2$	yellow	168	34.45 (34.89)	2.96 (2.70)	6.00 (6.26)	36.21 (35.72)	14.26 (13.26)

In thioureas, both nitrogen and sulfur may act as the donor atom. In order to ascertain the bonding site, we have recorded the infrared spectra (4000—200 cm^{-1}) of the ligand and their complexes (Table III). The ligand molecules are highly associated because of intermolecular hydrogen bonding

Table II

Molar conductance of a 0.002 M solutions in nitrobenzene and nitromethane at room temperature*

Complex	λ_m in nitrobenzene (Ohm^{-1} cm^2 mol^{-1})	λ_m in nitromethane (Ohm^{-1} cm^2 mol^{-1})
$SnCl_4$ *(detu)*$_2$	1.694	6.932
$SnBr_4$ *(detu)*$_2$	1.525	6.440
SnI_4 *(detu)*$_2$	3.389	7.587
$SnCl_4$ *(dbtu)*$_2$	2.168	6.779
$SnBr_4$ *(dbtu)*$_2$	1.119	6.371
$SnCl_4$ *(ditu)*	1.356	3.512
$SnBr_4$ *(ditu)*$_2$	1.966	4.612
SnI_4 *(ditu)*$_2$	2.000	7.457
$SnCl_4$ *(dptu)*$_2$	2.644	3.694
$SnBr_4$ *(dptu)*$_2$	3.631	5.841

* datu complexes are not sufficiently soluble in nitrobenzene and nitromethane

between the hydrogen of the NH group and the sulfur of the C=S group in the solid phase and even in concentrated solutions. To eliminate the effect of hydrogen bonding, the spectra of the ligands in dilute solutions have been compared with the spectra of the complexes in KBr.

The IR spectra of all the complexes show a marked lowering in the νN-H frequency, indicating co-ordination through nitrogen. Co-ordination through nitrogen should have some effect upon other related bands too, but, unfortunately, the normal vibrational modes in thioureas are strongly coupled and the majority of bands arise from group vibrations. The bands in the 1570—850 cm^{-1} range [16] have been attributed to νC=S-type group vibrations. Gosavi *et al.* [17] performed a normal co-ordinate analysis of N,N$^{|}$-dimethylthiourea and assigned various mixed bands in its spectrum. In N,N$^{|}$-dimethylthiourea the bands of group frequencies having a νC=S character (thioamide bands) were assigned at 1504, 1420, 1290 and 752 cm^{-1}. Recently, these group vibrations were assigned to absorptions at 1512—50, 1350, 1135—80 and 930—72 cm^{-1} in the IR spectra of various N,N$^{|}$-disubstituted thioureas [18]. The thioamide I band in N-allylthiourea has been assigned at 1442 cm^{-1} [13]. A strong band observed at about 1500 cm^{-1} in these thioureas can be assigned to thioamide I. This frequency is known to increase upon co-ordination through nitrogen [8, 12, 13]. In all the complexes this band lies at higher frequencies. The increase in the thioamide II (except in dbtu complexes) and νC=S + δNCS bands also indirectly supports nitrogen co-ordination [8, 13].

Table III

Assignments of IR bands of ligands and complexes

Complex	Assignments									
	νN—H	Thioamide I	Thioamide II	νC=S+ δNCS	νC—N+δNCN	Thioamide III	νC=S+ νC—N	δNCS	νSn—X	νSn—N
datu solid	3272s,b	1510sh		1240vs	1092vs	946vs	788m			
solution (CCl_4)	3440sh 3410vs	1500vs	1380s	1228s	1092sh	940vvs	780s*	552w,b		
$SnCl_4$ *(datu)*$_2$	3228vs 3056s	1540vs	1416s	1232s	1088s	938s	808m 782w	548s,b	338m	292w
$SnBr_4$ *(datu)*$_2$	3236vs 3056s	1542vvs	1414vs	1232s	1090s	940vs	812s 784w	544s,b	242s	300w
detu solid	3272vs,b 3124w 3044w	1482w	1384vs	1262vs	1058vs	944vvs	806vvs			
solution(CCl_4)	3435s	1498vs	1385vs	1288s	1058vs	935m	795vs*	564m,b		
$SnCl_4$ *(detu)*$_2$	3310vvs 3044w	1536vvs	1388vs	1320s	1050vvs	932vvs	804vvs	564vvs,b	298vvs	308sh
$SnBr_4$ *(detu)*$_2$	3312vvs	1532vvs	1388vs	1318m	1050vs	934vs	808vs	560vvs,b	228vs	310s
SnI_4 *(detu)*$_2$	3255vvs	1502vvs	1415w	1300m	1037s	920s	788s	550vvs,b		292s
dbtu solid	3260vs,b 3120m 3044m	1482s	1380vs	1288s	1088vs 1056s	938vvs	774vs			
solution(CCl_4)	3438s	1495vs	1385s	1282s	1085vs	945vs	766vs*	582m		
$SnCl_4$ *(dbtu)*$_2$	3324vvs	1538vs	1385m	1292m	1078s 1050w	945s	772s	576vs,b	318w 312vvs	256m
$SnBr_4$ *(dbtu)*$_2$	3306vvs	1532vs	1382w	1290m	1078w 1050w	940m	766m,b	556vs,b	229sh 222vs	276m

Table (contd)

ditu solid	3308s 3242s 3100w,b 3036s	1526vs	1392vs	1320vs	1050w	988vvs	748vs			
solution($CHCl_3$)	3422vvs	1498s	1392s	1304s		990s	748vs*	580s		
$SnCl_4$ *(ditu)*$_2$	3328vvs	1542vs	1400s	1324w	1028w	986s	746vs	572vs	312sh 305vvs 300 sh	274sh
$SnBr_4$ *(ditu)*$_2$	3312vvs	1528vvs	1398vs	1320m	1028s	980s	744vs	580s 560sh	216m	286s
SnI_4 *(ditu)*$_2$	3275vs 3236sh	1502vvs		1357s		960s	723vs	564vs 554sh		266s
dptu solid	3228vs 3058s 3040sh	1502vs	1350vs	1250vs	1078vs	940vs	770m 761m			
solution ($CHCl_3$)	3408s 3375s	1495vs	1358vs	1258w	1078m	942s	768sh* 760vs	558w		
$SnCl_4$ *(dptu)*$_2$	3324s 3224m	1534s 1500s	1398s	1284m	1080m	941s	780sh 766vs	540s	312vvs	**
$SnBr_4$ *(dptu)*$_2$	3362s 3228vs	1525vs 1498s	1396vs	1284m	1080m	940s	782m 764vs	520vs	231vs	288s

s = strong, m = medium, w = weak, vs = very strong, vvs = very very strong, sh = shoulder, b = broad

*nujol mull, ** overlapped by the broad and intense Sn—Cl band

The observed decrease in the frequency of the bands assigned to νCN + + δNCN in all cases except in N,N'-diphenylthiourea complexes is also in favour of co-ordination through nitrogen. The thioamide III band shows a decrease in frequency on complexation, however, in some complexes this band is only weakened in intensity. Previous workers have also observed such a change in the thioamide III band on nitrogen co-ordination [7, 8, 13].

The low-frequency thioamide band could not be observed in the IR spectra of thioureas in dilute solutions. The 806—748 cm^{-1} bands which arise from the vibrations consisting of νC=S and νC–N components after complexation, are shifted to higher frequencies or are virtually unchanged. However, in SnI_4 complexes of detu and ditu, the frequency changes in the opposite direction, which may be regarded as an evidence for co-ordination through sulfur, but a marked decrease in the νN–H frequency is in clear support of co-ordination through nitrogen. Actually, itis difficult to base any conclusion on changes in the vibration bands of the ligand where the observed bands of the ligand arise from group vibrations.

The δNCS frequency at about 550 cm^{-1} shows a decrease on complexation in all cases, except for $SnCl_4$ *(detu)*$_2$ in which it is unchanged. This is also in support of nitrogen co-ordination [3].

In N,N'-diallylthiourea, besides nitrogen and sulfur, the C=C double bond is also a potential bonding site. However, its νC=C frequency band at 1656 cm^{-1} remains unchanged after complexation, ruling out co-ordination through the double bond. From the above discussion, it is concluded that co-ordination in all the cases occurs through the nitrogen atom.

Far infrared spectra and structure of the complexes

The far infrared spectra in the 650—200 cm^{-1} range locate the νSn–X and νSn–N bands (Table III). The bands which are virtually unaffected upon changing the halogen are attributed to νSn–N modes. In the spectrum of the complexes, irrespective of the Lewis acid taken, we observed new bands in the 256—310 cm^{-1} region, which can be assigned to νSn–N. In the dptu complex of $SnCl_4$ this band is presumably overlapped by the broad and intense νSn–Cl mode.

Since the νSn–X bands are usually more intense than νSn–N and their frequency decreases as X is progressively changed in the sequence Cl → Br → I, these can easily be assigned. The νSn–I could not be observed in the spectral range studied. The probable geometry for these 1 : 2 (SnX_4 : ligand) complexes is octahedral, involving one of the nitrogen atoms of the thiourea ligand. The ligands should occupy either the *cis* or the *trans* positions in the octahedron. In these complexes, the presence of only one strong Sn–X stretching band is

indicative of a *trans*-octahedral geometry [19], however, in dbtu complexes and the $SnCl_4$ complex of ditu there is a slight splitting of this band and several bands are obtained, which are of weaker intensity and may be due to crystal field effects on a D_{4h} model.

*

We are grateful to Prof. W. RAHMAN, head of the Department of Chemistry, for providing the necessary facilities. One of us (T. A. K.) thanks the U. G. C. New Delhi for financial assistance.

REFERENCES

[1] BYSTROV, D. S., SUMAROKOVA, T. N., FILIMONOV, V. N.: Opt. Spectr. **9,** 460 (1960)
[2] CASSIDY, J. E., MOSER, W., DONALDSON, J. D., JELEN, A., NICHOLSON, D. G.: J. Chem. Soc. (A), 173 (1970)
[3] BAILEY, R. A., PETERSON, T. R.: Can. J. Chem., **46,** 3119 (1968)
[4] GENCHEV, M., ALEKSIEV, M., ALEKSIEVA, N.: Nature (Plovdiv), **3,** 41 (1970)
[5] SHUL'MAN, V. M., SAREL'EVA, Z. A., CHEREMISINA, J. M., VASIL'EV, Ya. V., ANUFRIENKO, V. F.: Izv. Sib. Otd. Akad. Nauk SSSR, Ser. Khim. Nauk, **1,** 77 (1972)
[6] GREENWOOD, N. N., ROBINSON, B. H.: J. Chem. Soc. (A), **1967,** 511
[7] LANE, T. J., YAMAGUCHI, A., QUAGLIANO, J. V., RAYAN, J. A., MIZUSHIMA, S.: J. Amer. Chem. Soc., **81,** 3824 (1959)
[8] SINGH, P. P., RIVEST, R.: Can. J. Chem., **46,** 2361 (1968)
[9] BIRCHALL, T., GILLESPIE, R. J.: Can. J. Chem., **41,** 2643 (1963)
[10] ZAIDI, S. A. A., SIDDIQI, Z. A.: J. Inorg. Nucl. Chem. **37,** 1806 (1975)
[11] RIVEST, R.: Can. J. Chem., **40,** 2234 (1962)
[12] JAIN, S. C., RIVEST, R.: J. Inorg. Nucl. Chem., **29,** 2787 (1967)
[13] SINGH, P. P., PANDE, I. M.: J. Inorg. Nucl. Chem., **34,** 591, 1131 (1972)
[14] G. BRAUER: Handbook of Preparative Inorganic Chemistry, p. 729. Academic Press (1963)
[15] GEARY, W. J.: Coord. Chem. Rev., **7,** 81 (1971)
[16] RAO, C. N. R.: Chemical Applications of Infrared Spectroscopy, p. 300. Academic Press (1963)
[17] GOSAVI, R. K., AGARWALA, U., RAO, C. N. R.: J. Amer. Chem. Soc. **89,** 235 (1967)
[18] MOHSEN, A., OMAR, M. E., OSMAN, S. A.: Pharmazie, **28,** 30 (1973)
[19] BEATTIE, I. R., WEBSTER, M., CHANTRY, G. W.: J. Chem. Soc., **1964,** 6172

S. A. A. ZAIDI
T. A. KHAN
K. S. SIDDIQI
Inorganic Division, Department of Chemistry,
Aligarh Muslim University,
Aligarh-202001, India.

Acta Chimica Academiae Scientiarum Hungaricae, Tomus 92 (4), pp. 395—402 (1977)

A PSEUDOEXACT PARAMETER METHOD FOR THE ANALYSIS OF INTRAMOLECULAR FORCE FIELDS. APPLICATION TO DEGENERATE VIBRATIONS OF SOME MOLECULES

T. R. ANANTHAKRISHNAN

(Department of Physics, St. Paul's College, Kalamassery-683104, India)

Received June 4, 1976

The normal co-ordinate transformation matrix L associated with a vibrational problem of order n is expressed in the parametric form so that its elements become functions of angular parameters Φ_{ij}. In order to solve higher-order vibrational problems, possessing insufficient experimental data, the possibility of imposing constraints on these parameters is analyzed in the light of the coupling they provide between the various symmetry co-ordinates in a normal mode. It is shown that constraints like $\Phi_{12} = \Phi_{13} = 0$ are best valid in the case of degenerate vibrations of $XY_3Z(C_{3v})$- and $XY_5(D_{3h})$-type molecules with experimental values of the Coriolis coupling constants ζ_{11} approximately equal to J_{11}, a term which is calculable purely from molecular geometry and atomic masses. The applicability of the constraint is illustrated in the case of CH_3F (whose force field is already well-established) and is used to fix the E' force field of AsF_5 (which is still poorly established due to the insufficiency of experimental data).

Introduction

A complete analysis of molecular vibrations requires unambiguous knowledge of the potential energy matrix F characterizing the intramolecular forces. In the general valence force field representation, the matrix F associated with a vibrational species of order 'n' involves $\frac{1}{2}\, n(n+1)$ elements and their evaluation with the 'n' vibrational frequencies is mathematically impossible. Recent work [1—5] indicates that one may require as many as four independent experimental data to fix unambiguously the force field associated with the simplest case of order $n = 2$. For higher-order problems this number would increase enormously, thus making the available experimental data insufficient for unambiguous calculation of force constants for most of the molecules [6, 7]. A profitable use of the Coriolis coupling constants ζ_{ii}, often available experimentally in the case of degenerate vibrations, for certain molecules is presented here through a pseudoexact method involving a physical approach to the mixing between symmetry co-ordinates in a normal mode.

Mixing parameters

The mixing of symmetry co-ordinates S in various normal modes Q is given by the eigenvector matrix L through the relation [8]

$$S = LQ \tag{1}$$

The parametric approach to the vibrational problem first suggested by TAYLOR [9] and later developed by many others [10—14] basically involves splitting of the matrix L into two parts, one (L_0) characteristic of the inverse kinetic energy matrix G and the other (C) a function of arbitrary parameters such that

$$L = L_0 C \tag{2}$$

The condition on L_0 is that it should obey the rel ation $L_0 \tilde{L}_0 = G$, and on C that it should be orthogonal. The matrix L_0, when taken in the lower triangular form possesses certain advantages [15], would involve only $\frac{1}{2} n(n+1)$ nonvanishing terms and can easily be generated through an equal number of equations from the G_{ij} elements as

$$G_{ij} = \sum_{k=1}^{n} (L_0)_{ik} (L_0)_{jk} \qquad i < j \tag{3}$$

The C matrix may be written as [12]

$$C = \Pi C_{ij}(\Phi_{ij}) \qquad i = 1, 2, 3 \ldots n \quad i < j \tag{4}$$

where the C_{ij}-s are elementary rotation matrices in the ij plane. (The iith and jjth elements are cos Φ_{ij}, the ijth element is —sin Φ_{ij}, the jith element is sin Φ_{ij}, all other diagonal elements are unity and all other off-diagonal elements are zero.)

The matrix C bears the key for the whole molecular dynamics since it enables the generation of the intramolecular force field [12—14] from the vibration frequencies ω_i as

$$(\tilde{L}_0)^{-1} C \Lambda \tilde{C} L_0^{-1} = F \tag{5}$$

Λ being a diagonal matrix of elements $\lambda_i = 4\pi^2 \omega_i^2$.

A normal mode of vibration Q_k would, in general, involve the largest contribution from S_k from among the different symmetry co-ordinates. It has been shown [16] that the vibrational frequencies corresponding to normal modes Q_i and Q_j become reversed as the value of Φ_{ij} varies from 0 to $\pi/2$ in a parameter space of $\frac{1}{2} n(n-1)$ dimensions. Thus, the parameter Φ_{ij} provides a measure of mixing between the symmetry co-ordinates S_i and S_j in a normal mode and may be called as 'mixing parameters' in this sense.

L matrix approximation and the mixing parameters

The setting of L_0 in the lower triangular form approximates the actual mixing between the symmetry modes in many cases [17]. This has been clearly established from its ability to provide excellent fit to many experimentally observable quantities, like vibrational amplitudes, centrifugal distortion constants and isotopic frequencies in many molecules [17—19]. Further, it is now well-established [17, 20, 21] that in the $n = 2$ cases involving a stretching (ν) and a bending (δ) vibration — which may be abbreviated as a $\nu\delta$ case — the latter is nearly pure, thus making the approximation $L_{12} = 0$ of considerable validity in most cases. Accounting for whatever deviation that may exist between the actual L and the one (L_0) under this approximation through C in Eq. (2), it has been found [1, 3, 4, 14] that C is almost nearly identical with a unit matrix in all the $\nu\delta$ cases so far analyzed with the use of sufficiently sensitive additional data, which in turn, upholds the superiority of the lower triangular model for L_0.

It has been shown by MULLER [21] that the extension of this approximation to $n = 3$ cases can be made by considering the problem as being made up of three $n = 2$ cases. Thus, in the most commonly encountered $\nu\nu\delta$ and $\nu\delta\delta$ cases, the suggested approximations are $L_{13} = L_{23} = 0$ and $L_{12} = L_{13} = 0$, respectively. These approximations can also be identified with Eq. (2) by setting $\Phi_{13} = \Phi_{23} = 0$ in the $\nu\nu\delta$ case and $\Phi_{12} = \Phi_{13} = 0$ in the $\nu\delta\delta$ cases. The existence of Φ_{12} and Φ_{23} in these two cases is a consequence of the stretch–stretch or bend–bend coupling being much more appreciable than the stretch–bend coupling.

The extension of MULLER's approximation to any higher-order problem can now be easily performed. The coupling between any two symmetry coordinates S_i and S_j is governed to a large extent by Φ_{ij} which, in turn, may be set to zero, provided that S_i and S_j correspond to stretching and bending vibrations, respectively, and L_0 is taken in the lower triangular form.

In principle, however, one may very much desire to estimate all the $\frac{1}{2}n(n-1)$ parameters Φ_{ij} by using additional experimental data which depend upon the L_{ij} elements. But even in cases where a set of independent and sensitive data like the Coriolis coupling constants or isotopic frequencies are available, they do not provide [22, 23] a sufficient number of equations for the unambiguous estimation of the Φ_{ij} values and the force field. As such, in the light of the approximation suggested by MULLER, one can try to set some of the Φ_{ij}'s to zero, thereby making the available additional experimental data sufficient enough for the solution of the problem.

Analysis of degenerate vibrations

In cases where the vibrations are degenerate, the first-order Coriolis coupling constants ζ_{ii} are often available from the analysis of the respective bands and can be related to the Φ_{ij} parameters as [1, 22]

$$\tilde{C}JC = \zeta \tag{6}$$

where $J = L_0^{-1}C^z\widetilde{L_0^{-1}}$ and C^z is the usual C matrix defined by MEAL and POLO [24]. It is known [22] that for all cases of $n > 2$, there would be infinite sets of force fields fitting the experimental data on vibrational frequencies ω_i and the Coriolis coupling constants ζ_{ii} thus leaving the problem still unsolvable. Setting constraints on the Φ_{ij} parameters provides a logical way out by virtue of their physical significance in the light of the coupling they provide between the various symmetry co-ordinates in a normal mode.

Illustration for $v\delta\delta$ cases

Degenerate vibrations of such higher-order cases very commonly encountered in literature are those associated with $XY_3Z(C_{3v})$- and $XY_5(D_{3h})$-type molecules. One of the normal modes in these types corresponds to stretching and the remaining two correspond to bending between the bonds, thus giving examples of $v\delta\delta$ cases.

Evidently, any a *priori* estimate of the magnitudes of L_{32} or L_{23} which characterise the mixing between the two bending modes would be difficult [21]. However, if the stretch–bend coupling can be taken as small, one can set $\Phi_{12} = \Phi_{13} = 0$, which would then yield

$$\zeta_{11} = J_{11} = C^z_{11}/G_{11} \tag{7}$$

Thus, in cases where J_{11} lies within the ranges of the experimental values of ζ_{11}, one can reasonably expect the constraint $\Phi_{12} = \Phi_{13} = 0$ to represent almost the actual case. The coupling between the two bending modes can then be determined easily from the value of Φ_{23} evaluated by using ζ_{22} or ζ_{33} data in Eq. (6).

As worked examples of the method, two specific cases, *viz.* degenerate vibrations of CH_3F and AsF_5, have been selected, where the condition $J_{11} = \zeta_{11}$ holds extremely well. The force field in CH_3F is already well-established [25] (by employing as many as 22 experimental data), hence this case may be viewed as an illustration of the method. The force field of AsF_5 is not still determined unambiguously (due to the lack of sufficient experimental data), hence, this case may be regarded as an application of the present method.

The equations for ζ_{22} and ζ_{33} emerging from Eq. (6) under the present constraint are

$$J_{22}\cos^2\Phi_{23} + J_{33}\sin^2\Phi_{23} + 2J_{23}\cos\Phi_{23}\sin\Phi_{23} = \zeta_{22} \tag{8}$$

$$J_{22}\sin^2\Phi_{23} + J_{33}\cos^2\Phi_{23} - 2J_{23}\cos\Phi_{23}\sin\Phi_{23} = \zeta_{33} \tag{9}$$

Along with Eq. (7) and the zeta sum rule, it can easily be seen that Eq. (8) or Eq. (9) should lead to the same value of Φ_{23} given by

$$\tan\Phi_{23} = \frac{-J_{23} \pm \sqrt{J_{23}^2 - (J_{22}-\zeta_{22})(J_{33}-\zeta_{22})}}{(J_{33}-\zeta_{22})} \tag{10}$$

$$\tan\Phi_{23} = \frac{+J_{23} \pm \sqrt{J_{23}^2 - (J_{22}-\zeta_{33})(J_{33}-\zeta_{33})}}{(J_{22}-\zeta_{33})} \tag{11}$$

The plus or minus signs of the square root in the above equations suggest two solutions for Φ_{23}, say Φ_{23A} and Φ_{23V}, which can be traced to the quadratic nature of Eqs (8) and (9). The corresponding two sets of force fields can be calculated from Eqs (4), (2) and (5). The two values of Φ_{23} and the two sets of force fields for the degenerate vibrations of CH_3F and AsF_5 are given in Tables I and II respectively along with the values reported earlier [25—27].

Table I

The E species force field of CH_3F fitting the experimental data on vibration frequencies and Coriolis coupling constants*

F_{ij}	Present method		Previous results	
	Set for $\Phi_{23A} = 5°\,7'$	Set for $\Phi_{23V} = 36°\,22'$	Set *A*	Set *B*
F_{11}	4.842 (5.371)	4.842 (5.368)	4.948±0.065 (5.422±0.054)	
F_{22}	0.469 (0.497)	0.392 (0.414)	0.470±0.006 (0.494±0.005)	(0.50)
F_{33}	0.724 (0.760)	0.857 (0.904)	0.722±0.009 (0.756±0.007)	(0.76)
F_{12}	−0.076 (−0.080)	−0.059 (−0.062)	−0.108±0.013 (−0.113±0.012)	
F_{13}	0.099 (0.120)	0.093 (0.098)	0.217±0.093 (0.244±0.084)	
F_{23}	−0.060 (−0.063)	0.023 (0.023)	−0.060±0.006 (−0.063±0.005)	(−0.09)

* The values in parentheses correspond to those obtained after unharmonicity corrections of the observed vibration frequencies.

All F_{ij}-s are in mdyn/A.

Set *A* is due to ALDOUS and MILLS [25] and Set *B* is due to MULLER *et al.* [28]

Table II

The E' species force field of AsF_5 fitting the experimental data on vibration frequencies and Coriolis coupling constants

F_{ij}	Present method		Previous results		
	Set for $\Phi_{23A} = -23° 20'$	Set for $\Phi_{23V} = 23° 20'$	Set *A*	Set *B*	Set *C*
F_{11}	5.368	5.473	5.38±0.5	5.37±0.58	5.29±0.25
F_{22}	0.524	0.171	0.64±0.14	0.18±0.05	0.15±0.05
F_{33}	2.022	2.022	1.83±0.31	2.02±0.78	2.21±0.08
F_{12}	0.045	−0.088	−0.13±0.16	−0.34±0.29	−0.24±0.15
F_{13}	0.213	0.510	0.0±1.0	0.0±1.0	0.01±0.05
F_{23}	0.855	−0.169	0.94±0.11	−0.19±0.39	0

F_{11} is in mdyn/A; F_{22}, F_{33} and F_{23} are in mdyn A; F_{12} and F_{13} are in mdyn.
Set *A* and Set *B* are due to HOSKINS and PERNG [27] and Set *C* is due to LEVIN [26]

The values of force constants corresponding to Φ_{23A} compare extremely well with the established values in the case of CH_3F. The slight deviations in the case of F_{12} and F_{13} elements are expected as a consequence of the nature of the approximation involved in this procedure. The values of F_{ij} elements that can be obtained by the pseudoexact high- and low-frequency separation (HFS) method [28] employing Coriolis coupling constants as additional data are also given in the table. The HFS method gives only three of the F_{ij} elements with a small deviation in the case of the interaction force constant.

The final results in the case of the E' species vibrations of AsF_5 are summarised in Table II. Different force fields fitting the observed frequency and Coriolis data in this case have been reported by LEVIN [26] and HOSKINS and PERNG [27]. The element F_{23} is constrained (by setting it equal to zero) in the set given by LEVIN, while the element F_{13} is constrained (in the range +1 to −1) in the set given by HOSKINS and PERNG. Further, LEVIN [26] has suggested an assignment opposite to the usual practice of setting the equatorial in-plane bending frequency greater than the axial bending frequency. We have employed the assignment suggested by LEVIN in the light of the recent work [22, 29, 30] rendering support to it. Interestingly enough, the two sets of force fields corresponding to Φ_{23A} and Φ_{23V} obtained by the present method lies well within the two sets (*A* and *B*) reported by HOSKINS and PERNG. This indicates that the sets *A* and *B* correspond to an assignment of frequencies as suggested by LEVIN.

HOSKINS and PERNG have discarded their *B* set as anomalous on the basis of the main argument that "$F_{33}(E') \approx 11F_{22}(E')$ is unreasonable". However, the calculation of potential energy contributions [31] to each symmetry

co-ordinate S_j from each normal vibrational mode Q_i given (as $\sum_k L_{ji}L_{ki}F_{jk}/\lambda_i$) in Table III seems to provide a still better way out since, of the two sets, the one corresponding to Φ_{23A} alone indicates large mixing between the two bending modes, which would explain the fluorine equivalence in the NMR spectrum of AsF_5 [27, 32].

Table III

Potential energy contributions to normal modes Q_i from symmetry co-ordinates Q_j corresponding to the two sets of force fields for AsF_5 (Table II) obtained by the present method

	Corresponding to Φ_{23A}			Corresponding to Φ_{23V}		
	S_1	S_2	S_3	S_1	S_2	S_3
Q_1	1	0	0	1	0	0
Q_2	0	0.753	0.247	0	0.933	0.067
Q_3	0	0.247	0.753	0	0.067	0.933

Conclusions

1. The method presented is only pseudoexact in the sense that it brings in a certain amount of decoupling of one of the normal modes from the remaining ones and is expected to work well in cases where such decoupling almost truly exists by virtue of the characteristic nature of vibrations, which is easily checked by the condition ζ_{11} (observed) $\approx J_{11}$ (calculated).

2. The method gives almost the correct values of force constants, though we do not employ a sufficient number of experimental data.

3. The method reflects to some extent the trends in the pseudoexact HFS method employing Coriolis data; however, the latter method [28] involves redefining of the G_{ij} and C^z_{ij} elements and gives only three of the F_{ij} elements as shown in Table I. The present method gives values for all the F_{ij} elements.

4. The method gives two solutions as a consequence of the quadratic nature of Eqs (8) and (9). However, as there are infinite sets of force fields [22] fitting the frequency and Coriolis data, the present state of affairs with two solutions definitely improves the situation. In fact, such multiplicities are inherent in any approach to the problem as already well-established [1—5] in the $n = 2$ cases.

5. The solution of such underdetermined cases is usually performed by constraining some of the F_{ij} elements. However, there exists no rigorous criterion for the choice of the F_{ij} elements to be thus constrained and the results obtained from different choices are often drastically different, thus

bringing in controversies and confusion [26, 27, 33]. The present solution in the case of AsF_5 indicates constraining F_{13} to be preferable.

The present approach of setting constraints on the mixing parameters seems more logical and physically meaningful.

*

It is pleasure to acknowledge the many interesting and helpful discussions with Dr. C. P. GIRIJAVALLABHAN in connection with this work.

REFERENCES

[1] ANANTHAKRISHNAN, T. R., ARULDHAS, G.: J. Mol. Struct., **13,** 163 (1972)
[2] HOY, A. R., STONE, J. M. R., WATSON, J. K. G.: J. Mol. Spectr., **42,** 393 (1972)
[3] ANANTHAKRISHNAN, T. R., GIRIJAVALLABHAN, C. P., ARULDHAS, G.: J. Mol. Struct., **16,** 149 (1973)
[4] ANANTHAKRISHNAN, T. R., GIRIJAVALLABHAN, C. P., ARULDHAS, G.: Indian J. Pure Appl. Phys., **11,** 648 (1973)
[5] ANANTHAKRISHNAN, T. R., ARULDHAS, G.: Acta Chim. (Budapest), **85,** 269 (1975)
[6] FADINI, A.: Z. Naturforsch., **24*a*,** 208 (1969)
[7] RUOFF, A., BURGER, H., BIEDERMANN, S.: Spectrochim. Acta. **27A,** 1359 (1971), **27A,** 1377 (1971)
[8] WILSON, E. B., DECIUS, J. C. CROSS, P. C.: Molecular Vibrations. McGraw-Hill, New York 1955
[9] TAYLOR, W. J.: J. Chem. Phys., **18,** 1301 (1950)
[10] PERSON, W. B., CRAWFORD, B.: J. Chem. Phys., **26,** 1295 (1957)
[11] TÖRÖK, F., PULAY, P.: Acta Chim. Acad. Sci. Hung., **44,** 287 (1965)
[12] TÖRÖK, F., PULAY, P.: J. Mol. Struct., **3,** 1 (1969)
[13] ALIX, A., BERNARD, L.: C. R. Acad. Sc. Paris, **270,** 151 (1970)
[14] ANANTHAKRISHNAN, T. R., ARULDHAS, G.: Proc. All-India Symposia on Physics Education and Research, Cochin University, Cochin 1976, pp. 125—150. Ed. KRISHNAPILLAI, M. G. and BABU JOSEPH, K.
[15] FREEMAN, D. E.: J. Mol. Spectr., **27,** 27 (1968)
[16] TÖRÖK, F.: Acta Chim. Acad. Sci. Hung., **52,** 205 (1967)
[17] ALIX, A., EYSEL, H. H., JORDANOV, B., KEBABCIOGLU, R., MOHAN, N., MULLER, A.: J. Mol. Struct., **27,** 1 (1975)
[18] ANANTHAKRISHNAN, T. R., ARULDHAS, G.: J. Mol. Struct., **23,** 316 (1974)
[19] MULLER, A., SCHMIDT, K. H., MOHAN, N.: J. Chem. Phys., **57,** 1752 (1972)
[20] PEACOCK, C. J., MULLER, A.: J. Mol. Spectr., **26,** 454 (1968)
[21] MULLER, A., PEACOCK, C. J.: J. Mol. Spectr., **30,** 338 (1969)
[22] ANANTHAKRISHNAN, T. R., ARULDHAS, G.: J. Mol. Struct., **26,** 1 (1975)
[23] TÖRÖK, F.: Acta Chim. Acad. Sci. Hung., **57,** 141 (1968)
[24] MEAL, J. H., POLO, S. R.: J. Chem. Phys., **24,** 1126 (1956)
[25] ALDOUS, J., MILLS, I. M.: Spectrochim. Acta, **18,** 1073 (1962)
[26] LEVIN, I. W.: J. Mol. Spectr., **33,** 61 (1970)
[27] HOSKINS, L. C., PERNG, C. N.: J. Chem. Phys., **55,** 5063 (1971)
[28] MULLER, A., RAI, S. N.: J. Mol. Struct., **24,** 59 (1975)
[29] BARTELL, L. S.: Inorg. Chem., **9,** 1594 (1970)
[30] WALKER, W.: J. Mol. Spectr., **43,** 411 (1972)
[31] PULAY, P., TÖRÖK, F.: Acta Chim. Acad. Sci. Hung., **47,** 273 (1966)
[32] MUETTERTIES, E. L., PHILIPS, W. D.: J. Amer. Chem. Soc., **81,** 1084 (1959)
[33] LOCKETT, P., FOWLER, W., WILT, P. M.: J. Chem. Phys., **53,** 452 (1970)

T. R. ANANTHAKRISHNAN; Kalamassery-683104, India

Acta Chimica Academiae Scientiarum Hungaricae, Tomus 92 (4), pp. 403—408 (1977)

CHEMISTRY OF LANTHANIDE CHELATES

SYNTHESIS AND PROPERTIES OF 2-*p*-TOLYLAMINO-4-*p*-TOLYLIMINO-2-PENTENE COMPLEXES OF THE TRIPOSITIVE LANTHANIDE IONS

M. MOHAN

(Department of Chemistry, N. R. E. C. College, Meerut University, Khurja (U.P.) — 203131, India)

Received January 5, 1976,
in revised form June 20, 1976

The reaction of 2-*p*-tolylamino-4-*p*-t olylimino-2-pentene with lanthanide (III) nitrates in anhydrous acetonitrile yields so lid compounds of the type $Ln(L)_n(NO_3)_3$ where Ln^{3+} = La, Pr, Nd, Sm, Gd, Dy, Er and Yb; L = 2-*p*-tolylamino-4-*p*-tolylamino-2-pentene and n = 3 or 4. The compounds have been characterized by analyses, magnetic and spectral studies. Magnetic susceptibilities of the new complexes, measured at room temperature, show little deviation from VanVleck values. Electronic spectra, at room temperature and at liquid nitrogen temperature, show slight and marked enhancement in the intensity of the bands. Nitrate ion co-ordination in several of the complexes is est ared data.

Introduction

Trivalent lanthanide nitrate chelates with 4-amino-3-pentene-2-one, 4-methylamino-3-pentene-2-one, 4-anilino-3-pentene-2-one and 2-phenylamino-4-phenylimino-2-pentene were recently synthesized and characterized in this laboratory [1—4]. The above study has now been extended to include the corresponding lanthanide chelates of the analogous ligand 2-*p*-tolylamino-4-tolylimino-2-pentene. The present paper reports the synthesis and characterization of the new trivalent lanthanide nitrate 2-*p*-tolylamino-4-*p*-tolylamino-2-pentene compounds.

Experimental

Materials. The anhydrous lanthanide (III) nitrates were prepared from lanthanide oxides by reported procedures [5]. Reagent-grade acetonitrile was dried and purified by distillation from phosphorus pentoxide. 2-*p*-tolylamino-4-tolylimino-2-pentene was prepared and characterized by the procedure described elsewhere [6].

Analyses. Carbon, hydrogen and nitrogen analyses were performed in the microanalytical laboratory of I. I. T. Kanpur-16, India. Metal estimations were carried out by known procedures [7]. A complete list of chelates and their analyses are given in Table I.

Magnetic measurements. Magnetic measurements at room temperature (299 K) were made on the pulverized complexes employing Gouy's method. Mercury (II) tetrathiocyanatocobaltate (II) (Xg 16.44×10^{-6} c. g. s. units at 293 K) was used as calibrant.

Table I

Analytical and magnetic data of lanthanide chelates

Compounds prepared*	Colour	Metal (%)		O (%)		H (%)		N (%)		Magnetic moment μ_{eff} (B.M.) at 299 K
		Calc.	Found	Calc.	Found	Calc.	Found	Calc.	Found	
$[La(L)_4NO_3](NO_3)_2$	White	9.64	9.70	63.28	63.30	6.38	6.40	10.69	10.70	Diamag.
$[Pr(L)_4NO_3](NO_3)_2$	Green	9.77	9.80	63.20	63.25	6.37	6.36	10.68	10.71	3.45
$[Nd(L)_4NO_3](NO_3)_2$	Violet	9.97	9.98	63 05	63.01	6.36	6.40	10.64	10.62	3.51
$[Sm(L)_4NO_3](NO_3)_2$	White	10.33	10.41	62.81	62.82	6.33	6.35	10.60	10.59	1.50
$[Gd(L)_4NO_3](NO_3)_2$	White	10.76	10.80	62.52	62.56	6.30	6.28	10.55	10.52	7.88
$[Dy(L)_4](NO_3)_3$	White	11.07	11.15	62.30	62.28	6.28	6.24	10.52	10.53	10.25
$[Er(L)_4](NO_3)_3$	Pink	11.37	11.39	62.09	62.08	6.25	6.28	10.48	10.51	9.32
$[Yb(L)_4](NO_3)_3$	White	11.73	11.76	61.84	61.80	6.23	6.26	10.44	10.47	4.23
$[La(L)_3(NO_3)_2](NO_3)$	White	11.96	12.10	58.87	58.86	5.93	6.00	10.84	10.90	Diamag.
$[Pr(L)_3(NO_3)_2](NO_3)$	Green	12.12	12.20	58.76	58.77	5.92	6.91	10.82	10.84	3.47
$[Nd(L)_3(NO_3)_2](NO_3)$	Violet	12.34	12.41	58.62	58.60	5.91	5.93	10.80	10.79	3.52
$[Sm(L)_3(NO_3)_2](NO_3)$	White	12.78	12.80	58.32	58.35	5.88	5.89	10.74	10.73	1.48
$[Gd(L)_3(NO_3)_2](NO_3)$	White	13.30	13.40	57 97	58.00	5.84	5.86	10.68	10.67	7.88
$[Dy(L)_3(NO_3)_2](NO_3)$	White	13.68	13.72	57 73	57.76	5.82	5.84	10.64	10.65	10.24
$[Er(L)_3(NO_3)_2](NO_3)$	Pink	14.04	14.12	57.49	57.50	5.79	5.77	10.57	10.58	9.31
$[Yb(L)_3(NO_3)_2](NO_3)$	White	14.46	14.50	57.22	57.25	5.77	5.78	10 54	10.59	4.23

* Designation of co-ordination sphere based on infrared spectra

Spectral measurements. The electronic spectra of all the complexes in DMF at room temperature were taken on a Cary-14 spectrophotometer. The IR spectra of the ligand and its lanthanide chelates were recorded on a Model 521 Perkin-Elmer spectrophotometer in potassium bromide. All samples were prepared under completely anhydrous conditions.

Synthesis. All reactions were performed in a dry box in an atmosphere of dry nitrogen gas. Tris and tetrakis lanthanide chelates of the type $Ln(L)_n(NO_3)_3$(Ln^{3+} = La, Pr, Nd, Sm, Gd, Dy, Er and Yb; $n = 3$ or 4; L = 2-*p*-tolylamino-4-tolylimino-2-pentene) were prepared by the direct reaction of the ligand with a lanthanide(III) nitrate in anhydrous acetonitrile. The ligand (0.05 mol for $n = 4$; 0.04 mol for $n = 3$) was dissolved in anhydrous acetonitrile and the solution was added dropwise to a well-stirred acetonitrile solution of 0.01 mol lanthanide nitrate. Precipitation of the product occurred immediately, but a completely stoichiometric product was obtained only after the suspension was heated under reflux for 8 hrs.

Results and discussion

All the lanthanide chelates are white to light yellow in colour, except those of praseodymium and neodymium, which are green and violet, respectively. The limited solubility of these chelates in various organic solvents did not permit the determination of the molecular weight and molar adsorbance. All the complexes show rapid decomposition of the organic part above 270 °C and are finally converted to oxide.

Magnetic susceptibility. Paramagnetic behaviour of the tripositive lanthanide ions is consistent with the presence of unpaired 4f electrons. Since these electrons are well-shielded from external influence both in their spin and orbital motion, the magnetic moment of a complex should indicate whether these 4f electrons take part in bond formation or not. The magnetic moments of all the lanthanide chelates, recorded in Table I, show little deviation from the VAN VLECK values [8] and from the values reported for 8-hydrated sulfates [9], indicating thereby that 4f electrons do not participate in bond formation in these chelates [10—12].

Electronic spectra. The line-like electronic spectra of lanthanide (III) ions result from inner 4f transitions, which are normally forbidden but allowed after the removal of degeneracy in the 4f orbitals by external crystal fields. The small splittings of the characteristic electronic bands are undoubtedly due to the effect of crystal fields upon the J levels of the central ion. The slight shifts in the bands have been attributed by JØRGENSON *et al.* [13—14] to the effect of these crystal fields upon certain parameters related to the interelectronic repulsion among the 4f electrons.

Typical spectral data for solutions of the chelates investigated in DMF are listed in Table II; for comparison, data for aqueous salt solutions are also given. Lanthanum(III) has no significant absorption in the visible region. The absorption bands of praseodymium(III) and neodymium(III) in the visible and near IR region appear to be due to transitions from the $^3H_4$ and $^4I_{9/2}$ ground level to the excited J levels of the 4f configuration, respectively. A red shift or nephelauxetic effect is observed in DMF solutions of the complexes. This is usually accepted as evidence of a higher degree of covalency

Table II

Electronic spectral bands (cm^{-1}) of lanthanide chelates

$PrCl_3$ in H_2O	$[Pr(L)_4NO_3](NO_3)_2$	$(1-\beta)$	$Pr[(L)_3(NO_3)_2](NO_3)$	$(1-\beta)$	Assignment
22 470	22 370	0.44×10^{-2}	22 380	0.40×10^{-2}	$^4H_4 \rightarrow {}^3P_2$
21 324	21 150	0.81×10^{-2}	21 170	0.72×10^{-2}	$\rightarrow {}^3P_1$
20 750	20 580	0.82×10^{-2}	20 600	0.72×10^{-2}	$\rightarrow {}^3P_0$
17 000	16 800	1.17×10^{-2}	16 820	1.05×10^{-2}	$\rightarrow {}^1D_2$
$NdCl_3$ in H_2O	$[Nd(L)_4NO_3](NO_3)_2$	$(1-\beta)$	$[Nd(L)_3(NO_3)_2](NO_3)$	$(1-\beta)$	Assignment
19 550	19 440	0.60×10^{-2}	19 456	0.48×10^{-2}	$^4I_{9/2} \rightarrow {}^2G_{9/2}$
17 360	17 250	0.63×10^{-2}	17 200	0.92×10^{-2}	$\rightarrow {}^4G_{5/2}$
					$^2G_{7/2}$
13 660	13 600	0.43×10^{-2}	13 520	1.02×10^{-2}	$\rightarrow {}^4S_{3/2}$
12 470	12 390	0.71×10^{-2}	12 420	0.40×10^{-2}	$\rightarrow {}^4F_{7/2}$
					$^4F_{5/2}$
$SmCl_3$ in H_2O	$[Sm(L)_4NO_3](NO_3)_2$	$(1-\beta)$	$[Sm(L)_3(NO_3)_2](NO_3)$	$(1-\beta)$	Assignment
24 870	24 690	0.72×10^{-2}	24 720	0.60×10^{-2}	$^6H_{5/2} \rightarrow {}^4F_{9/2}$
24 000	23 750	1.04×10^{-2}	23 800	0.83×10^{-2}	$\rightarrow {}^6P_{5/2}$
21 550	21 400	0.70×10^{-2}	21 500	0.23×10^{-2}	$\rightarrow {}^4I_{13/2}$

than in the aqueous complexes [13—14]. In all the complexes, a marked enhancement in the intensity of the bands has been observed.

IR spectra. Assignments for the nitrate absorptions based upon two possible symmetry types D_{3h} (free nitrate) and C_{2v} (co-ordinated nitrate) [15—17] are given in Table III. The identification of the sharp 1030 cm^{-1}

Table III

Assignment of bands in the regions of nitrate absorption (cm^{-1})

Assignment	$[Ln(L)_4NO_3](NO_3)_2$	$[Ln(L)_3(NO_3)_2](NO_3)$	$[Ln(L)_4](NO_3)_3$
$\nu_2(D_{3h})$	830(m)	825(m)	825(m)
$\nu_3(D_{3h})$	1350(sh)	1360(sh)	1360(s)
$\nu_1(C_{2v})$	1320(s)	1315(s)	—
$\nu_3(C_{2v})$	730(w)	735(w)	—
$\nu_4(C_{2v})$	1428(s)	1435(s)	—
$\nu_5(C_{2v})$	715(vw)	715(vw)	—
$\nu_6(C_{2v})$	800(m)	815(m)	—

band observed for a C_{2v} nitrate group was not possible, due to strong absorption by the NH groups of the co-ordinated ligand molecules.

The IR data indicate that all of the tris chelates contain both co-ordinated and ionic nitrate groups. A distinction between bidentate and monodentate nitrate co-ordination cannot be made on the basis of IR data alone, since both types of co-ordination reduce the symmetry of the nitrate group to C_{2v} [18]. It is also impossible on the basis of infrared data to determine the number of co-ordinated and ionic nitrate groups, thus, the co-ordination number of tris chelates may be 7, 8, 9 or 10. However, the assignment of two bidentate nitrate groups is reasonable, based on the bidentate behaviour of all three nitrate groups in tris(nitrato)bis(dipyridyl)lanthanum(III) [19].

The spectra for tetrakis chelates are of two distinct types. The heavier lanthanide chelates show nitrate absorptions corresponding only to D_{3h} nitrate groups. The fact that addition of a fourth molecule of ligand results in the displacement of co-ordinated nitrate groups from the co-ordination sphere is proof that the solid tetrakis chelates contain four molecules of co-ordinated ligands.

Typical infrared spectra for the tetrakis and tris chelates and for the free ligand in the region of the NH-stretching mode are presented in Fig. 1. Changes in nitrate absorption corresponding to nitrate co-ordination are accompanied by alternations in the NH-stretching region. The spectra of lighter

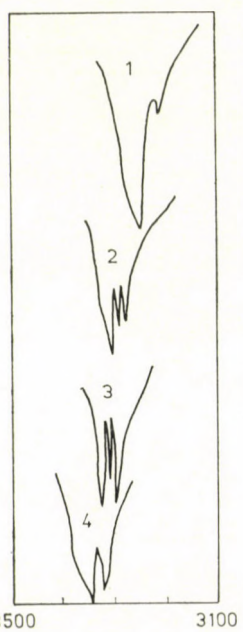

Fig. 1. IR Spectra of lanthanide(III) chelates and free ligand in the NH-stretching region: 1 – $[Ln(L)_4](NO_3)_3$; 2 – $[Ln(L)_4NO_3](NO_3)_2$; 3 – $[Ln(L)_3(NO_3)_2](NO_3)$; 4 – free ligand

tetrakis [La^{3+} to Gd^{3+}] chelates show a shift in the NH-stretching mode of about 40 cm^{-1} to lower frequencies relative to the same bands in the free ligand molecules. In the case of heavier tetrakis Dy^{3+}, Er^{3+} and Yb^{3+} complexes, which do not contain a co-ordinated nitrate group, the shift is 70 cm^{-1} to lower frequencies. The higher frequency component of the NH-stretching mode present in the spectra of the La^{3+} to Gd^{3+} tetrakis chelates disappears in that of the tetrakis Dy^{3+} E_r^{3+} and Yb^{3+} chelates. The spectra of tris chelates also show the same complications as those of the lighter tetrakis chelates. The shift is approximately 20 cm^{-1} in the tris chelates which contain two co-ordinated nitrate groups.

Alterations in the NH-stretching frequencies in these chelates and the large number of bands observed for the chelates containing co-ordinated C_{2v} nitrate were attributed to the overlapping of non-equivalent sets of NH-frequencies. The increase in the frequency of some NH groups may result from repulsion between the nitrogen end of the NH dipole and the co-ordinated nitrate ion [20] or poorer hydrogen bonding of the amino protons with the co-ordinated nitrate ions [21].

*

The author is grateful to Dr. P. C. GUPTA, Principal, N. R. E. C. College, Khurja for the facilities and encouragement.

REFERENCES

[1] MOHAN, M.: Gazz. Chim. Ital. (In press)
[2] MOHAN, M.: Acta Chim. (Budapest) (In press)
[3] MOHAN, M.: Acta. Cincia (In press)
[4] MOHAN, M.: Ann. Chim. (Rome), **65,** 533 (1975)
[5] MOELLER, T., AFTANDILIAN, V. D., CULLEN, G. W.: Inorg. Synt., **5,** 37 (1957)
[6] PARKS, J. E., HOLM, R. H.: Inorg. Chem., **7,** 1408 (1968)
[7] SRIVASTAVA, A. K., RANA, V. B., MOHAN, M., SWAMI, M. P., JAIN, P. C.: J. Inorg. Nucl. Chem., **37,** 723 (1975)
[8] VAN VLECK, J. H., FRANK, A.: Phys. Rev., **34,** 1494 (1929)
[9] YOST, D. M., RUSSEL, H., GARNER, C. S.: The Rare Earth Elements and their Compounds, Chapt. 2 Wiley, 1947
[10] KARAYANNIS, M., MIKULSK, C. M., MINKIEWICZ, J. V., PYTLEWSK, L. L., LABES, M. M.: J. Less-common Metals, **20,** 29 (1970)
[11] IANDELL, A.: Rare Earth Research Ed. E. V. KLEBER p. 135. Macmillan, London 1961
[12] DIDCHEMKOV, R., GORTSEMA, F. P.: J. Phys. Chem. Solids, **24,** 863 (1963)
[13] JØRGENSON, C. K., PAPPALARDO, R., RITTERHAUS, E.: Z. Naturf., **19A,** 424 (1964)
[14] JØRGENSON, C. K.: Acta Chem. Scand., **11,** 981 (1957)
[15] FERRARO, J. R.: J. Mol. Spectrosc., **4,** 99 (1960)
[16] GATEHOUSE, B. M., LIVINGSTONE, S. E., NYHOLM, R. S.: J. Chem. Soc., 4222 (1957)
[17] HERZBERG, G.: Infrared and Raman Spectra of Polyatomic Molecules, pp. 178—79. Van Nostrand, New York 1946
[18] WALKER, A., FERRARO, J. R.: J. Chem. Phys., **43,** 2689 (1965)
[19] AL-KARGHOULI, A. R., WOOD, J. S.: J. Amer. Chem. Soc., **90,** 6548 (1968)
[20] WATT, G. W., KLETT, D. S.: Inorg. Chem., **5,** 1278 (1966)
[21] FUJITA, J., NAKAMOTO, K., KOHAYASHI, M.: J. Amer. Chem. Soc., **78,** 3095 (1956)

M. MOHAN; Department of Chemistry, N.R.E.C. College, Meerut University Khurja (U. P.)-203131, India.

Acta Chimica Academiae Scientiarum Hungaricae, Tomus 92 (4), pp. 409—414 (1977)

EXCESS THERMODYNAMIC PROPERTIES OF MIXING DUE TO DIPOLAR INTERACTIONS

J. LISZI

(Research Group for Electrochemistry, Hungarian Academy of Sciences, Department of Physical Chemistry, University of Chemical Industries, Veszprém)

Received June 28, 1976

Using the grand partition function of binary liquid mixtures, formulas have been derived for the calculation of the dipolar parts of the excess free energy, internal energy and excess entropy of mixing. The formulas have also been extended for the case of multicomponent systems.

There are many attempts in the literature aimed at finding relationships between the dielectric and thermodynamic properties of liquid mixtures. FRANK [1] investigated the thermodynamics of a fluid substance in an electrostatic field. WADA [2] found a relationship between the dielectric constant and the heat of vaporization of non-polar liquids. BELL [3, 4, 5] studied the electrical energy of dipole molecules in different media. MARTIN [6] as well as MOELWYN-HUGHES and THORPE [7] considered the relation between the dielectric properties and the association of liquids. SURYANARAYANA and coworkers [8, 9, 10] studied the relation between the viscosity, internal pressure of liquids, azeotropism and the dielectric behaviour. COLE [11] examined the interactions of polar molecules. AMAYA [12] described the calculation of the electrostatic part of the thermodynamic excess functions due only to the dipole of the polar molecule in binary systems composed of polar and non-polar liquids. HÖRIG and BITTRICH [13] discussed the electrostatic parts of the thermodynamic excess functions, HASKELL [14] dealt with the same properties in terms of molar polarizations.

In the present paper a uniform description of the dipolar parts of the thermodynamic excess-free energy, internal energy and excess entropy of mixing have been calculated, using the grand partition function of binary liquid mixtures. The formulas for the case of multicomponent systems are also given.

The thermodynamic model used here is based on the ONSAGER theory [15] of the static relative permittivity. In the absence of an external electric field only the reaction field (**R**) induced by the dipoles of the polar molecules acts on the molecules of liquids. The energy (U) of a molecule having a permanent dipole moment μ in the field **R** [16] is

$$U = -\frac{\mu \cdot \mathbf{R}}{2} . \qquad (1)$$

With this energy expression the grand partition function for a binary mixture (Ω) is obtained

$$\Omega = \frac{N!}{N_1!\,N_2!}\left(q_1 \exp\left[\frac{\mu_1 \cdot \mathbf{R}_1}{2kT}\right]\right)^{N_1}\left(q_2 \exp\left[\frac{\mu_2 \cdot \mathbf{R}_2}{2kT}\right]\right)^{N_2}, \tag{2}$$

where $N = N_1 + N_2$ is the total number of molecules in the system, N_1 and N_2 are the numbers of the molecules of type 1 and 2, respectively, q is the molecular partition function, k is the BOLTZMANN constant, T is the thermodynamic temperature and the indices refer to the components.

The relationship between the free energy (F) and the partition function is

$$F = -kT \ln \Omega. \tag{4}$$

The grand partition function "before mixing":

$$\Omega^0 = \left(q_1 \exp\left[\frac{\mu_1 \cdot \mathbf{R}_1^0}{2kT}\right]\right)^{N_1}\left(q_2 \exp\left[\frac{\mu_2 \cdot \mathbf{R}_2^0}{2kT}\right]\right)^{N_2}, \tag{5}$$

where the index '0' refers to the pure substances. Equation (5) supposes that the mixing has no effect on the molecular partition functions and the permanent dipole moments. These latter values refer to the gas phase, the intermolecular forces are taken into consideration by the reaction field.

From Eqs (2), (4) and (5) the excess-free energy of mixing (ΔF^E) is

$$\Delta F^E = \frac{1}{2} N_1 \mu_1 \{R_1^0 - R_1\} + \frac{1}{2} N_2 \mu_2 \{R_2^0 - R_2\}. \tag{6}$$

For a mixture containing k components there results

$$\Delta F^E = \frac{1}{2} \sum_{i=1}^{k} N_i \mu_i (R_i^0 - R_i). \tag{7}$$

The relationship between the internal energy (E) and the partition function is

$$E = kT^2 \left(\frac{\partial \ln \Omega}{\partial T}\right)_V, \tag{8}$$

where V is the volume of the system. From Eqs (2), (5) and (8) there results for the energy of mixing

$$\begin{aligned} E - E_0 = \Delta E = \frac{1}{2}\Bigg\{ & N_1 \mu_1 \left[T\left\langle\left(\frac{\partial R_1}{\partial T}\right)_V - \left(\frac{\partial R_1^0}{\partial T}\right)_V\right\rangle + \langle R_1^0 - R_1\rangle\right] + \\ & + N_2 \mu_2 \left[T\left\langle\left(\frac{\partial R_2}{\partial T}\right)_V - \left(\frac{\partial R_2^0}{\partial T}\right)_V\right\rangle + \langle R_2^0 - R_2\rangle\right]\Bigg\}. \end{aligned} \tag{9}$$

For a mixture containing k components one obtains

$$\Delta E = \frac{1}{2} \sum_{i=1}^{k} N_i \mu_i \left[T \left\langle \left(\frac{\partial R_i}{\partial T} \right)_V - \left(\frac{\partial R_i^0}{\partial T} \right)_V \right\rangle + \langle R_i^0 - R_i \rangle \right]. \tag{10}$$

The excess entropy of mixing (ΔS^E) can be calculated by the following relation

$$T\Delta S^E = \Delta E - \Delta F^E. \tag{11}$$

Substituting from (6) and (9) into (11) we get

$$\Delta S^E = \left\{ N_1 \mu_1 \left\langle \left(\frac{\partial R_1}{\partial T} \right)_V - \left(\frac{\partial R_1^0}{\partial T} \right)_V \right\rangle + N_2 \mu_2 \left\langle \left(\frac{\partial R_2}{\partial T} \right)_V - \left(\frac{\partial R_2^0}{\partial T} \right)_V \right\rangle \right\}. \tag{12}$$

For a mixture containing k components there results

$$\Delta S^E = \frac{1}{2} \sum_{i=1}^{k} N_i \mu_i \left\langle \left(\frac{\partial R_i}{\partial T} \right)_V - \left(\frac{\partial R_i^0}{\partial T} \right)_V \right\rangle. \tag{13}$$

The reaction field strength can be expressed by measurable quantities. The reaction field strength of a polarizable dipole molecule [17] is

$$\mathbf{R} = \frac{f}{1 - \alpha f} \boldsymbol{\mu}, \tag{14}$$

where α is the molecular polarizability and f the reaction field factor. The last quantity from the ONSAGER theory [15] is

$$f = \frac{1}{r^3} \frac{2(\varepsilon - 1)}{2\varepsilon + 1}, \tag{15}$$

where r is the radius of the cavity and ε the static relative permittivity of the liquid. The radius of the cavity is given by the following relation [15]

$$\frac{4\pi}{3} \frac{N_A}{v} r^3 = 1 \tag{16}$$

where N_A is the AVOGADRO number, and v the molar volume of the liquid. From these last equations and from the definition of the internal refractivity (n) [18]

$$\frac{n^2 - 1}{n^2 + 2} = \frac{\alpha}{r^3} \tag{17}$$

one can get

$$\mathbf{R} = \frac{8\pi N_A}{9v} \frac{(n^2 + 2)(\varepsilon - 1)}{2\varepsilon + n^2} \boldsymbol{\mu}. \tag{18}$$

Adopting the notation

$$\Phi = \frac{(n^2 + 2)(\varepsilon - 1)}{2\varepsilon + n^2} \tag{19}$$

the reaction field strength is

$$R = \frac{8\pi N_A \mu}{9v} \Phi . \tag{20}$$

From equation (18)

$$\left(\frac{\partial R}{\partial T}\right)_V = \frac{8\pi N_A \mu}{9v} \left\{ \frac{\left(\frac{\partial \varepsilon}{\partial T}\right)_V (n^2 + 2)^2 + 2\left(\frac{\partial n^2}{\partial T}\right)_V (\varepsilon - 1)^2}{(2\varepsilon + n^2)^2} \right\} . \tag{21}$$

Using the notation

$$\varphi = \frac{\left(\frac{\partial \varepsilon}{\partial T}\right)_V (n^2 + 2)^2 + 2\left(\frac{\partial n^2}{\partial T}\right)_V (\varepsilon - 1)^2}{(2\varepsilon + n^2)^2} , \tag{22}$$

$$\left(\frac{\partial R}{\partial T}\right)_V = \frac{8\pi N_A \mu}{9v} \varphi . \tag{23}$$

results.

By equations (20) and (23) the mixing properties due to the dipolar interactions for a k-component system can be written in the following forms

$$\Delta E = \frac{4\pi N_A^2}{9} \sum_{i=1}^{k} x_i \mu_i^2 \left[T \left\langle \frac{\varphi}{v} - \frac{\varphi_i^0}{v_i^0} \right\rangle + \left\langle \frac{\Phi}{v} - \frac{\Phi_i^0}{v_i^0} \right\rangle \right], \tag{24}$$

$$\Delta F^E = \frac{4\pi N_A^2}{9} \sum_{i=1}^{k} x_i \mu_i^2 \left[\frac{\Phi_i^0}{v_i^0} - \frac{\Phi}{v} \right], \tag{25}$$

$$\Delta S^E = \frac{4\pi N_A^2}{9} \sum_{i=1}^{k} x_i \mu_i^2 \left[\frac{\varphi}{v} - \frac{\varphi_i^0}{v_i^0} \right] . \tag{26}$$

In these last equations the quantities without index refer to the mixture.

The application of the method described here is shown by the example of the n-heptane (1)-nitrobenzene (2) mixture. The author's experimental data referring to 20 °C are given in Table I. In the calculations the refractivity index referred to the sodium D line (n_D) was used instead of the internal refractivity. The temperature dependence of n_D is practically independent of the composition, $\left(\frac{\partial n_D^2}{\partial T}\right)_V \simeq 0.0015\ \mathrm{K}^{-1}$. The calculated data* are present-

* In the calculations the $\left(\frac{\partial n_D^2}{\partial T}\right)_V \simeq \left(\frac{\partial n_D^2}{\partial T}\right)_V$ as well as the $\left(\frac{\partial \varepsilon}{\partial T}\right)_P \simeq \left(\frac{\partial \varepsilon}{\partial T}\right)_V$ approximations were used [17].

ed in Table II. In Table III, for comparison's sake, the maximum values of the heat of mixing (ΔH_{max}) are given for some binary mixtures containing nitrobenzene.

Table I

Experimental data

x_2	ε	ϱ(g cm^{-3})	n_D	$\left(\frac{\partial\varepsilon}{\partial T}\right)_V$ (K^{-1})
0	1.90	0.6841	1.3888	0
0.1	3.44	0.7235	1.4042	0.007
0.2	4.98	0.7635	1.4203	0.020
0.3	7.29	0.8069	1.4372	0.035
0.4	9.85	0.8514	1.4527	0.052
0.5	12.29	0.9002	1.4690	0.071
0.7	20.00	1.0096	1.5014	0.121
0.8	24.48	1.0728	1.5189	0.150
0.9	29.74	1.1356	1.5361	0.180
1.0	34.74	1.1982	1.5532	0.203

Table II

Calculated energy functions

x_2	ΔE (Jmol^{-1})	ΔF^E(J mol^{-1})	$T\Delta S^E$(J mol^{-1})
0	0	0	0
0.1	263	231	32
0.2	480	369	111
0.3	593	434	159
0.4	646	470	176
0.5	687	485	202
0.7	522	387	135
0.8	383	281	102
0.9	200	149	51
1.0	0	0	0

Table III

Literary data

The pair of the nitrobenzene in the mixture	ΔH_{max} (J mol^{-1})
Benzene	265* [19]
1,2-dimethyl benzene	275* [19]
1,4-dimethyl benzene	289* [19]
Cyclohexane	1550** [20]

* 293 K
** 298 K

The comparison shows that the ΔE values in Table II can be considered as reasonable ones.

REFERENCES

[1] FRANK, H. S.: J. Chem. Phys., **23,** 2023 (1955)
[2] WADA, A.: Bull. Chem. Soc. Japan, **25,** 401 (1952)
[3] BELL, R. P.: Trans. Faraday Soc., **27,** 797 (1931)
[4] BELL, R. P.: J. Chem. Soc. **139,** 1371 (1931)
[5] BELL, R. P.: Trans. Faraday Soc., **31,** 1557 (1935)
[6] MARTIN, A. R.: Trans. Faraday Soc., **30,** 759 (1934)
[7] MOELWYN, E. A.-HUGHES, THORPE, P. L.: Proc. Roy. Soc., A277 423 (1964)
[8] SURYANARAYANA, C. V.: Monatsh. Chem. **91,** 139 (1960)
[9] SURYANARAYANA, C. V., GOVINDASWAMY, S.: Monath. Chem. **92,** 203 (1961)
[10] SURYANARAYANA, C. V., SOMASUNDARAM, K. M.: Z. Naturforschung, **15*a*,** 551 (1960)
[11] COLE, R. H.: J. Chem. Phys., **39,** 2602 (1963)
[12] AMAYA, K.: Bull. Chem. Soc. Japan, **34,** 1349 (1961)
[13] HÖRIG, H. J., BITTRICH, H. J.: Wiss. Z. T. H. Chemie, Leuna-Merseburg, **8,** 168 (1966)
[14] HASKELL, R. W.: J. Phys. Chem. **73,** 2916 (1969)
[15] ONSAGER, L.: J. Amer. Chem. Soc., **58,** 1486 (1936)
[16] FRÖCHLICH, H.: Theory of Dielectrics, 2nd ed., Oxford Press, Oxford 1957
[17] BÖTTCHER, C. J. F.: Theory of Electric Polarization; Revised by VAN BELLE, O. C., BORDEWIJK, P., RIP, A.: Vol. 1., Elsevier Sci. Publ. Co., Amsterdam, London, New York 1973
[18] HILL, N. E., WAUGHAN, W. E., PRICE, A. H., DAVIES, M.: Dielectric Properties and Molecular Behaviour; Van Nostrand Reinhold Co., London, New York, Toronto, Melbourne 1969
[19] Selected Data on Mixtures A (Ed. by H. V. KEHIAIAN), Vol. 1974. No. 3.
[20] AMAYA, K.: Bull. Chem. Soc. Japan, **34,** 1278 (1961)

János LISZI; H-8201 Veszprém P.O.B. 28.

Acta Chimica Academiae Scientiarum Hungaricae, Tomus 92 (4), pp. 415—419 (1977)

OXAZEPINES AND THIAZEPINES, III*

SYNTHESIS OF 2,3-DIHYDRO-2,4-DIPHENYL-1,5-BENZOTHIAZEPINES BY THE REACTION OF 2-AMINOTHIOPHENOL WITH CHALCONES SUBSTITUTED IN RING A

A. LÉVAI and R. BOGNÁR

(Institute of Organic Chemistry, Kossuth Lajos University, Debrecen)

Received April 14, 1976

The reaction of 2-aminothiophenol with twelve chalcones (**I**—**XII**), variously substituted in ring A, has been studied in hot, anhydrous toluene. It has been found that, depending on the substitution pattern of ring A, either β-phenyl-β-(2-aminophenylmercapto)propiophenones (**XIII**—**XVIII**) or 2,3-dihydro-2,4-diphenyl-1,5-benzothiazepines (**XXV**—**XXVIII**) are formed. The β-phenyl-β-(2-aminophenylmercapto)-propiophenones (**XIII**—**XVIII**) were converted into 2,3-dihydro-2,4-diphenyl-1,5-benzothiazepines (**XIX**—**XXIV**) by boiling them in methanolic solution in the presence of acetic acid catalyst.

The reactions of 2-aminothiophenol with α, β-unsaturated ketones, among them with chalcones, have been studied by several research groups, and numerous dihydro-1,5-benzothiazepines were synthesized in this way [1—5]. As a result of this work it has been ascertained that, depending on the reaction conditions, either dihydro-1,5-benzothiazepines or the addition products, *i. e.* β-(2-aminophenylmercapto)-ketones are obtained; the latter compounds can then be readily converted into the corresponding dihydro-1,5-benzothiazepines [3, 5]. These results are in accordance with a two-step reaction sequence, *viz.* first nucleophilic addition of the mercapto group to the β-carbon atom of the unsaturated ketone, followed by condensation of the amino and carbonyl groups to form the seven-membered hetero ring. The reaction conditions can significantly influence whether only the first, or also the second reaction step occurs [1, 3].

With chalcones, before our work, no attempts had been made at investigating how the substitution pattern of the aromatic rings of the chalcone used influences these reactions. In our experiments, we have studied the reactions of 2-aminothiophenol with chalcones variously substituted in rings A and B. Our previous paper [5] describes such reactions of chalcones substituted in ring B. In the present paper the reactions of 2-aminothiophenol with chalcones having different substituents in ring A will be reported.

Twelve chalcones (**I**—**XII**) were boiled, each for 3 hours, in anhydrous toluene with a small excess of 2-aminothiophenol and, depending on the substitution pattern, the following compounds were obtained.

* For Part II, see Ref. [5]

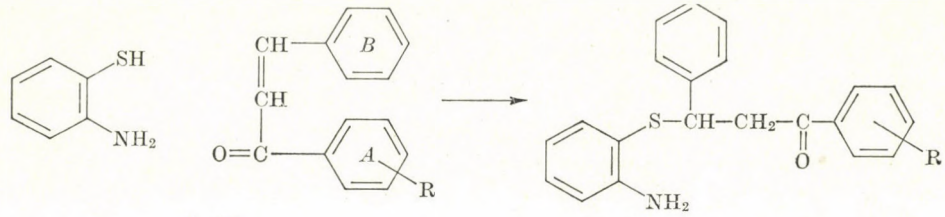

I–VI XIII–XVIII

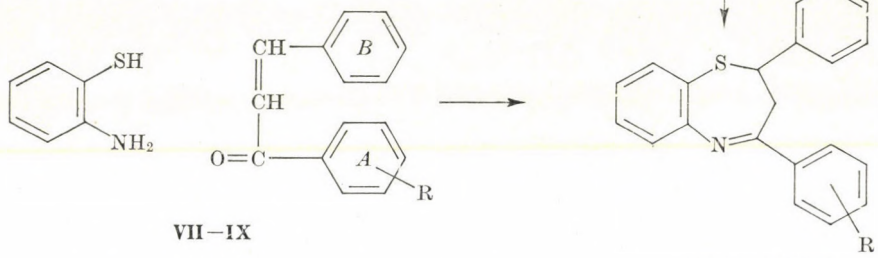

VII–IX XIX–XXVII

I, XIII, XIX: R = 4-CH_3
II, XIV, XX: R = 4-OCH_3
III, XV, XXI: R = 4-OH
IV, XVI, XXII: R = 4-F
V, XVII, XXIII: R = 4-Cl
VI, XVIII, XXIV: R = 3-Br
VII, XXV: R = 2-OH
VIII, XXVI: R = 2-OH, 4-OCH_3
IX, XXVII: R = 4-Br

If ring A has an electron donor (**I**—**IV**) or slightly electron-withdrawing (**V** and **VI**) substituent, which probably does not influence significantly the conjugation and/or the geometry of the molecule, the reaction takes place as in the case of unsubstituted chalcone [5] and β-phenyl-β-(2-aminophenylmercapto)propiophenones (**XIII**—**XVIII**) are formed. However, the presence of a hydroxyl group in *ortho* position (**VII** and **VIII**) can stabilize the plane of the carbonyl group and the double bond by chelation, or may result in quasi-protonation of the carbonyl group which, in turn, promotes the condensation step and thus the formation of the seven-membered hetero ring. Therefore, from compounds **VII** and **VIII** 2,3-dihydro-2,4-diphenyl-1,5-benzothiazepines (**XXV** and **XXVI**) are obtained directly.

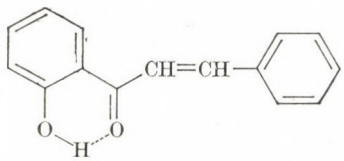

Of chalcones with a nitro group in ring A (**X**—**XII**) only the 3'-nitrochalcone (**XI**) could be made to react with 2-aminothiophenol under the above mentioned reaction conditions. This compound and the 4'-bromochalcone

(**IX**) gave directly the benzothiazepine (**XXVII** and **XXVIII**, respectively) in boiling toluene. In the case of these two compounds the electron-withdrawing substituent can polarize the carbonyl group to such an extent that both reaction steps take place in boiling toluene.

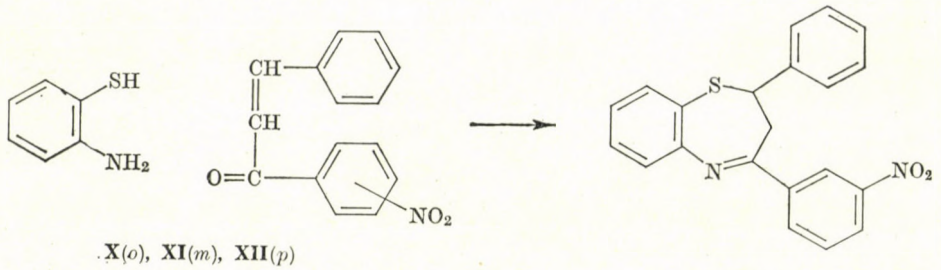

X(*o*), **XI**(*m*), **XII**(*p*)

XXVIII

Chalcones with an *ortho*- (**X**) or *para*-nitro group (**XII**) in ring A could not made to react with 2-aminothiophenol even during a longer reaction time (6 hrs). In the case of **X**, this inhibition may be due to a steric and a conjugation effect, *i. e.* the deformation of the plane of the $-(C=O)-CH=CH-$ chain, whereas a *para*-nitro group can upset the conjugation of the carbonyl group and the double bond so much that the nucleophilic addition of the mercapto group is hindered, the reason for the absence of the reaction thus being a conjugation effect.

The β-phenyl-β-(2-aminophenylmercapto)propiophenones (**XIII**—**XVIII**) were converted into 2,3-dihydro-2,4-diphenyl-1,5-benzothiazepines (**XIX**—**XXIV**) by boiling them in anhydrous methanol in the presence of acetic acid catalyst.

The C=O and NH_2 bands appearing in the infrared spectra of the β-phenyl-β-(2-aminophenylmercapto)propiophenones (**XIII**—**XVIII**), and the C=N band of 2,3-dihydro-2,4-diphenyl-1,5-benzothiazepines (**XIX**—**XXVIII**) unequivocally prove that these compounds have the structures ascribed them.

Experimental

M. p.'s are uncorrected.

IR spectra were obtained in KBr discs, with a UNICAM SP 200G instrument.

The chalcones were synthesized by the condensation of benzaldehyde and substituted acetophenones in alkaline ethanolic solution as described in the literature [6—11].

β-Phenyl-β-(2-aminophenylmercapto)propiophenones

The chalcone (**I**—**VI**) (10 mmoles) and 2-aminothiophenol (12 mmoles) were dissolved in dry toluene, and refluxed for 3 hrs in an apparatus provided with a water separator; the solvent was then removed in vacuum. The residue was crystallized from methanol to obtain compounds **XIII**—**XVIII** (Table I).

In such reaction conditions chalcones **VII**—**IX** and **XI** gave the benzothiazepines (**XXV**—**XXVIII**) (Table II).

Acta Chimica (Budapest) 92, 1977

Table I

Physical constants and analysis data of β-phenyl-β-(2-aminophenylmercapto)propiophenones

	M.p., °C	Yield, %	Overall formula	Molecular weight	Analysis, %					
					Calculated			Found		
					C	H	N	C	H	N
XIII	137—138	67.6	$C_{22}H_{21}ONS$	347.39	76.08	6.05	4.03	75.83	5.91	4.04
XIV	111—112	69.4	$C_{22}H_{21}O_2NS$	363.39	72.72	5.78	3.85	72.46	5.89	3.96
XV	177—178	65.7	$C_{21}H_{19}O_2NS$	349.36	72.20	5.44	4.01	72.23	5.58	4.17
XVI	115—116	65.6	$C_{21}H_{18}ONSF$	351.35	71.79	5.12	3.98	71.55	5.11	3.91
XVII	111—112	72.2	$C_{21}H_{18}ONSCl$	367.80	68.66	4.90	3.81	68.92	4.89	3.78
XVIII	101—102	75.3	$C_{21}H_{18}ONSBr$	412.26	61.16	4.36	3.39	61.93	4.41	3.31

Table II

Physical constants and analysis data of 2,3-dihydro-2,4-diphenyl-1,5-benzothiazepines

	M.p., °C	Yield, %	Overall formula	Molecular weight	Analysis, %					
					Calculated			Found		
					C	H	N	C	H	N
XIX	132—133	74.9	$C_{22}H_{19}NS$	329.37	80.24	5.77	4.25	80.52	5.85	4.19
XX	124—125	72.3	$C_{22}H_{19}ONS$	345.37	76.52	5.50	4.05	76.57	5.58	4.18
XXI	198—199	74.4	$C_{21}H_{17}ONS$	331.35	76.13	5.13	4.22	75.76	5.22	4.26
XXII	102—103	73.4	$C_{21}H_{16}NSF$	333.34	75.67	4.80	4.20	75.77	4.77	4.16
XXIII	134—135	84.2	$C_{21}H_{16}NSCl$	349.79	72.01	4.57	4.02	72.02	4.68	4.09
XXIV	113—114	88.8	$C_{21}H_{16}NSBr$	394.25	63.95	4.05	3.56	64.58	4.14	3.48
XXV	146—147	75.7	$C_{21}H_{17}ONS$	331.35	76.13	5.13	4.22	76.55	5.15	4.31
XXVI	165—166	63.8	$C_{22}H_{19}O_2NS$	361.37	73.13	5.26	3.87	73.43	5.35	3.98
XXVII	136—137	65.8	$C_{21}H_{16}NSBr$	394.25	63.95	4.05	3.56	63.61	4.15	3.53
XXVIII	126—127	43.0	$C_{21}H_{16}O_2N_2S$	360.34	69.97	4.44	7.77	69.83	4.55	7.65

2,3-Dihydro-2,4-diphenyl-1,5-benzothiazepines

β-Phenyl-β-(2-aminophenylmercapto)propiophenone (**XIII**—**XVIII**) (1.0 g) was refluxed for 1 hr in a mixture of anhydrous methanol (50 ml) and glacial acetic acid (1 ml). The product which separated after cooling was recrystallized from methanol: in this way compounds **XIX**—**XXIV** were prepared (Table II).

Table III

IR spectral data of β-phenyl-β-(2-aminophenylmercapto)propiophenones and 2,3-dihydro-2,4-diphenyl-1,5-benzothiazepines

Propiophenones				Thiazepines	
	$\nu C{=}O$ [cm^{-1}]		νNH_2 [cm^{-1}]		$\nu C{=}N$ [cm^{-1}]
XIII	1675		3370, 3475	**XIX**	1605
XIV	1668		3360, 3460	**XX**	1600
XV	1667		3358, 3458	**XXI**	1600
XVI	1680		3353, 3456	**XXII**	1600
XVII	1686		3357, 3455	**XXIII**	1610
XVIII	1684		3344, 3449	**XXIV**	1607
				XXV	1599
				XXVI	1600
				XXVII	1610
				XXVIII	1613

The authors' thanks are due to Dr. S. SZABÓ for the IR spectra and for his help in their evaluation, to Mrs. E. HAJNAL for her valuable assistance in the experimental work. The present work was sponsored by the Hungarian Academy of Sciences for which our gratitude is expressed.

REFERENCES

[1] RIED, W., MARX, W.: Ber. **90,** 2683 (1957)
[2] MUSKALO, L. K.: Obshch. Khim. **28,** 507 (1958)
[3] STEPHENS, W. D., FIELD, L.: J. Org. Chem. **24,** 1576 (1959)
[4] HIDEG-HANKOVSZKY, O., HIDEG, K.: Acta Chim. Acad. Sci. Hung. **68,** 403 (1971)
[5] LÉVAI, A., BOGNÁR, R.: Acta Chim. (Budapest) **88,** 293 (1976)
[6] KOSTANECKI VON, St., TAMBOR, J.: Ber. **32,** 1924 (1899)
[7] BARGELLINI, G., MONTI, L.: Gaz. chim. ital. **2,** 25 (1914); C. A. **9,** 447 (1915)
[8] WEYGAND, C., BAUER, E., GÜNTHER, H., HEYNEMANN, W.: Ann. **459,** 99 (1927)
[9] DILTHEY, W., NEUHAUS, L., SCHOMMER, W.: J. prakt. Chem. **123,** 235 (1929)
[10] BARNES, R. P., DODSON, L. B.: J. Am. Chem. Soc. **65,** 1585 (1943)
[11] MICHEL, J.: Bull. soc. chim. Belges **48,** 105 (1939), C. A. **33,** 7650 (1939)

Albert LÉVAI
Rezső BOGNÁR } H-4010 Debrecen KLTE

Acta Chimica Academiae Scientiarum Hungaricae, Tomus 92 (4), pp. 421—426 (1977)

THE ACYLATION OF 4,6-O-BENZYLIDENE-2--BENZYLOXYCARBONYLAMINO-2-DESOXY-D--GLUCONIC ACID[1]

GY. DEÁK, K. GÁLL-ISTÓK, J. HASKÓ-BREUER and P. SOHÁR*

*(Research Institute for Experimental Medicine of the Hungarian Academy of Sciences, Budapest and *Research Institute for Pharmaceutical Chemistry, Budapest)*

Received June 15, 1976

When 4,6-O-Benzylidene-2-benzyloxycarbonyl-D-glucosaminic acid was acylated in the usual manner, 2-benzyloxycarbonylamino-4,6-O-benzylidene-2,3-dideoxy-D-*erythro*-hex-2-enoic-1,5-lactone [**6**] was obtained in good yields.

When glucosaminic acid, regarded as an analogue of serine, was used as the amino acid component in peptide synthesis, it was observed that, owing to the interfering action of the hydroxyl groups, several methods generally applied such syntheses (DCC, active ester, mixed anhydride) failed even in the case of using 4,6-O-benzylidene glucosaminic acid, although work with this compound is more convenient than with glucosaminic acid itself. Another difficulty was that, owing to the nature of the compound, it is scarcely soluble in the apolar solvents generally used in peptide syntheses. Since protection of the hydroxyl groups by benzylation and *t*-butylation could not be employed, acylation was attempted.

The ethyl ester of 4,6-O-benzylidene-2-benzyloxycarbonylglucosaminic acid [4] was made to react with acetic anhydride or benzoyl chloride in anhydrous pyridine solution, according to the procedure suggested by Einhorn, when the respective 3,5-diacyl derivatives were obtained in satisfactory yields. However, acetylation of 4,6-O-benzylidene-2-benzyloxycarbonyl-glucosaminic acid carried out under similar conditions yielded a product different from the expected one. The same product was obtained when the acylation was accomplished in pyridine with benzoyl chloride or benzoic anhydride, or in acetic anhydride or benzoic anhydride in the presence of sodium acetate or sodium benzoate, respectively. The highest yield (80%) was achieved in the acylation process in acetic anhydride with sodium acetate.

In the IR spectrum of the product the bands characteristic of OH groups are absent, but the expected νCO band of the ester group did not appear either. However, there were new bands at 1725 cm^{-1} and 1645 cm^{-1}. Elemental analysis and molecular weight determination indicated the formula $C_{21}H_{19}O_6N$

[1] Preliminary communication, see Ref. [1]

which is by a fragment of composition $C_4H_8O_4$ less than the expected value.

The changes in the IR spectrum were not satisfactory to afford evidence for the decomposition of the benzylidene or benzyloxycarbonyl group under the conditions of the reaction. Therefore, in the subsequent acylations such a derivative of glucosaminic acid had to be chosen as the starting material whose IR spectrum clearly shows the presence of the arylidene group. For this purpose, the 4-chlorobenzylidene derivative was tried, since this group can be well detected in both elemental analysis and the IR spectra. The preparation procedure for this compound is shown in Scheme 1 (4).

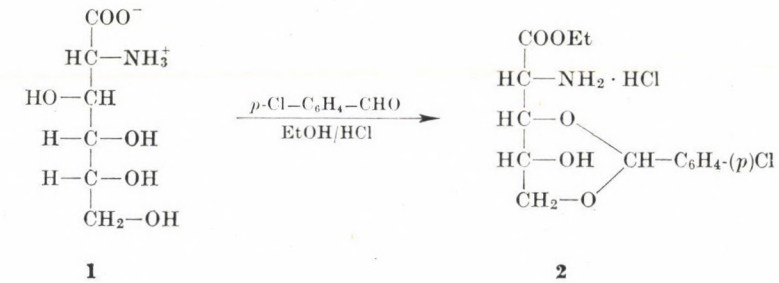

1 2

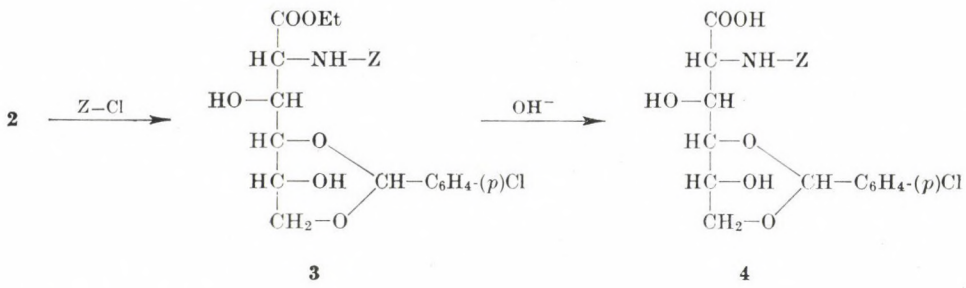

3 4

Z = $-C(=O)-O-CH_2-C_6H_5$

4,6-O-4'-Chlorobenzylidene-2-benzyloxycarbonyl-glucosaminic acid, synthesized first by us, was acylated with acetic anhydride in pyridine; the product had the same character as that obtained in the acylation of the parent compound.

The IR spectrum of the substance clearly showed the presence of intact arylidene and benzyloxycarbonyl groups after the reaction.

On the basis of these findings and the IR and NMR spectra [1], the product proved to be 2-benzyloxycarbonylamino-4,6-O-benzylidene-2,3-dideoxy-D-*erythro*-hex-2-enoic-1,5-lactone (6). The structure was also confirmed

by chemical methods: reaction with hydrazine hydrate yielded 1-benzyloxycarbonylamino-3,5-O-benzylidene-1,2-dideoxy-D-*erythro*-1-pentenecarboxylic acid hydrazide (**7**) (Scheme 2).

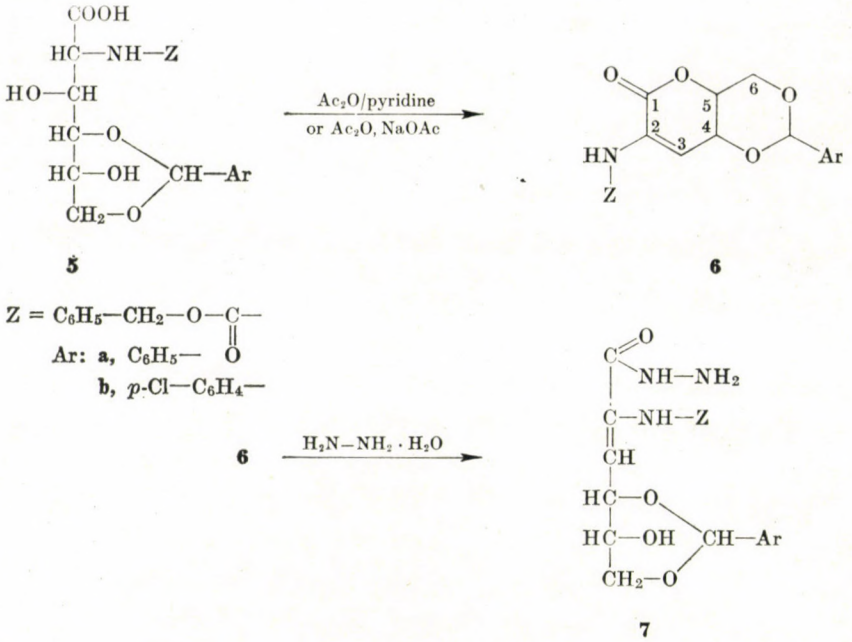

In view of these facts, during the acylation of the glucosaminic acid derivative, lactonization and β-elimination take place simultaneously, or subsequently. Lactonization must be of crucial importance in the β-elimination step, since in the acylation of the glucosaminic ester, where no lactonization is possible, β-elimination cannot be observed.

KUZUHARA and EMOTO [2] reported similar results on refluxing the N-benzamido derivative of benzylideneglucosaminic acid with an excess of acetic anhydride in absolute pyridine. In our experiments the conversion was observed at room temperature and it was also attempted to detect (or occassionally isolate) some intermediate by monitoring the course of the conversion. TLC and IR spectroscopy were used for this purpose, however, under various reaction conditions, always the starting material and the product could only be detected. This may indicate that the slow step in the reaction is lactonization, followed by the rapid elimination step.

Since the direct approach failed, the preparation of the acetylated glucosaminic acid derivative was attempted by starting from the acetylated derivative of such an ester of this compound, where the ester can be hydrolyzed selectively without affecting the acetyl groups. The dimethylaminoethyl ester

used by GREBEN *et al.* [3] seemed to be suitable, since it rapidly undergoes hydrolysis in 2—4% sodium hydrogen carbonate solution at room temperature. However, the dimethylaminoethyl ester of N-benzyloxycarbonyl-4,6-O-benzylidene-D-glucosaminic acid could not be prepared. Acid-catalyzed direct esterification could not be used because of the presence of the acetal bond in the compound. Establishing the ester bond by means of DCC could not be achieved because of lactonization caused by the reagent. Therefore, the preparation of the ester was tried by reacting the silver salt of the acid with dimethylaminoethyl bromide. However, the product obtained proved to be the N,N-dimethylaziridinium salt (**8**) of the starting acid (**5**) (Scheme 3). This shows

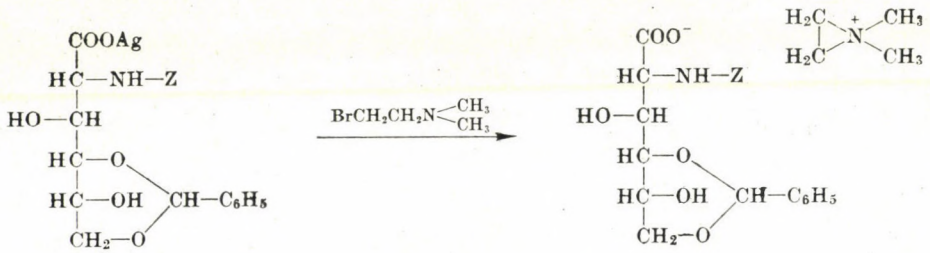

2 **8**

that the well-known cyclization reaction of dimethylaminoethyl bromide is more rapid than its reaction with the silver salt of the acid. Alcoholysis also failed in the preparation of the ester. When N-benzyloxycarbonyl-4,6-O-benzylidene-D-glucosaminic acid ethyl ester was allowed to react in absolute dimethylaminoethanol in the presence of trace amounts of metallic sodium without heating, no starting material could be detected in the solution by TLC after the dissolution of the substance. Since the expected product could not be isolated from the solution in pure state, the volatile components were removed in vacuum and the residual syrup was dissolved in absolute pyridine and acylated with an excess of acetic anhydride. When processing the mixture, the product expected could not be obtained, but, surprisingly, the dideoxy-lactone derivative (**6**) was isolated in 50% yield.

Experimental

4,6-O-(4'-Chlorobenzylidene)-glucosaminic acid ethyl ester. HCl (2)

Glucosaminic acid (3.3 g; 18 mmoles) was dissolved in absolute ethanol (35 ml) at room temperature with stirring, and freshly distilled and ground *p*-chlorobenzaldehyde (5.8 g; 40 mmoles) was added to it. Dry HCl gas was introduced into the solution for 4 min under stirring; the temperature rose to 65 °C and a clear yellow solution was obtained. The reaction mixture was allowed to cool under stirring; by the next day it partly solidified. Dry ether (40 ml) was added, the mixture was cooled to —20 °C for 3 hrs, then the solid was filtered off, washed

with dry ether and dried over Siccapent in a vacuum exsiccator. Recrystallization from a mixture of ethanol and ether (150 ml + 100 ml) gave a white crystalline substance in 62% yield, m. p. 185 °C (d.).

$C_{15}H_{21}Cl_2NO_6$ (382.25). Calcd. C 47.13; H 5.54; N 3.66; Cl 18.55. Found C 47.14; H 5.83; N 3.60; Cl 18.67%.

4,6-0-(4'-Chlorobenzylidene)-2-benzyloxycarbonylglucosaminic acid ethyl ester (3)

Compound **2** (14.2 g; 37.5 mmoles) was dissolved in water (250 ml) with stirring, chloroform (340 ml) was added to the solution, it was cooled to 0 °C, and then magnesium oxide (2.3 g; 57.7 mmoles) was added. In the next step, benzyloxycarbonyl chloride, (8.3 g) was added dropwise to the solution during 10 min at 0 °C under vigorous stirring. The pH had to be maintained at 8. Stirring was continued for 5 hrs at a temperature between 0° and +5 °C, then the excess benzyloxycarbonyl chloride was decomposed by stirring with pyridine (4 ml) for 5 min. The solution was acidified to pH 3 with 5*N* hydrochlorid acid, the two phases were separated in a separatory funnel and the aqueous phase was extracted with chloroform (2 × 50 ml). The combined chloroform phase was washed with 0.5*N* hydrochloric acid (2 × 300 ml), water (2 × 350 ml), 5% sodium hydrocarbonate (2 × 350 ml) and water (2 × 350 ml). Then it was dried over anhydrous sodium sulfate, filtered, the solvent removed, and the crude product crystallized from a mixture of ethyl acetate and petroleum ether. A white crystalline product was obtained in 75% yield (13.6 g), m. p. 166 °C.

$C_{23}H_{26}ClNO_8$ (479.92). Calcd. C 57.57; H 5.46; N 2.92; Cl 7.39. Found C 57.84; H 5.42; N 2.89; Cl 7.20%.

4,6-0-(4'-Chlorobenzylidene)-2-benzyloxycarbonylglucosaminic acid (4)

Compound **3** (7.2 g; 15 mmoles) was dissolved in methanol (720 ml) with stirring, the solution was cooled to 0 °C, then 1*N* sodium hydroxide (17.5 ml) was added with stirring which was then continued for 1 hr at 0 °C. The solution was filtered and evaporated to dryness in vacuum. The white solid was rubbed with water (10 ml). The suspension was acidified with 2*N* hydrochloric acid (6 ml), diluted with water (60 ml), cooled and filtered. The precipitate was washed with water (5 × 240 ml) until neutral, and then dried in air. After crystallization from a mixture of ethanol and petroleum ether, a white crystalline substance was obtained (4.4 g; 65%), m. p. 176—177 °C.

$C_{21}H_{22}ClNO_8$ (451.86). Calcd. V 55.81; H 4.91; N 3.30; Cl 7.85. Found C 55.62; H 5.12; N 3.38; Cl 7.67%.

1-Benzyloxycarbonylamino-3,5-0-(4'-chlorobenzylidene)-1,2-dideoxy-D-erythro--1-pentenecarboxylic acid hydrazide (7b)

Lactone **6b** (0.83 g; 2 mmoles) was dissolved in a mixture of methanol (15 ml) and dimethylformamide (15 ml), and hydrazine hydrate (0.5 ml) was added to the solution. The clear mixture was refluxed at 100 °C for 4 hrs, then allowed to stand at room temperature for 12 hrs; the crystalline hydrazide separated. After filtration and drying a white crystalline substance was obtained (0.3 g; 34%), m. p. 245 °C (d).

$C_{21}H_{22}ClN_3O_6$ (447.874). Calcd. C 56.31; H 4.95; N 9.38. Found C 56.34; H 5.19; N 9.35%.

Attempted preparation of 4,6-0-benzylidene-2-benzyloxycarbonylglucosaminic acid dimethylaminoethyl ester

4,6-O-Benzylidene-2-benzyloxycarbonylglucosaminic acid silver salt (1.67 g; 3 mmoles) was suspended in absolute chloroform (20 ml), cooled to 0 °C and a solution of dimethylaminoethyl bromide (0.45 g; 3 mmoles) in absolute chloroform (10 ml) at 0 °C was added to the reaction mixture in small portions during 1.5 hrs, with vigorous stirring. Stirring was continued for 2 hrs at 0 °C, then the mixture was allowed to stand at room temperature for 20 hrs. The silver bromide precipitate was removed by centrifuging. (0.55 g AgBr was obtained; the weight of 3 mmoles of AgBr is 0.56 g.) The chloroform solution was evaporated to dryness at room temperature to leave a pink solid foam (1.3 g), whose m. p. could not be determined.

The product which was presumably the aziridinium salt (0.5 g), was dissolved in water, the pH of the solution was adjusted to 3—4 with 2*H* HCl while cooling. The white precipitate (0.45 g; 82.5%) proved to be (**5**).

Acetylation in pyridine

Compound **5a** (1.23 g; 3 mmoles) was dissolved in absolute pyridine (12 ml), the clear solution was cooled to 0 °C, and acetic anhydride (0.68 g; 0.63 ml) (6 mmoles + 10% excess) was added to it. The clear solution was allowed to stand at room temperature for 72 hrs, poured into ice-water and acidifield to pH 3 with conc. HCl. The white precipitate was filtered off and washed with water until free from Cl^-. After drying, the substance was crystallized from ethyl acetate to obtain white crystalline 2-benzyloxycarbonylamino-4,6-O-benzylidine-2,3-dideoxy-D-*erythro*-hex-2-enoic lactone (**6a**) (0.8g; 77%), m. p. 190 °C (d).

$C_{21}H_{19}NO_6$ (381.38). Calcd. 66.14; H 5.02. Found C 65.83; H 5.30%.

Acetylation in acetic anhydride in the presence of sodium acetate

Acetic anhydride (8 ml) and anhydrous sodium acetate (0.5 g; 6 mmoles) were heated on a water bath for 5 min, then compound **5** (2.1 g; 5 mmoles) was added to it in small portions during 10 min. The mixture was stirred at 100 °C for 1 hr whereupon it became a jelly. The mass was rubbed with ice-water (30 ml), filtered off and washed with water until free from acid, and dried. Crystallization from ethyl acetate gave compound **6** (1.5 g; 80%).

Calcd. C 66.14; H 5.02; N 3.67. Found C 66.40; H 5.27; N 3.72%.

2-Benzyloxycarbonylamino-4,6-O-(4'-chlorobenzylidene)-2,3-dideoxy-D-erythro-hex-2-enoic lactone

Compound **5b** (4.2 g; 10 mmoles) was treated in absolute pyridine as described above. A white crystalline product 2.7 g; 65% was obtained, m. p. 205—206 °C.

$C_{21}H_{18}ClNO_6$ (415.83). Calcd. C 60.67; H 4.36; N 3.37; Cl 8.53. Found C 60.40; H 4.60; N 3.23; Cl 8.58%.

REFERENCES

[1] DEÁK, GY., GÁLL-ISTÓK, K., SOHÁR, P.: Acta Chim. (Budapest) **75,** 189 (1973)
[2] HIROYOSHI KUZUHARA, SAKAE EMOTO: Agr. Biol. Chem. (Tokyo) **26,** 334 (1962); C. A. **58,** 4638 (1963)
[3] GREBEN, A. E., MARTINOV, V. F., TITOV, M. I.: Zhurn. Obshch. Chim. **38,** 664 (1968)
[4] HOPE, D. P., KENT, P. W.: J. Chem. Soc. **1955,** 2831

Gyula DEÁK
Klára GÁLL-ISTÓK
Judit HASKÓ-BREUER
H-1083 Budapest, Szigony-u. 43.

Pál SOHÁR
H-1045 Budapest, Szabadságharcosok u. 47/49.

Acta Chimica Academiae Scientiarum Hungaricae, Tomus 92 (4), pp. 427—430 (1977)

INFRARED STUDIES ON SOME POWDER COPPER COMPLEXES

B. N. MISRA, S. D. SHARMA and S. K. GUPTA

(SHORT COMMUNICATION)

(Physics Department, University of Allahabad)

Received June 25, 1976

Amino acids exist as dipolar ions in the crystalline state. Empirical band assignments have been made for dipolar ions of glycine [1] α-alanine [2] and α-aminoisobutyric acid [3]. The infrared spectra of crystalline amino acids have been measured by KLOTZ and GRUEN [4] and THOMPSON *et al.* [5]. KRISHNAN and BALASUBRAMANIAN [6] also studied Raman spectra of amino acids in the crystalline state. In a complex, two glycinate ions co-ordinate to the metal by forming a trans-square planar structure:

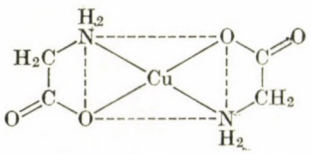

Copper has been found to have a similar surrounding in most of the copper complexes of amino acids. Oxygen of carboxylic group which is not co-ordinated to the metal are hydrogen-bonded either to amino group of neighbouring molecules or to water of crystallization or is bonded weakly to the metal of the neighbouring complex. Thus COO stretching frequencies of complexes of amino acids are affected by co-ordination as well as intermolecular interaction. In general, antisymmetric COO stretching frequency is much more sensitive to these influences than is the symmetric one. An increase in covalency of M–O bond leads to more asymmetrical carboxyl group and this increases the difference of frequencies between the two COO stretching bands.

All the chemicals used in preparation of the samples were high grade obtained from B. D. H. and Merck. Copper complexes with amino acids glycine, β-alanine, DL-methionine and L-asparagine were prepared as described in literature [7—9]. The samples were properly dried after purification. The first two samples are found to be soluble in water, while the latter two are insoluble. Solid complexes were studied in infrared region between 2—15 μ on a Perkin-Elmer Automatic Recording Spectrometer. The complexes were

intimately ground with KBr and then pellets were prepared of the mixture. These pellets were subjected to spectral analysis using pure KBr pellets as a blank.

The positions of all the absorption bands appearing in the spectra are measured and are shown in Table I, along with the intensity category. The difference of frequencies between the asymmetric and symmetric stretching

Table I

Position of different absorption bands observed in copper amino acid complexes

No.	Cu/glycine μ	Cu/β-alanine μ	Cu/DL methionine μ	Cu/L-asparagine μ
1	S 3.05	M 3.0	S 3.075	S 3.075
2	S 6.15	W 3.15	S 3.4	S 5.90
3	S 7.14	W 3.225	S 6.125	W 6.075
4	S 7.5	W 3.375	W 6.825	W 6.25
5	S 8.75	S 6.2	W 6.95	M 7.05
6	M 9.375	S 6.3	S 7.125	W 7.225
7	M 9.575	W 6.8	S 7.45	W 7.325
8	W 10.35	S 7.05	M 7.925	W 7.625
9	M 10.8	M 7.45	S 8.6	W 7.925
10		W 7.6	W 9.15	S 8.10
11		S 7.9	W 9.425	S 8.6
12		W 8.6	W 10.6	W 8.8
13		W 8.8	W 12.1	W 8.925
14		M 9.25	M 12.5	W 9.275
15		M 9.75	M 13.15	S 9.75
16		S 10.10	M 13.6	W 10.375
17		S 11.05	W 14.35	W 10.65
18		M 11.30		W 11.125
19		M 13.30		W 11.425
20				S 12.4
21				W 12.65

S — strong band, M — medium band and W — weak band

bands of COO in each sample has been calculated and this is proposed to be proportional to the covalent character of the copper oxygen bond in the sample (Table II).

It has been noted that all the complexes show strong absorption bands near 3.0μ. The positions of these bands vary from 3.0μ to 3.125μ. These have been assigned to NH_2 stretching vibrations. This region is carried for the de-

termination of the nature of copper to ligand bonding present in copper amino acid complexes. Appearance of N—H stretching absorption in our complexes in a higher wavelength region (3.0—3.125μ) compared to the range (2.94—3.13μ) for sodium salts of amino acids indicates the presence of N → Cu^{++} co-ordination. The absence of an absorption band near 5.8μ and the presence

Table II

Relative covalency in different copper complexes

Complex	V_{as} (COO)	V_s (COO)	$V_{as}-V_s$
Cu/glycine	6.153	7.140	0.987
Cu/β-alanine	6.300	7.05	0.75
Cu/DL-methionine	6.125	7.125	1.00
Cu/L-asparagine	6.25	7.05	0.80

of a very strong band in the region (6.15—6.25μ) indicate that the carboxyl to copper bond has a high degree of ionic character. This also indicates that the resonance in carboxylate ions is preserved so that the two carbon to oxygen bonds are equivalent and can be presented as 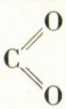 . A strong band at 5.9μ for Cu/L-asparagine suggests a covalency in the bonding between carboxyl group and copper in this complex.

The above observations of Cu-amino acid complexes are in accord with the evidence from X-ray crystal structure data of a square planar configuration of copper complexes. They show that linear *sp* metal bond orbitals are involved in the N-copper bonds in our complexes. The blue colour of the complexes also shows that the bonds are paramagnetic and the inner *d* orbitals are not used for bond formation. If this electrostatic bonding between copper and oxygen in the copper amino acid complexes is a general phenomenon and the bond formation takes place only with the outer *d* orbitals, it follows that complexes of the type $Cu(ligand)_2$ are always planar rather than tetrahedral. This has been found at least in all of the complexes studied here.

*

The authors SDS and SKG are thankful to CSIR for financial assistance.

REFERENCES

[1] Tsuboi, M., Onishi, K., Nakagawa, I., Shimanouchi, T., Mizushima, S.: Spectrochim. Acta., **12,** 253 (1958)
[2] Fukushima, K., Onishi, T., Shimanouchi, T., Mizushima, S.: Spectrochim. Acta., **14,** 236 (1959)
[3] Tsuboi, M., Takenishi, T.: Bull. Chem. Soc. Japan, **32,** 1044 (1959)

[4] KLOTZ, I. M., GRUEN, D. M.: J. Phys. Chem. **52,** 961 (1948)
[5] THOMPSON, H. W., NICHOLSON, D. L., SHORT, L. N.: Discuss. Faraday Soc. **9,** 222 (1950)
[6] KRISHNAN, R. S., BALASUBRAMANIAN, K.: Proc. Ind. Acad. Sci., **48***A*, 55, 138 (1958)
[7] FREEMAN, H. C., SNOW, M. R., NITTA, I., TOMITA, K.: Acta Crystallographica **17,** 1463 (1964)
[8] TOMITA, K.: Bull. Chem. Soc. Japan, **34,** 297 (1961)
[9] AULIFF, QUAGLIANO et al.: Inorg. Chem. **5,** 1996 (1966)

B. N. MISRA
S. D. SHARMA
S. K. GUPTA
Allahabad 211002, India

RECENSIONES

Topics in Current Chemistry. Managing Editor: F. Boschke. Vol. 62. Synthetic and Mechanistic Organic Chemistry

Springer-Verlag. Berlin, Heidelberg, New-York 1976. 258 pages

Volume 62 of the well-known and popular series covers three themes:

(1) F. MINISCI: *Homolytic Aromatic Substitutions.*

The discussion of homolytic aromatic substitution, proceeding *via* free radicals, is missing from most of the modern organic chemical textbooks. One of the reasons is that even the most extensively studied reaction of this kind, homolytic arylation, can be performed only with very poor selectivity.

However, radical substitutions were found in recent investigations both in the field of homocyclic and heterocyclic aromatic compounds, which proceed with excellent positional and substrate selectivities. This aroused the interest of synthetic chemists in processes of this kind. Moreover, the effect of polar factors on the reactivity of free radicals can be easily evaluated on suitable models, which facilitates the prediction of the course of the processes.

The Italian author discusses under consideration of these aspects in an absorbing way over 48 pages this undeservedly neglected field.

(2) J. B. HENDRICKSON: *A General Protocol for Systematic Synthesis Design.*

The synthesis of more complicated organic molecules can be regarded even today as an "art" rather than a science.

Efforts to change this situation and particularly to utilize computers for this purpose, have been multiplied in the last 10—15 years. For the use of computers, suitable protocols are needed. Professor Hendrickson describes on over 50 pages such a protocol, and this is followed by a table of 70 pages, containing the various patterns. Those attracted to the subject will read with great interest the concept elaborated during long years, which, however, as emphasized also by the author. cannot yet take adequately into consideration the stereochemical aspects.

(3) C. WENTRUP: *Rearrangements and Interconversions of Carbenes and Nitrenes.*

The Swiss author deals with reactions proceeding through the above intermediates, which are difficult to study. Of these reactions, primarily intramolecular processes proceeding in the gas phase are discussed, where the starting material of the nitrenes and carbenes is a diazo compound or azid.

It can be seen from the aforesaid that a rather narrow field is covered in the 78 pages available, which has its advantages and drawbacks. An advantage is that a detailed discussion, including even a complete gas chromatogram on p. 229, is given. However, it should be mentioned among the drawbacks that the field promised by the title is only partly covered.

All three chapters, based on the most modern literature, will not fail to interest the reader, so that the book as a whole can be recommended for study by organic chemists.

CS. SZÁNTAY

Theoretical Inorganic Chemistry, II. Vol. 65 of the series "Topics in Current Chemistry"

Springer-Verlag. Berlin, Heidelberg, New York 1976

The volume consists of three independent parts: K. BERNAUER: Diastereoisomerism and diastereoselectivity in metal complexes (36 pages); M. S. WRIGHTON: Photochemical reactions of co-ordination compounds (68 pages); A. ALBINI, H. KISCH: Complexing and activation of diazenes and diazo compounds (42 pages). Though the three parts are independent of one another, all three give a survey on recent results attained in a particular field of metal complex chemistry. Another common feature of the three parts is that the metal complexes discussed are of biological importance. Thus, for example, the stereoselectivity of co-ordination compounds is often brought into relationship with the well-known specific stereochemical behaviour of biological systems. In metal-containing enzymes metal ions have also a stereochemical function. In addition to increasing the probability of the reaction between the interacting molecules in the co-ordination sphere, metal ions also orient the reactions in a certain direction. Owing to the great complexity of the systems occurring in nature, their better understanding is often attempted by the study of model compounds. The knowledge of the stereospecific behaviour of the models (metal complexes) yields useful information for the study of biological systems. The importance of the co-ordination properties of diazenes, discussed in the third part, is due to the fact that, according to recent research, diazene complexes are presumably intermediates in biological nitrogen fixation. BERNAUER primarily summarizes results in conjunction with the diastereoselectivity of molecules, which have a single ligand with chiral properties. These may be bidentate (*e. g.* 1,2-diamines), tri-, quadri-, quinqe- and sexidentate ligands. Though many mixed ligand complexes have also been studied and their number is steadily increasing, experimental material available so far is insufficient for general conclusions. Bernauer examines on hand of several examples the requirements to be met by ligands located in the co-ordination sphere and thinks that the consideration of five parameters is decisive: (1) the nature of the ligand atoms; (2) the number and size of the chelate rings; (3) the mode of linkage of the chelate rings; (4) the type and position of the substituents; (5) the nature of the metal atoms. The first three parameters determine the geometry of the complex. The fourth parameter is a decisive factor with respect to chirality, determining the configuration of the complex, the conformation of the chelate rings and the absolute configuration of the asymmetric ligand atoms. As to the effect of the metal ion, the author thinks it important to collect as much information as possible on the influence of crystal field parameters, the charge of the metal and the ionic radius on the stereochemistry of metal complexes. Though the restricted number of optically active ligands strongly limits a systematic study of diastereoselectivity, BERNAUER draws useful conclusions from results known so far and marks out the advisable directions of future research. This part of the book cites 134 references.

The starting concept of WRIGHTON in discussing the photochemistry of transition metal complexes is the electron configuration (in the ground state and excited state). In the survey of photosubstitution reactions the reaction mechanisms are described. He discusses how Adamson's rules relevant to the direction of photosubstitution reactions can be supported in the light of MO and ligand field theories. Associative and dissociative types of reaction mechanisms are illustrated mainly by results obtained for Cr(III), Co(III), Rh(III) and Ir(III) complexes. He points out that in several cases there is an essential difference between the stereochemical processes of photosubstitution and thermal substitution. In further chapters of this part, WRIGHTON discusses the splitting of the metal–metal bond by photolysis in clusters, *cis-trans* isomerization by light during complex formation, and finally, photochemical redox reactions. The survey, comprising 196 references, is too compact, the divergence of the theme does not make possible the clear statement of the problems, and general conclusions drawn from results obtained so far are missing.

The third part of the book deals with the transition metal complexes of diazenes and diazo compounds. The novel character of the theme is reflected also by the fact that the 119 references given are, almost without exception, papers published later than 1970 (the first complex of this kind has been prepared in 1970). ALBINI and KISCH organize the survey clearly and logically. They refer to the electronic structure of diazenes and summarize also the results of quantum-chemical calculations relevant to diazenes. Complexes derived from diazenes are grouped as follows: mononuclear σ complexes, dinuclear σ complexes, Π cluster compounds, complexes formed by the splitting of the N=N bond. They describe briefly the preparation of the complexes belonging to the individual types, and evaluate the results of IR, UV, H-NMR, ^{13}C-NMR and X-ray diffraction investigations of the

compounds, pointing out in several cases also the inconsistencies between the results. Separate chapters deal with the reactions, primarily with the cycloaddition of complexes. It becomes evident from the results presented that, owing to the particular electronic structure of the diazeno group, various interactions can be observed in the complexes. The use of the complexes in catalytic processes seems promising. Results obtained in the cycloaddition reactions are of general importance from the point of view of the study of factors determining the photochemical and thermal reactions of co-ordinated ligands. Iron carbonyls activate the diazeno group to attack on unsaturated molecules, and this permits the convenient synthesis of new heterocyclic compounds. The reactions of diazeno complexes might be crucial steps in the incorporation of N_2 into organic compounds.

J. NAGY

INDEX

PHYSICAL AND INORGANIC CHEMISTRY

On the Mechanism of Cyclopentane Radiolysis, Cs. KESZEI, L. WOJNÁROVITS, G. FÖLDIÁK 329

Possibility of Coupling Polarization Measurements and Tracer Adsorption Measurements for the Study of Oxidation and Reduction Processes on a Platinum Electrode, Gy. HORÁNYI 351

Iterative Recalculation of Beta Integrals, J. SZŐKE, Á. I. KISS 367

Kinetics of the Complex Formation between Iron(III) and α-Oxy-α-dibutylphosphine-oxido-propionic Acid, A. MIFTAHOVA, L. DÓZSA, M. T. BECK 379

Identity of the Donor Atoms in N,N'-disubstituted Thiourea Complexes of Tin(IV) Halides, S. A. A. ZAIDI, T. A. KHAN, K. S. SIDDIQI 387

A Pseudoexact Parameter Method for the Analysis of Intramolecular Force Fields. Application to Degenerate Vibrations of some Molecules, T. R. ANANTHAKRISHNAN 395

Chemistry of Lanthanide Chelates. Synthesis and Properties of 2-*p*-tolylamino-4-*p*-tolylimino-2-pentene Complexes of the Tripositive Lanthanide Ions, M. MOHAN .. 403

Excess Thermodynamic Properties of Mixing Due to Dipolar Interactions, J. LISZI 409

ORGANIC CHEMISTRY

Oxazepines and Thiazepines, III. Synthesis of 2,3-Dihydro-2,4-diphenyl-1,5-benzothiazepines by the Reaction of 2-Aminothiophenol with Chalcones Substituted in Ring A, A. LÉVAI ᴮ BOGNÁR 415

The Acylation of 4,6-O-benzylidene-2-benzyloxycarbonylamino-2-desoxy-D-gluconic Acid, Gy. DEÁK, K. GÁLL-ISTÓK, J. HASKÓ-BREUER, P. SOHÁR 421

Infrared Studies on some Powder Copper Complexes, B. N. MISRA, S. D. SHARMA, S. K. GUPTA (Short communication) 427

RECENSIONES 431

Printed in Hungary

A kiadásért felelős az Akadémiai Kiadó igazgatója — Műszaki szerkesztő: Zacsik Annamária

A kézirat nyomdába érkezett: 1976. XII. 2 — Terjedelem 9,45 (A/5) ív, 38 ábra

77.3888 Akadémiai Nyomda, Budapest — Felelős vezető: Bernát György

ACTA CHIMICA

TOMUS 92

Fasciculus 1
Fasciculus 2
Fasciculus 3
Fasciculus 4

INDEX

AGARWAL, N. L., MITAL, R. L.: A Novel Synthesis of 12H-Benzo [A] Phenothiazin-5-ols and Their Esters 89
ANANTHAKRISHNAN, T. R.: A Pseudoexact Parameter Method for the Analysis of Intramolecular Force Fields. Application to Degenerate Vibrations of Some Molecules 395
ANSARI, NASEER AHMAD, s. SHAMEEM, M.
BAGYIN, L. s. MOHAI, B.
BECK, M. T. s. MIFTAHOVA, A.
BERNÁT, G., SOHÁR, P., LÁNG, K. L., GÖNDÖS, GY., GERA, L., PÁL, A.: Stereochemical Studies, XXVII. Studies on Cyclic 2-Hydroxycarboxylic Acids, VI. Neighbouring Hydroxyl Group Catalysis in the Alkaline Hydrolysis of Ethyl *Cis*- and *Trans*-2-hydroxycyclopentane-, Cyclohexane-, Cycloheptane- and Cyclooctanecarboxylates 178
BÉRCES, T.: Empirical Correlation Between the Potential Energy of Bond Dissociation and Bond Length 31
BESENYEI, G. s. MÓGER, D.
BLICKLE, T. s. POLINSZKY, K.
BOGNÁR, R. s. HORVÁTH, G.
BOGNÁR, R. s. LÉVAI, A.
CSERÉP, GY. s. KOVÁCS, A.
DEÁK, GY., GÁLL-ISTÓK, K., HASKÓ-BREUER, J., SOHÁR, P.: The Acylation of 4,6-O-benzylidene-2-benzyloxycarbonylamino-2-desoxy-D-gluconic Acid 421
DOLESCHALL, G., VÁNKAI, G.: 1,1,4-Triazines and Condensed Derivatives, XVII. Ethanolysis of 3-Methyltio-1,2,4-triazin-52(H)-one and a Novel Synthesis of 6-aza-2-thiouracil 323
DÓZSA, L. s. MIFTAHOVA, A.
EL-SAMABY, A. A. s. ISSA, R. M.
ERDEY-GRÚZ, T., HORÁNYI, GY., SZETEY, É.: Studies of Oxygen Overvoltage on Platinium Electrodes. The Interpretation of the Changes in Overvoltage under the Effect of Σ-Caprolactam (in German) 249
ETAIW, S. H. s. ISSA, R. M.
FAROOQI, A. S., s. ZAIDI, S. A. A.
FEHÉR, G. s. ZUBOVICS, Z.
FODOR, L. s. SZABÓ, J.
FÖLDIÁK, G. s. KESZEI, CS.
FÖLDIÁK G. s. KOVÁCS, A.
FÜLÖP, J. s. POLINSZKY, K.
GAÁL, GY. s. HORVÁTH, G.
GÁLL-ISTÓK, K. s. DEÁK, GY.
GERA, L. s. BERNÁTH, G.
GOEL, R. L. s. SING, P.
GÖNDÖS, GY. s. BERNÁTH, G.
GUDKOV, B. S. s. MAMALADZE, L. M.
GUPTA, S. K. s. MISRA, B. N.
GUTMAN, I.: The Relation Between Resonance Energy and Molecular Structure 65
HANKOVSZKY, O. H. s. HIDEG, K.
HASKÓ-BREUER, J. s. DEÁK, GY.

HIDEG, K., HANKOVSZKY, O. H., TIGYI, J.: Nitroxides, I. Sulfonic Esters of 4-Hydroxy--2,2,6,6-tetramethyl-piperidine 1-oxyl and Their Reaction with Nucleophilic Reactants 85
HINDAWAY, A. M., NASSAR, A. M. G., ISSA, R. M.: Preparation and IR Spectrophotometric Study of Charge-Transfer Complexes of 3,5-Dinitrobenzoic Acid with Aromatic Compounds 263
HORÁNYI, GY. s. ERDEY-GRÚZ, T.
HORÁNYI GY.: Possibility of Coupling Polarization Measurements and Tracer Adsorption Measurements for the Study of Oxidation and Reduction Processes on a Platinum Electrode 351
HORVÁTH G., GAÁL, GY., KEREKES, P., BOGNÁR, R.: Synthesis and Structure Investigations of Some 6-Substituted Dihydrocodeins and Dihydro-iso-codeins (in German) 311
ISSA, I. M. s. ISSA, R. M.
ISSA, R. M., EL-SAMANY, A. A., ISSA, I. M., ETAIW, S. H.: Electronic Absorption Spectra of Substituted Carbazoloquinones. Study of the Mechanism of Hexene Radiolysis, II. Investigation of *n*-Hexene Isomers with Additives 211
ISSA, R. M. s. HINDAWAY, A. M.
KEREKES, P. s. HORVÁTH, G.
KESZEI, CS., WOJNÁROVITS, L., FÖLDIÁK, G.: On the Mechanism of Cyclopentane Radiolysis 329
KHAN, T. A. s. ZAIDI, S. A. A.
KHULBE, K. C., MANN, R. S.: Structure of Vanadium-Phosphorus Oxide Catalysts 17
KIPERMAN, S. L. s. MAMALADZE, L. M.
KISS, A. B., SZONTAGH, E.: Infrared Spectrophotometric Studies on Aluminium Oxide Layers Prepared by Anodic Oxidation 129
KISS, Á. I. s. SZŐKE, J.
KISS, L.: Kinetic Equations fo Multistep Electrode Processes, III 113
KOVÁCS, A., CSERÉP. GY., FÖLDIÁK, G.: Study of the Mechanism of Hexene Radiolysis, I. Investigation of Cyclohexene in the Presence of Additives 117
KOVÁCS, A., CSERÉP, GY., FÖLDIÁK, G.: Study of the Mechanism of Hexene Radiolysis, II. Investigation of *n*-hexene Isomers with Additives 223
KOVÁCS, G. s. MÓGER, D.
LÁNG, K. L. s. BERNÁTH, G.
LÉVAI, A., BOGNÁR, R.: Oxazepines and Thiazepines, III. Synthesis of 2,3-Dihydro-2,4--diphenyl-1,5-benzothiazepines by the Reaction of 2-Aminothiophenol with Chalcones Substituted in Ring A 415
LISZI, J.: Excess Thermodynamic Properties of Mixing Due to Dipolar Interactions 409
MALLÁT, T. s. POLYÁNSZKY, É.
MAMALADZE, L. M., NEKRASOV, N. V., GUDKOV, B. S., KIPERMAN, S. L.: On the Mechanism of the Hydrogenation and Isotopic Exchange in the Alkylaromatic Hydrocarbons — Substituted Cycloalkanes System on Nickel 73
MANN, R. S. s. KHULBE, K. C.
MARKÓ, L. s. SPEIER, G.
MATHEW, J., TANDON, S. N.: Ion-Exchange Behaviour of Stannic Antimonate Separation of Some Metal Ions of Analytical Importance 1
MÁZOR, L.: Determination of Sulfur in Organic Compounds by the Hydropyrolysis Method 105
MENCZEL, GY.: Crystal and Molecular Structure of Decamethylbicyclo-Hexasiloxane, $Si_6O_7C_{10}H_{30}$ 9
MIFTAHOVA, A., DÓZSA, L., BECK, M. T.: Kinetics of the Complex Formation Between Iron (III) and α-oxy-α-dibutylphosphineoxido-propionic Acid 379
MISRA, B. N., SHARMA, S. D., GUPTA, S. K.: Infrared Studies on Some Powder Copper Complexes 427
MITAL, R. L. s. AGARWAL, N. L.
MÓGER, D., BESSENYEI, G., KOVÁCS, G., NAGY, F.: TPD Study of the Stability of H_2 Chemisorbed on Al_2O_3 and Pt 237
MOHAI, B., BAGYIN, L.: Thermolysis of Cyano Complexes, X. Synthesis and Thermal Decomposition of Quaternary Ammonium Hydrogen Cyanometallates (Regular Salts) (in German) 271
MOHAI, B., BAGYIN, L.: Thermolysis of Cyano Complexes, XI. Synthesis and Thermal Decomposition of Quaternary Ammonium Hydrogen Cyanometallates (Protonisation Complexes) (in German) 281

MOHAN, M.: Chemistry of Lanthanide Chelates. Synthesis and Properties of 2-*p*-tolylamino-4-*p*-tolylimino-2-pentene Complexes of the Tripositive Lanthanide Ions 403
NAGY, F. s. MÓGER, D.
NASSAR, A. M. G. s. HINDAWAY, A. M.
NEELAM SINGHAL s. ZAIDI, S. A. S.
NEKRASOV, N. V. s. MAMALADZE, L. M.
PÁL, A. s. BERNÁTH, G.
PETRÓ, J. s. POLYÁNSZKY, É.
POLINSZKY, K., BLICKLE, T., FÜLÖP, J., TŐRÖS, R., VAJDA, T.: The Optimation of Fermentation Processes by Means of the Propagation Curves of Microorganism Cultures (in German) 187
POLYÁNSZKY, É., MALLÁT, T., PETRÓ, J.: Electrochemical Investigations on Supported Palladium Catalysts 147
Recensiones 99, 201, 327, 431
SHAMEEM ANSARI, NASEER AHMAD: Bis-vanillin-*o*-phenylene Diamine Complexes of Rare Earths 27
SHARMA, S. D. s. MISRA, B. N.
SIDDIQUI, Z. A. s. ZAIDI, S. A. A.
SIDDIQUI, K. S. s. ZAIDI, S. A. A.
SIMON, Á. s. SPEIER, G.
SINGH, B. P. s. SINGH, P.
SINGH, C. S. s. SINGH, M. M.
SINGH, M. M., SINGH, C. S.: Anodic Oxidation of Potassium Oxalate in Sulfuric Acid on a Germanium Semiconductor-Electrolyte Interface 289
SINGH, P., SINGH, B. P., SINGH, V., GOEL, R. L.: Studies on Some Square Planar Complexes of N-5-Acetoacenaphthylidene-O-amino Phenol with Cu(II) Pt(II) and Pd(II) ... 143
SINGH, V. s. SINGH, P.
SOHÁR, P. s. BERHÁTH, G.
SOHÁR, P. s. SZABÓ, J.
SPEIER, G., SIMON, Á., MARKÓ, L.: The Reaction of Carbon Dioxide and Dioxygen with Dinitrogentris (Triphenylphosphine) Cobalt (0) 169
STERGIOPOULOS, Ch. s. WOLFRAM, W.
SZABÓ, J., FODOR, L., VARGA, I., VINKLER, E., SOHÁR, P.: Synthesis of 2*H*-1,3-benzothiazine Derivatives, II 317
SZETEY, É. s. ERDEY-GRÚZ, T.
SZŐKE, J., KISS, Á. I.: Iterative Recalculation of Beta Integrals 367
SZONTAGH, E. s. KISS, A. B.
TANDON, S. N. s. MATHEW, J.
TIGYI, J. s. HIDEG, K.
TOLDY, L. s. ZUBOVICS, Z.
TŐRÖS, R. s. POLINSZKY, K.
VÁNKAI, G. s. DOLESCHALL, G.
VAJDA, T. s. POLINSZKY, K.
VARGA, I. s. SZABÓ, J.
VINKLER, W. s. SZABÓ, J.
WOJNÁROVITS, L. s. KESZEI, Cs.
WOLFRAM, W., STERGIOPOULOS, CH.: Wettability of Gelatine Gels (in Russian) 167
ZAIDI, S. A. A., FAROOQI, A. S. NEELAM, SINGHAL: Spectal and Magnetic Studies on Copper (II) Complexes of Indazoles 49
ZAIDI, S. A. A., SIDDIQUI, Z. A.: Ionization of Inorganic Acid Anhydrides and Acid Halides in Chlorosulphuric Acid. "Formation of Oxycations" 57
ZAIDI, S. A. A., KHAN, T. A., SIDDIQUI, K. S.: Identity of the Donor Atoms in N,N'-disubstituted Thiourea Complexes of Tin (IV) Halides 387
ZUBOVICS, Z., FEHÉR, G., TOLDY, L.: Investigations on the Synthesis of 1,5-benzodiazepines (in German) 293

Les Acta Chimica paraissent en français, allemand, anglais et russe et publient des mémoires du domaine des sciences chimiques.

Les Acta Chimica sont publiés sous forme de fascicules. Quatre fascicules seront réunis en un volume (4 volumes par an).

On est prié d'envoyer les manuscrits destinés à la rédaction à l'adresse suivante:

Acta Chimica
H-1521 Budapest, Hongrie

Toute correspondance doit être envoyée à cette même adresse.

La rédaction ne rend pas de manuscript.

Le prix de l'abonnement est de $ 32,00 par volume.

Abonnement — en Hongrie à l'Akadémiai Kiadó (1363 Budapest, P.O.B. 24. C.C.B. (Bankszámla) 215 11488, à l'étranger à l'Entreprise pour le Commerce Extérieur «Kultúra» (1389 H-Budapest 62, P.O.B. 149, compte-courant No. 218 10990) ou à l'étranger chez tous les représentants ou dépositaires.

Die Acta Chimica veröffentlichen Abhandlungen aus dem Bereich der chemischen Wissenschaften in deutscher, englischer, französischer und russischer Sprache.

Die Acta Chimica erscheinen in Heften wechselnden Umfanges. Vier Hefte bilden einen Band. Jährlich erscheinen 4 Bände.

Die zur Veröffentlichung bestimmten Manuskripte sind an folgende Adresse zu senden:

Acta Chimica
H-1521 Budapest, Ungarn

An die gleiche Anschrift ist auch jede für die Redaktion bestimmte Korrespondenz zu richten.

Manuskripte werden nicht zurückerstattet. Abonnementspreis pro Band: $ 32,00.

Bestellbar für das Inland bei Akadémiai Kiadó (1363 Budapest, Postfach 24, Bankkonto Nr. 215 11488), für das Ausland bei Außenhandelsunternehmen »Kultúra« (1389 Budapest 62, P.O.B. 149. Bankkonto Nr. 218 10990) oder bei seinen Auslandsvertretungen und Kommissionären.

«Acta Chimica» издают статьи по химии на русском, английском, французском и немецком языках.

«Acta Chimica» выходят отдельными выпусками разного объема 4. выпуска составляют один том и за год выходят 4 тома.

Предназначенные для публикации рукописи следует направлять по адресу:

Acta Chimica
H-1521 Budapest, BHP

Всякую корреспонденцию в редакцию направляйте по этому же адресу.

Редакция рукописей не возвращает.

Подписная цена — $ 32,00 за том.

Отечественные подписчики направляйте свои заявки по адресу Издательства Академии Наук (1363 Budapest, P.O.B. 24, Текущий счет 215 11488), а иностранные подписчики через организацию по внешней торговле «Kultúra» (1389 H-Budapest 62, P.O.B. 149. Текущий счет 218 10990) или через ее заграничные представительства и уполномоченных.

Reviews of the Hungarian Academy of Sciences are obtainable at the following addresses:

AUSTRALIA
C.B.D. LIBRARY AND SUBSCRIPTION SERVICE, Box 4886, G.P.O., *Sydney N.S.W. 2001*
COSMOS BOOKSHOP, 145 Ackland Street, *St. Kilda (Melbourne), Victoria 3182*

AUSTRIA
GLOBUS, Höchstädtplatz 3, *1200 Wien XX*

BELGIUM
OFFICE INTERNATIONAL DE LIBRAIRIE, 30 Avenue Marnix, *1050 Bruxelles*
LIBRAIRIE DU MONDE ENTIER, 162 Rue du Midi, *1000 Bruxelles*

BULGARIA
HEMUS, Bulvar Ruszki 6, *Sofia*

CANADA
PANNONIA BOOKS, P.O. Box 1017, Postal Station "B", *Toronto, Ontario M5T 2T8*

CHINA
CNPICOR, Periodical Department, P.O. Box 50, *Peking*

CZECHOSLOVAKIA
MAD'ARSKÁ KULTURA, Národní třída 22, *115 66 Praha*
PNS DOVOZ TISKU, Vinohradská 46, *Praha 2*
PNS DOVOZ TLAČE, *Bratislava 2*

DENMARK
EJNAR MUNKSGAARD, Norregade 6, *1165 Copenhagen*

FINLAND
AKATEEMINEN KIRJAKAUPPA, P.O. Box 128, *SF-00101 Helsinki 10*

FRANCE
EUROPERIODIQUES S. A., 31 Avenue de Versailles, *78170 La Celle St. Cloud*
LIBRAIRIE LAVOISIER, 11 rue Lavoisier, *75008 Paris*
OFFICE INTERNATIONAL DE DOCUMENTATION ET LIBRAIRIE, 48 rue Gay-Lussac, *75240 Paris Cedex 05*

GERMAN DEMOCRATIC REPUBLIC
HAUS DER UNGARISCHEN KULTUR, Karl-Liebknecht-Strasse 9, *DDR-102 Berlin*
DEUTSCHE POST ZEITUNGSVERTRIEBSAMT, Strasse der Pariser Kommüne 3—4, *DDR-104 Berlin*

GERMAN FEDERAL REPUBLIC
KUNST UND WISSEN ERICH BIEBER, Postfach 46, *7000 Stuttgart 1*

GREAT BRITAIN
BLACKWELL'S PERIODICALS DIVISION, Hythe Bridge Street, *Oxford OX1 2ET*
BUMPUS, HALDANE AND MAXWELL LTD., Cowper Works, *Olney, Bucks MK46 4BN*
COLLET'S HOLDINGS LTD., Denington Estate, *Wellingborough, Northants NN8 2QT*
WM. DAWSON AND SONS LTD., Cannon House, *Folkestone, Kent CT19 5EE*
H. K. LEWIS AND CO., 136 Gower Street, *London WC1E 6BS*

GREECE
KOSTARAKIS BROTHERS, International Booksellers, 2 Hippokratous Street, *Athens-143*

HOLLAND
MEULENHOFF-BRUNA B.V., Beulingstraat 2, *Amsterdam*
MARTINUS NIJHOFF B.V., Lange Voorhout 9—11, *Den Haag*
SWETS SUBSCRIPTION SERVICE, 347b Heereweg, *Lisse*

INDIA
ALLIED PUBLISHING PRIVATE LTD., 13/14 Asaf Ali Road, *New Delhi 110001*
150 B-6 Mount Road, *Madras 600002*
INTERNATIONAL BOOK HOUSE PVT. LTD., Madame Cama Road, *Bombay 400039*
THE STATE TRADING CORPORATION OF INDIA LTS., Books Import Division, Chandralok, 36 Janpath, *New Delhi 110001*

ITALY
EUGENIO CARLUCCI, P.O. Box 252, *70100 Bari*
INTERSCIENTIA, Via Mazzé 28, *10149 Torino*
LIBRERIA COMMISSIONARIA SANSONI, Via Lamarmora 45, *50121 Firenze*
SANTO VANASIA, Via M. Macchi 58, *20124 Milano*
D. E. A., Via Lima 28, *00198 Roma*

JAPAN
KINOKUNIYA BOOK-STORE CO. LTD., 17-7 Shinjuku-ku 3 chome, Shinjuku-ku, *Tokyo 160-91*
MARUZEN COMPANY LTD., Book Department, P.O. Box 5050 Tokyo International, *Tokyo 100-31*
NAUKA LTD. IMPORT DEPARTMENT, 2-30-19 Minami Ikebukuro, Toshima-ku, *Tokyo 171*

KOREA
CHULPANMUL, *Phenjan*

NORWAY
TANUM-CAMMERMEYER, Karl Johansgatan 41—43, *1000 Oslo*

POLAND
WĘGIERSKI INSTYTUT KULTURY, Marszałkowska 80, *Warszawa*
CKP I W ul. Towarowa 28 *00-958 Warsaw*

ROUMANIA
D. E. P., *Bucureşti*
ROMLIBRI, Str. Biserica Amzei 7, *Bucureşti*

SOVIET UNION
SOJUZPETCHATJ — IMPORT, *Moscow*
and the post offices in each town
MEZHDUNARODNAYA KNIGA, *Moscow G-200*

SPAIN
DIAZ DE SANTOS, Lagasca 95, *Madrid 6*

SWEDEN
ALMQVIST AND WIKSELL, Gamla Brogatan 26, *101 20 Stockholm*
GUMPERTS UNIVERSITETSBOKHANDEL AB, Box 346, *401 25 Göteborg 1*

SWITZERLAND
KARGER LIBRI AG, Petersgraben 31, *4011 Basel*

USA
EBSCO SUBSCRIPTION SERVICES, P.O. Box 1943, *Birmingham, Alabama 35201*
F. W. FAXON COMPANY, INC., 15 Southwest Park, *Westwood, Mass, 02090*
THE MOORE-COTTRELL SUBSCRIPTION AGENCIES, *North Cohocton, N. Y. 14868*
READ-MORE PUBLICATIONS, INC., 140 Cedar Street, *New York, N. Y. 10006*
STECHERT-MACMILLAN, INC., 7250 Westfield Avenue, *Pennsauken* N. J. 08110

VIETNAM
XUNHASABA, 32, Hai Ba Trung, *Hanoi*

YUGOSLAVIA
JUGOSLAVENSKA KNJIGA, Terazije 27, *Beograd*
FORUM, Vojvode Mišiča 1, *21000 Novi Sad*

12. VIII. 1977 Index: 26.007